Oral Abstract Presentations

- Abstracts 1-23 will be presented on Thursday
- Abstracts 24-59 will be presented on Friday

PVD Moderated eAbstract Poster Session

- Abstracts 124, 300, 303, 313, 318, 337, 487, 496, 631 will be presented

Poster Abstract Presentations

- Abstracts 93 – 265 will be presented on Thursday
- Abstracts 299 – 468 will be presented on Friday
- Abstracts 473 – 643 will be presented on Saturday

1

Human Monocyte Diversity in Cardiovascular Disease Revealed by Mass Cytometry

Anouk A Hamers, Graham D Thomas, Cheryl Kim, La Jolla Inst for Allergy and Immunology, San Diego, CA; Anh T Nguyen, Chantel McSkimming, Angela M Taylor, Coleen A McNamara, Univ of Virginia, Charlottesville, VA; Catherine C Hedrick, La Jolla Inst for Allergy and Immunology, San Diego, CA

Background: Monocytes are critical to the initiation and development of atherosclerosis. To date, 3 distinct human monocyte subsets have been identified based primarily on their expression of the surface markers CD14 and CD16. With the emerging knowledge of myeloid-derived suppressor cells and other myeloid subsets, we hypothesized that monocytes are likely more heterogeneous in composition. Therefore, we set out to use the high dimensionality of mass cytometry to accurately identify and define monocyte subsets in blood of healthy humans and their changes in cardiovascular patients. Methods: Heparinized blood from 12 healthy donors and 15 patients with defined cardiovascular disease (CVD) based on angiography and gensini score was obtained and analyzed by CyTOF mass cytometry. We employed the Phenograph algorithm to cluster and identify all healthy monocyte subsets based on their phenotypes using a 40-marker mass cytometry panel. Results: Phenograph identified a total of 15 monocyte clusters in healthy human blood. By performing hierarchical clustering, we were able to group these clusters into 6 larger meta-clusters and found that most of these meta-clusters fall within the CD14 classical monocyte population, illustrating significant heterogeneity among this monocyte population. Cell numbers of one of these monocyte meta-clusters were significantly increased in blood from patients with CVD. We also identified two subsets of nonclassical monocytes in healthy donors. One of these subsets showed higher expression of the integrin CD61 and tetraspanin CD9, pointing to a possible role for this subset in patrolling and platelet activation. Conclusion: Monocytes are highly diverse with the conventional classical subset showing the most diversity. The numbers and frequencies of some of these monocyte subsets are changed in CVD. Studies to identify their functions in CVD should provide new information for the role of monocytes in CVD.

Disclosures: **A.A.J. Hamers:** None. **G.D. Thomas:** None. **C. Kim:** None. **A.T. Nguyen:** None. **C. McSkimming:** None. **A.M. Taylor:** None. **C.A. McNamara:** None. **C.C. Hedrick:** None.

2

Aorta Intima-Resident Macrophages Contribute to Atherosclerotic Lesion Initiation

Jesse W Williams, Brian T Saunders, Ki-Wook Kim, Washington Univ in St. Louis, Saint Louis, MO; Slava Epelman, Univ of Toronto, Toronto, ON, Canada; Kory Lavine, Bernd H Zinselmeyer, Gwendalyn J Randolph, Washington Univ in St. Louis, Saint Louis, MO

Atherosclerosis is an underlying cause of cardiovascular disease and a leading cause of mortality worldwide. Macrophage accumulation in atherosclerotic plaque, their uptake of cholesterol, and subsequent local death drive disease progression. Lipid-laden plaque macrophages are thought to be exclusively derived from blood monocyte progenitors that are recruited following endothelial damage induced by cholesterol exposure. In our current study, we focused on characterization of resident vascular macrophages that reside in the aortic intima in plaque-prone areas, previously identified as 'vascular dendritic cells'. Using en face whole-mount confocal microscopy of aortas, we confirm a uniform resident $CD64^+$ $CD11c^+$ $CX3CR1^+$ $MHCII^+$ macrophage population, which is present in C57/BL6 mice resistant to atherosclerosis. Importantly, they do not express dendritic cell restricted genes zBTB46 or L-myc. We find aortic macrophages require M-CSF and Flt3 signaling for survival, but are independent of CCR2, CCR7, and GM-CSF receptor signaling, making them a distinct myeloid population. Lineage-tracing and parabiosis approaches suggest these cells derive from definitive hematopoiesis and are then self-maintained independent of blood-progenitors. Using these characterization data, we developed a labeling strategy to identify resident from recruited macrophages during kinetic studies of lesion progression. We find that resident aortic macrophages are the first cells to take up lipid following high fat diet exposure and expand within the arterial wall to form the initial lesion bed. In the absence of resident macrophages early lipid deposition in the aortic arch is ablated. Finally, utilizing an intravital carotid artery imaging approach, we identify resident aortic macrophages to be potential mediators of monocyte recruitment through direct interactions with rolling monocytes on the endothelial surface under diseased

and steady-states. Overall, these results shift our understanding of the cellular mechanisms responsible for plaque construction and maintenance.

Disclosures: **J.W. Williams:** None. **B.T. Saunders:** None. **K. Kim:** None. **S. Epelman:** None. **K. Lavine:** None. **B.H. Zinselmeyer:** None. **G.J. Randolph:** None.

This Research has received full or partial funding support from the American Heart Association.

3

Cellular Contributions of the Circadian Clock in Atherogenesis

Xueling Li, Ling Ruan, Austin Bentley, Stephen Haigh, Yuqing Huo, Bhupesh Singla, Gabor Csanyi, David Stepp, David Fulton, **R. Daniel Rudic**, Medical Coll of Georgia of Augusta Univ, Augusta, GA

Atherosclerosis is a leading cause of death despite the improvements in lipid and blood pressure control. The circadian clock, a molecular network of genes and proteins that controls 24-hour timing, has emerged to have a surprising role in the control of metabolic and vascular function. Herein we examined the impact of circadian rhythm dysfunction in atherogenesis by implementation of vascular transplant and PCSK9 based approaches to induce accelerated lesion development in mice. We find that atherogenesis is exacerbated in Bmal1-KO aortic grafts immersed in the hypercholesterolemic milieu of $ApoE^{-/-}$ mice. To assess if atherosclerosis was 'circadian rhythm dependent' we subjected wild-type mice to a shortened light cycle (4L/4D) and induced atherosclerosis by intravenous injection of a human PCSK-9 adeno associated virus. Atherosclerosis in the jet-lagged PCSK-9 mice was robustly increased relative to the atherosclerosis observed in WT mice on a normal light cycle (12L/12D), providing further evidence that circadian rhythm and the circadian clock contribute to atherosclerosis. However, atherosclerosis is a complex disease that is the net result of interplay between intrinsic (vascular cells) and extrinsic mechanisms (metabolism, blood pressure, and hormones) and the importance of clock function in individual cell types is poorly understood. We found that deletion or silencing of key circadian transcription factors resulted in an enhanced inflammatory and pro-oxidant phenotype with diminished NO production and greater lipid uptake in both macrophages and endothelial cells. Loss of circadian function in smooth muscle cells similarly resulted in enhanced production of reactive oxygen species and greater cell proliferation. Surprising, the silencing of Bmal2 in endothelial cells resulted in greater lipid uptake in oxLDL treated HAEC as well as increased expression of markers of autophagy, suggesting that Bmal2 may orchestrate numerous output functions in different cell types. In conclusion, we find that the circadian clock and circadian rhythm have a profound impact on atherosclerosis, to influence vascular cell inflammatory and lipid uptake responses, and identify an unexpectedly prominent role for the side-partner of Bmal1, Bmal2.

Disclosures: **X. Li:** None. **L. Ruan:** None. **A. Bentley:** None. **S. Haigh:** None. **Y. Huo:** None. **B. Singla:** None. **G. Csanyi:** None. **D. Stepp:** None. **D. Fulton:** None. **R. Rudic:** None.

This Research has received full or partial funding support from the American Heart Association.

4

Deletion of Macrophage Low-density Lipoprotein Receptor-related Protein 1 (LRP1) Accelerates Atherosclerosis Regression by Increasing CCR7-dependent Egress of Plaque Macrophages

Paul Mueller, Oregon Health and Science Univ, Portland, OR; Lin Zhu, Vanderbilt Univ Medical Ctr, Nashville, TN; Illaria Giunzioni, Hagai Tavori, Oregon Health and Science Univ, Portland, OR; John M Stafford, MacRae Linton, Vanderbilt Univ Medical Ctr, Nashville, TN; Sergio Fazio, Oregon Health and Science Univ, Portland, OR

We previously showed that mice lacking macrophage LDL receptor-related protein 1 (LRP1) undergo accelerated lesion formation due to increased apoptosis, decreased efferocytosis, and enhanced macrophage transformation into the inflammatory M1 phenotype. *In vitro,* LRP1-deficient macrophages ($M\Phi LRP1^{-/-}$) show enhanced plasticity with exaggerated polarization towards either the inflammatory M1- or the anti-inflammatory M2-phenotype depending on the stimulant (LPS or IL-4, respectively). During atherosclerosis regression, the M2:M1 macrophage ratio increases as lesion M1 macrophages egress and inflammation resolves. Thus, we hypothesize that atherosclerosis regression is accelerated in $M\Phi LRP1^{-/-}$ mice via enhanced macrophage M2 polarization and CCR7-dependent M1 macrophage

egress. ApoE-/- mice on high fat diet for 12 weeks were reconstituted with bone marrow from wildtype (WT) or MΦLRP1$^{-/-}$ mice and then placed on chow diet for 8 weeks. In this model, apoE is reintroduced into circulation to correct the hyperlipidemia and induce regression of atherosclerotic lesions. A cohort of apoE$^{-/-}$ mice reconstituted with apoE$^{-/-}$ bone marrow served as baseline controls. Lesions in both WT and MΦLRP1$^{-/-}$ mice regressed relative to controls (11% and 22%, respectively; $p<0.05$), but MΦLRP1$^{-/-}$ lesions were 13% smaller than those of WT mice ($p<0.05$). LRP1 deletion increased M2 transformation of macrophages and a higher M2:M1 macrophage ratio ($p<0.01$) in the plaque. MΦLRP1$^{-/-}$ lesions contained 36% fewer M1 macrophages compared to WT ($p<0.01$). *In vivo* studies of reverse cholesterol transport (RCT) revealed that MΦLRP1$^{-/-}$ have a 1.4-fold higher RCT compared to WT mice ($p<0.01$). MΦLRP1$^{-/-}$ lesions contained 2.5-fold more CCR7^{+} macrophages relative to WT lesions ($p<0.01$), and in our *in vivo* egress assay 4.6-fold more CCR7^{+} macrophages were found in mediastinal lymph nodes. *In vitro*, M1-differentiated MΦLRP1$^{-/-}$ macrophages expressed 1.6-fold higher *Ccr7* mRNA compared to WT controls ($p<0.01$). Thus, the absence of macrophage LRP1 accelerates atherosclerosis regression due to enhanced transformation of macrophages into an anti-inflammatory M2 phenotype, increased cholesterol efflux, and increased CCR7-driven egress of M1 macrophages from lesions.

Disclosures: **P. Mueller:** None. **L. Zhu:** None. **I. Giunzioni:** None. **H. Tavori:** None. **J.M. Stafford:** None. **M. Linton:** None. **S. Fazio:** None.

5

The Contribution of Microbiome Alterations to Atherosclerotic Plaque Regression in Mice

Michael Garshick, Tessa Barrett, Felix Zhou, Martin Blaser, Edward Fisher, New York Univ Medical Ctr, New York CIty, NY

Objective: The human microbiome represents an underexplored driver of atherosclerosis. Alterations to the intestinal microbiome are associated with, systemic inflammation and upregulation of M1 macrophages (Mφ). Our study aims to determine if alterations to the intestinal microbiome by antibiotic treatment interferes with atherosclerotic plaque regression in mice.
Methods: *ApoE*$^{-/-}$ mice were fed a western diet for 16 weeks to develop complex atherosclerosis in aortic arches. These arches were transplanted into the abdominal aorta of wild-type (WT) mice to model clinical aggressive lipid management and promote plaque regression. To assess the contribution of the microbiome to plaque regression, aortic arches were transplanted in WT mice (n=4), and WT mice pulsed with tylosin (antibiotic, n = 4) 3 days pre-transplant and the duration of the experiment (5 days). Arches were also transplanted into *ApoE*$^{-/-}$ mice as a plaque progression control (n =4).
Results: Antibiotic treatment of WT mice with tylosin compared to control WT mice did not change circulating total cholesterol (TC, 57 ± 21 mg/dl vs. 46 ± 24 mg/dl, p = 0.5), or HDL-C (42 ± 8 mg/dl vs. 34 ± 11 mg/dl, p = 0.32). No statistically significant difference in plaque size (117,801 ± 70,921 μm^2 vs. 133,286 ± 19,871 μm^2 vs. 132,976 ± 40,347 μm^2, p = 0.88) or the absolute Mφ content (44,672 ± 27,154 μm^2 vs. 32,546 ± 21,226 μm^2 vs. 54,154 ± 22,418 μm^2, p = 0.47) was observed in WT mice which received tylosin, compared to control WT and *ApoE*$^{-/-}$ mice, respectively. The composition of the plaques however did change: When compared to the control *ApoE*$^{-/-}$ mice, WT recipient mice had a 26% reduction in the percent of the plaques occupied by Mφ, while WT mice receiving tylosin had only a 4% reduction (p = 0.07). There was a 20% difference between the percent of plaque Mφ content in the WT receiving tylosin, compared to WT controls (38% ± 4.3 vs. 30% ± 6.2, p = 0.07).
Conclusion: Tylosin-treated WT mice undergoing regression had Mφ enrichment in their plaques compared to WT controls. This study suggests that microbiome alterations can negatively influence plaque regression. Intestinal microbiome analysis and further studies are needed to confirm and extend this finding.

Disclosures: **M. Garshick:** None. **T. Barrett:** None. **F. Zhou:** None. **M. Blaser:** None. **E. Fisher:** None.

6

A Novel *in vivo* Endothelial Hierarchy from Progenitor to Mature Endothelial Cells Reveals Key SoxF-Dependent Differentiation Process

Jatin Patel, Elke J Seppanen, Mathieu Rodero, Ho Yi Wong, Prudence Donovan, Nicholas M Fisk, Mathias Francois, Kiarash Khosrotehrani, The Univ of Queensland, Brisbane, Australia

Background: The formation of new blood vessels during adult life is often explained by angiogenesis. However, an alternate proposal now suggests that neo-vessels form from endothelial progenitors able to assemble all the intimal layers of vessel structures. Our aim was to define vessel-resident endothelial progenitors *in vivo* in a variety of tissues in physiological (aorta, lung) and pathological (wounds, tumors) situations. **Methods and Results:** Using common endothelial markers (CD34, CD31, VEGFR2) with flow cytometry, three sub-populations of endothelial cells could be identified among VE-Cadherin+ and CD45- cells. These were termed an endovascular progenitor (EVP) harboring CD31lo VEGFR2lo giving rise to an intermediate CD31intVEGFR2lo transit amplifying (TA) and a definitive differentiated (D) CD31hiVEGFR2hi population. Confirmation of these populations was demonstrated via lineage tracing using *Cdh5cre ^{ERt2}/Rosa-YFP* reporter mice. Importantly, EVP cells arose from vascular resident beds that could not be transferred by bone marrow transplantation, marking their distinction for hematopoietic/myeloid origin. Furthermore, EVP displayed progenitor like status with a high proportion of cells in a quiescent cell cycle phase. Only EVP cells and not TA and D cells had self-renewal capacity as demonstrated by *in* vitro colony forming and transplant studies *in vivo* in Matrigel^{TM} plugs in recipient mice. Through whole RNA sequencing we demonstrated that EVP cells highly expressed genes related to progenitor function such as *Sox9*, *Il33, Egfr* and *Pdfgrα,* whereas D cells highly expressed genes related to differentiated endothelium including *Ets1&2*, *Gata2*, *Cd31, Vwf* and *Notch*. We also determined the *Sox18* transcription factor as having a significant role in defining the endothelial hierarchy, which we validated through lineage-tracing using S*ox18Cre^{ERt2}/Rosa-YFP* mice. In the absence of functional SOX18/SOXF, EVP progenitors were still present, but TA and D populations were significantly reduced. **Conclusion:** In summary, we have demonstrated the existence of an entirely novel endothelial hierarchy, from EVP to TA to D. This has been demonstrated by the self-renewal, differentiation and molecular profiling of an EVP.

Disclosures: **J. Patel:** Ownership Interest; Modest; Angiostem. **E.J. Seppanen:** None. **M. Rodero:** None. **H. Wong:** None. **P. Donovan:** None. **N.M. Fisk:** None. **M. Francois:** None. **K. Khosrotehrani:** Ownership Interest; Modest; Angiostem.

7

In vivo Transcriptional Profiling of Endothelial Cells Identifies Vascular Bed-Specific Changes Upon Lps-Induced Endotoxemia

Audrey Cleuren, Martijn van der Ent, Kristina Hunker, Hui Jiang, Andrew Yee, David Siemieniak, Santhi Ganesh, David Ginsburg, Univ of Michigan, Ann Arbor, MI

Endothelial cells (ECs) form a critical barrier between blood and parenchymal cells and play an important role in many pathologic conditions, including sepsis. ECs are highly adaptive to their microenvironment and also act as a critical responder to microbial pathogens. Though ECs are thought to display extensive heterogeneity, detailed profiling of the *in vivo* EC gene expression program has been limited by the challenges of isolating ECs from complex tissues and the phenotypic drift associated with manipulation and expansion of ECs *in vitro*. We applied an *in vivo* system in which a conditional hemagglutinin-epitope tag is targeted into the mouse ribosomal protein *Rpl22* locus and specifically activated in ECs, allowing immunoisolation of endothelial ribosome-associated mRNA. Both EC-selected and total mRNA from tissue lysates (brain, heart, kidney, liver and lung) were subjected to RNA sequencing followed by differential expression analysis to determine EC-enriched transcripts. These analyses were performed under physiologic conditions as well as in LPS injected mice to study transcriptional changes induced in ECs following endotoxin exposure. LPS-induced endotoxemia resulted in striking changes in the EC transcriptome (~800 per tissue), and included transcripts associated with known sepsis related pathophysiology, including impaired hemostasis, leukocyte recruitment and increased vascular permeability. Gene ontology analysis of transcriptional changes shared between ECs of different tissues identified cellular response to LPS among the highest enriched biologic processes (adjusted p-value 5.2E-5), together with immune (2.0E-14) and inflammatory responses (4.4E-12). Novel transcripts not previously associated with ECs or endotoxemia were also identified, as well as a subset of genes uniquely expressed in distinct vascular beds. In conclusion, our findings demonstrate remarkable heterogeneity of the EC transcriptome across multiple vascular beds *in vivo*. The EC response to endotoxin challenge is also highly heterogeneous across vascular beds and provides new insight into the endothelial response to infectious challenges, as well as identifying potentially useful biomarkers for the onset of sepsis and response to therapy.

Disclosures: **A. Cleuren:** None. **M. van der Ent:** None. **K. Hunker:** None. **H. Jiang:** None. **A. Yee:** None. **D. Siemieniak:** None. **S. Ganesh:** None. **D. Ginsburg:** None.

This Research has received full or partial funding support from the American Heart Association.

8

Endothelial TFEB Regulates Postischemic Angiogenesis via AMPKalpha Activation

Yanbo Fan, Haocheng Lu, Wenying Liang, Yanhong Guo, Ji Zhang, Tianqing Zhu, Yibai Hao, Univ of Michigan, Ann Arbor, MI; Minerva T Garcia-Barrio, Cardiovascular Res Inst, Morehouse Sch of Med, Atlanta, GA; Jifeng Zhang, Y Eugene Chen, Univ of Michigan, Ann Arbor, MI

***Rationale*:** Postischemic angiogenesis is critical to limit the ischemic tissue damage and improve the blood flow recovery. The regulation and the underlying molecular mechanisms of angiogenesis are not fully unraveled. Transcription factor-EB (TFEB) is emerging as a master gene for autophagy and lysosome biogenesis. However, the role of TFEB in the vascular disease is less understood.
***Objective*:** We aim to determine the role of endothelial TFEB in postischemic angiogenesis and underlying molecular mechanism**.**
***Methods and Results*:** In a murine hindlimb ischemic model, we demonstrated that TFEB was upregulated in the ischemic skeletal muscle tissue. Utilizing genetically-engineered endothelial cell (EC) specific TFEB transgenic mice, we investigated the function of TFEB in postischemic angiogenesis. We observed improved blood perfusion and increased capillary density in the EC-specific TFEB transgenic mice compared with the wild-type littermates ($n = 8$-9 for each group, $p < 0.01$). Furthermore, we found that blood flow recovery was attenuated in EC-selective TFEB deficient mice compared with control mice ($n = 8$-9 for each group, $p < 0.01$). In aortic ring cultures, we found that TFEB transgene significantly increased the vessel sprouting. Adenovirus-mediated TFEB overexpression promoted EC tube formation whereas small interfering RNA (siRNA)-mediated TFEB knockdown suppressed tube formation in ECs. Mechanistically, TFEB activated calcium/calmodulin-dependent protein kinase kinase-β and AMP-activated protein kinase (AMPK)-α signaling pathway. Through pharmacological inactivation and siRNA-mediated knockdown of AMPKα, we demonstrated that AMPKα is necessary for TFEB to regulate tube formation in ECs.
***Conclusions*:** In summary, our data demonstrate that TFEB is a positive regulator of angiogenesis through activation of AMPKα signaling, suggesting that TFEB constitutes a novel molecular target for ischemic vascular disease.

Disclosures: **Y. Fan:** Research Grant; Significant; AHA SDG award. **H. Lu:** None. **W. Liang:** None. **Y. Guo:** None. **J. Zhang:** None. **T. Zhu:** None. **Y. Hao:** None. **M.T. Garcia-Barrio:** None. **J. Zhang:** None. **Y. Chen:** Research Grant; Significant; NIH R01.

9

Smooth Muscle Cell Tgfbr2 Deletion in Mice Causes Aortic Hypercontractility and Impaired Endothelium-Dependent Relaxation

Jay Zhu, Univ of Washington, Seattle, WA; Fatos I Alp Yildirim, Istanbul Univ, Istanbul, Turkey; Stoyan N Angelov, Hao Wei, David Dichek, Univ of Washington, Seattle, WA

Background: Abnormal smooth muscle cell (SMC) TGF-β signaling is proposed as a critical driver in the development of thoracic aortic aneurysms and dissections (TAAD) associated with Marfan and Loeys-Dietz Syndromes as well as nonsyndromic TAAD. However, the mechanisms by which altered SMC TGF-β signaling causes TAAD are poorly understood. Others have proposed that loss of SMC TGF-β signaling causes TAAD by impairing SMC contractility, leading to aortic medial degeneration and dilation. However, mice generated in our lab with deficient SMC TGF-β signaling (due to SMC-specific deletion of the type II TGF-β receptor) have thicker aortic medias and increased mRNA encoding SMC contractile proteins. These observations predict increased contractility.
Methods & Results: We addressed this apparent contradiction experimentally by measuring vasomotor function (by tension myography) and contractile protein expression (by immunoblotting) in aortas of mice with normal or deficient SMC TGF-β signaling. Isolated aortic rings from mice with deficient SMC TGF-β signaling showed increased contraction to phenylephrine (Emax: 13.5 mN vs 7.8 mN in controls; $p<0.0001$; $n=19$-20) and potassium chloride (Emax: 7.5 mN vs 5.7 mN in controls; $p<0.0001$; $n=19$-20).

Moreover, levels of smooth muscle myosin heavy chain protein were at least as high in aortas with deficient SMC TGF-β signaling as in control aortas, consistent with their capacity to generate increased contractile force. Surprisingly, aortic segments from mice with deficient SMC TGF-β signaling also had impaired endothelium-dependent relaxation to acetylcholine (Emax: 37% vs 97% in controls; $p<0.0001$; $n=19$-20). Endothelium-independent relaxation to sodium nitroprusside was similar between the two groups. CD31 immunostaining of vessel segments revealed equivalent endothelial integrity in both groups.
Conclusion: Physiologic SMC TGF-β signaling is an important determinant of both SMC contractility and endothelial function. Disruption of physiologic SMC TGF-β signaling may lead to TAAD through direct effects on SMC as well as through indirect effects on endothelial function. Our results also suggest an unanticipated role for SMC TGF-β signaling in regulating endothelial-mediated vasomotor function.

Disclosures: **J. Zhu:** None. **F.I. Alp Yildirim:** None. **S.N. Angelov:** None. **H. Wei:** None. **D. Dichek:** None.

10

Endothelial FGF Protects Against Pulmonary Hypertension

Kel Vin Woo, Carla Weinheimer, Attila Kovacs, David Ornitz, Washington Univ, Saint Louis, MO

Pulmonary hypertension (PH) is a debilitating disease where 1 in 4 patients will die within five years of diagnosis. Pathologic changes of endothelial cell function, together with smooth muscle and adventitial hyperplasia increase pulmonary vascular resistance. Consequent elevation in right ventricular pressure ultimately causes right heart failure.
Expression of Fibroblast Growth Factor Receptors (FGFRs), FGFR1 and FGFR2, are elevated in lung samples from PH patients; however, the impact of these receptors on endothelial cell function, and endothelial to smooth muscle interaction is poorly understood.
We hypothesize that activation of endothelial FGFR1 and FGFR2 promotes endothelial cell survival, elaborating signals that protect against pulmonary hypertension via inhibition of smooth muscle cell recruitment.
We used the *Tie2-Cre* transgene to conditionally inactivate *Fgfr1* and *Fgfr2* in endothelial cells. Experimental mice with genotype *Tie2-Cre; Fgfr1$^{f/f}$; Fgfr2$^{f/f}$* (DCKO) and control *Fgfr1$^{f/f}$; Fgfr2$^{f/f}$* (DFF) were challenged with 10% hypoxia for 2 weeks. At the end, right ventricular pressure (RVp) was measured by cardiac catheterization. Compared to mice in normoxia, control littermates in hypoxia demonstrated significant increases in RVp, and RV to left ventricle + septum (LV+S) weight ratio, consistent with development of PH. DCKO mice demonstrate further elevation in RVp and an increase in the RV to LV+S weight ratio, demonstrating worsening PH. We also observed formation of plexiform lesions in DCKO mice, suggestive of a severe pathology. We found a previously unreported involvement of FGF10 in pulmonary hypertension. FGF10 expression was decreased in hypoxia-challenged DCKO mice as compared to both DCKO littermates on room air, and to hypoxia challenged DFF control mice.
Our data suggests that endothelial FGFR1 and FGFR2 activation may protect against pulmonary hypertension. Further studies are underway to elucidate the role of FGF10 and its mechanism in the pathology. We will also further identify associated FGF ligands, associated signaling mechanisms, and endothelial to smooth muscle interactions.

Disclosures: **K. Woo:** None. **C. Weinheimer:** None. **A. Kovacs:** None. **D. Ornitz:** None.

11

Effects of Canakinumab in Patients with Peripheral Artery Disease

Kerry S Russell, Denise Yates, Andrea Feller, Tianke Wang, Ping Chen, Timothy Clough, Laurence Colin, Novartis Insts for BioMedical Res, Cambridge, MA; Lucy LaPerna, Remington Davis, Columbus, OH; Mustafa M Shennak, Triumpharma, Amman, Jordan; Holger Lawall, Akademie fuer Gefaesskrankheiten, Hamburg, Germany; Sigrid Nikol, Asklepios Klinik St Georg, Hamburg, Germany; William Smith, NOCCR, Knoxville, TN; Thomas Forst, Profil Mainz, Mainz, Germany; Oliver J Mueller, Univ of Heidelberg, Heidelberg, Germany; John Hoekstra, Natl Clinical Res, Richmond, VA; Marek Piatek, Aspire Clinical Res, Glendale, AZ; Elizabeth V Ratchford, Johns Hopkins Univ, Baltimore, MD; Christopher M Kramer, Univ of Virginia Health System, Charlottesville, VA; Craig T Basson, Novartis Insts for BioMedical Res, Cambridge, MA

Background Peripheral artery disease (PAD) affects 8.5 million people in the US. PAD patients are at high risk for cardiovascular events, and their quality of life is often significantly impaired by decreased mobility. Interleukin-1β (IL-1β) may play an important role in this disease by promoting inflammatory responses that drive atherosclerotic plaque progression and impair vascular function. We sought to test whether interruption of IL-1β signaling would improve patient mobility and decrease plaque progression in the lower extremities. **Methods** 38 patients (mean age 65; 71% male) with symptomatic PAD (confirmed by ankle-brachial index) were randomized 1:1 to receive Canakinumab (150 mg subcutaneously) or placebo monthly for up to 12 months. Plaque volume in the superficial femoral artery (SFA) was assessed serially using 3.0T MRI. Mobility was assessed serially using the 6-minute walk test (maximum and pain-free walking distance). **Results** Canakinumab was safe and well-tolerated. 12 patients discontinued (8 placebo, 4 Canakinumab). MRI data (from 31 patients at 3 months; 21 patients at 12 months) showed no evidence of plaque progression in the SFA at either time point in placebo-treated patients; nor was there a change in plaque volume in the Canakinumab-treated group. There was a serial and significant improvement in placebo-adjusted maximum and pain-free walking distance observed as early as 3 months after treatment with Canakinumab (58-meter improvement over placebo in pain-free distance at 3 months, P=0.01). Two placebo-treated patients required peripheral vascular interventions due to progression of disease; however, no Canakinumab-treated patients required revascularization during the study. Canakinumab decreased markers of systemic inflammation (IL-6 and hsCRP). **Conclusions** Treatment with Canakinumab may improve maximum and pain-free walk distance in patients with symptomatic PAD. In conjunction with results soon to be reported for the CANTOS trial of Canakinumab for secondary prevention of cardiovascular events, additional studies may provide support that inhibition of IL-1β signaling can improve symptoms and function in this patient population with high unmet need.

Disclosures: **K.S. Russell:** Employment; Significant; Novartis Employee. **D. Yates:** Employment; Significant; Novartis Employee. **A. Feller:** Employment; Significant; Novartis Employee. **T. Wang:** Employment; Significant; Novartis Employee. **P. Chen:** Employment; Significant; Novartis Contracted Employee. **T. Clough:** Employment; Significant; Novartis Employee. **L. Colin:** Employment; Significant; Novartis Employee. **L. LaPerna:** Other; Significant; Investigator on Novartis-sponsored Trial. **M.M. Shennak:** Other; Significant; Investigator on Novartis-sponsored Trial. **H. Lawall:** Other; Significant; Investigator on Novartis-sponsored Trial. **S. Nikol:** Other; Significant; Investigator on Novartis-sponsored Trial. **W. Smith:** Other; Significant; Investigator on Novartis-sponsored Trial. **T. Forst:** Other; Significant; Investigator on Novartis-sponsored Trial. **O.J. Mueller:** Other; Significant; Investigator on Novartis-sponsored Trial. **J. Hoekstra:** Other; Significant; Investigator on Novartis-sponsored Trial. **M. Piatek:** Other; Significant; Investigator on Novartis-sponsored Trial. **E.V. Ratchford:** Other; Significant; Investigator on Novartis-sponsored Trial. **C.M. Kramer:** Other; Significant; Investigator on Novartis-sponsored Trial. **C.T. Basson:** Other; Significant; Novartis Employee.

12

Volume of Calcium in the Descending Thoracic Aorta Predicts All Cause Mortality Beyond Coronary Artery Calcium: The Multi-Ethnic Study of Atherosclerosis

Isac C Thomas, Matthew A. Allison, Nketi I. Forbang, Univ of California, San Diego, La Jolla, CA; Erin D. Michos, Johns Hopkins Univ, Baltimore, MD; WT Longstreth Jr., Univ of Washington, Seattle, WA; Nathan Wong, Univ of California, Irvine, CA; Wendy Post, Johns Hopkins Univ, Baltimore, MD; Michael H. Criqui, Univ of California, San Diego, La Jolla, CA

Introduction: Coronary artery calcium (CAC) volume and density differentially predict incident cardiovascular disease (CVD), with CAC density inversely associated with these outcomes. Whether similar associations exist between descending thoracic aortic calcium (DTAC) volume and density and all cause mortality (ACM) are unknown. We hypothesized that DTAC volume and density predict ACM independently of CAC.
Methods: The Multi-Ethnic Study of Atherosclerosis enrolled 6,814 participants free of clinical CVD at baseline and followed them for incident adverse events. Cardiac CT at baseline visualized the segment of the descending thoracic aorta posterior to the heart. Only participants with prevalent DTAC were included (necessary to evaluate DTAC density). DTAC and CAC volumes were natural log transformed to adjust for skewness. Cox regression models estimated the associations of DTAC volume and density with ACM after adjustment for age, gender, ethnicity, CVD risk factors, statin use, and CAC volume and density. The incremental predictive values of DTAC volume and density were evaluated by area under receiver operating characteristic (AUC) curves.
Results: Of the total cohort, 1,850 participants (27%) had prevalent DTAC and 491 deaths occurred over

10.3 years. In separate regression models, DTAC *volume* was independently associated with ACM after adjustment for CAC volume (HR 1.21 [95% CI 1.09-1.35]) and additional adjustment for CAC density (1.18 ([1.06-1.32]). After the same adjustments, DTAC *density* was not significantly associated with ACM (0.94 [0.84-1.06]). The AUC for the base Model 1 (risk factors + CAC volume) was 0.706 (0.680-0.732), which increased to 0.716 (0.690-0.742) with the addition of DTAC *volume* in Model 2 (p=0.03 compared to Model 1). Further addition of DTAC *density* in Model 3 did not improve the AUC significantly (0.717 [0.692-0.743], p=0.23 compared to Model 2).
Conclusions: In a cohort free of baseline clinical CVD, DTAC visualized on cardiac CT was common. When DTAC was present, DTAC volume (but not density) was independently associated with ACM. DTAC volume also significantly improved ACM risk prediction beyond risk factors and CAC volume.

Disclosures: **I.C. Thomas:** None. **M.A. Allison:** None. **N.I. Forbang:** None. **E.D. Michos:** None. **W. Longstreth:** None. **N. Wong:** None. **W. Post:** None. **M.H. Criqui:** None.

13

Inhibition of Nudt6 Stabilizes Advanced Atherosclerotic Plaques

Hong Jin, Yuhuang Li, Ekaterina Chernogubova, Alexandra Bäcklund, Stina Sellberg, Changyan Sun, Karolinska Inst, Stockholm, Sweden, Sweden; Albert Busch, Technical Univ Munich, Munich, Germany, Germany; Suzanne M Eken, Ljubica Perisic, Ulf Hedin, Karolinska Inst, Stockholm, Sweden, Sweden; Pavlos Tsantilas, Hans-Henning Eckstein, Jaroslav Pelisek, Technical Univ Munich, Munich, Germany, Germany; Lars Maegdefessel, Karolinska Inst, Stockholm, Sweden, Sweden

Natural antisense transcripts (NATs), a non-coding RNA subclass, being transcribed in antisense direction to protein coding genes, are an intriguing novel class of targetable modulators, exerting crucial effects on gene expression. Aim of the current study was to investigate the contribution of NATs to atherosclerotic plaque vulnerability.
Using laser capture micro-dissection, we isolated fibrous caps tissue of carotid artery plaques from 20 symptomatic patients with ruptured lesions *vs.* 20 samples from asymptomatic patients with stable lesions. A human transcriptome array (HTA; *GeneChip 2.0*) was used to profile the expression of all currently annotated RNA transcripts. Nucleoside diphosphate-linked moiety X motif 6 (NUDT6) was identified as one of the most significantly up-regulated transcripts in fibrous caps of ruptured lesions. Interestingly, NUDT6 is an established antisense RNA targeting the fibroblast growth factor 2 (FGF2). Of importance, FGF2 was among the most significantly down-regulated transcripts in ruptured lesions, corresponding to elevated NUDT6 expression.
In situ hybridization in both, human and mouse carotid atherosclerotic plaques, confirmed substantially higher expression levels of NUDT6 in ruptured lesions compared to stable. In addition, *in situ* hybridization revealed a distinct co-localization with smooth muscle cells (SMCs) in advanced plaques. Overexpression of NUDT6 in cultured human carotid artery SMCs effectively limited FGF2 on the mRNA as well as protein level. Furthermore, reduction of NUDT6 via siRNA stimulated proliferation and blocked apoptosis in SMCs. In an inducible atherosclerotic plaque rupture model using incomplete ligation and cuff placement on common carotid arteries of male *apoE*-/- mice, NUDT6 inhibition with gapmeRs was able to significantly improve SMC survival rates, leading to thicker fibrous caps, and to reduce the plaque rupture rate compared to scramble-gapmeR control-treated mice (22% *vs*. 63%, *p*= 0.03).
The present study presents NUDT6 as a novel crucial antisense regulator of fibrous cap stability through steering SMC survival *via* targeting its sense RNA transcript FGF2.

Disclosures: **H. Jin:** None. **Y. Li:** None. **E. Chernogubova:** None. **A. Bäcklund:** None. **S. Sellberg:** None. **C. Sun:** None. **A. Busch:** None. **S.M. Eken:** None. **L. Perisic:** None. **U. Hedin:** None. **P. Tsantilas:** None. **H. Eckstein:** None. **J. Pelisek:** None. **L. Maegdefessel:** None.

14

Characterization of the Oxidized Phospholipid Modification of Apolipoprotein(a) Kringle KIV10: Insights into the Site of OxPC Addition

Corey A Scipione, Robarts Res Inst, London, ON, Canada; Travis DeWolfe, James W Gauld, Univ of Windsor, Windsor, ON, Canada; Michael B Boffa, Western Univ, London, ON, Canada; Amir Ravandi, St. Boniface Hosp Res Ctr, Winnipeg, MB, Canada; Marlys L Koschinsky, Robarts Res Inst, London, ON, Canada

Elevated plasma levels of lipoprotein(a) (Lp(a)) are an independent and causal risk factor for coronary heart disease and aortic valve stenosis. Lp(a) consists of a low density lipoprotein (LDL)-like particle covalently linked to the unique glycoprotein apolipoprotein(a) (apo(a)). We have shown that apo(a) contains a covalent oxidized phosphocholine (oxPC) adduct on the KIV_{10} domain, and that perturbation of the strong lysine binding site (LBS) in this kringle results in a lack of covalent oxPC addition. We have implicated this modification in proinflammatory processes, such as the ability of apo(a) to induce interleukin-8 expression in macrophages. Apo(a) from Old World monkeys and apes lacks covalent oxPC modification and contains mutations in KIV_{10}, some of which impact the LBS. To identify the amino acids in human apo(a) that are covalently modified by oxPC, we mutagenized a KIV_{10}KV di-kringle apo(a) that contains covalent oxPC modification. We mutated to alanine all residues that are either substituted in primate apo(a) or that can act as acceptors for covalent oxPC addition. The resulting variants were then subjected to immunoblotting analysis with E06, an IgM antibody that binds to oxPC, and assessment of lysine-binding ability using affinity chromatography. Mutation of His33 to Ala abolishes oxPC modification of apo(a) while retaining the lysine binding ability of KIV_{10}. Thus, we have identified the long-sought location of the oxPC modification of apo(a). Molecular dynamic simulations of the oxPC-deficient mutant show no gross changes in the structure of KIV_{10}, in contrast to mutations that abolish both lysine binding ability and oxPC addition that result in a collapsed lysine binding pocket. Using mass spectrometry, we have also identified noncovalently-associated oxPC present on apo(a). Interestingly, the abundance of these species appears to be reduced in the apo(a) variant containing a mutation in the strong lysine binding site in KIV_{10}. Our findings allow the ability to assess the contributions to pathogenesis of the strong lysine binding site and oxPC modification of apo(a) kringle IV type 10 independently, and thus will enhance our understanding of the mechanisms by which Lp(a) contributes to atherothrombotic diseases.

Disclosures: **C.A. Scipione:** None. **T. DeWolfe:** None. **J.W. Gauld:** None. **M.B. Boffa:** None. **A. Ravandi:** None. **M.L. Koschinsky:** Consultant/Advisory Board; Modest; Lipoprotein(a) Foundation.

15

Serum Amyloid A is Not Just an HDL-Associated Lipoprotein

Patricia G Wilson, Joel C Thompson, Preetha Shridas, Frederick C de Beer, Nancy R Webb, **Lisa R Tannock**, Univ Of Kentucky, Lexington, KY

Serum Amyloid A (SAA) is traditionally thought to be only found with HDL; however, recently several groups have found that SAA is found on apoB-containing lipoproteins (LDL and VLDL) under some circumstances. The goal of this study was to determine the relative lipoprotein association of SAA. Native human acute phase SAA was isolated from acute phase plasma collected from patients undergoing cardiovascular bypass surgery; the SAA was purified and delipidated. Plasma was collected from a group of healthy, non-obese humans with low levels of SAA (< 2 mg/L) and lipoproteins (VLDL, LDL and HDL) were isolated by density gradient ultracentrifugation. The delipidated SAA (at 2 concentrations) was incubated in vitro with the various lipoprotein preparations then samples were re-isolated by fast protein liquid chromatography and SAA was analyzed by ELISA and immunoblot. When SAA was incubated with any single lipoprotein all of the SAA was found associated with that lipoprotein and none remained in a lipid-free form. When SAA was incubated with a mixture of VLDL, LDL and HDL (based on equal protein and corresponding to concentrations in plasma) a majority of SAA (50-60%) was found on HDL with the remaining SAA found on VLDL and LDL. When SAA first complexed to HDL was added to a mixture of SAA-free LDL and VLDL the majority of SAA remained with the HDL (76-86%) but 5-10% of the SAA was found on each of LDL and VLDL. When SAA first complexed to either apoB-containing lipoprotein was then added to a mixture of HDL and the other apoB-containing lipoprotein most SAA moved to HDL (55-70%) but the remainder was found on the apoB-containing particles. Thus, SAA can move between lipoprotein particles in vitro. To determine if the presence of SAA on apoB-containing lipoproteins had a functional effect we evaluated lipoprotein-proteoglycan binding affinity. Proteoglycan mediated lipoprotein retention in the vessel wall is thought to be one of the key steps in initiation of atherosclerosis. Compared

to SAA-free LDL or VLDL, the presence of SAA on apoB-containing lipoproteins caused increased proteoglycan binding affinity. Thus, SAA is not simply an HDL lipoprotein, but SAA can move between lipoprotein particles, and the presence of SAA on apoB particles may increase their atherogenicity.

Disclosures: **P.G. Wilson:** None. **J.C. Thompson:** None. **P. Shridas:** None. **F.C. de Beer:** None. **N.R. Webb:** None. **L.R. Tannock:** None.

16

Amyloidogenic Modifications of Apolipoprotein A-I Promote a Strong Pro-inflammatory Response in Macrophages, but Formation of Amyloid Fibrils Abrogates the Pro-inflammatory Effect

Andrzej Witkowski, Gary K Chan, Nancy J Li, UCSF Benioff Children's Hosp Oakland, Oakland, CA; Rui Lu, Shinji Yokoyama, Nutritional Health Science Res Ctr, and Dept of Food and Nutritional Sciences, Chubu Univ, Kasugai, Japan; **Giorgio Cavigiolio**, UCSF Benioff Children's Hosp Oakland, Oakland, CA

Inflammation is central to atherosclerosis, as inactivation of inflammation pathways strongly reduces atherosclerosis progression. Particulate matter, such as cholesterol crystals and amyloid materials, promotes release of the potent pro-inflammatory cytokine IL-1β in macrophages. Recently, it has been demonstrated that soluble substances that are precursors of particulate matter, such as free cholesterol, oxidized LDL and amyloidogenic peptides (i.e. amyloid-β, IAPP), can also induce an inflammatory response.
In this study, we investigated the interplay between oxidation of apolipoprotein A-I (apoA-I), amyloid formation, and the inflammatory response of macrophages. We previously reported that oxidation of apoA-I methionines (MetO-ApoA-I) promotes protein aggregation and formation of amyloid fibrils when MetO-ApoA-I is incubated at pH 6.0. In contrast, at physiological pH, MetO-ApoA-I remains soluble and perfectly functional, as it promotes cholesterol efflux from macrophages with the same efficiency of intact-ApoA-I. However, upon incubation of mouse bone marrow derived macrophages with soluble pre-fibrillar MetO-ApoA-I, levels of pro-IL-1β synthesis were more than 2-fold higher than those induced by intact-ApoA-I. In contrast, amyloid fibrils produced by MetO-ApoA-I did not increase the levels of pro-IL-1β synthesis compared to intact-ApoA-I. Furthermore, the pro-inflammatory effect was not observed in macrophages derived from MyD88/TRIF knock-out mice, indicating that the response is membrane TLR receptors-dependent. In contrast, the >2-fold increase (MetO-ApoA-I vs. intact-apoA-I) in pro-IL-1β synthesis was maintained in macrophages derived from CD36 knock-out mice. This observation suggests that the signaling pathway is not exclusively dependent on the TLR2/TLR6/CD36 membrane complex. Thus, in atherosclerotic lesions, oxidized apoA-I species that are amyloidogenic, but otherwise functional, may induce a pro-inflammatory response in macrophages. Amyloid fibril formation in contrast, could reduce, rather than exacerbate, the inflammatory burden produced by these pro-inflammatory apoA-I species by sequestering them in the form of inert amyloids.

Disclosures: **A. Witkowski:** None. **G.K.L. Chan:** None. **N.J. Li:** None. **R. Lu:** None. **S. Yokoyama:** None. **G. Cavigiolio:** None.

17

Apolipoprotein C-III Promotes Anti-Inflammatory Regulatory T Cell Phenotype Through Modulation of Intestinal Dendritic Cell Activation

Cayla N Rodia, Alison B Kohan, Univ of Connecticut, Storrs, CT

Apolipoprotein C-III (apoC-III) is a cardio-metabolic modulator in multiple tissues. Circulating apoC-III in humans is an independent risk factor for cardiovascular disease (CVD) because apoC-III increases circulating triglyceride (TG) through inhibition of the LDLR in the liver and lipoprotein lipase on the capillary endothelium. In the liver, apoC-III overexpression results in increased synthesis and secretion of more TG-rich VLDL. These actions increase the resident time and amount of atherogenic remnants in circulation. Paradoxically, apoC-III acts in the intestine to inhibit dietary fat absorption, a potentially beneficial action. Using human-apoC-III transgenic mice (hu-apoCIII^{tg} mice), which have increased circulating TG compared to C57Bl6/J littermate controls (WT), we have identified an increase in circulating IL-10 at basal conditions. Regulatory T cells (Tregs), a T cell subset that is known to delay atheroprogression, secrete the anti-inflammatory cytokine IL-10. Knowing that the immune system plays a dynamic role in atherogenesis, we asked whether apoC-III is a potential modulator of Tregs during a

western diet (WD) challenge. We subjected hu-apoCIII^{tg} and WT mice to 12 weeks of a WD and through flow cytometry, found significantly increased circulating and intestinal Tregs in hu-apoCIII^{tg} mice compared to WT. Hu-apoCIII^{tg} intestinal gene expression showed increases in TGF-β and maintenance of IL-10 and FOXP3, key Treg-related genes, after the WD compared to WT. We hypothesized that apoC-III may act in the intestine to induce tolerance to dietary antigens through dendritic cell (DC) activation and subsequent differentiation of naïve T cells to the Treg phenotype. Using flow cytometry of the lamina propria, we saw increased activation of intestinal DCs, in hu-apoCIII^{tg} mice at basal and WD-challenged conditions suggesting that intestinal DCs are influenced by apoC-III overexpression. These results suggest that apoC-III may influence Treg differentiation or proliferation through alteration of intestinal DC activation. **The phenotype we have uncovered in hu-apoC-III^{tg} mice suggests a link between apoC-III overexpression, dietary fat absorption, and the immune system, and that this may be protective against inflammation.**

Disclosures: **C.N. Rodia:** None. **A.B. Kohan:** None.

18

APOBEC1 Complementation Factor: A Novel Regulator of Triglyceride Metabolism

Jennie Lin, Donna Conlon, Xiao Wang, Daniel J Rader, Kiran Musunuru, Univ of Pennsylvania, Philadelphia, PA

A recent human rare-variant study on plasma lipids has identified a missense mutation in the *A1CF* (APOBEC1 complementation factor) gene that significantly associates with TG levels. Expressed in the liver and small intestine, *A1CF* encodes an RNA binding protein that facilitates APOBEC1's editing of *APOB* mRNA, introducing a premature stop codon that yields apoB-48. Surprisingly, despite the importance of apoB-48 in plasma lipid metabolism, prior studies have shown that *APOBEC1* deficiency itself does not alter plasma TG levels. Therefore, we hypothesize that A1CF regulates TG metabolism independently of its role in *APOB* mRNA editing. To evaluate this hypothesis, we used CRISPR-Cas9 to generate whole-body *A1cf* knockout mice (*A1cf* $^{-/-}$), knock-in mice homozygous for the TG-associated Gly398Ser mutation (*A1cf*$^{GS/GS}$), and *A1cf* $^{-/-}$ rat hepatoma cell lines. Both *A1cf*$^{GS/GS}$ and *A1cf* $^{-/-}$ mice had significantly increased fasting plasma TG compared to controls (1.71-fold, N = 22-27, $P = 1.5 \times 10^{-3}$; and 1.67-fold, N = 15-27, $P = 1.8 \times 10^{-3}$ respectively), recapitulating the human TG phenotype and demonstrating that A1CF loss of function leads to hyperTG. Supporting our hypothesis that this occurs independently of APOBEC1 function, apoB-48 was detected by immunoblot in the plasma and small intestines of *A1cf* $^{-/-}$ and *A1cf*$^{GS/GS}$ mice without a significant shift in apoB-100/apo-B48. TG clearance was not decreased in *A1cf* $^{-/-}$ mice during an oral fat tolerance test (N = 12), but A1CF deficiency did result in increased TG secretion *in vivo* (1.34-fold, N = 12, $P < 0.001$), consistent with an observed increase in VLDL-apoB secretion by *A1cf* $^{-/-}$ hepatoma cells (1.55-fold, $P < 0.001$). We performed RNA-seq of *A1cf* $^{-/-}$ and wild-type mouse livers, and while differential expression analysis did not yield candidate mechanisms to explain the TG phenotype, we detected 167 alternative splicing (AS) events (delta PSI > 10). We validated several AS events for metabolism genes such as *Khk* and *Hmgcl* by RT-PCR, identifying A1CF's previously unknown role as a regulator of AS events with clear metabolic relevance. In summary, we have demonstrated in our functional follow-up of a human rare-variant study that A1CF modulates TG metabolism through entirely novel mechanisms independent of *APOB* mRNA editing.

Disclosures: **J. Lin:** None. **D. Conlon:** None. **X. Wang:** None. **D.J. Rader:** None. **K. Musunuru:** None.

19

Selective BET Inhibitors Are Useful for Normalizing Inflammation Leading to Reduced Cardiovascular Disease (CVD) in Humans

Ewelina Kulikowski, Laura Tsujikawa, Sarah Atwell, Eric Campeau, Sylwia Wasiak, Christopher Halliday, Jan Johansson, Mike Sweeney, **Norman C Wong**, Resverlogix Corp., Calgary, AB, Canada

Apabetalone (RVX-208) a bromodomain extra-terminal (BET) inhibitor selectively binds the 2nd ligand domain within a BET protein thus displacing it from acetylated lysine marks on histone tails. In clinical trials of ~1000 patients, many (n=499) of whom with CVD when given 200 mg/d RVX-208 had a 55% relative risk reduction in major adverse cardiac events (MACE) vs placebo. This benefit of RVX-208 may stem from ability of BET inhibition (BETi) to calm inflammation, metabolism, coagulation and complement

pathways with well-known roles in CVD risks. These potential benefits of RVX-208 underlie BETonMACE a phase 3 CVD events trial. Of major interest is the anti-inflammatory (AI) effects seen in clinical data showing BETi lowers CRP by 28% in RVX-208 treated patients (n=331). RVX-208 lowered IL-6 and MCP-1 U937 cells exposed to LPS in a dose and time dependent manner by 90 and 85%, respectively within 24 hrs. RVX-208 displaced BET proteins BRD2-4 from chromatin. These AI effects underpin studies of RVX-297 a more potent cousin of RVX-208 that lowered IL-6 and MCP-1 in LPS stimulated U937 cells by 95 and 80% respectively within 24 hrs. In ChIP assays, RVX-297 also displaced BET protein BRD4 and pol II from promoters of cytokine genes IL-6 and IL-1β that mediate inflammation. Together, data from studying RVX-208 and -297 show both BET inhibitors displace transcription factors from promoter DNA that control expression of inflammatory genes (IGs) with key roles in CVD. Importance of BETi displacement of BRD4 and pol II from DNA becomes clear when added to the fact that cellular response to inflammation requires immediate and robust expression of defined set of IGs. For this rapid transcriptional response, the cell places chromatin structures upstream of IGs called super-enhancers (SE) or latent enhancers (LE) that act as molecular sinks for attracting BET proteins such as BRD4. The placement of a SE or LE adjacent to a promoter that controls a IG recruits this gene to the response against an inflammatory insult. Thus targeting BET proteins including BRD4 with a selective BETi may have broad effects on many genes or pathways by crippling SE or LE mediated cellular response to the inflammatory component of CVD. This mechanism may have potential implications to other inflammatory diseases.

Disclosures: **E. Kulikowski:** Employment; Significant; Resverlogix Corp. Ownership Interest; Significant; Resverlogix Corp. **L. Tsujikawa:** Employment; Significant; Resverlogix Corp. Ownership Interest; Significant; Resverlogix Corp. **S. Atwell:** Employment; Significant; Resverlogix Corp. Ownership Interest; Significant; Resverlogix Corp. **E. Campeau:** Employment; Significant; Resverlogix Corp. Ownership Interest; Significant; Resverlogix Corp. **S. Wasiak:** Employment; Significant; Resverlogix Corp.. Ownership Interest; Significant; Resverlogix Corp. **C. Halliday:** Employment; Significant; Resverlogix Corp.. Ownership Interest; Significant; Resverlogix Corp. **J. Johansson:** Employment; Significant; Resverlogix Corp. Ownership Interest; Significant; Resverlogix Corp. **M. Sweeney:** Employment; Significant; Resverlogix Corp. Ownership Interest; Significant; Resverlogix Corp. **N.C. Wong:** Employment; Significant; Resverlogix Corp. Ownership Interest; Significant; Resverlogix Corp.

20

Resolution Phenotype of Monocytes and Macrophages is Altered in Peripheral Arterial Disease

Melinda S Schaller, Laura Menke, Mian Chen, Warren J Gasper, S. Marlene Grenon, Michael S Conte, Univ of California, San Francisco, San Francisco, CA

Introduction: Peripheral arterial disease (PAD) is a chronic disease characterized by systemic inflammation. Monocytes (Mo) and macrophages play a central role in vascular inflammation and its resolution. We hypothesize that impaired resolution in PAD results in poor clinical outcomes.
Methods: Resolution phenotype was assessed by phagocytic activity of leukocytes, Mo cell surface markers, and cytokine profiling of Mo-derived macrophages (MDM). Phagocytosis and cell-surface markers were determined by flow cytometry. MDMs were generated from peripheral blood mononuclear cells via density gradient centrifugation. Cytokines were measured by ELISA following MDM differentiation and subsequent stimulation with LPS.
Results: Circulating Mo and neutrophils (PMN) isolated from PAD patients (n=9) demonstrated significantly lower phagocytic activity (Mo: >30%, p<.001; PMN: >25%, p<.01, Fig. 1) as compared to healthy subjects (HS) (n=14). Cell-surface marker analysis demonstrated a higher proportion of the pro-inflammatory intermediate Mo subset ($CD14^{++}16^{+}$, 1.8-fold, p=.04) in PAD compared to HS. MDM from PAD subjects retain their intrinsic inflammatory program by producing more IL-6 (PAD 3138±2676 ng/mL, HS 731±854 ng/mL p=.03) and IL-1β (PAD 244±236 ng/mL, HS 24.1±23.8 ng/mL p=.04) than those from HS. Upon stimulation with LPS, MDM from PAD subjects secrete more IL-6 (PAD 23353±22483 ng/mL, HS 5097±5836 ng/mL p=.05) than those from HS.
Conclusions: Circulating Mo and PMN in patients with PAD have substantially lower phagocytic activity as well as a greater proportion of the pro-inflammatory intermediate Mo subset compared to HS. MDM preserve their elevated inflammatory state throughout culture and retain a heightened response upon latter stimulatory cues. Collectively these data demonstrate a heightened inflammatory and impaired resolution phenotype in PAD that has potential implications for disease progression and response to interventions.

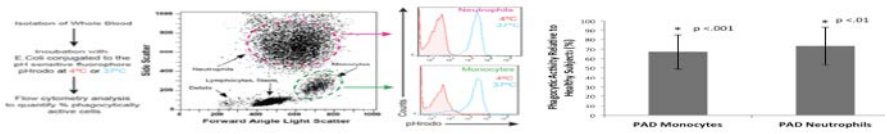

Disclosures: **M.S. Schaller:** None. **L. Menke:** None. **M. Chen:** None. **W.J. Gasper:** None. **S. Grenon:** None. **M.S. Conte:** None.

21

Endothelial Epsins Promote LPS-Induced Inflammation During Septic Shock

Hong Chen, Harvard Medical Sch, Boston Children's Hosp, Boston, MA

Introduction: Sepsis is caused by a deleterious host response to infection, which is primarily responsible for further injury of host tissue and cause of organ dysfunction. Despite significant progress, the pathophysiology of sepsis and the underlying regulatory mechanisms are still not fully understood. We have established that endothelial epsins play a pivotal role in mediating internalization and degradation of Thrombomodulin after LPS challenge.
Hypothesis: Given LPS triggers “cytokine storm” that causes hyper-permeability in the endothelium of lungs and excessive inflammation, we assessed the hypothesis that epsins play a role in promoting endothelial permeability and augmenting inflammation.
Methods and Results: Using innovative tissue-specific inducible epsins double knock out animal models, we investigated the role for epsins during sepsis. We administered lethal dose of LPS into endothelial-specific inducible epsins mutant mice, myeloid cell-specific epsins mutant mice, and platelet-specific epsins mutant mice (n>10). We uncover a potent protective role for endothelial epsins deficiency against the development of LPS-induced sepsis, whereas deletion of epsins in myeloid cells offers 40% ~ 50% of protection, and loss of epsins in platelets exhibits no protection. We further show that endothelial epsin-deficiency upregulates Thrombomodulin surface protein expression by preventing its internalization and subsequent degradation induced by LPS exposure. Sustained surface Thrombomodulin activity subsequently impaired the heightened Tissue Factor expression and activation that usually occurs in response to LPS. Given LPS challenge mimics chronic inflammatory conditions, we show endothelial epsin-deficiency downregulates LPS-induced proinflammatory cytokine production and suppresses endothelial hyper-permeability in lungs assessed by ELSA and Evans Blue perfusion, respectively.
Conclusions Endothelial epsins depletion inhibits septic shock after LPS challenge by protecting Thrombomodulin against internalization and degradation, blocking proinflammatory cytokine production and inhibiting endothelial leakage in the lungs, highlighting the therapeutic potential for targeting epsins during sepsis.

Disclosures: **H. Chen:** None.

This research has received full or partial funding support from the American Heart Association.

22

Crosstalk Between Phosphotidylinositol-4,5 Bisphosphonate-3 Kinase Pathway and Mitogen-Activated Protein Kinase Pathway Regulates Platelet Activation and Protein Synthesis via Phosphoinositide-Dependent Kinase-1

Bhanu Kanth Manne, Univ of Utah, Salt Lake City, UT; Patrick Münzer, Univ of Tübingen, Tübingen, Germany; Rachit Badolia, Temple Univ, Philadelphia, PA; Andrew S. Weyrich, Univ of Utah, Salt Lake City, UT; Satya P Kunapuli, Temple Univ, Philadelphia, PA; Oliver Borst, Univ of Tuebingen, Tuebingen, Germany; Matthew Rondina, Univ of Utah, Salt Lake City, UT

Phosphoinositide-dependent protein kinase 1 (PDK1) is known to regulate PAR4 induced platelet activation and thrombus formation through GSK3β. However, whether PDK1 signaling also involves the ADP receptor and, if so, downstream functional consequences are unknown. We employed both pharmacologic (e.g. the selective PDK1 inhibitor, BX795) and genetic (platelet specific deletion of PDK1) approaches to dissect the role of PDK1 in ADP-induced platelet activation and protein synthesis. Inhibition of PDK1 with BX795 reduced 2MeSADP-induced platelet aggregation by abolishing thromboxane generation. Similar results were observed in PDK1$^{-/-}$ mice (Fig A). Inhibition of PDK1 protected mice from collagen and epinephrine-induced pulmonary embolism (Fig B). PDK1 was also necessary for the phosphorylation of MEK1/2, Erk1/2 and cPLA2, indicating that PDK1 regulates an upstream kinase in MAPK pathway. We next identified that this upstream kinase is Raf1 (necessary for the phosphorylation of MEK1/2), as pharmacologic inhibition and genetic ablation of PDK1 was sufficient to prevent Raf1 phosphorylation (Fig C). Pharmacologic inhibition and genetic ablation of PDK1 blocked MAPK- and mTORC1-dependent protein synthesis in platelets through a mechanism requiring the phosphorylation of eIF4E and S6K. Concordantly, PDK1 is necessary for signal-dependent synthesis of the protein bcl3, which is under mTORC1-dependent control (Fig C). Taken together, our findings show for the first time that PDK1, a master kinase in the PI3K pathway, directly governs thromboxane generation, thrombosis, and protein synthesis in platelets through regulating MAPK and mTORC1 pathways.

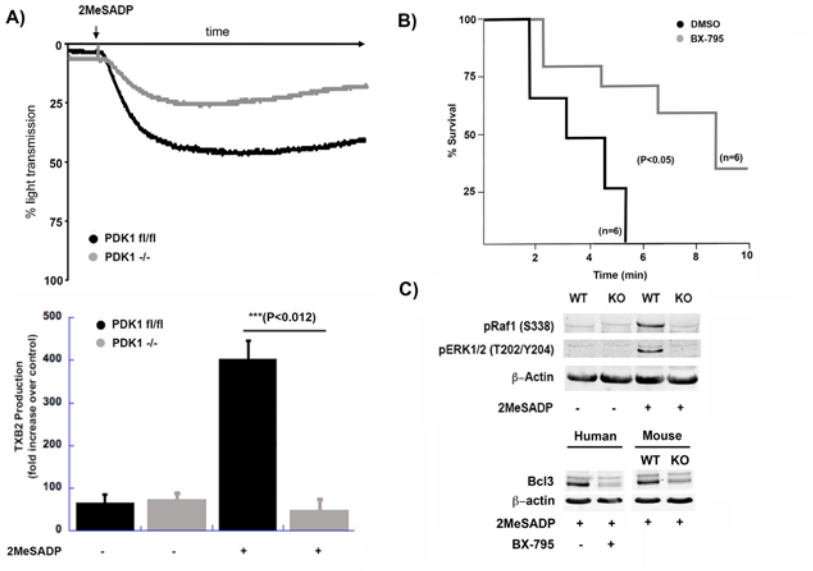

Disclosures: **B. Manne:** None. **P. Münzer:** None. **R. Badolia:** None. **A. Weyrich:** None. **S. Kunapuli:** None. **O. Borst:** None. **M. Rondina:** None.

23

Identification of NCF4 as a Novel Regulator in Arterial Remodeling and Advanced Atherosclerosis

Alexandra Bäcklund, Karl Gertow, Hong Jin, Lina Olsson, Maria Gonzalez-Diez, Maria Sabater-Lleal, Rona J Strawbridge, Bengt Sennblad, John Öhrvik, Karolinska Inst, Stockholm, Sweden; Delilah Zabaneh, Sonia Shah, Fabrizio Veglia, Ctr Cardiologico Monzino, IRCCS, Milan, Italy; Lasse Folkersen, Bruna Gigante, Karin Leander, Max Vikström, Angela Silveira, Karolinska Inst, Stockholm, Sweden; Gualtiero I Colombo, Ctr Cardiologico Monzino, IRCCS, Milan, Italy; Anders Gabrielsen, Ulf Hedin, Anders Franco-Cereceda, Gabrielle Paulsson-Berne, Karolinska Inst, Stockholm, Sweden; Kristiina Nyyssönen, Tomi-pekka Tuomainen, Kai Savonen, Rainer Rauramaa, Univ of Eastern Finland, Kuopio, Finland; Andries J Smit, Univ of Groningen, Groningen, Netherlands; Philippe Giral, Assistance Publique - Hopitaux de Paris, Paros, France; Elmo Mannarino, Univ of Perugia, Perugia, Italy; Sander W van der Laan, Gerard Pasterkamp, Univ Medical Ctr, Utrecht, Netherlands; Göran K Hansson, Per Eriksson, Karolinska Inst, Stockholm, Sweden; Damiano Baldassarre, Elena Tremoli, Ctr Cardiologico Monzino, IRCCS, Milan, Italy; Ulf de Faire, Karolinska Inst, Stockholm, Sweden; Steve E Humphries, Univ Coll London, London, United Kingdom; Anders Hamsten, Rikard Holmdahl, Lars Maegdefessel, Karolinska Inst, Stockholm, Sweden

Arterial wall remodeling is a central multifactorial process in the development and progression of cardiovascular diseases. We employed an approach aimed at observing genetic variants associated with the progression of carotid intima-media thickness (cIMT) in order to identify novel pathways effecting vessel remodeling. This was achieved by conducting gene-centric analysis of 400,000 variants in 3,042 subjects with repeated cIMT measurements.
Rs16997464 on chr22 intergenic between neutrophil cytosolic factor-4 (*NCF4)* and colony stimulating factor 2 receptor beta (*CSF2RB*) was associated with cIMT progression at array-wide significance ($p < 4.5x10^{-7}$). The potential causative genes within this locus were investigated using a human vascular and non-vascular tissue biobank. Expression of 9 genes near rs16997464, were analyzed with the most significant association being with *NCF4* in aortic adventitia. The effect of the variant on the function of the *NCF4* gene product was further analyzed by comparing the oxidative burst capacity of neutrophils from subjects with different rs16997464 genotypes. We observed that neutrophils homozygous for the minor T allele, associated with slower cIMT progression, produced more extracellular ROS than neutrophils homozygous for the G allele, indicating a functional effect of rs16997464 on the *NCF4* gene product $p40^{phox}$, a component of the NADPH oxidase 2 complex (NOX2).
In parallel, we investigated if the chr22 locus also influenced the cellular composition of the atherosclerotic plaque, by utilizing data from the Athero-Express Biobank. Here we found that the minor T allele associated with a higher smooth muscle cell (SMC) content in the plaque. Finally, using a partial ligation model in mice where *ncf4* is mutated, resulting in a reduced but not absent NOX2-associated ROS formation, we observed a reduced neointima formation in the *ncf4*-mutated strain compared with wild-type littermates.
Thus, this study identified rs16997464 in the *NCF4-CSF2RB* locus as a novel genetic determinant of cIMT progression, and provides evidence suggesting that *NCF4* is involved in SMC proliferation and alteration of vessel wall pathophysiology.

Disclosures: **A. Bäcklund:** None. **K. Gertow:** None. **H. Jin:** None. **L. Olsson:** None. **M. Gonzalez-Diez:** None. **M. Sabater-Lleal:** None. **R.J. Strawbridge:** None. **B. Sennblad:** None. **J. Öhrvik:** None. **D. Zabaneh:** None. **S. Shah:** None. **F. Veglia:** None. **L. Folkersen:** None. **B. Gigante:** None. **K. Leander:** None. **M. Vikström:** None. **A. Silveira:** None. **G.I. Colombo:** None. **A. Gabrielsen:** None. **U. Hedin:** None. **A. Franco-Cereceda:** None. **G. Paulsson-Berne:** None. **K. Nyyssönen:** None. **T. Tuomainen:** None. **K. Savonen:** None. **R. Rauramaa:** None. **A.J. Smit:** None. **P. Giral:** None. **E. Mannarino:** None. **S.W. van der Laan:** None. **G. Pasterkamp:** None. **G.K. Hansson:** None. **P. Eriksson:** None. **D. Baldassarre:** None. **E. Tremoli:** None. **U. de Faire:** None. **S.E. Humphries:** None. **A. Hamsten:** None. **R. Holmdahl:** None. **L. Maegdefessel:** None.

24

Abca1 Agonist Cs6253 Reverses Apoe4-Driven Alzheimer's Disease with Concomitant Changes in Plasma and Brain Apoe And Apoj

Jan O Johansson, Artery Therapeutics, San Ramon, CA; Anat Boehm-Cagan, The Sagol Sch of Neuroscience, Tel Aviv, Israel; John K Bielicki, Lawrence Berkeley Lab, Berkeley, CA; Daniel M Michaelson, The Sagol Sch of Neuroscience, Tel Aviv, Israel

Background: Apolipoprotein E4 (apoE4) is associated with perturbed lipid metabolism and elevated risk for CVD and Alzheimer's disease (AD). Data suggests impact of both non-brain and brain apoE on risk to develop AD. Homozygosity for apoE4 increases AD risk approximately 10-fold. Brain apoE4particles are smaller and less lipidated than brain apoE2 or apoE3. ApoE is lipidated by ATP Binding Cassette A1 (ABCA1) and both proteins are synthesized predominantly in astrocytes. We hypothesized that enhancing apoE4 lipidation by an ABCA1 agonist, CS6253, would have AD therapeutic actions. Methods and results: Astrocyte cholesterol efflux is highly responsive to stimulation by exogenous CS6253 peptide. Time-course showed that basal [3H]cholesterol efflux from cells to serum-free medium was compromised in apoE4 astrocytes. Incubating with peptide CS6253 (10 µg/mL) showed 6-fold improvement in [3H] cholesterol efflux to serum-free medium containing either apoE4 or E3 astrocytes. CS6253 crossed the BBB and was found to co-localize with astrocytes in hippocampus. CS6253 i.p. injection (20 mg/kg/48h for 6 weeks) in apoE4 Targeted Replacement mice significantly lowered apoJ in plasma and the brain. The distribution of serum apoE4 on HPLC to smaller lipoproteins was seen rendering similar profile to apoE3. Plasma apoA-I levels, cholesterol and triglyceride levels were unchanged. Lipidation of apoE in brain was compromised in apoE4 compared to apoE3 mice and CS6253 treatment increased apoE4 lipidation. CS6253 treatment prevented cognition decline and development of the brain AD pathological phenotype. CS6253 treatment decreased Aβ42 and P-tau and increased levels of VGluT1 and apoER2.

Cognitive decline was fully prevented in apoE4 mice by CS6253 treatment as assessed by novel object recognition and Morris water maze. Conclusion: ABCA1 agonist treatment by CS653 resulted in improved apoE4 lipidation in cells and in mice. Six weeks treatment counteracted apoE4 driven AD with regard to phenotype and cognition. The data point to the potential therapeutic utility of CS6253 in apoE4 AD.

Disclosures: **J.O. Johansson:** Employment; Significant; Artery TX. Ownership Interest; Significant; ARTERY TX. **A. Boehm-Cagan:** None. **J.K. Bielicki:** Other Research Support; Significant; Sponsored Research Agreement. Ownership Interest; Modest; Artery Tx. **D.M. Michaelson:** Other Research Support; Significant; Sponsored Research Agreement. Ownership Interest; Modest; Artery Tx.

25

Ultrasound Cavitation Mediated Gene Delivery of ApoAI to the Artery Wall for Modulating Plaque Content

Azzdine Ammi, Devon Christian, Jonathan Lindner, **Hagai Tavori**, Oregon Health & Science Univ, Portland, OR

Gene therapy is a potential approach for inhibiting many of the processes that occur during atherogenesis, particularly when targeting key molecular regulators that have multiple adverse downstream signaling pathways. Local expression of human-apoAI in the artery wall has been shown to protect against atherosclerosis in mice, without affecting systemic HDL levels. We hypothesized that focal gene delivery in arterial plaque is possible using ultrasound (US)-mediated cavitation of acoustically-active cationic microbubble gene carriers. Lipid-shelled cationic microbubbles (MB) with a decafluorobutane gas core were prepared. Bicistronic plasmids (luciferase with either GFP or apoAI) were charge coupled to the MB and injected intravenously in 12 $LDLR^{-/-}$ mice fed high-fat diet for 8 weeks. The thoracic aortic root was exposed to US at 1.6MHz, a pulsing interval of 1Hz, and a mechanical index of 1.3 in order to produce repetitive cavitation of MB. *In vivo* optical imaging showed a focal luciferase activity only at the site of UMGD starting from a day after the procedure and lasting for 7-10 days. Activity was subsequently localized to the aortic root on *ex vivo* optical imaging. Immunohistochemistry of the aortic root confirmed luciferase transfection of both endothelial cells of the aortic root and base of the aortic cusps, and intramural cells in atherosclerotic lesions, likely macrophages. We further show that gene therapy with the luciferase-apoAI plasmid, results in migration of cells to the thymus 6-8 days after transfection. These results indicate that local US-mediated gene therapy approach for controlling atherosclerosis is feasible in this pre-clinical model.

Disclosures: **A. Ammi:** None. **D. Christian:** None. **J. Lindner:** None. **H. Tavori:** None.

This research has received full or partial funding support from the American Heart Association.

26

Identification of a Novel Gene, DENND5B, Associated With Plasma High Density Lipoprotein Levels and Intestinal Fat Absorption

Scott M Gordon, Zhihong Yang, Milton Pryor, Michael Mendelson, Daniel Levy, Alan T Remaley, Natl Insts of Health, Bethesda, MD

In an effort to identify novel high density lipoprotein (HDL) receptors expressed by the liver, a bacteriophage library expressing liver cDNA fragments was used to screen for clones that bind to HDL. The gene DENND5B showed significant enrichment for HDL binding over 3 cycles of biopanning, with negative selection against low density lipoprotein binding. Although little is known about the recently described DENN-domain containing family of proteins, some members act as guanine nucleotide exchange factors involved in the activation of Rab proteins and membrane trafficking. To examine the influence of DENND5B on HDL physiology, a DENND5B knockout mouse was generated using a custom zinc finger nuclease. $DENND5B^{-/-}$ mice had decreased plasma total cholesterol (-30.9%, $p < 0.0001$) and phosphatidylcholine (-31.4%, $p < 0.0001$). When plasma was analyzed by size-exclusion chromatography, the lipid effects were attributed entirely to decreased HDL. When fed western diet for 4 months, $DENND5B^{-/-}$ mice showed significantly smaller increases in plasma lipids and body weight compared to wild type mice. After sacrifice, $DENND5B^{-/-}$ mice were found to have a distended small intestine that was whitish in color. To evaluate fat absorption, mice were given an oral gavage of vegetable oil (10 uL/gram body weight) and plasma lipids were measured at 0, 2, and 4 hours post-

gavage. DENND5B$^{-/-}$ mice had significantly reduced plasma triglyceride ($p < 0.05$) and free fatty acids ($p < 0.01$) in response to oil gavage compared to wild type mice. To identify a possible role for this gene in human lipoprotein metabolism, we examined gene expression data from 5,458 participants in the Framingham Heart Study. Consistent with the mouse data, a significant negative relationship exists between DENND5B expression and plasma HDL-C ($p = 4.82 \times 10^{-5}$). In summary, using a phage display screening approach, we have identified a novel gene associated with circulating HDL levels in mice and humans. Additionally, in a homozygous knockout mouse model, a defect in intestinal fat absorption is present. Future studies will be aimed at evaluating the influence of this gene on HDL function, fat absorption, and atherosclerotic disease burden.

Disclosures: **S.M. Gordon:** None. **Z. Yang:** None. **M. Pryor:** None. **M. Mendelson:** None. **D. Levy:** None. **A.T. Remaley:** None.

27

ApoA-I Improves Lymphatic Function Through a Platelet-Dependent Mechanism in Atherosclerotic Mice

Andreea Milasan, François Dallaire, Gabriel Jean, Jean-Claude Tardif, Yahye Merhi, Montreal Heart Inst / Inst de Cardiologie de Montreal, Montreal, QC, Canada; Mary Sorci-Thomas, Medical Coll of Wisconsin, Milwaukee, WI; **Catherine Martel**, Montreal Heart Inst / Inst de Cardiologie de Montreal, Montreal, QC, Canada

Rationale. Lymphatic vessels (LVs) are now recognized as prerequisite players in the modulation of cholesterol removal from the artery wall in experimental conditions of plaque regression, and a particular attention has been brought on the role of the collecting LVs in early atherosclerosis-related lymphatic dysfunction. Whereas recent findings revealed that apoA-I restores the neovascularization capacity of the lymphatic system during tumor necrosis factor-induced inflammation, the effect of apoA-I on collecting LV function during atherosclerosis has not been tested. **Objective.** In the present study, we address whether and how apoA-I can enhance collecting LV function in atherosclerosis-associated lymphatic dysfunction. **Methods and results**. A 6-week systemic treatment with lipid-free apoA-I enhanced lymphatic transport and abrogated collecting lymphatic vessel permeability in atherosclerotic Ldlr$^{-/-}$ mice when compared to control. As injection of apoA-I has been shown to protect wild-type mice against flow restriction-induced thrombosis, and that platelets are identified as key elements in the maintenance of lymphatic vessel integrity via their interaction with lymphatic endothelial cells (LECs), we have tested whether the effects of apoA-I could be mediated through a platelet-dependent mechanism. Our *in vivo* results show that apoA-I kinetics in lymph reflected that of blood. *Ex vivo* experiments performed with washed platelets isolated from mouse blood reveal that apoA-I decreased thrombin-induced but not podoplanin-induced platelet aggregation. Whereas this result suggests that apoA-I limits platelet thrombotic potential in blood but not in lymph, we demonstrate that treatment of human LECs with apoA-I increases the adhesion of bridge-like platelets on human LECs. **Conclusions**. Our results suggest that apoA-I can mediate beneficial effects on lymphatic function by promoting platelet adhesion to the lymphatic endothelium and consequently restore collecting LV integrity. Altogether, we bring forward a new pleiotropic role for apoA-I in lymphatic function and unveil new potential therapeutic targets for the prevention and treatment of atherosclerosis.

Disclosures: **A. Milasan:** None. **F. Dallaire:** None. **G. Jean:** None. **J. Tardif:** None. **Y. Merhi:** None. **M. Sorci-Thomas:** None. **C. Martel:** None.

28

Apolipoprotein A-I Vascular Gene Therapy Provides Durable Protection from Atherosclerosis in Hyperlipidemic Rabbits

Bradley K Wacker, Nagadhara Dronadula, Lianxiang Bi, Alexis Stamatikos, David A Dichek, Univ of Washington, Seattle, WA

Background Gene therapy, delivered directly to the vascular wall, could potentially protect against atherosclerotic lesion growth or regress existing lesions. Previously, we demonstrated that infusion of HDAdApoAI [a helper-dependent adenoviral vector (HDAd) expressing apolipoprotein (apo) A-I] in carotid arteries of fat-fed rabbits reduced early carotid atherosclerosis development (4 wk after vector infusion). Here we tested whether the same HDAd could protect long-term against more severe atherosclerosis.

Methods 25 fat-fed rabbits underwent bilateral carotid gene transfer [HDAdApoAI on one side; control vector (HDAdNull) on the other, with sides randomized]. Postoperatively, diets were adjusted to maintain plasma cholesterols of 200-800 mg/dl. This protocol yields large lipid- and macrophage-rich lesions. 6 mo later, carotids were harvested for analyses of DNA, RNA, protein, cholesterol, and histology (H&E, oil red O), or immunostaining for macrophages, muscle actin, T-cells, ICAM-1 and VCAM-1. **Results** Vector genomes persisted equally in HDAdApoAI and HDAdNull-infused arteries; however, apoA-I mRNA was detected only in HDAdApoAI-infused arteries. HDAdApoAI-infused arteries had ~60% less median intimal lesion volume than HDAdNull-infused arteries, with concomitant reductions (40-75%) in intimal lipid, macrophage, smooth muscle cell, VCAM-1 and ICAM-1. We used within-rabbit paired analyses to control for high correlations of lesion size and composition between left and right carotids of the same rabbit. 19 of 25 rabbits had smaller lesions in HDAdApoAI-infused vs HDAdNull-infused arteries; median decreased intimal area between paired carotids in the same rabbit was 30% (P<0.03). Within individual rabbits, intimal lipid, macrophage, smooth muscle cell, VCAM-1 and ICAM-1 were all less in HDAdApoAI arteries (median 23-36% less; P<0.05 for all except ICAM-1). **Conclusions** Vascular gene therapy with HDAdApoAI reduced lesion development and decreased intimal lipid, macrophage, and adhesion molecule expression 6 mo after treatment. Vector genomes and apo A-I mRNA remained high at 6 mo. A single application of vascular gene therapy durably retards development of atherosclerosis, even in a setting of severe hyperlipidemia.

Disclosures: **B.K. Wacker:** None. **N. Dronadula:** None. **L. Bi:** None. **A. Stamatikos:** None. **D.A. Dichek:** None.

29

Chronic Stress Predisposes to Thrombosis by Abnormal Megakaryopiesis: Protective Effect of Apocynin

Leonardo Sandrini M, Ctr Cardiologico Monzino, IRCCS, Milano, Italy; Alessandro Ieraci, Elisa Turra, Univ degli Studi di Milano, Milano, Italy; Patrizia Amadio, Ctr Cardiologico Monzino, IRCCS, Milano, Italy; Maurizio Popoli, Univ degli Studi di Milano, Milano, Italy; Elena Tremoli, **Silvia Stella Barbieri**, Ctr Cardiologico Monzino, IRCCS, Milano, Italy

Introduction: Psychological stress (e.g. anxiety and depression) has been identified as an important trigger of acute coronary syndromes (ACS), as a consequence of enhanced coagulation and of hyper-reactive platelets. Changes in redox balance, alteration of genes regulating antioxidant systems, including NADPH oxidase, and increased production of reactive oxygen species (ROS) have been measured in both chronic stress and ACS. However, the mechanisms by which chronic stress affects platelet activation and predisposes to thrombosis are not well known. **Hypothesis:** We hypothesized that Apocynin, an inhibitor of NADPH oxidase influences the alteration of megakaryopoiesis and activation of platelets induced by chronic stress in mice. **Methods and Results:** We show the NADPH/$NADP^+$ ratio in bone marrow (BM) of mice exposed to forced swimming for 4 days (5 min twice/day) is markedly reduced compared to control mice, and that Apocynin treatment (2.4 mg/ml in drinking water for 4 days) prevents this alteration. Chronic stress leads to an abnormal megakaryopoiesis increasing the number of BM megakaryocytes (MKs) and affecting circulating platelets. MKs of stressed mice show an advanced maturation state (e.g. nuclear/cytoplasmic ratios and expression of CD42d), and an enhanced ability to produce ROS. Interestingly, a higher number of large and reticulated platelets with marked functional activation (e.g. integrin $\alpha_{IIb}\beta 3$ and P-selectin expression, and platelet/leukocyte aggregates) is detected after chronic stress. In addition, Apocynin prevents ROS MKs generation and decreases the total number of MKs without affecting the percentage of $CD42d^+$ cells. Finally, the inhibitor of NADPH oxidase activity reduces the hyper-activation of platelets and the enhanced susceptibility to FeCl3-induced arterial thrombosis in stressed mice.**Conclusion:** Apocynin treatment, reducing ROS generation in MKs, restores the physiological bone marrow megakaryopoiesis and platelet behaviour, and it prevents the detrimental effect of chronic stress on atherothrombosis. These data suggest a potential use of NADPH oxidase inhibitors in the occurrence of thrombosis associated with chronic stress. Studies in human will verify the clinical impact of these findings.

Disclosures: **L. Sandrini:** None. **A. Ieraci:** None. **E. Turra:** None. **P. Amadio:** None. **M. Popoli:** None. **E. Tremoli:** None. **S. Barbieri:** None.

30

Tissue Factor Pathway Inhibitor α Inhibits Prothrombinase via a Three-Step Mechanism

Jeremy P Wood, Alan E. Mast, Blood Ctr of Wisconsin, Milwaukee, WI

TFPIα inhibits early forms of the prothrombinase complex (factor Xa (FXa), factor Va (FVa)), though the inhibitory mechanism is not entirely understood. One step of inhibition is a high affinity interaction between a TFPIα C-terminal basic region (BR) (252-LIKTKRKRKK-261) and an acidic region (AR) present in FXa-activated and platelet-released forms of FVa. We investigated two additional potential mechanistic steps: (1) binding of the second Kunitz-type inhibitory domain (K2) of TFPIα to the FXa active site; and (2) the function of uncharged residues L252, I253, and T255 within the BR, which are evolutionarily conserved, suggesting they have activity. Direct inhibition of FXa was investigated using TFPIα with an altered K2 (TFPI-R107A) incapable of binding FXa. TFPI-R107A inhibited purified prothrombinase 17-fold weaker than TFPIα (IC50 = 30.6nM vs. 1.8nM) and did not inhibit FXa-initiated thrombin generation in platelet-rich plasma (PRP). Therefore, direct binding of FXa and K2 is required for efficient inhibition of prothrombinase under physiological conditions. Similarly, the role of L252, I253, and T255 was investigated by substituting them with alanine (TFPI-AAKA). The IC50 for prothrombinase inhibition by TFPI-AAKA was 10.4nM, and it had reduced inhibitory activity in PRP, revealing that these residues are also required for efficient prothrombinase inhibition. The role of L252, I253, and T255 was further probed using the peptide LIKTKRKRKK, which inhibited purified prothrombinase (IC50 = 1.0μM) and thrombin generation in PRP at 1μM. AAKAKRKRKK had very little activity in either assay (~20% prothrombinase inhibition with 225μM peptide), but bound the FVa AR equivalently to LIKTKRKRKK (K_d= 5.9nM and 6.0nM, respectively). Thus, the basic residues are responsible for AR binding, while a second step, mediated by L252-T255, is necessary for inhibitory activity. These residues may be necessary for displacement of FXa from FVa, as proposed by Bunce et al. We propose that prothrombinase inhibition by TFPIα involves three steps: (1) the TFPIα BR basic residues bind the FVa AR; (2) residues L252-T255 block prothrombinase assembly; and (3) K2 binds the FXa active site. All three steps are required for physiologic inhibition of prothrombinase by TFPIα.

Disclosures: **J.P. Wood:** None. **A.E. Mast:** Research Grant; Significant; Novo Nordisk. Honoraria; Modest; Siemins.

31

Platelet Plasminogen Activator Inhibitor-1 is Regulated by a Major Chromosome 5 eQTL in Inbred Mice

Amy E Siebert, Stephanie C Verbeek, Alexander J Johnston, Marisa A Brake, Oakland Univ, Rochester, MI; Audrey C Cleuren, Univ of Michigan, Ann Arbor, MI; Jill M Johnsen, Univ of Washington, Seattle, WA; Amy Banes-Berceli, Fabia U Battistuzzi, **Randal J Westrick**, Oakland Univ, Rochester, MI

Decreased fibrinolytic activity is strongly associated with cardiovascular disease. Plasminogen activator inhibitor-1, (PAI-1, Serpine1) is a major circulating fibrinolysis inhibitor, >80% of which is found in platelets. Platelet PAI-1 (pPAI-1) is produced by the megakaryocytes and packaged directly into platelets, thus it is distinct from plasma PAI-1. Plasma PAI-1 levels have been extensively studied and consistently linked with cardiovascular disease. However, variation in pPAI-1, either in the presence or absence of cardiovascular disease, is unknown. To study PAI-1 expression, we surveyed ten mouse strains for pPAI-1 antigen. In particular, the LEWES/EiJ mouse strain had significantly increased pPAI-1 (and Serpine1 mRNA), with an average concentration of 3.1 pg/μg total platelet protein compared to C57BL/6J (B6), which had an average pPAI-1 concentration of 0.4 pg/μg total protein (q=0.0018). Outcrossing LEWES/EiJ x C57BL/6J produced F1 mice with average pPAI-1 levels of 1.6 pg/μg total protein (q=0.0018), suggesting a semidominantly-inherited Serpine1 regulatory effect. To identify pPAI-1 regulatory regions, we produced 48 F2 mice, measured pPAI-1 levels and genotyped 12 (with <0.4 pg/μg total protein) and 12 (with >1.0 pg/μg total protein) using the Mouse Universal Genotyping Array (MegaMUGA). QTL analysis revealed several candidate regions including a major significant 14.4 megabase locus (128.2-142.6 megabases) on Chromosome 5 (LOD score = 4.81). The Serpine1 gene resides within this candidate interval, strongly suggesting that a Serpine1 cis-eQTL is responsible for pPAI-1 expression differences between LEWES/EiJ and C57BL/6J. Identifying pPAI-1 expression control elements offers insights into platelet-specific gene expression and identifies a putative therapeutic target for modulating hemostasis.

Disclosures: **A.E. Siebert:** None. **S.C. Verbeek:** None. **A.J. Johnsen:** None. **M.A. Brake:** None. **A.C. Cleuren:** None. **J.M. Johnsen:** None. **A. Banes-Berceli:** None. **F.U. Battistuzzi:** None. **R.J. Westrick:** None.

This research has received full or partial funding support from the American Heart Association.

32

Ly6C^{Lo} Monocyte/Macrophages Are Essential for Thrombus Resolution in a Murine Model of Venous Thrombosis

Andrew S Kimball, Cathy Luke, Qing Cai, Andrea Obi, Univ of Michigan, Ann Arbor, MI; Farouc Jaffer, Harvard Univ, Boston, MA; Katherine Gallagher, Peter Henke, Univ of Michigan, Ann Arbor, MI

Venous thrombosis (VT) results in vein wall injury by promoting inflammation and fibrosis leading to venous reflux, swelling, pain, and potentially, recurrent thrombosis. While prior work has shown that infiltrating leukocytes are important for VT resolution, as of yet, the precise roles of different leukocyte subsets are not well understood. Monocyte/macrophages (Mo/MΦs) are essential for the repair and resolution of tissue injury in other models, and come in inflammatory (Ly6C^{Hi}) or pro-resolution (Ly6C^{Lo}) subtypes. We hypothesized that infiltrating Mo/MΦs would be critical to VT resolution. In order to study this *in vivo*, we utilized a conditional macrophage depletion technique, using CD11b-DTR mice, to examine the effects of Mo/MΦs in a murine model of stasis VT by inferior vena cava ligation. Administration of 10ng/g diphtheria toxoid (DTx) every 48 hours by intra-peritoneal injection in CD11b-DTR mice resulted in an 89% and 55% decrease in circulating monocytes at 24hrs and 48hrs, respectively. When compared to saline controls, DTx injection had no effects on thrombogenic response or IVC thrombus cell populations in C57BL/6 control mice. At 8 days' post-ligation, DTx treated CD11b-DTR mice had preferentially decreased vein wall-thrombus Ly6C^{Lo} Mo/MΦs as compared with controls. DTx treated mice had significantly larger thrombi (1.7-fold) and less TGF-β, FSP-1, and plasminogen by western immunoblotting (all P-values ≤ 0.01). Consistent with a reduction in Ly6C^{Lo} Mo/MΦs was a significant decrease in cellular TGF-β by intra-cellular flow cytometry. These findings suggest that Ly6C^{Lo} Mo/MΦs are essential for normal VT resolution and may promote thrombus resolution via a plasminogen-mediated mechanism.

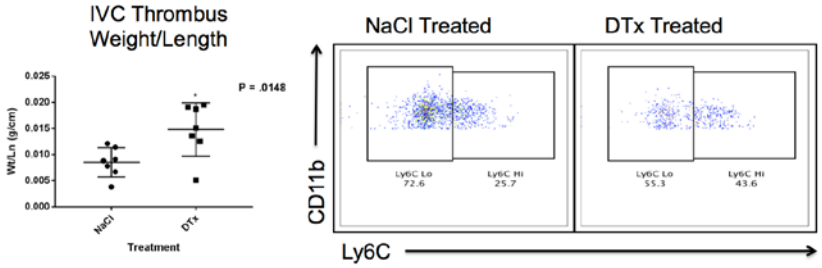

Disclosures: **A.S. Kimball:** None. **C. Luke:** None. **Q. Cai:** None. **A. Obi:** None. **F. Jaffer:** None. **K. Gallagher:** None. **P. Henke:** None.

33

Activated Protein C Light Chain Provides an Extended Binding Surface for Anticoagulant Cofactor Protein S

Jose A Fernandez, Xiao Xu, Ranjeet K Sinha, Laurent O Mosnier, **John H Griffin**, The Scripps Res Inst, La Jolla, CA

Plasma protein S whose deficiency is linked to increased risk for thrombosis provides anticoagulant cofactor activity for activated protein C (APC) by enhancing rates of inactivation of factors Va and VIIIa. Previous APC mutagenesis studies showed that residues 35-39 in the gamma-carboxyglutamic acid domain are required for normal interactions with protein S, indicating the APC Gla domain binds protein

S. Here we used mutagenesis of APC to interrogate the surface of APC's light chain to identify the extended binding surface for protein S. We characterized the ability of protein S to enhance the anticoagulant activity of multiple recombinant APC variants using factor Xa-1-stage clotting assays using normal pooled plasma and protein S-depleted plasma. Mutations of residues L38, K43, I73, F95, and W115 in APC significantly reduced protein S's cofactor activity. An APC variant carrying all of these five mutations lost all of protein S cofactor activity. On the crystallographic structure of APC, these five residues delineate an extended surface on only one side of the APC light chain that identifies the putative protein S binding site which is found on a face that is opposite APC's catalytic triad site. Each of the APC variants with single or multiple L38, K43, I73, F95, and W115 mutations showed a normal ability to cleave SEAP-labeled PAR1 at Arg 41 and Arg 46, implying that the protein S-binding surface does not bind EPCR or PAR1. In summary, mutagenesis studies identify an extended surface on a single face of APC's light chain for binding protein S. This knowledge will enable design and interpretation of new APC biologics with enhanced translational value.

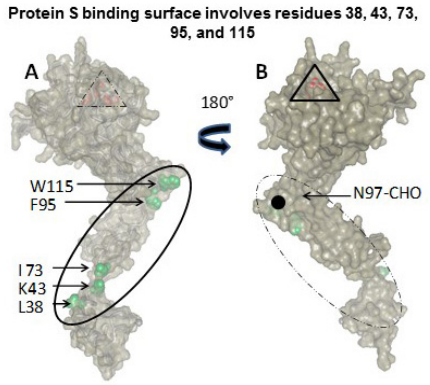

Disclosures: **J.A. Fernandez:** None. **X. Xu:** None. **R.K. Sinha:** None. **L.O. Mosnier:** None. **J.H. Griffin:** None.

34

Methotrexate Inhibits Vein Wall Scarring in Experimental Deep Vein Thrombosis: Implications for the Post-Thrombotic Syndrome

Lang Wang, Guanming Qi, Chase W. Kessinger, Harkamal S. Jhajj, Wenzhu Li, Cardiovacular Res Ctr, Div of Cardiology at Massachusetts General Hosp, Boston, MA; Peter K. Henke, Dept of Vascular Surgery, Univ of Michigan, Ann Arbor, MI; Farouc A. Jaffer, Cardiovacular Res Ctr, Div of Cardiology at Massachusetts General Hosp, Boston, MA

Background: Despite anticoagulant therapy, the post-thrombotic syndrome (PTS) remains a frequent, morbid complication of deep venous thrombosis (DVT). There are no effective clinical approaches beyond anticoagulation to prevent and mitigate PTS, which is driven by inflammation, impaired thrombus resolution, and vein wall scarring leading to valvular reflux. Methotrexate (MTX) is a FDA-approved antimetabolite drug that exerts multiple anti-inflammatory actions. Here we investigate the effects of MTX on vein wall scarring, a key mediator of PTS, in experimental murine DVT. Methods: Stasis VT was established by inferior vena cava complete ligation in C57Bl6 mice (n=60) on day 0. MTX (0.7 mg/kg) or PBS was intraperitoneal injected daily from day 1 to sacrifice. Thrombus burden, vein wall scarring, inflammatory gene expression and macrophage content were assessed at multiple timepoints. Results: MTX decreased Carstairs' and picrosirius red-assessed vein wall thickness by 36.52% on day 8 (n=6 for each group, $p<0.05$ vs PBS). Macrophage recruitment in the vein wall was inhibited by MTX at day 8 ($p<0.05$ vs. PBS). MTX further inhibited vein wall mRNA expression of inflammatory markers CD68 and cathepsin B ($p<0.05$ vs. PBS). At day 4, neutrophil infiltration in the vein wall was similar in both groups ($p>0.05$). Thrombus burden, weight, length and mass were similar for both groups on both day 4 ($p>0.05$) and day 8 ($p>0.05$). Conclusions: MTX attenuates vein wall scarring in association with the macrophage-mediated inflammatory response in VT, without impairing thrombus resolution. MTX administration following DVT may offer a new translatable approach to reduce the post-thrombotic syndrome.

Disclosures: **L. Wang:** None. **G. Qi:** None. **C.W. Kessinger:** None. **H.S. Jhajj:** None. **W. Li:** None. **P.K. Henke:** None. **F.A. Jaffer:** None.

35

Predictors and Etiologies of 30-Day Readmission Rate in Patients with Pulmonary Embolism: A National Population-Based Cohort Study

Saman Setareh-Shenas, Alejandro Lemor, Daniel Castaneda Mayorga, Mount Sinai St. Luke's Hosp & Mount Sinai West Hosp, New York, NY; Alonso Alvarado, Univ de San Martin de Porres, Santa Anita, Peru; Eyal Herzog, Mount Sinai St. Luke's Hosp & Mount Sinai West Hosp, New York, NY

Background: The hospitalization rates of patients with pulmonary embolism (PE) has been on the rise. However, there is limited data recognizing the etiologies and predictors of early readmission rate in this patient population.
Methods: We utilized the National Readmission Database (NRD) 2013, subset of the Healthcare Cost and Utilization Project (HCUP) sponsored by the Agency for Healthcare Research and Quality (AHRQ). PE was identified using ICD 9 code (415.1X) as primary diagnosis. Co-morbidities identified by "CM_" variables provided by NRD. Primary outcome was identified as predictors of 30-day readmission rates and secondary outcomes as the leading etiologies and trends of readmission rate. To identify predictors of outcome, a two level hierarchical logistical model was used.
Results: We analyzed 76,994 patients with primary diagnosis of PE. Total of 11.6% (8,934) patients were readmitted within 30 days of index hospitalization. Significant predictors of readmission were associated with end stage renal disease, drug abuse, chronic lung disease, congestive heart failure, and gastrointestinal bleed during primary admission. In addition, female gender, those admitted to teaching hospital and with longer length of stay (LOS) had higher 30-day readmission rate. Remarkably, elderly age (age>75 years) was not associated with increase in readmission rates. The leading etiologies besides DVT/PE for readmission were sepsis/septic shock, cancer, heart failure and pneumonia.
Conclusion: The rising hospitalization rate of patients with pulmonary embolism, imposes a higher burden on the cost of health care. We identified important predictors and etiologies of 30-day readmission rate. These findings may help in prevention of hospital readmissions and may decrease the cost of care.

Charactertistics of readmited patients in their first admission	
Readmitted once	7909 (10.3%)
Readmitted more than once	1021 (1.3 %)
Age (mean)	63.7
Female	55.1%
Hypertension	62.5%
Diabetes Mellitus	27.9%
Congestive Heart Failure	20.5%

Predictors of readmission	OR	p value
Lengh of stay >= 3 days	1.35	<0.001
Peripheral Vascular Disease	1.03	0.5
Gastrointestinal Bleed	1.22	0.03
End stage renal disease	1.62	<0.001
Age > 75 yrs	0.98	0.47
Drug abuse	1.67	<0.001
Chronic Lung Disease	1.16	<0.001
Hypertension	1.06	0.03
Congestive Heart Failure	1.36	<0.001
Female	1.10	<0.001
Teaching Hospital	1.13	<0.001
Estimated median household income of residents in the		
US$ 1 - 39,999	Reference	
US$ 40, 000 - 50, 999	0.82	<0.001
US$ 51, 000 - 65,999	0.77	<0.001
US$ More than 66, 000	0.75	<0.001

Etiologies for readmission		
	Number	Percentage
DVT/PE	1051	11.8%
Sepsis/Septic Shock	660	7.4%
Cancer	569	6.4%
Heart Failure (systolic or diastolic)	482	5.4%
Pneumonia	402	4.5%
Gastrointestinal Bleed	359	4.0%
Acute respiratory failure	242	2.7%
COPD	237	2.7%
Chest pain	216	2.4%
Acute Kidney Injury	208	2.3%
Anemia	138	1.5%
CVA	134	1.5%
Pleural Effusion	129	1.4%
Atrial fibrillation	120	1.3%
Syncope/ Hypotension/ Dizziness	116	1.3%
Urinary Tract Infection	115	1.3%
Hematoma	105	1.2%
Cellulitis	97	1.1%
Acute myocardial infarction	92	1.0%

Disclosures: **S. Setareh-Shenas:** None. **A. Lemor:** None. **D. Castaneda Mayorga:** None. **A. Alvarado:** None. **E. Herzog:** Speakers Bureau; Modest; Astra Zeneca, Daiichi Sankyo, Bristol Myers Squibb.

36

Factor XII RNAi-based Therapeutic as a Prophylactic Anti-thrombotic Therapy

Stacey Melquist, Tao Pei, Holly Hamilton, Qili Chu, Casi Schienebeck, Christine Chapman, Collin Hagen, Megan Walters, Tracie Milarch, Zach Trilling, Aaron Andersen, Gary Christensen, Jeff Casper, Crystal Klas, Julia Hegge, Zhen Li, Steven Kanner, Arrowhead Pharmaceuticals, Madison, WI

Introduction: Current anticoagulants effectively prevent thromboembolic (TBE) events, but unmet medical need remains due to elevated risk of major bleeding events, particularly where Factor Xa inhibitors are

contraindicated. Factor XII (F12) zymogen initiates the intrinsic coagulation pathway through both autocleavage and Factor XI cleavage. F12 deficient mice show protection from induced thrombosis without increased bleeding risk. F12 deficiency in humans is not associated with increased bleeding risk, suggesting F12 is not essential for hemostasis. Methods: Hepatocyte-targeted RNA interference (RNAi) triggers for reducing liver F12 expression were developed for subcutaneous (SQ) administration. Specific rodent/human/non-human primate (NHP) cross-reactive RNAi triggers were designed *in silico* and screened for knockdown activity *in vitro* and in wild-type mice. Structure activity relationship (SAR) studies of active RNAi triggers identified optimal modifications for lead identification. Candidate RNAi triggers were evaluated for activity and safety in NHPs. In addition, candidate RNAi triggers were evaluated for activity in two rodent models of thrombosis and bleeding risk. Results: F12 RNAi triggers exhibited significant and sustained knockdown of serum F12 levels in both mice and NHPs. SAR studies enabled identification of a candidate lead molecule that demonstrated >95% knockdown after a single 1 mg/kg dose in mice. Evaluation of two SQ doses of this RNAi trigger in NHPs demonstrated >93% knockdown of serum F12 levels at nadir with durable knockdown of >90% for over 5 weeks after the final dose. Concomitant increases in coagulation biomarker aPTT were observed, consistent with functional F12 depletion. Both arteriovenous shunt studies in rats and $FeCl_3$-induced TBE studies in mice exhibited prevention of clot formation after F12 knockdown. Importantly, F12 knockdown did not increase bleeding times in explicit hemostasis studies in mice. Conclusions: Development of a SQ-administered F12-specific RNAi trigger offers potential for a novel, infrequently dosed prophylactic treatment for TBE without increased bleeding risk. Administration by medical personnel would eliminate adherence concerns inherent to current therapies.

Disclosures: **S. Melquist:** Employment; Significant; Arrowhead Pharmaceuticals. **T. Pei:** Employment; Significant; Arrowhead Pharmaceuticals. **H. Hamilton:** Employment; Significant; Arrowhead Pharmaceuticals. **Q. Chu:** Employment; Significant; Arrowhead Pharmaceuticals. **C. Schienebeck:** Employment; Significant; Arrowhead Pharmaceuticals. **C. Chapman:** Employment; Significant; Arrowhead Pharmaceuticals. **C. Hagen:** Employment; Significant; Arrowhead Pharmaceuticals. **M. Walters:** Employment; Significant; Arrowhead Pharmaceuticals. **T. Milarch:** Employment; Significant; Arrowhead Pharmaceuticals. **Z. Trilling:** Employment; Significant; Arrowhead Pharmaceuticals. **A. Andersen:** Employment; Significant; Arrowhead Pharmaceuticals. **G. Christensen:** Employment; Significant; Arrowhead Pharmaceuticals. **J. Casper:** Employment; Significant; Arrowhead Pharmaceuticals. **C. Klas:** Employment; Significant; Arrowhead Pharmaceuticals. **J. Hegge:** Employment; Significant; Arrowhead Pharmaceuticals. **Z. Li:** Employment; Significant; Arrowhead Pharmaceuticals. **S. Kanner:** Employment; Significant; Arrowhead Pharmaceuticals.

37

Centrosome Destabilization Through the Ubiquitin-Proteasome Pathway Regulates Proplatelet Production

Kellie R Machlus, Prakrith Vijey, Thomas Soussou, Joseph E Italiano Jr., Harvard Medical Sch, Boston, MA

BACKGROUND: Proteasome inhibitors such as bortezomib, a chemotherapeutic used to treat multiple myeloma, induce thrombocytopenia within days of initiation. The mechanism for this thrombocytopenia has been tied to data revealing that proteasome activity is essential for platelet formation. The major pathway of selective protein degradation uses ubiquitin as a marker that targets proteins for proteolysis by the proteasome. This pathway is previously unexplored in megakaryocytes (MKs).
OBJECTIVES: We aim to define the mechanism by which the ubiquitin-proteasome pathway affects MK maturation and platelet production.
RESULTS: Pharmacologic inhibition of proteasome activity blocks proplatelet formation in megakaryocytes. To further characterize how this degradation was occurring, we probed distinct ubiquitin pathways. Inhibition of the ubiquitin-activating enzyme E1 significantly inhibited proplatelet formation up to 73%. In addition, inhibition of the deubiquitinase proteins UCHL5 and USP14 significantly inhibited proplatelet formation up to 83%. These data suggest that an intact ubiquitin pathway is necessary for proplatelet formation.
Proteomic and polysome analyses of MKs undergoing proplatelet formation revealed a subset of proteins decreased in proplatelet-producing megakaryocytes, consistent with data showing that protein degradation is necessary for proplatelet formation. Specifically, the centrosome stabilizing proteins Aurora kinase (Aurk) A/B, Tpx2, Cdk1, and Plk1 were decreased in proplatelet-producing MKs. Furthermore, inhibition of AurkA and Plk1, but not Cdk1, significantly inhibited proplatelet formation in vitro over 83%.

CONCLUSIONS: We hypothesize that proplatelet formation is triggered by centrosome destabilization and disassembly, and that the ubiquitin-proteasome pathway plays a crucial role in this transformation. Specifically, regulation of the AurkA/Plk1/Tpx2 pathway may be key in centrosome integrity and initiation of proplatelet formation. Determination of the mechanism by which the ubiquitin-proteasome pathway regulates the centrosome and facilitates proplatelet formation will allow us to design better strategies to target and reverse thrombocytopenia.

Disclosures: **K.R. Machlus:** None. **P. Vijey:** None. **T. Soussou:** None. **J.E. Italiano:** None.

This research has received full or partial funding support from the American Heart Association.

38

Neutrophil-Derived S100a8 and S100a9 Promotes Reticulated Thrombocytosis and Atherogenesis in Diabetes

Prabhakara R Nagareddy, Univ of Alabama at Birmingham, Birmingham, AL; Michael J Kraakman, Man Kit Sam Lee, Annas Al-Sharea, Dragana Dragoljevic, Baker IDI Heart and Diabetes Inst, Melbourne, Australia; Jeffery Berger, Ira Goldberg, New York Univ, New York, NY; Andrew Murphy, Baker IDI Heart and Diabetes Inst, Melbourne, Australia

Platelets play a critical role in atherogenesis and thrombosis-mediated myocardial ischemia, processes that are accelerated in diabetes. It remains unknown if hyperglycemia promotes platelet production and whether this contributes to enhanced atherothrombosis. Here we show that in response to hyperglycemia, neutrophil-derived S100A8/A9 interacts with the receptor for advanced glycated end-products (RAGE) on hepatic Kupffer cells resulting in increased production of interleukin-6 (IL-6), a pleiotropic cytokine implicated in inflammatory thrombocytosis. IL-6 acts on hepatocytes to enhance the production of thrombopoietin, which in turn interacts with its cognate receptor, c-MPL on megakaryocytes and bone marrow progenitor cells to promote their expansion and proliferation resulting in reticulated thrombocytosis. Lowering blood glucose using a sodium-glucose co-transporter 2 inhibitor (dapagliflozin), depleting neutrophils/Kupffer cells or inhibiting S100A8/A9 binding to RAGE (paquinimod) all reduced diabetes-induced thrombocytosis. Inhibiting S100A8/A9 also decreased atherogenesis in diabetic mice. Finally, we show that patients with type 2 diabetes have reticulated thrombocytosis, which correlates with glycated hemoglobin, and also have increased plasma S100A8/A9 levels. These studies provide novel insights into the mechanisms that regulate platelet production and may help to develop strategies to improve on current antiplatelet therapies and to reduce cardiovascular disease risk in diabetes.

Disclosures: **P.R. Nagareddy:** None. **M. Kraakman:** None. **M. Lee:** None. **A. Al-Sharea:** None. **D. Dragoljevic:** None. **J. Berger:** None. **I. Goldberg:** None. **A. Murphy:** None.

39

Myeloid Klf2 Regulates Arterial and Venous Thrombosis

Lalitha Nayak, Stephanie Lapping, Neelakantan Vasudevan, Alvin H. Schmaier, Case Western Reserve Univ, Cleveland, OH; Nigel Mackman, Univ of North Carolina Sch of Med, Chapel Hill, NC; Mukesh K. Jain, Case Western Reserve Univ, Cleveland, OH

Experimental, clinical and pathological studies have indicated an important link between inflammation and thrombosis. However, the precise mechanisms regulating myeloid cell function and the importance of various myeloid lineages involved in thrombosis remain incompletely defined. Published work from our group shows that a systemic deficiency of KLF2 renders animals susceptible to thrombosis. Using conditional knockouts, we examined the role of myeloid KLF2 in thrombosis. Carotid thrombosis assay (Rose Bengal model) show a robust reduction in time to occlusion in MY-K2-KO mice. No difference was noted in complete blood counts and coagulation assays between MY-K2-KO and control mice. Adoptive transfer of KLF2-KO neutrophils significantly shortened the time to occlusive thrombosis in control mice compared with the occlusion time in control mice given control neutrophils. No change in thrombosis time was noted in MY-K2-KO mice transfused with either control or KLF2-KO neutrophils. Neutrophil depletion with Ly6G antibody reversed the prothrombotic phenotype in MY-K2-KO mice and prolonged thrombosis time while no change was noted in thrombosis time in control mice following neutropenia. MY-K2-KO mice also developed significantly larger venous clot burden as compared to controls (complete ligation of inferior vena cava model). KLF2 deleted neutrophils demonstrated significantly increased tissue factor

(TF) expression and activity. KLF2 deleted monocytes did not reveal change in TF expression as compared to controls. MY-K2-KO neutrophils also demonstrated increased generation of neutrophil extracellular traps and increased expression of neutrophil elastase (NE) and myeloperoxidase (MPO) as compared to controls. Other enzymes reported as important to the generation of NETs were not altered. TF, NE and MPO promoter-luciferase reporter assays demonstrated that KLF2 overexpression significantly abrogates p65-induced promoter activity. Collectively these studies identify neutrophil KLF2 as an important regulator of both arterial and venous thrombosis and illuminate the molecular mechanisms involved suggesting that modulation of neutrophil KLF2 may alter thrombosis.

Disclosures: **L. Nayak:** None. **S. Lapping:** None. **N. Vasudevan:** None. **A.H. Schmaier:** None. **N. Mackman:** None. **M.K. Jain:** None.

40

Platelet Fragmentation During the Hemostatic Response and its Prevention by a P2Y12 Antagonist

Maurizio Tomaiuolo, Chelsea N Matzko, Izmarie Poventud-Fuentes, Leonard Nettey, Brad A Herbig, John W Weisel, Scott L Diamond, Lawrence F Brass, Timothy J Stalker, Univ of Pennsylvania, Philadelphia, PA

Previous studies using intravital microscopy have shown that hemostatic plugs formed in the mouse microvasculature have a characteristic architecture in which the extent of platelet activation reflects gradients in the distribution of platelet agonists radiating outwards from the injury site. In that setting, we found minimal overlap of thrombin and ADP signaling, with thrombin primarily responsible for robust platelet activation close to the injury site and $P2Y_{12}$-mediated ADP signaling resulting in accumulation of minimally activated platelets. Here we have taken these studies a major step forward by integrating fluorescence with scanning electron microscopy. Hemostatic plugs produced by needle injury in mouse jugular veins were imaged *in situ* 1 to 20 min after injury. The results show with unprecedented detail what could only be inferred previously, showing that platelet size, morphology and packing density vary remarkably depending on spatial localization within the hemostatic plug. The intraluminal and extravascular portions of the hemostatic mass presented distinct architectures. A large mass comprised almost exclusively of platelets was observed on the interior surface of the vein. Platelets closest to the injury edge had a highly activated morphology, including P-selectin surface expression, dense packing and platelet fragmentation, while those farther from the injury edge often remained discoid. In contrast, the extravascular portion of the hemostatic mass was rich in densely-packed, platelet-derived fragments intertwined with fibrin. Hemostatic plugs from mice treated with a $P2Y_{12}$ inhibitor were significantly smaller. The platelet activation gradient described above was less apparent and, notably, fragmentation of the platelets close to the injury edge was not observed with the inhibitor present. In conclusion, our findings indicate that 1) the development of a platelet activation gradient is a conserved feature of the hemostatic response across different vessels, 2) fragmentation of platelets closest to the injury site occurs very rapidly following injury, and 3) clinically relevant platelet signaling pathways play a role in regulating its formation.

Disclosures: **M. Tomaiuolo:** None. **C.N. Matzko:** None. **I. Poventud-Fuentes:** None. **L. Nettey:** None. **B.A. Herbig:** None. **J.W. Weisel:** None. **S.L. Diamond:** None. **L.F. Brass:** Research Grant; Significant; The Medicines Company. **T.J. Stalker:** Research Grant; Significant; The Medicines Company.

This research has received full or partial funding support from the American Heart Association.

41

Transcriptional Networks Specifying Homeostatic and Pro-Inflammatory Programs of Gene Expression in Human Aortic Endothelial Cells

Casey E Romanoski, Univ of Arizona, Tucson, AZ; Nicholas T Hogan, Univ of Rochester, Rochester, NY; Michael Whalen, Lindsey K Stolze, Univ of Arizona, Tucson, AZ; Michael T Lam, Univ of California San Diego, La Jolla, CA; James R Springstead, Univ of Western Michigan, Kalamazoo, MI; Christopher K Glass, Univ of California San Diego, La Jolla, CA

Endothelial cells are critical determinants of vascular homeostasis and inflammation, but transcriptional mechanisms specifying their identities and functional states remain poorly understood. Here, we report a

genome-wide assessment of regulatory landscapes in primary human aortic endothelial cells (HAECs) under basal and activated conditions, enabling inference of transcription factor networks that direct homeostatic and pro-inflammatory programs of gene expression. We provide evidence that AP1, ETS, and GATA transcription factors play key roles in establishing HAEC identity by co-binding at many enhancers associated with EC-specific genes. We further demonstrate that exposure of HAECs to oxidized phospholipids or pro-inflammatory cytokines results in signal-specific alterations in enhancer landscapes that are associated with coordinated binding of CEBPD, IRF1 and NFkB. Collectively, these findings identify cis-regulatory elements and corresponding trans-acting factors that contribute to endothelial cell identity and their specific responses to pro-inflammatory stimuli.

Disclosures: **C.E. Romanoski:** None. **N.T. Hogan:** None. **M. Whalen:** None. **L.K. Stolze:** None. **M.T. Lam:** None. **J.R. Springstead:** None. **C.K. Glass:** None.

42

Control of Macrophage Cholesterol Efflux and Atherogenesis by the Noncoding RNA MeXis

Tamer Sallam, Marius Jones, Brandon J Thomas, Xiaohui Wu, Thomas Gilliland, Kevin Qian, Jaspreet Sandhu, David Salisbury, David Casero, Cynthia Hong, Ayaka Ito, Antonio Castrillo, Stephen Smale, Peter Tontonoz, David Geffen Sch of Med at UCLA, Los Angeles, CA

The ligand-dependent nuclear receptor LXR regulates the expression of genes involved in responses to excess cholesterol including Abca1. Macrophage-specific cholesterol efflux driven by Abca1 has been causally linked to the prevention and reversal of heart disease, but therapeutic strategies for targeting efflux pathways in macrophages have been elusive. Here, we define a novel regulatory axis controlling macrophage responses to cholesterol overload. We identify the lncRNA MeXis as an amplifier of LXR-dependent Abca1 gene transcription in macrophages. MeXis interacts with and guides the promoter binding of nuclear receptor transcriptional coactivators. Loss of MeXis in murine immune cells has a marked impact on chromosome architecture at the Abca1 locus, impairs cellular responses to cholesterol overload, and accelerates the development of atherosclerosis. Our findings identify MeXis as a transcriptional gatekeeper that modifies the actions of LXR in lipid-dependent control of macrophage gene expression. It is conceivable that therapeutic approaches that enhance MeXis activity might augment reverse cholesterol transport and reduce foam cell formation.

Disclosures: **T. Sallam:** None. **M. Jones:** None. **B.J. Thomas:** None. **X. Wu:** None. **T. Gilliland:** None. **K. Qian:** None. **J. Sandhu:** None. **D. Salisbury:** None. **D. Casero:** None. **C. Hong:** None. **A. Ito:** None. **A. Castrillo:** None. **S. Smale:** None. **P. Tontonoz:** None.

This research has received full or partial funding support from the American Heart Association.

43

Cholesterol Efflux Pathways Suppress Inflammasome Activation in Mice and Humans

Marit Westerterp, Univ of Groningen, Groningen, Netherlands; Panagiotis Fotakis, Columbia Univ, New York, NY; Mireille Ouimet, New York Univ, New York, NY; Andrea E. Bochem, Academic Medical Ctr, Amsterdam, Netherlands; Hanrui Zhang, Matthew M. Molusky, Wei Wang, Sandra Abramowicz, Nan Wang, Carrie L. Welch, Muredach P. Reilly, Columbia Univ, New York, NY; Erik S. Stroes, Academic Medical Ctr, Amsterdam, Netherlands; Kathryn J. Moore, New York Univ, New York, NY; Alan R. Tall, Columbia Univ, New York, NY

Plasma high-density-lipoprotein (HDL) has several anti-atherogenic properties, including its key role in functioning as acceptor for ATP-binding cassette A1 and G1 (ABCA1 and ABCG1) mediated cholesterol efflux. We have shown previously that macrophage *Abca1/g1* deficiency accelerates atherosclerosis, by enhancing foam cell formation and inflammatory cytokine expression in atherosclerotic plaques. Macrophage cholesterol accumulation activates the inflammasome, leading to caspase-1 cleavage, required for IL-1β and IL-18 secretion. Several studies have suggested that inflammasome activation accelerates atherogenesis.
We hypothesized that macrophage *Abca1/g1* deficiency activates the inflammasome. In *Ldlr*$^{-/-}$ mice fed a Western type diet (WTD), macrophage *Abca1/g1* deficiency increased IL-1β and IL-18 plasma levels (2-fold; P<0.001), and induced caspase-1 cleavage. Deficiency of the inflammasome components *Nlrp3* or *caspase-1* in macrophage *Abca1/g1* knockouts reversed the increase in plasma IL-18 levels (P<0.001),

indicating these changes were inflammasome dependent. We found that macrophage *Abca1/g1* deficiency induced caspase-1 cleavage in splenic $CD115^+$ monocytes and $CD11b^+$ macrophages. While mitochondrial ROS production or lysosomal function were not affected, macrophage *Abca1/g1* deficiency led to an increased splenic population of monocytes (2.5-fold; $P<0.01$). Monocytes secrete ATP, and as a result, ATP secretion from total splenic cells was increased (2.5-fold; $P<0.01$), likely contributing to inflammasome activation. *Caspase-1* deficiency decreased atherosclerosis in macrophage *Abca1/g1* deficient *Ldlr*$^{-/-}$ mice fed WTD for 8 weeks (225822 vs 138606 μm^2; $P<0.05$). Of therapeutic interest, one injection of reconstituted HDL (100 mg/kg) in macrophage *Abca1/g1* knockouts decreased plasma IL-18 levels ($P<0.05$). Tangier disease patients, with a homozygous loss-of-function for ABCA1, showed increased IL-1β and IL-18 plasma levels (3-fold; $P<0.001$), suggesting that cholesterol efflux pathways also suppress inflammasome activation in humans. These findings suggest that macrophage cholesterol efflux pathways suppress inflammasome activation, possibly contributing to the anti-atherogenic effects of HDL treatment.

Disclosures: **M. Westerterp:** None. **P. Fotakis:** None. **M. Ouimet:** None. **A.E. Bochem:** None. **H. Zhang:** None. **M.M. Molusky:** None. **W. Wang:** None. **S. Abramowicz:** None. **N. Wang:** None. **C.L. Welch:** None. **M.P. Reilly:** None. **E.S. Stroes:** None. **K.J. Moore:** None. **A.R. Tall:** None.

44

Failure of Protective Autoimmunity in Mouse and Human Atherosclerosis

Dennis Wolf, Teresa Gerhardt, La Jolla Inst for Allergy and Immunology, La Jolla, CA; Nathaly Anto Michel, Univ Heart Ctr Freiburg, Freiburg, Germany; Bjarke Hansen, Immundex Corp., Copenhagen, Denmark; Alessandro Sette, La Jolla Inst for Allergy and Immunology, La Jolla, CA; Andreas Zirlik, Univ Heart Ctr Freiburg, Freiburg, Germany; Marc K Jenkins, Univ of Minnesota Medical Sch, Minneapolis, MN; Klaus Ley, La Jolla Inst for Allergy and Immunology, La Jolla, CA

Background: In atherosclerosis, $CD4^+$ T helper cells recognize auto-antigens including ApoB, the main protein in low-density lipoprotein (LDL). However, atherosclerosis-specific, auto-reactive $CD4^+$ T cells have not been detected *in vivo*, and their function is unknown. *Methods and Results:* We have previously identified peptides derived from mouse ApoB that bind with high affinity to the MHC class II molecule of C57BL/6 mice (I-A^b). We designed and validated a new multimer of a recombinant MHC-II molecule fused to one ApoB auto-epitopes, P6 (TGAYSNASSTESASY, P6:I-A^b), that enabled detection of low-affinity, P6-reactive $CD4^+$ T cells. Using this P6:I-A^b multimer, we identified ApoB-reactive $CD4^+$ T cells in healthy, young C57BL/6 mice that were predominately differentiated T-regulatory cells (T_{regs}) and expressed IL-10, a known atheroprotective cytokine. This population was detectable in lymph nodes and already showed a memory phenotype in young animals without atherosclerosis. In *Apoe*$^{-/-}$ mice, adoptively transferred ApoB P6-specific T_{regs} accumulated in the aorta and draining lymph nodes and gave rise to pathogenic T_H1 and T_H17 cells. This phenotypic switch was caused by enhanced plasticity of antigen-specific T_{regs} as evidenced by multiple clusters of intermediate T_{reg}-T_{eff} phenotypes in single cell RNA sequencing of 4485 antigen-specific $CD4^+$ T cells. In the plaque, many T cells were ex-T_{regs} as identified by a FoxP3 lineage tracker mouse, suggesting that atherosclerosis-specific $CD4^+$ T cells lost their regulatory capacity. Vaccination with P6 maintained a protective phenotype in antigen-specific T_{regs} and protected from atherosclerosis. In humans, ApoB-specific $CD4^+$ T cells from atherosclerotic patients showed the same cytokine patterns found in mouse $CD4^+$ T cells, suggesting that autoimmunity to ApoB is protective first, but later gives rise to a pathogenic $CD4^+$ T cell response that aggravates atherosclerosis. *Conclusion:* Protective T-regulatory cells recognizing peptide antigens of ApoB exist in naïve mice, protect against atherosclerosis, but convert into pathogenic T_H1 and -17 cells during the natural course of disease in mice and humans. These results call for immunomodulatory therapies to maintain protective autoimmunity.

Disclosures: **D. Wolf:** None. **T. Gerhardt:** None. **N. Anto Michel:** None. **B. Hansen:** None. **A. Sette:** None. **A. Zirlik:** None. **M.K. Jenkins:** None. **K. Ley:** None.

45

Endothelial Aryl Hydrocarbon Receptor Nucleatranslator (Arnt) is a Novel Regulator of Cardiac Endothelial Barrier Integrity in Diabetes

Maura Knapp, Mei Zheng, Nikola Sladojevic, Univ of Chicago, Chicago, IL; Qiong Zhao, Inova Heart and Vascualr Inst, Falls Church, VA; Konstaintin G Birukov, James K Liao, **Rongxue Wu**, Univ of Chicago, Chicago, IL

Background: Diabetes leads to endothelial barrier dysfunction and altered endothelial permeability, which results in increased cardiovascular risk. ARNT, also known as HIF-1β, a transcription factor that functions as a master regulator of glucose homeostasis, has been implicated in diabetes. Endothelial-specific ARNT deletion (ArntΔEC) in mice is embryonically lethal, with hemorrhage occurring in the heart during the embryonic stage. However, the particular role of endothelial ARNT(ecARNT) in diabetes is largely unknown. We have found a significant decrease in ARNT expression in both diabetic rodent endothelial cells and diabetic human hearts. We hypothesize that a loss of ecARNT mediates endothelial barrier dysfunction during diabetes. Methods and Results: We generated inducible endothelial specific ARNT knockout mice (ecARNT-/-) by crossing mice with loxP sequences flanking exon 6 of ARNT with Cre ERT2 mice under the VE-cadherin promoter. A 90% deletion of ecARNT was achieved following two weeks of oral tamoxifen administration. ecARNT-/- mice exhibit severe blood vessel leakage, which is restricted to the heart, suggesting a distinct function for ecARNT in different tissues. Cardiomyopathy is evident 6 months after ARNT deletion. *In vitro*, trans-endothelial electrical resistance (TER) and transwell assays have confirmed endothelial barrier disruption in cardiac microvascular endothelial cells (CMEC) isolated from both ecARNT-/- hearts and diabetic (DB/DB) mouse hearts. To determine the underlying mechanisms by which ARNT may regulate endothelial barrier function, we performed DNA sequencing on CMEC isolated from control, ecARNT-/-, and DB/DB mice. Data suggest a significant increase in TNFa signaling, including ELAM-1 and ICAM-1 in CMEC isolated from ecARNT-/- CMEC and diabetic CMEC. Moreover, use of anti-TNFa antibody rescues endothelial barrier dysfunction in CMEC isolated from ecARNT-/- mice. Taken together, these results suggest that a reduction in ecARNT during diabetes may mediate endothelial barrier dysfunction through a TNFa signaling pathway. Conclusion: ecARNT is a critical mediator of endothelial barrier function and could potentially serve as a therapeutic target for diabetic cardiovascular diseases.

Disclosures: **M. Knapp:** None. **M. Zheng:** None. **N. Sladojevic:** None. **Q. Zhao:** None. **K. Birukov:** None. **J. Liao:** None. **R. Wu:** None.

This research has received full or partial funding support from the American Heart Association.

46

The Effects of Membrane Cholesterol on Vascular Smooth Muscle Cell Stiffness and Adhesion to Fibronectin

Josh Childs, Zhongkui Hong Hong, Univ of South Dakota, Sioux Falls, SD

Atherosclerosis remains a major cause of cardiovascular disease (CVD). Cholesterol has been identified as a major contributor to the cause of atherosclerosis. It is well known that the cholesterol accumulation in macrophage-derived foam cells is the major component of atherosclerotic plaque. However, growing evidences suggests that cholesterol loading into vascular smooth muscle cells (VSMC) in atherosclerosis is much larger than previously known, and about 40% of total foam cells in the atherosclerotic plaque are VSMC-derived. Cholesterol may not only contribute as the fatty deposition in the atherosclerotic lesion, but also play a critical role in the VSMC migration toward the intima of the blood vessel wall. In addition, the arterial wall becomes stiffer during atherosclerosis altering the micromechanical environment experienced by the VSMCs leading to changes in VSMC stiffens, adhesion, and phenotype. Migration of VSMCs is a complex process including proliferation and phenotypic switching of VSMCs, thus contributing too many changes in cell membrane adhesion molecules. We tested the hypothesis that membrane cholesterol in VSMCs may play an important role in $\alpha_5\beta_1$-integrin mediated adhesion, and alter the sensory function of VSMCs to ECM mechanical properties. In this study cholesterol manipulation was achieved using methyl-β-cyclodextrin, and gel substrates with varying stiffness were used to mimic the changing environment in atherosclerosis. Atomic force microscopy (AFM) was used to determine integrin-fibronectin adhesion force and cell stiffness. A custom-written MATLAB program was used to interpret the elasticity of the VSMC cytoskeleton and adhesion force. Cellular adhesion was measured for 50%-70% confluent cells with a sample size of 50 cells on a fibronectin coated AFM stylus probe. Our results show

that there is a significant decrease in α5β1-integrin adhesion of VSMCs on substrates above 9 kPa upon membrane cholesterol depletion. Additionally, mechanotransduction of VSMCs upon cholesterol depletion is less efficient. In conclusion, cell membrane cholesterol and extracellular mechanical signals may synergistically regulate cellular mechanical functions of VSMCs and their migration in the progression of atherosclerosis.

Disclosures: **J. Childs:** None. **Z. Hong:** None.

This research has received full or partial funding support from the American Heart Association.

47

FXR1 Regulates Inflammatory MRNA Stability and VSMC Proliferation by Modulation of HuR Activity

Allison Herman, Ross England, Dale Haines, Sheri Kelemen, Mitali Ray, Michael V Autieri, Lewis Katz Sch of Med, Philadelphia, PA

Vascular smooth muscle cells (VSMC) play a critical role in the etiology and progression of many vascular diseases including atherosclerosis and restenosis. Our laboratory has found that one anti-inflammatory interleukin, IL-19, is atheroprotective and can decrease vascular inflammation by reduction in mRNA stability of inflammatory transcripts by reduction of activity of HuR, an mRNA stability protein. HuR translocates from the nucleus to the cytoplasm where it recognizes AU-rich elements present almost exclusively in the 3'UTR of pro-inflammatory genes. Proteins and pathways which limit HuR translocation are understudied, but may reduce inflammatory mRNA stability. Using MASS SPEC to identify HuR-interacting proteins under different inflammatory conditions, we identified one protein, Fragile X-related protein (FXR1), which interacts with HuR in inflammatory, but not basal conditions, a novel interaction. FXR1 mRNA expression is enhanced in muscle cells, but nothing has been reported on expression of FXR1 in VSMC or function for FXR1 in vascular disease. The FXR1 promoter contains multiple cholesterol-response elements, and in this study we demonstrate that FXR1 expression is increased in injured arteries and TNFα and oxLDL stimulated human VSMC, but also by IL-19. RNA EMSA demonstrates that FXR1 directly interacts with ARE in 3'UTR. SiRNA knock down of FXR1 in VSMC increases stability of inflammatory mRNA and protein abundance as well as VSMC proliferation, while overexpression of FXR1 reduces both their abundance and stability in addition to reducing proliferation. Since FXR1 appears to be a novel repressor of inflammatory proteins, and is also induced by IL-19, our overall hypothesis is that FXR1 expression and HuR interaction is an inflammation responsive, counter-regulatory mechanism to reduce abundance of pro-inflammatory proteins and therefore reduce inflammation.

Disclosures: **A. Herman:** None. **R. England:** None. **D. Haines:** None. **S. Kelemen:** None. **M. Ray:** None. **M.V. Autieri:** None.

48

Role of Receptor for Advanced Glycation End Products (RAGE) in Regression of Diabetic Atherosclerosis

Laura M Senatus, Raquel Lopez-Diez, Jianhua Liu, Huilin Li, Gurdip Daffu, Qing Li, Karishma Rahman, Yuliya Vengrenyuk, Tessa Barrett, NYUMC, New York, NY; Richard Friedman, Columbia Univ, New York, NY; Ravichandran Ramasamy, Edward Fisher, AnnMarie Schmidt, NYUMC, New York, NY

Atherosclerosis is a chronic inflammatory disorder. Both progression and regression of atherosclerosis are adversely affected by diabetes. A key player in these processes is Receptor for Advanced Glycation End Products (RAGE). RAGE is a multiligand cell surface macromolecule, which binds ligands enriched in atherosclerotic plaques, such as advanced glycation endproducts (AGEs). RAGE is expressed on a wide array of cell types implicated in cardiovascular disease, such as endothelial cells, and inflammatory cells such as macrophages. The cytoplasmic domain of RAGE binds to the formin molecule DIAPH1 and DIAPH1 is required for RAGE ligands to activate cell signaling responses. RAGE acts as a key mediator of oxidative and inflammatory signaling pathways that are involved in atherosclerosis. We tested mechanisms of impaired regression of atherosclerosis in a murine model of aorta transplantation and found that deletion of *Ager* or *Diaph1* in diabetic mice recipients of *Ldlr* null mice atherosclerotic aortas accelerates atherosclerosis regression and significantly reduces the lesional macrophage content when

compared to diabetic wild-type recipient mice. The antiatherosclerotic effects in diabetic *Ager* null mice and diabetic *Diaph1* null mice include reduced RAGE ligand AGEs in transplanted aortas, with reduced expression of a range of proatherogenic factors, including reactive oxygen species and inflammatory cytokines implicated in leukocyte recruitment and activation. We employed RNA sequencing to identify the key transcriptional events by which RAGE mediates its effects in donor or recipient macrophages in diabetic regressing plaques. Our results suggest that critical gene expression profiles, including those genes involved in inflammation, endothelial dysfunction, oxidative stress, monocyte/macrophage fate (recruitment, differentiation, proliferation), signal transduction and lipid metabolism, are beneficially modulated, at least in part, via *Ager* deletion in atherosclerosis regression. Taken together, these data increase our understanding of the role of RAGE in diabetic atherosclerosis, particularly in macrophages, and may provide avenues for therapeutic strategies to accelerate regression of atherosclerosis in diabetes.

Disclosures: **L.M. Senatus:** None. **R. Lopez-Diez:** None. **J. Liu:** None. **H. Li:** None. **G. Daffu:** None. **Q. Li:** None. **K. Rahman:** None. **Y. Vengrenyuk:** None. **T. Barrett:** None. **R. Friedman:** None. **R. Ramasamy:** None. **E. Fisher:** None. **A. Schmidt:** None.

49

Adipose-Specific Knockout of *Trib1* Reduces Plasma Lipids and Diet-Induced Insulin Resistance, and Increases Circulating Adiponectin

Mikhaila A Smith, Univ of Pennsylvania, Philadelphia, PA; Jian Cui, Columbia Univ, New York, NY; Sumeet A Kheterpal, Daniel J Rader, Univ of Pennsylvania, Philadelphia, PA; **Robert C Bauer**, Columbia Univ, New York, NY

Tribbles-1 (TRIB1) was recently identified through genome-wide association studies as a novel mediator of plasma lipids and coronary artery disease in humans. While subsequent in vivo mouse work confirmed a role for hepatic TRIB1 in these associations, little is known about metabolic roles for extra-hepatic Trib1. Interestingly, SNPs near the *TRIB1* gene are significantly associated with circulating adiponectin levels in humans, suggesting a metabolic role for adipose *TRIB1*. To further investigate this, we generated adipose-specific *Trib1* KO mice (Trib1_ASKO) by crossing Trib1 cKO mice to transgenic Adiponectin-Cre mice. Chow-fed Trib1_ASKO mice exhibited no differences in adipose tissue mass and overall body mass as compared to control littermates (N=8/group). However, Trib1_ASKO mice had reduced total (-16.9%, $p<0.01$), HDL (-16.7%, $p<0.01$), and non-HDL cholesterol (-17.3%, $p=0.068$), as well as plasma triglycerides (-28.6%, $p<0.001$) as compared to WT mice. Trib1_ASKO mice also had increased plasma adiponectin levels, a finding more pronounced in female mice (+33.3%, $p<0.001$) than in males (+16.4%, $p=0.072$). Despite this increase, transcript levels of *adipoQ* were moderately decreased in Trib1_ASKO mice, suggesting a post-transcriptional mode of regulation. Transcript and protein levels of C/EBPα, the best described target of *Trib1* and a key regulator of adipogenesis, remained unchanged. To further investigate the metabolic consequences of adipose-specific KO of *Trib1*, WT and Trib1_ASKO mice were fed high-fat diet (HFD, 45% kCal fat) for 12 weeks to induce obesity. HFD-fed Trib1_ASKO mice had reduced fasting plasma glucose (-22.3%, $p<0.05$), insulin (-38.2%, $p<0.05$), and glucose tolerance (-19.8% AUC, $p<0.05$) compared to control mice. Body mass and fat mass of HFD-fed Trib1_ASKO mice remained unchanged from WT, and the reductions in plasma lipids and increase in plasma adiponectin persisted in the HFD-fed state. In summary, we present here the first in vivo validation of the human genetic association between *TRIB1* and plasma adiponectin, and provide evidence suggesting that adipose *TRIB1* contributes to the genetic associations observed in humans between *TRIB1* and multiple metabolic parameters.

Disclosures: **M.A. Smith:** None. **J. Cui:** None. **S.A. Kheterpal:** None. **D.J. Rader:** None. **R.C. Bauer:** None.

This research has received full or partial funding support from the American Heart Association.

50

TLR2 Plays A Key Role in Platelet Hyperreactivity and Accelerated Thrombosis Associated With Hyperlipidemia

Sudipta Biswas, Alejandro Zimman, Detao Gao, Tatiana Byzova, Eugene Podrez, Cleveland Clinic Fndn Learner Res Inst, Cleveland, OH

Introduction. Platelet hyperreactivity, common in many pathophysiological conditions, is associated with increased atherothrombotic risk. Platelet hyperreactivity, specifically in dyslipidemia, has been mechanistically linked to accumulation in circulation of specific oxidized phospholipids ($oxPC_{CD36}$), ligands for pattern-recognition receptor CD36. Although significant progress in understanding of CD36 mediated signaling in platelets has been made in recent years, many details of the molecular mechanism are still missing.
Hypothesis. CD36 is known to cooperate with other receptors in cells such as macrophages during inflammation and apoptosis. Moreover, we have recently reported that platelets can also respond to oxidation specific epitopes via Toll Like Receptors. So, we hypothesized that TLRs may have a role in $oxPC_{CD36}$ induced platelet activation.
Methods and Results. In this study, using *in vitro* approaches as well as mice with genetic deletion of MyD88 or TLRs, we demonstrate that TLR2 is required for platelet activation by $oxPC_{CD36}$. $oxPC_{CD36}$ induce formation of CD36/TLR2/TLR6 complex in platelets and downstream signaling via TIRAP-MyD88-IRAK1/4-TRAF6, which leads to platelet integrin activation via the SFK-Syk-PLCγ2 pathway. Studies in hyperlipidemic *ApoE*$^{-/-}$ mice have demonstrated that TLR2 deficiency abolishes platelet hyperreactivity and accelerated thrombosis induced by hyperlipidemia. At the same time, no effect of TLR2 deficiency on platelet activation nor thrombosis was observed in normolipidemic mice.
Conclusions. Taken together, our studies reveal that TLR2 plays a key role in platelet hyperreactivity and the prothrombotic state in the settings of hyperlipidemia by sensing a wide range of endogenous lipid-peroxidation ligands and activating innate immune signaling cascade in platelets.

Disclosures: **S. Biswas:** None. **A. Zimman:** None. **D. Gao:** None. **T. Byzova:** None. **E. Podrez:** None.

This research has received full or partial funding support from the American Heart Association.

51

A Critical Role for Outside-In Signaling of Integrin AlphaIIIb/Beta3 in Shear-Dependent Platelet Microvesicle Formation and Phosphatidylerine Exposure

Aiming Pang, Yujie Cui, Michael Keegan Delaney, Aleksandra Stojanovic-Terpo, Xiaoping Du, Dept of Pharmacology,Univ of Illinois at Chicago, Chicago, IL

Platelets promote coagulation mainly by exposing membrane phosphatidylserine (PS) and releasing PS-expressing microvesicles (MV). We have recently shown that PS exposure and MV release induced by platelet agonists requires shear stress. To identify the receptor responsible for the shear-dependent signaling leading to PS exposure and MV release, we compared platelets from $\beta_3^{-/-}$ mice and wild-type mice in MV release and PS exposure under defined shear stress introduced using a cone-plate rheometer. MV release and PS exposure were determined using flow cytometry. Shear-dependent PS exposure and MV release were significantly suppressed in β_3-/- platelets. Similarly, Wild type platelets treated with integrin antagonists also showed defective PS exposure and MV release. These data indicate an important role for the ligand binding function of integrin αIIb/β3 in shear-dependent MV release and PS exposure. To determine whether the role of integrin αIIb/β3 is due to its outside-in signaling, β_3-/- platelets were transplanted with wild type β_3 or a mutant β_3 with the critical Gα13 binding site of the β_3 cytoplasmic domain (EEE) changed to alanines (AAA), which was previously shown to selectively abolish outside-in signaling of $\alpha IIb/\beta_3$. Transplantation of wild type β_3 rescued the defective MVs release and PS exposure of β_3-/- platelets. In contrast, AAA mutant failed to rescue these defects. Consistently, wild type platelets treated with the selective inhibitor of Gα13-integrin interaction, inhibited integrin outside-in signaling and also PS exposure and MV release under shear stress. Furthermore, we also showed that the inhibition of Src, which is important in outside-in signaling downtream of Gα13, also abolished shear-dependent MV release and PS exposure. These data suggest that integrin outside-in signaling mediated by the Gα13-β_3 interaction and Src-dependent signaling pathway plays an important role in transmitting shear-induced mechanical signals leading to MV release and PS exposure in activated platelets.

Disclosures: **A. Pang:** None. **Y. Cui:** None. **M.K. Delaney:** None. **A. Stojanovic-Terpo:** None. **X. Du:** None.

52

IkB Kinase beta is a Key Modulator of Platelet Function, and the Remodeling of CARMA1-Bcl10-MALT1 Complex Formation

Zubair A Karim, Univ of Texas at El Paso, El Paso, TX

Secretion plays an important role in platelet function, and hence the secretory machinery offers a unique target to modulate thrombogenesis. We previously established that IκB kinase (IKK)-β is phosphorylated upon platelet activation, regulates their SNARE machinery, and involves CBM (CARMA1, Bcl10, and MALT1) complex formation. However, the detailed role of IKKβ in platelet function, the mechanism by which it regulates CBM complex formation and downstream effector activation remain elusive. Using a knockout mouse model system (*IKK*$\beta^{flox/flox}$-PF4Cre), we first showed that IKKβ plays a vital role in thrombus formation, and that it does so, in part, by regulating platelet functional responses, including dense and alpha granule release, αIIbβ3 activation, and PS exposure. Furthermore, we observed defects in compound fusion, platelet spreading, actin remodeling, and clot retraction. To this end, under clot retraction conditions in the knockout platelets, 7S complex formation was found to be inhibited. In terms of its signaling, using knockout platelets, we observed that IKKβ is required for the recruitment of Bcl10/MALT1 to CARMA1 upon platelet activation, i.e., CBM complex formation, and that this was due to the defective phosphorylation of Bcl10 and the IKKγ polyubiquitination. In conclusion, our data shows that IKKβ is a key regulator of platelet activation, *in vitro* and *in vivo*, and the remodeling of the CBM complex. Furthermore, our findings indicate that inducible clustering of signaling mediators and the formation of higher-order multi-protein complexes (i.e., the CBM complex) is a dynamic process, that supports nonlinear signaling networks and is important for platelet activation.

Disclosures: **Z.A. Karim:** None.

53

Ablation of Thrombin Signaling in Platelets but Not in Endothelial Cells Impairs Hemostasis in a Mouse Model of Spontaneous Gastrointestinal Bleeding

Stephen J Wilson, Maria M Stevens, Shaun R Coughlin, Univ of California, San Francisco, San Francisco, CA

Human PAR1 is expressed in endothelial cells as well as in platelets where it facilitates the response to thrombin and platelet activation. Vorapaxar, a PAR1 antagonist, prevents myocardial infarction and stroke in patients with prior MI or peripheral arterial disease at a cost of increased bleeding risk. Par1 is also highly expressed in endothelial cells in mice, and Par1-deficiency is associated with bleeding in the mouse embryo at midgestation. Additionally, known actions of endothelial PAR1 activation suggest pro-hemostatic functions. This raises the question of whether inhibition of PAR1 function in endothelial cells (in addition to PAR1 inhibition in platelets) contributes to the bleeding risk associated with Vorapaxar treatment. Our previous work demonstrated that Par1 deficiency results in loss of thrombin signaling in mouse endothelial cells but not mouse platelets, while Par4 deficiency ablated thrombin-induced platelet activation in mice. Thus, mice allow us to separate loss of thrombin signaling in platelets from loss of thrombin signaling in endothelial cells. Accordingly, we used Apc min/+ mice, which develop intestinal polyposis and spontaneous GI bleeding, as a model to determine whether loss of thrombin signaling in platelets (Par4 KO) or endothelial and other cells (Par1 KO) exacerbates spontaneous bleeding. Hematocrit and other hematologic parameters were measured biweekly from 7 weeks through 15 weeks of age. Hematocrits in mice wild-type for Apc were stable over this period (41.48 ± 0.48 at 7 weeks; 40.48 ± 0.37 at 15 weeks, n=15). Hematocrits in Apc min/+ mice fell approximately linearly from 37.06 ± 0.82 at 7 weeks to 14.39 ± 1.12 at 15 weeks (n=15). Hematocrits in Par1-deficient Apc min/+ mice were indistinguishable from those in Apc min/+ without Par deficiency (14.39 ± 1.12 vs 14.47 ± 1.66 at 15 weeks; n=6-15). By contrast, Par4-deficient Apc min/+ mice were already severely anemic at 7 weeks compared to Apc min/+ mice (19 ± 2.0 vs 39 ± 3.6; $p<0.01$, n=4). Par-dependent differences in polyp count and size were not detected. Taken together, our results suggest that loss of thrombin signaling in platelets promotes spontaneous GI bleeding in the Apc min model while loss of thrombin signaling in endothelial cells is without effect in this system.

Disclosures: **S.J. Wilson:** Research Grant; Significant; Merck. **M.M. Stevens:** None. **S.R. Coughlin:** Research Grant; Significant; Merck.

54

ML355 in Prevention of Thrombosis in vivo with Minimal Effects on Hemostasis

Reheman Adili, Katherine Mast, **Michael Holinstat**, Univ of Michigan, Ann Arbor, MI

12-lipoxygenase (12-LOX) has been demonstrated to regulate platelet function, hemostasis, and thrombosis *ex vivo*, supporting a key role for 12-LOX in regulation of *in vivo* thrombosis. While pharmacologically targeting 12-LOX *in vivo* has been a challenge to date, the recent development of the 12-LOX selective inhibitor, ML355, as an effective antiplatelet therapeutic *in vivo* was assessed. ML355 potently inhibited thrombin and other agonist-induced platelet aggregation *ex vivo* in washed human platelets and inhibited downstream oxylipin production of platelet 12-LOX as confirmed by Mass spectrometry analysis. *Ex vivo* flow chamber assays confirmed that human platelet adhesion and thrombus formation at arterial shear over collagen was attenuated in human whole blood treated with ML355 to a greater extent compared to aspirin. *In vivo*, PK assessment of ML355 showed reasonable 12-LOX plasma levels 12 hours following administration of ML355. $FeCl_3$-induced injury of the mesenteric arterioles resulted in less stable thrombi in 12-LOX$^{-/-}$ mice and ML355-treated WT mice resulting in impairment of vessel occlusion. Additionally, ML355 dose-dependently inhibited laser-induced thrombus formation in the cremaster arteriole thrombosis model in WT, but not in 12-LOX$^{-/-}$ mice. Importantly, hemostatic plug formation and bleeding following treatment with ML355 were not affected in response to laser ablation on the saphenous vein or in a cremaster microvasculature laser-induced rupture model. Our data strongly supports 12-LOX as a key determinant of platelet reactivity *in vivo* and inhibition of platelet 12-LOX with ML355 may represent a new class of antiplatelet therapeutics.

Disclosures: **R. Adili:** None. **K. Mast:** None. **M. Holinstat:** None.

55

Disruption of *PCSK9* Using a Targeted Base Editing Strategy

Alexandra C. Chadwick, Kiran Musunuru, Univ of Pennsylvania, Philadelphia, PA

Proprotein convertase subtilisin/kexin type 9 (PCSK9) increases blood low-density lipoprotein (LDL) cholesterol by acting as an LDL receptor antagonist, thereby impairing LDL particle clearance. Since genetic disruption of *PCSK9* is linked to reduced risk of coronary heart disease (CHD), our recent work has sought to permanently knock out the gene by using new genome editing technology. Recently reported “base editors” introduce point mutations at specific locations in the genome without the need for DNA double-strand breaks and, thus, with a lowered incidence of off-target effects. These base editors build on the CRISPR-Cas9 system by tethering an RNA-editing domain to a nickase version of Cas9, allowing for specific C◊T and/or G◊A base alterations. In this study, we used the “BE3” base editor (which uses the APOBEC-1 RNA-editing domain) to specifically target codons encoding tryptophans (TGG) or glutamines (CAG or CAA) to introduce nonsense mutations (producing stop codons TAG, TGA, or TAA) into human *PCSK9*. The number of testable targets was increased by introducing specific point mutations into the BE3 construct (D1135V, R1335Q, T1337R in the Cas9 portion of BE3) to alter the protospacer adjacent motif (PAM) from NGG to NGA. Using HEK293 cells, we individually targeted a number of codons spanning the first seven exons in *PCSK9* and identified several efficient targets. Most notably, the codons encoding glutamine 278 and glutamine 302 could be altered to stop codons in ~50% of alleles, as determined by the CEL-I nuclease mismatch assay and Sanger sequencing. We then targeted glutamine 278 in human induced pluripotent stem cells (iPSCs) and demonstrated base editing to introduce nonsense mutations into *PCSK9*, albeit at a lower efficiency than in HEK293 cells. As a next step towards translation to human patients, we are targeting *Pcsk9* in the mouse liver *in vivo* with BE3. Base editing may prove to be an efficient, safer strategy than standard CRISPR-Cas9 genome editing and holds promise as a strategy for the prevention of CHD.

Disclosures: **A.C. Chadwick:** None. **K. Musunuru:** None.

56

Coronary Artery Disease Risk Alleles at the *LIPA* Locus are Associated With Higher Levels of Its mRNA and Enzymatic Activity in Human Macrophages

Hanrui Zhang, Chenyi Xue, Muredach P Reilly, Columbia Univ, New York City, NY

GWASs have identified *LIPA,* encoding lysosomal acid lipase (LAL), as a novel locus for coronary artery diseases (CAD) but not lipid traits. Meta-analyses revealed that CAD risk alleles rs1412444T and rs2246833T (clustered in intron 2/3 in high LD, r^2=0.985) were associated with higher *LIPA* mRNA in monocytes. It is, however, unclear whether the risk alleles are associated with increased *LIPA* mRNA or LAL enzymatic activity in monocyte-derived macrophages (HMDM), the cell type playing critical roles in atherogenesis. Fine mapping of the *LIPA* region through our CARDIoGRAM+C4D consortium confirmed that the original GWAS SNPs showed the strongest signals. Both SNPs were enriched for H3K27Ac marks and binding sites for PU.1 and CEBPβ in HMDM, suggesting potential regulatory roles. *LIPA* mRNA and LAL activity were higher in HMDM of risk allele carriers (by Kruskal-Wallis test). *LIPA* mRNA was reduced by M1(LPS/IFNγ)-activation and increased by M2(IL-4)-activation. The eQTL relationship of *LIPA* was present in M1- and M2-activated HMDM, suggesting the activity of genetic determinants of *LIPA* expression was retained during macrophage activation. We performed allele-specific expression analysis with RNA-seq of HMDM from 30 subjects of European ancestry (EA) (~70M uniquely-mapped reads/sample) genotyped by Illumina Infinium Multi-Ethnic Global BeadChip imputed with 1000G Phase 3 v5. rs1051338 is within an annotated exon, in high LD with the GWAS lead SNPs (r^2=0.859 in EA), and had consistent allelic expression favoring G allele, which is on the same haplotype as the risk alleles of the GWAS SNPs. In addition, *LIPA* mRNA was higher in human coronary arteries with atherosclerotic plaque. Immunostaining showed that LAL was abundant within the extracellular space of human atherosclerotic intima and also co-localized with CD68+ macrophages. In summary, the results support a novel, potentially pro-atherogenic role for monocyte-macrophage *LIPA* gain-of-function in CAD.

Disclosures: **H. Zhang:** None. **C. Xue:** None. **M.P. Reilly:** None.

This research has received full or partial funding support from the American Heart Association.

57

The Epigenetic Enzyme Kdm6b Controls the Pro-Fibrotic Transcriptome Signature of Foam Cells

Annette E Neele, Koen H Prange, Marten A Hoeksema, Saskia van der Velden, Academic Medical Ctr, Amsterdam, Netherlands; Tina Lucas, Stefanie Dimmeler, Inst of Cardiovascular Regeneration, Ctr for Molecular Med, Frankfurt, Germany; Esther Lutgens, Jan Van den Bossche, Menno P de Winther, Academic Medical Ctr, Amsterdam, Netherlands

Aim: Foam cells are a key hallmark of atherosclerotic lesion formation. Within the atherosclerotic lesion macrophages scavenge modified lipoproteins and thereby acquire their foam cell characteristics. Besides their foam cell phenotype, macrophages can have specific inflammation regulatory functions in atherosclerotic lesions. Epigenetic pathways are crucial for monocyte to macrophage differentiation and activation. The H3K27 demethylase Kdm6b (also known as Jmjd3) is regulated in response to various triggers and regulates several modes of macrophage activation. Given the crucial role of macrophage foam cells in atherosclerosis, we here studied Kdm6b in peritoneal foam cells in order to identify regulated pathways. **Material and Methods:** A myeloid deficient Kdm6b mice (LysMCre-Kdm6b$^{fl/fl}$) was generated and bone marrow of Kdm6b^{wt} or Kdm6b^{del} mice was transplanted to irradiated Ldlr$^{-/-}$ mice which were fed a high fat diet for 9 weeks to induce foam cell formation. Peritoneal foam cells from Kdm6b^{del} or Kdm6b^{wt} mice were isolated and used for RNA-sequencing analysis. **Results:** Among the list of downregulated genes many genes involving fibrosis were affected in Kdm6b deficient foam cells including *Collagen* genes (*Col1a1*, *Col1a2*), *Alpha smooth muscle actin* (*Acta2*) and *Fibronectin-1* (*Fn1*). Pathway analysis on downregulated genes (*P*-value < 0.05) indicated that pathways involved in epithelial to mesenchymaltransition (EMT) (*q*-value=10^{-13}) and extracellular matrix organization (*q*-value=10^{-4}) were significantly downregulated. Pro-fibrotic pathways were thus strongly suppressed in Kdm6b deleted foam cells. Analysis of published datasets of foam cells showed that foam cell formation induces these pro-fibrotic characteristics. Overlay of both data sets indicated that fibrotic genes which are induced upon foam cell formation, are reduced in the absence of Kdm6b. These data suggest that foam cell formation induces a pro-fibrotic gene signature in a Kdm6b-dependent manner. **Conclusion:** We identified Kdm6b as a novel regulator of the pro-fibrotic signature of peritoneal foam cells.

Disclosures: **A.E. Neele:** Research Grant; Significant; The Netherlands Heart Foundation (CVON 2011/ B019: Generating the best evidence-based pharmaceutical targets for atherosclerosis [GENIUS]). **K.H.M. Prange:** None. **M.A. Hoeksema:** None. **S. van der Velden:** None. **T. Lucas:** None. **S. Dimmeler:** None. **E. Lutgens:** Research Grant; Significant; REPROGRAM (EU Horizon 2020). **J. Van den Bossche:** Research Grant; Significant; Junior Postdoc grant from the Netherlands Heart Foundation (2013T003) and a VENI grant from ZonMW (91615052). **M.P.J. de Winther:** Research Grant; Significant; REPROGRAM (EU Horizon 2020), Spark-Holding BV (2015B002), the European Union (ITN-grant EPIMAC), e Netherlands Heart Foundation (CVON 2011/ B019: Generating the best evidence-based pharmaceutical targets for atherosclerosis [GENIUS]).

58

Hypercholesterolemia Accelerates the Ageing of Hematopoietic Stem Cells by a Tet1 Dependent Pathway

Guodong Tie, Jinglian Yan, Lyne Khair, Amanda Tutto, Louis Messina, UMASS Medical Sch, Worcester, MA

Rationale: Hypercholesterolemia, a major risk factor for cardiovascular disease, also increases all-cause mortality. Previous work from our lab and others has shown that hypercholesterolemia induces an oxidant stress-dependent accelerated ageing of hematopoietic stem cells (HSCs) that shortens the telomeres of both HSCs and WBCs. However, little is known about the underlying epigenetic mechanism.
Objective: We found that hypercholesterolemia causes an oxidant stress-dependent downregulation of Tet1 and so we hypothesize that hypercholesterolemia accelerates the ageing of HSCs through a Tet1 dependent epigenetic pathway. Identifying the mechanisms by which hypercholesterolemia accelerates the ageing of HSCs may provide clues to understanding how hypercholesterolemia increases all-cause mortality in divergent clinical studies.
Methods and Results: RT-PCR showed that the expression of Tet1 was specifically downregulated in HSCs isolated from $ApoE^{-/-}$ mice. FACS analysis showed that the frequency of total HSCs was significantly higher in $Tet1^{-/-}$ mice than those in WT control, while the long-term and side populations of HSCs in $Tet1^{-/-}$ mice were significantly fewer than those in WT mice. The reconstitution capacity of total HSCs in $Tet1^{-/-}$ mice was significantly less than that of WT mice. In contrast, long term HSCs from $Tet1^{-/-}$ mice showed higher reconstitution capacity than that of long term HSCs from WT mice. Restoration of the Tet1 expression in $Tet1^{-/-}$ HSCs effectively restored the LT-HSC population as well as the reconstitution capacity of total HSCs. RT-PCR showed that the expression of p19 and p21 were upregulated in HSCs from $Tet1^{-/-}$ mice. DNA pyrosequencing did not show significant change in DNA methylation status in the promoter region of p19 and p21, while ChIP-PCR indicated that Tet1 deficiency facilitated the accumulation of the H3K4m3 modifications of p19 and p21.
Conclusion: Tet1-dependent epigenetic regulation is critical to maintain a healthy HSC compartment. Hypercholesterolemia induced downregulation of Tet1. Tet1 increased the expression of p19 and p21, and thereby reduces the long-term HSC population, resulting accelerated ageing in HSCs.

Disclosures: **G. Tie:** None. **J. Yan:** None. **L. Khair:** None. **A. Tutto:** None. **L. Messina:** None.

59

Wall Layer-Specific Gene Expression Profile of Coding and Non-Coding Transcripts in Abdominal Aortic Aneurysms

Moritz Lindquist Liljeqvist, Rebecka Hultgren, Christina VIllard, Malin Kronqvist, Per Eriksson, Joy Roy, Karolinska Instt, Stockholm, Sweden

Objective: To identify coding and non-coding transcripts and gene sets that are differentially expressed and enriched, respectively, in the media and adventitia of abdominal aortic aneurysms (AAA). **Methods**: Aortic tissue samples from 76 patients with AAA and 13 transplant donors (controls) were collected from the Stockholm AAA Biobank (STAAAB) and analyzed with Affymetrix HTA 2.0 microarrays. All samples were divided into intimal/medial and adventitial wall layers. Differential expression, adjusted for age and gender, and orthogonal partial least squares discriminant analysis (OPLS-DA) were performed with R. Gene set enrichment analysis (GSEA) was performed for annotated transcripts against the Molecular Signatures Database. **Results**: When controls were compared with AAAs, 9379 transcripts were differentially expressed in the tunica media and 3982 in the adventitia. Comparing adventitia and media,

7915 and 13154 transcripts were differentially expressed for AAAs and controls, respectively. Using OPLS-DA, significant separation could be made for all these comparisons. However, the difference between wall layers was less pronounced in AAA. Hallmark gene sets that were transmurally increased in AAA included allograft rejection and responses to interferon gamma and alpha and tumor necrosis factor alpha, whereas gene sets related to metabolism and sex hormone responses were downregulated. Gene sets upregulated in the AAA media, compared with its adventitia, included angiogenesis, complement and hypoxia. In controls, the media, compared with the adventitia, expressed mitotic spindle and myogenesis gene sets. **Conclusions:** The gene expression profiles of AAAs and controls are distinct and differ between wall layers. While inflammation is transmural in the AAA, hypoxia and angiogenesis are increased in the media. These results are in line with, and yield additional detail to, research published previously.

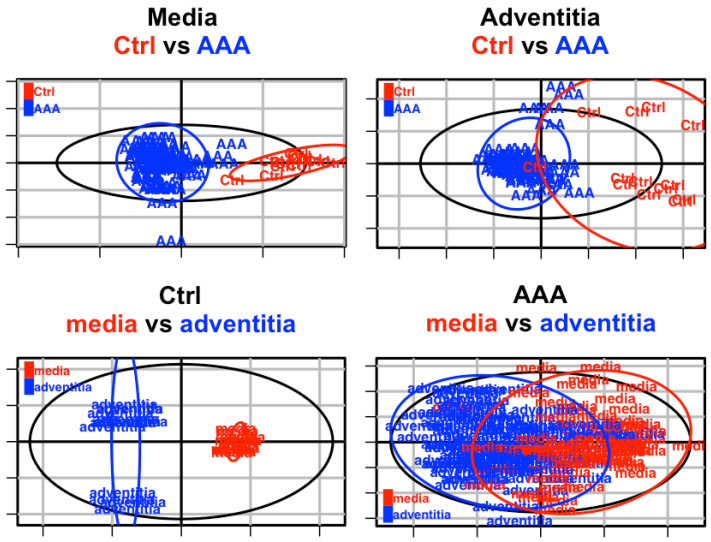

Disclosures: **M. Lindquist Liljeqvist:** None. **R. Hultgren:** None. **C. VIllard:** None. **M. Kronqvist:** None. **P. Eriksson:** None. **J. Roy:** None.

124

Safety of Carotid Endarterectomy and Carotid Stenting in the Early Period After the Neurologic Index Event - Results from the German Quality Assurance Registry on > 50,000 Patients

Pavlos Tsantilas, Andreas Kühnl, Lars Maegdefessel, Klinikum Rechts der Isar, Technical Univ of Munich, Munich, Germany; Thomas König, Thorben Breitkreuz, AQUA - Inst for Applied Quality Improvement and Res in Health GmbH, Göttingen, Germany; Christoph Knappich, Sofie Schmid, Michael Kallmayer, Alexander Zimmermann, Hans-Henning Eckstein, Klinikum Rechts der Isar, Technical Univ of Munich, Munich, Germany

Objectives: Current guidelines recommend that carotid endarterectomy (CEA) should be performed within two weeks after the neurologic index event in patients with a 50-99% symptomatic carotid artery stenosis (sCS). Safety of early CEA and early carotid artery stenting (CAS) within those two weeks remains unclear. This study aims to analyze the safety of CEA and CAS in sCS in Germany. **Methods:** By German law all extracranial carotid procedures have to be documented prospectively in a nationwide quality assurance registry. We analysed data on 56,336 CEAs (68% male, mean age 71 years (SD ± 9.6) and 4,726 CAS (68% male, median age 70 years (SD ± 9.8) treated between 2009-2014 for sCS. The patient cohort was divided into four time interval groups (I: 0-2 days, II: 3-7 days, III: 8-14 days and IV: 14-180 days respectively). Primary endpoint was the combined in-hospital stroke and mortality rate. We excluded all emergency CEAs (stroke-in-evolution, acute occlusion) and all procedures for recurrent carotid stenosis from this analysis. We performed chi-squared tests and a multivariable multilevel Poisson-regression analysis to estimate adjusted risk ratios (RR). **Results:** The procedural combined stroke and mortality rate was 3.0% (157 of 5198)/6.0% (33 of 550) in group I, 2.5% (480 of 19,117)/4.4% (70 of 1579) in group II, 2.6% (427 of 16,205)/2.4% (30 of 1244) in group III and 2.3% (370 of 15,759)/3.0% (40 of 1344) in group IV respectively. In the multivariable regression analysis the time interval was no independent risk factor for patients treated by CEA. However, CAS was associated with a decreased periprocedural risk when performed 8-14 days (group III) after the index event vs. group I (0-2 days) (RR 0.47, 95% CI 0.28-0.79). No significance was found comparing time group II vs. I (RR 0.80, 95% CI0.52-1.24) and IV vs. I (RR 0.64, 95% CI 0.39-1.05). **Conclusion:** Time interval between neurologic event and CEA has no significant influence on the perioperative stroke and mortality rate. CAS was associated with a higher risk when performed early. In accordance with the guidelines, CEA remains to be the treatment of choice in the early period after cerebral ischemia.

Disclosures: **P. Tsantilas:** None. **A. Kühnl:** None. **L. Maegdefessel:** None. **T. König:** None. **T. Breitkreuz:** None. **C. Knappich:** None. **S. Schmid:** None. **M. Kallmayer:** None. **A. Zimmermann:** None. **H. Eckstein:** None.

300

Targeting IL-1β Protects from Aortic Aneurysms Induced by Disrupted TGFβ signaling in SMCs

Daniela Carnevale, Sapienza Univ of Rome and IRCCS Neuromed, Pozzilli (IS), Italy; Raimondo Carnevale, IRCCS Neuromed, Pozzilli (IS), Italy; Francesco Da Ros, Univ of Padova, Pozzilli (IS), Italy; Giuseppe Cifelli, Manuel Casaburo, Roberta Iacobucci, Lorenzo Carnevale, Marialuisa Perrotta, IRCCS Neuromed, Pozzilli (IS), Italy; Giorgio Bressan, Univ of Padova, Padova, Italy; Giuseppe Lembo, Giuseppe Lembo, Sapienza Univ of Rome and IRCCS Neuromed, Pozzilli (IS), Italy

Aortic aneurysms represent a life-threatening condition because of the current lack of effective treatment, with therapeutic options limited to emergency surgery. Aneurysm formation is typically associated with extracellular matrix remodeling and persistent inflammation. Although the molecular mechanisms underlying aortic pathology remain largely unclear, TGFβ signaling is unquestionably implied and its downstream target Smad4 showed protective functions for maintenance of aortic walls' integrity. Using mice with smooth muscle cells (SMCs) specific deletion of *Smad4* in the adult (*Smad4*-SMC^{iko}), developing spontaneous aneurysms, we investigated the molecular mechanisms activated by dysregulation of TGFβ signaling. Structural disarrangement of ascending aorta media in *Smad4*-SMC^{iko}

mice was clearly appreciated early after Smad4 deletion as discrete breaks of elastic lamellae. Interestingly, the islands of damage evidenced in the aorta of *Smad4*-SMC^{iko} were enriched of immune infiltrate, mainly composed by monocytes/macrophages, as indicated by flow cytometry and immunofluorescence. We then analyzed several pathways downstream to Smad4 inhibition, finding a selective activation of NF-kB/IL-1β pathway in SMCs. This danger signal released by SMCs later recruits innate immunity, hence arising inflammation. In order to test the relevance of this pathway in the formation of aneurysms induced by TGFβ dysregulation, we deleted *Smad4* in SMCs of mice with *Il1r1 null* background (*Smad4*-SMC^{iko};*Il1r1*$^{-/-}$). Serial ultrasonographic analyses revealed that ablation of IL1 receptor 1 protected mice with the SMCs deletion of *Smad4* from the progression of pathology and improved their overall survival. In the end, to test the translational potential of our findings, we neutralized IL-1β signaling with the clinically relevant murine version of the FDA-approved clinical drug canakinumab. During a time course of 16 weeks, while a weekly administration of control immunoglobulins did not change aneurysm progression in *Smad4*-SMC^{iko} mice, treatment with anti-IL-1β antibody significantly hampered aneurysm formation in the aorta. These findings identify a mechanistic target for controlling aneurysms progression induced by disrupted TGFβ signaling.

Disclosures: **D. Carnevale:** None. **R. Carnevale:** None. **F. Da Ros:** None. **G. Cifelli:** None. **M. Casaburo:** None. **R. Iacobucci:** None. **L. Carnevale:** None. **M. Perrotta:** None. **G. Bressan:** None. **G. Lembo:** None. **G. Lembo:** None.

303

Increased Endogenous Hydrogen Sulfide Protects Against Vein Graft Disease

Kaspar Trocha, Ming Tao, Alban Longchamp, Brigham & Women's Hosp, Boston, MA; Michael Macarthur, James Mitchell, Harvard Sch of Public Health, Boston, MA; C. Keith Ozaki, Brigham & Women's Hosp, Boston, MA; Margreet R. de Vries, Dept of Surgery, Leiden Univ Medical Ctr, Leiden, Netherlands

Objective: Vein graft failure secondary to intimal hyperplasia remains a challenge. Hydrogen sulfide (H_2S) is produced endogenously by cystathionine γ-lyase (CGL) in endothelial cells, and as a gasotransmitter holds numerous beneficial vascular effects. We thus hypothesized that increased endogenous H_2S would attenuate the vascular response to injury. Here, we leveraged a CGL transgenic overexpressing mouse model to test the potential of increased endogenous H_2S to attenuate the vascular response to injury in a vein graft model. **Approach and Results:** A murine carotid-interposition cuff technique vein graft model was employed, including an artificial bacterial chromosome-based CGL transgenic (Tg) strain with an extra copy of the CGL gene locus randomly inserted in the genome. CGL^{Tg} mice were fed a high-fat/high-cholesterol diet, implanted with a vein graft from CGL^{Tg} donors (n=8), and compared to wild-type (WT) controls (n=7; WT/ WT conduits); all on C57BL/6 background. Grafts were imaged *in vivo* with ultrasound biomicropscopy and harvested after 28 days. CGL^{Tg} mice demonstrated an approximate two-fold increase in serum H_2S production capacity (lead acetate assay) compared to controls. The CGL^{Tg} mice exhibited a significant decrease in their intimal thickness (p=<0.05, Fig.A) and intimal/medial+adventia ratios (p=<0.05, Fig.B) 28 days after implantation. *In vivo* biomicroscopy was supportive: CGL^{tg} mice had a larger mean luminal diameter relative to WT controls (p=<0.05, Fig.C). **Conclusion:** Elevated endogenous H_2S production reduces the fibroproliferative response to vein graft arterialization. Manipulation of this gasotransmitter's biology stands as a novel approach to impact the durability of vascular reconstructions.

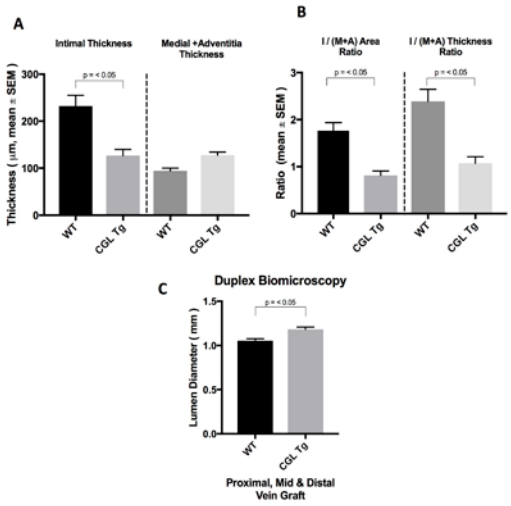

Disclosures: **K. Trocha:** None. **M. Tao:** None. **A. Longchamp:** None. **M. Macarthur:** None. **J. Mitchell:** None. **C. Ozaki:** None. **M. R. de Vries:** None.

This research has received full or partial funding support from the American Heart Association.

313

Protective Roles of Small GTP-Binding Protein GDP Dissociation Stimulator Against Angiotensin II-Induced Thoracic Aortic Aneurysm Formation and Rupture in Mice -A Possible Novel Therapeutic Target

Masamichi Nogi, Kimio Satoh, Shun Kudo, Junichi Omura, Nobuhiro Kikuchi, Taijyu Satoh, Shinichiro Sunamura, Ryo Kurosawa, Tohmohiro Ohtsuki, Kazuhiko Numano, Kota Suzuki, Hiroaki Shimokawa, Tohoku Univ Graduate Sch of Med, Sendai, Japan

Background: Statins reduce the incidence and development of thoracic aortic aneurysm (TAA) and rupture. We have previously identified that small GTP-binding protein GDP dissociation stimulator (SmgGDS) is a crucial mediator of the pleiotropic effects of statins. ***Methods and Results:*** To examine the role of SmgGDS in TAA formation, Apoe$^{-/-}$ and Apoe$^{-/-}$SmgGDS$^{+/-}$ (DKO) mice were infused with angiotensin II (AngII, 1,000 ng/min/kg) for 4 weeks. There was no significant difference in blood pressure between the 2 genotypes in response to the AngII treatment. However, during the follow-up, 36% of DKO mice died suddenly due to TAA rupture, whereas there was no TAA rupture in Apoe$^{-/-}$ mice (P<0.05, n=14 each). Histological analysis of DKO mice showed dissections of major thoracic aorta in the early phase of AngII infusion (day 3~5). We performed ultrasound imaging every week to follow the serial changes in aortic diameters. Diameter of the ascending aorta was progressively and significantly increased in DKO mice compared with Apoe$^{-/-}$ mice (1.64±0.06 vs. 1.43±0.05 mm at 4 weeks, P<0.05, n=14 each), whereas that of the abdominal aorta was comparable between the 2 genotypes. Indeed, there was no significant difference in the incidence of AngII-induced abdominal aortic aneurysm (AAA) formation between the 2 genotypes (both 75%). Western blotting demonstrated that AngII-induced activations of JNK and ERK were significantly higher in the thoracic aorta of DKO mice compared with Apoe$^{-/-}$ mice (P<0.01, n=6 each). For mechanistic analyses, we primary cultured aortic smooth muscle cells (AoSMCs) from the 2 genotypes. After AngII (100 nM) treatment for 24 hours, DKO AoSMCs showed significantly increased JNK activity, cyclophilin A secretion, and oxidative stress levels compared with Apoe$^{-/-}$ AoSMCs (P<0.01, n=6 each). Interestingly, AngII-induced upregulation of Nrf2, a master regulator of cellular responses against environmental stresses, was significantly less in DKO AoSMCs compared with Apoe$^{-/-}$ AoSMCs (P<0.01, n=6). Finally, expressions of matrix metalloproteinase-2 and -9 were significantly increased in DKO AoSMCs compared with Apoe$^{-/-}$ AoSMCs. ***Conclusions:*** These results suggest that SmgGDS is a novel therapeutic target for the prevention and treatment of TAA.

Disclosures: **M. Nogi:** None. **K. Satoh:** None. **S. Kudo:** None. **J. Omura:** None. **N. Kikuchi:** None. **T. Satoh:** None. **S. Sunamura:** None. **R. Kurosawa:** None. **T. Ohtsuki:** None. **K. Numano:** None. **K. Suzuki:** None. **H. Shimokawa:** None.

318

Modulation of Neointimal Hyperplasia Severity in Rats by Commensal Microbial Transfer

Cori A. Cason, Northwestern Univ, Chicago, IL; Thomas M. Kuntz, Neil Gottel, Univ of Chicago, Chicago, IL; Liqun Xiong, Qun Jiang, Northwestern Univ, Chicago, IL; Eugene B. Chang, Jack A. Gilbert, Univ of Chicago, Chicago, IL; Karen J Ho, Northwestern Univ, Chicago, IL

Neointimal hyperplasia is a major contributor to restenosis after arterial interventions. The genetic and environmental mechanisms underlying the variable propensity for neointimal hyperplasia between individuals are not well understood. One possible modulator could be commensal gut microbes. To address whether microbes mediate neointimal hyperplasia, we cohoused genetically different rats (Lewis [LE] and Sprague-Dawley [SD]) which harbor different commensal microbes and compared neointimal hyperplasia 2 weeks after carotid angioplasty in the cohoused and non-cohoused cohorts. Cohousing is a means of microbial transfer between cage inhabitants. We observed that differences in neointimal hyperplasia between non-cohoused LE and SD rats (median intima+media [I+M] area 0.12 mm^2 LE vs. 0.26 mm^2 SD, P<.0001;Mann-Whitney) were mitigated when rats are cohoused for 1 month (Figure 1A), suggesting an environmental effect that outweighs the genetic influence. Specifically, I+M area decreased by 23% in SD rats that were cohoused with LE rats (P<.0001;Mann-Whitney), and there was a trend towards a 10% increase in I+M area in cohoused LE rats. To identify specific bacteria associated with the change in neointimal hyperplasia, we monitored fecal bacteria over time using 16S rRNA sequencing. Principal component analysis revealed that fecal samples from cohoused rats diverged from non-cohoused rats in both strains (P<.001 SD, P=.008 LE;PERMANOVA) (Figure 1B). The greatest change was cohoused SD samples becoming similar to non-cohoused LE samples over time, which correlates with the carotid morphometric data. Comparative analysis showed that abundance of the bacterial genera Peptococcus and Blautia negatively correlated with I+M area in both strains (P<.001;Fisher z transform, Bonferroni corrected, Spearman's ρ -0.8 for both). Ongoing studies will further delineate the potential causative relationship between these microbes and neointimal hyperplasia.

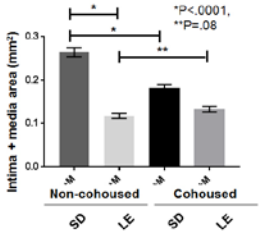

Figure 1A. Intima and media area of carotid arteries in non-cohoused and cohoused rats 2 weeks after angioplasty. N=4-6 rats per group.

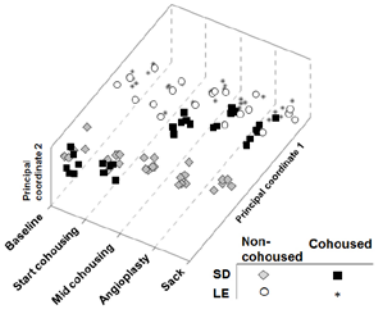

Figure 1B. Principal component analysis of 16S sequences from fecal samples from non-cohoused and cohoused rats at 5 timepoints, showing divergence of cohoused SD samples from non-cohoused SD samples to become similar to LE samples. Percent variation explained by coordinate 1 and 2 is 13.7% and 5.6%, respectively. N=4-6 rats per group.

Disclosures: **C.A. Cason:** None. **T.M. Kuntz:** None. **N. Gottel:** None. **L. Xiong:** None. **Q. Jiang:** None. **E.B. Chang:** None. **J.A. Gilbert:** None. **K.J. Ho:** None.

337

Kidney Injury Affects Metabolism and Modification of Apolipoprotein A1 Promoting Renal Lymphangiogenesis

Jianyong Zhong, Hai-Chun Yang, Yohei Tsuchida, Vanderbilt Univ Medical Ctr, Nashville, TN; Taiji Matsusaka, Tokai Univ, Shimizu, Japan; Agnes Fogo, MacRae Linton, Sean Davies, Valentina Kon, Vanderbilt Univ Medical Ctr, Nashville, TN

Kidney disease causes ApoAI/HDL to lose their vasculoprotective effects. A likely mechanism for the protective loss is modification of ApoAI/HDL reactive carbonyls which are increased. Kidney injury increases reactive carbonyls and permits more ApoAI to escape into the glomerular ultrafiltrate. We examined how apoAI was metabolized in the injured proteinuric kidney. Nphs1-hCD25 mice (NEP25) expressing human CD25 in podocytes were injured by immunotoxin, LMB2. Six weeks after LMB2, we assessed urinary excretion and intrarenal localization of ApoAI and examined the renal lymphatic network

with podoplanin. In vitro, we studied proximal tubular cells (PTC) and lymphatic endothelial cells (LEC) exposed to ApoAI or modified ApoAI (IsoLG-ApoAI). NEP25 mice developed glomerulosclerosis, increased urinary excretion of albumin and ApoAI with high molecular weight forms of ApoAI appearing in urine of injured mice assessed by western blot. Proteinuric kidneys had more ApoAI and VEGFC staining that localized to tubular epithelial cells and showed a dramatically more dense and complex lymphatic network than wild type mice. ApoAI localized to lymphatic vessels. Cultured PTC and LEC responded differently to normal and isolevuglandin (IsoLG)-modified ApoAI. In PTC, IsoLG-ApoAI promoted more ApoAI uptake and VEGFC secretion, a powerful lymphaniogenic stimulus. In LEC, IsoLG-ApoAI led to greater cell viability, migration and ROS production than normal ApoAI. Notably, supernatant of PTC exposed to ApoAI secreted a high molecular weight form of ApoAI. In conclusion, injury that disrupts the glomerular filtration barrier causing proteinuria also leads to a dramatic increase in filtered ApoAI followed by greater uptake by the proximal tubules, interstitium and lymphatic vessels. Proximal tubules can modify ApoAI and activate tubular secretion of VEGFC, which in turn promotes renal lymphangiogenesis and encourages delivery of kidney-modified ApoAI into circulation.

Disclosures: **J. Zhong:** None. **H. Yang:** None. **Y. Tsuchida:** None. **T. Matsusaka:** None. **A. Fogo:** None. **M. Linton:** None. **S. Davies:** None. **V. Kon:** None.

487

Systemic Administration of Target-Seeking, Vessel Penetrating Recombinant Decorin Fusion Protein, Car-DCN, Reduces Severity of Abdominal Aortic Aneurysm in Mice

Yue (Steve) Shen, Valerio Russo, Matthew Zeglinski, Stephanie Sellers, Zhengguo Wu, Cameron Oram, Stephanie Santacruz, Yulia Merkulova, Christopher Turner, Keerit Tauh, Hongyan Zhao, Tatjana Bozin, Lubos Bohunek, Haishan Zeng, Michael Seidman, Bruce McManus, Univ of British Columbia, Vancouver, BC, Canada; R Chris Bleackley, Univ of Alberta, Edmonton, AB, Canada; Erkki Ruoslahti, 7.Cancer Res Ctr, Sanford-Burnham Prebys Medical Discovery Inst, La Jolla, CA; Tero A Järvinen, 9.Sch of Med, Univ of Tampere & Dept of Orthopedics & Traumatology, Tampere Univ Hosp, Tampere, Finland; David Granville, Univ of British Columbia, Vancouver, BC, Canada

Objective: Decorin (DCN) is a small leucine-rich proteoglycan that mediates collagen fibrollogenesis, organization, and tensile strength. DCN is reduced in abdominal aortic aneurysm (AAA) through a Granzyme B-dependent mechanism resulting in vessel wall instability and aneurysm formation. A recombinant decorin fusion protein CAR-DCN was engineered with an extended C-terminus comprised of CAR homing peptide that recognizes inflammatory blood vessels and penetrates deep into the vessel wall. In the present study, we sought to evaluate the role of systemically administered CAR-DCN in AAA progression and rupture rate in a murine model.
Approach and Results: To induce aneurysm, apolipoprotein E knockout (ApoE-KO) mice were infused with 28 days of angiotensin II (AngII). CAR-DCN or vehicle was systemically administrated until day 15. We observed a significant increase in the survival of CAR-DCN-treated mice (93%) compared to vehicle controls (60%). Although the incidence of AAA onset was similar between vehicle and CAR-DCN groups, the severity of aneurysm in the CAR-DCN group was significantly reduced. Furthermore, histological analysis revealed that CAR-DCN treatment significantly increased DCN and collagen levels in aortic walls compares to vehicle controls.
Conclusions: CAR-DCN administration attenuated the severity of Ang II-induced AAA in mice by reinforcing the vessel wall. CAR-DCN may represent a novel therapeutic strategy to attenuate AAA progression and rupture.

Disclosures: **Y. Shen:** None. **V. Russo:** None. **M. Zeglinski:** None. **S. Sellers:** None. **Z. Wu:** None. **C. Oram:** None. **S. Santacruz:** None. **Y. Merkulova:** None. **C. Turner:** None. **K. Tauh:** None. **H. Zhao:** None. **T. Bozin:** None. **L. Bohunek:** None. **H. Zeng:** None. **M. Seidman:** None. **B. McManus:** None. **R.C. Bleackley:** None. **E. Ruoslahti:** None. **T.A.H. Järvinen:** None. **D. Granville:** Ownership Interest; Significant; D.J.G. is the Founder and Chief Scientific Officer of viDA Therapeutics Inc..

496

Genetic Neutrophil Deficiency Ameliorates Cerebral Ischemia-Reperfusion Injury

Ryan A Frieler, Yutein Chung, Jianrui Song, Thomas M Vigil, Richard M Mortensen, Univ of Michigan, Ann Arbor, MI

Background: Neutrophils respond rapidly to cerebral ischemia and are thought to contribute to inflammation-mediated injury during stroke. Neutralizing antibodies and inhibition of neutrophil chemotactic molecules can be protective during models of stroke, but many of these techniques have the potential to result in cross-reactivity and non-specificity with other immune cell types. Using myeloid Mcl1 knockout mice as a model of genetic neutrophil deficiency, we investigated the contribution of neutrophils to stroke pathophysiology. **Methods:** Myeloid Mcl1 knockout mice were subjected to transient 90-min middle cerebral artery occlusion and infarct size was assessed by MRI after 24 hours reperfusion. Immune cell mobilization and infiltration was assessed by flow cytometry after 24 hours reperfusion. **Results:** We found that myeloid Mcl1 knockout mice had significantly reduced infarct size when compared to heterozygous and wild type control mice ($MyMcl1^{+/+}$: 78.0 mm^3; $MyMcl1^{+/-}$: 83.4 mm^3; $MyMcl1^{-/-}$: 55.1 mm^3). This was accompanied by a nearly complete absence of neutrophils in the ischemic hemisphere of myeloid Mcl1 knockout mice. Although myeloid Mcl1 knockout mice were protected from cerebral infarction, no significant differences in the expression of inflammatory genes were detected. Inhibition of neutrophil chemotaxis using CXCR2 pepducin treatment partially reduced neutrophil mobilization and recruitment to the brain after stroke, but did not reduce infarct size 24 hours after transient MCA occlusion. **Conclusions:** These data confirm that neutrophils have an important role in infarct development during stroke pathophysiology and suggest that complete deficiency, but not partial inhibition, is necessary to prevent neutrophil-mediated injury during stroke.

Disclosures: **R.A. Frieler:** None. **Y. Chung:** None. **J. Song:** None. **T.M. Vigil:** None. **R.M. Mortensen:** None.

631

Nox1-Mediated CREB Promotes Gremlin1-Induced Endothelial Cell (EC) Proliferation

Daniel de Jesus, Sanghamitra Sahoo, Anastasia Gorelova, Maria Eugenia Cifuentes-Pagano, Patrick Pagano, Univ of Pittsburgh, Pittsburgh, PA

Background: Pulmonary arterial hypertension (PAH) is a devastating, rapidly degenerating disease characterized by lung vascular cell proliferation/remodeling and elevated vascular pressure leading to right heart failure. We previously showed that BMP antagonist-Gremlin1 elicits pulmonary endothelial cell (EC) proliferation in response to hypoxia, a stimulus that recapitulates in vivo changes occurring in human PAH also leading to vascular cell proliferation and remodeling. NADPH oxidase-derived reactive oxygen species (ROS) purportedly play a critical role in PAH; yet the mechanisms by which they propagate the disease are scant. Other studies show that the cAMP response element protein (CREB) is activated by ROS and modulates cell proliferation. We postulated that Nox1-mediated CREB activation leads to Gremlin1 expression promoting human pulmonary arterial EC (HPAEC) proliferation.
Method: HPAECs were subjected to 24 hrs hypoxia (1% O_2) vs. normoxia (21% O_2). Nox1, Nox2, Nox4, active CREB (pCREB), Gremlin1 and active Smads1/5/8 (pSmads) were evaluated by Western blot. Superoxide anion ($O_2^{\bullet-}$) changes were assessed using cytochrome C. To evaluate whether CREB binds to Gremlin1 promoter, chromatin immunoprecipitation (CHIP) was performed.
Results: Hypoxia upregulated Nox1 (58% increase vs. normoxia, $p<0.0001$) but did not affect Nox2 and 4 levels. Hypoxia induced $O_2^{\bullet-}$ (13.6±1.5 vs. 18.3±0.6 nmol/min*mg, normoxia v. hypoxia, respectively, $p<0.05$). Furthermore, hypoxia increased pCREB (66% vs. normoxia, $p<0.05$), and Gremlin1 (39% increase vs. normoxia) whereas it decreased pSmads 1/5/8 (50% reduction vs. normoxia, $p<0.05$). Nox1 siRNA decreased pCREB (48% reduction vs. hypoxia alone, $p=0.08$). Finally, preliminary data show CREB binding to the Gremlin1 promoter.
Discussion: In the present study, we found that hypoxia-induced HPAEC $O_2^{\bullet-}$ derived from Nox1 appears to mediate CREB activation, and subsequent promotion of Gremlin1 expression. Taken together, our data are consistent with CREB mediating Nox1-Gremlin1 signaling in hypoxia-induced EC proliferation.

Disclosures: **D. de Jesus:** None. **S. Sahoo:** None. **A. Gorelova:** None. **M. Cifuentes-Pagano:** None. **P. Pagano:** None.

93

Endothelial A Disintegrin and Metalloprotease 10 Deficiency Enhances Murine Atherosclerosis Development

Kosta Theodorou, Emiel van der Vorst, Cardiovascular Res Inst Maastricht, Maastricht Univ, Maastricht, Netherlands; Timo Rademakers, Jaap van Buul, Sanquin Res and Landsteiner Lab, Amsterdam, Netherlands; Michael Lehrke, Corinna Lebherz, Dept of Internal Med, RWTH Aachen Univ, Aachen, Germany; Daniela Dreymüller, Andreas Ludwig, Inst for Pharmacology and Toxicology, RWTH Aachen Univ, Aachen, Germany; Jacob Bentzon, Ctr Nacional de Investigaciones Cardiovasculares Carlos III, Madrid, Spain; Erik Biessen, **Marjo Donners**, Cardiovascular Res Inst Maastricht, Maastricht Univ, Maastricht, Netherlands

Through shedding of various membrane molecules, including adhesion molecules and chemokines, A Disintegrin And Metalloproteinase 10 (ADAM10) could regulate endothelial permeability and leukocyte recruitment, critical processes in inflammatory diseases like atherosclerosis. Indeed, proteomic analysis on mouse endothelial cell sheddome revealed ±300 differentially regulated proteins upon ADAM10 inhibition, of which 10% appeared involved in permeability and leukocyte transmigration. Accordingly, *in vitro* inhibition of endothelial ADAM10 decreased neutrophil adhesion and transmigration under flow. To evaluate the causal role of endothelial ADAM10 in atherosclerosis development, we used wildtype or endothelial ADAM10-deficient ($ADAM10^{fl/fl}$/Tie2-Cre; in brief $ADAM10^{del}$) mice. Mice were rendered atherogenic by adeno-associated virus-mediated overexpression of PCSK9, resulting in persistent LDL receptor knockdown and hyperlipidemia after high cholesterol diet feeding (HCD). Surprisingly, after 12 weeks of HCD diet feeding, $ADAM10^{del}$ mice showed significantly larger (±45%) and more advanced atherosclerotic lesions, with intraplaque hemorrhage in the brachiocephalic artery. Necrotic core area was increased (±87%) and macrophage content decreased (±49%). No differences were observed in granulocyte and collagen content. In contrast to the *in vitro* findings, *in vivo* endothelial permeability, leukocyte adhesion and extravasation, as assessed by intravital multiphoton microscopy, were all increased. In conclusion, this study reveals an unexpected protective effect of endothelial ADAM10 in atherosclerosis development. The underlying mechanisms remain to be determined.

Disclosures: **K. Theodorou:** None. **E. van der Vorst:** None. **T. Rademakers:** None. **J. van Buul:** None. **M. Lehrke:** None. **C. Lebherz:** None. **D. Dreymüller:** None. **A. Ludwig:** None. **J. Bentzon:** None. **E. Biessen:** None. **M. Donners:** Research Grant; Significant; Dutch Heart Foundation grant (2012 T079), Professor's fund of the Limburg University Fund.

94

Deficiency of Epsins in Macrophages Ameliorates Atherosclerosis by Attenuating Inflammation

Megan L Brophy, Yunzhou Dong, Hao Wu, Kai Song, Ashiqur Rahman, Aiyun Wen, Sukyoung Kwak, Scott Wong, Kenneth Krygier, Boston Children's Hosp, Boston, MA; Klaus Ley, La Jolla Inst for Allergy and Immunology, La Jolla, CA; Hong Chen, Boston Children's Hosp, Boston, MA

Background Atherosclerosis is caused by the immune and inflammatory cell infiltration of the vascular wall, leading to enhanced inflammation and lipid accumulation. Understanding the molecular mechanisms underlying this disease is critical for the development of new therapies. Our recently studies demonstrate that endothelial epsins, a family of ubiquitin-binding endocytic adaptors are critical regulators of atherosclerosis. However, whether epsins in macrophages play a role in regulating vascular inflammation is unknown. We hypothesize that epsins in macrophages promote inflammation to facilitate atherogenesis.
Methods and Results We engineered myeloid cell-specific epsins double knockout mice (Mϕ-DKO) on an ApoE-/- background fed western diet. Strikingly, these mice exhibited reduced atherosclerotic lesion formation, diminished immune and inflammatory cell recruitment to aortas and reduced cleaved caspase 3 staining but increased α-SMA staining within aortic root sections. Epsin deficiency hindered foam cell formation, suppressed the pro-inflammatory M1 macrophage phenotype but increased the anti-inflammatory macrophage phenotype, and enhanced efferocytosis in primary macrophages. Mechanistically, we show that epsin loss specifically increases total and surface levels of LRP-1, a protein with anti-inflammatory properties without altering levels of LDL scavenger receptors. We further show that

epsin and LRP-1 interact via epsin's UIM domain. Oxidized LDL treatment increased LRP-1 ubiquitination and subsequent binding to epsin while mutation of cytoplasmic lysine residues attenuated LRP-1 ubiquitination, suggesting that epsin promotes the ubiquitin-dependent internalization and degradation of LRP-1. Importantly, Mϕ-DKO/ApoE null mice on LRP-1 heterozygous background restored atherosclerosis, suggesting that epsin-mediated LRP-1 downregulation in macrophages plays a pivotal role in propelling atherogenesis.
Conclusions Macrophage epsins promote atherogenesis, in part, by facilitating pro-inflammatory macrophage recruitment and potentiating foam cell formation by downregulating LRP-1, implicating that targeting epsin in macrophages may serve as a novel therapeutic strategy to treat atheroma.

Disclosures: **M.L. Brophy:** None. **Y. Dong:** None. **H. Wu:** None. **K. Song:** None. **A. Rahman:** None. **A. Wen:** None. **S. Kwak:** None. **S. Wong:** None. **K. Krygier:** None. **K. Ley:** None. **H. Chen:** None.

This research has received full or partial funding support from the American Heart Association.

95

MiRNA-210 Enhances Fibrous Cap Stability in Advanced Atherosclerotic Lesions

Suzanne M Eken, Hong Jin, Ekaterina Chernogubova, Yuhuang Li, Nancy Simon, Changyan Sun, Greg Korzunowicz, Albert Busch, Alexandra Bäcklund, Cecilia Österholm, Anton Razuvaev, Thomas Renné, Karolinska Instt, Stockholm, Sweden; Hans H Eckstein, Jaroslav Pelisek, Technical Univ Munich, Munich, Germany; Per Eriksson, Maria Gonzalez Diez, Ljubica Matic Perisic, Karolinska Instt, Stockholm, Sweden; Isabel N Schellinger, Uwe Raaz, Univ Göttingen, Göttingen, Germany; Nicholas J Leeper, Stanford Univ Sch of Med, Palo Alto, CA; Göran K Hansson, Gabrielle Paulsson-Berne, Ulf Hedin, Lars Maegdefessel, Karolinska Instt, Stockholm, Sweden

In the search for markers and modulators of vascular disease, miRNAs have emerged as potent therapeutic targets. We investigated miRNAs of clinical interest in patients with unstable carotid stenosis at risk of stroke. Utilizing patient material from the Biobank of Karolinska Endarterectomies (BiKE), we profiled miRNA expression in symptomatic versus asymptomatic patients with high-grade carotid artery stenosis. A PCR-based miRNA of plasma, sampled at the carotid lesion site, identified eight deregulated miRNAs (miR-15b, -29c, -30c/d, -150, -191, -210 and -500). miR-210 was the most significantly downregulated miRNA in local plasma material. Laser-capture microdissection as well as *in situ* hybridization revealed a distinct localization of miR-210 in the fibrous caps of atherosclerotic lesions and showed reduced miR-210 expression in the unstable fibrous cap. We confirmed that miR-210 directly targets the tumor suppressor gene adenomatous polyposis coli (APC), thereby affecting Wnt signaling and regulating vascular smooth muscle cell survival, as well as differentiation, in advanced atherosclerotic lesions. Substantial changes in arterial miR-210 were detectable in two rodent models of vascular remodeling and plaque rupture. Modulating miR-210 *in vitro* and *in vivo* improved fibrous cap stability with implications for vascular disease. We discovered that an unstable carotid plaque at risk of stroke is characterized by low expression of miR-210. miR-210 contributes to stabilizing carotid plaques through inhibition of APC, ensuring vascular smooth muscle cell survival. We present local delivery of miR-210 as a therapeutic approach for prevention of atherothrombotic disease.

Disclosures: **S.M. Eken:** None. **H. Jin:** None. **E. Chernogubova:** None. **Y. Li:** None. **N. Simon:** None. **C. Sun:** None. **G. Korzunowicz:** None. **A. Busch:** None. **A. Bäcklund:** None. **C. Österholm:** None. **A. Razuvaev:** None. **T. Renné:** None. **H.H. Eckstein:** None. **J. Pelisek:** None. **P. Eriksson:** None. **M. Gonzalez Diez:** None. **L. Matic Perisic:** None. **I.N. Schellinger:** None. **U. Raaz:** None. **N.J. Leeper:** None. **G.K. Hansson:** None. **G. Paulsson-Berne:** None. **U. Hedin:** None. **L. Maegdefessel:** None.

96

Melatonin Prevents Atherosclerosis via Regulating NLRP3 Inflammasome: The Role of Sirt3 Signaling

Sai Ma, Jiangwei Chen, Zhenli Luo, Dept of Cardiology, Xijing Hosp, Xi'an, China; Yabin Wang, Feng Cao, Dept of Cardiology, Chinese PLA General Hosp, Beijing, China

Introduction: NLRP3 inflammasome mediated inflammatory factors secretion is critically involved in atherosclerosis (AS). Melatonin has anti-inflammatory properties. However, it is unknown whether

melatonin is beneficial in AS.
Hypothesis: Melatonin plays a beneficial role in AS by decreasing NLRP3 inflammasome activation in macrophages.
Methods: AS model was induced with high fat diet in apoE$^{-/-}$ mice. Plaque stability was examined with historical staining. *In vitro* study was performed in ox-LDL treated RAW264.7 cells. NLRP3 inflammasome activation, inflammatory factors secretion, mitochondrial ROS generation, autophagy, mitophagy indexes and potential signaling pathways were investigated.
Results: Historical staining results showed that melatonin treatment markedly alleviated AS plaque progression. Despite of unchanged protein expression, Sirt 3 activity was elevated in plaque tissue in melatonin treated mice. Melatonin attenuated NLRP3 inflammasome activation and inflammatory factors secretion in ox-LDL treated macrophages, while this protective effect was abolished by Sirt3-siRNA. Mitochondrial ROS (mitoROS), which was an inducer for NLRP3 inflammasome, was reduced by melatonin through the elimination of damaged mitochondria (mitophagy). Similar with Sirt3-siRNA, autophagy inhibitor 3-MA also abolished the effects of melatonin on mitoROS clearance, indicating the crucial role of autophagy and mitophagy in melatonin caused NLRP3 inactivation. Furthermore, melatonin protected against AS via Sirt3/FoxO3/Parkin signaling pathway.
Conclusions: Melatonin prevented atherosclerotic progression. Melatonin reduced mitochondrial ROS through the activation of autophagy and mitophagy, thereby attenuating NLRP3 inflammasome activation in macrophages. Moreover, the protective effect of melatonin was mediated by Sirt3/FoxO3/Parkin signaling pathway. Our study provides insight into a new therapeutic target for AS.

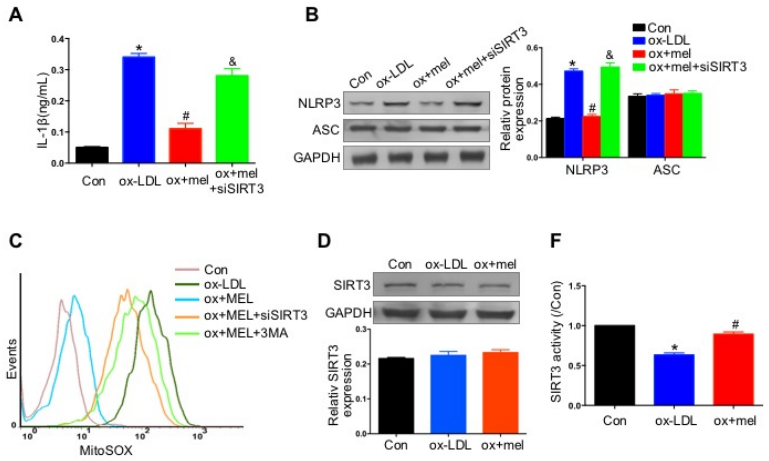

Disclosures: **S. Ma:** None. **J. Chen:** None. **Z. Luo:** None. **Y. Wang:** None. **F. Cao:** None.

97

Genotype to Phenotype: Function of Common Noncoding and Rare Coding Variants In *ANGPTL3*

Xiao Wang, Univ of Pennsylvania, Philadelphia, PA; Avanthi Raghavan, Harvard Medical Sch, Boston, MA; A. Christina Vourakis, Alexandra E Sperry, Harvard Univ, Cambridge, MA; Wenjun Li, Wenjian Lv, Alexandra C Chadwick, Kiran Musunuru, Univ of Pennsylvania, Philadelphia, PA

Human genetics studies have demonstrated a strong link between *ANGPTL3*, which encodes lipoprotein lipase inhibitor Angiopoietin-like 3, and blood lipid phenotypes. Rare nonsense *ANGPTL3* mutations were identified in patients with familial combined hypolipidemia, while common variants at the *ANGPTL3* locus have been found by genome-wide association studies (GWASs) to associate with lower triglycerides (TGs) and low-density lipoprotein cholesterol. In light of the seemingly favorable clinical consequences of ANGPTL3 deficiency, we established an experimental framework to identify (1) causal common variants that regulate *ANGPTL3* expression and (2) rare missense mutations that disrupt *ANGPTL3* function. Using massively parallel reporter assays, we profiled the regulatory activity of all the common variants linked ($r^2 \geq 0.5$) to the lead GWAS SNP in the *ANGPTL3* locus and found that rs10889356 demonstrated

significant allele-specific enhancer activity. To validate this finding, we used CRISPR-Cas9 to alter the SNP in a human pluripotent stem cell line. When differentiated into hepatocytes, altered cells displayed a 67% increase in *ANGPTL3* expression (n = 4 wild-type and 4 mutant clones, P = 0.007). CRISPR interference using each of three guide RNAs targeting the SNP in HepG2 cells also substantially increased *ANGPTL3* expression. These findings support rs10889356-*ANGPTL3* as a causal SNP-gene set. Next, we examined the coding regions of *ANGPTL3* in 20,000 sequenced individuals and sought to experimentally define rare missense variants using a mouse model. We used CRISPR-Cas9 to generate *Angptl3* knockout mice, which exhibited decreased TG (61%, $P < 0.001$) and decreased cholesterol (31%, $P < 0.002$). We reconstituted the knockout mice to normal expression levels with adenoviruses expressing either wild-type *ANGPTL3* or missense variant *ANGPTL3*. So far we have assessed 28 rare missense variants computationally predicted to be deleterious, of which only 10—D42N, K58E, S117P, P264S, Q286H, L315S, L360Q, T383I, T383S, and Y417C—were validated as loss-of-function (conferring <25% of wild-type activity as assessed by changes in both TG and cholesterol levels), underscoring the need for functional characterization of variants of uncertain significance.

Disclosures: **X. Wang:** None. **A. Raghavan:** None. **A. Vourakis:** None. **A.E. Sperry:** None. **W. Li:** None. **W. Lv:** None. **A.C. Chadwick:** None. **K. Musunuru:** None.

98

Chronic Kidney Disease-Associated Atherosclerosis is Attenuated by Dual Inhibition of microRNA-92a and microRNA-489

Carrie Wiese, Zhi-Qi Xu, Youmin Zhang, Yan Guo, Jianyong Zhong, Marisol Ramirez, Wanying Zhu, Valentina Kon, Kasey Vickers, Vanderbilt Univ, Nashville, TN

Chronic kidney disease (CKD) subjects have an increased risk of developing cardiovascular disease, namely atherosclerosis. Endothelial dysfunction and inflammation are linked to the development of these diseases and recent work has identified a number of microRNAs (miRNAs) involved in these pathologies. As such, endothelial miRNAs are potential novel therapeutic targets to prevent and treat atherosclerosis. This study identified elevated aortic endothelial miR-92a-3p and miR-489-3p levels in a mouse model of CKD-associated atherosclerosis, *Apoe*$^{-/-}$ mice with 5/6 nephrectomy. A combinatorial miRNA inhibition strategy resulted in the loss of both miR-92a-3p and miR-489-3p in the endothelium and significantly reduced the atherosclerotic lesion area by 33%. Total RNA sequencing of the aortic endothelium identified many altered genetic pathways and metabolic processes in response to *in vivo* miRNA loss-of-function, including inflammation, phospholipid metabolism, and protein degradation pathways. Results suggest that the reduction in atherosclerosis levels were not likely to be linked to alterations in plasma cholesterol levels or kidney function since these physiological parameters were not improved upon miRNA inhibition. Nevertheless, novel miRNA targets were identified to be significantly elevated in the aortic endothelium that may reduce inflammation leading to the improved physiological phenotype. *Fam220a*, a negative regulator of signal transducer and activator of transcription 3 (STAT3) phosphorylation, mRNA levels were significantly reduced in CKD-atherogenic mice compared to controls, but miRNA inhibition *in vivo* blocked the *Fam220a* repression. Moreover, gene reporter (luciferase) assays with site-directed mutagenesis confirmed *FAM220A* as a direct target of miR-92a-3p. Furthermore, *FAM220A* mRNA levels were repressed in human coronary artery endothelial cells (HCAEC) with miR-92a-3p over-expression, which resulted in increased phosphorylation of STAT3. Collectively, these results suggest that endothelial miR-92a-3p and miR-489-3p are novel therapeutic targets to treat CKD-associated atherosclerosis.

Disclosures: **C. Wiese:** None. **Z. Xu:** None. **Y. Zhang:** None. **Y. Guo:** None. **J. Zhong:** None. **M. Ramirez:** None. **W. Zhu:** None. **V. Kon:** None. **K. Vickers:** None.

100

Lower Probability of Aortic Aneurysm Diagnosis Among Patients With Chronic Cannabis Exposure, An Analysis of the 2012-2014 National Inpatient Survey

Adeyinka C Adejumo, Univ. of Massachusetts Medical Sch, Worcester, MA; Samson Alliu, Maimonides Medical Ctr, Brooklyn NY, NY; Oluwole M Adegbala, Englewood Hosp and Medical Ctr, Englewood, NJ; Nnaemeka E Onyeakusi, Bronx-Lebanon Hosp Ctr, Bronx, NY; Tokunbo O Ajayi, Johns Hopkins Med, Howard County General Hosp, Columbia, MD; Akintunde M Akinjero, Englewood Hosp and Medical Ctr,

Englewood, NJ; Adetoro T Okafor, MPH Epidemiology program, Univ of Minnesota, Minneapolis, MN; Edgar Lichstein, Maimonides Medical Ctr, Brooklyn NY, NY

Introduction: Cannabis is a commonly utilized recreational substance which contains numerous bioactive agents. As more states legalize the use of marijuana, it's effect on various disease conditions is expected to become more pronounced. Cannabis' anti-inflammatory effects could suppress pro-inflammatory conditions. For example, chronic inflammation with extracellular matrix degradation resulting in weakness and abnormal dilatation of the aortic wall is a hallmark of Aortic Aneurysm. We, therefore, hypothesized that cannabis users would have less prevalence of aortic aneurysms.Objective: To identify the relationship between chronic cannabis use (CU) and diagnosis of aortic aneurysms (AA) among hospitalized patients.Methods: After selecting patients who were 55 years and above from 2012 to 2014 National Inpatient Sample database, we identified those who had a diagnosis of Aortic Aneurysm and those who utilize Cannabis. We then stratified the CU into two groups: nondependent (NDU) and dependent users (DU). Using logistic regression, we estimated the Odds Ratio (AOR) after controlling for numerous factors.Results: In our total 10,461,694 sample, 99.6% (10,419,972) are non-users, 0.37% (38,514) are nondependent users and 0.03% (3,208) are dependent users. About 3.21% (336,202) of the patients had a diagnosis of AA versus 96.79% (10,125,492) without a diagnosis of AA. Compared to non-users of cannabis, the odds of AA is about 35% less among CU (AOR 0.66[0.62-0.71]), 40% less among DU (aOR 0.58[0.44-0.76]), and 33% less among NDU (AOR 0.67[0.62-0.72]). The odds of AA was lower in females (AOR 0.61[0.60-0.610]), but higher in many conditions such as: among >=65 years (AOR 1.16[1.15-1.17]), tobacco users (AOR 1.18[1.17-1.19]), predisposing hereditary conditions (AOR 5.31[4.60-6.13]), and atherosclerosis (AOR 3.04[3.00-3.08]).Conclusions: Our result shows that Cannabis use is associated with less occurrence of AA. Cannabidiol, an anti-inflammatory alkaloid in Cannabis could potentially suppress the release of proteolytic inflammatory mediators which might be responsible for the gradual weakening of the vascular walls. We recommend more basic research to evaluate this effect of Cannabidiol.

Disclosures: **A.C. Adejumo:** None. **S. Alliu:** None. **O.M. Adegbala:** None. **N.E. Onyeakusi:** None. **T.O. Ajayi:** None. **A.M. Akinjero:** None. **A.T. Okafor:** None. **E. Lichstein:** None.

101

Dipeptidylpeptidase-iv Inhibition Using MK626 Attenuates BAPB/AT2 Induced Murine Aneurysm

John S Byrne, Emily Chen, Mansoor Husain, Maral Ouzounian, Clint Robbins, Thomas Lindsay, Univ of Toronto, Toronto, ON, Canada

The dearth of effective treatments to diminish aneurysm progression is a recognized clinical challenge. Modulation of the glucagon-like peptide-1 (GLP-1) pathway is a recent addition to anti-diabetic management regimes, and has pleiotropic effects to inhibit arterial wall macrophage infiltration, a key pathological event in aneurysmal disease. We therefore hypothesized that inhibition of endogenous breakdown of GLP-1, using the dipeptidylpeptidase-IV inhibitor MK626, would attenuate BAPN/AT2 induced murine aneurysm.
Eight-week-old C57/Bl6 mice received two weeks of oral beta-aminoproprionononitrile (BAPN) and four weeks of angiotensin-2 (AT2) via mini-osmotic pump. MK626 3mg/kg in methylcellulose vehicle was administered daily and compared to control methylcellulose vehicle. At four weeks, whole aortas were dissected and photomicrographed. Cross sections of aorta were stained using H&E and EVG. Compared to wild-type, BAPN/AT2 caused dilatation of the aorta from the ascending to the suprarenal segment ($p<0.002$) with infrarenal sparing ($p=0.77$). Focal aneurysmal dilatation reproducibly occurred in the suprarenal aorta (wild-type diameter 0.93±0.03mm, n=8; BAPN/AT2 diameter 2.26±0.12, n=8; $p<0.0001$). Treatment with MK626 attenuated dilatation of the descending aorta compared to controls (BAPN/AT2 control 1.26±0.05mm, n=8; MK626 1.07±0.05mm, n=10; $p=0.03$). The focal suprarenal aneurysmal dilatation was significantly reduced by treatment with MK626 (BAPN AT2 control 2.26±0.34mm, n=8; MK626 1.66±0.32mm, n=10; $p=0.0001$). BAPN/AT2 induced aortic aneurysm was associated with excess matrix deposition, increased medial thickness, and elastic fibre fragmentation. Modulation of the GLP pathway using the dipeptidylpeptidase-IV inhibitor MK626 attenuates aneurysm in a BAPN/AT2 induced murine model.

Disclosures: **J.S. Byrne:** None. **E. Chen:** None. **M. Husain:** None. **M. Ouzounian:** None. **C. Robbins:** None. **T. Lindsay:** None.

102

A Novel Swine Model of Infrarenal Abdominal Aortic Aneurysm

Jonathan M Cullen, Guanyi Lu, Gang Su, Robert Hawkins, Anna Fashandi, Michael Spinosa, William Montgomery, Morgan Salmon, Ashish Sharma, Gorav Ailawadi, Gilbert Upchurch Jr., Univ of Virginia, Charlottesville, VA

Introduction
A reproducible large animal model for abdominal aortic aneurysms (AAAs) does not exist. This study sought to develop a large animal AAA model in swine using β-aminopropionitrile (BAPN), a lysyl oxidase inhibitor, an enzyme responsible for collagen cross-linking. We hypothesized that elastase/collagenase perfusion and balloon dilatation in combination with BAPN administration would result in AAA formation.
Methods
Uncastrated Yorkshire male swine were fed BAPN (0.12g/kg) daily for one week prior to surgery and continued throughout the experiment. After anesthesia, the aorta was exposed from the renal arteries to the aortic bifurcation. The infrarenal aorta was cannulated via the caudal mesenteric artery and an aortic angioplasty was performed to dilate the aorta to 200% of its original diameter. Next, a 30 mL solution consisting of 500 units of elastase and 8,000 units of Type I collagenase was perfused into the infrarenal aorta for 10 minutes. This solution was also then topically applied for 10 minutes. The abdomen was irrigated and closed. Antibiotics and analgesic medications were administered.
Results
BAPN-fed swine sacrificed at 28 days (n=5) had a 101% increase in infrarenal aorta diameter compared with day 0 (p=0.008). Swine (n=4) sacrificed at 7 and 14 days showed an increase of 114 and 75%, respectively. Histologically on day 28, collagen decreased by 20% and smooth muscle cell expression decreased by 40% (p=0.0001) in the aortic wall compared with control suprarenal aorta. Infrarenal aortas also showed a strong predilection for M1-polarized macrophages (MCP-1 positive staining, p=0.0165) compared with M2 macrophages (Arg-1 positive staining). MMP2 activity by zymography (p=0.0127) and IL-18 by array was also significantly increased (p=0.0202) on day 28 in the infrarenal AAA.
Conclusions
Compared with previous large animal AAA models, this model using conventional techniques including balloon dilatation, elastase/collagenase perfusion, in addition to oral BAPN led to robust AAA with similar molecular and histologic changes to those seen in human AAA. This novel swine AAA model may serve as a much-needed link that will allow for the progression of studies from rodents to humans.

Disclosures: **J.M. Cullen:** None. **G. Lu:** None. **G. Su:** None. **R. Hawkins:** None. **A. Fashandi:** None. **M. Spinosa:** None. **W. Montgomery:** None. **M. Salmon:** None. **A. Sharma:** None. **G. Ailawadi:** None. **G. Upchurch:** None.

103

Socioeconomic Factors and Illicit Drug Use Affect Time to Presentation in Ascending Aortic Dissection

Tanya Doctorian, Sean Khorami, Jie Ren, Kaiser Permanente Fontana Medical Ctr, Fontana, CA

Objectives: Ascending aortic dissection (AoD) is the most lethal condition involving the aorta. Despite increased awareness of AoD among clinicians and improvements in diagnostic imaging and treatment, the mortality and morbidity rates of this condition remain high. To further optimize outcomes, symptom onset and its impact on presentation is needed. The objective of this study was to determine whether socioeconomic factors and legal or illegal drug use were associated with delays in presentation of ascending AoD patients.
Methods: In this study, 186 patients with complete data presenting with ascending AoD from 2007 to 2016 to 2 tertiary hospitals were retrospectively studied. Symptom-onset-to-hospital-arrival time was analyzed for: legal and illegal substance use, ethnicity, insurance status, gender, and marital status. Symptom onset time was identified by review of medical records and emergency services data. Statistical analysis was carried out to compare differences in time to presentation between groups.
Results: See tables 1 and 2
Conclusions: In this cohort, illicit drug use and tobacco use were associated with significant barriers to presentation in patients with ascending AoD. In addition, ascending AoD patients who were female, Hispanic, uninsured, and widowed presented significantly later than the other patient groups. Contrary to expectation, alcohol use was not associated with pre-hospital delays. Enhanced public awareness and

targeted education to these vulnerable patient groups are necessary to decrease pre-hospital delays, reduce barriers to presentation, and further improve clinical outcomes in ascending AoD patients.

Table 2: Socioeconomic Factors

	Percentage of Population	Symptom onset to Presentation time {median (min – max)} in hours	P-value
Gender			
Male	82%	2 (0.5 – 168)	Reference
Female	28%	4 (0.5 – 168)	0.003
Ethnicity			
White/Caucasian	34%	2 (0.5 – 48)	Reference
Black	30%	4 (0.5 – 168)	0.022
Hispanic/Latino	19.80%	8 (0.5 – 168)	0.003
Asian	12.6%	6 (0.5 – 168)	0.053
Other	3.60%	2 (0.5 – 5)	0.301
Insurance Status			
Private insurance	54%	2 (0.5 – 168)	Reference
Uninsured	7.5%	8 (4 – 168)	0.001
Medicare/Medicaid	38.5%	3 (1 – 44)	0.412
Marital status			
Married	60.5%	2 (0.05 – 168)	Reference
Divorced	9.9%	3 (0.05 – 24)	0.217
Widowed	7.2%	24 (1 – 168)	<0.001
Single/Never Married	22.4%	4 (0.5 – 168)	0.027

Table 1: Legal and Illegal Substance Use

	Percentage of population	Symptom onset-to-presentation time {median (min-max)} in hours	P-value
Smokers			
Never	50.0%	2 (0.5 – 48)	Reference
Current	23.5%	8 (2 – 336)	<0.001
Past	27.90%	2 (0.5 – 144)	0.001
Alcohol			
Never	86.2%	3 (0.5 – 8)	Reference
Current	10.8%	4 (1 – 133)	0.06
Past	3.0%	1 (1 – 4)	0.416
Methamphetamine, Cocaine, or Marijuana abuse			
Never	89.6%	2 (0.5 – 8)	Reference
Current	9.1%	8 (1 – 366)	0.001
Past	1.3%	4 (1 – 4)	0.406

Disclosures: **T. Doctorian:** None. **S. Khorami:** None. **J. Ren:** None.

104

Prevalence of Abdominal Aortic Aneurysm in Multi-Vessel Coronary Artery Disease

Rikin Kadakia, Veterans Affair Salem Medical Ctr / Virginia Tech Sch of Med, Roanoke, VA; Amitabh Parashar, Veterans Affair Salem Medical Ctr / Virginia Tech - SOM, Roanoke, VA

Background: Abdominal aortic aneurysm (AAA) is the 10th leading cause of death in the United States. USPSTF recommends screening for AAA on men ages 65 to 75 years who have ever smoked. However, recent literature suggests an increased prevalence of AAA in patients with multi-vessel coronary artery disease (CAD) irrespective of age. Additionally, CAD with AAA share common risk factors. AAA rupture or repair on patients less than 65-year-old have not been documented. **Objective**: We conducted a single center retrospective review of all patients at the Salem VA Medical Center, Virginia who completed an

abdominal ultrasound (US) for AAA screen in 2013. The goal of the current study was to identify the prevalence of AAA through routine US screen in veteran population compare with the prevalence of AAA in patients with multi-vessel CAD. Additionally to identify specific trends in high-risk population. **Method**: Cohort A included 634 patients for primary screening of AAA. Cohort B included 132 patients who had multi-vessel CAD based on coronary catherization were reviewed for incidental AAA on any abdominal imaging. Medical records were reviewed; demographics were collected including age, gender, HTN, DLD, DM, tobacco use, presence of AAA, and size. **Conclusion**: Cohort B had 19.3% (26/135) prevalence of AAA, verses Cohort A had 7.7% (49/634), a statistically difference P (0.008). Cohort B, 13.3% (6/26) were less than 65-years-old verses 25% (20/88) were over 65 years old. Cohort A with AAA 34.5% (17/49) of patients had documented CAD - Number of coronary vessels conferred to a greater risk of AAA, 2 vessel CAD 10.3% (6/58), 3 vessel CAD 7.3% (10/73), 4 vessel CAD 100% (1/1). This result supports the growing concern for AAA in patients with multi-vessel CAD, thus should be considered as an independent risk factor for AAA. Patients with multi-vessel CAD should be screened sooner than current recommended guidelines.

Results:

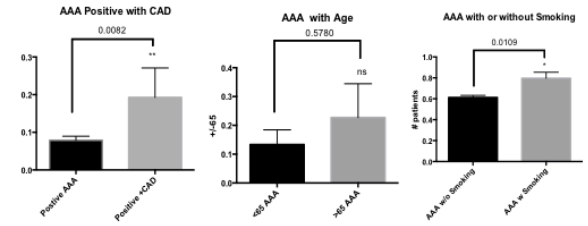

CAD/AAA vs. AAA screen/AAA

CAD/AAA >65 age vs. CAD/AAA >6

AAA screen w/ Smoke vs. w/o smoking

Cohort B	26/135 (19.3%)
Cohort A	49/634 (7.7%)
Cohort A with history of CAD	17/49 (34.5%)

Cohort B <65 years	6/26 (13.3%)
Cohort A >65 years	20/88 (25%)

Cohort B, 1 vessel CAD w/ AAA	0/1 (0%)
Cohort B, 2 vessel CAD w/ AAA	6/58 (10.3%)
Cohort B, 3 vessel CAD w/ AAA	10 / 73 (7.3%)
Cohort B, 4 vessel CAD w/ AAA	1/1 (100%)

Disclosures: **R. Kadakia:** None. **A. Parashar:** None.

105

Association of Viscoelastic Material Properties and Extracellular Matrix Remodeling in Human Abdominal Aortic Aneurysmal Tissue

Doran S Mix, Sandra A Toth, Univ of Rochester Sch of Med and Dentistry, Rochester, NY; Ibrahima Bah, Univ of Rochester, Rochester, NY; Michael C Stoner, Bruce I Goldman, Univ of Rochester Sch of Med and Dentistry, Rochester, NY; Mark Buckley, Univ of Rochester, Rochester, NY; Scott J Cameron, Michael S Richards, Univ of Rochester Sch of Med and Dentistry, Rochester, NY

Objectives: Predicting rupture of abdominal aortic aneurysm (AAA) requires knowledge of both the rate of extracellular matrix (ECM) degradation and the pulsatile stress on the aortic tissue. The activity of matrix metallopeptidase 9 (MMP9) and its inhibitor, TIMP1, are associated with alterations in aortic ECM but it is unknown if these changes effect the dynamic viscoelastic properties. We hypothesize that increased levels of MMP9 within AAA tissue will be associated with a greater dynamic modulus (E*), as a surrogate of increased aortic wall stress.
Methods: Human aneurysmal aortic tissue was obtained at the time of open AAA repair (n=11) and age-matched non-aneurysmal cadavers (n=10). Uniaxial viscoelastic material properties were measured in the circumferential orientation under physiologic preload (110 mmHg) and cyclic strain (± 5%@1Hz). Quantitative histologic and immunohistochemistry were preformed using Fiji imaging software. Aortic MMP9 and TIMP1 content and activity were quantified using western blot and zymography.
Results: E* was greater (1862±464 vs 1362±405 kPa, p=0.02) in the AAA tissue as compared to non-aneurysmal tissue. AAA tissue contained less elastin (6.7±6.7 vs 23.4±8.7%, p=0.01) and a greater

collagen/elastin ratio (19.9±20.6 vs 2.3±2.5%, p=0.05). Immunohistochemistry revealed 200% greater MMP9 content in the AAA tissue (Figure A & B, 0.61 vs 0.03%, p=0.03). Increased MMP9 content was confirmed using a western blot (0.43 vs 0.06 AU, p<0.01). No difference in relative MMP9 activity (4307 vs 2324 AU, p=0.25) or level of TIMP1 (0.03 vs 0.02, p=0.6) were observed. There was a positive linear correlation (Figure C, r^2=0.47) between E* and MMP9 as determined by quantitative immunohistochemistry.
Conclusions: Our data suggests a positive relationship between E* and MMP9 content. Increased tissue stiffness may trigger MMP9 production resulting in a positive-feedback loop, progressively increasing aortic wall stress and rupture risk.

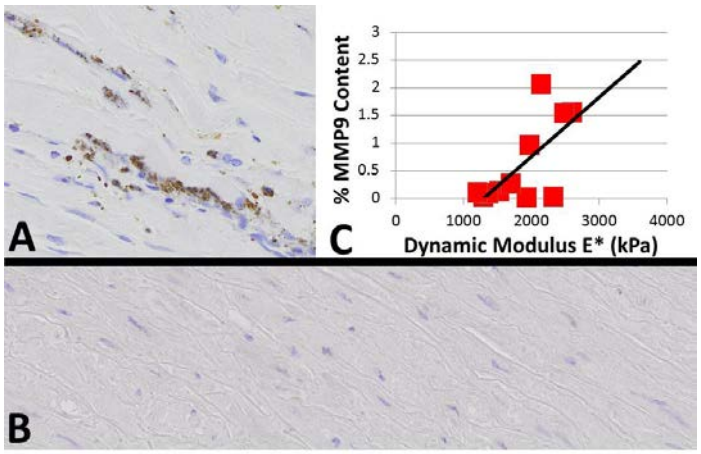

Figure A: Immunohistochemistry staining of MMP9 in AAA tissue (brown inclusions)
Figure B: Immunohistochemistry staining with paucity of MMP9 in non-AAA tissue
Figure C: Positive correlation between dynamic modulus E* and MMP9 content

Disclosures: **D.S. Mix:** None. **S.A. Toth:** None. **I. Bah:** None. **M.C. Stoner:** None. **B.I. Goldman:** None. **M. Buckley:** None. **S.J. Cameron:** None. **M.S. Richards:** None.

106

Receptor Interacting Kinase 1 Contributes to Pathogenesis of Abdominal Aortic Aneurysm by Causing Smooth Muscle Cell Necroptosis as Well as Inflammation

Noel M Phan, Ting Zhou, Qiwei Wang, Kartik Gupta, Conner Feldman, Univ of Wisconsin-Madison, Madison, WI; K. Craig Kent, Ohio State Univ Coll of Med, Columbus, OH; Bo Liu, Univ of Wisconsin-Madison, Madison, WI

Objectives
Abdominal aortic aneurysm (AAA), the progressive weakening and dilatation most commonly occurred in the infrarenal segment of aorta, is a common aortic disease associated with high lethality. Currently, there is no approved pharmacological treatment to effectively slow aneurysm growth or prevent rupture. We have recently demonstrated that inhibition of receptor interacting protein kinase 1 (RIP1), a critical mediator of necroptosis and apoptosis, attenuates aneurysm pathogenesis in a mouse elastase AAA model. Here, we tested whether RIP1 is also required for aneurysm formation in hypercholesterolemia mice stressed with Angiotensin II (AngII).
Methods
Apolipoprotein E-deficient mice were infused with 1000 ng/kg/min of AngII for 28 days. The RIP1 inhibitor Necrostatin-1s (Nec-1s, 1.6 mg/kg/day) was administered via daily intraperitoneal (IP) injection. An aneurysm is defined as aortic expansion in the suprarenal ≥50% over infrarenal diameter.
Results
The incidence of aneurysm formation was significantly lower in Nec-1s treated group compared to the DMSO group (33.35 vs 90.5%). Additionally, Nec-1s reduced aortic expansion (DMSO: 55.40±13.80%, Nec-1s: 121.1±16.44%, p<0.05 unpaired student's *t* test). The number of mice that died prior to 28 days (due to aortic rupture) were comparable between DMSO and Nec-1 groups. Histological analysis showed preserved elastin fibers in aortae from Nec-1s treatment vs DMSO treatment. Immunohistochemical and immunofluorescence staining revealed that Nec-1s decreased the abundance of CD68+ cells as well as CD3+ T-cells but relative higher number of CD206 positive M2 macrophages in the aneurysm prone

aortae. In vitro, Nec-1s attenuated smooth muscle necroptosis but stimulated biosynthesis of elastin. Furthermore, Nec-1s inhibited chemotaxis of monocytes/macrophages.
Conclusions
Our data demonstrate that RIP1 contributes to aneurysm pathophysiology through regulation of cell death and inflammation infiltration. Being a small chemical molecule that is highly selective for RIP1, Necrostatin-1s may serve as a suitable drug treatment for AAAs.

Disclosures: **N.M. Phan:** None. **T. Zhou:** None. **Q. Wang:** None. **K. Gupta:** None. **C. Feldman:** None. **K. Kent:** None. **B. Liu:** None.

107

Increased Peak Wall Stress in Women with Abdominal Aortic Aneurysms

Eric Shang, Cleveland Clinic Fndn, Cleveland, OH; Grace Wang, Ronald Fairman, Benjamin Jackson, Hosp of the Univ of Pennsylvania, Philadelphia, PA

OBJECTIVE: Women with abdominal aortic aneurysms (AAA) exhibit more rapid aneurysm growth and greater rupture risk at equivalent diameters relative to men. Evidence suggests that biomechanical peak wall stress (PWS) derived from finite element analysis of AAAs is a superior predictor of rupture compared to maximum transverse diameter (MTD). This study aimed to investigate differences in the calculated PWS of AAAs between men and women.
METHOD**:** Men (n=35) and women (n=35) with infrarenal AAAs with 45-55mm MTD undergoing CTA were identified. Customized image processing algorithms extracted patient-specific AAA geometries from raw DICOM images. The resulting aortic reconstructions incorporated patient-specific and regionally resolved aortic wall thickness, intraluminal thrombus, and wall calcifications. Aortic models were loaded with 120mmHg blood pressure using commercially available FEA solvers.
RESULTS**:** Peak wall stress was found to be significantly higher in women (299±51 vs 257±53 kPA, P=0.001, see Figure). Neither MTD (50.5±3.1 vs 49.8±2.9 mm, P=0.34), mean aortic wall thickness (2.38±0.52 vs 2.34±0.50 mm, P=0.69), nor wall thickness at location of PWS (2.36±0.60 vs 2.20±0.46 mm, P=0.20) varied by sex. While there were no sex-associated differences in aneurysm volume (86.6±27.0 vs 94.8±25.5 cm^3, P=0.76) or intraluminal thrombus volume (14.2±11.7 vs 16.3±13.4 mm, P=0.33), women's AAAs had significantly increased maximum Gaussian curvature (0.032±0.011 vs 0.025±0.015 mm^{-2}, P=0.03).
CONCLUSION**:** Comparably sized AAAs in women were shown to have significantly higher peak wall stress. Maximum gaussian curvature, a measure of aneurysm morphology, was significantly different between the two groups. These results suggest that men and women possess distinct aneurysm geometries, and that PWS-derived rupture risk prediction may provide a more reliable estimator of rupture risk in all patients.

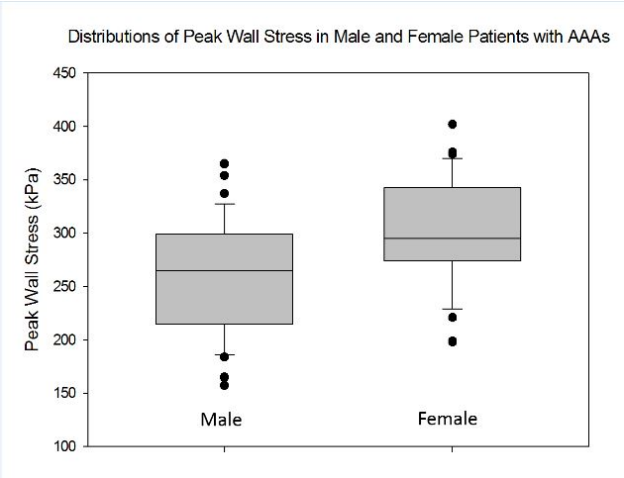

Disclosures: **E. Shang:** None. **G. Wang:** None. **R. Fairman:** None. **B. Jackson:** None.

108

Deletion of Lrp1 In SMCS Differentially Alters Susceptibility of Distinct Vascular Beds to BAPN-Induced Aneurysm and Dissection Formation

Areck A Ucuzian, Ctr for Vascular & Inflammatory Diseases, Dept of Surgery, Univ of Maryland Sch of Med, Baltimore, MD; Selen C Catania, Ctr for Vascular & Inflammatory Diseases, Dept of Physiology, Univ of Maryland Sch of Med, Baltimore, MD; Subhradip Mukhopadhyay, Rajabrata Sarkar, Dudley S Strickland, Ctr for Vascular & Inflammatory Diseases, Dept of Surgery, Univ of Maryland Sch of Med, Baltimore, MD

Lysyl oxidase (LOX) inhibition by β-aminopropionitrile (BAPN) induces aortic aneurysm and dissection (AD). The LDL receptor-related protein 1 (LRP1) is an endocytic receptor that plays a key role in maintaining the structural integrity of vessels. Deletion of LRP1 in vascular smooth muscle cells (smLRP1 -/-) in mice induces fully penetrant and spontaneous aneurysms with aging. The objective of this study was to investigate the role of smLRP1 in modulating the susceptibility of various vascular beds to BAPN-induced AD. Wild-type (WT) and smLRP1 -/- mice were treated with BAPN supplemented in drinking water (3g/L). After 4-16 weeks, the vessels were analyzed histologically and with micro-CT. Abnormal elastic lamellae were identified throughout the vasculature of both the BAPN-treated WT and smLRP1 -/- cohorts. smLRP1 -/- mice were more susceptible to aneurysm formation after 8 (p=0.035) or 16 weeks (p=0.043) of treatment. Aneurysms in BAPN-treated WT mice were localized to the aorta, while aneurysms in BAPN-treated smLRP1 -/- mice were localized to the visceral and iliac arteries (Table). Histologic and radiographic evidence of AD was detected in the ascending and descending thoracic aorta in BAPN and AngII (subcutaneous,1µg/kg/min, 24 hrs)-treated WT mice, but not in BAPN and Ang II-treated smLRP1 -/- mice (Figure). Thoracic ruptures were more prevalent in the BAPN-treated WT group and abdominal ruptures were more prevalent in the BAPN-treated smLRP1 -/-group (p=0.02). In summary, these data demonstrate that genetic deletion of LRP1 in SMCs differentially alters the susceptibility of distinct vascular beds to the development of aneurysm and dissection upon LOX inhibition.

	WT, BAPN	smLRP1 -/-, BAPN	*p-value*
Aortic Aneurysm	5/13 (38%)	0/12 (0%)	*0.016*
Other Aneurysm	0/13 (0%)	11/12 (92%)	*< 0.0001*

Table) Distribution of aneurysm formation in BAPN-treated WT and smLRP1 -/- mice.

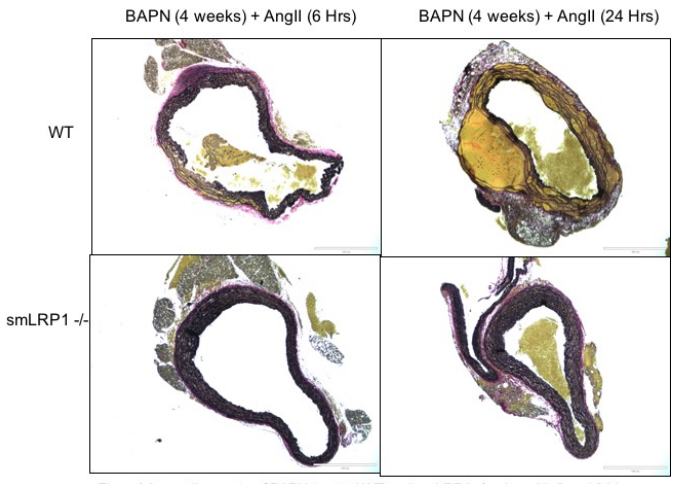

Figure) Ascending aorta of BAPN-treated WT and smLRP1 -/- mice with 6 and 24 hours of AngII treatment. EVG, Mag 10x.

Disclosures: **A.A. Ucuzian:** None. **S.C. Catania:** None. **S. Mukhopadhyay:** None. **R. Sarkar:** None. **D.S. Strickland:** None.

109

Tumor Necrosis Factor Inducible Gene 6 Protein (TSG-6) is Highly Expressed in Human Abdominal Aortic Aneurysms

S. Keisin Wang, Linden Green, Jie Xie, Raghu Motaganahalli, Andres Fajardo, Cliff Babbey, IU Sch of Med, Indianapolis, IN; Robert McCready, St. Francis Hosp, Indianapolis, IN; Michael Murphy, IU Sch of Med, Indianapolis, IN

Objective
The formation of an abdominal aortic aneurysm (AAA) is characterized by a dominance of pro-inflammatory forces that result in smooth muscle cell apoptosis, extra-cellular matrix degradation, and progressive diameter expansion. Additional defects in the anti-inflammatory response may also contribute to AAA progression, however have yet to be characterized robustly. Here, we describe the role of the anti-inflammatory cytokine TSG-6 (TNF-stimulated gene-6) in AAA formation.
Methods
Blood and aortic tissue samples were collected from patients undergoing elective AAA screening and open surgical AAA repair. Aortic specimens collected were preserved for IHC or immediately assayed after tissue homogenization. Cytokine concentrations in tissue and plasma were assayed by ELISA. All immune cell populations were assayed using FACS analysis. *In vitro,* macrophage polarization from monocytes were performed with young, healthy donor PBMCs.
Results
TSG-6 was found to be abnormally elevated in both the plasma and aorta of patients with AAA compared to healthy and risk-factor matched non-AAA donors. We observed the highest tissue concentration of TSG-6 in the less diseased proximal and distal shoulders compared to the central aspect of the aneurysm. IHC localized the majority of TSG-6 to the tunica media with minor expression in the tunica adventitia of the aortic wall. Higher concentrations of both M1 and M2 macrophages where also observed in the aortic wall, however M1/M2 ratios were unchanged from healthy controls. Additionally, we observed no difference in M1/M2 ratios in the peripheral blood of risk-factor matched non-AAA and AAA patients. Interesting, TSG-6 inhibited the polarization of the anti-inflammatory M2 phenotype *in vitro*.
Conclusions
AAA formation results from an imbalance of inflammatory forces causing aortic wall infiltration of mononuclear cells leading to resultant vessel breakdown. From our results, we suggest TSG-6 is elevated in the AAA patient as a compensatory anti-inflammatory feedback mechanism. However, it's effects may be abrogated by defects in CD44, its cognate receptor or downstream signaling pathways, future areas for investigation.

Disclosures: **S. Wang:** None. **L. Green:** None. **J. Xie:** None. **R. Motaganahalli:** None. **A. Fajardo:** None. **C. Babbey:** None. **R. McCready:** None. **M. Murphy:** None.

111

Effect of Thyroxin Treatment on Carotid Intima Media Thickness (CIMT) Reduction in Patients With Subclinical Hypothyroidism (SCH)-A Meta-Analysis of Randomized Clinical Trials

Yugandhar Kandimalla, Ocala Regional Medical Ctr, Ocala, FL; **Muhammad Aziz**, Baptist Health South Florida, Miami, FL; Archana Machavarapu, Ocala Regional Medical Ctr, Ocala, FL; Rehan Malik, Adnan Younus, Baptist Health South Florida, Miami, FL; Aaron Jaffe, Ocala Regional Medical Ctr, Ocala, FL; Rana Jaber, Huwad Choudhry, Samantha Ronderos, Nadia Paz, Emir Veledar, Khurram Nasir, Baptist Health South Florida, Miami, FL

BACKGROUND: Research shows that subclinical hypothyroidism (SCH) is related to increased carotid intima media thickness (CIMT), a surrogate marker of stroke and subclinical cardiovascular disease (CVD). It is controversial whether SCH should be treated or not to reduce risk of stroke and CVD morbidity and mortality. The aim of this meta-analysis was to determine whether SCH is associated with an increase in CIMT as compared to Euthyroidism (EU) and whether thyroxin therapy in SCH can reverse

the change in CIMT.
METHODS: Two independent reviewers did an extensive database search up to December 2016. Total of 12 randomized clinical trials discussed effect of thyroxin treatment on CIMT values at pre-and-post treatment in SCH subjects.
RESULTS: CIMT was significantly higher among SCH (n=280) as compared to EU controls (n=263) at baseline, pooled standardized mean difference (SMD) of CIMT was 0.44 mm [95%CI 0.14, 0.74], SE=0.15; p=0.004 with heterogeneity I^2= 65%. After treatment with thyroxin in SCH subjects (n=314), there was a statistically significant decrease in CIMT from pre-to-post treatment, pooled SMD of CIMT decrease was [SMD -0.32; 95%CI (-0.47, -0.16), SE=0.08; p<0.0001, with heterogeneity I^2= 2%], and was no longer different from EU controls [SMD 0.13 mm; 95% CI (-0.04, 0.30); p= 0.14; I^2 = 27%]. The total cholesterol, triglycerides, and low density lipoprotein were higher in SCH as compared to EU controls and decreased significantly after treatment with thyroxin.
CONCLUSION: This meta-analysis shows that thyroxin therapy in SCH subjects significantly decreases CIMT and improves lipid profile, modifiable risk factors for stroke and CVD. Thyroid hormone replacement in SCH subjects might have a role in slowing down or preventing progression of atherosclerosis.

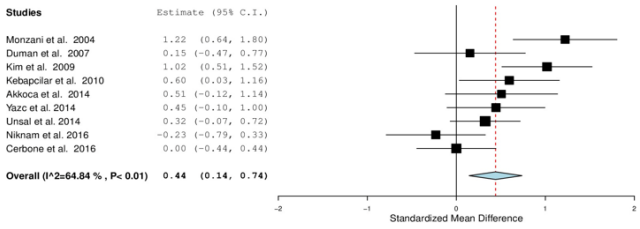

Fig a. SMD with 95% CI of carotid intima–media thickness (CIMT) in SCH and EU at baseline using random effect model.

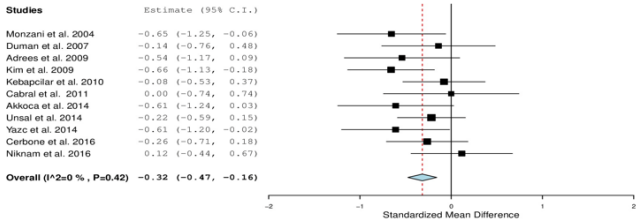

Fig b. SMD with 95% CI of carotid intima–media thickness (CIMT) at pre-to-post thyroxin Rx. in subjects with SCH using fixed effect model.

Disclosures: **Y. Kandimalla:** None. **M. Aziz:** None. **A. Machavarapu:** None. **R. Malik:** None. **A. Younus:** None. **A. Jaffe:** None. **R. Jaber:** None. **H. Choudhry:** None. **S. Ronderos:** None. **N. Paz:** None. **E. Veledar:** None. **K. Nasir:** None.

112

Exploring Sleep Disturbance Among Patients With Symptomatic Peripheral Artery Disease: Results From the Project Voice Pilot Study

Timothy Craven, Donna Keith, Justin Hurie, Gabriela Velazquez-Ramirez, Randolph Geary, Matthew Edwards, Wake Forest Sch of Med, Winston-Salem, NC; Matthew Corriere, Univ of Michigan, Ann Arbor, MI

Background: Sleep disturbance is an important determinant of both mental and physical health-related quality of life (QOL). Associations between sleep disturbance and subclinical cardiovascular disease have been described but little is known about it among patients with symptomatic PAD. We studied sleep disturbance in symptomatic PAD patients using a wearable device for 30 days.
Methods: Patients with claudication confirmed by ABI<0.9 were recruited to participate. Participants received walking exercise instruction, a wearable device to track walking activity and sleep, and an iPad with access to a PAD-specific digital health platform with educational materials and patient surveys.

Participants set personal walking goals, received weekly telephone follow up, and completed quality of life instruments [Walking Impairment Questionnaire (WIQ) and VascuQol-6] at baseline and post-completion. Poisson regression was used to examine associations between number of nights with sleep interruption, patient characteristics and survey responses.
Results: Twenty participants enrolled and completed the study; 35% were female; 30% were African American. Mean age was 69±9 years; mean ABI was 0.69±0.14. Over a mean study period of 34±6 days, sleep data were recorded an average of 28±6 days and walking activity on 12±10 days. Mean nights of interrupted sleep was 1.3±1.8; 8 participants (40%) had sleep interruption at least one night. No associations were observed between daily walking activity or VascuQol-6 scores and sleep disturbance. Increases in sleep disturbance were associated with higher (i.e., more severe) WIQ distance (P=0.02) and stair (P=0.03) scores at baseline, and WIQ distance (P=0.03), speed (P=0.002) and overall (P=0.009) scores at study completion.
Conclusions: These observations suggest that sleep disturbance impacts walking, disability and QOL among people with symptomatic PAD. Further investigation is warranted to characterize sleep disturbance among patients with both claudication and critical limb ischemia, evaluate associations with disease severity, and explore utility as a treatment outcome.

Disclosures: **T. Craven:** None. **D. Keith:** None. **J. Hurie:** None. **G. Velazquez-Ramirez:** None. **R. Geary:** None. **M. Edwards:** None. **M. Corriere:** Research Grant; Significant; Vascular Cures.

113

Glucose Metabolic Disorders in Aging-Associated Microglial NADPH Oxidase 2 Activation and Oxidative Damage of Cerebral Microvasculature and Neurons

Li Geng, Jian-Mei Li, Univ of Reading, Reading, United Kingdom

Aging has been recognised to be a major risk factor for the development of cardiovascular and neurodegenerative diseases and growing evidence suggests a role for oxidative stress. A Nox2-containing NADPH oxidase has been reported to be a major source of reactive oxygen species (ROS) generation in the vascular system and in the brain. However, the role of Nox2 enzyme in aging-related metabolic disorders and vascular neurodegeneration remains unclear. In this study, we used age-matched wild-type (WT) and Nox2-deficient ($Nox2^{-/-}$) mice on a C57BL/6 background at young (3-4 month) and aging (20-24 month) to investigate the role of Nox2 in aging-related oxidative stress, metabolic disorders and cerebral vascular dysfunction. There was an aging-related increase in blood pressure in WT mice (126 mmHg for young and 148 mmHg for aging) ($P<0.05$); however the blood pressure was well maintained without significant change in $Nox2^{-/-}$ aging mice. Compared to young WT mice, WT aging mice had significantly high levels of fasting serum insulin and this was accompanied with delayed clearance of glucose ($P<0.05$) indicating insulin resistance. In contrast, there was no indication of insulin resistance for $Nox2^{-/-}$ aging mice. We then examined aging-related brain oxidative stress. Compared to WT young mice, there were significant increases (2.7±0.7 folds) in the levels of ROS production by WT aging brain tissue homogenates as detected by lucigenin-chemiluminescence and DHE fluorescence. Increased ROS production in WT aging brain was accompanied by a significant increase (1.8±0.3 folds) in the Nox2 expression detected mainly in the microglial cells (labelled by Iba-1) and decreases in brain capillaries (labelled by CD31) (2.4±0.8 folds) and neurons (labelled by Neu-N) (2.9±0.5 folds) (all $P<0.05$). Knockout of Nox2 abolished aging-associated increases in brain ROS production and significantly reduced the aging-related pathophysiological changes in the brain. In conclusion, aging-associated metabolic disorders play a crucial role in aging-associated Nox2 activation and vascular neurodegeneration. Nox2-containing NADPH oxidase represents a valuable therapeutic target for oxidative stress-related brain microvascular damage and neurodegeneration.

Disclosures: **L. Geng:** None. **J. Li:** None.

114

Calf Muscle Oxygen Saturation During Standardized Treadmill Testing in Patients with Intermittent Claudication

Hernan Hernandez, Univ of Nebraska Medical Ctr, Omaha, NE; Molly Schieber, Univ of Nebraska Omaha, Omaha, NE; Holly K DeSpiegelaere, Veterans' Affairs Nebraska-Western Iowa Healthcare Systems, Omaha, NE; Katyarina E Brunette, Kyung-Soo Kim, Constance Mietus, Univ of Nebraska Medical Ctr, Omaha, NE; Sarah Baker, Sara Myers, Univ of Nebraska Omaha, Omaha, NE; George P Casale, Iraklis Pipinos, Univ of Nebraska Medical Ctr, Omaha, NE

Objectives: Leg muscle hypoxia during walking is believed to be a key mechanism underlying the exercise intolerance of claudicating patients but detailed data on the changes exercise produces in the kinetics of leg muscle oxygenation are limited. Our objective was to record the calf muscle oxygen saturation (MO_2S) at rest, during treadmill exercise and during recovery from exercise in patients with chronic claudication.
Methods: We recruited 19 claudicating patients. The MO_2S of the gastrocnemius was recorded with the Moxy near-infrared spectroscopy monitor (Hutchinson, MN). We measured resting MO_2S for a period of three minutes and then performed a Gardner, standardized treadmill test. We recorded claudication onset time (COT) and peak walking time. We also measured the MO_2S recovery for 30 minutes following the end of the TT or until muscle saturation reached a steady state.
Results: Table I summarizes our results. Patients started experiencing a decrease in their MO_2S 18.8 sec after initiation of TT; approximately 28 steps covering 16.8 meters. COT occurred when calf MO_2S had dropped to 23.7%. Patients reached their minimum (14.1%) MO_2S, 340.5 sec into the TT. During the post-TT recovery period, MO_2S rebounded initially to 65.1% at 689.4 sec and 407.1 sec later it declined to a steady-state level of 56.3%, both above the pre-TT baseline reading. This relative hyperoxic state persisted for the duration of the post-exercise recording period ($\geq$30 min).
Conclusions: Our study objectively demonstrates considerable, walking-induced changes in MO_2S in patients with claudication. During walking, MO_2S drops quickly and the calf muscles experience substantial hypoxia while after the end of walking, MO_2S rebounds above the baseline state and the leg muscles remain relatively hyperoxic beyond 30 min. This study provides much needed data concerning the kinetic patterns of muscle oxygenation claudicating patients experience in their everyday lives.

Table I.

Parameter	Mean +/- Standard Error
Resting muscle oxygen saturation	43.7% +/- 2.4%
Time to muscle oxygen saturation drop below resting level during treadmill test	18.8s +/- 4.0s
Minimum muscle oxygen saturation during standardized treadmill test	14.1% +/- 2.6%
Time to minimum saturation during treadmill test	340.5s +/- 68.8s
Claudication onset time	220.9s +/- 31.8s
Muscle oxygen saturation at claudication onset time	23.7% +/- 4.0%
Peak walking time	530.4s +/- 65.7s
Muscle oxygen saturation at peak walking time	23.1% +/- 3.8%
Maximum muscle oxygen saturation during post-treadmill recovery	65.1% +/- 4.0%
Time to maximum muscle saturation after exercise stopped	689.4s +/- 125.2s
Muscle oxygen saturation during the steady state period ($\geq$30 minutes) of post-treadmill recovery	56.3% +/- 3.8%
Time between post-treadmill recovery maximum and steady state saturations	407.1s +/- 109.7s

Disclosures: **H. Hernandez:** None. **M. Schieber:** None. **H.K. DeSpiegelaere:** None. **K.E. Brunette:** None. **K. Kim:** None. **C. Mietus:** None. **S. Baker:** None. **S. Myers:** None. **G.P. Casale:** None. **I. Pipinos:** None.

115

Microvascular Response to Ramipril in Peripheral Artery Disease

Constance J Mietus, Peter Karvelis, Timothy Lackner, Hernan Hernandez, Univ of Nebraska Medical Ctr, Omaha, NE; Holly DeSpiegelaere, VA Nebraska-Western Iowa Healthcare System, Omaha, NE; Feng Xie, Thomas Porter, Iraklis Pipinos, George P Casale, Univ of Nebraska Medical Ctr, Omaha, NE

Background: The myopathy of Peripheral Artery Disease (PAD), a consequence of ischemia caused by atherosclerotic plaques in arteries supplying the legs, is characterized by myofiber degeneration and fibrosis of the vascular walls and extramyofiber matrix. In association with fibrosis we have found a robust expression of the profibrotic cytokine TGFβ1 in vascular smooth muscle cells. Additionally, we have observed microvascular endothelial "swelling" in PAD muscle. Published data indicate that inhibitors of the angiotensin system reduce fibrosis in multiple organ systems and improve walking performance, in diverse patient populations. We hypothesize that "swelling" of microvasculature endothelial cells represents abnormal accumulation of basement membrane Collagen Type IV (Col-IV) and that treatment with Ramipril will improve the microvasculature. **Methods and Results:** Gastrocnemius biopsies of PAD patients at Fontaine Stage II (N=5) before and after six months of Ramipril intervention and control patients (N=4) were labeled with an antibody specific for Col-IV. Images were acquired with an automated wide-field microscope and then processed with Image Pro Plus® and AutoQuant® deconvolution software. We used Col IV label to measure wall thickness and lumen diameter of 230 to 360 microvessels per patient, with a custom MatLab program based on the Expectation Maximization algorithm coupled with a Gaussian Mixture Model. Microvessel wall thickness was significantly greater ($p < 0.04$) in PAD patients before (1.54 ± 0.04 μ) and after (1.61 ± 0.06 μ) Ramipril treatment compared to control (1.42 ± 0.02). Lumen diameter was significantly greater ($p < 0.02$) in Post-Ramipril (3.49 ± 0.04 μ) compared to Pre-Ramipril (3.18 ± 0.08 μ) and control (3.00 ± 0.11 μ) patients. **Conclusions**: The increase of microvessel lumen diameter with Ramipril treatment is expected to increase microvascular perfusion and thereby improve walking distance. Our study will be expanded to increase cohort size and evaluate the association of microvascular measurements with microperfusion determined by Contrast Enhanced Ultrasonography and with walking performance.

Disclosures: **C.J. Mietus:** None. **P. Karvelis:** None. **T. Lackner:** None. **H. Hernandez:** None. **H. DeSpiegelaere:** None. **F. Xie:** None. **T. Porter:** None. **I. Pipinos:** None. **G.P. Casale:** None.

116

Oral Administration of Resolvin D1 Attenuates Early Inflammation Following Vascular Injury in a Rat Carotid Angioplasty Model

Giorgio Mottola, Evan Werlin, Bian Wu, Mian Chen, Anuran Chatterjee, Melinda Schaller, Michael S Conte, UCSF, San Francisco, CA

Introduction. Inflammation ensuing from vascular injury promotes intimal hyperplasia (IH) and restenosis. Resolvin D1 (RvD1) is a specialized pro-resolving lipid mediator derived from docosahexaenoic acid that attenuates IH *in vivo* when delivered locally to the vessel wall in animal models. We tested the hypothesis that RvD1 *per os* in a peri-procedural regimen could blunt the local response to an arterial injury.
Methods. Carotid angioplasty was performed on Sprague-Dawley rats (n=46) fed with either RvD1 (0.5μg/Kg) or vehicle through oral gavage bid, starting from the day before the injury until POD3 when arteries were harvested. To study the pharmacokinetics and bioactivity of oral RvD1, rats underwent blood draws after one dose. RvD1 was measured in plasma via EIA after solid phase extraction, while whole blood was tested in a phagocytosis assay (fluorescently labeled *E. Coli*) using flow cytometry and cAMP levels in the thoracic aorta were measured by ELISA. Carotids were harvested for frozen sections (stained using an anti-CD45, an anti-Myeloperoxidase (MPO), an anti-Ki67 Ab or dihydroethidium (DHE)) and mRNA (analyzed via RT-PCR).
Results. RvD1 plasma concentration peaked (1.18nM) 3h after oral gavage (n=3) at which point we concurrently observed an increase in circulating monocyte phagocytosis and cAMP within the aorta in RvD1-treated rats vs. vehicle (n=3-4). Oral RvD1 modulated local arterial inflammation by reducing

CD45+, MPO+ (Fig. 1A) Ki67+ cells, and DHE staining intensity (n=5). Oral RvD1 also reduced expression of multiple pro-inflammatory genes within the injured vessels (Fig. 1B; n=12-16). Conclusion. RvD1 increases in rat plasma after oral gavage and acts on circulating monocyte phagocytosis and aortic cAMP levels. At the vascular injury site, oral RvD1 attenuated leukocyte recruitment, ROS production, cell proliferation and pro-inflammatory gene expression. Ongoing studies seek to address subsequent effects on IH and remodeling.

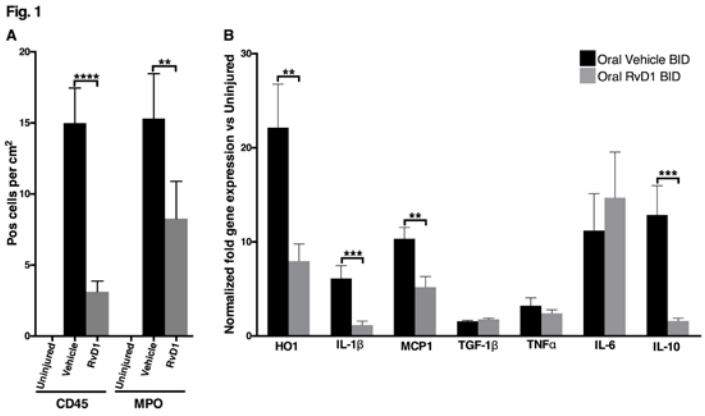

Disclosures: **G. Mottola:** None. **E. Werlin:** None. **B. Wu:** None. **M. Chen:** None. **A. Chatterjee:** None. **M. Schaller:** None. **M.S. Conte:** Research Grant; Significant; Grant from Metagenics in related area of research.

This research has received full or partial funding support from the American Heart Association.

117

Statin Use Improves Limb Salvage After Intervention for Peripheral Arterial Disease

Gaurav Parmar, Zdenek Novak, Benjamin J Pearce, Mark A Patterson, Emily Spangler, Marc A Passman, Adam W Beck, Univ of Alabama at Birmingham, Birmingham, AL

Background: Statin use is recommended in patients with peripheral arterial disease (PAD) due to its morbidity and mortality benefits. However, the effect of statins on limb salvage in PAD is unclear. We examined the effect of statins on survival and limb salvage among PAD patients undergoing surgical or endovascular intervention. **Methods:** PAD patients were identified who underwent intervention between 2009 and 2010. Information was collected from electronic medical records and the Social Security Death Index. Univariate analysis was used to determine predictors of ongoing statin use. Survival and freedom from amputation were determined using KM plots and adjusted hazard ratios by Cox regression. **Results:** A total of 488 PAD patients underwent surgical (n=297) or endovascular (n=191) intervention. 39% were African-American, 44% were female, 41% received statins, 56% received antiplatelet medications, 26% received oral anticoagulants, 9% required a major amputation, and 11% died during follow-up of up to 88 months. Statin users were more often male (p=0.03), caucasian (p=0.03), smokers (p<0.01), and had higher comorbidities such as CAD (p<0.01), hypertension (p<0.01), and diabetes (p<0.01). Antiplatelet use was not associated with amputations (p=0.13), but did lower mortality (p<0.01). Dual antiplatelet therapy did not show any benefit over monotherapy for mortality (p=0.3) or amputations (p=0.4). Statin use was associated with lower mortality (p=0.04), and improved limb salvage (hazard ratio, 0.3; 95% confidence interval, 0.2-0.6) after adjusting for severity of disease as well as antiplatelet and anticoagulation use. **Conclusion:** Statin use in PAD patients with interventions was associated with improved limb-salvage and survival. Despite existing guidelines, statin therapy was disappointingly low in our PAD population, and efforts will be made to increase use across our health system.

Figure: Effects of statin and antiplatelets on overall survival and limb salvage.

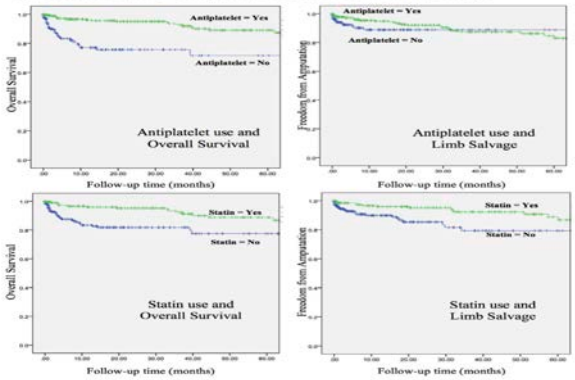

Disclosures: **G. Parmar:** None. **Z. Novak:** None. **B.J. Pearce:** None. **M.A. Patterson:** None. **E. Spangler:** None. **M.A. Passman:** None. **A.W. Beck:** None.

118

Angina Patients Improve Physical Fitness in 18 Days

Francisco E Ramirez, Neil Nedley, Nedley Clinic, Weimar, CA; Albert Sanchez, Weimar Inst, Weimar, CA

Background Angina patients can have difficulty with physical activity. It is known that physical exercise could be beneficial for patients suffering from angina. We document the effect that lifestyle interventions have on metabolic equivalents (MetS). MetS is related to oxygen consumed at rest, higher MetS indicates better physical fitness.
Methods A medical residential program took place in the Sierra Mountains in Placer County in California. Patients were referred by their physician or came by themselves to the not for profit program. The program included plant-based meals, stress management, spiritual help, chaplaincy, psychological, physical and medical therapies. Every patient was evaluated by a board certified physician who also conducted a stress test on participants. The stress test was done before and after the program. The Bruce protocol was followed for the stress test, the test gave the initial and final MetS measurements. Patients were monitored daily and every patient did some level of physical exercise according their physical condition. For females 60+ years old a MetS of 5 or less are considered very poor fitness while a MetS of 9 is considered good. For males 60+ MetS of 6 are considered very poor while a MetS of 10 is considered good.
Results From 12 years of data 2030 patients participated of the program, from those, n=82 had the diagnosis of angina and they also had a before and after stress test results. Those 82, 50% were females, 47.5% were Caucasian, 20.7% Black and 19.5% Hispanic. Average age for males was 62.2, SD 10.4 and mean age for females was 65.6, SD 11.8. For the females baseline MetS were mean 6.1, SD 2.3, median 6, mode 6, min 2, max 11. End MetS were 7.2, SD 2.6, median 7, mode 5, min 3, max 13. T-test reported significant change t(40)=-6.4, p<.001**.** For the males baseline MetS were mean 7.5, SD 2.6, median 7, mode 7, min 2.5, max 12. End MetS were mean 8.9, SD 2.7, median 9, mode 7, min 4.5, max 15.2. T-test indicates significant change t(40)=-4.9, p<.001. Many patients reported less angina events during the program.
ConclusionThe increase in MetS is a clear indication that the fitness level of these patients improved. The end MetS of this group is related to better prognosis since an increase of MetS means better exercise capacity and may decrease mortality.

Disclosures: **F.E. Ramirez:** None. **N. Nedley:** Ownership Interest; Modest; Nedley Health Solutions. **A. Sanchez:** None.

119

Protective Effects of Chloroquine on Ischemic and Nutrient Depleted Muscle are Mediated by HMGB1 and Caspase-1

Ulka Sachdev, Xiangdong Cui, Qian Sun, Edith Tzeng, Alex Chen, Melanie Scott, Univ of Pittsburgh Medical Ctr, Pittsburgh, PA

Introduction: Millions of Americans are at risk for amputation from severe peripheral arterial disease (PAD) when surgery is not possible. Pro-regenerative and angiogenic agents may improve outcome in that setting. Chloroquine (CQ) promotes wound healing in scleroderma but has not been tested in PAD. CQ promotes healing of ischemic muscle, increases muscle high mobility group box 1 (HMGB1), an inflammatory, pro-angiogenic protein, and activates caspase-1 in myoblasts. We hypothesize that HMGB1 mediates protective effects of CQ and is regulated by caspase-1 in muscle. Controlled rather than indiscriminate release of HMGB1 from damaged muscle may be protective during ischemia.
Methods: C2C12 myoblasts in low serum were treated with CQ (0-50μM) ± Ac-YVAD-cmk (10 μg/ml), a caspase-1 inhibitor. HMGB1 release in supernatants was measured using ELISA. Cytotoxicity was assessed by comparing spontaneous lactate dehydrogenase (LDH) activity in culture media from control, treated and maximally lysed cells. CQ (50μg/ml) or placebo treated wild-type and inducible HMGB1 knockout (iHMGB1KO) mice underwent unilateral femoral artery ligation (FAL). Laser Doppler perfusion imaging (LDPI) before and 1,7,14 and 21d after FAL was reported as % improvement over time. ANOVA was used to assess statistical significance among groups.
Results: CQ (5-10uM) attenuated spontaneous LDH leak after 12h from serum-depleted myoblasts ($p < 0.01$, N=3), and modestly increased HMGB1 release ($p < 0.001$, N=3). Ac-YVAD-cmk reversed the cytoprotective effects of CQ, significantly raising both LDH activity to 55% of maximal activity and HMGB1 in the supernatant. Compared to d1 post FAL, CQ improved perfusion recovery in WT mice by 300-800% over 21 days ($p<0.03$, N=7/group), but not in iHMGB1KO mice.
Conclusion: We present the novel finding that in nutrient-depleted myoblasts, caspase-1 mediates the survival benefits of CQ and regulates HMGB1 release. In turn, HMGB1 is critical for CQ's beneficial effects on perfusion after FAL, another stress condition. Regulated HMGB1 release may be immunomodulatory, regenerative and modifiable with drugs like CQ. Altering survival and inflammatory pathways through CQ may present a novel therapeutic strategy in PAD.

Disclosures: **U. Sachdev:** Research Grant; Modest; K08HLI03899 (NHLBI). **X. Cui:** None. **Q. Sun:** None. **E. Tzeng:** None. **A. Chen:** None. **M. Scott:** None.

121

Role of Oxidative State in Endothelial Cells During Arteriogenesis

Bandana Shrestha, Christopher B. Pattillo, Louisiana Health Science Ctr -Shreveport, Shreveport, LA

Peripheral vascular disease (PVD), a common cardiovascular disease causes reduced blood flow to the limbs, ischemia related complications and in severe cases amputations. Atherosclerotic plaque formations result in ischemia from gradual occlusion of blood vessels followed by shunting of blood through collateral arteries increasing their arteriolar size for perfusion compensation (arteriogenesis). This change in shear flow and friction in the surrounding arteries and vasodilation affects the underlying blood vessels thereby activating signaling pathways including VEGFR2, NO and NF-κB, increased inflammation and remodeling of endothelial and smooth muscle cells. However, this important compensatory mechanism is affected adversely due to increased oxidative stress which leads to defective arteriogeneis and worsened PVD complications. Typically, antioxidants such as glutathione (GSH) regulates the oxidative stress within cells by reducing Reactive Oxygen Species (ROS) while being oxidized into glutathione disulfide (GSSG), hence maintaining an optimum GSH:GSSG ratio. Our experiments with arterial ligation models using transgenic mice with modified Gclm (modulatory subunit of an enzyme for GSH synthesis) showing Gclm-/- (KO) mice having severely diminished GSH levels (~80%), Gclm +/- (HET) mice having slightly decreased (~20%) and wild type mice with highest levels of GSH implicate a delicately balanced ratio (as seen with Gclm+/- mice) to increased blood flow and reperfusion, an important regulation during arteriogenesis. Additionally, GSH:GSSG levels can lead to post translational modification such as cysteine glutathionylation which is known to protect cysteine residues from oxidation as well as regulate the function of various proteins. Our studies in Human Aorta Endothelial cells (HAECs) have implicated a relationship between varying GSH:GSSG ratios, resulting glutathionylation and VEGFR2 phosphorylation, an important player in arteriogenesis. Hence, a critical balance between

the reductive and oxidative cellular environments drives optimal VEGFR2 signaling to mediate arteriogenic remodeling due to increased shear and oxidant stress.

Disclosures: **B. Shrestha:** None. **C.B. Pattillo:** None.

This research has received full or partial funding support from the American Heart Association.

122

Supervised Exercise Therapy for Claudication Modulates Global Profiles of Plasma Lipid Mediators

Aeron Small, Univ of Pennsylvania, Philadelphia, PA; Kamil Borokowski, Univ of California, Davis, CA; Sarah Ratcliffe, Erin Englund, Zoltan Arany, Univ of Pennsylvania, Philadelphia, PA; John Newman, Univ of California, Davis, CA; Thomas Floyd, Stony Brook Univ, New York, NY; Emile Mohler, Scott Damrauer, Univ of Pennsylvania, Philadelphia, PA

Background: Lipid mediators are complex molecules that demonstrate an association to inflammatory states including atherosclerotic vascular disease. Peripheral artery disease (PAD) is an atherosclerotic disease of the distal aorta and lower extremity arteries. Supervised walking therapy (SWT) is the mainstay of treatment for PAD and is hypothesized to improve claudication by suppressing inflammatory activation. **Objectives**: We sought to examine how lipid mediators were impacted by treadmill testing in PAD, and to identify lipid mediators that were altered by SWT. **Methods:** Plasma samples were collected before and after Gardner treadmill testing (GTT) in individuals with PAD; participants underwent 12 weeks of SWT and were retested. Lipid mediators were isolated using Ostro Sample Preparation Plates (Waters; Milford, MA) and quantified by UPLC-MS/MS. **Results**: Thirty-six participants had complete sets of plasma for analysis. The median age was 67 years (IQR: 62 - 71); there were 55 men (73%) and the median ABI was 0.64 (IQR: 0.55 - 0.76). The median peak walking time prior to SWT was 7.4 min (IQR: 4.8 - 10.3 min), which increased to 11.9 min (IQR: 8.4 - 17.1) after SWT ($p < 10^{-4}$). Discriminant analysis showed clear separation of pre- and post- GTT and pre- and post- SWT samples based on global lipid profiles (Figure 1). Cluster analysis demonstrated 13 distinct clusters of lipid mediators; those clusters containing carbon and arachidonic acid epoxides, and vicinal diols were significantly (FDR <5%) impacted by the interaction between SWT and GTT. **Conclusions**: Lipid mediator profiles manifested unique response patterns to treadmill testing and were modified by supervised walking therapy. These data suggest that lipid mediators play an active role in the biology underlying improvements in lower extremity symptoms associated with SWT and may offer a novel target for therapeutic manipulation.

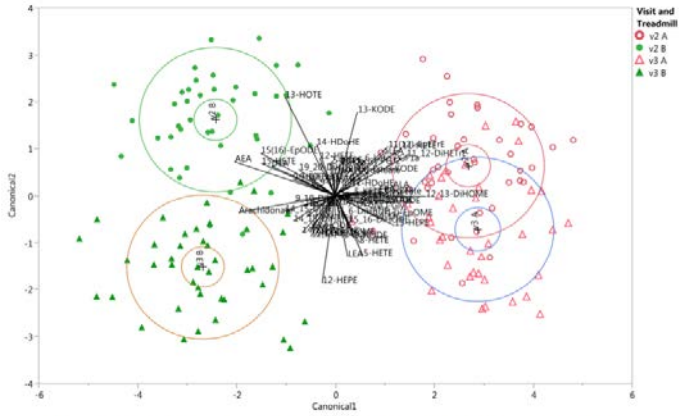

Figure 1: Discriminant analysis of the subject range scaled data. Data were Log transformed prior to the scaling. Legend: circles – pre-walking therapy; triangles – post-walking therapy; red – post-treadmill; green – pre-treadmill.

Disclosures: **A. Small:** None. **K. Borokowski:** None. **S. Ratcliffe:** None. **E. Englund:** None. **Z. Arany:** None. **J. Newman:** None. **T. Floyd:** None. **E. Mohler:** None. **S. Damrauer:** None.

123

Perivascular Adiponectin Attenuates the Neointimal Response Potentially via Modulation of Hydrogen Sulfide

Kaspar Trocha, Ming Tao, Brigham & Women's Hosp, Boston, MA; Michael Macarthur, Harvard Sch of Public Health, Boston, MA; Alban Longchamp, Brigham & Women's Hosp, Boston, MA; Humberto Trevino, Harvard Sch of Public Health, Boston, MA; Margreet R. de Vries, Dept of Surgery, Leiden Univ Medical Ctr, Leiden, Netherlands; James Mitchell, Harvard Sch of Public Health, Boston, MA; C. Keith Ozaki, Brigham & Women's Hosp, Boston, MA

Objective: Intimal hyperplasia (IH) limits the durability of vascular interventions. Perivascular adipose serves as scaffolding for vessels and also as a source of adipokines, including adiponectin (APN). The globular domain of adiponectin (gAPN) has high affinity for endothelial AdipoR1 receptors and holds beneficial roles in vascular adaptations. Hydrogen sulfide (H_2S) is a vasculo-protective gasotransmitter produced by cystathionine γ-lyase (CGL), and low circulating H_2S levels associate with human vascular disease. We therefore hypothesized that APN knockout (KO) mice would be predisposed to IH, and that local administration of gAPN would protect APN KO mice from IH. Furthermore, we evaluated potential links between APN and H_2S in these effects. **Approach and Results:** Wildtype (WT, n=7) and APN KO (n=8) mice maintained on high fat diet were subject to carotid focal stenosis. An additional group of APN KO mice (n=7) were treated by local injection of gAPN suspended in Matrigel. Carotids were harvested 28 days following surgery and analyzed 400-2800μm proximal to the stenosis microscopically. IH area was significantly increased at 400μm in APN KO mice compared to WT (p=<0.05, Fig. A), while gAPN significantly attenuated intimal area compared to untreated KO mice (p=<0.05, Fig. B). This finding was coupled with significant (p=<0.05, Fig. C) decrease in pre-operative baseline serum H_2S production capacity in APN KO (lead acetate assay) compared to WT. Serum collected upon harvest trended toward increased H_2S production capacity in APN KO mice treated with gAPN (Fig. D). Kidney CGL expression (Western) revealed a trend for increased in CGL expression in the gAPN group (Fig. E). **Conclusion:** In a focal stenosis model APN KO mice demonstrated increased distal IH; when administered locally, gAPN significantly attenuated IH. These data also uncover a reduction in H_2S production capacity in APN KO mice, providing a novel potential link between these potent vasomediators.

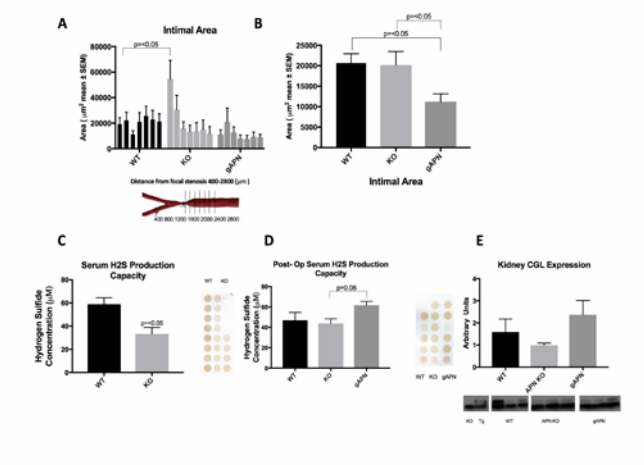

Disclosures: **K. Trocha:** None. **M. Tao:** None. **M. Macarthur:** None. **A. Longchamp:** None. **H. Trevino:** None. **M. R. de Vries:** None. **J. Mitchell:** None. **C. Ozaki:** None.

This research has received full or partial funding support from the American Heart Association.

124 will be presented in the PVD Moderated eAbstract Poster Session. The abstract content is located on page 38.

125

Association Between Abo Blood Group, Von Willebrand Factor and Factor VIII in Patients Undergoing Vascular Surgery

Francisco Ujueta, Michael A Nardi, Yu Guo, Adriana Perez, Maya Rubin, Mark Adelman, Caron B Rockman, Jeffrey S Berger, New York Langone Medical Ctr, New York, NY

Background: ABO blood groups have been associated with functional effects on factor VIII (FVIII), von Willebrand factor (vWF) and incident atherothrombosis. This study sought to examine the association between ABO blood type, FVIII and vWF in patients undergoing vascular surgery. **Method:** This is a retrospective analysis of data from a cohort of 181 patients undergoing elective vascular surgery. ABO blood type, FVIII and vWF was measured before surgery. The primary end point was the occurrence of MACE (defined as myocardial necrosis, myocardial infarction, stroke or death) within 30-days after surgery. Multivariable logistic regression modeling was used to estimate odds of MACE. **Results**: The mean age was 71.6 ± 9.8 and 29% were female. Non-O blood type was present in 105 patients (70 A, 27 B, 8 AB) and type O in 76 patients. Non-O had higher FVIII (128.2 ± 44.7 vs 112.4 ± 42.4, P<0.001) and vWF (176.0 ± 54.0 vs 133.2 ± 41.0, P<0.001) than type O. Thirty day MACE occurred in 38 (21.0%) patients; 25% in non-O and 15.8% in type O (P=0.13). After adjustment for age, sex, race, prior coronary artery disease and heart failure, patients with non-O blood type (vs. O) had a higher incidence of 30-day MACE (odds ratio 2.1, 95% CI 0.9 to 5.1, P=0.08) although statistical significance was not reached. There was no significant association between FVIII and vWF and 30-day MACE. **Conclusions**: Non-O blood type was associated with higher levels of FVIII and vWF and a trend towards increased 30-day MACE in patients undergoing vascular surgery. Larger studies across of ABO blood groups and perioperative events in different types of surgeries are warranted.

Disclosures: **F. Ujueta:** None. **M.A. Nardi:** None. **Y. Guo:** None. **A. Perez:** None. **M. Rubin:** None. **M. Adelman:** None. **C.B. Rockman:** None. **J.S. Berger:** None.

126

Diabetes Influences Circulating FAS in Patients with Carotid Artery Stenosis

Mohamed A Zayed, Malik Darwish, Uzma Naim, Luis A Sanchez, Clay F Semenkovich, Washington Univ Sch M, Saint Louis, MO

Plasma lipid abnormalities associated with diabetes are thought to contribute to atherogenesis and overall cardiovascular morbidity. Fatty Acid Synthase (FAS), an essential multiunit enzyme that catalyzes the synthesis of long-chain fatty acids from acetyl-CoA and malonyl-CoA, was recently found to circulate in the plasma (pFAS). Since FAS is essential for the lipogenic functions of the liver and adipose tissue, and its tissue expression is altered in the setting of diabetes, we sought to evaluate whether pFAS is a biomarker for arterial occlusive disease in diabetic patients. To test this hypothesis, we compared the activity of pFAS in the fasting serum in a relatively homogenous group of 15 diabetic (DM) and 15 non-diabetic (NDM) patients who are undergoing carotid endarterectomy (CEA). We also evaluated pFAS in 15 additional control patients who have no evidence of arterial occlusive disease. Among selected patients, DM patients were more likely to have hypertension and receive metformin compared to NDM patients (P<0.05). Control patients who have no evidence of arterial occlusive disease were all <60 years old, and none had cardiovascular morbidities. DM patients undergoing CEA demonstrated a 39% increase in pFAS activity compared to NDM patients undergoing CEA (P=0.04), and a 91% increase compared to control patients (P<0.001). Similarly, on Western blot analysis DM patients demonstrated an average 27% increase compared to control patients (P=0.4). pFAS did not correlate with fasting plasma glucose, LDL, HDL, or total cholesterol, but demonstrated a modest correlation with fasting plasma triglycerides (R^2=0.4, P=0.03). These findings suggest pFAS activity is altered in DM patients with carotid artery stenosis, and correlates with specific plasma lipid profiles suggestive of overall cardiovascular morbidity.

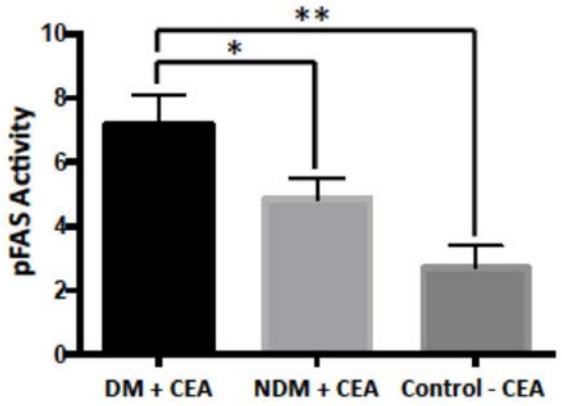

Disclosures: **M.A. Zayed:** None. **M. Darwish:** None. **U. Naim:** None. **L.A. Sanchez:** None. **C.F. Semenkovich:** None.

127

Colchicine Attenuates Vein Wall Scarring in Murine Venous Thrombosis: Implications for Limiting the Post-Thrombotic Syndrome

Guanming Qi, **Chase W. Kessinger**, Adam Mauskapf, Harkamal S. Jhajj, Massachusetts General Hosp, boston, MA; Peter Henke, Univ of Michigan, Ann Arbor, MI; Farouc A. Jaffer, Massachusetts General Hosp, boston, MA

Objective In this study, we investigated the effects of colchicine on vein wall inflammation and scarring, and thrombus burden/VT resolution, key drivers of the PTS. **Methods** Inferior vena cava (IVC) stasis VT were created in C57BL/6 mice (n=60). Colchicine (0.2 or 0.02 mg/kg for high or low dose, respectively) was administered daily via intraperitoneal injection starting 24 hours after VT initiation. At VT timepoints of day 4, 8 and 14, mice were sacrificed and VT were resected for measurements of thrombus. Picrosirius-red staining of VT sections assessed vein wall thickness. Serial sections were processed for Carstairs fibrin staining and immunostaining. The number of vein wall fibroblasts and macrophages per 5 high-power fields (400×) were calculated. **Results** Colchicine significantly decreased venous thrombus-induced vein wall scarring at Day 8 (PBS 71.53±6.97μm, Col lo 55.11±5.48μm, Col hi 46.84±2.03μm; n=5 per group; PBS vs Col lo, $P < 0.01$; Col lo vs Col hi, $P < 0.05$) and at Day 14 (PBS 55.29±8.97μm, Col lo 45.20±2.73μm, Col hi 42.68±3.57μm; n=4-7 per group; PBS vs Col lo, $P < 0.05$; PBS vs Col hi, $P < 0.05$; Col lo vs Col hi, $P > 0.05$). Colchicine reduced the number of vein wall F4/80+ macrophages (PBS vs Col hi, 73.33±8.63 vs 55.87±8.07, n=5 per group, $P < 0.01$) and FSP1+ cells (PBS vs Col hi, 73.80±8.01 vs 41.60±8.37, n=5 per group, $P < 0.01$) in DVT D8. Also, colchicine reduced RNA expression of both profibrotic (collagen I, collagen III, procollagen I, procollagen III, FSP1) and proinflammatory (IL-1β, CD68) markers in DVT D8 (n=8 per group, $P < 0.05$). Of note, despite possessing anti-inflammatory actions, colchicine did not impair VT resolution (measured by thrombus mass) at D4 PBS vs Col hi, 27.00±5.11 vs 23.47±6.03mg/cm, n=9-12 per group, $P > 0.05$) nor at D8 (PBS vs Col hi, 19.05±5.23 vs 15.58±6.52mg/cm, n=12 per group, $P > 0.05$). **Conclusion** The FDA-approved agent colchicine reduces experimental VT-induced vein wall scarring without impairing thrombus resolution. Anti-scarring effects may be related to attenuated inflammation of fibrotic mediators in the vein wall and adherent thrombus. Colchicine may offer a clinically viable option to reduce the post-thrombotic syndrome induced by deep vein thrombosis.

Disclosures: **G. Qi:** None. **C.W. Kessinger:** None. **A. Mauskapf:** None. **H.S. Jhajj:** None. **P. Henke:** None. **F.A. Jaffer:** None.

This research has received full or partial funding support from the American Heart Association.

128

LRP1 Deletion in Smooth Muscle Cells of the Outer Aortic Media Promotes Angiotensin II-induced Thoracic Aortic Aneurysm

Hisashi Sawada, Debra L Rateri, Univ of Kentucky, Lexington, KY; Mark W Majesky, Univ of Washington Sch of Med, Seattle, WA; Alan Daugherty, Univ of Kentucky, Lexington, KY

Objective: Low-density lipoprotein receptor-related protein 1 (LRP1) is a multifunctional protein that is linked to several vascular pathologies. LRP1 deletion in smooth muscle cells (SMCs) accelerates angiotensin II (AngII)-induced thoracic aortic aneurysm (TAA). In association with TAA formation, there is medial thickening that is characterized by a transmural gradient in which pathology progressively increases from lumen to adventitial aspect. We hypothesized that deletion of LRP1 in the outer medial layers of the proximal thoracic aorta has a pivotal role in the pathogenesis of TAA. The aim of this study was to determine whether LRP1 deletion in the outer media accelerates AngII-induced TAA formation.
Methods and Results: SMCs in the outer media of the ascending aorta are derived from the second heart field, as demonstrated by lineage tracing studies using Cre under the control of Mef2c. Therefore, we used Mef2c-driven Cre to delete LRP1 in SMCs of the outer medial layers. Female LRP1 flox/flox mice were bred to male Mef2c-Cre1/0 mice to generate study mice. We first confirmed LRP1 deletion in Cre1/0 mice by both immunostaining and Western blot. LRP1 was expressed ubiquitously across smooth muscle cells of all aortic medial layers in Cre 0/0 mice. In mice expressing Mef2c-Cre, aortic LRP1 protein was detected only in SMCs of the inner laminar medial layers. Western blotting demonstrated LRP1 protein abundance in Cre expressing mice was reduced by 43%. Saline or AngII (1,000 ng/kg/min) was infused by subcutaneous osmotic pumps for 28 days into 12 - 14 week-old male Cre0/0 and 1/0 mice. As expected, systolic blood pressure increased similarly in both AngII-infused Cre 0/0 and 1/0 mice compared to saline-infused mice. Aortic rupture occurred within 3 to 10 days after AngII infusion in 17% of AngII-infused Cre 0/0 mice, while LRP1 deletion in Cre 1/0 mice increased aortic rupture to 27%. Aortic diameter in the survivors was significantly increased in Cre1/0 mice compared to Cre0/0 mice. Histologically, elastin fragmentation was detected in the aorta of AngII-infused Cre 0/0 mice and greater in Cre1/0 mice.
Conclusion: LRP1 in second heart field-derived SMCs of the outer media may play a critical role in the pathogenesis of TAA.

Disclosures: **H. Sawada:** None. **D.L. Rateri:** None. **M.W. Majesky:** None. **A. Daugherty:** None.

129

The Role of Mechanosensing and Fak Pathway in Acute Aortic Dissections in the *Myh11*^{R247c} Mouse Model

Shanzhi Wang, Callie Kwartler, Univ of Texas Medical Sch at Houston, Houston, TX; Teddy Zhang, Rice Univeristy, Houston, TX; Andrew Peters, Dianna Milewicz, Univ of Texas Medical Sch at Houston, Houston, TX

Thoracic aortic dissections (TAD) are a cause of premature deaths. The major risk factors for TAD are hypertension (HTN) and genetic variants. Here we used an engineered mouse model with a homozygous *Myh11* missense variant (*Myh11*^{R247C}) in the motor head of the smooth muscle myosin heavy chain to identify signaling pathways that lead to TAD. ***Results:*** The *Myh11*^{R247C} alteration decreases aortic contractility but does not cause aortic disease in mice. When hypertension is induced by feeding the mice L-NAME and a high salt diet, blood pressures were both significantly increased within 2 weeks in wildtype (WT) and mutant mice. About 20% of mutant mice (4/22) died within 2 weeks but none of the WT mice (0/13) died (p=0.1). Necropsy identified pericardial tamponade due to a retrograde dissection in the ascending aorta as the cause of death in the mutant mice. Electron microscopy analyses found abnormal formation of focal adhesions (FAs) in the mutant mice compared with WT, leading to greater distortion of FAs in the mutant mice when HTN was induced. RNA sequencing and pathway analysis of the *Myh11*^{R247C} aortas identified the FA signaling as the major pathway altered with HTN. Phosphorylated FAK was increased in *Myh11*^{R247C} aortas at baseline compared with WT, and increased further in *Myh11*^{R247C} aortas with HTN induction. To activate FA signaling, explanted smooth muscle cells (SMCs) were seeded on fibronectin-coated plates. Levels of phosphorylated regulatory light chain were dramatically increased in mutant SMCs compared with WT, presumably to compensate for the defective myosin motor. Apoptosis markers, Bid and Bax, were also increased. To determine if FAK signaling and elevated apoptosis were involved in aortic dissection in the mutant mice, either a FAK inhibitor

(PF573228) or p53 inhibitor (pifithrin-α) were administered 7 days before and during HTN induction. Both treatments completely prevent dissection deaths (P=0.03 and 0.05). In contrast, when prosurvival pathways were inhibited using a tyrosine kinase inhibitor, imatinib, dissection deaths significantly increased (p=0.002). ***Conclusion:*** These data indicated aberrant mechanosensing through focal adhesions leading to increased apoptosis trigger aortic dissections in the *Myh11*^{R247C} mouse model.

Disclosures: **S. Wang:** None. **C. Kwartler:** None. **T. Zhang:** None. **A. Peters:** None. **D. Milewicz:** None.

This research has received full or partial funding support from the American Heart Association.

130

The Diversity of Coronary Artery and Myocardial Infarction in Mice

Jiqiu Chen, Delaine K. Ceholski, Lifan Liang, Roger Hajjar, Mount Sinai Sch of Med, New York, NY

Low reliability and reproducibility in heart failure research has been a major concern. The purpose of the present study is to explore factors that affect model consistency of myocardial infarction (MI) in mice. **Methods**: MI was induced by left coronary artery (LCA) ligation. Echocardiography was used to measure cardiac function after MI. The coronary artery was casted with resin and visualized with fluorescent imaging in ex vivo. LCA characteristics and MI size were analyzed individually in each animal. MI size was correlated with LV function by echocardiography. **Results:** Coronary anatomy varies widely amongst animals, posing challenges for surgical ligation and resulting in inconsistent MI size data post-ligation. The length of coronary arterial trunk, level of bifurcation, number of branches, and territory supplied by these branches were unique in every animal. When the main LCA trunk was ligated, this resulted in a large MI, but when a single branch was ligated, MI size varied significantly due to differing levels of LCA ligation and differing amounts of territory supplied by the branches. During the ligation procedure, nearly 40% of LCAs were not grossly visible to the surgeon. In these situations, the surgeon commonly blindly sutures a wider and deeper area of tissue in an attempt to ensure that the LCA is caught and ligated. Paradoxically, these situations have greater odds of resulting in smaller MIs. **Conclusion**: The current study offers evidence of anatomical LCA diversity and the problems this poses for creating a consistent heart failure model by LCA ligation in mice. Carefully recognizing the inevitable individual variation of coronary anatomy in mice is essential to restoring reliability of the LCA ligation model of heart failure.

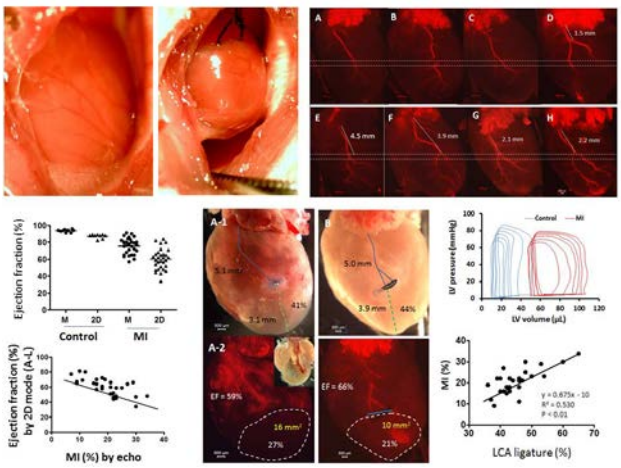

Disclosures: **J. Chen:** None. **D.K. Ceholski:** None. **L. Liang:** None. **R. Hajjar:** None.

131

Could One Define "FARD Score (Female, Aging, Respiratory & D-Dimer)" in Regard to Deep Vein Thrombosis in Cases with Immobilization?

Koichi Sato, Kazuhiko Hanzawa, Takeshi Okamoto, Ayako Nagasawa, Kenji Aoki, Osamu Namura, Masanori Tsuchida, Niigata Univ Graduate Sch of Medical and Dental Sciences, Niigata, Japan

<Objectives> With 17 sub-analyses, this prospective study aimed at evaluating the prevalence and indicators of deep vein thrombosis (DVT) associated with pulmonary embolism (PE) in patients immobilized on admission to internal medical wards. <Methods> In sub-groups (with more than 20 cases) of the 189 consecutive patients immobilized for more than 48 hours after admission (screening), we studied the significance of the major clinical factors in relation to whether DVT was identified with ultrasonography. If D-dimer level was positive (≥ 1.0 μg/ ml) in each case, chest enhanced CT was performed. <Results> With regard to 16 PE cases (8.5%) of the 189 cases, incidence of PE was higher in the groups of elderly patients (14%, 9 of 63 cases), of women (12%, 13 of 111 cases) and of patients with respiratory disease (9%, 3 of 33 cases) than in the other sub-groups. Among 77 DVT cases (40%) of the 189 cases, the groups of patients with respiratory disease (13 DVT cases), with gastro-intestinal disease (13 DVT cases) and with renal disease (13 DVT cases) included respectively more than those with the other diseases, in addition to the group of patients with malignant disease (15 DVT cases). In the groups of patients with abdominal disease (52%, 14 of 27 cases), central venous catheter (50%, 12 of 24 cases) and advanced age (49%, 31 of 63 cases), ratios of DVT cases were higher than in the other sub-groups. In patients with renal disease (P=0.01) and in women (P=0.02), D-dimer level was higher in DVT cases than in non-DVT cases whereas, in the groups with abdominal disease (P=0.72) and with respiratory disease (P=0.49), D-dimer level was essentially comparable between in DVT cases and in non-DVT cases. Only in the group of elderly patients, the prevalence of DVT was higher above-knee than below-knee. Multiple presence of DVT (20 of 77 DVT cases) was associated with presence of pulmonary embolism (P=0.09) in DVT cases. <Conclusions> In DVT cases with immobilization, practical risk factors of pulmonary embolism could be Female, Aging (older than 70 years, classified possibly), Respiratory disease and, in women, high D-dimer level.

Disclosures: **K. Sato:** None. **K. Hanzawa:** None. **T. Okamoto:** None. **A. Nagasawa:** None. **K. Aoki:** None. **O. Namura:** None. **M. Tsuchida:** None.

132

Glomerular Podocyte Damage is Mitigated by Normal HDL and ApoA1

Yohei Tsuchida, Jianyong Zhong, Vanderbilt Univ Medical Ctr, Nashville, TN; G.M. Anantharamaiah, Univ of Alabama at Birmingham, Birmingham, AL; MacRae Linton, Haichun Yang, Valentina Kon, Vanderbilt Univ Medical Ctr, Nashville, TN

We and others have shown that chronic kidney disease (CKD) disrupts the normally beneficial effects of apoAI/HDL on many different cell types. Proteinuria which characterizes CKD is a hallmark of glomerular podocyte injury and a powerful risk factor for cardiovascular disease (CVD). Although the glomerular filtration barrier normally limits direct contact of lipoproteins with podocytes, disruption in the filtration barrier promotes such interactions. We therefore investigated the effects of normal HDL and ApoAI on injured podocytes and compared these effects to HDL isolated from subjects with CKD.
Primary podocytes were isolated from wild type mice. The cells were exposed to puromycin (PAN, 100ug/ml) with and without HDL isolated from controls with normal kidney function, individuals with CKD, normal ApoA1 (EMD Millipore Company), and ApoA-I mimetic peptide L-4F. We assessed podocyte viability and proliferation (colorimetrically), cellular production of superoxide (ROS)(HPLC), membrane lipid rafts, phosphorylated caveolin-1 (Cav-1)(western blot).
PAN significantly altered ROS production, cell viability, proliferation. ApoA1 or HDL^{Cont}, but not HDL^{CKD}, significantly improved each of these responses. In addition, L-4F increased podocyte viability (0.60±0.04 PAN vs 0.65±0.04 PAN+L-4F) and HDL^{Cont}, but not HDL^{CKD}, normalized the significant increase in PAN-induced Cav-1 phosphorylation (0.65±0.04 vs 0.81±0.05 vs 0.70±0.09, respectively).
We conclude that podocyte damage including ROS production, cellular membrane and functions can be mitigated by normal HDL or its primary lipoprotein, ApoA1, findings that parallel beneficial functions of HDL/ApoA1 on other cell types. By contrast, HDL of subjects with CKD do not provide similar benefit.

	Cell viability	Cell proliferation	ROS production (pmol/mg)
PAN (-)	0.47±0.02	0.48±0.05	0.98±0.05
PAN (+)	0.37±0.03*	0.34±0.02*	1.84±0.05*
PAN (+)/ApoAI	0.41±0.02 †	0.44±0.04 †	1.30±0.03 †
PAN (+)/HDL^{Cont}	0.41±0.03 †	0.43±0.07 †	1.29±0.05 †
PAN (+)/HDL^{CKD}	0.40±0.06	0.41±0.06	1.48±0.04 †#

Mean ± SD, * vs. PAN (-), † vs. PAN(+), # vs. PAN(+)/HDL^{Cont}

Disclosures: **Y. Tsuchida:** None. **J. Zhong:** None. **G. Anantharamaiah:** None. **M. Linton:** None. **H. Yang:** None. **V. Kon:** None.

140

Comparison of Major Complication of Oral Anticoagulants in Non-Valvular Atrial Fibrillation: Systematic Review and Meta-Analyses

Hong Seok Lee, Univ of California, Riverside, Riverside, CA

Background: Oral anticoagulants known as a novel oral anticoagulant have been used for the management of non -valvular atrial fibrillation. There was no enough study regarding the efficacy and safety of three major new oral anticoagulants. We assessed major three oral anticoagulants in terms of major bleeding complication and stroke prevention by meta-analyses studies comparing those drugs. **Method:** Relevant studies were identified through electronic literature searches of MEDLINE, EMBASE, Cochrane library, and clinicaltrials.gov (from inception to February 24, 2016). RevMan and ITC software were used for direct comparisons, respectively. **Results**:
Apixaban (N=6020), versus dabigatran(N=12038), apixaban versus rivaroxaban(N=8503) and rivaroxaban versus dabigatran were analyzed directly. There was significantly higher major bleeding risks in apixaban compared to dabigatran (both 110mg and 150mg) after adjusting baseline bleeding risk (Relative risk 3.41, 95% confidence interval(2.61 to 4.47) in 110mg, (5.62, 4.83 to 6.54) in 150mg. Intracranial bleeding risk in apixaban was significantly higher than in dabigatran (10.5, 6.10 to18.01). However, apixaban had less GI bleeding risk compared to dabigatran (0.80 , 0.65 to 0.98) and also had less ischemic stroke risk (0.31,0.22 to 0.42). Rivaroxaban showed higher major bleeding risk than dabigatran 110mg (2.34 , 1.81 to 3.03), however, Rivaroxaban had less bleeding risk compared to dabigatran 150mg (0.41, 0.35 to 0.46). Dabigatran 110mg and 150mg had less GI bleeding risk compared to rivaroxaban (0.31 , 0.24 to 0.39) and (0.23,0.17 to 0.29) respectively. Ischemic stroke risk was also decreased in dabigatran110mg (0.46, 0.38 to 0.57). and 150mg (0.66 ,0.52 to 0.83). **Conclusion:** Observed oral anticoagulants were associated with various complications. Overall, apixaban had higher intracranial bleeding risk than dabigatran. The highest GI bleeding risk in rivaroxaban compared to apixaban and dabigatran. Ischemic stroke risk was the highest in dabigatran. In conclusion, we may use those oral anticoagulant based on risks rates, however, a larger study with longer follow-up is needed to corroborate findings.

Disclosures: **H. Lee:** None.

141

Inhibition of Coagulation Factor Xa Attenuates Myocardial Ischemia Reperfusion Injury in Mice

Jens Posma, Jelle Posthuma, Rene Van Oerle, Maastricht Univ, Maastricht, Netherlands; Stefan Heitmeier, Bayer, Wuppertal, Germany; Hugo Ten Cate, Henri Spronk, Maastricht Univ, Maastricht, Netherlands

Background: Ischemic/reperfusion (I/R) injury substantially effects the outcome of myocardial infarction (MI). Current reperfusion therapy does not sufficiently prevent injury caused by microvascular thrombo-inflammation. Coagulation proteases mediate inflammation via protease activated receptors. FXa induced thrombin generation is the key step in the coagulation cascade. We **hypothesize** that inhibition of FXa by rivaroxaban attenuates I/R injury after MI. **Methods:** Male WT c57BL/6 mice (age 8-9 weeks, n=8 per group) underwent surgical ligation of the left anterior descending coronary artery 7 days prior to experimentation. Next, the ligature was tightened for 1h to induce ischemia and loosened either at 4h

(early), or at 4 weeks (late), to allow reperfusion. The intervention consisted of 2 rivaroxaban (1.6 mg/kg) i.v.-injections or placebo (0.9%NaCl) after 15min of ischemia and 5min of reperfusion. In the early model. the area at risk (AAR) was visualized through Evans blue and differentiated from the area of infarction (AOI) through triphenyl tetrazolium chloride staining. Plasma cardiovascular markers were quantified using Luminex Multiplex. In the late model, LVEF was measured 10min pre-ischemia and 4 weeks' post-reperfusion utilizing echocardiography. **Results:** The rivaroxaban treatment group showed signs of diminished myocardial damage as indicated by reduced median AOI/AAR (41%[IQR34-48] vs. control 62%[IQR52-67] $p<0.001$). This was supported by a better preserved LVEF after 4 weeks of reperfusion (25%[IQR19-31] vs. control (16%[IQR12-21]). Although not significantly different, plasma E-Selectin, PECAM-1, PAI-1, proMMP9, and thrombomodulin showed a trend to increased levels upon treatment with rivaroxaban. **Conclusion:** FXa inhibition by rivaroxaban significantly reduces myocardial I/R injury in mice and may provide long term preservation of LVEF. Raised cardiovascular markers suggest increased tissue remodeling and phenotypical alteration of endothelial cells after rivaroxaban treatment. These results suggest that coagulation proteases (i.e. FXa) play a relevant role in I/R injury during MI, most likely through activation of protease activated receptors.

Disclosures: **J. Posma:** None. **J. Posthuma:** None. **R. Van Oerle:** None. **S. Heitmeier:** Employment; Modest; Bayer. **H. Ten Cate:** None. **H. Spronk:** None.

142

Biomimetic Recombinant Thrombomodulin Conjugate and Its Anticoagulant Activity

Lin Wang, Rui Jiang, **Xue-Long Sun**, Cleveland State Univ, Cleveland, OH

Thrombomodulin (TM) is an endothelial cell membrane protein that acts as a major cofactor in the protein C (PC) anticoagulant pathway. To closely mimic membrane protein structural feature of TM, we proposed a membrane-mimetic re-expression of recombinant TM onto liposome. The EGF-like domains 4-6 of TM (TM_{456}) are essential for PC activation. A recombinant TM containing TM_{456} and an azidohomoalanine at C-terminus was expressed in *E. coli*. The biomimetic liposomal recombinant TM conjugate was prepared by conjugation of the recombinant TM_{456}-azide with liposome *via* orthogonal chemistry and confirmed with Western blotting and PC activation activity. The liposomal recombinant TM_{456} conjugate showed a 2-fold higher PC activation activity than that of the recombinant TM_{456} alone, which indicated that the lipid membrane has a beneficiary effect on the recombinant TM_{456}'s activity. Also, the liposomal recombinant TM_{456} conjugate showed higher stability and longer plasma half-life than TM_{456}. Moreover, the liposomal recombinant TM_{456} conjugate showed *in vivo* anticoagulant activity by decreasing the mortality in a thrombin-induced thromboembolism mouse model. The reported liposomal TM_{456} conjugate mimics endothelial TM structure and anticoagulant activity and may serve as an anticoagulant agent candidate for future development.

Disclosures: **L. Wang:** None. **R. Jiang:** None. **X. Sun:** None.

This research has received full or partial funding support from the American Heart Association.

143

Bridging the Gender Gap: Sex Differences in Von Willebrand Factor Aptamer Inhibition Across Species

David L Dornbos III, Debra G Wheeler, Jeanne Green, Nicholas Venetos, Allyson Huttinger, Spencer Talentino, Nicholas Musgrave, Cheyenne Jones, Jay L Zweier, Shahid M Nimjee, The Ohio State Univ, Columbus, OH

Introduction: A gender gap exists in stroke, with increased morbidity and mortality in women. The underlying mechanisms remain unknown, although differences in platelet biology may play a role. Inhibition of the interaction between VWF and GP 1B-IX-V has demonstrated thrombolytic efficacy.
Hypothesis: We hypothesized that sex differences in reperfusion after stroke were attributable to the VWF-GP IB-IX-V axis, and inhibition of this interaction would yield clear discrepancies.
Methods: Adult wild-type (C57BL/6J) mice were anesthetized, the right carotid artery exposed and baseline carotid flow obtained by Doppler. Thrombosis was induced with a $FeCl_3$ patch. After 20-minute stabilization, mice were intravenously administered vehicle (n, male=12, female=8) or VWF aptamer. Aptamer (0.5 mg/kg) administration was assessed using a bolus (5 min; n, male=5, female=8) method.

Given the minimal observed thrombolytic effect in females, a continuous infusion (45 min; n, female=5) was also attempted.
Next, blood from male (n=8) and female (n=8) adult wild-type beagles was mixed with VWF aptamer (control, 6.25 nM, 12.5 nM, 25 nM, and 100 nM), and platelet reactivity was assessed (Platelet Function Analyser-100). Statistical analysis was performed using a two-way ANOVA with multiple comparisons.
Results: Bolus VWF aptamer restored carotid blood flow in male mice (Figure 1), compared to females ($p<0.001$) and vehicle ($p<0.01$). With continuous infusion, reperfusion in female mice was significantly higher than vehicle ($p<0.01$).
Male canines (264.3 ± 70.3 s) demonstrated significantly more platelet inhibition ($p<0.01$) than females (175.3 ± 83.2 s) at the 12.5 nM VWF aptamer concentration.
Conclusions: Following VWF inhibition, *in vivo* thrombolytic efficacy in mice is gender dependent, while *ex vivo* platelet activity varies in canines. The mechanisms underlying these differences in platelet biology are unclear, but this indicates that the VWF-GP IB-IX-V axis plays a role.

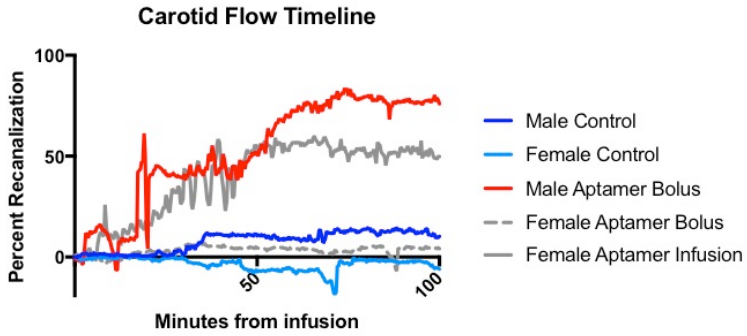

Disclosures: **D.L. Dornbos:** None. **D.G. Wheeler:** None. **J. Green:** None. **N. Venetos:** None. **A. Huttinger:** None. **S. Talentino:** None. **N. Musgrave:** None. **C. Jones:** None. **J.L. Zweier:** None. **S.M. Nimjee:** None.

145

Bench Evaluation of Diagnostic and Coronary Guide Catheters in the Radial and Femoral Paths

Mark C Arokiaraj, Pondicherry Inst of Medical Sciences, Pondicherry, India

Aims: To evaluate the pushability and trackability of the angiographic and guide catheters in the femoral and radial paths. To identify the factors influencing engagement and the performance of angiograms and angioplasty in the radial and femoral paths. **Methods and Results** Cordis diagnostic and guide catheters were evaluated in the radial and femoral paths. The paths were created after evaluating the angles and diameters of the path till coronary ostia. The apparatus is shown in the picture below. Force transmission was evaluated by proximal force, distal force and the ratio of the forces. Trackability was evaluated by force and distance transmission analysis. The mean ratio of proximal to distal force transmission in femoral approach was 0.28 (± 0.13) for diagnostic, and 0.51(± 0.11) for guide catheters. The mean ratio of distal/proximal force transmission in the radial track was 0.63 (± 0.07) for angiographic catheters, and 0.58 (± 0.06) for guide catheters. This lesser ratio in the femoral is desirable for better torque control ($\delta\pi$) of catheter, which is inversely proportional to time (δt). The trackability of the catheters was good in the radial track with an unique restriction at 74 cm out of the total 81cm. This correlates anatomically with the brachiocephalic trunk to aortic arch bend. Also, the angular momentum and velocity applying the right hand thumb rule was directed towards left shoulder. In the femoral path the trackablity of the catheters was good upto the end of the path, which is near the coronary ostium. These parameters indirectly correlate with the duration of the procedure and contrast usage. **Conclusion** The trackabiity in the radial path was restricted to 74 cm out of 81 cm. The force transmission ratio in the femoral is lesser. However, this would result in better torque control of catheters by the femoral approach.

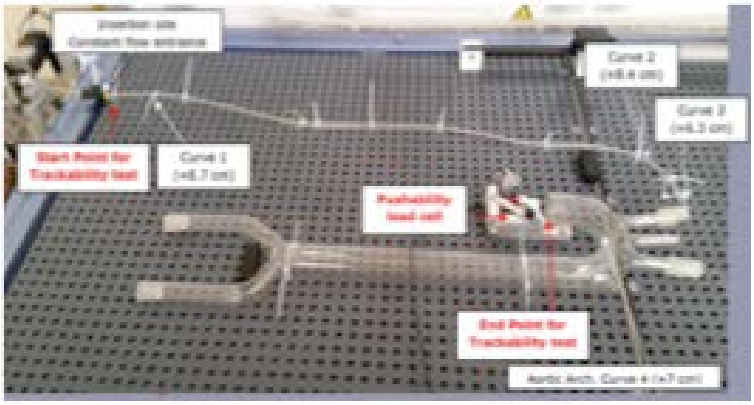

Disclosures: **M.C. Arokiaraj:** None.

146

Deficiency of Cystathionine beta Synthase Alters Blood Brain Barrier Integrity and Exacerbates Cerebral Ischemia Reperfusion Injury in Mice

Sean X Gu, Vijay Sonkar, Univ of Iowa, Iowa City, IA; Warren D Kruger, Fox Chase Cancer Ctr, Philadelphia, PA; Teodoro Bottiglieri, Baylor Res Inst, Dallas, TX; Steven R Lentz, Sanjana Dayal, Univ of Iowa, Iowa City, IA

Hyperhomocysteinemia is a risk factor for stroke; however the mechanisms by which elevated homocysteine leads to stroke are poorly defined. In a murine model of cystathionine beta synthase (CBS) deficiency, we investigated whether mild to severe elevation in plasma total homocysteine (tHcy) increases susceptibility to cerebral infarction and if this phenotype is associated with loss of blood brain barrier (BBB) integrity. We studied male *Cbs*-/- mice conditionally expressing a zinc-inducible mutated human *CBS*$^{(I278T)}$ transgene along with *Cbs*+/- and *Cbs*+/+ littermates at 10-14 weeks of age. The human transgene was allowed to express only until weaning to overcome the early mortality of *Cbs*-/- mice. Experimental stroke was induced with middle cerebral artery occlusion for one hour followed by 24 hours of reperfusion. TTC stained coronal sections were used to quantify the infarcted area. BBB integrity was assessed prior to injury using a standard Evan's blue (EB) infusion method. Leakage of EB was quantified in brain homogenates and normalized to brain weight. Mild to severe increases in plasma tHcy were observed in *Cbs*+/- and *Cbs*-/- mice (6.1±0.3 and 309±18 µM, respectively) compared with *Cbs*+/+ littermates (3.1±0.6 µM, P<0.01). Both *Cbs*+/- and *Cbs*-/- mice exhibited significant increases in infarct size following ischemia-reperfusion injury as compared to *Cbs*+/+ mice (12.2±3% in *Cbs*+/+ mice vs. 35.1±7.7% in *Cbs*+/- and 27.7±7.8% in *Cbs*-/- mice, P<0.05). A significant increase in EB extravasation was observed in *Cbs*+/- and *Cbs*-/- mice (3.8±0.8 and 4.8±0.2 µg/g, respectively) compared to *Cbs*+/+ mice (1.7±0.4 µg/g, P<0.05). The similarity in extent of cerebral infarction observed in *Cbs*+/- and *Cbs*-/- mice suggests a threshold effect and that a mild increase in tHcy is enough to disrupt BBB integrity and produce a severe stroke phenotype in experimental murine models.

Disclosures: **S.X. Gu:** None. **V. Sonkar:** None. **W.D. Kruger:** None. **T. Bottiglieri:** None. **S.R. Lentz:** None. **S. Dayal:** None.

This research has received full or partial funding support from the American Heart Association.

147

Plasma Factor XIII Binding to Cold-stored Platelets Results in Increased Fibrin Crosslinking and Clot Strength

Prajeeda M Nair, Shaunak G Pandya, Shatha F Dallo, Univ of Texas at San Antonio, San Antonio, TX; Kristin M Reddoch, Robbie K Montgomery, Inst of Surgical Res, Sam Houston, TX; Heather F Pidcoke, Terumo BCT, Lakewood, CO; Andrew P Cap, Inst of Surgical Res, San Antonio, TX; Anand K Ramasubramanian, San Jose state Univ, San Jose, CA

Currently, platelets (PLTs) stored at room temperature (RT) for 5-7 days with gentle agitation are exclusively used for transfusion although FDA recently clarified that apheresis PLTs stored at 4°C for up to 72 hours may be used for treating active hemorrhage. We have demonstrated that cold (4C) storage of PLT is an attractive alternative to RT storage since it better preserves the PLT metabolic reserves, *in vitro* responses to agonists of activation, aggregation and physiologic inhibitors, as well as adhesion to thrombogenic surfaces. In this study, we tested the hypothesis that 4C-stored PLT will form clots with mechanical strength superior to those from RT-stored PLT due to higher hemostatic potential. From rheological measurements, we observed that the clots formed from 5 day 4C-stored PLTs are significantly stiffer (elastic modulus) and stronger (critical stress) than those formed from RT-stored PLT but comparable to fresh PLT (Fig. A). We also observed from ultrastructural microscopy that the fibrin fibers in clots from cold-stored PLT were thinner with more branch points than those from RT-stored PLTs, indicating the presence of increased crosslinks (Fig. B, C). Finally, molecular analysis revealed an increase FXIII transglutaminase activity due to the binding of plasma FXIII/fibrinogen to the surface of 4C-stored PLTs (Fig D).In conclusion, we have shown that cold-induced plasma FXIII binding to PLT surface result in increased fibrin crosslinking and enhanced clot strength. Our data, together with the benefit of reduced risk of late thrombosis due to their rapid clearance *in vivo*, underscores the consideration of 4C-stored PLT for acute response to hemorrhage.**Figure 1** (A) RT-stored platelets form clots with less stiffness (n=5); (B) Representative SEM images of clots (n=3) (C) Clots from 4C-stored platelets have higher cross-linking density (n=5) (D) In FXIII-deficient plasma, 4C-stored platelets form clots with higher stiffness than fresh platelets (n=4)

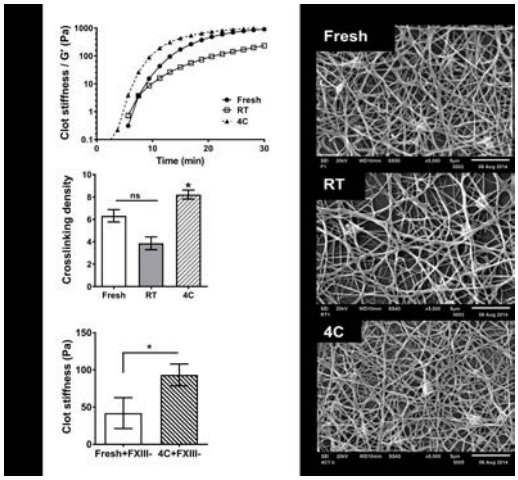

Disclosures: **P.M. Nair:** None. **S.G. Pandya:** None. **S.F. Dallo:** None. **K.M. Reddoch:** None. **R.K. Montgomery:** None. **H.F. Pidcoke:** None. **A.P. Cap:** None. **A.K. Ramasubramanian:** None.

148

Difference in Neointimal Coverage Pattern Between Zotarolimus Eluting Stents and Everolimus Eluting Stents Using Optical Coherence Tomography: A Meta-Analysis

Vivek Yarlagadda, AtlantiCare Regional Medical Ctr, Atlantic City, NJ; Pradyumna Agasthi, Moorehouse Sch of Med, Atlanta, GA; Aneese Chaudhary, Sivakanth Aloor, Eric Chang, Morehouse Sch of Med, Atlanta, GA; Kwan Lee, Banner Univ Medical Ctr-South, Tucson, AZ; Gautam Kumar, Emory Univ, Atlanta, GA; Rajesh Sachdeva, Morehouse Sch of Med, Atlanta, GA

Background: Late stent thrombosis in drug eluting stents (DES) is attributed to poor endothelialization of struts. Second generation DES have shown superior safety profile and efficacy in comparison to first generation DES. We conducted a meta-analysis to compare the neointimal coverage patterns between Zotarolimus eluting stents (ZES) and Everolimus eluting stents (EES) using optical coherence tomography (OCT).
Methods: We searched online databases for studies comparing the neointimal thickness (NIT), %malapposed strut per stent (MSS) or % uncovered strut per stent (USS) between ZES and EES using OCT. Studies included inte mmeta-analysis, OCT was performed >6 months after stent deployment. A calculation of weighted standardized mean difference (SMD) in NIT, MSS and USS between ZES and EES groups was calculated. Residual maximum likelihood (REML) metaregression was performed on smokers, diabetes mellitus (DM), hypertension, (HTN) dyslipidemia (DLD), and age and sex covariates.
Results: A total of 6 studies enrolling 327 patients which met inclusion criteria were included in the meta-analysis. 400 stents including 184 ZES and 216 EES were analyzed by OCT. The median of mean age in years, male sex, smokers, DM, HTN and DLD in the ZES group was 60.7(59.5 - 60.9), 76.7% (71.4 - 77.3), 38.7% (18.2 - 45.8), 36.4% (23.3 - 37.5), 63.6% (60 - 66.6), 66.7% (47.9 - 68.4) versus 62.6(59.8 - 65.3), 63.9% (63.6 - 82.1), 30% (17.2 - 47.2), 31.8% (25 - 36.1), 69.4% (59.1 - 75.9), 70% (48.9 - 70.7) in the EES group respectively. The unweighted median NIT, MSS and USS in the ZES group are 127.5 µm (108.8 - 152.2), 0.7% (0.7 - 0.9), 1.8% (0.2 - 3.5) vs 117.4 µm (108.5 - 128.5), 0.3% (0.2 - 1.3), 2.3% (0.9 - 3.5) in the EES group respectively. The weighted SMD of NIT, MSS and USS in the ZES vs EES groups are -0.22 (95%CI -1.12; 0.67) P = 0.63, -0.51(95% CI -1.78; 0.77), P = 0.44, -1.26 (95%CI -2.83; 0.31). None of the above mentioned covariates accounted for statistical insignificance except age for NIT. As age increases, the SMD increases for NIT and was not significant for MSS and USS.
Conclusion: No significant difference was noted in the NIT, MSS and USS between both groups. This suggests that the neointimal coverage patterns are similar in ZES and EES groups.

Disclosures: **V. Yarlagadda:** None. **P. Agasthi:** None. **A. Chaudhary:** None. **S. Aloor:** None. **E. Chang:** None. **K. Lee:** None. **G. Kumar:** None. **R. Sachdeva:** None.

149

Phosphatidylserine Promotes Thrombosis in Pediatric CPB Model

Andrew D Meyer, Anjana Raghunath, Patricia Heard, Univ of Texas Health, San Antonio, TX; Robin Kamucheka, Crystal Lafleur, Michael Scherer, US Army Inst for Surgical Res, San Antonio, TX; Andrew P Cap, US Army Inst For Surgical Res, San Antonio, TX

Over 18,000 children per year receive cardiopulmonary bypass (CPB) surgery. Unfortunately, common CPB-related thrombotic complications continue to result in significant mortality and morbidity. Previous ex-vivo CPB studies using animal blood document an increase in platelet-derived microparticles (PMPs), which are small (0.1-1 micron) membrane vesicles that may be 50 to 100-fold more pro-coagulant than activated platelets. Our hypothesis is that increased duration and magnitude of shear stress in an ex-vivo pediatric CPB circuit increases the generation of PMP expressing pro-thrombotic phosphatidylserine. We constructed an ex-vivo CPB circuit that circulates heparinized human blood from healthy adult volunteers for six hours at pediatric flow rates (*e.g.,* 0.3, 0.5, and 0.7 L/min). Our protocol normalizes each run through the circuit to a normal hematocrit, pH, ionized calcium, and an activated clotting time of 180 to 220 sec. An aliquot of static blood controls is maintained in a similar test environment without CPB circuitry. PMP-PS (CD41a+/phosphatidylserine[PS]) concentration and pro-coagulant function are measured in platelet-depleted plasma using high-resolution flow cytometry (BS FACS Canto II with PMT) and STA®-Procoag-PPL. Thrombin generation (*e.g.*, calibrated automated thrombogram) and clot formation (*e.g.*, thromboelastography) further define the coagulation function of pump-produced PMP-PS. At 0.5 L/min the circuit generates an exponential increase in PMP-PS and decreasing PPL clot time compared to static blood control (p<0.001, Figure 1, n=4). Platelet count, prothrombin time, and activated

partial thromboplastin time do not change over time. Results also document an increase in peak thrombin potential and clot formation that correlate strongly with the increase in PMP-PS. PMP-PS may be a clinically relevant biomarker and therapeutic target to decrease life-threatening CPB surgery coagulation complications.

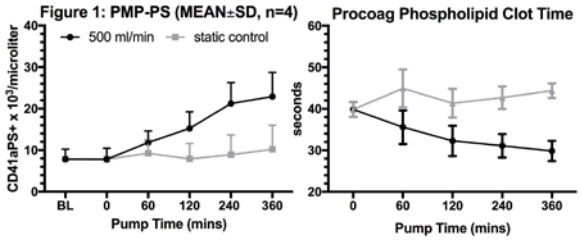

Disclosures: **A.D. Meyer:** Research Grant; Modest; DOD CCCRP Grants. Research Grant; Significant; NHLBI K23, AHA Grant-In-Aid. **A. Raghunath:** None. **P. Heard:** None. **R. Kamucheka:** None. **C. Lafleur:** None. **M. Scherer:** None. **A.P. Cap:** Employment; Significant; DOD.

150

Hypoxia and Ischemia Promote a Maladaptive Platelet Phenotype

Scott J Cameron, Doran S Mix, Sara K Ture, Rachel Schmidt, Amy Mohan, Sandra Toth, Michael C Stoner, David J Field, Kristina L Modjeski, Criag N Morrell, Univ of Rochester Medical Ctr, Rochester, NY

Background: An understudied area of platelet biology is that ischemic diseases such as peripheral vascular disease (PVD) can alter the platelet phenotype, and this may lead to unpredictable effects of anti-platelet agents.
Methods: Isolated murine and human platelets were exposed to a reduced oxygen environment (hypoxia chamber, 5% O_2). Platelet activation was assessed as mean fluorescence intensity (MFI) of surface p-selectin by flow cytometry, and morphologic changes by confocal microscopy. A murine model of critical limb ischemia (CLI) was used to assess changes in platelet activity in wild-type (WT) and in platelet ERK5$^{-/-}$ mice. Limb blood flow was assessed by laser Doppler imaging. Hypoxia was additionally examined in mice by unilateral pneumonectomy. Western blotting was used to assess protein expression.
Results: In human platelets *ex vivo* at 5% O_2, platelet activation increased to 5076 MFI±409 from 3548 MFI±187 at 20% O_2 (P=0.005). With the ERK5 inhibitor XMD892, platelet activation at 5% O_2 decreased from 5677 MFI±312 to 3175 MFI±247 (p=0.001). In a murine model of PVD, enhanced platelet activation was sustained for weeks vs. sham, and limb blood flow in platelet ERK5$^{-/-}$ mice one week after ischemia was augmented by 26%: 0.61±0.03 vs 0.87±0.03 vs, WT mice (p=0.0002), with 50% less platelet activity. In mice with unilateral pneumonectomy vs. sham surgery, observed hypoxia was accompanied by increased platelet ERK5 activation coincident with enhanced platelet activation. In patients with CLI, augmented platelet activation in spite of aspirin treatment was observed via the thromboxane and the PAR1 receptors, and especially via $P2Y_{12}$ receptor.
Conclusions: Hypoxia and ischemic tissue injury, such as with critical limb ischemia, change the phenotype of the platelet, promoting a pro-thrombotic state that is partly dependent on platelet ERK5. Platelet phenotype and function should be better characterized in ischemic diseases.

Disclosures: **S.J. Cameron:** None. **D.S. Mix:** None. **S.K. Ture:** None. **R. Schmidt:** None. **A. Mohan:** None. **S. Toth:** None. **M.C. Stoner:** None. **D.J. Field:** None. **K.L. Modjeski:** None. **C.N. Morrell:** None.

151

Parsimonious Model for the Detection of Acute Coronary Thrombus

Alok R Amraotkar, Shahab Ghafghazi, Patrick J Trainor, Andrew P DeFilippis, Univ of Louisville, Louisville, KY

Background: There is limited data to determine accuracy and precision of detecting acute coronary thrombus via angiography. **Objective**: To build a parsimonious model for the prediction of acute coronary

thrombus from four commonly used angiographic characteristics (spherical, ovoid, or irregular filling defect; abrupt vessel cutoff with persistence of contrast; intraluminal staining; any coronary filling defect). **Methods**: Angiographic Core Laboratory (Baltimore, Maryland) evaluated angiograms of 80 acute MI / stable CAD subjects in blinded fashion. Outcome was defined as presence of thrombus by histological examination. Multivariable generalized linear modeling was conducted to determine best combinations of characteristics for discriminating between lesions with a histologically confirmed thrombus versus lesions without a histologically confirmed thrombus. **Results**: A best-fit parsimonious model revealed that individual presence of abrupt vessel cutoff with persistence of contrast (O.R=16, P<0.0001) or any coronary filling defect (O.R=84, P<0.0001), or both in concurrence (O.R=105, P<0.0001) (Figure 1 and Table 1), was most significantly associated with the presence of coronary thrombus. **Conclusions**: Modeling suggests that the presence of abrupt vessel cutoff with persistence of contrast or any filling defect, individually or in concurrence, is significantly associated with acute coronary thrombus, and therefore warrants validation in an independent cohort.

Figure 1: Angiographic Characteristics Constituting Best-Fit Parsimonious Model

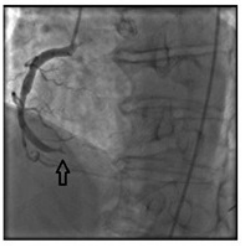

Abrupt Vessel Cutoff with Persistent Contrast

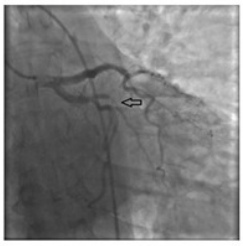

Any Coronary Filing Defect

Table 1 – Multivariable Best-Fit Parsimonious Model for Detecting Thrombotic Lesions

Characteristics	Estimate	Standard Error	Odds Ratio (95% CI)	P-Value
Abrupt Vessel Cutoff with Persistence of Contrast	2.791	0.572	16.3 (5.31, 50) *	**<0.0001**
Any Coronary Filling Defect	4.432	0.897	84.1 (14.9, 474) *	**<0.0001**
Abrupt Vessel Cutoff with Persistence of Contrast ***AND*** Any Coronary Filling Defect	4.656	1.102	105.2 (12.1, 911.9) *	**<0.0001**

* Odds ratio estimates for: Present v/s all other (Absent/Undetermined)

Disclosures: **A.R. Amraotkar:** None. **S. Ghafghazi:** None. **P.J. Trainor:** None. **A.P. DeFilippis:** None.

This research has received full or partial funding support from the American Heart Association.

152

Pre-chemotherapy Lymphocyte Count as a Predictor of Venous Thromboembolism in Patients With Gastric Cancer

Harry E Fuentes, Luis H Paz, John Stroger Hosp, Chicago, IL; Diana M Oramas, Univ of Illinois at Chicago, chicago, IL; Xavier A Andrade, Ahmed Al-Ogaili, John Stroger Hosp, Chicago, IL; Alfonso X Tafur, NorthShore Univ HealthSystem, Evanston, IL

Background: VTE is a largely preventable leading cause of mortality among patients with cancer. Gastric cancer (GC) is one of the most pro-thrombotic solid tumors. The use of effective prophylaxis for cancer-associated thrombosis CAT is anchored on reliable VTE risk stratification. Pre-chemotherapy lymphocytes (PCL) are associated with both arterial and venous thrombosis and play an important role in the thrombogenic pathway; however, their clinical significance in GC CAT is unknown. **Aim:** To test PCL as a predictor of VTE in patients with gastric cancer
Methods: Single institution chart review of GC treated patients (2010-15). VTE events were objectively confirmed in all cases by imaging. Active cancer was defined as biopsy positive metastatic disease or on chemotherapy. Demographic variables, PCL and potential confounding variables were independently

extracted. We present continuous variables as median (interquartile range). Categorical variables are expressed as percentages. SPSS version 23 was used and Chi-square, Mann-Whitney U, and logistic regression with forward modeling were applied.
Results: We included 112 patients in the analysis who were 58 (51-64) year-old, predominantly male (66%), with adenocarcinoma (84%), and advanced disease (59%). The follow-up was 21.3 months (9.5 - 42.6). VTE occurred in 13 (12%) patients: 4 extremity, 4 splanchnic and 5 pulmonary embolisms. Median PCL was 1.6 (1.0 - 2.1). We selected PLC > 1.75 as optimal cutoff based on the ROC performance for new VTE (sensitivity of 70% and specificity of 67%). PCL >1.75 was an independent predictor of VTE (OR: 4.9; 95%CI: 1.3-18.1; p=0.02) after adjusting for body mass index, performance status and cancer stage. **Conclusion**: PCL independently predicted VTE occurrence among patients with GC. Pending external validation, PCL could be implemented in risk stratification strategies specific to GC thromboprophylaxis

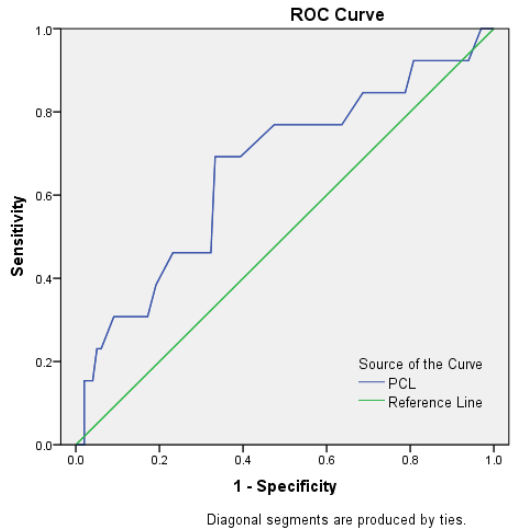

Disclosures: **H.E. Fuentes:** None. **L.H. Paz:** None. **D.M. Oramas:** None. **X.A. Andrade:** None. **A. Al-Ogaili:** None. **A.X. Tafur:** None.

153

IL-17 Amplifies Thrombosis in a Mouse Model of DVT

Benjamin N Jacobs, Yogen Kanthi, Danica Petrovic-Djergovic, Hui Liao, David J Pinsky, Univ of Michigan, Ann Arbor, MI

Background Immune cells are known to participate in thrombosis. A subset of IL-17 producing T-cells plays a role in the inflammatory dysregulation of inflammatory bowel disease, malignancy, and acute graft rejection. IL-17 resides at the interface between innate and adaptive immunity, exerting pro-inflammatory effects via induction of cytokines and cellular adhesion molecules, with consequent neutrophil activation and mobilization. Inflammatory properties of endothelium itself direct T-cell plasticity, and we have previously demonstrated that endothelial CD39 is an important inflammatory regulator via degradation of pro-inflammatory nucleotides. It is unknown whether IL-17 affects development of thrombosis in deep veins. **Hypothesis** IL-17 released from T-cells augments deep venous thrombosis, through endothelial CD39-driven T-cell phenotype switching. **Methods** A uniform non-occluding ligature around the infrarenal IVC was used to model DVT. CD39 haploinsufficient (CD39+/-) mice were used, as full knockouts demonstrate baseline platelet reactivity abnormalities affecting thrombosis. Mice were sacrificed at 48 hours and IVC and thrombus harvested. IL-17 protein was measured using western blotting and immunohistochemistry and inflammatory cells in vein wall were identified by flow cytometry. **Results** CD39 +/- mice had increased thrombus mass compared to wild-type animals (p=0.02), with a corresponding increase in IL-17. In CD39 +/- mice, immunohistochemistry of thrombus indicated increased inflammatory cell infiltration, expression of VCAM-1 and IL-17. In vitro confirmation of effect of IL-17 dosing of HUVEC induced a 2-fold induction of E-Selectin (p<0.0001) and a 1.25 fold induction of ICAM-1 (p=0.0002) by qPCR; P-Selectin was not different (p=0.6). Flow cytometric analysis of vein wall

after thrombus induction indicated increased infiltration of neutrophils (2.5-fold), monocyte-macrophage (2-fold), and T-cells (1.5 fold) in CD39 +/- mice compared with controls. **Conclusion** Decreased expression of CD39 is associated with a pro-thrombotic phenotype in CD39 haploinsufficient mice, resulting in increased IL-17 within the IVC, inducing Selectin- and CAM-driven pathways of inflammatory cell infiltration after thrombosis.

Disclosures: **B.N. Jacobs:** None. **Y. Kanthi:** None. **D. Petrovic-Djergovic:** None. **H. Liao:** None. **D.J. Pinsky:** None.

154

Bridging to Warfarin with Direct Oral Anticoagulant Agents

Luis Diaz Quintero, Alfonso Tafur, Northshore Univ Healthsystem, Evanston, IL

Background Anticoagulation bridging using LMWH remains a common practice to mitigate the Warfarin's delayed onset of action. However, LMWH often creates resistance from patients given cost, fear to injections, or in patients already on direct oral anticoagulant agents (DOACs), cost coverage that demand agent change. In such circumstances, the possibility of bridging using DOACs has been adopted.
Aim To characterize the outcomes and cost benefit for patients who were bridged to Warfarin using a DOAC.
Methods We identified a case series of patients who used DOACs for bridging to Warfarin. Primary outcome was major hemorrhage and thrombosis recurrence identified 30 and 60 days after initial bridging therapy was initiated. Categorical variables were presented as percentages, continuous variables as median and range. Chi Square or Student T were used as appropriate.
Results A total of nineteen patients were included (Men = 42%, Age = 66.3 (32-93), BMI = 29 (19.5-44.6)). Twelve patients received Apixaban (63%), and seven patients received Rivaroxaban (37%). Reasons to avoid low molecular weigh heparin were patient's preference (53%), changing indication (32%), interaction (10%), and cost (5%) The average time for successful bridging was 13.2 days (5-29). No episodes of major bleeding, deep venous thrombosis, pulmonary embolism or minor bleeding were registered after 30 and 60 days of initiation of bridging therapy. Average cost of bridging therapy with DOAC was 158.3 USD (Range 21.1-407.9). Estimated cost of bridging therapy with LMWH and current pricing would have been 652.4 US dollars (294-1421).
ConclusionBridging strategy with direct oral anticoagulant agents seems to be a safe, cost-effective approach in patients receiving oral Warfarin. Moreover, this alternative is reasonable for patients with aversion or lack of social support to administer injections. A larger study is necessary to further explore these findings.

Disclosures: **L. Diaz Quintero:** None. **A. Tafur:** None.

160

Multiscale Entropy of Photoplethysmographic Pulse Amplitudes of Bilateral Fingertips Varies by Hand Dominance and Diabetes Status

Gen-Min Lin, Chieh-Ming Yang, Hsien-Tsai Wu, Natl Dong-Hwa Univ, Hualien, Taiwan

Objective: Multiscale entropy (MSE) of photoplethysmographic (PPG) pulse amplitudes may reflect cardiovascular health. In addition, poor glycemic control and weak handgrip strength are related to microvascular dysfunction in diabetes. We hypothesized that MSE of PPG pulse amplitudes between dominant and non-dominant hand may differ by diabetes status. **Methods:** Of a middle-to-old aged and right hand-dominant population free of prior cardiovascular disease, we matched age, sex, and weight to select the unaffected (no type 2 diabetes, n =36), the well-controlled diabetes (HbA1c <8%, n =22), and the poorly-controlled diabetes (HbA1c ≥8%, n =22) groups. MSEs were calculated from simultaneous consecutive 1,500 resting PPG pulse amplitudes of bilateral index fingers. The small- and large-scale MSEs were defined as the average of scales 1 to 3 (MSE_{1-3}) and scales 4 to 10 (MSE_{4-10}), respectively. Intra- and inter-groups comparisons were performed by 1- and 2-sample t tests. **Results:** The inter- and intra-groups mean pulse amplitudes did not differ. In contrast, the pulse wave velocity was higher in the two diabetes groups, but was similar between two hands in each group. The dominant hand MSE_{4-10} was lower in the poorly-controlled diabetes compared with the unaffected and well-controlled diabetes groups (1.25 vs. 1.52 and 1.49, p=0.001 and 0.017, respectively); whereas the non-dominant hand MSE_{4-10} was lower in the well- and poorly-controlled diabetes groups than the unaffected (1.31 and 1.26 vs. 1.54,

p=0.007 and 0.002 respectively). There was no intra-groups difference in MSE_{4-10}, but a higher MSE_{1-3} of dominant hand than that of non-dominant hand in the well-controlled diabetes (1.30 vs. 1.07, p=0.05). **Conclusion:** Diabetes status and hand activity are related to the MSE of PPG pulse amplitudes. The MSE indexes differed between two hands with euglycemia indicated that local physical inactivity might be an independent contributor to diabetic microvascular dysfunction.

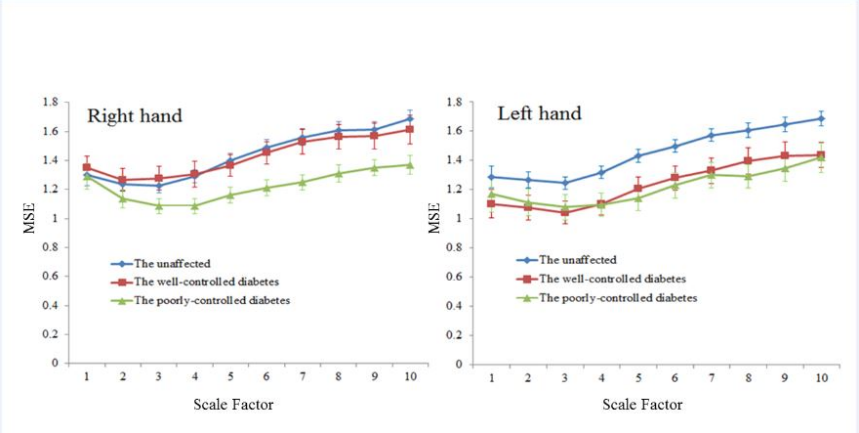

Disclosures: **G. Lin:** None. **C. Yang:** None. **H. Wu:** None.

161

Diet-Induced Obesity Links to Breast Cancer Progression via LPA/PKD-1-CD36 Signaling Axis-Mediated Microvascular Remodeling

Ye Yuan, Liuyi Dong, Blood Res Inst, Blood Ctr of Wisconsin, Milwaukee, WI; Irene Aguilera-Barrantes, Dept of Pathology, Medical Coll of Wisconsin, Milwaukee, WI; Yiliang Chen, Rong Yuan, Blood Res Inst, Blood Ctr of Wisconsin, Milwaukee, WI; Roy Silverstein, **Bin Ren**, Blood Res Inst, Blood Ctr of Wisconsin; Dept of Med, Medical Coll of Wisconsin, Milwaukee, WI

Background Obesity increases breast cancer (BC) risk. However, the molecular links by which obesity promotes BC progression remain largely unknown. Lysophosphatidic acid (LPA) produced excessively in obesity is a lipid signaling mediator essential for vascular remodeling, angiogenesis and BC progression, in which protein kinase D1 (PKD-1) and angiogenic regulator CD36 play an important role. **Hypothesis** Obesity promotes microvascular remodeling and angiogenesis for BC progression via LPA/PKD-1-CD36 signaling axis. **Methods** The hypothesis was tested in tumor-associated endothelial cells (TAECs), BC cells and a diet-induced obesity (DIO) mouse model. Lentiviral transduction, qPCR, Western blotting and Halo pull-down assays, angiogenesis profiling and immunofluorescence and immunohistochemical assays were applied for analysis of gene and protein expression, and relevant signaling pathways. Seahorse Bioscience Extracellular Flux Analyzer was used to detect cellular mitochondrial respiration. **Results** LPA/PKD-1-CD36 signaling was a *bona fide* BC promoter via stimulating microvascular remodeling in chronic DIO. ER^+ breast cancer grew faster and larger in the DIO mice than in the lean control, specifically accompanied by enhanced microvascular remodeling in a syngeneic ER^+ BC model. The expression of vascular endothelial cell growth receptor 2, and endothelial differentiation gene 2/LPA receptor 1 (Edg2/LPA_1), and phospho-PKD-1 also increased, accompanied by CD36 downregulation in the tumor endothelium. TAECs exposed to LPA showed sustained nuclear PKD-1 phosphorylation, and elevated mRNA levels of ephrin B2, and reduced CD36 mRNA expression, along with increased proliferation, which was inhibited by a selective PKD inhibitor. Finally, LPA/PKD-1 signaling changed mitochondrial respiration in ECs and breast adenocarcinoma cells. **Conclusion** These studies suggest that LPA/PKD-1-CD36 signaling axis links DIO to BC progression via stimulation of arteriolar remodeling of microvasculature in the tumor microenvironment. The axis-mediated changes in cellular metabolism may promote the microvascular remodeling process. Targeting this signaling axis could provide an additional novel therapeutic strategy against breast cancer.

Disclosures: **Y. Yuan:** None. **L. Dong:** None. **I. Aguilera-Barrantes:** None. **Y. Chen:** None. **R. Yuan:** None. **R. Silverstein:** None. **B. Ren:** None.

This research has received full or partial funding support from the American Heart Association.

162

Perivascular Adipose Tissue Controls Insulin-Mediated Microvascular Recruitment and Skeletal Muscle Glucose Uptake in vivo

Alexander H Turaihi, Yvo M Smulders, Victor WM van Hinsbergh, John S Yudkin, Etto C Eringa, VUmc, Amsterdam, Netherlands

Introduction: Insulin-mediated microvascular recruitment (IMVR) regulates postprandial delivery of substrates to insulin-sensitive tissues. We have previously proposed that perivascular adipose tissue (PVAT) controls vascular function through “vasocrine”, i.e. vessel-to-vessel, signaling (Lancet 2005; 365: 1817-20). Here we tested this hypothesis by evaluating the effect of physical separation of local PVAT from muscle arteries on IMVR in vivo.
Methods: In lean C57/Bl6 mice we removed PVAT from the gracilis artery (GA) and adjacent parts of the femoral artery (Removed), incised the skin of the hindlimb (Sham) or did not apply surgery (Intact). Mice underwent combined contrast enhanced ultrasonography and intravital microscopy to measure IMVR and GA diameter, respectively, during the hyperinsulinemic-euglycemic clamp. PVAT vasodilatory capacity was examined ex vivo using pressure myography of muscle resistance arteries. Local muscle glucose uptake was examined in vivo using 18Fluorodeoxyglucose (^{18}FDG) tracer in mice undergoing insulin clamp in PET-CT scanner.
Results: All mice had comparable peripheral insulin sensitivity. In vivo, insulin increased GA diameter (p=0.001) of the Intact (14.5% ± 6%) and Sham (20.0% ± 5%) compared to the Removed (2.0% ± 7%). Muscle IMVR was higher (p=0.007) in the Intact (35.7% ± 31%) and the Sham (42.1% ±12%) compared to the Removed (-4.8% ± 7%). Insulin-induced ^{18}FDG uptake was higher in the Sham hindlimb muscle compared to the Removed. Ex vivo, insulin [2.0 nM] increased GA diameter in the presence of PVAT (26.2% ± 25%; p=0.03) but not in absence of PVAT (0.3% ±12%).
Conclusion: We provide proof that local PVAT depots regulate muscle perfusion and glucose uptake in vivo. These data highlight the importance of PVAT in vascular function in normal physiology and metabolic diseases.

Disclosures: **A.H. Turaihi:** None. **Y.M. Smulders:** None. **V.W. van Hinsbergh:** None. **J.S. Yudkin:** None. **E.C. Eringa:** None.

164

The Effects of Resveratrol Treatment on Vascular Function in Type 2 Diabetes Mellitus

Ji-Yao Zhang, Monika Holbrook, Elika Inagaki, Bihua Feng, Dorae Ko, Robert M. Weisbrod, Reena Bastin, Margaret Stathos, Rosa Breton-Romero, Jessica Fetterman, Naomi M. Hamburg, Boston Univ Sch of Med Whitaker Cardiovascular Inst, Boston, MA

Patients with diabetes mellitus (DM) have abnormal vascular function characterized by premature aging and aortic stiffness. In animal models of metabolic disease, the plant-derived polyphenol, resveratrol, decreases arterial stiffness through SirT1 activation. Therefore, we hypothesized that resveratrol would improve vascular function and activate SirT1 in patients with DM. We performed a randomized, double-blind, placebo-controlled crossover study of resveratrol supplementation in 57 patients with DM (age 56±8 years, female 52%, African-American 67%, BMI 31.7±4.4 kg/m^2). Patients consumed resveratrol 100 mg/d for 2 weeks followed by 300 mg/d for 2 weeks or a matched placebo containing no polyphenols with a two-week wash-out period between treatments. In the overall study group, there was a trend toward lower carotid-femoral pulse wave velocity (CFPWV) with resveratrol treatment (P=0.18). In a subset of patients with high arterial stiffness at baseline, resveratrol treatment lowered CFPWV without a change in systemic blood pressure consistent with reduced central aortic stiffness (Figure). Brachial artery flow-mediated dilation, reactive hyperemia, and pulse amplitude tonometry did not change. In a subset of 7 patients, we collected venous endothelial cells by J-wire biopsy and observed a trend toward increased SirT1 activity with resveratrol treatment. Our findings suggest that resveratrol supplementation may reverse arterial stiffening in patients with DM potentially through activation of endothelial SirT1 activity.

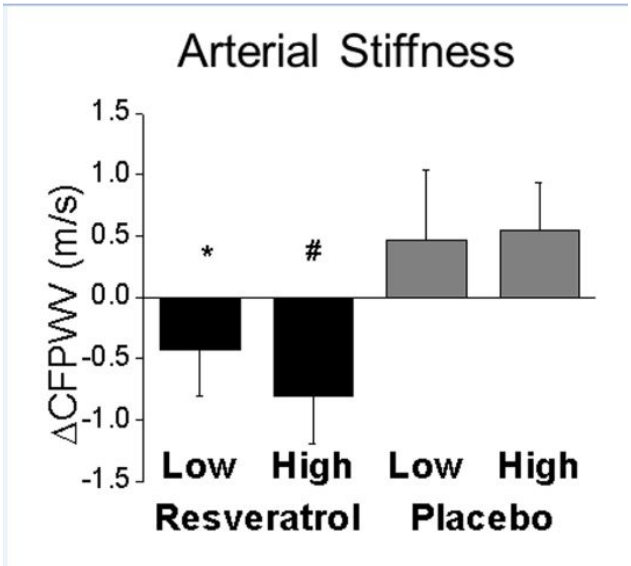

Disclosures: **J. Zhang:** None. **M. Holbrook:** None. **E. Inagaki:** None. **B. Feng:** None. **D. Ko:** None. **R.M. Weisbrod:** None. **R. Bastin:** None. **M. Stathos:** None. **R. Breton-Romero:** None. **J. Fetterman:** None. **N.M. Hamburg:** None.

This research has received full or partial funding support from the American Heart Association.

165

Functional Consequences of a Lysosomal Acid Lipase Variant Associated With Coronary Artery Disease

Trent D Evans, Reece Clark, In-Hyuk Jung, Arturo Alisio, Nathan O Stitziel, Babak Razani, Washington Univ in St. Louis, St. Louis, MO

Two tightly linked common intronic variants at the *LIPA* locus (which encodes for Lysosomal Acid Lipase - LAL) are present in nearly one-third of the population and are known to increase the risk of coronary artery disease (CAD) by 13-17% in large-scale genome-wide association studies. LAL mediates the hydrolysis of cholesteryl esters and patients with rare loss-of-function mutations develop hypercholesterolemia and CAD. However, these common *LIPA* variants are non-coding, not associated with lipid abnormalities, and result in increased *LIPA* transcripts in monocytes, a constellation of findings that has hindered further mechanistic understanding. We have discovered a previously unrecognized coding variant in tight linkage with the intronic variants that is equally associated with CAD risk. This coding variant involves a shift from a nonpolar to polar amino acid (T16P) in the predicted signal peptide region of LAL, providing a highly biologically plausible link to altered enzyme trafficking and function. We hypothesized that the coding variant is the causative SNP by altering LAL subcellular distribution and enzyme activity with functional consequences in lipid handling. In monocytes isolated from a large cohort of human patients, we show the coding variant leads to both increased *LIPA* mRNA expression and LAL enzyme activity in whole-cell lysates. To more precisely implicate the coding variant's effects on LAL function, we studied several *in vitro* overexpression models assessing the coding variant in the absence of the intronic variants. We show the T16P alteration is sufficient to alter LAL trafficking away from the lysosome with a portion favoring the secretory pathway. These findings have important implications for macrophage lipid handling in the atherosclerotic plaque and provide a novel mechanism for one of the most common genomic variants in cardiovascular disease.

Disclosures: **T.D. Evans:** None. **R. Clark:** None. **I. Jung:** None. **A. Alisio:** None. **N.O. Stitziel:** None. **B. Razani:** None.

166

Acceleration of Diabetic Wound Healing with Adipose Derived Stem Cells, Endothelial Differentiated Stem Cells and Topical Conditioned Medium Therapy in a Swine Model

Robin F. Irons, Kevin W. Cahill, Deviney A. Rattigan, Joseph H. Marcotte, Marc W. Fromer, Shaohua Chang, Ping Zhang, Kathryn C. Behling, Spencer A. Brown, Jeffrey P. Carpenter, Francis J. Caputo, Cooper Univ Hosp, Camden, NJ

Objectives: The goal of our study is to investigate the effect of adipose derived stem cells (ASCs), endothelial differentiated (ED) ASCs, and various conditioned medium (CM) on wound healing in a diabetic swine model.
Methods: Diabetes was induced in 4 male Yorkshire pigs via intravenous injection of 150 mg/kg Streptozotocin. Pig ASCs were harvested and cultured in either M199 or EGM-2 medium with 30 mm glucose. Fourteen circular dorsal wounds (5 cm diameter; 5 mm depth) were created. Duplicate wounds were treated with one of 4 cell-based therapies by injection of 5 million (M) ASCs, 10M ASCs, 5M ED ASCs, or 10M ED ASCs on day 0 and half the initial dose on day 15. Wounds assigned to the topical CM therapy were covered with 2 cc of either serum free M199 primed by ASCs or Human Umbilical Vein Endothelial Cells every 3 days. One set of wound was designated as control. Wounds were assessed at day 0, 10, 15, 20 and 28. Animals were sacrificed on day 28. Image J software was used to evaluate percent wound healing.
Results: On day 10, 15, 20 and 28 there was a significant increase in percent wound closure rates in both cell-based treatments when compared to control ($p<0.05$, **Figure 1**). All treatments displayed significant increase in wound closure rates on day 28 when compared to control. Histology revealed a decrease in dermal inflammatory cells and improved restoration of normal skin architecture in therapeutic treatment groups when compared to untreated controls.
Conclusions: Cellular therapy with ASCs, ED ASCs and topical CM accelerate diabetic wound healing in the swine model. Cellular therapy may provide the greatest benefit, as cells may continuously supply growth factors and adapt to the evolving microcellular environment as the wound progresses through the various phases of healing

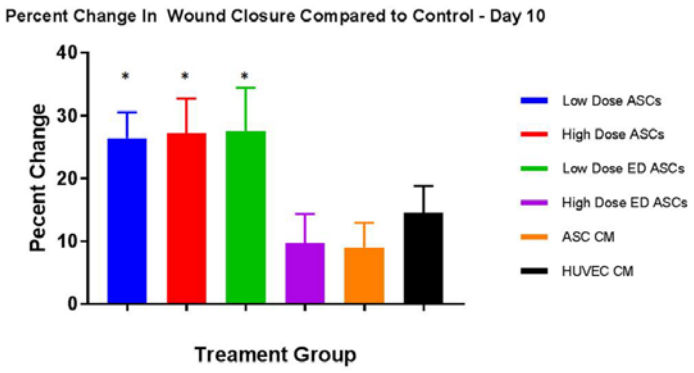

Disclosures: **R.F. Irons:** None. **K.W. Cahill:** None. **D.A. Rattigan:** None. **J.H. Marcotte:** None. **M.W. Fromer:** None. **S. Chang:** None. **P. Zhang:** None. **K.C. Behling:** None. **S.A. Brown:** None. **J.P. Carpenter:** None. **F.J. Caputo:** Research Grant; Significant; The Cooper Foundation Research Grant.

167

Vascular Tissue Engineering in Diabetes

Agneta Simionescu, Jhilmil Dhulekar, Zoltan Hajdu, Dan Simionescu, Clemson Univ, Clemson, SC

Tissue engineered blood vessels based on biological scaffolds seeded with autologous cells are currently being developed, but very little information exists regarding their fate in the complex diabetic environment. Diabetes is a major risk factor for vascular diseases as elevated levels of blood glucose and lipids interact irreversibly with long-lived proteins, such as collagen and elastin from the blood vessel wall, via oxidation and crosslinking, resulting in formation of advanced glycation end products (AGEs) and vascular

stiffening. Vascular cells respond to diabetic environment by dysfunction and pathological remodeling, contributing to the onset and progression of vascular disease. These changes result in activation of inflammation, impaired healing, fibrosis, and calcification. Our hypothesis is that by reducing the level of AGEs in the cell milieu and stabilizing the matrix, vascular cells will positively contribute to the vascular wall remodeling. Therefore, acellular scaffolds prepared from renal arteries were treated with penta galoyl glucose (PGG), an antioxidant elastin-binding polyphenol, and seeded with adipose stem cells (ASCs) isolated from streptozotocin-induced diabetic rats. Constructs were analyzed for AGE formation, inflammation, and calcification after subnormal implantation as autologous cell seeded grafts, as well as by end-to-end anastomoses to the aorta. PGG-treated scaffolds showed good patency, undetectable dilatation and well-preserved elastin. ASCs seeded on scaffolds diminished macrophage infiltration, while simultaneously allowed M2 macrophage polarization. PGG-treatment and ASC seeding inhibited scaffold calcification and expression of osteogenic proteins. In conclusion, the antioxidative properties of PGG and the immunomodulatory properties of ASCs prevented vascular wall deterioration under the hostile diabetic milieu.

Disclosures: **A. Simionescu:** None. **J. Dhulekar:** None. **Z. Hajdu:** None. **D. Simionescu:** None.

168

Role of Beta-Carotene Conversion to Vitamin a in Atherosclerosis

Jaume Amengual, Felix Zhou, Tessa J Barrett, New York Univ, New York City, NY; Johannes von Lintig, Case Western Reserve Univ, Cleveland, OH; Edward A Fisher, New York Univ, New York City, NY

Beta-carotene (BC) is the natural precursor of vitamin A, a potent gene regulator involved in cellular homeostasis and immune system. Vitamin A is formed by the action of the enzyme BC oxygenase 1 (BCO1), which is mostly expressed in the intestine and the liver. Whereas ingested BC is present in large amounts in human plasma and tissues, wild-type mice do not accumulate BC in significant amounts. To study the role of circulating BC and its conversion to vitamin A in atherosclerosis, we crossed *Ldlr*$^{-/-}$ mice with *Bco1*$^{-/-}$ mice. When compared to *Ldlr*$^{-/-}$mice, *Ldlr*$^{-/-}$/*Bco1*$^{-/-}$ mice fed a Western Diet containing BC (WD-BC) accumulate large amounts of BC in plasma, liver, and in atherosclerotic lesions. To study the role of BCO1 in the conversion BC to vitamin A in myeloid cells, as well as in plaque macrophages, we performed bone marrow transplant experiments (BMTs) using wild-type or *Bco1*$^{-/-}$ mice as a donor, and *Ldlr*$^{-/-}$/*Bco1*$^{-/-}$ as a recipient mice. After BMTs, recipient mice were fed WD-BC for 16 weeks. Gene expression analyses on circulating monocytes and T-cells of mice receiving *Bco1*$^{-/-}$ myeloid cells showed a pro-inflammatory phenotype in comparison to those that received wild-type cells (monocytes; IL-1β~1.5 fold increase, T-cells; FoxP3~1 fold decrease). Overall, these results indicate that BCO1 regulates the inflammatory status of myeloid cells through the conversion of circulating BC to vitamin A.

Disclosures: **J. Amengual:** Research Grant; Significant; Recipient of an AHA-SDG to study Beta-carotene & atherosclerosis. **F. Zhou:** None. **T.J. Barrett:** None. **J. von Lintig:** None. **E.A. Fisher:** None.

This research has received full or partial funding support from the American Heart Association.

169

A Non-Viral Functionalized Nanoparticle Based Hepatocyte-Targeting Cholesteryl Ester Hydrolase Gene Delivery Strategy for Potential Alleviation of Atherosclerosis

Hongliang He, Michael Lancina, Jing Wang, William Korzun, Hu Yang, Shobha Ghosh, Virginia Commonwealth Univ, Richmond, VA

Current atherosclerosis treatment strategies primarily focus on limiting further cholesteryl ester (CE) accumulation within the plaques by reducing plasma LDL-cholesterol levels (the primary source of plaque CE) using multiple strategies. No therapy is currently available to enhance the removal of CE, a crucial step to reduce the burden of existing disease. Increasing hepatic CE hydrolysis by adenovirus or transgene mediated over-expression of CE hydrolase (CEH) enhances final elimination of cholesterol from the body and is anti-atherosclerotic. In an effort to advance towards application of this anti-atherosclerotic strategy, in the present study we developed a non-viral hepatocyte-specific platform, namely, galactose-functionalized polyamidoamine (PAMAM) dendrimer G5.0 (Gal-G5) for delivery of CEH expression vector via the hepatocyte-specific asialoglycoprotein receptor (ASGPR). ASGPR is triggered by binding of galactose residues and facilitates receptor-mediated endocytosis of large molecules across

the hepatocyte plasma membrane. The data presented herein show increased specific uptake of Gal-G5 by hepatocytes *in vitro* (See Figure, Panel A) and liver *in vivo* (Panel B). Gal-G5 mediated delivery of CEH expression vector upregulated CEH expression in hepatocytes (Panel C), led to increased intracellular hydrolysis of HDL-CE and subsequent conversion/secretion of released FC into bile acids (Panel D). Gal-G5 mediated increased CEH expression in the liver significantly increased the flux of FC from HDL-CE into bile (Panel E) as well as feces (Panel F). These data are consistent with adenovirus or transgene-mediated over-expression of CEH and are likely to be anti-atherogenic. In conclusion, the development of this relatively non-toxic and efficient liver-specific gene delivery platform is an encouraging step towards clinical translation of strategies to enhance hepatic processes involved in final elimination of cholesterol from the body.

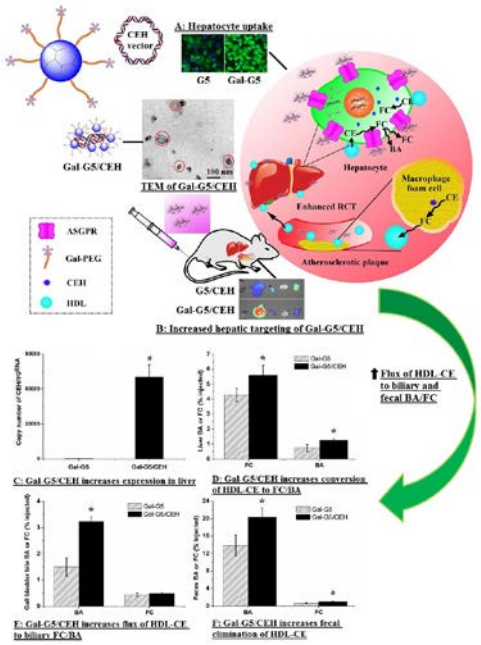

Disclosures: **H. He:** None. **M. Lancina:** None. **J. Wang:** None. **W. Korzun:** None. **H. Yang:** None. **S. Ghosh:** None.

170

Glucose Oxidation by Pyruvate Dehydrogenase Ameliorates Cradiomyocytes Contractility in Response to Hypoxic Stress

Dongyang Chu, Thomas Rousselle, Courtney Cates, **Ji Li**, Univ of Mississippi Medical Ctr, Jackson, MS

Introduction: Pyruvate dehydrogenase (PDH) plays a key role in aerobic energy metabolism and occupies a central crossroad between glycolysis and the tricarboxylic acid cycle. Dichloroacetate (DCA), a PDH activator, has been revealed to increase glucose oxidation and reduce myocardial infarct size during ischemia and reperfusion.
Hypothesis: Cardiac PDH activation plays a critical role in modulation of cardiomyocytes contractility and calcium signaling in response to hypoxia.
Methods: Mechanical properties and intracellular Ca^{2+} homeostasis were measured in isolated cardiomyocytes by IonOptix system. The stress signaling was evaluated using immunoblotting and immunoprecipitation analysis.
Results: PDH activator DCA treatment significantly protects cardiomyocytes from hypoxia-induced contractile dysfunction as measured by maximal velocity of shortening (+dL/dt) and relengthening (−dL/dt), peak height and peak shortening (PS) amplitude, time-to-90% relengthening (TR90) in cardiomyocytes. However, DCA treatment did not show any protective effects on contractile functions of isolated cardiomyocytes from the cardiomyocyte specific PDH KO mouse hearts under hypoxic conditions. Intriguingly, the rise of intracellular Ca^{2+} levels and intracellular ATP levels have no significant difference among wild type (WT) and PDH KO cardiomyocytes with and without DCA treatment. The results demonstrated that cardiomyocyte PDH KO does not affect cardiomyocyte contractility under

normal physiological conditions, but significantly impaired the contractile functions of isolated cardiomyocytes under hypoxic conditions. Furthermore, the immunoblotting results showed that hypoxia triggered phosphorylation of AMP-activated protein kinase (AMPK) in isolated cardiomyocytes, but the AMPK phosphorylation was significantly impaired in PDH KO cardiomyocytes. DCA treatment clearly augmented ischemic AMPK phosphorylation in the isolated wild type (WT) but not in PDH KO cardiomyocytes.
Conclusions: The glucose oxidation by pyruvate dehydrogenase (PDH) plays a critical role in cardiomyocyte contractility in response to hypoxic stress. PDH agonist DCA could be used for improve contractile function of cardiomyocytes under hypoxic insults.

Disclosures: **D. Chu:** None. **T. Rousselle:** None. **C. Cates:** None. **J. Li:** None.

This research has received full or partial funding support from the American Heart Association.

171

Lysosomal Response Tocholesterol Loading is Altered in DBA/2 Mouse Foam Cells Which May Explain Impairedautolysosome Formation and Lipid Droplets Clearance

Peggy Robinet, Alexander M Alzayed, Jonathan D Smith, Cleveland Clinic Fndn, Cleveland, OH

In a previous study, we identified autolysosome formation as the limiting step for turnover of cholesterol esters in lipid droplets of macrophage foam cells from the athero-sensitive DBA/2 strain compared to the athero-resistant AKR mouse strain. As autophagosome formation was similar in these two strains, we hypothesized that the lysosomal response to acetylated LDL (AcLDL) loading may be defective in DBA/2 vs. AKR foam cells. For all our studies, we cultured AKR and DBA/2 macrophages with or without AcLDL for 24h. AcLDL loaded DBA/2 vs. AKR cells exhibited a 40 to 50% decrease in lysosome number as measured by staining cells with Lysotracker or an anti-Lamp1 antibody, respectively. Lysosomal degradation capacity was assayed by cell incubation with Alexa647-DQ-ovalbumin, and we observed that AcLDL loading led to a 15% decrease in lysosomal capacity in DBA/2 foam cells ($p<0.001$) while it had no effect in AKR cells. Also, unloaded and loaded AKR cells had higher degradation capacity than DBA/2 cells (31% and 43%, respectively, $p<0.001$) which couldn't be explained by a change in lysosomal pH. As the transcription factor TFEB is a key regulator for lysosome biogenesis and function, we analyzed TFEB protein expression by western blot. Upon loading, TFEB was increased in AKR (48%) but not DBA/2 cells leading to a 45% higher TFEB level in AKR vs. DBA/2 foam cells ($p<0.05$). AKR and DBA/2 macrophages were labeled with a TFEB antibody and the nucleus to cytoplasm fluorescence intensity ratio was assessed. AcLDL loading led to a 37% increase in TFEB nuclear localization in AKR foam cells vs. unloaded cells ($p<0.001$) with no effect in DBA/2 macrophages. These results were confirmed by western blot after cellular fractionation. In conclusion, we found that DBA/2 vs. AKR foam cells have altered TFEB processing that may explain decreased lysosome number and function and impaired autolysosome formation in DBA/2 cells.

Disclosures: **P. Robinet:** None. **A.M. Alzayed:** None. **J.D. Smith:** None.

This research has received full or partial funding support from the American Heart Association.

172

Abcg1 Regulates Pulmonary Surfactant Metabolism in Mice and Men

Thomas Q de Aguiar Vallim, Elinor Lee, David J Merriott, Univ of California, Los Angeles, Los Angeles, CA; Christopher N Goulbourne, Columbia Univ, New York, NY; Joan Cheng, Angela Cheng, Univ of California, Los Angeles, Los Angeles, CA; Ayelet Gonen, Univ of California, San Diego, La Jolla, CA; Elisa N Palldino, Saint Louis Univ, St. Louis, MO; Katayun Barmak, Columbia Univ, New York, NY; David A Ford, Saint Louis Univ, St. Louis, MO; Tisha Wang, Univ of California, Los Angeles, Los Angeles, CA; Angel Baldan, Saint Louis Univ, St. Louis, MO; **Elizabeth J Tarling**, Univ of California, Los Angeles, Los Angeles, CA

Inflammation is a hallmark characteristic of many diseases, including atherosclerosis and respiratory distress, and it is also a stereotypical response of the innate immune system to pathogens. Given the central role both inflammation and lipid homeostasis play in disease progression, defining the immune and lipid signaling pathways is key in identifying new strategies for therapeutic intervention. The ATP

Binding Cassette (ABC) transporter ABCG1 is highly expressed in pulmonary type 2 cells, alveolar macrophages and immune cells. We, and others, have demonstrated that loss of ABCG1 attenuates atherosclerotic lesion progression, and profoundly impacts B cell and natural antibody homeostasis. ABCG1-deficient mice accumulate pulmonary surfactant, lamellar-body loaded type 2 cells, lipid-loaded macrophages, B-1 lymphocytes and immunoglobulins, clearly demonstrating the ABCG1 has a critical role in pulmonary homeostasis. We have identified a variant in the ABCG1 promoter in patients with pulmonary alveolar proteinosis, that results in impaired activation of ABCG1 by the liver X receptor alpha. We have generated mice that lack ABCG1 specifically in either type 2 cells or macrophages, and show that loss of ABCG1 from both cell types has specific effects on pulmonary lipid and immune homeostasis. These results establish a critical role for type 2 cell ABCG1 in controlling surfactant and lipid homeostasis in the lung and in the pathogenesis of human lung disease.

Disclosures: **T.Q. de Aguiar Vallim:** None. **E. Lee:** None. **D.J. Merriott:** None. **C.N. Goulbourne:** None. **J. Cheng:** None. **A. Cheng:** None. **A. Gonen:** None. **E.N.D. Palldino:** None. **K. Barmak:** None. **D.A. Ford:** None. **T. Wang:** None. **A. Baldan:** None. **E.J. Tarling:** None.

This research has received full or partial funding support from the American Heart Association.

174

The Use of Next-Generation Sequencing to Detect Copy Number Variation in the Molecular Diagnosis of Familial Hypercholesterolemia

Michael A Iacocca, Western Univ, London, ON, Canada; Jian Wang, Robarts Res Inst, London, ON, Canada; Jacqueline S Dron, Western Univ, London, ON, Canada; John F Robinson, Adam D McIntyre, Matthew R Ban, Robarts Res Inst, London, ON, Canada; Henian Cao, Western Univ, London, ON, Canada; Robert A Hegele, Robarts Res Inst, London, ON, Canada

Background: Familial hypercholesterolemia (FH) is a common monogenic disorder of lipoprotein metabolism, characterized by elevated LDL cholesterol and increased risk for premature cardiovascular disease. Efforts to provide a molecular diagnosis of FH are trending towards the use of targeted next-generation sequencing (NGS) panels to interrogate canonical FH-associated genes—*LDLR*, *APOB*, and *PCSK9*—for clinically relevant small-scale variants. However, large-scale copy number variants (CNVs) or "deldup" variants constitute 10-15% of *LDLR* variants in many cohorts. Because these are not routinely accessible by NGS, a second assay, namely multiplex-ligation dependent probe amplification (MLPA), is currently required to screen for them. To increase efficiency and decrease costs associated with identifying the genetic causes for FH, use of a single platform to detect both small and large-scale variants would be extremely beneficial in a clinical setting.
Objective: Here we determine the accuracy of NGS bioinformatic tools in identifying CNVs.
Methods: In 313 clinically ascertained, unrelated patients with at least possible FH per the Dutch Lipid Clinic Network (DLCN) criteria, we sequenced canonical FH-associated genes using our targeted NGS panel (LipidSeq™). These patients were also assayed using MLPA. The CNV analysis tool (VarSeq® Golden Helix, Inc.) was run using the NGS data generated for each patient. Concordance between the NGS tool and standard MLPA was subsequently determined.
Results: We evaluated a subset of 99 FH individuals: 19 were positive while 80 were negative for a *LDLR* mutation using MLPA. Our CNV analysis using bioinformatically processed NGS data compared to MLPA yielded 2 out of 19 false negatives and 0 out of 80 false positives. This translates to a sensitivity of 89% and a specificity of 100% for our NGS approach, considering MLPA as the current 'gold standard'.
Conclusions: Analysis of deeply resequenced targeted NGS data for the identification of CNVs in FH shows excellent potential to become a standard diagnostic test for those with suspected FH, potentially eliminating the need for secondary MLPA analysis. Future applications of this NGS tool may also allow for novel CNV screening in additional FH-associated genes.

Disclosures: **M.A. Iacocca:** None. **J. Wang:** None. **J.S. Dron:** None. **J.F. Robinson:** None. **A.D. McIntyre:** None. **M.R. Ban:** None. **H. Cao:** None. **R.A. Hegele:** None.

175

Glycosylated Hemoglobin is Associated with Coronary Plaque Burden in Psoriasis Beyond Cardiovascular Risk Factors

Jonathan H Chung, Anshuma Rana, Amit K Dey, Joshua P Rivers, Abhishek Chaturvedi, Joseph B Lerman, Justin A Rodante, Charlotte L Harrington, Martin P Playford, Marcus Y Chen, David A Bluemke, Nehal N Mehta, NIH, Bethesda, MD

Introduction: Psoriasis (PSO), a chronic inflammatory disease associates with increased metabolic and cardiovascular (CV) risk. Dysglycemia may contribute to the increased risk of CV disease observed in psoriasis. Therefore, the aim of this study was to characterize whether dysglycemia assessed by hemoglobin A1c (HbA1c) is associated with subclinical coronary artery disease in psoriasis.
Hypothesis: We hypothesized that total burden (TB) of coronary artery plaque and non-calcified burden (NCB) would be associated with HbA1c values in psoriasis independent of cardiovascular risk factors.
Methods: Consecutive psoriasis patients (n=103) and age and sex matched controls (n=42) underwent CCTA (Toshiba, 320-detector row) for coronary plaque characterization. TB and NCB were quantified using QAngio (Medis, The Netherlands). Fasting blood samples were collected on the same day to get HbA1c values. The relationship of HbA1c with TB and NCB was analyzed using multivariable regression models (STATA 12).
Results: PSO patients were middle-aged, predominantly male, had a low CV risk by FRS and had mild to moderate skin disease (Table 1). HbA1c levels were elevated in psoriasis compared to controls (P=0.007). Furthermore, total (P=0.02) and non-calcified (P=0.04) burden were elevated in psoriasis as compared to controls. HbA1c directly associated with TB (β=0.21; P=0.001) and NCB (β=0.18; P=0.004); a relationship which persisted beyond CV risk factors (TB and NCB: β *=0.22;* P=0.01).
Conclusions: HbA1c was associated with total and non-calcified burden in psoriasis population independent of CV risk factors. These findings underscore the importance of screening for glycemic abnormalities to mitigate CV disease risk in patients with psoriasis.

Table 1: Demographics and clinical data of study groups.

Parameter	Psoriasis (n=103)	Control (n=42)	p value
Demographics and medical history			
Age, years	48.4 ± 12.5	40.2 ± 13.4	matched
Male	63 (61)	28 (67)	matched
Ethnicity, whites	79 (77)	31 (74)	---
Hypertension	21 (20)	8 (19)	0.86
Hyperlipidemia	36 (35)	12 (29)	0.46
Type 2 diabetes mellitus	9 (9)	3 (7)	0.75
Current smoker	14 (14)	1 (2)	**0.04**
Lipid treatment	28 (27)	8 (19)	0.30
Waist-to-hip ratio	0.97 (0.92-1.03)	0.94 (0.89-0.98)	**0.045**
Clinical and laboratory values			
Systolic blood pressure, mmHg	120.9 ± 14.9	110.8 ± 10.2	**<0.001**
Framingham risk score	2 (1-4)	1 (1-4)	0.05
Total cholesterol, mg/dL	182.8 ± 40.6	179.2 ± 37.2	0.31
HDL cholesterol, mg/dL	56.5 ± 17.4	57.2 ± 17.9	0.41
LDL cholesterol, mg/dL	103.2 ± 31.7	95.9 ± 30.7	0.10
Triglycerides, mg/dL	97 (68-141)	93 (73-140)	0.90
HbA1c, %	5.6 ± 0.6	5.4 ± 0.5	**0.007**
Insulin, mIU/mL	15.2 ± 15.8	12.5 ± 10.5	0.15
Glucose, mg/dL	100.6 ± 15.4	93.0 ± 10.9	**0.002**
HOMA-IR	2.6 (1.5-4.6)	2.3 (1.3-3.4)	0.17
Psoriasis Severity and Treatment			
PASI score	7.7 (5.2-13.2)	---	---
Systemic/biologic treatment	32 (31)	---	---
Coronary Burdens			
Total burden, mm^2 (X100)	1.12 ± 0.43	1.02 ± 0.35	**0.02**
Non-calcified burden, mm^2 (X100)	1.09 ± 0.43	1.01 ± 0.36	**0.04**
Dense calcified burden, mm^2 (X100)	0.03 ± 0.06	0.01 ± 0.02	**0.02**

All values are expressed as Mean ± SD and Median (IQR) for continuous variables and N (%) for categorical variables. t-test and Mann-Whitney test for continuous variables, Pearson's Chi-square test for categorical variables. HOMA-IR: Homeostasis model assessment of insulin resistance. PASI: Psoriasis area severity index.

Disclosures: **J.H. Chung:** None. **A. Rana:** None. **A.K. Dey:** None. **J.P. Rivers:** None. **A. Chaturvedi:** None. **J.B. Lerman:** None. **J.A. Rodante:** None. **C.L. Harrington:** None. **M.P. Playford:** None. **M.Y. Chen:** None. **D.A. Bluemke:** None. **N.N. Mehta:** None.

179

Computational Modelling Of Early Atherosclerotic Plaque Structure Reveals The Role Of The Rate Of Lipid Deposition On Plaque Structure And Growth Rate

Ishraq Uddin, Mary R Myerscough, Univ of Sydney, Sydney, Australia

Much current research on inflammation in atherosclerosis focuses on specific cellular and biochemical processes as isolated phenomena. There is scope, therefore, for an integrated approach that examines the interactions between the various mechanisms involved in early plaque growth. An in silico modelling approach is promising in this regard as multiple biological processes can easily be incorporated into the model and used to simulate early plaque growth under a variety of conditions. We present a computational model to simulate early plaque growth and test the hypothesis that higher rates of lipid deposition in the artery wall will cause accelerated plaque growth and influence the plaque's morphology and composition.
We formulate a mathematical model based on the observed interactions between macrophages, pro-atherogenic extracellular lipid, lipid accumulated by macrophages, and apoptotic cells/cellular debris. This basic model incorporates several key processes including monocyte recruitment, phagocytosis, proliferation, apoptosis, lipid cytotoxicity, and cell migration. The model is used to computationally simulate how the early development of the plaque is influenced by its physiological environment, focusing in particular on the rate of lipid influx into the artery wall. Individual simulations yield a profile of how cells and lipids are spatially distributed over the plaque, and how this distribution and the total plaque size evolve in time.
The model qualitatively suggests that the rate of lipid deposition has a key influence on early plaque morphology and behaviour. Specifically, increasing the rate of lipid deposition (simulating higher fat diets) accelerates the rate of plaque growth. The ratio of apoptotic cells to active macrophages also increases with distance from the endothelium, with the ratio becoming more pronounced in older plaques. The computational model provides a novel methodology with which to capture the dynamics and structure of early atherosclerotic plaques, and provides a foundation on which to build models that can account for further aspects of the relevant biology, including plaque regression and necrotic core formation.

Disclosures: **I. Uddin:** None. **M.R. Myerscough:** Research Grant; Significant; Dynamics of atherosclerotic plaque formation, growth and regression; Myerscough M, Macaskill C; Australian Research Council (ARC)/Discovery Projects (DP)., Continuum models of atherosclerotic plaques; Myerscough M, Byrne H; DVC Research/International Research Collaboration Award (IRCA)..

180

Chronic Myelogenous Leukemia Cell Viability is Differentially Regulated by LXR Activation, HDL-associated Proteins, and LDL

Catherine J Andersen, Lydia Dupree, Adam Doerr, Layra Cintron-Rivera, Kristina Murray, Nicholas Ragonesi, Fairfield Univ, Fairfield, CT

LXR activation and HDL exert anti-cancer effects, albeit to varying degrees depending on cancer type and model. One of the mechanisms by which LXR and HDL impair cancer cell growth is through mediation of cellular cholesterol and phospholipid efflux, thereby limiting the availability of essential lipids for rapidly proliferating cells. Thus, the variability in LXR- and HDL-mediated anti-cancer effects may in part be due to differences in 1) HDL functionality and 2) the ability to induce expression of LXR target genes involved in lipid efflux and homeostasis due to adaptive shifts in cancer cell metabolism. Interestingly, serum amyloid A (SAA), a pro-inflammatory acute phase protein shown to be elevated in cancer, infection, and obesity, has recently been shown to differentially increase and decrease cholesterol efflux, despite its ability to displace apoA1 on HDL. Therefore, we investigated the effects of LXR activation, lipoproteins (HDL and LDL) and HDL-associated proteins (apoA1 and SAA) on the viability of chronic myelogenous leukemia cells - a cancer model previously unstudied in regards to cholesterol metabolism. Treatment of cells with the LXR agonist TO901317 (1μM, 5μM, and 10μM) significantly increased ABCA1 mRNA expression at 24hr and 72hr, in addition to dose-dependently decreasing HMG-CoA reductase and anti-apoptotic Bcl-xL mRNA expression. Changes in TO901317-induced gene expression corresponded to time- (24hr, 48hr, 72hr) and dose-dependent decreases in cell viability and average cell size. Interestingly, the addition of HDL to cell cultures with or without TO901317 treatment did not affect K562 cell viability, whereas LDL dose-dependently increased cell viability. Conversely, human-derived apoA1 (25 μg/mL) or HDL + apoA1 drastically reduced TO901317-treated

K562 cell viability after 48hr and 72hr. K562 cell viability was modestly decreased by SAA (10 µg/mL) treatment, with greater decreases observed in cells treated with SAA + HDL. These findings suggest that LXR activation, HDL-associated proteins, and LDL differentially regulate chronic myelogenous leukemia cell viability.

Disclosures: **C.J. Andersen:** None. **L. Dupree:** None. **A. Doerr:** None. **L. Cintron-Rivera:** None. **K. Murray:** None. **N. Ragonesi:** None.

181

Insulin Receptor Signaling Regulates ApoA-I Secretion from Hepatocytes

Ailing Ji, Xuebing Wang, Lisa Bennett, David B Graf, Gregory A Graf, Deneys R van der Westhuyzen, Univ of Kentucky, Lexington, KY

The aim of the study was to assess the effect of insulin receptor (IR) signaling on hepatic apoA-I metabolism. The experimental approach was to compare hepatic apoA-I expression, secretion and cellular localization in IRfl/fl mice and LIRKO mice in which hepatic insulin receptors were specifically deleted by AAV delivered Cre-recombinase. Results showed that IR mRNA and protein levels were markedly reduced in the livers of LIRKO mice compared to control IRfl/fl mice. As expected, LIRKO mice exhibited decreased glucose tolerance and reduced hepatic insulin signaling. Knockdown of hepatic IR decreased plasma HDL cholesterol and apoA-I levels. Whereas apoA-I mRNA levels were similar in LIRKO and control hepatocytes, apoA-I protein levels were increased in both the liver and primary hepatocytes isolated from LIRKO mice. In contrast to apoA-I, apoE and apoB protein levels in the liver and in cultured hepatocytes, as well as in the plasma, were similar in LIRKO and control mice. ApoA-I accumulation in LIRKO hepatocytes was associated with a decreased rate of apoA-I secretion. Immunofluorescence staining demonstrated that apoA-I accumulated in LIRKO hepatocytes in membrane bound inclusions. These inclusions shared markers characteristic of early, late and recycling endosomes, and of lysosomes. We conclude that IR-mediated insulin signaling plays an important role in hepatic apoA-I secretion and consequent nascent HDL formation. Reduced apoA-I secretion from liver into the circulation may contribute to the lower HDL levels typically associated with insulin resistance.

Disclosures: **A. Ji:** None. **X. Wang:** None. **L. Bennett:** None. **D.B. Graf:** None. **G.A. Graf:** None. **D.R. van der Westhuyzen:** None.

182

Use of a Nanoparticle Delivery System to Rescue Macrophage Lysosomal Dysfunction in Atherosclerosis

Xiangyu Zhang, Washington Univ Sch of Med, St. Louis, MO; Guru Raja Vulugundam, Univ of Illinois at Urbana-Champaign, Urbana, IL; Gregory Lanza, Washington Univ Sch of Med, St. Louis, MO; Dipanjan Pan, Univ of Illinois at Urbana-Champaign, Urbana, IL; Babak Razani, Washington Univ Sch of Med, St. Louis, MO

Atherosclerotic vascular disease remains the leading cause of death in the United States with the majority of mortality due to coronary artery disease and myocardial infarction. Dysfunction in the macrophage lysosomal system, such as reduced acidity or diminished lysosomal degradative capacity, inhibits the clearance of excess cellular debris or atherogenic lipids present in atherosclerotic plaques and has emerged as an important contributor to plaque progression. Thus, devising strategies to rescue this macrophage lysosomal dysfunction is a novel therapeutic measure. Nanoparticles are subcellular spherical structures ranging from 1-100 nm in size and prepared from natural or synthetic polymers. Injected nanoparticles tend to undergo opsonization, a process which favors macrophage binding, internalization by phagocytosis, and trafficking to lysosomes. In order to use nanoparticles as a macrophage lysosome delivery platform, we developed acid-eluting PLGA (poly-Lactide-co-Glycolic acid) or PLA (polylactic acid) nanoparticles to both maintain lysosomal acidity as well as potentially deliver encapsulated lysosomal enzymes to macrophages in vitro and in vivo. We show that fluorescence-labeled PLGA nanoparticles can be successfully trafficked to lysosomes of murine bone marrow derived macrophages and rescue increases in lysosomal pH instigated by Bafilomycin A1, a disruptor of lysosomal proton gradient. This lysosomal acidification can also rescue the degradative capacity of macrophage lysosomes as gauged by enhanced proteolysis of fluorescent-conjugated ovalbumin. Finally, we demonstrate that acidic nanoparticles injected intravenously into mice can be internalized in splenic

macrophages as well as macrophages of the atherosclerotic plaque. Taken together, our data support the use of this technology as a strategy to rescue macrophage lysosomal dysfunction in the treatment of atherosclerosis.

Disclosures: **X. Zhang:** None. **G.R. Vulugundam:** None. **G. Lanza:** None. **D. Pan:** None. **B. Razani:** None.

183

Loss of Notch1 Signaling in Endothelial Cells Suppresses Progression of Atherosclerosis

Zhao-Jun Liu, Yan Li, Leiming Zhang, Manuela M Regueiro, Yuntao Wei, Omaida C Velazquez, Univ of Miami, Miami, FL

Introduction. Notch signaling plays pivotal roles in vascular development and cardiovascular disease. Our previous studies showed that the Notch pathway is activated in luminal endothelial cells (EC) at atherosclerotic plaques and results in pro-inflammatory response and senescence of EC, implicating a potential involvement of Notch signaling in atherosclerosis. Here, we investigate the role of Notch signaling in atherosclerosis using genetic mouse model with inducible endothelial cell-specific Notch1 gene deletion on an ApoE-deficient background.
Methods. A genetically engineered mouse model, *Notch1*$^{FLOX/FLOX}$*/VE-cadherin-CreER*^{T2}*/ApoE*$^{-/-}$*,* which is a Tamoxifen-inducible endothelial cell-specific Notch1 gene knockout mouse on atherosclerosis-prone ApoE-deficient background, was established. Mice were fed with high-fat-diet (HFD) along with or without Tamoxifen treatment (i.p. 2 mg/day for 5 consecutive days) starting from 4-wk old and terminated on 16-wk old. Aortas were harvested to study the effects of loss of Notch1 signaling in endothelial cells on the progression of aortic atherosclerosis. Deletion of Notch1 in endothelial cells was validated by immunostaining. Aortic plaque burden was evaluated by quantification of proportion of total aorta containing atherosclerosis detected by Oil-Red-O and hematoxylin-eosin staining using computer-aided image analysis. Blood was tested to measure lipid profile.
Results. Notch1 is deleted from endothelial cells in Tamoxifen-treated mice. Loss of endothelial Notch1 signaling significantly decreased aortic plaque burden [n=10 (Tamoxifen -) and 12 (Tamoxifen +), $P<0.05$]. The serum levels of total cholesterol, HDL, LDL, triglycerides and glucose were comparable between Tamoxifen-treated and -untreated mice.
Conclusions. Inactivation of endothelial Notch1 signaling inhibits atherosclerotic plaque formation. The decrease in atherosclerosis was not due to changes in the serum levels of total cholesterol, HDL, LDL, triglycerides and glucose. Our findings demonstrate that loss of Notch1 signaling in endothelial cells suppresses progression of atherosclerosis. It highlights Notch1 signaling as an emerging therapeutic target for the treatment of atherosclerosis.

Disclosures: **Z. Liu:** None. **Y. Li:** None. **L. Zhang:** None. **M.M. Regueiro:** None. **Y. Wei:** None. **O.C. Velazquez:** None.

184

Adenylate Cyclase Type 9 Promotes Atherosclerosis in Mice

Yohann Rautureau, Vanessa Deschambault, Geneviève Brand, Marie-Eve Higgins, Mélanie Mecteau, Kurunradeth Uy, Daniel Rivas, Samaneh Samami, Gaétan Mayer, Eric Rhéaume, Jean-Claude Tardif, Montreal Heart Inst, Montreal, QC, Canada

Polymorphisms in the ADCY9 gene, coding for adenylate cyclase type 9, determine atherosclerotic cardiovascular responses to the CETP inhibitor dalcetrapib in patients. ADCY9 is broadly expressed and involved in various immune cell functions and inflammatory responses. Our objective is to determine the role of ADCY9 in the development of atherosclerosis in the absence of CETP.
We used 8-12 week-old wild-type (WT, n=25) or *Adcy9*-inactivated (*Adcy9*^{Gt}, n=21) male mice. To induce hypercholesterolemia and atherosclerosis, mice were infected with an adeno-associated virus coding for a gain-of-function mutant of *Pcsk9* (*Pcsk9*^{D377Y}) and were fed an atherogenic high-cholesterol diet for 16 weeks in absence or presence of dalcetrapib treatment (200 mg/kg/day). Percent atherosclerotic lesion area (PALA) in the whole aorta was quantified using *en face* Oil Red O plaque staining. We used VCAM-1 immunofluorescence staining (n=6 per group) in atherosclerotic lesions of the aortic root to quantify inflammation. We also measured aortic root accumulation of macrophages and vascular smooth muscle cells by immunofluorescence imaging of CD68 and smooth muscle actin (SMA), respectively, in plaque

lesions. We also quantified blood leukocytes in normocholesterolemic WT and *Adcy9*^{Gt} mice by flow cytometry analysis of CD45^{+} cells.
In hypercholesterolemic animals, *Adcy9*^{Gt} mice showed a 60% decrease in atherosclerotic lesions (PALA: 2.7±0.5%) compared to WT mice (6.5±0.7%, P<0.01). Dalcetrapib treatment, in these mice without CETP, did not modify significantly the reduction (63%) of PALA in *Adcy9*^{Gt} mice (2.9±0.4%) compared to WT (7.6±1.6%, P<0.01). Macrophage content was reduced by 55% from 17.8±2.8% in WT to 7.2%±1.9% in *Adcy9*^{Gt} mice (P<0.05), while SMA staining was similar. VCAM-1 expression also tended to be decreased, from 5.7±3.3% in WT to 2.0±0.4% in *Adcy9*^{Gt} mice (P=0.0598). CD45^{+} blood leukocytes were reduced by 35.4% in *Adcy9*^{Gt} compared to WT normocholesterolemic mice (P<0.01).
Adcy9 inactivation in mice (without CETP) results in large reductions of atherosclerosis and plaque macrophage and in decreased VCAM-1 expression. These results support the ADCY9 genotype-dependent clinical effects of dalcetrapib.

Disclosures: **Y. Rautureau:** None. **V. Deschambault:** None. **G. Brand:** None. **M. Higgins:** None. **M. Mecteau:** None. **K. Uy:** None. **D. Rivas:** None. **S. Samami:** None. **G. Mayer:** None. **E. Rhéaume:** None. **J. Tardif:** Research Grant; Significant; Amarin, Astra-Zeneca, DalCor, Eli Lilly, Esperion, Ionis, Merck, Pfizer, Roche, Sanofi, Servier. Honoraria; Significant; DalCor, Pfizer, Sanofi, Servier. Other; Modest; Patent genotype dependent effects of dalcetrapib, Equity in DalCor.

185

Transgenic Overexpression of Alanine-glyoxylate Aminotransferase 2 in Mice Lowers Asymmetric Dimethylarginine and Improves Vasomotor Function

Roman N. Rodionov, Univ Ctr for Vascular Med, Technische Univ Dresden, Dresden, Germany; Dmitri Burdin, Dept of General Physiology, Saint-Petersburg State Univ, Saint-Petersburg, Russian Federation; Silke Brilloff, Univ Ctr for Vascular Med, Technische Univ Dresden, Dresden, Germany; Vladimir Todorov, Dept of Nephrology, Technische Univ Dresden, Dresden, Germany; Natalia Jarzebska, Univ Ctr for Vascular Med, Technische Univ Dresden, Dresden, Germany; Jens Martens-Lobenhoffer, Inst of Clinical Pharmacology, Otto-von-Guericke Univ, Magdeburg, Germany; Anja Hofmann, Henning Morawietz, Div of Vascular Endothelium and Microcirculation, Technische Univ Dresden, Dresden, Germany; Karl Hilgers, Nada Cordasic, Johannes Jacobi, Dept of Nephrology and Hypertensiology, Univsklinikum Erlangen, Erlangen, Germany; Renke Maas, Inst of Clinical and Experimental Pharmacology and Toxicology, Friedrich-Alexander Univ, Erlangen, Germany; YingJie Chen, Cardiovascular Div, Dept of Med, Univ of Minnesota, Minnesota, MN; Stefanie M. Bode-Böger, Inst of Clinical Pharmacology, Otto-von-Guericke Univ, Magdeburg, Germany; Christian P. Hugo, Bernd Hohenstein, Dept of Nephrology, Technische Univ Dresden, Dresden, Germany; Norbert Weiss, Univ Ctr for Vascular Med, Technische Univ Dresden, Dresden, Germany

Background: It has been demonstrated in various studies that ADMA (asymmetric dimethylarginine), an inhibitor of nitric oxide synthase, is associated with the increased risk of cardiovascular diseases. There are two known pathways of ADMA metabolism: hydrolysis to citrulline by dimethylarginine dimethylaminohydrolases (DDAH) and transamination by alanine-glyoxylate aminotransferase 2 (AGXT2) with formation of asymmetric dimethylguanidino valeric acid (ADGV). The second pathway is still poorly understood. The goal of the current study was to test the hypothesis that transgenic overexpression of AGXT2 leads to lowering of plasma levels of ADMA and improvement of vasomotor function. **Methods and Results**: We generated transgenic mice (TG) with ubiquitous overexpression of *AGXT2* under control of the chicken beta actin (CAG) promoter. qPCR and Western Blot were used to confirm the ubiquitous expression of the transgene. HPLC-MS/MS was used to generate biochemical data. Systemic ADMA levels were decreased by 15% (p<0.05) in the TG mice, whereas ADGV plasma levels were six times higher in comparison with wild type animals (p<0.001). Heart and lung of TG animals exhibited 2 times lower tissue ADMA content in comparison with wild type littermates (p<0.05). In further experiments, we crossed the AGXT2 TG mice with DDAH1 KO mice and showed that upregulation of AGXT2 protects DDAH1 KO mice from elevation of plasma ADMA levels and restores endothelium-dependent vasodilation in aortic rings. In the current experiments we are assessing whether AGXT2 overexpression also protects DDAH1 KO mice from hypertension. **Conclusion**: In the current study we demonstrated that upregulation of AGXT2 leads to lowering of ADMA levels and improvement of endothelium-dependent relaxation *in vivo* in the settings of DDAH1 deficiency. AGXT2 thereby may be a potential drug target for long-term reduction of systemic ADMA levels in cardiovascular pathologies. This is especially important, because all the efforts to develop pharmacological ADMA-lowering interventions by means of upregulation of DDAH have not been successful so far.

Disclosures: **R.N. Rodionov:** None. **D. Burdin:** None. **S. Brilloff:** None. **V. Todorov:** None. **N. Jarzebska:** None. **J. Martens-Lobenhoffer:** None. **A. Hofmann:** None. **H. Morawietz:** None. **K. Hilgers:** None. **N. Cordasic:** None. **J. Jacobi:** None. **R. Maas:** None. **Y. Chen:** None. **S.M. Bode-Böger:** None. **C.P.M. Hugo:** None. **B. Hohenstein:** None. **N. Weiss:** None.

186

Cyp8b1 Ablation Prevents Western Diet-Induced Weight Gain and Hepatic Steatosis due to Impaired Fat Absorption

Enrico Bertaggia, Columbia Univ, New York, NY; Kristian K Jensen, Jose Castro-Perez, Merck Res Labs, Kenilworth, NJ; Yimeng Xu, Robin B Chan, Columbia Univ, New York, NY; Liangsu Wang, Merck Res Labs, Kenilworth, NJ; Rebecca A Haeusler, Columbia Univ, New York, NY

Bile acids (BAs) are cholesterol derivatives that are well-known for their role in facilitating intestinal lipid absorption. Furthermore, they can regulate glucose and lipid metabolism by activating nuclear and cell surface receptors. Insulin resistance is correlated with alterations in bile acid composition, in particular higher levels of 12α-hydroxylated BAs. These BA species are generated by the enzyme Cyp8b1. We hypothesized that elevated levels of 12α-hydroxylated BAs could be a link between insulin resistance and defects of lipid metabolism. To study the role of Cyp8b1 in the regulation of lipid metabolism, we used Cyp8b1 deficient mice-which are unable to produce 12α-hydroxy BAs-and challenged them with a western type diet. We found that Cyp8b1-/- mice gained less weight compared to controls, which was entirely accounted for by fat mass. Triglyceride and cholesterol accumulation in the liver of Cyp8b1-/- mice were also strongly reduced. We found that these improvements were due to reduced lipid absorption in the intestine of Cyp8b1-/- mice, which could be rescued by replenishing the pool with taurocholic acid. The lipid malabsorption resulted in higher caloric excretion in the feces, due to excess excretion of hydrolyzed dietary lipids. When we fed the mice with a fat-free diet, these differences between genotypes were normalized, confirming the central role of BA composition-not just overall levels-in intestinal lipid absorption and whole-body lipid homeostasis. Based on these findings, it is possible that reducing 12α-hydroxy BAs could be a therapeutic option for the control of obesity and lipid homeostasis.

Disclosures: **E. Bertaggia:** None. **K.K. Jensen:** Employment; Modest; Merck employee. **J. Castro-Perez:** Employment; Modest; Merck Employee. **Y. Xu:** None. **R.B. Chan:** None. **L. Wang:** Employment; Modest; merck employee. **R.A. Haeusler:** None.

187

Genetic Targeting at Apolipoprotein E Locus to Knockdown Scavenger Receptor Class B Type I in Mice: Characterization of a Novel Mouse Model of Coronary Heart Disease

Hong Chen, Sheng Hu, Xing Yu Huo, Li Yuan Zhu, Qing Wan, Xiao Yan Ma, Chuan Sheng Xu, Hui Feng Hao, Fuwai Hosp, Beijing, China; Wei Jun Jin, SUNY Downstate Medical Ctr, NY, NY; Miao Wang, Fuwai Hosp, Beijing, China

Background—Scavenger Receptor Class B Type I (SRBI) is the key player mediating HDL-dependent reverse cholesterol transport (RCT) in hepatocyte, and SRBI mutation causes coronary heart disease (CHD) in humans. Mice lacking SRBI and apolipoprotein E (apoE), fed on chow diet, develop cardinal features of CHD and succumb to premature death. However, the application of this model is limited due to the short lifespan, early onset of CHD symptom, the difficulty to maintain genetic mutations at two different loci, and infertility. The latter may be related to adrenal SRBI deficiency. Methods and Results—A genetic mouse model, named as $SRBI^{KD}$ $ApoE^{-/-}$ was produced by using CRISPR/Cas9 technique, in which an SRBI knock-down cassette (at both mRNA and proteins levels) is inserted downstream of the indogenous apoE promoter, thus abolishing apoE expression. Real-time PCR and Western blot characterization showed that SRBI expression in liver was significantly reduced (33% vs. 100% by RT-PCR, 0.5% vs. 100% by WB, P<0.001), but no significant difference was found in other examined tissues. $SRBI^{KD}$ $ApoE^{-/-}$ mice are fertile and do not exhibit pre-mature cardiovascular death on chow diet up to 10 months. Compared to $ApoE^{-/-}$ mice, $SRBI^{KD}$ $ApoE^{-/-}$ mice showed significant increase in serum HDL-C (3.11 vs 1.70 mmol/L, P<0.01), whereas serum triglyceride or LDL-C was similar (triglyceride: 0.87 vs. 0.9 mmol/L; LDL-C: 8.35 vs. 7.74 mmol/L). When treated with high-fat diet (HFD: 21% fat, 0.2% cholesterol in weight, n=6/group) for 8 weeks (starting at 8-week old), $SRBI^{KD}$ $ApoE^{-/-}$ mice gained significantly more

weight than ApoE$^{-/-}$ mice(P<0.05 for females), and exhibited higher weight ratio of heart to body than that of ApoE$^{-/-}$ mice (females: 6.51% vs. 5.16%, P=0.051; males: 6.54% vs. 4.64%, P<0.01). Splenomegaly was observed more frequently in these mice than in ApoE$^{-/-}$ mice (females: 17.7% vs. 5.99%, P<0.001; males: 6.12% vs. 3.99%, P<0.01).

Disclosures: **H. Chen:** None. **S. Hu:** None. **X.Y. Huo:** None. **L.Y. Zhu:** None. **Q. Wan:** None. **X.Y. Ma:** None. **C.S. Xu:** None. **H.F. Hao:** None. **W.J. Jin:** None. **M. Wang:** None.

188

Angiopoietin-Like Protein 4 is a HDL Component For HDL Metabolism snd Function in Non-Diabetic Participants and Type-2 Diabetic Patients

Longyan Yang, Caiguo Yu, Xuhong Wang, Shasha Yuan, Lijie Zhang, Jianan Lang, Dong Zhao, **Yingmei Feng**, Beijing Key laboratory of Diabetes Prevention and Res, Beijing, China

Objectives: Angiopoietin-like protein 4 (angptl4) is a potent lipoprotein lipase inhibitor and present in HDLs in mice and human. Plasma levels of ANGPTL4 were increased in type-2 diabetic (T2DM) patients. However, it is not defined whether ANGPTL4 in HDLs could participate in HDL metabolism and affect its function in T2DM. Methods: Non-diabetic (n=201) and T2DM patients (n=185) were analyzed in the study. Angptl4 levels in the circulation and HDLs were quantified by ELISA. HDL components were measured. HDLs were isolated to assess cholesterol efflux or subjected to endothelial lipase (EL)-expressing HEK293 cells to study the kinetic of EL hydrolysis *in vitro*. Results: The levels of angptl4 in the plasma and HDLs were 1.7- and 2.0-fold higher in T2DM patients than non-diabetic controls (p<0.0001 for both). When angptl4-containing HDLs were subjected onto HEK 293 cells expressing EL, phospholipid and triglyceride were dramatically hydrolyzed in HDLs with medium- and high-levels of angptl4 when compared with those having lowest angptl4 levels in HDLs in T2DM patients (p<0.05 for phospholipid; p<0.01 for triglyceride), but it did not occur in HDLs isolated from healthy controls (p>0.62 for both).Cholesterol hydrolysis was comparable and independent of angptl4 levels in HDLs in both groups. Multivariate-adjusted analysis demonstrated that per one doubling increase of ANGPTL4 levels in HDLs, the changes amounted to +0.27% cholesterol efflux (p=0.03), +0.06 μg/mL apoA-I (p=0.09) and -9.41 μg/L SAA (p=0.02) in non-diabetic controls. In T2DM patients, the corresponding estimates were -0.06% cholesterol efflux (p=0.10), -0.06 μg/mL apoA-I (p=0.38) and +3.64 μg/L SAA (p=0.72). Conclusions: Angptl4 in HDLs protected HDLs from hydrolysis and maintained HDL function in non-diabetic controls. Resulting from increased circulating angptl4 levels in T2DM, angptl4 levels in HDLs were elevated that compromised its inhibitory effect on EL, leading to increased HDL hydrolysis and dysfunction.

Disclosures: **L. Yang:** None. **C. Yu:** None. **X. Wang:** None. **S. Yuan:** None. **L. Zhang:** None. **J. Lang:** None. **D. Zhao:** None. **Y. Feng:** None.

189

Improved Triglyceride-Rich Lipoprotein Clearance In Human Apolipoprotein A-Ii Knockin Rabbits

Tomonari Koike, Yui Koike, Dongshan Yang, Jun Song, Jie Xu, Univ of Michigan, Ann Arbor, MI; Jianglin Fan, Univ of Yamanashi, Chuo city, Japan; Jifeng Zhang, Y. Eugene Chen, Univ of Michigan, Ann Arbor, MI

Apolipoprotein A-II (apoA-II) is a second major apolipoprotein in HDL particles, which account for 15-20 % of total HDL protein in human. Compared with apolipoprotein A-I (apoA-I) which is a most major apolipoproteins in HDL, physiological role of apoA-II is not fully understood. We previously reported that overexpression of apoA-II in rabbits significantly suppressed cholesterol-rich diet induced atherosclerosis. Because rabbits are the animal of naturally deficient in apoA-II, so it becomes a good animal model to study the functions of apoA-II. To elucidate the role of apoA-II independent from apoA-I in HDL on lipid metabolism and atherogenesis, we generated a rabbit model in which the human apoA-II was knocked in to rabbit apoA-I locus by TALEN technology. The model was confirmed by genomic PCR, sequencing, RT-PCR and proteomics. With this model, we found that the triglyceride (TG) levels are significantly lower in homozygote than that in wild type control. The results of lipoprotein analysis using ultracentrifugation and FPLC also show that TG-rich lipoproteins were lower in homozygote than that of wild type. TGs were not increased in homozygote even after feeding of food. Small LDL and HDL2 particles were increased in homozygote rabbits. In addition, increased apoE was shown in HDL3 particle from homozygote. These

results suggest that apoA-II knock-in has critical roles in the metabolism of TG-rich lipoproteins. Roles of apoA-II only HDLs from homozygote on cholesterol efflux and atherogenesis are under investigation.

Disclosures: **T. Koike:** None. **Y. Koike:** None. **D. Yang:** None. **J. Song:** None. **J. Xu:** None. **J. Fan:** None. **J. Zhang:** None. **Y. Chen:** None.

190

The Role of Hepatic FoxO Transcription Factors in HDL-Mediated Reverse Cholesterol Transport

Samuel X Lee, Columbia Univ Medical Ctr, New York, NY; Markus Heine, Christian Schlein, Univ Medical Ctr Hamburg Eppendorf, Hamburg, Germany; Rajasekhar Ramakrishnan, Jing Liu, Ido Haimi, Henry Ginsberg, Columbia Univ Medical Ctr, New York, NY; Joerg Heeren, Franz Rinninger, Univ Medical Ctr Hamburg Eppendorf, Hamburg, Germany; Rebecca Haeusler, Columbia Univ Medical Ctr, New York, NY

Insulin resistance and type 2 diabetes are associated with low levels of high-density lipoprotein-cholesterol (HDL-C). The insulin-repressible FoxO transcription factors are potential mediators of insulin's effect on HDL-C. FoxOs mediate a substantial portion of insulin-regulated transcription, and poor FoxO repression is thought to contribute to the excessive glucose production in diabetes. In this work, we show that mice with liver-specific triple FoxO knockout (L-FoxO1,3,4), which are known to have reduced hepatic glucose production, also have increased HDL-C. This was associated with decreased expression of HDL-C clearance factors, scavenger receptor class B type I (SR-BI) and hepatic lipase, and defective selective uptake of HDL-cholesteryl ester by the liver. The phenotype could be rescued by re-expression of SR-BI. These findings demonstrate that hepatic FoxOs are required for cholesterol homeostasis and HDL-mediated reverse cholesterol transport to the liver.

Disclosures: **S.X. Lee:** Research Grant; Significant; NIH F31 Grant: F31HL132484. **M. Heine:** None. **C. Schlein:** None. **R. Ramakrishnan:** None. **J. Liu:** None. **I. Haimi:** None. **H. Ginsberg:** None. **J. Heeren:** None. **F. Rinninger:** None. **R. Haeusler:** None.

191

Adipocyte Procollagen C-endopeptidase Enhancer Protein 2 (PCPE2) Influences Lipid Metabolism Secondary to Changes in Expression and Function of Scavenger Receptor Class B Member 1 (SR-BI)

Elisa C Maruko, Michael Tschannen, Pengyuan Liu, Shirng-Wern Tsaih, Medical Coll of Wisconsin, Milwaukee, WI; Craig A Glastonbury, Kerrin Small, King's Coll London, London, United Kingdom; Sushma Kaul, Hao Xu, Kaniz Fatema, Michael J Thomas, Mary G Sorci-Thomas, Medical Coll of Wisconsin, Milwaukee, WI

Scavenger receptor class B member 1 (SR-BI) functions as a HDL receptor and stimulates reverse cholesterol transport (RCT) via selective uptake of HDL cholesterol esters (HDL-CE). Procollagen c-endopeptidase enhancer protein 2 (PCPE2) is an extracellular matrix glycoprotein encoded by the PCOLCE2 gene and most highly expressed in adipose tissue, heart, and aorta. PCPE2 has been suggested to be atheroprotective secondary to mechanisms involved in lipid metabolism. Our lab previously reported that SR-BI mediated cholesterol ester uptake is reduced in the absence of PCPE2 despite its increased expression levels. Subsequent HDL turnover studies suggested an overall reduction in catabolism, consistent with larger HDL particles observed, is responsible for the paradox. More recently, human data from the TwinsUK study showed strong correlations between PCOLCE2 and adipose tissue distribution with BMI included as a covariate. Furthermore, despite similar overall body weights, our lab observed a significant reduction in visceral fat pad development in PCPE2-deficient mice fed a Western diet for 25 weeks when compared to wild type mice. In addition, our lab has generated PCPE2 knockout cell lines from murine preadipocyte 3T3-L1 cells ($PCPE2^{-/-}$ 3T3-L1) and Chinese hamster ovary (CHO) cells using CRISPR-Cas9 and siRNA technology, respectfully. In addition to both cell lines showing increased SR-BI expression, differentiated $PCPE2^{-/-}$ 3T3-L1 cells have impaired lipid droplet formation. To elucidate the relationship between PCPE2 and SR-BI function and their effects on adipose tissue development, we performed RNA sequencing on visceral adipose tissue from PCPE2-deficient male mice fed a Western diet for 12 weeks. Genes exhibiting significant expression alterations (FDR <0.026) compared to wild type were further analyzed via Ingenuity Pathway Analysis (IPA). Differential expression analysis of diseases and functions related to changes in SR-BI expression highlighted permutations of a number of lipid modulating genes. Overall, changes in SR-BI related

metabolic pathways secondary to PCPE2 deficiency appear to play a crucial role linking SR-BI mediated cholesterol ester uptake to adipocyte biology.

Disclosures: **E.C. Maruko:** None. **M. Tschannen:** None. **P. Liu:** None. **S. Tsaih:** None. **C.A. Glastonbury:** None. **K. Small:** None. **S. Kaul:** None. **H. Xu:** None. **K. Fatema:** None. **M.J. Thomas:** None. **M.G. Sorci-Thomas:** None.

192

Intra-Individual Temporal Variation of Lipid and Apolipoprotein Levels in Patients With Type II Diabetes Mellitus and Normolipidemic Individuals

Bryan A Parks, Susan Kuklenyik, David Schieltz, Christopher Toth, Michael Andrews, Jeffrey Jones, Michael Gardner, Jon Rees, Lisa McWilliams, John R Barr, Ctrs for Disease Control and Prevention, Atlanta, GA

Hypertriglyceridemia is frequently observed with diabetes mellitus (DM) and is associated with increased cardiovascular disease (CVD) risk. In conditions of insulin deficiency or resistance, increased levels of free fatty acids are seen by the liver, which trigger increased lipogenesis and secretion of triglyceride (TG) rich lipoprotein (TRL) particles. However, a high number of specific ApoC-III on TRL particles suppress their return to the liver leading to a continuous circulation of highly atherogenic TRL remnants. To better understand the effect of intra-individual temporal variations on the differentiation of lipid and apolipoprotein profiles in DM vs. normal individuals, a small time course study over a 4 week period was performed on 3 normolipidemic, and 3 type II DM patients. Our laboratory has developed a method to separate lipoproteins based on hydrodynamic size coupled with mass spectrometry based analysis. Whole serum and lipoprotein size fractions were analyzed for 8 apolipoproteins (ApoA-I, ApoA-II, ApoA-IV, B-100, ApoC-I, ApoC-II, ApoC-III and E) and non-polar lipids (FC, CE, TG) while monitoring other proteins (ApoD, ApoM, CETP, LCAT, PLTP, PON1 and SAA4). In whole serum over the course of 4 weeks, ApoA-IV levels of DM vs. normal subjects differed the most, 3.2 (0.7) vs. 1.8 (0.4) µM, respectively, more significantly than intra-group or intra-individual variations. On the contrary, significantly lower whole serum levels were found for FC, CE, ApoM and PON1 (Prob<0.01). HDL-ApoC-III/LDL-ApoC-III was also lower in DM vs. normal subjects, 3.0 (1.9) vs. 7.2 (4.1). By metrics of molar ratio measured in 20-35 nm LDL fractions, the most significant difference was found between DM vs. normal subjects in ApoC-III/ApoB-100 (1.8 (0.6) vs. 0.9 (0.3)), C-II/ApoB-100 (0.8 (0.4) vs. 0.4 (0.2)) and ApoE/ApoC-III (0.11 (0.09) vs. 0.24 (0.15)). These LDL composition differences indicate lower lipase activity and inhibition of LDL uptake. However, no significant differences were observed in these molar ratios as function of LDL particle size. In conclusion, due to less significant temporal deviations, apolipoprotein molar ratios are a more useful and informative measure of CVD risk in DM subjects than LDL size distribution characteristics.

Disclosures: **B.A. Parks:** None. **S. Kuklenyik:** None. **D. Schieltz:** None. **C. Toth:** None. **M. Andrews:** None. **J. Jones:** None. **M. Gardner:** None. **J. Rees:** None. **L. McWilliams:** None. **J.R. Barr:** None.

193

Remnant-Like Particle Cholesterol, Low-Density Lipoprotein Triglyceride and Incident Cardiovascular Disease in the Atherosclerosis Risk in Communities Study: Can Genetic Variants Provide New Insights on Triglycerides and Atherogenic Lipoproteins?

Anum Saeed, Baylor Coll of Med, Houston, TX; Eleana Feofanova, Bing Yu, Univ of Texas Health Sciences Ctr, Houston, TX; Salim S. Virani, Wensheng Sun, Vijay Nambi, Baylor Coll of Med, Houston, TX; Gerardo Heiss, Univ of North Carolina, Chapel Hill, NC; Cameron S Guild, Univ of Mississippi, Jackson, MS; Josef Coresh, Johns Hopkins Bloomberg Sch of Public Health, Baltimore, MD; Eric Boerwinkle, Univ of Texas Health Sciences Ctr, Houston, TX; Christie M Ballantyne, Ron Hoogeveen, Baylor Coll of Med, Houston, TX

Recent genetic studies have focused on the atherogenicity of remnant-like particle cholesterol (RLPC) with paucity of data on TGs in LDL (LDL-TG). We examined the association of RLPC and LDL-TG with incident CVD and the genetic variants associated with their levels in the biracial ARIC study. Fasting plasma RLPC and LDL-TG were measured by automated homogeneous assays (Denka Seiken, Tokyo) in 9334 men and women without prevalent CVD at baseline. Incident CHD and stroke over 16-y follow-up were obtained from medical records. Associations between LDL-TG and RLPC and the

genomic variants (Illumina HumanExome Beadchip) were assessed using single variant analysis for common variants and gene-based burden tests for rare variants. Variants with minor allele frequency >1% were analyzed individually.
RLPC and LDL-TG were correlated with elevated TG (r=0.85 and 0.64, p<0.0001). In minimally adjusted analyses, both were associated with CVD risk, but after adjusting for traditional CVD risk factors including lipids, only LDL-TG was positively associated with incident CHD (HR 1.28 [95% CI 1.10-1.50]) and stroke (HR 1.47 [95% CI 1.13-1.92]; p<0.01). Single variant tests showed a common *APOE* variant (rs7412) had the strongest association with LDL-TG and RLPC in both races ($p<5x10^{-8}$). Since rs7412 defines apoE isoforms, we assessed *APOE* haplotypes and found E2/2 was associated with reduced LDL-TG and increased RLPC (Fig).
Although elevated TGs are associated with increased RLPC and LDL-TG, only LDL-TG remained significant for CVD risk in multivariable-adjusted models. ApoE2 locus variants were associated with RLPC and LDL-TG, but individuals with apoE2/E2 had decreased LDL-TG and increased RLPC. These findings, and prior studies showing that apoE2 is associated with lower CVD risk, suggest that the increased risk of CVD with high TGs may be related more to LDL-TG than RLPC. Further research is needed to understand whether LDL-TG plays a causal role in CVD and is a target for therapy.

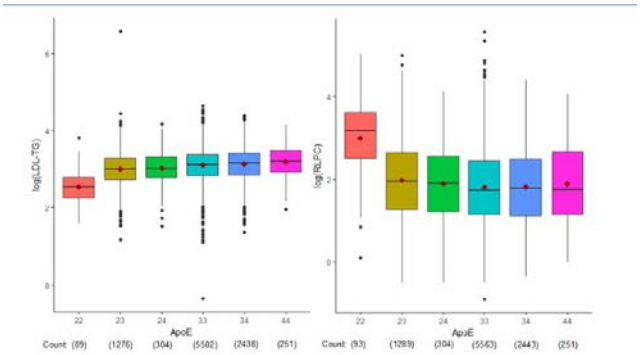

Figure 1: ApoE haplotypes and association with log LDL-TG (left) and RLPC (right)

Disclosures: **A. Saeed:** None. **E. Feofanova:** None. **B. Yu:** None. **S.S. Virani:** None. **W. Sun:** None. **V. Nambi:** Research Grant; Modest; Troponin based (Roche for provisional patent) and Siemens for adjudication of events for a troponin assay. **G. Heiss:** None. **C.S. Guild:** None. **J. Coresh:** None. **E. Boerwinkle:** None. **C.M. Ballantyne:** None. **R. Hoogeveen:** Research Grant; Modest; Denka Seiken, Co.

194

Lipid and Apolipoprotein Size Profile Differences Between Low and High Body Mass Index Individuals in Response to Fat Challenge

David Schieltz, Zsuzsanna Kuklenyik, Bryan A. Parks, Michael Gardner, Christopher Toth, Jeffrey Jones, Michael Andrews, Jon Rees, Lisa McWilliams, John Barr, Jim L. Pirkle, Ctrs for Disease Control and Prevention, Atlanta, GA

Clearance of elevated triglycerides (TG) level in response to fat challenge is a clinically significant indicator of CVD risk. HDL can play a key role in facilitating TG metabolism explaining the reverse correlation of HDL levels with CVD risk. In this study 6 individuals, low BMI (21-25) and 3 high BMI (30-49) were challenged with a meal containing ~90 g of total fat. Blood samples were drawn in fasting state before meal and 3 times after meal in 2, 4 and 6 hours. Serum was analyzed by a quantitative, multiplexed analytical workflow which included analysis of whole serum and the separation of lipoproteins by asymmetric flow field-flow fractionation where fractions were collected with 1 nm increments of 7-15 nm (HDL), 20-30 nm (LDL) and >30 nm lipoprotein classes. Dynamic light scattering was used to determine hydrodynamic size in each size fraction. Whole serum and individual fractions were analyzed to determine concentrations of apolipoproteins (apo A-I, A-II, A-IV, B, C-I, C-II, C-III and E), and non-polar lipids (FC, CE and TG), using two parallel liquid chromatography tandem mass spectrometry methods developed in our laboratory. In whole serum, the total TG levels for low and high BMI donors, relative to pre-meal levels (57-137 mg/dL and 111-183 md/dL), peaked at between the 2 and 4 hours post meal (103-214 mg/dL and 210-309 mg/dL). LCAT were lower (20%) and CETP levels were higher (30%), in

low vs high BMI groups, but did not show change in repose to the fat challenge. In both low and high BMI groups, the most significant change between pre-meal and post-meal after 2 hours occurred in HDL-ApoC-I, HDL-ApoC-II, and HDL-ApoC-III levels mainly in the HDL size range of 9-12 nm (medium HDL) and at 13-16 nm (large HDL), with concurrent TG increase observed in LDL and remnant fractions (Prob-|t|=0.01 0.07). After 6 hours post-meal, HDL-ApoE and HDL-ApoC-II levels were significantly lower than pre-meal, however HDL-ApoA-II was significantly higher in the high BMI group. These finding indicate that during fat challenge, first HDL particles collect ApoC-I, ApoC-II and ApoC-III to provide cofactors for regulation of TG metabolism, but then lose these ApoC and ApoE proteins with time. High levels of ApoA-II in the high BMI subjects may be due to altered lipoprotein lipase function.

Disclosures: **D. Schieltz:** None. **Z. Kuklenyik:** None. **B.A. Parks:** None. **M. Gardner:** None. **C. Toth:** None. **J. Jones:** None. **M. Andrews:** None. **J. Rees:** None. **L. McWilliams:** None. **J. Barr:** None. **J.L. Pirkle:** None.

196

Acute Phase Response Transcription Factor CREBH Mediates Metabolic Inflammation to Hepatic VLDL Overproduction and Hyperlipidemia

Yongyan Song, Miaoyun Zhao, Rituraj Khound, **Qiaozhu Su**, Univ of Nebraska-Lincoln, Lincoln, NE

Hyperlipidemia is a major complication of insulin-resistant states, such as obesity and type 2 diabetes, and contributes to an increased risk of cardiovascular disease. One key mechanism underlying the hyperlipidemia in metabolic syndrome is the overproduction of apolipoprotein B (apoB), the essential structural protein of the triglyceride-rich lipoproteins, such as very-low-density lipoproteins (VLDL) and chylomicrons. Currently, the underlying mechanisms for the overproduction of VLDL in metabolic syndrome are not fully understood. In this study, we demonstrated that the cAMP responsive element binding protein H (CREBH), an acute phase transcription factor, enhanced VLDL assembly and secretion by upregulating apoB expression, which contributed to hyperlipidemia associated metabolic inflammation. Specifically, we showed that over-expression of CREBH significantly induced mRNA and protein expression of apoB in McA-7777 cells. A luciferase assay further revealed that the presence of CREBH positively enhanced the activity of the apoB gene promoter. Genetic depletion of CREBH in mice resulted in significant reduction in expression of hepatic apoB mRNA. Moreover, challenging mice with a fat load via oral gavage upregulated VLDL secretion in wild type but not in the CREBH-null mice, suggesting the essential role of CREBH in apoB expression. Inflammatory cytokine TNFα treatment activated hepatic CREBH expression in wild type mice which subsequently enhanced hepatic apoB biosynthesis and VLDL secretion. This phenotype was not observed in CREBH-null mice. Metabolic inflammation induced by LPS or HFD also resulted in overproduction of apoB and hyperlipoproteinemia in wild type but not in CREBH-null mice. **Conclusion**: This study demonstrated that, for the first time, CREBH could be a mediator between metabolic inflammation and hepatic VLDL overproduction in chronic metabolic disorders. This novel finding establishes CREBH as the first transcription factor that regulates apoB expression on the transcription level and the subsequent VLDL biosynthesis in response to metabolic inflammation, and further provides novel mechanistic insight into the pathogenesis of hyperlipidemia in metabolic syndrome.

Disclosures: **Y. Song:** None. **M. Zhao:** None. **R. Khound:** None. **Q. Su:** None.

197

Characterization of the Effects of Angiopoietin-Like 3 on Plasma Lipids and Lipoproteins in Humans

Jessica Minnier, Sergio Fazio, Michael Shapiro, Oregon Health & Science Univ, Portland, OR; Sotirios Tsimikas, Univ of California at San Diego, La Jolla, CA; Marcello Arca, Sapienza Univ of Rome, Rome, Italy; **Hagai Tavori**, Oregon Health & Science Univ, Portland, OR

Angiopoietin-like 3 (ANGPTL3) deficiency due to loss-of-function (LOF) gene mutations causes familial combined hypobetalipoproteinemia type 2 (FHBL2) in homozygotes and compound heterozygotes, with a lipid phenotype much milder in heterozygotes. We aim to determine whether a critical reduction in plasma ANGPTL3 levels is a major determinant of FHBL2 lipid phenotype. We studied 126 subjects from 19 families with ANGPTL3 LOF mutations. Individuals homozygous for mutations in ANGPTL3 manifest the full FHBL2 phenotype of reduced total cholesterol, triglycerides, very low-density lipoprotein (VLDL), low-density lipoprotein (LDL) and high-density lipoprotein (HDL) cholesterol (-C) and particle concentration (-

p), and LDL size. Heterozygotes only displayed with low total cholesterol, HDL-C, HDL-p and VLDL-p compared with non-carriers. Using multivariate adaptive regression splines, we found that: (*i*) total cholesterol, triglycerides, LDL-C, HDL-C, HDL-p, and LDL size correlated with ANGPTL3 but only for levels below 25% of normal (<60 ng/dl); (*ii*) VLDL-p and LDL-p correlate with ANGPTL3 irrespective of its plasma levels; and (*iii*) homozygotes exhibited reduced levels of mature proprotein convertase subtilisin/kexin type 9 (PCSK9), a known regulator of plasma LDL-C levels. These results indicate that the full FHBL2 phenotype seen in homozygous carriers of LOF mutations in ANGPTL3 is caused by a critical reduction of more than 75% of its plasma levels, thus uncovering the relationship between mutation status, plasma ANGPTL3 concentrations, and the lipid phenotype. Furthermore, our study suggests that the low plasma LDL seen in homozygous carriers of ANGPTL3 LOF mutations is mediated by the modulation of plasma PCSK9.

Disclosures: **J. Minnier:** None. **S. Fazio:** None. **M. Shapiro:** None. **S. Tsimikas:** None. **M. Arca:** None. **H. Tavori:** None.

This research has received full or partial funding support from the American Heart Association.

200

Functional Mapping of the 8q24 Noncoding Region Reveals Enhancer Elements and Association Between GWAS SNPs and *TRIB1* Gene Expression

Andrea M Berrido, Mikhaila A Smith, Nicholas J Hand, Christopher D Brown, Daniel J Rader, Univ of Pennsylvania, Philadelphia, PA; **Robert C Bauer**, Columbia Univ, New York, NY

Single nucleotide polymorphisms (SNPs) in the human 8q24 locus have repeatedly been associated by genome-wide association studies (GWAS) with multiple human metabolic traits such as plasma lipids and coronary artery disease. These SNPs lie in a non-coding region ~30kb downstream of the gene Tribbles-1 (*TRIB1*). While a large body of in vivo evidence from *Trib1* gain- and loss-of-function mouse models strongly supports *TRIB1* as the gene of interest at this locus, there has been no demonstrated association between SNPs in the GWAS region and the expression of the neighboring *TRIB1* gene to date. To address this, we performed RNA-seq and genome-wide genotyping on 42 human cadaveric liver samples, and next performed allele-specific expression (ASE) analysis of the *TRIB1* locus in 23 samples that harbored heterozygous coding SNPs in the *TRIB1* gene, allowing for allelic discrimination. While subjects homozygous for the major allele of the lead GWAS SNP (rs2954029) had even allelic expression (p=0.29 by non-parametric t-test), samples heterozygous for the minor allele at rs2954029 exhibited imbalanced allelic expression (p<0.0005). This finding suggests that SNPs in the *TRIB1* locus do affect *TRIB1* gene expression; however, it remains unclear which SNP(s) is causal. To that end, we used ENCODE data from primary hepatocytes and HepG2 cells to identify 10 genomic regions of interest that contained SNPs with significant GWAS p-values and epigenetic markers consistent with enhancer activity. Two regions (R2, R9) exhibited strong enhancer activity when cloned in front of a minimal promoter driving a luciferase reporter (pGL4.23), increasing luciferase activity 2-5-fold as compared to empty vector (p<0.05). Introduction of the minor alleles at three separate candidate SNPs in R2 reduced enhancer activity. In summary, we show that common variation in the 8q24 GWAS locus does affect *TRIB1* gene expression, as measured by ASE in human livers. We also identified multiple enhancer elements that exhibit reduced activity when the minor alleles of GWAS SNPs are introduced into them. We are currently pursuing modification of the endogenous locus in HepG2 cells via CRISPR/Cas genome editing to further elucidate the roles of both these enhancer elements and the SNPs contained in them.

Disclosures: **A.M. Berrido:** None. **M.A. Smith:** None. **N.J. Hand:** None. **C.D. Brown:** None. **D.J. Rader:** None. **R.C. Bauer:** None.

This research has received full or partial funding support from the American Heart Association.

201

Generation of Photoactivatable apoA I to Study HDL Transport in vivo Reveals Impaired HDL Recirculation in a Murine Model of Psoriasis

Li-Hao Huang, Bernd H Zinselmeyer, Chih-Hao Chang, Brian T Saunders, Brian S Kim, Washington Univ Sch of Med, St. Louis, MO; Helge Wiig, Univ of Bergen, N-5009 Bergen, Norway; Michael J Thomas, Mary G Sorci-Thomas, Medical Coll of Wisconsin, Milwaukee, WI; Gwendalyn J Randolph, Washington Univ Sch of Med, St. Louis, MO

HDL is cardioprotective, but plasma HDL levels do not necessarily predict cardiovascular outcomes. The major HDL-associated protein apoA-I picks up its cholesterol from cells within extravascular compartments to return it to plasma and then bile. Yet, tools are lacking to quantify the important step of HDL transit through extravascular spaces. Here, we developed recombinant photoactivatable apoA-I to quantify endogenous HDL recirculation. Using the tool, we studied HDL passage through skin in healthy mice versus those with experimental psoriasis, wherein collagen density increased in the skin in a $CD4^+$ T cell-dependent manner. In control mice, photoactivated HDL mobilized to plasma within 2 h but was retained in collagen-enriched skin of mice with psoriasis. These data suggest that cardiovascular comorbidity in psoriasis might be linked to T cell-mediated structural changes in skin that impedes systemic recirculation of HDL. This new tool is likely to find wide application in HDL research.

Disclosures: **L. Huang:** None. **B.H. Zinselmeyer:** None. **C. Chang:** None. **B.T. Saunders:** None. **B.S. Kim:** None. **H. Wiig:** None. **M.J. Thomas:** None. **M.G. Sorci-Thomas:** None. **G.J. Randolph:** None.

202

Synergistic Protective Effects of Statin and Angiotensin Receptor Blocker for the Progression of Atherosclerosis

Seul-gee LEE, Sung-Kyung Bong, Yonsei Univ, Seoul, Korea, Republic of; Oh-Hyun Lee, Choongki Kim, Jaewon Oh, Sungha Park, Sang-Hak Lee, Jung-Sun Kim, Yonsei Univ Coll of Med, Seoul, Korea, Republic of

Objective: Both statin and angiotensin receptor blocker (ARB) are well known to prevent the progression of atherosclerosis. However, the additive effects of anti-atherosclerosis at early period are not fully investigated. Therefore, we tried to investigate whether an anti-atherosclerotic effect of statin and ARB could be synergistic and clarify its mechanisms. **Methods:** Atherosclerotic plaques were developed at 23 rabbits' iliac arteries with a high cholesterol (HC) diet and balloon inflation. We applied with 5 different treatment for 4 weeks; group 1 [n=5, HC diet]; group 2 [n=3, a regular chow diet]; group 3 [n=5, HC diet and rosuvastatin (R, 10 mg/kg)]; and group 4 [n=5, HC diet and olmesartan (O, 20 mg/kg)]; group 5 [n=5, HC diet and R + O]. End of the period, optical coherence tomography (OCT) was performed to detect the plaque characteristics and all tissues were harvested for histological evaluation. **Results:** Histological analysis demonstrated that atherosclerotic plaque lesions (Intima/plaque ratio, %) were decreased in the combination group compared to the statin (p=0.001) or ARB group (p=0.17). The macrophage infiltration of RAM11 staining was not significantly different between combination and each treatment group (mean±SEM=31.8±4.8% (R+O) vs. 38.1±6.53% (R), p=0.35 or 35.1±2.9% (O), p=0.62). Relative area of macrophage M1 polarization (iNOS staining) was significantly lower in the combination group compared to ARB group (3.2±0.5% (R+O) vs. 4.6 ±0.4% (R), p=0.09 or 5.2±1.0% (O), p=0.03). M2 macrophage polarization (Arg-1 staining) revealed increase in the combination group compared to each treatment group (17.7±3.0% (R+O) vs. 7.9±0.7% (R), p=0.002 or 11.9±2.8% (O), p=0.05) **Conclusion:** The combination of statin and ARB appeared more beneficial effects to reduce plaque formation, which may be associated with modulation of macrophage subtype in early period.

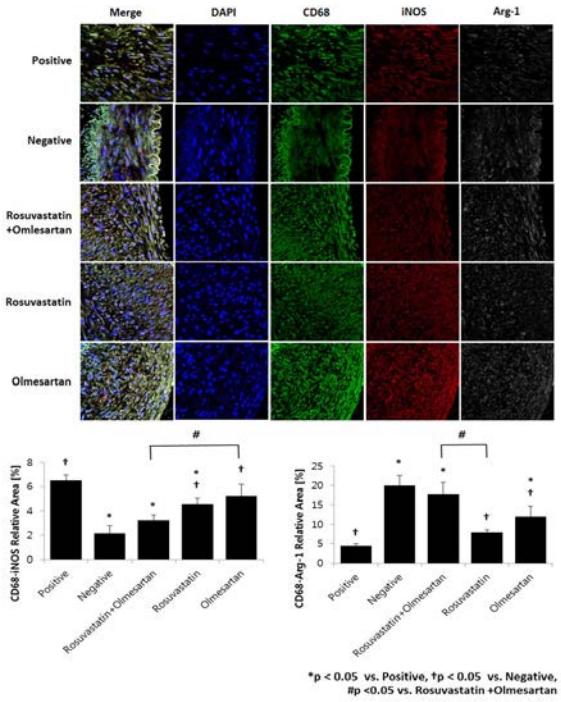

Disclosures: **S. Lee:** Research Grant; Significant; NRF-2014R1A1A2055584. **S. Bong:** Research Grant; Significant; 2014R1A1A2055584. **O. Lee:** None. **C. Kim:** None. **J. Oh:** None. **S. Park:** None. **S. Lee:** None. **J. Kim:** Research Grant; Significant; 2014R1A1A2055584.

203

Role of Glucagon Receptor Signalling in PCSK9 Regulation

Stefano Spolitu, **Lale Ozcan**, Columbia Univ, New York, NY

Excessive glucagon receptor action in hepatocytes is a major contributing factor to type 2 diabetes (T2D). Accordingly, there has been great interest in developing glucagon receptor antagonists (GRAs) as a treatment for T2D. Although phase 2 clinical trials have shown that GRAs effectively lower blood glucose in T2D subjects, they increase plasma low density lipoprotein (LDL) cholesterol levels, which has presented a significant block to their development. In this context, recent studies have suggested that cholesterol and proprotein convertase subtilisin/kexin type 9 (PCSK9) levels can be regulated by fasting and perhaps glucagon, but in-depth mechanistic insight is lacking. In order to test the functional importance of hepatic glucagon action on lipid metabolism, we silenced glucagon receptor (GcgR) in obese mice using AAV8-H1-shGcgr to silence the receptor in hepatocytes. Consistent with previous reports, this treatment effectively lowered blood glucose in obese mice without a change in body weight. Moreover, GcgR silencing, like GRAs in humans, significantly increased plasma LDL cholesterol. In search for the mechanism, we found that inhibition of GcgR significantly lowered hepatic LDL-receptor protein levels and increased both hepatic PCSK9 and circulating PCSK9. To determine causation, we treated GcgR-silenced mice with a neutralizing monoclonal antibody against PCSK9 and found that this intervention restored hepatic LDL-receptor protein levels and prevented the increase in LDL cholesterol. Further mechanistic work revealed that GcgR silencing in hepatocytes did not increase *Pcsk9* mRNA. Rather, blocking GcgR increased the half-life of PCSK9 protein by suppressing signalling through exchange protein activated by cAMP 1 (Epac1). In particular, the ability of GcgR silencing to increase PCSK9 and suppress LDL receptor protein levels was mimicked by hepatocytes lacking Epac1. Thus, GcgR signalling through Epac1 appears to have critical effects on processes that regulate cholesterol metabolism through PCSK9. These new findings have important implications for the lipid metabolism effects of hepatic glucagon signalling in both normal physiology and metabolic disease, and for the development of safer GRA-like drugs to treat T2D.

Disclosures: **S. Spolitu:** None. **L. Ozcan:** None.

204

Prioritizing Genome-Wide Association Study Lipid Loci With Global Gene Networks

Jennifer Nguyen, **Brian W Parks**, Univ of Wisconsin-Madison, Madison, WI

Large genome-wide association studies (GWAS) conducted in humans by the Global Lipids Genetics Consortium (GLGC) have identified more than 150 genome-wide significant loci that are associated with variation in plasma lipid levels (cholesterol, LDL/HDL-cholesterol, and triglycerides). Some loci contain genes with well-described roles in lipid metabolism, such as *CETP*, *LDLR*, and *APOB*; however, for many genome-wide significant loci, there is no clear causal gene. To test the hypothesis that lipid genes in the liver are co-regulated, we constructed global co-expression gene networks from genome-wide gene expression data obtained from the livers of multiple independent mouse genetic crosses. All together, we constructed global gene networks from eight distinct studies, representing more than 800 unique mice of diverse genetic backgrounds. For all studies analyzed, we identified a module (or sub-network) of genes that is significantly enriched ($p<1x10^{-15}$) functionally for cholesterol biosynthesis and metabolism genes. This module ranges in size from 70 to 824 genes across the eight studies and contains all genes involved in the cholesterol biosynthesis pathway (*Acat2, Hmgcs2, Hmgcr, Lss, Sc5d, etc.*). This module also contains many genes involved in the regulation of cholesterol metabolism, such as *Ldlr*, *Pcsk9*, and *Insig1*. Because of the significant enrichment of cholesterol genes in this module, we have begun to cross-reference all genes in the module against the GLGC lipid GWAS data. Through this analysis, we have identified genes of unknown function that are clearly located within genome-wide significant lipid loci as well as sub-threshold (suggestive significant) lipid loci. Among the genes we identified was *Sestrin1*, which was located within a clear sub-threshold locus associated with plasma cholesterol (rs12206606; $p=1.4 \times 10^{-5}$). In conclusion, our studies provide a framework to identify causal genes within reported lipid GWAS loci as well as to identify novel sub-threshold loci associated with variations in lipids among humans. We illustrate the approach by identifying *Sestrin1* within a sub-threshold locus associated with plasma cholesterol levels and show that *Sestrin1* is transcriptionally regulated in the liver by dietary cholesterol.

Disclosures: **J. Nguyen:** None. **B.W. Parks:** None.

205

Inhibition of Angiopoietin-Like 3 Expression is a Potential Mechanism of Activation of Lipoprotein Lipase and of Lipid Lowering by Metformin

Li Lin, Jamie R Burke, Northeast Ohio Medical Univ, Rootstown, OH; Werner J Geldenhuys, West Virginia Univ, Morgantown, WV; **Prabodh Sadana**, Northeast Ohio Medical Univ, Rootstown, OH

Dyslipidemias associated with primary lipid disorders or secondary to abnormal glucose metabolism are commonly seen metabolic disorders in the clinic. Of special interest is the diabetic dyslipidemia and its growing prevalence. Interestingly, metformin, a commonly used anti-diabetic drug also has potent lipid lowering activity. However, the mechanisms associated with this metformin activity are poorly understood. A key protein regulating the plasma lipid homeostasis is the enzyme lipoprotein lipase (LPL) which is found lining the capillary endothelium in tissue capillary beds. LPL hydrolyses the core triglycerides (TGs) of chylomicrons and very-low density lipoprotein (VLDL). Angiopoietin-like 3 (ANGPTL3), a secretory protein derived from liver, inhibits the lipolytic activity of LPL, resulting in an increase in plasma TGs. We investigated whether metformin regulates LPL and in effect plasma lipids, via regulation of ANGPTL3 in the liver. A single dose (150mg/kg) treatment of metformin for twenty-four hours in mice resulted in an increase in the LPL activity in plasma. Since metformin is frequently used in type 2 diabetes which is characterized by insulin resistance, a condition compounded by dietary fatty acids, we studied the relationship between metformin and ANGPTL3 in a human liver cell line treated with palmitic acid. Treatment with palmitic acid mimicked the conditions of insulin resistance in the liver and elevated the expression of ANGPTL3 in the liver which was inhibited by co-treatment with metformin. Gene and protein expression assays revealed a potent inhibition of ANGPTL3 expression and secretion from the hepatocytes upon treatment with metformin. We examined the role of sirtuin 1 (SIRT1)/adenosine monophosphate activated kinase (AMPK) in the metformin regulation of ANGPTL3 and observed that even though activation of SIRT1/AMPK axis inhibited the expression of ANGPTL3, metformin inhibition of ANGPTL3 was independent of SIRT1/AMPK as revealed by pharmacological inhibition and gene knockdown approaches. Our studies suggest that a potential mechanism of lipid lowering activity of

metformin is the inhibition of expression of ANGPTL3, which results in an increase in LPL activity and a lowering of plasma lipids.

Disclosures: **L. Lin:** None. **J.R. Burke:** None. **W.J. Geldenhuys:** None. **P. Sadana:** None.

206

Intestinal LXR Directs Absorbed Lipids to Storage

Amnon Schlegel, Univ of Utah, Salt Lake City, UT

Post-prandial hypertriglyceridemia has emerged as a cardiovascular risk factor with limited therapeutic options. We have taken genetic and physiological approaches to identify and characertize novel factors that regulate intestinal lipid handling in the hope of revealing cellular pathways that dampen delivery of dietary lipids, opening the therapeutic window to blunting post-prandial lipid excursions. Liver X receptors (Lxrs) are master regulators of cholesterol catabolism, driving the elimination of cholesterol from the periphery to the lumen of the intestine. These nuclear hormone receptors are activated by oxysterol, ligands that accumulate when excess cholesterol is present. Loss of *nr1h3* function causes anticipated gene regulatory changes and cholesterol intolerance, collectively reflecting high evolutionary conservation of zebrafish Lxra function. Intestinal *nr1h3* activation delays transport of absorbed neutral lipids, with accumulation of neutral lipids in enterocyte cytoplasmic droplets, as visualized with histological stains, live fluorescent lipid probes, and ultrastructural analyses. This delay in transport of ingested neutral lipids protects animals over-expressing *nr1h3* in the intestine from hypercholesterolemia and hepatic steatosis induced by a high-fat diet. On a gene regulatory level, Lxra induces expression of *acsl3a*, which encodes acyl-CoA synthetase long-chain family member 3a, a lipid droplet-anchored protein that directs fatty acyl chains into lipids. We have identified a gene regulatory network in enterocytes whereby the pace of delivery of dietary lipids is gated by Lxrs. Development of pharmacological agents to activate Lxrs has been hindered by synthetic Lxr agonists' induction of hepatic lipogenesis and hypertriglyceridemia. The development of intestine-limited Lxr agonists could be of therapeutic value in blunting post-prandial hypertriglyceridemia.

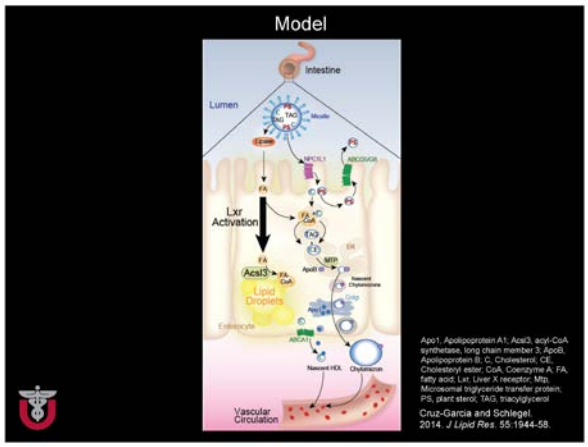

Disclosures: **A. Schlegel:** None.

This research has received full or partial funding support from the American Heart Association.

207

ApoC-II Mimetic Peptide Blunts Post-Prandial Hypertriglyceridemia in Mice

Anna Wolska, Toshihiro Sakurai, Denis Sviridov, Milton Pryor, Lipoprotein Metabolism Section, Natl Heart, Lung, and Blood Inst, Natl Insts of Health, Bethesda, MD; Larry Lo, Soumitra Ghosh, Madhav Devalaraja, Corvidia Therapeutics, Waltham, MA; Alan T. Remaley, Lipoprotein Metabolism Section, Natl Heart, Lung, and Blood Inst, Natl Insts of Health, Bethesda, MD

Post-prandial hypertriglyceridemia is as an important CVD risk factor. We recently described an apoC-II mimetic peptide (18A-CII) that activates LPL and lowers plasma TG in apoC-II-KO mice. To investigate 18A-CII as a therapy for post-prandial hyperTG, we investigated its effect on several mouse models after a fat challenge test. After an oral gavage with vegetable oil (10 µL/gram), plasma TG increased by 3 h in C57BL/6 mice by at least 5-fold but when mice were injected 30 min before gavage with 18A-CII (1 µmoL/kg; IP or SQ), the post-prandial TG rise was almost completely blunted. Similar results were found in apoE-KO mice, indicating that the effect of 18A-CII is independent of apoE. 18A-CII did not appear to work at the level of TG absorption, because it also rapidly accelerated plasma clearance of TG after IP injection of 20% Intralipid. Addition of exogenous LPL to plasma samples collected after IP injection with Intralipid revealed that lipoprotein particles from mice treated with 18A-CII were better substrates for LPL. The rise in plasma TG after IP injection of Intralipid was only partially blocked by about 50% when mice were co-injected with the LPL inhibitor Triton WR1339, indicating that 18A-CII also works by an LPL-independent mechanism. Incubation of human plasma with exogenous 18A-CII at doses comparable to that achieved *in vivo* in mice showed that 18A-CII binds to all lipoproteins, including HDL and causes the displacement of apoC-I and apoC-III. Furthermore, the *in vitro* inhibition of LPL from the addition of exogenous apoC-III could be overcome by adding 18A-CII at a molar ratio of at least 1:10 compared to apoC-III. In summary, the18A-CII mimetic peptide at relatively low doses can accelerate the clearance of post-prandial TG after a fat load. It does so in part by activating LPL but also by relieving the inhibition of LPL by apoC-III and possibly by also blocking the other known LPL-independent effects of apoC-III and possibly apoC-I in delaying the post-prandial clearance of TG.

Disclosures: **A. Wolska:** Research Grant; Significant; Corvidia Therapeutics, Waltham, MA, USA. **T. Sakurai:** Research Grant; Significant; Corvidia Therapeutics, Waltham, MA, USA. **D. Sviridov:** Research Grant; Significant; Corvidia Therapeutics, Waltham, MA, USA. **M. Pryor:** Research Grant; Significant; Corvidia Therapeutics, Waltham, MA, USA. **L. Lo:** Ownership Interest; Significant; Corvidia Therapeutics, Waltham, MA, USA. **S. Ghosh:** Consultant/Advisory Board; Significant; Corvidia Therapeutics, Waltham, MA, USA. **M. Devalaraja:** Ownership Interest; Significant; Corvidia Therapeutics, Waltham, MA, USA. **A.T. Remaley:** Research Grant; Significant; Corvidia Therapeutics, Waltham, MA, USA.

208

Isolevuglandin, a Highly Reactive γ-ketoaldehyde Formed from the Isoprostane Pathway, Induces Deleterious Structural and Functional Consequences to High-density Lipoprotein

Linda S Zhang, Vanderbilt Univ, Nashville, TN; Huan Tao, Vanderbilt Medical Ctr, Nashville, TN; Tiffany Pleasent, Meharry Medical Coll, Nashville, TN; Mark S. Borja, Children's Hosp Oakland Res Inst, Oakland, CA; Michael N Oda, Children's Hosp Oakland Res Inst, Oakland, TN; W. Gray Jerome, Patricia G. Yancey, Vanderbilt Medical Ctr, Nashville, TN; L. Jackson Roberts II, Vanderbilt Univ, Nashville, TN; MacRae F. Linton, Vanderbilt Medical Ctr, Nashville, TN; Sean S. Davies, Vanderbilt Univ, Nashville, TN

Recent evidence suggest that cardiovascular disease (CVD) risk depends on levels of functional HDL particles, not HDL-cholesterol. In CVD, increased oxidative stress generates reactive lipid species that alter HDL function. Isolevuglandins (isoLGs), generated in parallel to isoprostanes, are extremely reactive to lysine residues of proteins and headgroups of phosphatidylethanolamine (PE). Importantly, IsoLG protein and PE adducts are elevated in atherosclerosis. Recently, our group observed a 42% reduction of atherosclerotic lesion size when salicylamine (SAM), a small molecule scavenger of reactive dicarbonyls including IsoLG, was administered to $LDLr^{-/-}$ mice. Little is known about the consequences of IsoLG to HDL function. The aim of this study is to compare effects of IsoLG on apolipoprotein crosslinking, morphology and size of HDL to its functions: cholesterol efflux, apoA-I exchange and anti-inflammation. Human HDL was incubated overnight at 37ºC with IsoLG. Thioglycolate-induced intraperitoneal macrophages were harvested from $apoE^{-/-}$ mice. IsoLG crosslinked structural apolipoproteins, apoA-I and apoA-II, starting at 0.3 mol IsoLG per mol apoA-I (0.3 eq). HDL modified with 3 eq IsoLG formed subpopulations of two distinct sizes, 6-13 nm and 16-23 nm. A 40.6±0.04% decrease in ^{3}H-cholesterol

efflux from macrophages was observed at 1 eq IsoLG compared to unmodified control HDL. At this IsoLG concentration, HDL-ApoA-I exchange was reduced (P<0.01, n=4), from 47.4±2.8% with control HDL to only 24.8±5.8%, suggesting that IsoLG inhibited apoA-I from disassociating from HDL to interact with ABCA1. Intriguingly, IsoLG inhibited HDL's protection against LPS-stimulated inflammatory response in macrophages at 0.03 eq as shown by IL-1β and TNFα mRNA expression comparable to LPS alone. At 0.1 eq IsoLG, HDL becomes pro-inflammatory, as indicated by a 927±309% increase in IL-1β mRNA expression (P<0.001). Unlike cholesterol efflux, these effects occurred independent of HDL apolipoprotein crosslinking. We report a novel pathway by which HDL becomes dysfunctional, by mechanisms involving IsoLG-mediated alterations of HDL proteins and structure. Future studies will pinpoint how IsoLG modifies HDL proteins (or lipids) to alter its function.

Disclosures: **H. Tao:** None. **T. Pleasent:** None. **M.S. Borja:** None. **M.N. Oda:** None. **W. Jerome:** None. **P.G. Yancey:** None. **L. Roberts:** None. **M.F. Linton:** None. **S.S. Davies:** None.

209

An XX Sex Chromosome Complement Promotes the Development of Obesity, Hypercholesterolemia and Atherosclerosis in Male and Female *Ldlr*$^{-/-}$ Mice Fed a Western Diet

Yasir Alsiraj, Sean Thatcher, Heba M. Ali, Ryan Temel, Alan Daugherty, Lisa Cassis, Univ of Kentucky, Lexington, KY

Background: Underlying mechanisms contributing to sexual dimorphism of cardiovascular diseases are not well understood. Sex hormones are primary contributors to sexual dimorphism of cardiovascular diseases. By comparison, little is known regarding the contribution of genes on sex chromosomes (XX and XY) to sexual dimorphism of cardiovascular diseases, even though the X chromosome contains around 5% of the human genome. In this study, we hypothesized that genes on sex chromosomes influence the development of obesity, hypercholesterolemia and atherosclerosis. ***Methods and Results:*** Transgenic male mice with deletion of *Sry* from the Y-chromosome expressing *Sry* on autosomes (8-12 weeks of age) were bred to female *Ldlr*$^{-/-}$ mice to generate female and male mice with an XX or an XY sex chromosome complement (FXX, FXY, MXX, MXY). Mice were fed a Western diet (Teklad TD88137) for 3 months. XX mice exhibited increased body weight compared to mice with an XY sex chromosome complement, regardless of gonadal sex (FXX, 41.2 ± 2.4; FXY, 31.7 ± 2.5 g; P<0.05; MXX, 51.5 ± 1.2; MXY, 41.7 ± 1.8 g; P<0.05). Moreover, XX mice had increased serum cholesterol concentrations, regardless of gonadal sex (FXX, 2501 ± 192; FXY, 890 ± 141 mg/dl; P<0.05; MXX, 3814 ± 344; MXY, 1297 ± 385 mg/dl; P<0.05). Elevations in serum lipids were manifest as increased VLDL and LDL-cholesterol. The extent of atherosclerosis in aortic arch was significantly increased in XX compared to XY mice (XXF, 37 ± 2.1; XYF, 20 ± 3.2; XXM, 38 ± 3.6; XYM, 24 ± 3.6 % lesion surface area; P<0.05). In the aortic sinus, atherosclerotic lesion surface area was significantly increased in XX mice, regardless of gonadal sex (FXX, 60.4 x 10^4 ± 3.6 x 10^4; FXY, 32.4 x 10^4 ± 3.8 x 10^4 μm^2; P<0.05; MXX, 67.1 x 10^4 ± 9.6 x 10^4; MXY, 36.2 x 10^4 ± 3.7 x 10^4 μm^2; P<0.05). ***Conclusion:*** Results demonstrate that an XX sex chromosome complement promotes diet-induced obesity, hypercholesterolemia and atherosclerosis regardless of gonadal sex. Future studies will identify the role of genes on the X or Y chromosome as mechanisms for these effects.

Disclosures: **Y. Alsiraj:** None. **S. Thatcher:** None. **H. M. Ali:** None. **R. Temel:** None. **A. Daugherty:** None. **L. Cassis:** None.

This research has received full or partial funding support from the American Heart Association.

210

Milk Fat Globule Epidermal Growth Factor VIII Mediates Vascular Remodeling by Increasing Inflammation and Smooth Muscle Activation

Ting-Hein Lee, Chang-Gung Univ, Kwei-Shan Tao-Yuan, Taiwan; Shigekazu Nagata, Biochemistry & Immunology,Immunology Frontier Res Ctr, Osaka Univ, Osaka, Japan; Kamran Atabai, Dept of Med and Cardiovascular Res Inst, UCSF, San Francisco, CA; **Hou-Yu Chiang**, Chang-Gung Univ, Kwei-Shan Tao-Yuan, Taiwan

Vascular remodeling, defined as a change in the geometry of the vessel wall, occurs in the pathological process of vascular diseases, like atherosclerosis, hypertension and restenosis. The resulting neointimal

formation is a part of a reparative response including thrombosis, inflammatory cell infiltration, vascular smooth muscle cell (VSMC) proliferation and migration, which lead to the stenosis of blood vessels and the restricted blood flow. Milk fat globule epidermal growth factor VIII (Mfge8), a secreted glycoprotein, is well-characterized for its capacity of assisting the clearance of apoptotic cells in vascular system. Recently, Mfge8 has been identified as a pivot relay between pro-inflammatory signals and activated VSMCs, contributing to intima-media thickening of the vessel wall by promoting VSMC proliferation and migration in aged arteries. We have noted intense Mfge8 expression in the endothelial cells and VSMCs of the carotid artery following ligation injury in mice, suggesting that Mfge8 may regulate the two characteristics of vascular remodeling, inflammatory cell infiltration and VSMC activation, in response to low blood flow. To elucidate the functions of Mfge8 in a flow-induced model of vascular remodeling, a complete carotid ligation was conducted in wild-type (WT) or Mfge8 knockout (KO) mice. Morphometric analysis demonstrated that genetic deletion of Mfge8 in mice reduces carotid intima and media thickening compared to WT mice. Deficiency of Mfge8 prevented VSMC phenotypic modulation, as evidenced by the decreased expression of smooth muscle myosin heavy chain and attenuated cell proliferation in tunica media after ligation injury. VSMCs transfected with SiRNA against Mfge8 migrated slower than in controls as early as 0.5 days post-platelet-derived growth factor (PDGF) stimulation. Further, Mfge8-null mice showed a dramatic decrease in leukocyte infiltration into the vessel wall. Collectively, in a flow-induced model of vascular remodeling, Mfge8 plays a crucial role in VSMC migration and proliferation, as well as inflammatory cell accumulation, thereby regulating neointimal formation.

Disclosures: **T. Lee:** None. **S. Nagata:** None. **K. Atabai:** None. **H. Chiang:** None.

211

Response Gene to Complement 32 Deficiency Protects Endothelial Cell From Inflammation and Attenuates Atheroslcerosis

Xiao-Bing Cui, Jun-Na Luan, Kun Dong, The Univ of Georgia, Athens, GA; Yongyi Wang, Shanghai Jiaotong Univ, Shanghai, China; Sisi Chen, Wendy T Watford, Shi-You Chen, The Univ of Georgia, Athens, GA

Response gene to complement 32 (RGC-32) is involved in diet-induced obesity and hepatic steatosis. Therefore, we hypothesized that RGC-32 plays a role in atherosclerosis. Our current study showed that RGC-32 expression was dramatically induced in endothelial cells (ECs) of the atherosclerotic lesions from both apolipoprotein E-deficient ($ApoE^{-/-}$) mice and diseased human arteries. RGC-32 deficiency ($Rgc32^{-/-}$) significantly attenuated the high-fat diet-induced and spontaneously developed atherogenesis in $ApoE^{-/-}$ mice without affecting the serum lipid profiles. In addition, $Rgc32^{-/-}$ decreased the macrophage content without affecting fibrous cap size. $Rgc32^{-/-}$ in bone marrow cells had no effect on atherosclerosis development, and $Rgc32^{-/-}$ mice transplanted with wild-type (WT) bone marrow cells exhibited decreased atherosclerotic lesion area and macrophage infiltration, suggesting that RGC-32 in resident vascular cells plays a critical role in the atherogenesis. $Rgc32^{-/-}$ decreased the expression of intercellular adhesion molecule 1 (ICAM-1) and vascular cell adhesion molecule 1 (VCAM-1) in ECs both *in vivo* and *in vitro*, resulting in a decreased monocyte-EC interaction. Mechanistically, RGC-32 regulated ICAM-1 and VCAM-1 transcription via activation of nuclear factor (NF)-κB. It appeared that RGC-32 interacted with NF-κB, which facilitated NF-κB binding to ICAM-1 and VCAM-1 promoters. Indeed, blockade of NF-κB activity by its selective inhibitor ammonium pyrrolidinedithiocarbamate blocked RGC-32-induced ICAM-1 and VCAM-1 expression. In conclusion, RGC-32 promoted atherogenesis by inducing monocyte-EC interaction through NF-κB-dependent induction of endothelial ICAM-1 and VCAM-1 expression.

Disclosures: **X. Cui:** None. **J. Luan:** None. **K. Dong:** None. **Y. Wang:** None. **S. Chen:** None. **W.T. Watford:** None. **S. Chen:** None.

This research has received full or partial funding support from the American Heart Association.

212

Endothelium-Specific Deletion of Epsins Attenuates Atherosclerosis in ApoE-deficient Mouse Model Through Stabilization of IP3 Receptor 1 and Maintaining ER Homeostasis

Yunzhou Dong, Megan L Brophy, Aiyun Wen, Lili Yu, Hao Wu, Kai Song, Ashiqur Rahman, Scott Wong, Sukyoung Kwak, Kenneth Krygier, Hong Chen, Boston Children's Hosp, Boston, MA

Background Atherosclerosis is caused in part by endothelial dysfunction due to ER stress. Understanding the mechanisms that cause ER stress and endothelial dysfunction are essential in establishing new therapies to treat atherosclerosis. Epsins are endocytic adaptor proteins that mediate the internalization of plasma membrane receptors. However, whether epsins affect atherosclerosis remains unknown. To this end, we assessed the hypothesis that endothelial epsins play a critical role in regulating atherosclerosis.
Methods and Results In an ApoE-deficient murine model, endothelial-specific double knockout mice (EC-iDKO/ApoE-/-) significantly attenuated atherosclerotic lesion and macrophage infiltration in the aortic root and arch compared to ApoE-/- mice fed Western diet for ten weeks. To elucidate underlying mechanisms, mass spectrometry analysis identified IP3R1 as one of major interactors of epsins upon exposure to oxLDL. We show that epsins bind IP3R1 and facilitate its degradation in the endothelium. Downregulation of IP3R1 by atherosclerosis promoting agents augmented ER stress in primary mouse aortic endothelial cells. In line with these findings from mouse studies, in human atherosclerotic lesion, IP3R1 is dramatically downregulated and decrease in IP3R1 expression is associated with increased ER stress. Conversely, loss of epsins stabilized IP3R1, attenuated ER stress, reduced expression of P-selectin, adhesion molecules, and chemoattractant MCP-1 in primary mouse aortic endothelial cells. Molecular mapping analysis revealed that epsin's UIM domain is critical in facilitating the degradation of IP3R1. Delivery of a synthetic UIM peptide conjugated with atheroma-targeting Lyp-1 peptide significantly attenuated atherosclerosis in ApoE-/- animal models by stabilizing IP3R1 and maintaining ER homeostasis. Importantly, atherosclerotic lesion was restored in EC-iDKO/ApoE-/- mice by breeding them onto an endothelial-specific IP3R1 heterozygous background, suggesting that endothelial epsins promote atheroma progression in part by mediating IP3R1 degradation.
Conclusions Our data identified a novel mechanism of epsins in regulating atherosclerosis and provide a potential target to treat atherosclerosis.

Disclosures: **Y. Dong:** None. **M.L. Brophy:** None. **A. Wen:** None. **L. Yu:** None. **H. Wu:** None. **K. Song:** None. **A. Rahman:** None. **S. Wong:** None. **S. Kwak:** None. **K. Krygier:** None. **H. Chen:** None.

This research has received full or partial funding support from the American Heart Association.

213

Deletion of Epha2 Reduces Fibroproliferative Remodeling in Atherosclerosis and Vascular Smooth Muscle

Alexandra C Finney, Jonette M. Green, Mohammad A Rana, Louisiana State Univ Health Sciences Ctr, Shreveport, Shreveport, LA; Steven D. Funk, Washington Univ Sch of Med, St. Louis, MO; James G. Traylor, A. Wayne Orr, Louisiana State Univ Health Sciences Ctr, Shreveport, Shreveport, LA

Advanced atherosclerosis involves the recruitment of vascular smooth muscle cells, leading to smooth muscle-mediated fibroproliferative remodeling and plaque stiffening. We previously demonstrated the neuronal guidance receptor EphA2 shows enhanced expression in murine and human atherosclerosis, and EphA2 deletion in atherosclerosis-prone ApoE knockout mice attenuates lesion formation and endothelial cell activation in models of atherosclerosis. We now demonstrate deletion of EphA2 attenuates plaque progression to advanced stages associated with diminished smooth muscle content. While contractile smooth muscle cells show minimal EphA2 expression *in vitro* and *in vivo*, transition to the synthetic phenotype results in enhanced EphA2 expression and luciferase reporter activity *in vitro* and in atherosclerotic lesions. Furthermore, forced expression of EphA2 in quiescent smooth muscle cells is sufficient to suppress contractile smooth muscle markers, suggesting a role for EphA2 in smooth muscle phenotypic switch. Depletion of EphA2 results in significant reductions in proliferation within atherosclerotic plaques and in smooth muscle cells with associated reductions in serum-induced ERK and Akt signaling. Conversely, overexpression of EphA2 enhances smooth muscle proliferation *in vitro*, suggesting EphA2 is sufficient to drive proliferation. EphA2-deficient mice show reductions in plaque fibrosis and matrix remodeling. Consistent with this, depletion of EphA2 in vascular smooth muscle cells

exhibit a significant reduction in matrix deposition. Together these data suggest a role for EphA2 in smooth muscle-mediated fibroproliferative remodeling, representing the first link between EphA2 signaling and smooth muscle function in atherosclerosis.

Disclosures: **A.C. Finney:** None. **J.M. Green:** None. **M.A. Rana:** None. **S.D. Funk:** None. **J.G. Traylor:** None. **A. Orr:** None.

This research has received full or partial funding support from the American Heart Association.

214

Immune Response Biomarkers Characterize Endothelial Injury and Predict Acute Coronary Syndrome

Douglas S Harrington, Univ. of Southern California, Irvine, CA; Americo Simonini, Cedars Sinai, Los Angeles, CA

Acute Coronary Syndromes (ACS) are caused by free-radical mediated endothelial injury. Soft unstable coronary artery wall lesions form that can rupture causing thrombosis and obstruction. Three software systems (Akaike, Bayesian, Drop-in Deviance) tested 45 biomarkers and global risk factors to predict risk of ACS. A novel 9 protein algorithm was developed in 3 unique longitudinal, outcome-based studies and independently verified in MESA (Multiethnic Study of Atherosclerosis). The proteins selected include CTACK (Cutaneous T-Cell Attracting Chemokine)-homing of memory t-cells to tissue injury site; EOTAXIN (Eosinophil Chemotactic Protein)-attracts eosinophils to endothelial injury facilitating fibrin removal; MCP-3 (Monocyte Chemotactic Protein 3)-attracts monocytes and modulates activity; IL-16 (cytokine)-chemoattractant and modulator of T cell activation; sFAS (soluble FAS Ligand)-suppresses apoptosis; FAS Ligand (transmembrane protein tumor necrosis factor family member) induces apoptosis; HGF (Hepatocyte Growth Factor)-acts on epithelial cells and endothelial cells for angiogenesis, tumorogenesis, and tissue regeneration/repair; HDL (High-density Lipoprotein)-reverse cholesterol transport and inhibits oxidation, inflammation, endothelial activation, coagulation, and platelet aggregation; HbA1c (Hemoglobin A1c)-three-month average plasma glucose concentration. We conclude that the selection of biomarkers associated with endothelial damage and immune system response correlates with risk of ACS and reflects the underlying pathophysiology. Further studies are warranted.

Disclosures: **D.S. Harrington:** Employment; Significant; Co-CEO Predictive Health Diagnostics. Consultant/Advisory Board; Significant; laboratory Director Telomere Diagnostics. **A. Simonini:** None.

215

Rac-Signaling as a Critical Determinant of IL-1beta-Dependent Atherosclerotic Calcification

Abigail L Healy, Warren Alpert Medical Sch at Brown Univ, Providence, RI; Nicolle Ceneri, Yale Cardiovascular Res Ctr, New Haven, CT; Chris Mantsounga, Alan R Morrison, Warren Alpert Medical Sch at Brown Univ, Providence, RI

Coronary artery disease caused by atherosclerosis is the leading cause of morbidity and mortality in the world. Calcification of atherosclerotic plaque has predictive value in terms of cardiovascular event risk and mortality. Plaque calcium composition appears critical to determining cardiovascular risk; microcalcification has been associated with more vulnerable plaque phenotypes, while somewhat paradoxically, densely calcified plaque is associated with more stable disease. Inflammation can influence calcification of plaque, but immune modulators of plaque calcification are minimally defined. Rac1 and Rac2 are small GTPases that influence cytokine expression in plaque macrophages. We have defined a Rac-based signaling mechanism that regulates macrophage IL-1β expression. Using an atherosclerotic-prone mouse model, we identified that progressive calcification depends on altered Rac expression and activation (GTP-binding) through consequent effects on macrophage IL-1β production and IL-1R signaling. IL-1β production and its downstream signaling were critical determinants of atherosclerotic plaque calcification. In short, Rac2 expression determined the degree of Rac1 GTP-binding, acting as a brake on Rac1-dependent IL-1β production, whereas macrophage IL-1β production and atherosclerotic calcification depended on myeloid Rac1. Therapeutic inhibition of macrophage Rac-mediated IL-1β expression has the potential to be a treatment strategy for progressive, inflammatory atherosclerotic calcification.

Disclosures: **A.L. Healy:** None. **N. Ceneri:** None. **C. Mantsounga:** None. **A.R. Morrison:** None.

216

Hdac2 Modulates Atherosclerosis

Deepesh Pandey, Daijiro Hori, Yohei Nomura, Anil Bhatta, Dan Berkowitz, Lew Romer, Johns Hopkins Univ, Baltimore, MD

Objective: We recently described a novel regulatory role for histone deacetylase 2 (HDAC2) in vascular endothelial cell protection against the known endothelial injury stimulus Oxidize Low Density Lipoprotein (OxLDL). The goal of current study is to determine the effects of endothelial-specific HDAC2 overexpression on endothelial dysfunction and atherogenesis *in vivo*.
Approach and Results:
To study the effect of endothelial HDAC2 overexpression on vascular function and atherogenesis, we generated and characterized an endothelial specific human HDAC2 overexpressing transgenic mouse (HDAC2-Tg) under the control of the tie2 promoter. The founder HDAC2-overexpressing mice appear to have a normal phenotype- normal weight, mean arterial blood pressure (MAP) and pulse wave velocity (PWV). Isolated intact aortas from endothelial-specific overexpressing HDAC2 transgenic mice (HDAC2-Tg) exhibited a healthier vascular function profile with higher nitric oxide levels and less OxLDL-mediated vascular dysfunction. Further, we induced atherogenesis in C57BL6 and HDAC2-Tg mice by injecting adeno-associated viruses (AAV) encoding PCSK9 (D377Y) under the control of a liver-specific promoter by tail vein injection followed by high fat diet regimen for 12 weeks and measured endothelium-dependent vasorelaxation in isolated blood vessels, pulse wave velocity, an index of vascular stiffness and mean arterial blood pressure. HDAC2-Tg exhibited protected endothelial dependent vascular relaxation and no significant changes in MAP and PWV as compared to control mice.
Conclusion: HDAC2 is a critical regulator of endothelial function. Overexpression or activation of HDAC2 represents a novel therapy for endothelial dysfunction and atherosclerosis.

Disclosures: **D. Pandey:** Research Grant; Significant; AHA 16SDG27340010. **D. Hori:** None. **Y. Nomura:** None. **A. Bhatta:** None. **D. Berkowitz:** None. **L. Romer:** None.

This research has received full or partial funding support from the American Heart Association.

217

LOX-1 Primarily Contributes to M1 Macrophage Induced Foam Cell Formation

Branimir Popovic, Univ of Pittsburgh, Pittsburgh, PA; Antonella Millin, Univ of Udine, Udine, Italy; Deenadayalan Bakthavatsalam, Texas Heart Inst, Houston, TX; Murugesan Velayutham, Univ of Pittsburgh, Pittsburgh, PA; Steven Post, Univ of Arkansas for Medical Sciences, Little Rock, AR; Shanmugam Nagarajan, Univ of Pittsburgh, Pittsburgh, PA

Objectives: Modified LDL uptake by macrophages (Mϕ) leading to foam cell formation is an early event in atherosclerosis. Recent studies suggest that Mϕ polarization contributes to the progression of atherosclerosis. Therefore, we investigated the hypothesis that macrophage plasticity affects modified LDL uptake and subsequent foam cell formation.
Approach & Results: Bone marrow-derived Mϕ were treated with LPS and IFNγ or IL-4 to induce Mϕ polarization to M(LPS/IFNγ or M1) and M (IL4 or M2) phenotypes. Foam cell formation was determined after incubating M(LPS/IFNγ) and M(IL4) Mϕ with oxidized-LDL. Our results show that formation of foam cells was marginally increased in M(IL4) Mϕ compared to un-polarized M(-) Mϕ. However, accumulation of neutral lipids was higher in M(LPS/IFNγ) Mϕ compared to M(IL4) Mϕ indicating that foam cell formation is enhanced by polarization to pro-inflammatory M(LPS/IFNγ) Mϕ. Interestingly, mRNA and protein expression of CD36, one of the major scavenger receptors, were lower in M(LPS/IFNγ) Mϕ compared to un-polarized Mϕ. To assess the specific contribution of CD36, foam cell formation was assessed in Mϕ isolated from CD36-deficient mice. Notably, oxidized-LDL uptake and foam cell formation in CD36-deficient M(LPS/IFNγ) Mϕ was similar to M(LPS/IFNγ) Mϕ from wild type mice. This indicates that CD36 does not mediate the increased foam cell formation in M(LPS/IFNγ) Mϕ. We therefore examined expression of LOX-1, another scavenger receptor implicated in foam cell formation. We found that both mRNA and protein expression for LOX-1 increased several fold in M(LPS/IFNγ) Mϕ. We also showed that

TLR4-mediated NF-κB activation is the primary mechanism for the increased LOX-1 expression and foam cell formation in M(LPS/IFNγ) polarized Mϕ.

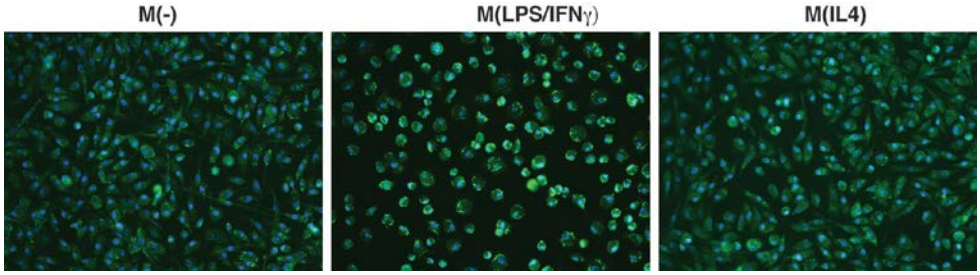

Conclusion: Macrophage plasticity, specifically polarization of Mϕ to pro-inflammatory M(LPS/IFNγ) phenotype promotes foam cell formation, which has implications for the progression of atherosclerosis.

Disclosures: **B. Popovic:** None. **A. Millin:** None. **D. Bakthavatsalam:** None. **M. Velayutham:** None. **S. Post:** None. **S. Nagarajan:** None.

218

Early Identification of Individuals on Dangerous Atherosclerotic Trajectories

Jeffrey K Raines, Harvard Medical Sch, Homestead, FL

Background: Atherosclerosis is a process that involves: (i) smooth muscle cell migration, (ii) intima thickening, (iii) loss of lumen, and (iv) other complex wall changes which occur in advance of blood flow alterations.
Methods: Working from the tenets that early atherosclerosis reduces Local Arterial Compliance and the upper extremity arteries, and even the carotid arteries, do not reflect disease in the coronary arteries due to differences in distribution of elastin, collagen, and smooth muscle between these beds, the major technical challenge was to devise an accurate method to measure Local Arterial Volume (Δ volume), since the parameter to assess atherosclerosis, is defined as Δ volume / Δ pressure.
Results The Soteria Cardiac Platform was developed, clinically tested, manufactured, and is now in clinical distribution. The Platform measures arterial compliance at the femoropopliteal distribution. The flagship Platform Module is the ***Soterogram***. This technology was awarded 8 United States Patents, cleared by the FDA for a National Launch on 05-31-14, and uses CPT and ICD-10 Codes supported by CMS required for Carrier payments in physician offices, clinics, and hospitals. The Platform has been in active clinical use for 22 months with over 10,000 procedures performed. The procedures are noninvasive, rapid, and inexpensive when compared to other techniques. The results obtained from the Platform have been documented to be extremely useful in diagnosis and management. The accuracy of the testing is very high with False Positive Rates and False Negative Rates of 3%, each. Interesting data has been assembled over the development and clinical periods. Besides the obvious diagnostic value, one example of ancillary data is an explanation of why females are protected from atherosclerosis early in life and develop a more aggressive form of atherosclerosis later in life.
Conclusions The Platform is now in active clinical use and has the potential of reducing cardiovascular morbidity and mortality by accurate and early identification of individuals at risk for atherosclerosis. The Platform involves Primary and Secondary Prevention and maybe used to monitor the success of therapy. Proper distribution of this technology has proven to be a very challenging task.

Disclosures: **J.K. Raines:** Ownership Interest; Significant; Technology Developer.

219

Deficiency of the T Cell Regulator Cbl-B Aggravates Atherosclerosis by Inducing CD8$^+$ T Cell-Mediated Macrophage Death

Tom T. Seijkens, Univ of Amsterdam, Amsterdam, Netherlands; Holger Winkels, Ludwig Maximilian's Univ Munich, Munich, Germany; Marion Gijbels, Univ of Amsterdam, Amsterdam, Netherlands; Jan A Kuivenhoven, Univ of Groningen, Groningen, Netherlands; Ljubica Perisic, Gabrielle Paulsson-Berne, Karolinska Univ Hosp, Stockholm, Sweden; Ulf Hedin, Karolinska Univ Hosp, s, Sweden; Goran K Hansson, Karolinska Univ Hosp, Stockholm, Sweden; Christian Weber, Norbert Gerdes, Ludwig Maximilian's Univ Munich, Munich, Germany; Menno P de Winther, Esther Lutgens, Univ of Amsterdam, Amsterdam, Netherlands

Aims: The E3-ligase CBL-B (*Casitas B-cell Lymphoma-B*) is an important negative regulator of T cell activation that is also expressed in macrophages. T cells and macrophages mediate atherosclerosis, but their regulation in this disease remains largely unknown; thus, we studied the function of CBL-B in atherogenesis.
Methods and Results: Here we investigated the effect of CBL-B deficiency in hyperlipidemic *Apoe*$^{-/-}$ mice in atherosclerosis. At the age of 20 weeks, chow diet-fed *Cbl-b*$^{-/-}$*Apoe*$^{-/-}$ mice showed a significant increase in plaque area in the aortic arch, due to greater macrophage infiltration. *Cbl-b*$^{-/-}$*Apoe*$^{-/-}$ macrophages displayed strong recruitment towards MCP1 and showed an increase in oxidized (ox)LDL uptake. In the aortic root of the same *Cbl-b*$^{-/-}$*Apoe*$^{-/-}$ mice, where more advanced plaques were present than in the aortic arch, plaque area rose by 40%, accompanied by a dramatic change in plaque phenotype. Plaques contained fewer macrophages, had larger necrotic cores, and harboured more CD8$^+$ T cells. The CD8$^+$ T cells of *Cbl-b*$^{-/-}$*Apoe*$^{-/-}$ mice were less susceptible to apoptosis and less resistant to Treg suppression. The increase in CD8$^+$ T cells in the plaque effected greater macrophage apoptosis, resulting in enhanced necrotic core formation. Moreover, CBL-B gene expression was downregulated in human atherosclerotic plaques, and positively correlated with FoxP3 expression, indicating an atheroprotective effect.
Conclusion: CBL-B is an important regulator of innate and adaptive immune reactions in atherosclerosis, by mediating macrophage recruitment and activation, CD8$^+$ T cell activation, and CD8$^+$ T cell-induced macrophage death in atherosclerotic plaques.

Disclosures: **T.T.P. Seijkens:** None. **H. Winkels:** None. **M. Gijbels:** None. **J.A. Kuivenhoven:** None. **L. Perisic:** None. **G. Paulsson-Berne:** None. **U. Hedin:** None. **G.K. Hansson:** None. **C. Weber:** None. **N. Gerdes:** None. **M.P.J. de Winther:** None. **E. Lutgens:** None.

220

Obesity Drives the Decline in Large HDL Subspecies Among Male Adolescents

Amy Sanghavi Shah, Anna Heink, Hannah Sexmith, Lawrence Dolan, Cincinnati Children's Hosp, Cincinnati, OH; Scott Gordon, Natl Insts of Health, Bethesda, MD; Jane Khoury, Deborah Elder, Cincinnati Children's Hosp, Cincinnati, OH; W. Sean Davidson, Univ of Cincinnati, Cincinnati, OH

We have shown that adolescents with type 2 diabetes have an altered HDL subspecies profile, characterized by a depletion of large apoE rich HDL particles. We have also shown a significant inverse relationship between this profile and arterial stiffness suggesting that the loss of these particles is associated with early atherosclerosis. We sought to evaluate known risk factors (that contribute to the depletion of large HDL subspecies in adolescents. We evaluated the contributions of obesity, insulin resistance and diabetes to loss of large HDL particles, in five adolescent groups (n=20 per group) with highly specific phenotypes. Insulin resistance was defined by fasting insulin levels and HOMA-IR Adolescent groups were: lean insulin sensitive (normal body mass index (BMI) with no insulin resistance; lean insulin resistant (normal BMI with insulin resistance), obese insulin sensitive (obese BMI with no insulin resistance), obese insulin resistant (obese BMI with insulin resistance), and with type 2 diabetes (obese with insulin resistance and type 2 diabetes by the American Diabetes Association criteria). Stored plasma from each participant was fractionated using gel filtration chromatography to isolate HDL subspecies. The mean age of the cohort was 17.9 ± 1.6 years. Groups did not differ in age and race (50% Caucasian, 50% African American, all male). Large rich HDL subspecies declined significantly across each group from lean insulin sensitive, to lean insulin resistant, to obese insulin sensitive, to obese insulin resistant to type 2 diabetes ($p<0.0001$). An inverse relationship was also seen for small HDL particles ($p<0.0001$). Medium size particles did not differ across groups. These data were confirmed by nuclear

magnetic resonance spectroscopy. Obesity explained ~50%, insulin resistance ~ 25%, and diabetes ~10% of the decline in large particles between lean insulin sensitive to type 2 diabetes participants. Twenty percent remained unexplained. Obesity appears to drive the decline in large atheroprotective HDL particles in male adolescents. However, contributions of insulin resistance and type 2 diabetes are evident. Whether weight loss reverses this profile and has the potential to improve cardiovascular risk remains to be determined.

Disclosures: **A.S. Shah:** None. **A. Heink:** None. **H. Sexmith:** None. **L. Dolan:** None. **S. Gordon:** None. **J. Khoury:** None. **D. Elder:** None. **W. Davidson:** None.

221

B-1b Cells Produce IgM to Malondialdehyde-Modified Low Density Lipoprotein in Perivascular Adipose Tissue in Response to Immunization And Attenuate Diet Induced Atherosclerosis

Prasad Srikakulapu, Aditi Upadhye, Sam M Rosenfeld, Kaivon Kouhestani, Melissa Marshall, Univ of Virginia, Charlottesville, VA; Thomas A Prohaska, Joseph L Witztum, Univ of California San Diego, La Jolla, CA; Coleen A McNamara, Univ of Virginia, Charlottesville, VA

Background: B-1b cells are capable of long-lasting IgM memory and secrete more IgM, particularly malondialdehyde-modified low density lipoprotein (MDA-LDL) specific IgM than B-1a cells after transfer into hyperlipidemic $Rag1^{-/-}$ mice. Id3 is a basic helix-loop-helix protein and dominant negative inhibitor of E proteins. B cell specific Id3 deficiency ($Id3^{BKO}$) increases B-1b cell numbers systemically and provides atheroprotection. Adipose tissue is a source of B-1b-derived IgM and regulates inflammatory cytokine production from M1 macrophages locally. Perivascular adipose tissue (PVAT) has been implicated in regulation of atherosclerosis. However, the effect of B cell specific Id3 deficiency on B-1 cell responses in PVAT is not yet known. Also, whether these B-1b cells respond to MDA-LDL immunization is unknown.**Hypothesis:** B-1b cells are present in PVAT and produce MDA-LDL specific IgM in PVAT, and immunization with MDA-LDL can enhance B-1b-mediated atheroprotection.**Methods and Results:** Flow Cytometry and Enzyme-Linked ImmunoSpot (ELISPOT) analysis of PVAT of normal chow diet fed young mice demonstrated that ApoE.$Id3^{BKO}$ mice have significantly higher numbers of B-1b cells and IgM secreting cells but not B-2 and B-1a cell numbers in PVAT compared to ApoE.$Id3^{WT}$ mice. ELISPOT demonstrated that the % of MDA-LDL specific IgM of total IgM secreting cells was significantly greater in PVAT, but not in spleen or bone marrow, of ApoE.$Id3^{BKO}$ mice compared to ApoE.$Id3^{WT}$ mice, suggesting that modified lipids such as MDA-LDL in plaques and PVAT may stimulate local B-1b cells to secrete MDA-LDL specific IgM. Adoptive transfer of B-1b cells into ApoE.$Rag1^{-/-}$ mice followed by MDA-LDL+PPS3 (pneumococcal polysaccharide) immunization, increased plasma IgM to MDA-LDL after 2 weeks and significantly attenuated atherosclerosis after 16 weeks of Western diet compared to PBS injected mice and B-1b cells transferred mice with PBS immunization. **Conclusion:** B-1b cells produce IgM to MDA-LDL in PVAT. MDA-LDL immunization increased IgM to MDA-LDL after two weeks and attenuated diet-induced atherosclerosis. Taken together, results suggest that B-1b cells may regulate atherosclerosis through both local and systemic IgM production.

Disclosures: **P. Srikakulapu:** None. **A. Upadhye:** None. **S.M. Rosenfeld:** None. **K. Kouhestani:** None. **M. Marshall:** None. **T.A. Prohaska:** None. **J.L. Witztum:** None. **C.A. McNamara:** None.

222

Utility of Non-Contrast, Non-EKG Gated Multi-Detector Computed Tomography to Rule Out Obstructive Coronary Artery Disease in Heart Transplant Recipients

Akanksha Thakkar, Hilda Mariana Gonzalez-Bonilla, Alpana Senapati, Nakul Gupta, Paulino Alvarez, Su Min Chang, Houston Methodist Hosp, Houston, TX

Background Annual or biannual coronary angiography is recommended after heart transplantation. This is associated with radiation and contrast exposure in addition to being invasive. Absence of coronary calcium on CT in non-transplanted patients has a high negative predictive value (NPV) to rule out obstructive CAD. Objective To determine whether the absence of coronary calcium on non-contrast, non-gated MDCT has a high NPV to rule out obstructive CAD in heart transplant recipients. Methods We included patients with a non-contrast, non-gated chest CT within 1 year of undergoing a coronary angiogram from 2006 to 2016. Obstructive CAD was defined as stenosis >50%. Coronary artery calcium scores (CACS) were calculated by the Agatston method using the syngo.via platform (Siemens

Healthcare GmbH, Germany). For analysis, CACS were categorized based on a) presence or absence of coronary calcium (i.e., CACS=0 or CACS>0) or b) severity of calcification (i.e., CACS=0, CACS 0-100 and CACS>100). Results We reviewed 76 consecutive angiograms and corresponding CTs. Prevalence of obstructive CAD was 9.2% (n=7). Prevalence of CACS=0 was 89.5% (n=68) of which 5 had obstructive CAD presenting a NPV of 93%. 8 patients had CACS>0 of which 2 had obstructive CAD on angiogram (positive predictive value=25%). CACS was found to correlate with severity of CAD by angiography($p<0.05$). Of 7 angiograms with obstructive CAD, stenosis >50% was found in 10 vessels - 5 LAD, 1 D1, 1 LCx, 2 OM branches and 1 RCA. Calculating CACS enabled detection of 1/5 LAD lesions; lesion in D1 was detected as an LAD lesion; lesions in the OM branches and RCA were not detected. Conclusion Absence of coronary calcium on MDCT has a high NPV in ruling out obstructive CAD in heart transplant recipients. However, only 2/10 obstructive lesions on angiogram had calcification plaques detected on corresponding vessels on CT. The clinical significance of this is yet to be determined.

Disclosures: **A. Thakkar:** None. **H. Gonzalez-Bonilla:** None. **A. Senapati:** None. **N. Gupta:** None. **P. Alvarez:** None. **S. Chang:** None.

223

CXCR4 Regulates B1 Cell Localization, Proliferation, Survival, and Atheroprotective IgM Production

Aditi Upadhye, Prasad Srikakulapu, Anh Nguyen, Chantel McSkimming, Univ of Virginia, Charlottesville, VA; Sotirios Tsimikas, Univ of California, San Diego, La Jolla, CA; Angela Taylor, Coleen McNamara, Univ of Virginia, Charlottesville, VA

Background: B1 cells exert protective effects in atherosclerosis through production of anti-inflammatory natural IgM antibodies that recognize oxidation-specific epitopes, such as MDA-LDL, present in diseased arteries. The bone marrow, spleen, and omental fat are known niches for B1 antibody production. However, the mechanisms underlying B1 localization to these sites and B1 antibody production are currently unclear.
Methods and Results: To identify key immune mediators that may be relevant to atherosclerosis, our lab has correlated surface marker expression on peripheral blood mononuclear cells with clinical markers of atherosclerosis in a human cohort. Expression of the chemokine receptor CXCR4 on circulating B1 cells associates with decreased plaque burden in coronary arteries and increased plasma levels of anti-MDA-LDL IgM antibodies. To study the role of CXCR4 in modulating B1 cell function, we generated mice with B cell-specific loss of CXCR4 on the atherogenic $ApoE^{-/-}$ background ($CXCR4^{BKO}$). Chow-fed, 8-week-old $CXCR4^{BKO}$ mice demonstrate fewer B1 cells (N=6-8, $p<0.0001$) and IgM antibody-secreting cells (N=6, $p=0.004$) in the bone marrow, and reduced plasma total IgM levels (N=6-8, $p=0.04$), relative to littermate controls ($CXCR4^{WT}$). To determine the role of CXCR4 on the B1 cell subset specifically, we adoptively transferred $CXCR4^{WT}$ or $CXCR4^{BKO}$ B1 cells into lymphocyte-deficient $Rag1^{-/-}ApoE^{-/-}$ mice. After 16 weeks of Western diet feeding, recipient mice given $CXCR4^{BKO}$ B1 cells demonstrate significantly reduced plasma IgM levels (n=5-7, $p=0.02$), and fewer donor B1 cells in the spleen, peritoneal cavity, and omental fat compared to recipients given $CXCR4^{WT}$ B1 cells. Few to no donor cells were detected in the bone marrow. To determine whether CXCR4 has a role in B1 cell proliferation or survival, BrdU incorporation and expression of the death receptor FasR were assayed in $CXCR4^{WT}$ and $CXCR4^{BKO}$ B1 cells. B1 cells from $CXCR4^{BKO}$ mice display heightened BrdU incorporation (n=4, $p=0.005$), yet have increased expression of FasR (n=4, $p=0.01$) relative to $CXCR4^{WT}$ B1 cells.
Conclusion: Our data demonstrate novel roles for CXCR4 in regulating several processes in B1 cells, including proliferation and survival, consequently impacting production of IgM.

Disclosures: **A. Upadhye:** None. **P. Srikakulapu:** None. **A. Nguyen:** None. **C. McSkimming:** None. **S. Tsimikas:** None. **A. Taylor:** None. **C. McNamara:** None.

This research has received full or partial funding support from the American Heart Association.

224

TRAF-STOP-RHDL-Nanoparticles Reduce Atherosclerosis

Claudia M van Tiel, Tom T Seijkens, Pascal J Kusters, Academic Medical Ctr, Amsterdam, Netherlands; Barbara Zarzycka, Cardiovascular Res Inst Maastricht, Maastricht, Netherlands; Oliver Soehnlein, Inst for Cardiovascular Prevention, Munich, Germany; Marion J Gijbels, Academic Medical Ctr, Amsterdam, Netherlands; Francois Fay, Translational and Molecular Imaging Inst, New York, NY; Boris Bleijlevens, Academic Medical Ctr, Amsterdam, Netherlands; Norbert Gerdes, Inst for Cardiovascular Prevention, Munich, Germany; Menno P de Winther, Academic Medical Ctr, Amsterdam, Netherlands; Gerry A Nicholaes, Cardiovascular Res Inst Maastricht, Maastricht, Netherlands; Willem J Mulder, Academic Medical Ctr, Amsterdam, Netherlands; Christian Weber, Inst for Cardiovascular Prevention, Munich, Germany; Esther Lutgens, Academic Medical Ctr, Amsterdam, Netherlands

Background: Inhibition of the costimulatory CD40-CD40L receptor/ligand dyad drastically reduces atherosclerosis. However, its long-term blockage can result in immune suppression. We recently identified small molecule inhibitors that block the interaction between CD40 and TNF Receptor Associated Factor (TRAF) 6 (TRAF-STOPs), while leaving CD40-TRAF2/3/5 interactions intact, thereby preserving CD40-mediated immunity. We investigated the potential of the TRAF-STOPs to treat atherosclerosis. **Results:** Treatment of ApoE-/- mice with either TRAF-STOP 6877002 or 6860766 reduced both initial and established atherosclerosis and induced a stable plaque phenotype with increased collagen and VSMC content, decreased lipid core, and a decrease in macrophage number. There were no signs of immune suppression or toxicity. In vitro experiments showed that the TRAF-STOPs reduced inflammation in macrophages, but not in T- or B cells, endothelial cells or vascular smooth muscle cells. Intravital microscopy demonstrated that the TRAF-STOPs reduced monocyte recruitment to the plaque. The CD36-mediated uptake of ox-LDL by macrophages and foam cell formation was also inhibited by TRAF-STOPs. Transcriptomics analysis and Ingenuity pathway analysis of TRAF-STOP-treated bone marrow-derived macrophages revealed that the top ranking canonical pathways for both TRAF-STOPs involved pro-inflammatory immune responses and cholesterol biosynthesis. 6877002 also affected cell cycle regulation. Surface plasmon resonance experiments and mutation studies demonstrated that 6877002 and 6860766 had a different interaction site within the TRAF6 C-domain, which explained the additional effect of 6877002. To target TRAF-STOPs specifically to macrophages, 6877002 was incorporated into rHDL nanoparticles. Flowcytometry and fluorescent microscopy demonstrated accumulation of rHDL-6877002 in plaque macrophages after a single dosis. Six weeks of rHDL-6877002 treatment reduced atherosclerosis in ApoE-/- mice. **Conclusions:** TRAF-STOP 6877002 and 6860766 can overcome the current limitations of long-term CD40 and CD40L inhibition and nanoparticle-mediated delivery TRAF-STOP to plaque macrophages may become a future therapy for atherosclerosis.

Disclosures: **C.M. van Tiel:** None. **T.T. Seijkens:** None. **P.J. Kusters:** None. **B. Zarzycka:** None. **O. Soehnlein:** None. **M.J. Gijbels:** None. **F. Fay:** None. **B. Bleijlevens:** None. **N. Gerdes:** None. **M.P.J. de Winther:** None. **G.A. Nicholaes:** None. **W.J. Mulder:** None. **C. Weber:** None. **E. Lutgens:** None.

226

C-type Lectin Receptor Clec9a on Cd8a+ Dendritic Cells Promotes the Development of Atherosclerosis in Mice

Haddad Yacine, Charlotte Lahoutte, INSERM UMR-970, Paris, France; Marc Clément, Dept of Med Div of Cardiovascular Med, Cambridge, United Kingdom; Ludivine Laurans, Sarvenaz.Metghalchi Sarvenaz.Metghalchi, Lynda Zeboudj, Andreas Giraud, Xavier Loyer, Marie Vandestienne, Julien Wain-Hobson, Bruno Esposito, Stephane Potteaux, Hafid Ait-Oufella, INSERM UMR-970, Paris, France; Caetano Reis e Sousa, The Francis Crick Inst, london, United Kingdom; Alain Tedgui, Ziad Mallat, Soraya Taleb, INSERM UMR-970, Paris, France

Necrotic core formation during the development of atherosclerosis is associated with a chronic inflammatory response and promotes accelerated plaque development and instability. We hypothesized that sensing of necrotic cells by CLEC9A, a C-type lectin receptors selectively expressed by the CD8α$^+$ subset of dendritic cells (CD8α$^+$DCs), plays a determinant role in the inflammatory response of atherosclerosis.
Reconstitution of lethally-irradiated Ldlr-/- with bone marrow from CLEC9A-/- mice significantly reduced atherosclerotic lesion size in aortic root after 5 weeks of high fat diet (HFD) (-45%, p=0,0059) and after 7

weeks of HFD (-40%, p=0,0017), as compared to mice transplanted with wild-type bone marrow-derived cells. However, no effect of CLEC9A was observed after 13 weeks of HFD (p=0,4996), suggesting early effect of CLEC9A on atherosclerosis development.
The same phenotype was observed in 20-week-old Apoe-/-CLEC9A-/- compared to Apoe-/- mice put on chow diet (-50%, p=0,0022).
Interestingly, an increase of IL-10 expression (+60%, p=0,0093) was observed in spleens of mice deficient for CLEC9A. Furthermore, the beneficial effect observed in CLEC9A-/- was abolished in CLEC9A-/-IL-10-/- compared to IL-10-/- (p=0,4452). Moreover, a specific deletion of Clec9a in CD8α$^+$DC cells significantly increases Il10 expression, reduces macrophage and T cell contents within the lesions, and significantly limits the development of atherosclerosis. In conclusion, our results identify a new role of Clec9a in regulating vascular inflammation and atherosclerosis development and potentially identify a new target for disease modulation.

Disclosures: **H. Yacine:** None. **C. Lahoutte:** None. **M. Clément:** None. **L. Laurans:** None. **S. Sarvenaz.Metghalchi:** None. **L. Zeboudj:** None. **A. Giraud:** None. **X. Loyer:** None. **M. Vandestienne:** None. **J. Wain-Hobson:** None. **B. Esposito:** None. **S. Potteaux:** None. **H. Ait-Oufella:** None. **C. Reis e Sousa:** None. **A. Tedgui:** None. **Z. Mallat:** None. **S. Taleb:** None.

227

Megalin Regulates Angiotensinogen and Contributes to Atherosclerosis

Feiming Ye, Zhejiang Univ The Second Hosp, Hangzhou, China; Deborah Howatt, Univ of Kentucky, Lexington, KY; Adam Mullick, Mark Grahan, Ionis Pharmaceuticals, Carlsbad, CA; Anju Balakrishnan, Craig Vander Kooi, Univ of Kentucky, Lexington, KY; A.H. Jan Danser, Erasmus MC, Rotterdam, Netherlands; Jian-An Wang, Zhejiang Univ The Second Hosp, Hangzhou, China; Alan Daugherty, Hong Lu, Univ of Kentucky, Lexington, KY

Objective: Angiotensinogen (AGT) is the only substrate of the renin-angiotensin system to generate angiotensin peptides, including angiotensin II (AngII), a critical contributor to atherosclerosis. AGT interacts with megalin in proximal convoluted tubules of kidney. The purpose of this study was to determine effects of megalin on AGT, AngII, and atherosclerosis in mice.
Methods and Results: Male C57BL/6 mice were injected subcutaneously with vehicle (PBS) or megalin second generation antisense oligonucleotides (ASO) for 5 weeks. Inhibition of megalin was confirmed by more than 80% reduction of megalin mRNA in kidney. Urine was collected using metabolic cages after 5 weeks of vehicle or ASO injections. At termination, blood was collected with EDTA and protease inhibitor cocktail to measure plasma concentrations of renin and AngII, respectively. Urine AGT and renin concentrations were profoundly increased, accompanied by reduction of renal, but not plasma, AngII production. To determine whether megalin inhibition influences atherosclerosis, male LDL receptor -/- mice were injected with vehicle, control ASO, or megalin ASO for 13 weeks. Western diet was started 1 week after the first injection and continued for 12 weeks. Atherosclerosis was quantified by en face analysis of the aortic intimal surface from the ascending aorta to 3 mm proximal to the left subclavian artery branch. Megalin ASO administration led to more than 70% reductions of megalin mRNA in kidney. Consistent with the effects in C57BL/6 mice, AGT concentrations were significantly higher in urine (Vehicle, control ASO and megalin ASO groups: 85 ± 10, 109 ± 71, and 4616 ± 637 ng/ml, respectively; P<0.001 by one way ANOVA with Holm-Sidak method). Plasma total cholesterol concentrations did not differ among groups. Megalin inhibition reduced atherosclerotic lesion area compared to the other two groups (Percent lesion area in Vehicle, control ASO and megalin ASO groups: 23 ± 2, 20 ± 2, 12 ± 1 %, respectively; P < 0.001 by one way ANOVA with Holm-Sidak method).
Conclusions: Inhibition of megalin increased urine AGT and renin, reduced renal AngII concentrations, and diminished hypercholesterolemia-induced atherosclerosis in mice.

Disclosures: **F. Ye:** None. **D. Howatt:** None. **A. Mullick:** Employment; Modest; Employee of Ionis Pharmaceuticals. **M. Grahan:** Employment; Modest; Employee of Ionis Pharmaceuticals. **A. Balakrishnan:** None. **C. Vander Kooi:** None. **A. Danser:** None. **J. Wang:** None. **A. Daugherty:** None. **H. Lu:** None.

228

The Establishment of a Novel Atherosclerosis Regression Model in Mice

Chaojun Tang, Lijie Ren, Yifei Liu, Yinyan Wang, Yiren Cao, Lei Wang, Fan Wu, Tao You, **Li ZHU male**, Soochow Univ, Suzhou, China

Background: Inhibition of plaque progression by various anti-atherosclerotic drugs is a canonical aspect underlying their therapeutic efficacy. Although existed animal models of plaque regression are available for drug evaluation, they are either highly invasive or time-consuming. We therefore aimed to establish a practical method to study the mechanism of atherosclerosis regression based on hemodynamic regulation of atherosclerosis. Methods: A carotid plaque regression model in mice was developed based on the previously described model. Briefly, a single slipknot was applied to all three branches of the left carotid artery (LCA) in ApoE$^{-/-}$ mice. After 2 weeks on HFD, the blood flow in LCA was reconstructed by slipknot release. Mice were housed for additional 4 weeks. Carotid ultrasonography was used to verify successful induction of disturbed flow and the reconstruction of the blood flow. Atherosclerotic plaques were stained with Sudan IV. The infiltration of smooth muscle cells and macrophages were determined by immunofluorescence staining. Results: Histology studies demonstrated similar cellular components and lipid deposition between the d-flow induced plaques in the LCA in WT mice and atherosclerotic plaques in aorta of ApoE$^{-/-}$ mice on HFD. However, a significantly higher proportion of SMC (n=5, p<0.0001) and lower macrophage infiltration (n=6, p=0.0056) were observed in the induced carotid plaques compared to the aortic plaques. After the release of the knots, an abrupt increase in flow velocity indicated a successful restoration of blood flow from the LCA to its branches. At this point, the restored flow in ligated LCA was still lower compared to the untied right carotid artery (RCA). After the procedure, mice were given chew diet for additional 4 weeks and blood flow was re-accessed using carotid ultrasonography. Results showed no significant difference of blood flow between LCA and RCA, indicating nearly complete regression of carotid atherosclerosis. Conclusion: We have established a highly reproducible atherosclerosis regression model with less invasiveness and genetic independence that supplies a practical tool for evaluation of anti-atherosclerotic drugs and for the pathophysiology of atherosclerosis regression.

Disclosures: **C. Tang:** Research Grant; Significant; NSFC 81670134, NSFC 31300781. **L. Ren:** None. **Y. Liu:** None. **Y. Wang:** None. **Y. Cao:** None. **L. Wang:** None. **F. Wu:** None. **T. You:** None. **L. Zhu:** Research Grant; Significant; NSFC 81370373.

229

Mucosal Immunity Shapes the Lipoprotein Small-RNA Fingerprint from Commensal, Dietary and Environmental Microbiota

Ryan M Allen, Marisol A. Ramirez-Solano, Wanying Zhu, Shilin Zhao, Quanhu Sheng, Kasey Vickers, MacRae Linton, Vanderbilt Univ Medical Ctr, Nashville, TN

Cardiovascular disease (CVD) is a leading cause of mortality in developed countries and is a frequent comorbidity of numerous metabolic and inflammatory diseases that demands more effective therapies. Dyslipidemias are a classical risk factor for CVD, but emerging alternative functions of lipoproteins have implicated them in novel narratives for the pathophysiology of many diseases that warrant further study. Our lab has identified functional, intercellular gene regulatory networks mediated by extracellular transport of microRNAs (miRNA) by lipoproteins. Here, we quantified the landscape of small RNAs (sRNA) on human and animal lipoproteins and discovered that most lipoprotein-sRNAs are derived from microorganisms of multiple kingdoms, primarily bacteria. Based on these observations, our over-arching hypothesis is that lipoprotein-sRNA signatures are shaped by the interface of host tissues with resident, environmental and dietary microbiota, and likely participate in unique gene regulation networks that contribute to complex (patho)physiological traits. To investigate this hypothesis, we developed a sRNA-sequencing analysis pipeline that identifies and quantifies both host and non-host sRNAs. Using this bioinformatic tool, we identified and validated a number of lipoprotein-sRNAs derived from bacteria that are similar in size to miRNAs with identical seed regions, termed Doppelganger (Dopl)-miRNAs. We hypothesized that mucosal immunity contributes to non-host sRNAs on lipoproteins, as mucosal linings are a primary interface between host tissues and microorganisms. To this end, we investigated the lipoprotein-sRNAs of mice lacking the polymeric immunoglobulin receptor (pIgR$^{-/-}$), which is devoid of polymeric IgA and IgM at mucosal linings and models human respiratory and intestinal diseases. We report a global increase in lipoprotein-miRNAs juxtaposed with a profound decrease in bacterial sRNA

and Dopl-miRNAs from specific taxa. This work unfurls novel links between microbiota, mucosal immunity, and lipoprotein-sRNA gene networks and emphasizes the potential for novel nucleic-acid based therapeutics.

Disclosures: **R.M. Allen:** None. **M.A. Ramirez-Solano:** None. **W. Zhu:** None. **S. Zhao:** None. **Q. Sheng:** None. **K. Vickers:** None. **M. Linton:** None.

This research has received full or partial funding support from the American Heart Association.

233

Genetic Evidence for Overlap in the Pathogenesis of Peripheral Artery Disease and Coronary Artery Disease

Derek Klarin, Massachusetts General Hosp, Boston, MA; Aeron Small, Univ of Pennsylvania Medical Ctr, Philadelphia, PA; Jie Huang, VA Boston Healthcare System, Boston, MA; Julie Lynch, VA Salt Lake City Healthcare System, Salt Lake City, UT; Shipra Arya, Emory Univ Sch of Med, Atlanta, GA; Themistocles L. Assimes, Stanford Univ Sch of Med, Stanford, CA; Pradeep Natarajan, Massachusetts General Hosp, Boston, MA; Danish Saleheen, Univ of Pennsylvania Medical Ctr, Philadelphia, PA; Sekar Kathiresan, Massachusetts General Hosp, Boston, MA; Daniel J Rader, Univ of Pennsylvania Medical Ctr, Philadelphia, PA; John Concato, Yale Univ Sch of Med, New Haven, CT; J. Michael Gaziano, Kelly Cho, VA Boston Healthcare System, Boston, MA; Yan Sun, Peter W Wilson, Emory Univ Sch of Med, Atlanta, GA; Kyong-Mi Chang, Univ of Pennsylvania Medical Ctr, Philadelphia, PA; Christopher J O'Donnell, VA Boston Healthcare System, Boston, MA; Philip S Tsao, Stanford Univ Sch of Med, Stanford, CA; Scott M Damrauer, Univ of Pennsylvania Medical Ctr, Philadelphia, PA; VA Million Veteran Program

Introduction: Peripheral artery disease (PAD) is thought to share atherosclerotic biologic mechanisms and traditional risk factors with coronary artery disease (CAD). Although significant progress has been made in identifying genetic contributors to CAD, genetic factors underlying PAD remain largely uncharacterized. The aim of our study was to evaluate the shared genetic architecture between PAD and CAD. **Hypothesis:** DNA sequence variants associated with CAD risk are also associated with PAD. **Methods:** We analyzed the electronic health records from 239,621 U.S. Veterans of European ancestry with available imputed genetic data from the VA Million Veteran Program. Within this cohort we identified 16,364 participants with PAD, and 67,636 with CAD. We constructed additive weighted genetic risk scores (GRS) of 57 DNA sequence variants previously associated with CAD at genome-wide significance. We standardized the GRS to have a mean of zero and standard deviation (SD) of 1, and assessed the strength of its association with PAD through logistic regression. Models were adjusted for age, sex, and 7 principal components of ancestry. In a mediation analysis, we then included CAD status in the model to examine if these genetic associations remained significant after accounting for a CAD diagnosis. **Results:** The CAD GRS was significantly associated with clinical CAD [OR = 1.22 per SD increase in GRS, (95%CI: 1.21 -1.23, Z-Score = 44.5, $P < 2 \times 10^{-16}$)]. The CAD GRS was also significantly associated with PAD [OR = 1.12 per SD increase in GRS, (95%CI: 1.10-1.14, Z-Score = 14.5, $P < 2 \times 10^{-16}$)]. This magnitude of association was attenuated when further adjusting for CAD in the regression model but remained strongly significant [OR = 1.05 per SD increase in GRS, (95%CI: 1.03-1.07, Z-Score = 6.2, $P = 5.6 \times 10^{-10}$)]. **Conclusions:** In the largest single cohort of CAD and PAD cases worldwide, we found that a genetic risk score of DNA sequence variants associated with risk for CAD are also associated with risk of PAD, even after accounting for the presence of coronary atherosclerosis. These data suggest significant overlap in the mechanisms underlying development of atherosclerosis within both the peripheral and coronary arterial beds.

Disclosures: **D. Klarin:** None. **A. Small:** None. **J. Huang:** None. **J. Lynch:** None. **S. Arya:** None. **T.L. Assimes:** None. **P. Natarajan:** None. **D. Saleheen:** None. **S. Kathiresan:** Employment; Modest; Regeneron, Merck, Celera, Novartis, Bristol-Myers Squibb, Sanofi, AstraZeneca, Alnylam, Eli Lilly, Leerink, Catabasis. Research Grant; Modest; Regeneron, Bayer. Consultant/Advisory Board; Modest; Regeneron. **D.J. Rader:** Consultant/Advisory Board; Modest; Merck. **J. Concato:** None. **J. Gaziano:** None. **K. Cho:** None. **Y. Sun:** None. **P.W.F. Wilson:** None. **K. Chang:** None. **C.J. O'Donnell:** None. **P.S. Tsao:** None. **S.M. Damrauer:** None.

234

Interleukin 2 Promotes Proliferation and Migration in Vascular Smooth Muscle Cells

Spencer Barnhill, Prakash Arumugam, John Matsuura, Wright State Univ, Dayton, OH; Scott Berceli, Univ of Florida, Gainesville, FL; Katie Carroll, Lucile Wrenshall, Wright State Univ, Dayton, OH

Interleukin-2 (IL-2) is primarily known as a soluble cytokine that regulates T cell responses. We previously reported, however, that IL-2 is retained in the extracellular matrix by association with perlecan, a heparan sulfate proteoglycan (HSPG). Perlecan is the main HSPG in vascular basement membranes, and previous studies from our laboratory demonstrated that, in human arteries, vascular smooth muscle cells (VSMC) are surrounded by perlecan-bound IL-2. We also noted that IL-2 deficient mice lose SMCs with age, leading to widened esophagi and aortic aneurysms. Given this information, we hypothesized that IL-2 has a direct impact on VSMC, and that VSMC express functional IL-2 receptors (IL-2R). We therefore examined both protein and mRNA expression of each of the three IL-2R subunits (alpha, beta, gamma) on human VSMC grown from arterial explants. These VSMC expressed SMC actin, smooth muscle myosin heavy chain, and when quiescent, smoothelin. Protein expression was assessed by in cell Western and by Western blot analysis. Receptor expression was evaluated under distinct culture conditions, which yielded highly proliferative, intermediate, or quiescent VSMC. Contractile protein expression was low, intermediate, or high, respectively, consistent with the characteristics of proliferating vs quiescent SMCs. Each phenotype expressed all 3 subunits of the IL-2R. IL-2 subunits appeared to follow a cytoskeletal pattern in cells expressing high levels of contractile proteins. Western blot analysis of VSMC lysates revealed expression of all 3 receptors at molecular weights identical to lysates from a T cell line. VSMCs also expressed mRNA for each receptor subunit. Functionally, IL-2 promoted migration (using a Boyden chamber assay) and proliferation in a dose dependent fashion. Because excess proliferation and migration are critical to intimal hyperplasia, we asked whether IL-2 levels change under conditions known to generate intimal hyperplasia. In a rabbit model, IL-2 mRNA increased in venous grafts exposed to high flow for 2h. IL-2 levels, by Western blot, were also increased in human hyperplastic veins. In conclusion, these data show that VSMC have functional IL-2R, and suggest that IL-2 may contribute to the development of intimal hyperplasia.

Disclosures: **S. Barnhill:** None. **P. Arumugam:** None. **J. Matsuura:** None. **S. Berceli:** None. **K. Carroll:** None. **L. Wrenshall:** None.

235

Interaction Between a Macrophage Chemokine Receptor, CCR2, and Its Ligand Plays a Crucial Role in Macrophage Recruitment Aand Regulated Inflammation in Normal Wound Healing

Anna E Boniakowski, Andrew Kimball, Amrita Joshi, Ron Allen, Matt Schaller, Peter Henke, Beth Moore, Steve Kunkel, Katherine Gallagher, Univ of Michigan, Ann Arbor, MI

BACKGROUND: Wound healing in chronic diseases, such as type 2 diabetes (T2D), is impaired due to dysregulated inflammation. Innate immune cells, particularly macrophages, play a significant role in regulated inflammation following tissue injury. After injury, CCR2+ monocytes are recruited to the peripheral wound. This recruitment is mediated in part by the CCR2 ligand, CCL2. Thus, we hypothesized that the CCL2/CCR2 interaction is vital for normal wound healing and appropriate inflammation, and that this signaling cascade is impaired in T2D. METHODS: $CCR2^{-/-}$ mice and littermate controls underwent 4mm hindlimb wounds, and wound closure was compared daily. Wound macrophages (CD3-CD19-NK1.1-CD11b+ cells) were analyzed on day 3 by flow cytometry for intracellular cytokine production. Adoptive transfer was performed using blood CD11b+ cells from WT C57BL/6 or $CCR2^{-/-}$ mice isolated by magnetic sorting and transferred into $CCR2^{-/-}$ mice via tail vein injection. Mice were then wounded and wound closure was compared between the two groups. C57BL/6 mice were maintained on normal or high fat diet for 12-14 weeks, wounds were created, and CD11b+ cells were isolated from wounds on day 2. ELISA for CCL2 was performed. RESULTS: $CCR2^{-/-}$ mice showed significantly impaired wound healing on days 2-7 compared with littermate controls. Macrophages isolated on day 3 from wounds of $CCR2^{-/-}$ mice expressed significantly less inflammatory cytokines (IL-1β, TNF-α) by qPCR. Flow cytometry analysis revealed less Ly6C hi macrophages in the wounds, as well as macrophages that made significantly less IL-1β, NOS2, and TNF-α. When adoptive transfer was performed, wound healing was restored to normal in the mice that received WT compared to those that received $CCR2^{-/-}$ CD11b+ cells ($P< 0.01$). Since CCR2 is important for normal wound inflammation, and we have previously shown that inflammation is impaired in the diet-induced obese (DIO) mice, we examined CCL2 in DIO wounds. CCL2

was significantly decreased in DIO wound macrophages on day 2. CONCLUSION: Appropriate CCR2/CCL2 interaction plays a crucial role in macrophage recruitment and regulated inflammation in normal wound healing. Impairment in CCR2/CCL2 signaling may be responsible, in part, for delayed early inflammation in T2D.

Disclosures: **A.E. Boniakowski:** None. **A. Kimball:** None. **A. Joshi:** None. **R. Allen:** None. **M. Schaller:** None. **P. Henke:** None. **B. Moore:** None. **S. Kunkel:** None. **K. Gallagher:** None.

236

Carbon Monoxide Mediated Changes in Macrophages are Regulated by Vagal Activation

Karim Salem, Guiying Hong, Andrew Leake, Ankur Aggarwal, Univ of Pittsburgh, Pittsburgh, PA; Edith Tzeng, VA Medical Ctr, Pittsburgh, PA

Introduction:
Carbon monoxide (CO) has potent vasoproective effects in vivo through changes in macrophage (MΦ) function. Because of these marked changes, we examined the vagal cholinergic anti-inflammatory pathway in regulating the actions of inhaled CO. We previously showed that vagotomy inhibited the ability of inhaled CO to prevent intimal hyperplasia following arterial injury in rats. We now hypothesize that the anti-inflammatory effects of inhaled CO can be blocked through pharmacologic vagal inhibition.
Methods:
Sprague-Dawley rats (3 rats/group) were treated with inhaled CO (250 parts per million) for 1 hr or remained in room air. Some were injected with atropine (0.05 mg/kg SQ) 1 hr prior to and just prior to inhaled CO treatment. Peritoneal macrophages (MΦ) were collected 1 hr after CO treatment or comparable time period in control rats and were cultured overnight under standard conditions. Media from these cells were collected for Western blot analysis for high mobility box group 1 (HMGB1) and VEGF.
Results:
MΦ isolated from CO treated rats released increased levels of HMGB1 and VEGF into the media compared to MΦs from air treated rats (1.7 and 4 fold increase, respectively; Fig.). These molecules mediate the proendothelial actions of inhaled CO. MΦs isolated from atropine treated rats showed a mild reduction of HMGB1 and VEGF secretion. In contrast, MΦ from atropine and CO treated rats showed a significant inhibition of HMGB1 release ($P<0.01$ vs. all other treatment groups) and a trend toward significance in the reduction in VEGF release (Fig.).
Conclusions:
Inhaled CO activates vagal signaling to mediate changes in MΦ behavior. Inhibition of vagal signaling with atropine blocked the changes in MΦ induced by inhaled CO, confirming the importance of the vagus nerve in mediating the vasoprotective actions of CO. These findings suggest the potential ability to reproduce the therapeutic actions of CO through pharmacologic vagal stimulation.

Disclosures: **K. Salem:** None. **G. Hong:** None. **A. Leake:** None. **A. Aggarwal:** None. **E. Tzeng:** Research Grant; Significant; VA Merit Award.

237

The Role of Lymphocyte Specific Protein-1 in the Phenotypic Switch of Smooth Muscle Cells After Arterial Injury

Mirnal A Chaudhary, Go Urabe, Alex Hayden, Sarah Franco, Xudong Shi, Lian Wang-Guo, Univ of Wisconsin-Madison, Madison, WI; K Craig Kent, The Ohio State Univ, Columbus, OH

Background: After vascular injury, vascular smooth muscle cells (SMCs) switch from a differentiated contractile state to synthetic de-differentiated phenotype which contributes to the pathophysiology of restenosis. Experimental data generated by our lab indicate that TGF-β downregulates contractile proteins and stimulates migration. To understand how TGF-β promotes SMC phenotypic switch in injured arteries, we performed an Affymetrix Array analysis and identified Lymphocyte Specific Protein-1 (LSP1) among other upregulated genes. LSP1 is known to play a role in neutrophil extravasation, however the role of LSP1 within SMCs is unknown. We hypothesize that LSP1 contributes to SMC pathophysiological behavior through changes in cell architecture and migration *in-vivo* and *in-vitro.* Methods and Results: After carotid artery angioplasty, male Sprague-Dawley rats were sacrificed at 3, 7, and 14 days after injury for immunohistochemistry. Immunofluorescence staining revealed a unique upregulation of LSP1 within the neointima, media, and adventitia at 7 and 14 days, but not at 3 days after injury. Confocal

images revealed that the LSP1 positive cells minimally express α-SMA (Pierson's Coefficient, r=.017). Additional characterization experiments using immune cell markers CD3 and CD45 show no co-localization with LSP1 positive cells. To mimic the *in-vivo* neointimal cells and vascular injury induced de-differentiation *in-vitro*, rat A10 cells were treated with solvent or PDGF-bb (10 ng/mL). Quantitative RT-PCR demonstrated an upregulation of LSP1 mRNA after 24 hrs of PDGF-BB stimulation. Using Western Blotting, we confirm an upregulation of LSP1 protein after 48 hrs of PDGF-BB stimulation. Lastly, we performed nuclear and cytoplasmic fractionation followed by Western Blotting which demonstrated that LSP1 is remained within cytoplasmic fraction of the A10 cell after treatment with PDGF-BB. Conclusion: These results demonstrate that LSP1 is increased *in-vivo* after balloon injury, and *in-vitro* after PDGF-BB stimulation. Experiments to characterize the identity of these LSP1 cells *in-vivo* are in process, with future *in-vitro* experiments to focus on the role of LSP1 phosphorylation as a part of cytoskeletal remodeling and cellular migration.

Disclosures: **M.A. Chaudhary:** None. **G. Urabe:** None. **A. Hayden:** None. **S. Franco:** None. **X. Shi:** None. **L. Wang-Guo:** None. **K. Kent:** None.

238

Sub-Endothelial Matrix Targeted Liposomal Nanoparticles For Vascular Therapeutics

Jonathan S Cudnik, Phillip C West, Richard K Fisher, UT Graduate Sch of Med, Knoxville, TN; Sam Mattern-Schain, Michael Best, Univ of Tennessee Knoxville, Knoxville, TN; Stacy S Kirkpatrick, Michael B Freeman, Oscar H Grandas, Deidra J Mountain, UT Graduate Sch of Med, Knoxville, TN

Objectives: Vascular intervention results in intimal denudation, exposure of the sub-endothelial matrix, and subsequent intimal hyperplasia (IH), under the control of numerous remodeling mechanisms. Reduction of IH-induced restenosis may be achieved by manipulation of these remodeling pathways through targeted molecular inhibition. Spatially-controlled nanoparticles designed to co-localize to exposed sub-endothelial matrices could provide an optimal delivery system for targeted vascular therapeutics. To his end, we aimed to develop the framework for a surface-modified liposomal drug delivery platform designed to preferentially bind collagen type IV. **Methods:** Non-targeted control liposomes (NTL) were formed with bulk DOPC-PEG, 30% cholesterol, and 0.1 mol% Rhodamine-DOPE. DSPE-PEG-DBCO lipids were conjugated to peptides previously shown to bind collagen IV via copper-free click chemistry and inserted at 5 mol% to form collagen-targeting liposomes (CTL), either at hydration (PreCTL) or by post-insertion via micellar transfer (PostCTL). Peptide conjugation was confirmed by MALDI-TOF, and liposomes were characterized by DLS and electrophoretic mobility. Liposome binding was assayed on collagen IV matrices dried at 3ug/cm^2 and quantified by fluorescence at 0-24hr static 37°C incubation. **Results:** All liposome formulations exhibited a narrow size distribution (~100nm) and neutral-low positive charge. CTLs demonstrated a significant increase in binding vs. NTLs (Fig1). **Conclusions:** CTLs demonstrated significant affinity for collagen IV binding in a static environment compared with NTLs. Future studies aim to optimize the binding capacity of CTLs via further lipid modifications and under flow conditions mimicking vessel wall hemodynamics. Considering the efficacy demonstrated here, CTLs show promise as the framework for a spatially-controlled drug delivery platform for future application in targeted vascular therapeutics.

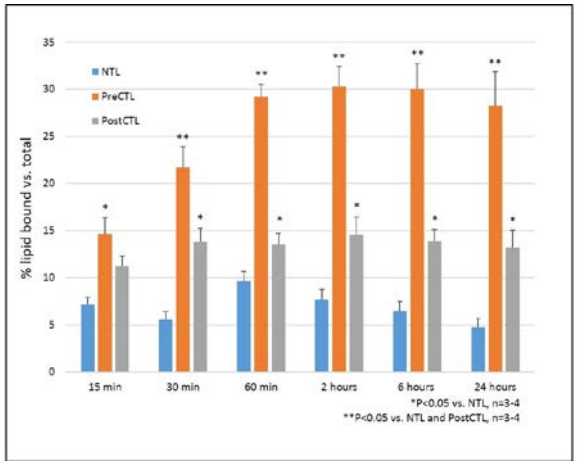

Disclosures: **J.S. Cudnik:** None. **P.C. West:** None. **R.K. Fisher:** None. **S. Mattern-Schain:** None. **M. Best:** None. **S.S. Kirkpatrick:** None. **M.B. Freeman:** None. **O.H. Grandas:** None. **D.J.H. Mountain:** None.

239

Parthanatos is Involved in Hydrogen Peroxide Induced Vascular Smooth Muscle Cell Death

Conner C Feldman, Ting Zhou, Noel Phan, Bo Liu, Univ of Wisconsin, Madison, WI

Objectives
Oxidative stress underlies major vascular diseases including atherosclerosis and abdominal aortic aneurysm. Hydrogen peroxide (H2O2) is widely used to trigger oxidative stress in vitro for the study of apoptosis. However, we have previously shown that vascular smooth muscle cells (SMCs) respond to high concentrations (>1 mM) of H2O2 with necrosis. Traditionally regarded as incidental form of cell death, necrosis can occur through different mechanisms mediated by distinct intracellular signaling networks. The precise knowledge of death pathway is essential to the design of therapeutic strategy targeting cell death. The goal of the current study is to determine how H2O2 induces necrosis in SMCs.
Methods
Mouse vascular aortic smooth muscle cell line, MOVAS, were treated with 3mM H2O2 for 2 hours, after which cell death was analyzed using flow cytometry and protein expression determined via western blot.
Results
SMCs underwent apoptosis and necrosis in response to 0.3 and 3 mM H2O2, respectively. The 3mM H2O2 group died via a caspase-independent mechanism. Expression of common autophagy-associated proteins were unaffected. Additionally, different autophagy activators and inhibitors only moderately facilitated the pro-necrotic effect of H2O2. The H2O2-induced necrosis was not affected by necroptosis inhibitors including necrostatin-1s or by SiRNA silencing of necroptosis mediators RIP1, RIP3 and MLKL. Furthermore, ferroptosis and CypD inhibitors did not provide protection from necrosis induced by H2O2. In contrast, the necrotic response was attenuated by the PARP-1 inhibitor 3-aminobenzamide (37.10±13.72% vs 82.05±0.64%). Moreover, an *PARP1* siRNA also reduced necrosis. PARP-1 is the central mediator of a necroptosis mechanism called parthanatos.
Conclusions
Our data demonstrates that parthanatos constitutes a major mechanism underlying the necrotic response to high concentrations of H2O2. Current studies delineate the involvement of parthanatos in myocardial ischemia/reperfusion injury, cardiovascular ailments, and atherosclerosis. The present study may provide a new perspective on targeting PARP-1 for the protection of SMCs and likely cardiac myocytes against oxidative stress.

Disclosures: **C.C. Feldman:** None. **T. Zhou:** None. **N. Phan:** None. **B. Liu:** None.

This research has received full or partial funding support from the American Heart Association.

240

TGFβ-Activated Kinase 1 is Required for Arteriovenous Fistula Maturation

Haidi Hu, Takuya Hashimoto, Hualong Bai, Jianming Guo, Toshihiko Isaji, Bogdan Yatsula, Jeans M Santana, Tambudzai Kudze, Alan Dardik, Yale Univ Sch of Med, New Haven, CT

Objectives*:* Arteriovenous fistulae (AVF) remain the optimal conduit for hemodialysis access but continue to have high rates of primary failure to mature. Transforming growth factor-β-activated kinase 1 (TAK1) plays important roles in regulation of extracellular matrix (ECM) production and deposition as well as inflammatory signaling and prevention of apoptosis; however the function of TAK1 in mechanotransduction in response to hemodynamic changes such as occur during AVF maturation is not well understood. Since deposition of ECM is critical to AVF maturation, we hypothesized that TAK1 is a critical regulator of AVF maturation. ***Methods***: Aortocaval fistulae were created via needle puncture in wild-type (WT) C57BL/6J mice. AVF diameter was serially assessed weekly by duplex ultrasound; AVF were harvested at days 7 or 21 for histological analysis using computerized morphometry, as well as qPCR and Western blot. Some mice were treated with either the TAK1 inhibitor 5Z-7-oxozeaenol (OZ, 0.5mg/kg/day, 7 days) or Lentiviral TAK1 ShRNA (1x 10^8 pfu/ml; adventitial transduction). Mouse lung endothelial cells (MLECs) were exposed to laminar shear stress (3 or 20 dyne/cm^2, 1h); TAK1 signaling

was detected by Western blot and immunofluorescence. ***Results***: TAK1 mRNA expression was increased at days 7 and 21 in AVF (2.0-fold; day 21; $p<0.05$) compared with sham controls. In AVF treated with OZ there was reduced fistula diameter ($p=0.0059$) and wall thickness ($p=0.031$) at day 21, as well as reduced collagen and fibronectin deposition ($p<0.05$), compared to controls. TAK1 knockdown with ShRNA also showed reduced fistula diameter at day 21 ($p<0.05$), compared to controls. MLECs exposed to arterial magnitudes of laminar shear stress showed increased TAK1 phosphorylation and downstream signaling ($p<0.05$) compared to MLECs exposed to venous shear stress or static conditions, which was reduced in cells either pretreated with OZ ($p<0.0001$) or transfected with TAK1 ShRNA ($p<0.05$). ***Conclusions***: TAK1 regulates ECM production during AVF maturation. Strategies to alter TAK1 function in vivo may be a novel therapeutic approach to improve AVF maturation.

Disclosures: **H. Hu:** None. **T. Hashimoto:** None. **H. Bai:** None. **J. Guo:** None. **T. Isaji:** None. **B. Yatsula:** None. **J.M. Santana:** None. **T. Kudze:** None. **A. Dardik:** None.

241

An Increased Response to Injury by Smooth Muscle Cells of Human Veins at Valve Sites

Shinsuke Kikuchi, Asahikawa Medical Univ, Asahikawa, Japan; Lihua Chen, Kevin Xiong, Univ of Washington, Seattle, WA; Yukihiro Saito, Nobuyoshi Azuma, Asahikawa Medical Univ, Asahikawa, Japan; Gale Tang, Michael Sobel, Univ of Washington, Seattle, WA; Thomas Wight, Benaroya Res Inst, Seattle, WA; **Richard D Kenagy**, Univ of Washington, Seattle, WA

Objective: Venous valves are prone to injury, thrombosis and fibrosis. We compared the behavior and gene expression of smooth muscle cells (SMCs) in the valve sinus vs non-valve sites to elucidate biological differences associated with vein valves.
Methods: SMC migration was measured using 2.5 mm^2 explants of the intima/media of valve sinus segments (without valve leaflets) vs. non-valve segments of human saphenous veins. Proliferation and death of SMCs was determined by staining for Ki67 and TUNEL, respectively. Proliferation and migration of passaged valve vs non-valve SMCs was determined by cell counts and using microchemotaxis chambers. Global gene expression in valve vs non-valve intima/media was determined by RNA-Seq.
Results: Valve SMCs demonstrated greater proliferation within tissue explants compared to non-valve SMCs (19.3±5.4% vs. 6.8±2.0% Ki67 positive nuclei at 4 days, respectively; mean ± SEM, 5 veins; P<.05). This was also true for migration (18.2±2.7 vs. 7.5±3.0 migrated SMCs/explant at 6 days, respectively; 24 veins, 15 explants/vein; P<.0001). Cell death was not different (39.6±16.1% vs. 41.5±16.0% TUNEL positive cells, respectively, at 4 days, 5 veins). Cultured valve SMCs also proliferated faster than non-valve SMCs in response to PDGF-BB (2.9±0.2 vs. 2.1±0.2 fold of control, respectively; P<.001; N=5 vein's paired cells). This was also true for migration (6.5±1.2 vs. 4.4±0.8 fold of control, respectively; P<.001; N=7 vein's paired cells). Blockade of FGF2 inhibited the increased responses of valve SMCs, but had no effect on non-valve SMCs. Exogenous FGF2 increased migration of valve, but not non-valve SMCs. Unexpectedly, blockade of FGF2 did not block migration of valve or non-valve SMCs from tissue explants. 37 genes were differentially expressed by valve compared to non-valve intimal/medial tissue (11 veins).
Conclusions: Valve, compared to non-valve, SMCs have greater rates of migration and proliferation, which may in part explain the propensity for pathological lesion formation in valves. While FGF2 mediates these effects in cultured SMCs, the mediators of these stimulatory effects in valve wall tissue remain unidentified. Here, the newly identified differentially expressed genes may play a role.

Disclosures: **S. Kikuchi:** None. **L. Chen:** None. **K. Xiong:** None. **Y. Saito:** None. **N. Azuma:** None. **G. Tang:** None. **M. Sobel:** None. **T. Wight:** None. **R.D. Kenagy:** None.

242

MMP-3 Promotes SMC Transformation During Medial Artery Calcification

Tonghui Lin, Beth Israel Deaconess Medical Ctr/Harvard Medical Sch, Boston, MA; Xue-lin Wang, Beth Israel Deaconess Medical Ctr, Boston, MA; Sara Zettervall, Yujun Cai, Alyssa Flores, Raul J. Guzman, Beth Israel Deaconess Medical Ctr/Harvard Medical Sch, Boston, MA

Objective- Medial artery calcification is associated with increased cardiovascular morbidity and mortality. It occurs with diabetes and chronic kidney disease. We have previously demonstrated that the matrix metallopeptidase 3 (MMP-3) is strongly induced in arterial calcification. We also showed that MMP-3

inhibition decreases calcium accumulation in vascular SMCs and that MMP-3 deficient mice develop less medial calcification than wildtype controls. In this series of continuing experiments, we evaluate the effects of MMP-3 on SMCs phenotypic transformation in *vitro* and in *vivo.* ***Methods and Results-*** Confluent rat aortic smooth muscle cells (RASMCs) cultured in calcification medium containing elevated calcium and phosphate levels for 7 days showed increased MMP-3 activity, decreased expression of the SMC markers SM-actin and SM-MHC, and increased expression of the bone markers alkaline phosphatase (ALP) and osterix (Osx). Cells were next exposed a selective MMP-3 inhibitor 2(EMD Millipore). In the presence of inhibitor, MMP-3 activity (MMP-3 activity assay kit, Abcam) was significantly decreased. Additionally, SMC osteogenic transformation was prevented as demonstrated by maintenance of SM22α and SM-MHC expression with reduction of ALP and Osx expression. In confirmatory experiments, MMP-3 reduction with siRNA inhibited the calcification of SMC that were exposed to calcification medium. We next evaluated phenotypic marker expression in MMP-3 knockout and wild-type mice injected with vitamin D_3, a model of medial artery calcification. At 7 days after injection, expression of the SMC marker gene SM-MHC was significantly greater in MMP-3 KO mice than controls, while bone cell marker genes (Runx2, ALP, Osx) were decreased as measured by qPCR. Deletion of MMP-3 thus inhibited the osteogenic transformation of medial SMCs in vitamin D_3-treated mice suggesting that it may control calcification via local effects within the arterial wall. ***Conclusion-*** Together these findings suggest that MMP-3 promotes medial artery calcification through local effects on the phenotypic state of vascular SMCs, and further, that it may serve as a therapeutic target to reduce calcification and improve outcomes in our PAD patient population.

Disclosures: **T. Lin:** None. **X. Wang:** None. **S. Zettervall:** None. **Y. Cai:** None. **A. Flores:** None. **R.J. Guzman:** None.

243

Neutrophil-Mediated Inflammation Drives Sickle Cell Vasculopathy

Derick Okwan, Laura Hansen, Giji Joseph, Daiana Weiss, David R Archer, Emory Univ Sch of Med, Atlanta, GA; W Robert Taylor, Emory Univ Sch of Med, Veterans Affairs Medical Ctr, Atlanta, GA

Objectives: Many of the clinical complications associated with sickle cell disease (SCD), such as stroke, pain crises, proliferative retinopathy, renal and heart failure, can be attributed to repeated bouts of vascular insufficiency, yet the detailed mechanisms of vascular repair following injury are largely unknown in SCD. Given our previous work showing the importance of reactive oxygen species in neovascularization, we aimed to delineate the immune mechanisms of oxidative stress during vascular repair in a humanized sickle cell mouse model (SS) in comparison to wildtype (AA). **Methods:** We performed limb ischemia (HLI) in mice by ligation of the femoral artery to evaluate vascular dysfunction in sickle cell mice. Vascular recovery was ascertained using weekly LASER Doppler perfusion imaging (LDPI) for 28 days. Voluntary running wheel test was used to determine spontaneous motor function recovery. **Results:** There was significant diminution in functional collateral vessel formation in SS mice following HLI as evaluated by LDPI (76 ±13 % recovery in AA vs 34±10 % recovery in SS by day 28, $p < 0.001$ n=8 per group). This was characterized by dysfunctional Moyamoya-like sprouting vessels with impaired spontaneous motor function recovery in SS. Specifically, AA mice recovered 98% motor function by day 28 following HLI, vs 36% in SS mice, $p < 0.001$. The phenotype was associated with persistent neutrophils in the hind limb muscle of SS mice up to 28 days, a time point by which all neutrophils were cleared in AA mice. Consequently, there was a 2.45 fold increased production of hydrogen peroxide in SS mice ischemic hind limbs at day 28, compared to AA mice ($p< 0.05$). Importantly, *in vivo* depletion of neutrophils improved functional collateral vessel formation in the SS mice. **Conclusions:** Our data suggest that neutrophil-mediated excessive inflammation and oxidative stress drive dysfunctional collateral vessel formation in SS mice following ischemic injury. Targeting neutrophils may improve vascular dysfunction in SS disease.

Disclosures: **D. Okwan:** None. **L. Hansen:** None. **G. Joseph:** None. **D. Weiss:** None. **D.R. Archer:** None. **W. Taylor:** None.

244

Distinct Regulation of Fat and Dachsous Cadherins in Response to Arterial Injury

Dario F Riascos-Bernal, Longyue L Cao, Prameladevi Chinnasamy, Albert Einstein Coll of Med, Bronx, NY; Rong Hou, St. Louis Univ Hosp, St. Louis, MO; Nicholas E Sibinga, Albert Einstein Coll of Med, Bronx, NY

Molecular mechanisms that control the activities of vascular smooth muscle cells (VSMCs) in the diseased or injured arterial wall remain incompletely understood. The atypical cadherin FAT1 is prominently expressed in VSMCs after vascular injury. In recent work, we found that processing of FAT1, a type I transmembrane protein, releases its intracellular domain, the FAT1ICD; in turn, FAT1ICD fragments accumulate in mitochondria and interact with electron transport complexes I and II to restrict VSMC respiration and control cell growth and neointimal formation. We hypothesized that FAT1 processing (and therefore these VSMC activities) is controlled by extracellular ligands that may interact physically via FAT1's extended cadherin repeat or transmembrane domains. FAT4 and Dachsous 1 (DCHS1) are leading candidates for such interactions, but these proteins have not been studied in VSMCs or vascular injury response. Accordingly, we analyzed expression profiles of FAT4 and Dachsous 1 (DCHS1) during the vascular response to injury, using a rat carotid artery balloon injury model. Interestingly, FAT4 transcripts increased transiently after injury, peaking at day 7 (6.99±0.21-fold over baseline, P<.001), in a pattern reminiscent of FAT1. In contrast, DCHS1 levels decreased by day 3 after injury (0.49±0.02-fold of baseline, P<.001), remained low through day 14, and recovered by day 30. Physical interactions of FAT4 either with DCHS1 or with FAT1 have both been reported previously; therefore, decreased DCHS1 coincident with increased FAT4 suggest an increase in FAT4 availability and/or interaction with FAT1 during injury response. How this increase in FAT4 affects FAT1 function and VSMC metabolism and growth is the subject of ongoing investigation. FAT1 induction and processing after vascular injury represent an important novel molecular mechanism by which VSMC metabolism and growth are controlled after vascular injury. Increased availability of FAT4 cadherin due to FAT4 induction together with DCHS1 downregulation after vascular injury provides a likely upstream regulatory mechanism to govern FAT1 activities.

Disclosures: **D.F. Riascos-Bernal:** None. **L.L. Cao:** None. **P. Chinnasamy:** None. **R. Hou:** None. **N.E.S. Sibinga:** None.

This research has received full or partial funding support from the American Heart Association.

245

Non-Invasive *in vivo* Assessment of the Re-Endothelialization Process Using Ultrasound Biomicroscopy in the Rat Carotid Artery Balloon Injury Model

Samuel Röhl, Linnea Eriksson, Robert Saxelin, Mariette Lengquist, Kenneth Caidahl, Ulf Hedin, Anton Razuvaev, Karolinska Instt, Stockholm, Sweden

Objective
Ultrasound BioMicroscopy (UBM), or high-frequency ultrasound, is a novel technique used for assessment of anatomy and physiology small research animals. In this study, we evaluate the UBM assessment of the re-endothelialization process following denudation of the carotid artery in rats.
Methods
Ultrasound BioMicroscopy data from three different experiments were analyzed. A total of 66 rats of three different strains (Sprague-Dawley, Wistar and Goto-Kakizaki) were included in this study. All animals were subjected to common carotid artery balloon injury and examined with UBM 2 and 4 weeks after injury. Re-endothelialization in UBM was measured as the length from the carotid bifurcation to the distal edge of the intimal hyperplasia. *En face* staining with Evans-blue dye was performed upon euthanization at 4 weeks after injury followed by tissue harvest for morphological and immunohistochemical evaluation.
Results
A significant correlation (Spearman r=0.63,p<0.0001) and an agreement according to Bland-Altman test was identified when comparing all measurements of re-endothelialization in high frequency ultrasound and *en face* staining. Analysis by animal strain revealed a similar pattern and a significant growth in re-endothelialization length measured in UBM from 2 to 4 weeks could be identified. Immunohistochemical staining for von Willebrand factor confirmed the presence of endothelium in the areas detected as re-endothelialized by the ultrasound assessment.
Conclusion

Ultrasound BioMicroscopy can be used for longitudinal in vivo assessment of the re-endothelialization following arterial injury in rats.

Disclosures: **S. Röhl:** None. **L. Eriksson:** None. **R. Saxelin:** None. **M. Lengquist:** None. **K. Caidahl:** None. **U. Hedin:** None. **A. Razuvaev:** None.

246

TGF-β1 and TGFBR2 Polymorphisms With ISH

Xiaoying Zhang, Shasha Yu, Wencai Chen, Jianfei Ren, Ningbo Medical Treatment Ctr Lihuili Hosp, Ningbo, Zhejiang, China; **Xiaofeng Chen**, Taizhou Hosp, Wenzhou Medical Univ, Taizhou, Zhejiang Province, China

Background and Objective: Isolated systolic hypertension (ISH) is characterized by increased aortic stiffness and associated with a significantly increased risk of cardiovascular morbidity and mortality. It has been reported that elevated plasma transforming growth factor-beta 1(TGF-β1) levels predicted development of hypertension. However, little is known about the association of TGF- β 1 pathway gene polymorphisms and ISH. The aim of the present study was to study the association of transforming growth factor-beta 1(TGF-β1) and its receptor 2(TGFBR2)functional gene polymorphisms with isolated systolic hypertension (ISH). **Methods and Results:** One hundred and three consecutive ISH patients and 169 healthy controls were recruited in this study. All subjects were genotyped for TGFβ1-869T/C, TGFBR2-3779A/G and TGFBR2-1444C/G by the technology of polymerase chain reaction-restriction fragment length polymorphism (PCR-RFLP) and then confirmed by direct sequencing. No significant difference in genotype (and allele) frequency of TGFβ1-869T/C, TGFBR2-3779A/G and TGFBR2-1444C/G polymorphisms were observed between ISH group and healthy group (p>0.05). **Conclusion:** Our findings suggest that TGFβ1-869T/C, TGFBR2-3779A/G and TGFBR2-1444C/G polymorphisms may not be associated with susceptibility of isolated systolic hypertension in Chinese population.

Disclosures: **X. Zhang:** None. **S. Yu:** None. **W. Chen:** Research Grant; Significant; Ningbo Natural Science Foundation under #2014A610281. **J. Ren:** Research Grant; Significant; Ningbo Natural Science Foundation under #2014A610281. **X. Chen:** None.

247

The Association of the Serotonin Transporter Polymorphism LL-Genotype with Non-Syndromic Mitral Valve Prolapse Requiring Surgery at a Younger Age

Kathryn H Driesbaugh, The Children's Hosp of Philadelphia, Philadelphia, PA; Juan B Grau, Univ of Ottawa Heart Inst, Ottawa, ON, Canada; Eric K Lai, Emanuela Branchetti, Univ of Pennsylvania, Philadelphia, PA; Nancy Rioux, Valley Hosp, Ridgewood, NJ; Farrah Alkhaleel, Nathan Frick, Univ of Pennsylvania, Philadelphia, PA; Robert J Levy, The Children's Hosp of Philadelphia, Philadelphia, PA; **Giovanni Ferrari**, Univ of Pennsylvania, Philadelphia, PA

Background: Non-syndromic mitral valve prolapse (MVP) is a highly prevalent heart valve disease that is treated surgically when indicated by clinical deterioration. Serotonin (5HT)-related valvulopathies have been reported; however, 5HT has not been shown to be directly associated with MVP. A polymorphism (5-HTTLPR), with a 44-base micro-insertion/deletion in the promoter of the 5HT transporter (SERT) gene, is present in all human populations studied. 5-HTTLPR, with designated long (L) or short (S) alleles, has been reported to have an impact on SERT expression in non-cardiac valve studies. We hypothesized that MVP surgical patients may have an altered distribution of 5-HTTLPR, resulting in SERT expression levels associated with an increased risk of disease progression. **Methods:** 201 MVP surgical patients were recruited under an IRB approved protocol; DNA extraction followed by genomic fragment analysis was performed to determine allelic frequencies. qRT-PCR of SERT and related genes was carried out on RNA extracted from available MVP tissue (N=64). A RT2 Profiler microarray study for 84 genes associated with human dopamine and 5HT signaling was also performed (N=44). **Results:** MVP surgical patients had an overall frequency of LL-32%, LS-50%, and SS-18%. The frequency of 5-HTTLPR-LL was significantly increased in males under 55 years of age (N=19/41, 47.6%) (*p=0.04*) compared to the rest of the population. Interestingly, the LL patients had the lowest SERT expression levels per qRT-PCR compared to LS and SS. A similar expression pattern was also noted for another 5HT transporter, vesicular monamine transporter-2 (VMAT2), with the lowest expression in the LL specimens. Expression of 5HT receptors 2A and 2B were comparable between genotypes in the MVP samples analyzed. Similarly,

microarray studies demonstrated tight regulation of 5HT-associated genes, but with LS/SS patients expressing >2-fold more SERT than LL. **Conclusion:** 5-HTTLPR-LL is associated with MVP surgery at a younger age in men, with relatively lower expression of both SERT and VMAT2, suggesting a reduced capacity for transporter processing of 5HT. The 5-HTTLPR-LL genotype may constitute a novel risk factor useful for identifying MVP patients more likely to have rapid disease progression.

Disclosures: **K.H. Driesbaugh:** None. **J.B. Grau:** None. **E.K. Lai:** None. **E. Branchetti:** None. **N. Rioux:** None. **F. Alkhaleel:** None. **N. Frick:** None. **R.J. Levy:** None. **G. Ferrari:** None.

248

Comparative Transcriptomic Analysis of Smooth Muscle Cells and Endothelial Cells Identifies Distinct Signaling Networks Following Inflammatory Challenges

Bowen Wang, Ohio State Univ, Columbus, OH; Xiaokang Pan, Pennsylvania State Univ, University Park, PA; Mengxue Zhang, Xudong Shi, Univ of Wisconsin-Madison, Madison, WI; Lian-Wang Guo, K Craig Kent, Ohio State Univ, Columbus, OH

Background: Drug-eluting devices have shown promising outcomes in patients receiving endovascular procedures, particularly in managing post-intervention restenosis that often leads to failure of the reconstructions. However, emerging evidences have revealed increased thrombogenic risk associated with the use of drug-eluting stents and balloons. It has been widely acknowledged that the major culprit responsible for the observed thrombosis events is the non-selective damage of the anti-restenotic compounds on vascular endothelial cells (ECs), which, under physiological conditions, serve as the protective barrier for maintaining vascular homeostasis. Given the clinical relevance, there is an urgent need for a therapeutic agent that could confer selective management of smooth muscle cells (SMCs) without damaging ECs. However, by far the differential mechanisms in the two cell types underlying their distinct cellular behaviors toward pathogenic stimuli are poorly understood. Thus, a systematic and comparative analysis of their cellular dynamics at the transcriptomic level is needed. Methods and Results: Human primary aortic SMCs and ECs were starved and then stimulated with 2 pro-inflammatory cytokines (TNF-α and IL-1β), which are well-established inducers of SMCs' proliferative and migratory phenotypes while simultaneously damaging ECs. Samples were then subject to RNA sequencing. We developed a customized algorithm to evaluate the differential responses and transcriptomic network dynamics in the two cell types, and successfully identified multiple gene modules that contain functionally related genes that possibly are involved in the distinct regulations of SMCs versus ECs post inflammatory challenges. Conclusions: Our study provides the first comprehensive analysis of the differential transcriptomic dynamics between SMCs and ECs following inflammatory challenges, which are prominent contributors to the pathogenesis of both restenosis and thrombosis following vascular injury. Our data identify several module groups of genes that could serve as potential targets to achieve differential modulation of the pathophysiologies of SMCs versus ECs. Further studies are warranted to validate the contributions of these genes.

Disclosures: **B. Wang:** None. **X. Pan:** None. **M. Zhang:** None. **X. Shi:** None. **L. Guo:** None. **K.C. Kent:** None.

This research has received full or partial funding support from the American Heart Association.

249

Potential Tissue-specific Interactions Between Inflammation and Canonical Tgfβ Signaling in Marfan Syndrome

Rebecca L Black, Carolyn M Roos, Michael A Hagler, Nassir M Thalji, Bin Zhang, Grace C Verzosa, Jordan D Miller, Mayo Clinic, Rochester, MN

Marfan syndrome is a connective tissue disorder frequently driven by mutations in the fibrillin-1 gene (Fbn1). This results in multiple aberrant cardiovascular phenotypes, including aortic aneurysm and mitral valve prolapse. While the molecular changes underlying aortic aneurysm formation have been extensively studied, the molecular underpinnings of mitral valve prolapse in this syndrome remain poorly understood. Therefore, we hypothesized that smad2/3 phosphorylation would be significantly increased in both aorta and mitral valve from $Fbn1^{+/1037G}$ mice with Marfan syndrome and associated with impaired anti-inflammatory signaling in both tissues. We used young (3 months) mice that were wild-type ($Fbn1^{+/+}$) or

fibrillin-1 mutant ($Fbn1^{+/1037G}$) and fed a normal chow diet. qRT-PCR was used to measure mRNA levels in aortic arch and mitral valve tissue, and fluorescent immunohistochemistry to evaluate changes in canonical TGFβ signaling. Consistent with previous reports, TGF-β1 mRNA levels were increased in $Fbn1^{+/1037G}$ compared to wild-type mice in both aorta and mitral valve. Interestingly, while p-SMAD2/3 protein levels were increased in aorta from $Fbn1^{+/1037G}$ mice, we were surprised to find that p-SMAD2/3 protein levels were decreased in mitral valve from $Fbn1^{+/1037G}$ mice compared their wild-type littermates. Given the emerging role of inflammatory signaling in accelerated development of Marfan phenotypes, we sought to determine whether there were compensatory or maladaptive changes in IL10 (a known inhibitor of p-SMAD2/3). In aorta, IL10 mRNA levels were decreased in $Fbn1^{+/1037G}$ compared to $Fbn1^{+/+}$mice, suggesting a maladaptive response. In contrast, IL10 levels in mitral valve tissue were significantly increased in $Fbn1^{+/1037G}$ mice compared to their wild-type littermates, suggesting a compensatory/protective response. Collectively, these data suggest that tissue-specific changes in IL10 levels may modulate p-SMAD2/3 signaling in aorta and mitral valve, which may be a key permissive step in the onset of Marfan-related phenotypes. Future work to experimentally determine the role of IL10 in the regulation of canonical and non-canonical TGFβ signaling and the penetrance of Marfan-associated phenotypes is warranted.

Disclosures: **R.L. Black:** None. **C.M. Roos:** None. **M.A. Hagler:** None. **N.M. Thalji:** None. **B. Zhang:** None. **G.C. Verzosa:** None. **J.D. Miller:** None.

250

Four-And-A-Half LIM Domain Protein 2 Plays a Critical Role in Spleen T-Cell Dependent Antibody Response

Talin Ebrahimian, David Simon, France Dierick, Maryam Heidari, Alexandre Orthwein, Koren K Mann, Stephanie Lehoux, Lady Davis Inst, Montreal, QC, Canada

Background: Four-and-a-half LIM domain protein 2 (FHL2) is an adaptor molecule that regulates signalling cascades and gene transcription. We have uncovered vasculoprotective and atheroprotective effects of FHL2 knockout in mice. Since B cells could regulate these processes, we investigated the potential role of FHL2 in B cell function and activity. **Methods and results:** Under basal conditions, FHL2-/- mice presented a mild splenomegaly (84.0±9.0 vs 68.0±5.0mg), associated with bigger spleen follicles (1.6 fold) and higher proportions of spleen B cells (56.0±2.0 vs 40.0±9.0%) vs WT mice. Flow cytometry confirmed significantly higher ($p<0.05$) proportions of B cells in the follicles (Fo)(CD23+CD21lo/int) (77.0±1.0 vs 67.0±3.0%) and the marginal zone (Mz)(CD23-,CD21+)(7.0±1.0 vs 2.5±1.0%) of FHL2-/- vs WT mice. Mice were injected with sheep red blood cells (SRBC) to elicit a T cell-dependent B cell activation. SRBC did not influence Fo and Mz B cell numbers, but it did affect germinal center (GC) formation. GCs are zones within Fo where T cells activate B cells to produce high affinity antibodies. SRBC induced a 5- and 2.5-fold increase in B cells (GL7+) within FHL2-/- and WT GCs, respectively. However, there was no increase in plasma IgG1 levels in FHL2-/- mice in response to SRBC, whereas a 3-fold increase was observed in WT mice (1158±227 vs 2943±226ng/ml; $p<0.05$). Instead, plasma IgM levels were higher in FHL2-/- than WT SRBC mice. Moreover, SRBC only induced a modest, 1.3-fold fold increase in Fo T helper cells (CXCR5+PD1+) in FHL2-/- compared with a 6-fold increase in WT. Nevertheless, FHL2-/- B cells successfully proliferated and underwent class switch recombination in response to LPS, anti-CD40 and IL-4 in vitro, indicating that these cells were not defective. **Conclusion:** These results suggest that FHL2 plays a critical role in spleen antibody production in response to a T-dependent antigen, possibly by affecting activation or antigen presentation by Fo T helper cells.

Disclosures: **T. Ebrahimian:** None. **D. Simon:** None. **F. Dierick:** None. **M. Heidari:** None. **A. Orthwein:** None. **K.K. Mann:** None. **S. Lehoux:** None.

251

Loss of Endothelial E Prostanoid Receptor 4 Exacerbates Wire-Injury Induced Neointimal Formation

Huifeng Hao, Sheng Hu, Hong Chen, Miao Wang, State Key Lab of Cardiovascular Disease, Fuwai Hosp, Natl Ctr for Cardiovascular Diseases, Chinese Acad of Medical Sciences, Beijing, China

Prostanoids, which are synthesized from the cyclooxygenase cascade and inhibited by nonsteroidal anti-inflammatory drugs, participate in vascular remodeling. Deletion of microsomal prostaglandin (PG) E

synthase-1 increases prostacyclin and attenuates injury-induced neointimal formation in mice. The role of E prostanoid receptor 4 (EP4) in vascular response to injury is unknown. Using an inducible Cre-LoxP-based approach, we generated the endothelial-restricted EP4 knockout mice (cKO) and their littermate controls (Ctl). After tamoxifen treatment, one side femoral arteries of the mice were subjected to wire-injury. Twenty-eight days later, the femoral arteries were harvested and the neointima formation were evaluated. Deletion of endothelial EP4 strikingly exacerbated intima area and the ratio of intima to media area, without affecting media area. Treatment of wild type mice with AE1-329, a selective EP4 agonist, significantly reduced neointimal hyperplasia after wire-injury. Mechanistically, activation of endothelial EP4 signaling with AE1-329 promoted endothelial cell proliferation. Notably, the adhesion of leukocytes to endothelial cells was significantly inhibited by AE1-329 treatment. Collectively, endothelial EP4 may protect against vascular remodeling via enhancing endothelial repair and reducing leukocytes adhesion to the endothelium.

Disclosures: **H. Hao:** None. **S. Hu:** None. **H. Chen:** None. **M. Wang:** None.

252

ABR-238901 Promotes Cardiac Repair After Myocardial Infarction by Reducing Inflammation and Increased Presence of "Reparatory" Macrophages Trough Blockage of Alarmin Complex S100a8/9

Goran Marinković, CRC, Malmo, Lund Univ, Malmö, Sweden; Laura Winkler, Lisa Kefene, Van Andel Inst, Grand Rapids, MI; Jan Nilsson, CRC, Malmo, Lund Univ, Malmö, Sweden; Stefan Jovinge, Van Andel Inst, Grand Rapids, MI; Schiopu Alexandru, CRC, Malmo, Lund Univ, Malmö, Sweden

Objective: Myocardial infarction (MI) is an ischemic injury of the heart leading to excessive local inflammation. The alarmin complex S100A8/9 is potently upregulated locally and systemically after MI and promotes the influx of neutrophils and monocytes into the myocardium. We studied whether S100A8/A9 inhibition with the blocking compound ABR-238901 might reduce inflammation and improve myocardial function after MI.
Methods: MI was induced by left coronary artery ligation in 8-12 weeks old mice. Echocardiography was used to assess left ventricular function.
Results: Two days after MI, mice treated with ABR-238901 i.p. showed improved ejection fraction in comparison with buffer-treated animals, and had significantly decreased numbers of neutrophils and monocytes in the blood. More importantly, the presence of neutrophils and monocytes in the myocardium was reduced, leading to lower numbers of infiltrating macrophages. After 7 days of continuous treatment, cardiac function and the total counts of neutrophils and monocytes in blood and heart became similar in the two groups. However, the numbers of reparatory $F4/80^{+}MerTK^{hi}Ly6C^{low}$ macrophages were lower in the hearts of ABR-238901 treated mice after 7 days. In contrast, we found that a balanced treatment strategy using ABR-238901 for 3 days followed by 4 days buffer increased the numbers and the proliferative capacity of this macrophage subset, promoting cardiac repair.
Conclusion: We report that 3-day blockage of S100A8/9 has beneficial effects on cardiac function in the immediate period after an MI and enhances the presence of reparatory macrophages in the myocardium.

Disclosures: **G. Marinković:** None. **L. Winkler:** None. **L. Kefene:** None. **J. Nilsson:** None. **S. Jovinge:** None. **S. Alexandru:** None.

253

The Direct Renin Inhibitor Aliskiren Prevents Endothelial Dysfunction in Spontaneously Hypertensive Rat Aortas

Gary Tse, Xiaoyu Tian, Yu Huang, Jack Wong, The Chinese Univ of Hong Kong, Shatin, Hong Kong

Introduction: Hypertension is a significant medical problem. Aliskiren is a novel anti-hypertensive agent that inhibits renin directly. We tested the hypothesis that aliskiren prevents endothelial dysfunction in spontaneously hypertensive rats (SHRs).
Methods: SHRs and age-matched Wistar Kyoto (WKY) rats were randomly divided and subjected to oral administration of aliskiren (10 mg/kg/day) or vehicle for 8 weeks. Blood pressure was monitored bi-weekly by a tail-cuff method. After an initial equilibration period, each ring was contracted by elevated KCl (60 mmol/L) to ensure a level of contractility suitable for subsequent experimentation. To examine endothelium-dependent relaxations in phenylephrine-contracted rings, two consecutive concentration-response curves to acetylcholine (ACh; 3 nmol/L -30 µmol/L) were constructed. In some phenylephrine-

contracted rings without intact endothelium, sodium nitroprusside (SNP; 3 nmol/L – 10μmol/L) were applied cumulatively to the bathing solution to test the sensitivity of vascular smooth muscle cells (VSMCs) to NO.
Results: Aliskiren reduced systolic blood pressure (SBP) to 155.6 ± 1.87 mmHg as compared to 165.3 ± 3.2 mmHg in vehicle-treated SHRs (n = 7), while chronic aliskiren administration did not affect SBP in WKY rats. SHR aortas with endothelium relaxed less in response to different concentrations of ACh than age-matched WKY rat aortas and ACh failed to cause relaxations of aortic rings without endothelium. By contrast, endothelium-independent relaxations caused by sodium nitroprusside (SNP) were comparable in aortas from SHR and WKY rats. Chronic aliskiren administration improved endothelium-dependent dilatations of aortas from SHRs compared to vehicle-treated SHRs, but this was unaffected in WKY rats. Endothelium-independent relaxations to SNP were not significantly different in aortas from the four treatment groups.
Conclusions: Aliksiren reduces blood pressure and improves endothelium-dependent dilatations of SHRs.
Figure 1. Effects of 8-week treatment of aliskiren on acetylcholine (ACh)-induced endothelium-dependent dilatations in SHR **(A)** and WKY **(B)** aortas. Results are mean ± SEM of 7 experiments. *p<0.05.

Disclosures: **G. Tse:** Employment; Significant; Croucher Foundation of Hong Kong. Research Grant; Significant; Croucher Foundation of Hong Kong. **X. Tian:** None. **Y. Huang:** None. **J. Wong:** None.

254

Kawasaki Disease Vasculitis in Mice Develop Myocardial Fibrosis After Adrenergic Stimulation

Harry H. H. Matundan, Jon Sin, Masanori Abe, Magali Noval Rivas, Michael C. Fishbein, Thomas A. Lehman, Roberta A. Gottlieb, **Moshe Arditi**, Cedars-Sinai Medical Ctr, Los Angeles, CA

Background: Kawasaki disease (KD) is the most common cause of acquired cardiac disease among US children and causes coronary artery aneurysms (CAA) in 25% of untreated patients. CAAs can result in myocardial ischemia, infarction, and even death. Other long-term sequelae from KD include extensive remodeling of CAA leading to stenosis and endothelial (EC) dysfunction. Acute KD is also associated with myocarditis that can cause arrhythmias, which can be fatal and may lead to long-term myocardial dysfunction and fibrosis, areas of KD research that are severely neglected. These myocardial changes may persist for decades after the acute illness and closely correlate with long-term myocardial sequelae. **Objective**: To investigate long-term myocardial dysfunction, including myocardial fibrosis and coronary microvascular lesions in the KD vasculitis mouse model. **Methods:** Mice were injected with *Lactobacillus casei* cell wall extract (LCWE) to induce KD vasculitis, coronary arteritis, and myocarditis at 1 week. Five weeks later, control or KD mice were injected with isoproterenol (ISO), a beta agonist, for 10 consecutive days to induce pharmacologically mediated exercise, followed by sacrifice and analysis. Cardiac hypertrophy was measured by calculating heart weight normalized to tibia length. Myocardial fibrosis was determined by Masson's trichrome staining of the myocardium and myocardial function was measured by serum BMP levels and ventricular ejection fraction by MRI. **Results:** KD significantly increased the risk of cardiac hypertrophy and increased myocardial fibrosis, diminished ejection fraction and increased BMP following prolonged pharmacologic exercise (ISO), compared with controls. Post KD pharmacologic exercise-induced myocardial fibrosis was associated with significant reduction in the expression of the EC marker CD31 in the myocardium. This KD induced myocardial fibrosis was IL-1-dependent as the IL-1R KO mice were protected. **Conclusions:** Pharmacologic stress (exercise) leads to cardiac hypertrophy and chronic myocardial fibrosis in the LCWE-induced acute KD vasculitis mouse model, a process that involves IL-1 signaling and diminished microvascular circulation in the myocardium. **Supported by NIH grant AI 072726 to MA**

Disclosures: **H.H. Matundan:** None. **J. Sin:** None. **M. Abe:** None. **M. Noval Rivas:** None. **M.C. Fishbein:** None. **T.A.J. Lehman:** None. **R.A. Gottlieb:** None. **M. Arditi:** None.

256

Differential Biomechanical Regulation of Vein Graft Endothelial CD39 by Pulsatile Radial Forces

Yogendra Kanthi, Vinita Yadav, Kinsey Vear, Benjamin N Jacobs, Yibai Hao, Hui Liao, David J Pinsky, Univ of Michigan Health System, Ann Arbor, MI

Saphenous veins are frequently used bypass grafts in coronary & peripheral artery bypass surgery, but are more prone to failure than arterial grafts due to adverse remodeling. The endothelium senses radial and linear biomechanical forces exerted by blood flow. Thin-walled venous blood flow *in situ* is non-pulsatile until transposed as an arterial graft. The impact of cyclic stretch from pulsatile distention on the vein wall is not well elucidated. CD39 is a potent ecto-enzyme at the blood:vessel interface regulating vascular thrombo-inflammation by dissipating extracellular ATP & ADP. We recently identified that vascular CD39 expression can be induced by laminar shear stress. However, the response of CD39 to cyclic stretch during vein graft arterialization remains unknown. We *hypothesized that the vasculo-protective enzyme CD39 is induced by the venous endothelium in response with pulsatile stretch.*
Methods: Primary human saphenous vein endothelial cells (HSVEC) were exposed to cyclic stretch *in vitro*, mimicking arterial & vein graft patterns. CD39 transcript & protein expression were quantified. Ecto-ATPase and -ADPase activity of CD39 on HSVEC were quantified with a malachite green assay. CD39 haploinsufficient (*Cd39*$^{+/-}$) & WT mice underwent carotid bypass surgery with a vein graft, & subsequent neointimal hyperplasia was compared.
Results: High (16%, 1 Hz) and low (5%, 1 Hz) levels of cyclic stretch of HSVEC elicited distinct patterns of CD39 expression. *Cd39* mRNA remained unchanged after 48h of low or high stretch (n=6,each). Low-level cyclic stretch did not alter CD39 protein expression (n=6,each). In stark contrast, 16% cyclic stretch induced increases in CD39 protein expression after 24h (60%) and 48h (130%) compared with static controls (n=6 each,$P<0.05$). CD39-dependent ATP & ADP hydrolysis increased by 60% & 100% in HSVEC following high-level cyclic stretch (n=4, $p<0.005$). Preliminary murine vein graft model studies suggest that CD39-deficiency exacerbates vein graft neointimal hyperplasia compared to WT controls.
Conclusions: We have identified CD39 as a novel, stretch-responsive endothelial ecto-enzyme in human saphenous veins, which may represent a protective response to venous distention from arterial stretch patterns.

Disclosures: **Y. Kanthi:** None. **V. Yadav:** None. **K. Vear:** None. **B.N. Jacobs:** None. **Y. Hao:** None. **H. Liao:** None. **D.J. Pinsky:** None.

257

Activation of the Renin-Angiotensin II-Aldosterone-System Leads to Increase in Protein Disulfide Isomerase

Pablo Lopez, Yaritza Inostroza-Nieves, Jamie Rosado, Lorena Rivera-Gonzalez, Alexandra Lozano, Dept of Biochemistry, San Juan Bautista Sch of Med, Caguas, PR; Alicia Rivera, Dept of Lab Med, Boston Children's Hosp and Dept of Pathology and Harvard Medical Sch, Boston, MA; Patricia Pulido-Perez, Natl Autonomous Univ of Mexico, Mexico DF, Mexico; Joshua Cazares, Dept of Molecular and Cellular Biology, Univ of California, Merced, CA; Enrique Torres-Rasgado, Faculty of Med, Univ of Puebla, Puebla, Mexico; Akira Nishiyama, Dept of Pharmacology, Kagawa Medical Univ, Kagawa, Japan; Ricardo Pérez-Fuentes, Faculty of Med, Univ of Puebla, Puebla, Mexico; Rudy M. Ortiz, Dept of Molecular and Cellular Biology, Univ of California, Merced, CA; Jose R. Romero, Div of Endocrinology, Diabetes and Hypertension, Dept of Med, Brigham and Women’s Hosp, and Harvard Medical Sch, Boston, MA

Activation of the Renin-Angiotensin-Aldosterone-System (RAAS) is proposed to play a role in the development of insulin resistance and type II diabetes. Angiotensin II (AngII) is a principal effector molecule that binds AT1 receptors (AT1R) in various tissues. Recent data shows that activated endothelial cells secrete protein disulfide isomerase (PDI), a multifunctional protein that has been shown to be critical to the initiation and regulation of thrombus formation. However, the effects of RAAS on PDI regulation are unknown. We hypothesized that RAAS activation would lead to increased PDI levels thus contributing to inflammation. First, we studied the in vitro effects of AngII on EA.hy926 human endothelial cells and measured PDI activity. Our results show that AngII increased PDI activity; an event that was blocked by preincubation with 0.5 M losartan, an AT1R antagonist (ARB) ($P<0.05$, n=6). We then studied the in vivo effects of exogenous AngII infusion in Sprague–Dawley rats under the following conditions: (1) control; (2) AngII infused; (3) AngII + ARB. In these rats, AngII infusion led to significant increases in

plasma PDI levels that were partially prevented by ARB treatment (P<0.05, n>5). We then studied the obese Otsuka Long Evans Tokushima Fatty (OLETF) (n = 6/group) rats, a model of naturally increased AngII and RAAS mediated insulin resistance and hypertension. OLETF and their lean strain controls were randomly assigned to the following groups: (1) untreated Long Evans Tokushima Otsuka (lean, control); (2) untreated OLETF; (3) OLETF + ARB. Our results show that OLETF rats had increased insulin resistance and significantly greater circulating PDI activity than control rats (P<0.05) that was likewise blocked by ARB treatment (P<0.05). To assess the relevance to humans of these findings we measured circulating PDI levels in patients with type 2 diabetes. In our cohort, PDI activity was significantly greater in patients with type 2 diabetes than non diabetics (P<0.001, n=134). Our data suggest that RAAS activation represents a novel mechanism for PDI secretion. Thus we posit that PDI may contribute to the deleterious effects of RAAS-mediated vascular disease.

Disclosures: **P. Lopez:** None. **Y. Inostroza-Nieves:** None. **J. Rosado:** None. **L. Rivera-Gonzalez:** None. **A. Lozano:** None. **A. Rivera:** None. **P. Pulido-Perez:** None. **J. Cazares:** None. **E. Torres-Rasgado:** None. **A. Nishiyama:** None. **R. Pérez-Fuentes:** None. **R.M. Ortiz:** None. **J.R. Romero:** None.

258

Mir-155 Mitigates Acute Oscillatory Shear Stress (OSS)-Induced Vascular Inflammation and Barrier Dysfunction Through Down Regulation of the AT1R-ETS1 Pathway

Islam Mohamed, Sheena Thomas, Roy Sutliff, Nick Willet, Charles Searles, Emory Univ, Decatur, GA

Introduction: Shear stress forces play an integral role in dictating the vascular wall response to changes in blood flow, induction of pro-inflammatory response and hence development of atherosclerosis. Previously, our group and others have identified an inverse relationship between microRNA-155 (miR-155) and AT1R expression and/or activity in atheroprone areas of chronic low magnitude oscillatory shear stress (OSS) in vasculature and in-vitro.
Hypothesis: we hypothesized that acute induction of OSS mediates vascular inflammation and dysfunction, via activation of the AT1R-ETS1 pathway and dysregulation of miR-155.
Methods: 12-week old C57B/6J mice were subjected to abdominal aortic coarctation (AAC), a unique model of acute induction of acute OSS, for 3 days. Downstream segments of acute OSS were compared to upstream unidirectional shear stress (USS) segments of the thoracic aorta using RT-PCR, western blot analysis and unpaired student t-test.
Results: Acute OSS resulted in vascular inflammation evidenced by upregulation of the AT1R-ETS1 pathway and several of its downstream targets including phosphorylated ERK2, MCP-1 and VCAM-1 in OSS segments compared with USS. This was associated with loss of EC barrier function as evaluated by extravasation of Evans-blue dye assay along with increased expression of MMP3 and MMP9 in in OSS segments compared with USS. However, vascular miR-155 expression was also higher in OSS segments compared with USS (n=6-12, P<0.05). Nevertheless, tail vein injections of miR-155 overexpressing lentivirus particles after AAC resulted in further upregulation of miR-155 expression and inverse downregulation of the AT1R-ETS1 pro-inflammatory pathway and MMPs 3 and 9 expression in OSS segments compared with USS versus scramble control (n=5-6, P<0.05).
Conclusions: Despite the early upregulation of the shear-sensitive miR-155, our data suggest that it could serve as a negative feedback regulator to acute OSS-induced upregulation of the pro-inflammatory AT1R-ETS1 pathway. Further studies are in progress to evaluate the effect of exogenous miR-155 on OSS-induced oxidative stress and vascular dysfunction, which can serve as the basis for developing novel miRNA-based therapeutic modalities.

Disclosures: **I. Mohamed:** None. **S. Thomas:** None. **R. Sutliff:** None. **N. Willet:** None. **C. Searles:** None.

259

Phenotype Switch and Altered Mechanosignaling in Vascular Smooth Muscle Cells From Marfan Syndrome Mice

Patricia Nolasco, Carolina G Fernandes, Univ of São Paulo/ Heart Inst, São Paulo, Brazil; Mariana S Ferraz, Univ of São Paulo/ Physics Inst, São Paulo, Brazil; Lazaro R Soares, UFBA/IMS, Vitória da Conquista, Brazil; Adriano M Alencar, Univ of São Paulo/ Physics Inst, São Paulo, Brazil; Francisco R Laurindo, Univ of São Paulo/ Heart Inst, São Paulo, Brazil

Background: Mechanisms whereby fibrillin-1 gene mutations promote aortic aneurysms in Marfan Syndrome (MFS) are complex. Vascular smooth muscle cells (VSMC) are crucial to aneurysm pathophysiology through (1) support of mechanical homeostasis, in which contractile VSMC connect extracellular matrix to shield synthetic VSMC against high mechanical loads and (2) key effects of synthetic VSMC on extracellular matrix organization. However, little is known about VSMC phenotypic adaptation and response to mechanical loading in MFS development.Methods: We investigated phenotypic patterns and response to cyclic stretch in VSMC cultured from aortae of wild-type (WT) mice or MFS mice bearing mgΔ^{lpn} mutation, which develop aortic dilation/thickening from the first month of age, accelerated after 6 months. We studied VSMC from 8-9 week-old mice to focus on early disease stages. VSMC remained either static or underwent 10% cyclic stretching (1Hz, 8h). Protein expression/morphology were evaluated by Western and confocal analyses. We also performed Traction Force Microscopy to assess force distribution profile. Results: There were significant phenotypic changes in MFS-VSMC vs. WT, with loss of fusiform shape and enhanced spreading, promoting ≈7-fold increased in cell area vs. WT ($p<0.001$, n=5) and >60% decrease in calponin expression vs. WT ($p<0.05$, n=3). Also, MFS-VSMC had a 10-fold greater expression of endoplasmic reticulum stress marker Grp78 (n=2). Cyclic stretch promoted expected increase in synthetic phenotype markers in WT-VSMC but an opposing contractile phenotype switch in MFS-VSMC, with decreased calponin and pFAK expression and increased stress fiber buildup. Cyclic stretch promoted similar increase in Grp78 expression in WT vs. MFS-VSMC. MFS-VSMC showed ca.60% lower capacity to generate adhesive force and extracellular matrix contractile momentum ($p<0.003$, n=10), associated with lower deformation energy *in vitro* (9,16 vs. 1,67 pJ, $p<0.004$, n=6).Conclusions: MFS associate with important deregulation of VSMC phenotypic adaptations, which may impact on their force development and disrupt force distribution in aorta.

Disclosures: **P. Nolasco:** None. **C.G. Fernandes:** None. **M.S.A. Ferraz:** None. **L.R.S. Soares:** None. **A.M. Alencar:** None. **F.R.M. Laurindo:** None.

260

Monocyte to Macrophage Conversion is Guided by Isoform Switching of the Actin Capping Protein Y-Adducin

Jurriën Prins, Ruben G de Bruin, Anton Jan van Zonneveld, Eric P van der Veer, Leiden Univ Medical Ctr, Leiden, Netherlands

Background: Modulation of cellular function necessitates a versatile utilization of the transcriptome, thereby altering the proteome. These functional adaptations are post-transcriptionally guided by RNA-binding proteins (RBP), which confer cells with the capacity to rapidly respond to various stimuli and stressors. We recently discovered a pivotal role for the RBP Quaking (QKI) in directing the conversion of monocytes into macrophages, with in particular alternative splicing of pre-mRNAs critically impacting the acquisition of a pro-inflammatory phenotype. Computational analysis indicated that this differentiation process was dependent on dynamic mobilization of the actin cytoskeletal network, which prompted us to focus our attention on an exclusion event of exon 13 at the C-terminus of the actin-capping protein gamma-Adducin (ADD3). At present, the functional consequences of ADD3 isoform switching are unknown.
Methods and Results: Stimulation of primary human monocytes with GM-CSF initially led to a decrease in ADD3 mRNA expression while ADD3 exon 13 usage was preserved. However, mRNA expression was restored upon differentiation towards the pro-inflammatory macrophage phenotype (t=3 days), while exon 13 inclusion strikingly dropped from 47.2% ± 10.5 to 7.7% ± 2.6 ($p=0.0387$, n=3). Having previously shown that QKI protein expression increases upon conversion to a macrophage, we sought to pinpoint whether QKI specifically regulates this ADD3 splicing event. Therefore, we mutated the QKI binding site (ACUAA → ACGAA) proximal to exon 13 using an ADD3 minigene. These studies revealed that disrupting the capacity for QKI to bind at this intronic sequence almost completely abolished exon 13

splicing (ACGAA: 94.9% ± 0.0025 inclusion vs. ACUAA: 2.0% ± 0.0009 inclusion; p<0.0001, n=3). Using predictive bioinformatics tools, exclusion of exon 13 was found to induce conformational changes in ADD3 protein structure. We subsequently utilized atomic force microscopy to study actomyosin dynamics and cell stiffness, pressure and tension in monocytes overexpressing the distinct ADD3 isoforms. **Conclusions:** QKI-mediated splicing of ADD3 triggers an isoform switch that impacts monocyte and macrophage function by altering the actin cytoskeleton.

Disclosures: **J. Prins:** None. **R.G. de Bruin:** None. **A. van Zonneveld:** None. **E.P. van der Veer:** None.

261

EBP50/NHERF-1 Regulates Basal and TNFα-induced Mitochondrial Dynamics in Vascular Smooth Muscle Cells

Vera Procaccia, Callen Wallace, Catherine Corey, Claudette St. Croix, Sruti Shiva, Alessandro Bisello, Univ of Pittsburgh, Pittsburgh, PA

Mitochondrial dysfunction has been associated with the phenotypic switch of VSMC and vascular disease. Changes in mitochondrial dynamics (fission and fusion) are linked to VSMC proliferation and metabolism during vascular remodeling. Mitochondrial fission and fusion are regulated by several key molecules, including dynamin-related protein 1 (Drp1) and mitofusin2 (Mfn2). We previously showed that scaffolding Ezrin-radixin-moesin binding phosphoprotein of 50 kDa (EBP50/NHERF1) increases inflammatory responses and proliferation of VSMC. These actions are mediated by the activation of PKCζ under inflammatory stimuli and the stabilization of the S-phase kinase associated protein 2 (Skp2), a component of an E3 ligase that promotes proliferation. Thus, EBP50 knockout (EBP50$^{-/-}$) mice are protected neointimal hyperplasia following arterial injury. Here we test the hypothesis that EBP50 regulates mitochondrial dynamics and responses to inflammatory stimuli in vascular smooth muscle cells (VSMC). We found that EBP50 knockdown, by decreasing Skp2 levels, increased FoxO1 stability and nuclear localization leading to higher mitofusin-2 (Mfn-2) expression. In contrast, inhibition of FoxO1 reduced Mfn2 levels. High resolution morphological analysis with both TEM and confocal microscopy revealed that mitochondria were more elongated in EBP50$^{-/-}$ than WT VSMC. In WT VSMC, TNFα induced PKCζ-mediated phosphorylation of Drp1. In contrast, EBP50$^{-/-}$ VSMC exhibited significantly reduced Drp1 phosphorylation following TNFα treatment. Live-cell 3D imaging followed by morphological analysis showed that TNFα elicited rapid and significantly greater mitochondria fragmentation in WT compared to EBP50$^{-/-}$ VSMC. Finally, EBP50$^{-/-}$ VSMC exhibited lower extracellular acidification rate (ECAR) than WT VSMC consistent with their lower proliferation. Collectively, these findings delineate a new mechanism of regulation of mitochondrial dynamics by the scaffolding protein EBP50 in response to inflammatory stimuli. Therefore EBP50 can be viewed as a potential therapeutic target for vascular proliferative diseases.

Disclosures: **V. Procaccia:** None. **C. Wallace:** None. **C. Corey:** None. **C. St. Croix:** None. **S. Shiva:** None. **A. Bisello:** Research Grant; Significant; AHA grant.

This research has received full or partial funding support from the American Heart Association.

262

Drebrin Regulates Aortic Remodeling in Angiotensin II-Induced Hypertension

Lisheng Zhang, Jiao-Hui Wu, Tai-Qin Huang, Igor Nepliouev, Leigh Brian, Zhushan Zhang, Nathan P Rudemiller, Steven D Crowley, Neil J Freedman, **Jonathan A Stiber**, Duke Univ Medical Ctr, Durham, NC

The actin-binding protein, Drebrin, is upregulated in response to arterial injury and reduces smooth muscle cell migration/proliferation through its interaction with the actin cytoskeleton. Because hypertensive aortic remodeling involves smooth muscle cell (SMC) activation and synthesis of extracellular matrix, we tested the hypothesis that Drebrin inhibits this process. To determine the effect of Drebrin deficiency in SMCs on hypertensive aortic remodeling, we induced hypertension by implanting osmotic mini-pumps to infuse angiotensin II (Ang II, 1000 ng/kg/min) or vehicle (0.9% NaCl) continuously for 28 days in SM22-α Cre$^{+/-}$;*Dbn*$^{flox/flox}$ mice (SMC-*Dbn*$^{-/-}$ mice) and controls. Blood pressure (BP) responses to Ang II treatment were assessed by telemetry. After completion of Ang II infusion, the degree of aortic remodeling was assessed by computerized tomography of histologic cross-sections of the

proximal ascending aorta. Despite observing no difference in the extent of Ang II-induced hypertension in SMC-*Dbn*$^{-/-}$ mice compared with controls, SMC-*Dbn*$^{-/-}$ mice exhibited a significant increase in medial hypertrophy and outward remodeling. Wall thickness/body weight was increased by 61 ± 2% ($p<0.01$) in SMC-*Dbn*$^{-/-}$ mice compared with controls, and lumen area/body weight was increased by 102 ± 9% ($p<0.01$). Cellular proliferation and matrix deposition were increased in the proximal aortas of Ang II-treated SMC-*Dbn*$^{-/-}$ mice compared with controls as evidenced by increased immunoreactivity for PCNA, p-ERK, and Collagen I. SMC loss of Drebrin also resulted in increased Ang II-induced pro-inflammatory signaling as evidenced by increased expression of VCAM-1, p-P65 and MMP-9 and increased CD68 positive cellular proliferation in response to chronic Ang II infusion. We conclude that SMC loss of Drebrin augments adverse aortic remodeling in angiotensin II-induced hypertension.

Disclosures: **L. Zhang:** None. **J. Wu:** None. **T. Huang:** None. **I. Neppliouev:** None. **L. Brian:** None. **Z. Zhang:** None. **N.P. Rudemiller:** None. **S.D. Crowley:** None. **N.J. Freedman:** None. **J.A. Stiber:** None.

This research has received full or partial funding support from the American Heart Association.

263

Thrombin-Mediated Human Aortic Endothelial Barrier Dysfunction Alters Microrna Pathways Involved in Cell Survival, Injury, and Cancer

Christine M Wardell, McMaster Univ, Hamilton, ON, Canada; John Harlock, Theodore Rapanos, Dept of Surgery, Div of Vascular Surgery, McMaster Univ, Hamilton, ON, Canada; Alison Fox-Robichaud, Peter Gross, Thrombosis and Atherosclerosis Res Inst, McMaster Univ, Hamilton, ON, Canada; Kathryn L Howe, Dept of Surgery, Div of Vascular Surgery, McMaster Univ, Hamilton, ON, Canada

Introduction Endothelial cells (EC) must maintain an effective physiologic barrier in a highly dynamic environment. Capable of regulating other cells within the vasculature (e.g. smooth muscle cells), ECs govern response to injury and inflammation. microRNAs (miR) are emerging as critical regulators of vascular disease, implicating EC miRs in homeostasis maintenance. Increased EC permeability has been documented in atherosusceptible regions of the aorta suggesting it plays a role in disease development, but whether this is a cause or consequence is unknown.
Hypothesis We hypothesized EC barrier dysfunction is a critical event that perpetuates chronic vascular disease via altered miR profiles.
Methods Human aortic endothelial cells (HAEC) cultured in transwells were exposed to thrombin (0.5, 1, 2U/ml) and permeability measured by fluorescence flux across monolayers at 90 minutes. Total HAEC RNA was isolated at various timepoints with individual miR transcripts counted using nanoString nCounter® (n=6 samples). miR that was altered >2-fold compared to controls were analyzed using nSolver™ software and Ingenuity® Pathway Analysis (IPA).
Results Thrombin exposure increased EC permeability to 130±8.4% of untreated controls (2U/ml thrombin; $p<0.05$; n=16 transwells). Heatmaps from miR counts showed extensive miR profile changes in response to thrombin (n=6 samples (control, 90min, 4h, 24h)). Using IPA, miRs were clustered based on seed regions and matched with experimentally confirmed mRNA targets. At all timepoints, mRNA targets were shown to be most involved in cancer and injury disease pathways, with top cellular functions identified as cell movement, proliferation, growth, and survival.
Conclusions In response to a permeability insult, HAEC miR levels are significantly altered. Although our preliminary data need to be further substantiated, they highlight a possible mechanism whereby EC barrier dysfunction is a critical event that perpetuates chronic vascular disease. In this way, we might envision a scenario not unlike cancer (which has been compared to atherosclerosis), where an initial appropriate endothelial repair response becomes dysregulated in the context of ongoing injury (e.g. permeability) in atherosusceptible regions.

Disclosures: **C.M. Wardell:** None. **J. Harlock:** None. **T. Rapanos:** None. **A. Fox-Robichaud:** None. **P. Gross:** None. **K.L. Howe:** None.

264

Protein Disulfide Isomerase A1 is a Central Hub for Redox Regulation of VSMC Phenotype

Joao Wosniak Jr, Renata Castro Gonçalves, Leonardo Yuji Tanaka, Univ of Sao Paulo/Heart Inst, São Paulo, Brazil; Daniela Bertolini Zanatta, Bryan Eric Strauss, Cancer Inst of Sao Paulo State, São Paulo, Brazil; Francisco Rafael Laurindo, Denise Castro Fernandes, Univ of Sao Paulo/Heart Inst, São Paulo, Brazil

OBJECTIVE: Vascular smooth muscle cell (VSMC) phenotype switch depends on extrinsic/intrinsic cues including NOX NADPH oxidase-linked redox signaling. Growth factor-triggered NOX1 expression/activity requires the chaperone oxidoreductase protein disulfide isomerase-A1 (PDI). Acute PDI overexpression induces agonist-independent NOX1 expression. PDI is required for VSMC migration and cytoskeleton organization, and extracellular PDI supports expansive vascular remodeling via cytoskeleton reshaping. Such PDI effects led us to hypothesize that PDI may orchestrate VSMC phenotypic alterations.**APPROACH AND RESULTS:** In primary VSMC, PDI silencing spontaneously decreased differentiation marker expression. Transfection with a doxycycline-inducible lentiviral vector encoding PDI showed that sustained PDI overexpression (72h) enhanced actin branching pattern vs. baseline (anisotropy index, 0.103±0.019 vs. 0.220±0.027, 72h vs. 0h, mean±SEM, N=5, P<0.05), increased cell length and induced expression of differentiation marker calponin (2-fold, 72h vs 0h, N=5, P<0.05), alpha-actin and smoothelin, which were abrogated upon catalase incubation. Intracellular superoxide enhanced upon 48h of PDI overexpression (2-hydroxyethidium levels, 0.998±0.102 vs. 2.887±0.227 AU, N=4, P<0.05) and was NOX1-dependent, based on inhibition with GKT136901 (by 48%) or NOXA1ds peptide (by 54%) (N=6, P<0.05). Increased NOX1 mRNA occurred early after PDI overexpression (74%, 24h vs. 0h, N=4, P<0.05), while NOX4 mRNA was upregulated only after long-term PDI induction (100%, 72h vs. 0h, N=4, P<0.05). In rabbit restenosis model exhibiting strong PDI upregulation (12-fold at day 14 after injury), ex vivo PDI silencing 7 or 14 days after injury reversed PCNA expression, while promoting increased NOX1 and decreased NOX4 mRNA levels (+54% and -45%, respectively, siPDI vs. siSCR, N=3, P<0.05 for both).**CONCLUSIONS:** While short-term PDI overexpression supports NOX1 activation/expression, sustained PDI overexpression drives NOX4 expression and VSMC differentiation. Effects on cytoskeleton, NOX1/4 activation and temporal control of NOX1/4 expression suggest a central role for PDI as a hub for redox-mediated VSMC phenotype regulation.

Disclosures: **J. Wosniak Jr:** None. **R.C. Gonçalves:** None. **L.Y. Tanaka:** None. **D.B. Zanatta:** None. **B.E. Strauss:** None. **F.R.M. Laurindo:** None. **D.C. Fernandes:** None.

265

FXR1 Regulates Inflammatory MRNA Stability and VSMC Proliferation by Modulation of HuR Activity

Allison Herman, Ross England, Dale Haines, Sheri Kelemen, Mitali Ray, Michael V Autieri, Lewis Katz Sch of Med, Philadelphia, PA

Vascular smooth muscle cells (VSMC) play a critical role in the etiology and progression of many vascular diseases including atherosclerosis and restenosis. Our laboratory has found that one anti-inflammatory interleukin, IL-19, is atheroprotective and can decrease vascular inflammation by reduction in mRNA stability of inflammatory transcripts by reduction of activity of HuR, an mRNA stability protein. HuR translocates from the nucleus to the cytoplasm where it recognizes AU-rich elements present almost exclusively in the 3'UTR of pro-inflammatory genes. Proteins and pathways which limit HuR translocation are understudied, but may reduce inflammatory mRNA stability. Using MASS SPEC to identify HuR-interacting proteins under different inflammatory conditions, we identified one protein, Fragile X-related protein (FXR1), which interacts with HuR in inflammatory, but not basal conditions, a novel interaction. FXR1 mRNA expression is enhanced in muscle cells, but nothing has been reported on expression of FXR1 in VSMC or function for FXR1 in vascular disease. The FXR1 promoter contains multiple cholesterol-response elements, and in this study we demonstrate that FXR1 expression is increased in injured arteries and TNFα and oxLDL stimulated human VSMC, but also by IL-19. RNA EMSA demonstrates that FXR1 directly interacts with ARE in 3'UTR. SiRNA knock down of FXR1 in VSMC increases stability of inflammatory mRNA and protein abundance as well as VSMC proliferation, while overexpression of FXR1 reduces both their abundance and stability in addition to reducing proliferation. Since FXR1 appears to be a novel repressor of inflammatory proteins, and is also induced by IL-19, our

overall hypothesis is that FXR1 expression and HuR interaction is an inflammation responsive, counter-regulatory mechanism to reduce abundance of pro-inflammatory proteins and therefore reduce inflammation.

Disclosures: **A. Herman:** None. **R. England:** None. **D. Haines:** None. **S. Kelemen:** None. **M. Ray:** None. **M.V. Autieri:** None.

266

Extracellular Hemoglobin from Stored Rbcs Binds Ago2 And Delivers Functional Microrna to Endothelial Cells

Appesh N Mohandas, Sheena A Thomas, Kimberly A Rooney, Adam J Mitchell, John D Roback, Charles D Searles, Emory Univ, Atlanta, GA

Red blood cell (RBC) transfusion is among the most common clinical therapies. Prior to transfusion, packed RBCs (PRBCs) may be stored for up to 42 days. During storage, RBCs undergo many changes, including hemolysis and the release of extracellular hemoglobin (Hb). Prior work has shown that endothelial cells exposed to free hemoglobin demonstrate upregulation of inflammatory and anti-inflammatory pathways including elevated ICAM-1, VCAM-1 and E selectin, as well as elevated Hemeoxygenase-1 and bilirubin levels. Our work tests the hypothesis that extracellular Hb from stored RBCs can transfer functional microRNA to endothelial cells.
Stored RBCs (age 30-42 days) were obtained from the Emory University Hospital Blood Bank. Extracellular Hb was obtained from lysed RBCs. Binding of Argonaute 2 (Ago2) to Hb was assessed by immunoprecipitation (IP) of Hb-alpha followed by Western blot for Ago2. In addition, microRNA was extracted from the Hb immunoprecipitate. Levels of miR-451, -16, -584, and -92 were assessed by RT-qPCR analysis. Lastly, human aortic endothelial cells (HAECs) were treated with Hb from RBC lysates. After treatment, Qiazol was used to extract RNA from washed cells, and levels of miR-451 and target genes were measured by RT-qPCR and Western analysis.
We found that Ago2, a crucial component of the RISC complex that executes the regulatory function of microRNA, co-immunopreciptated with Hb from RBC lysates. We also observed that miR-451, a microRNA known to be abundant in RBCs, was highly abundant in Hb immunoprecipates. Furthermore, miR-16, -584 and -92 could also be amplified from Hb immunoprecipitates. Endothelial cells treated with extracellular Hb from RBC lysates for 36 hours had a dramatic increase in levels of miR-451 and a significant decrease in mRNA abundance of genes known to be targets of miR-451, including ATF2 (p-value=0.03), CAV1 (p-value=0.02), and MIF (p-value=0.005). HAECs treated with extracellular Hb for 72 hours had decreased protein levels of ATF2 (p-value=0.01) and CAV1 (p-value=0.003). In conclusion, previous work has shown that extracellular Hb can have direct effects on endothelial cells; our data show, for the first time, that extracellular Hb also serves as a vehicle for the cell-to-cell delivery of microRNA.

Disclosures: **A.N. Mohandas:** None. **S.A. Thomas:** None. **K.A. Rooney:** None. **A.J. Mitchell:** None. **J.D. Roback:** None. **C.D. Searles:** None.

299

Effect of Low-Dose versus Very-Low-Dose Rivaroxaban on Stroke and Major Bleeding Among Atrial Fibrillation Patients Undergoing Percutaneous Coronary Intervention: A Bivariate Analysis on the Net Clinical Benefit

Jolanta Marszalek, Louis A. Weiss Memorial Hosp, Chicago, IL; Sara Mehrsefat, Johns Hopkins Univ, Sch of Med, Baltimore, MD; Gerald Chi, Beth Israel Deaconess Medical Ctr, Harvard Medical Sch, Boston, MA

Background: Among atrial fibrillation (AF) patients undergoing percutaneous coronary intervention (PCI), both low-dose and very-low-dose rivaroxaban plus antiplatelets had similar rates of stroke and major bleeding compared to triple therapy.
Methods: To assess the risk-benefit profile of two rivaroxaban dosing strategies with a spectrum of non-inferiority margin, a previously described method of bivariate analysis was used. In the PIONEER AF-PCI trial, 2,124 patients were randomized to three groups and followed for 12 months: 1) low-dose rivaroxaban (15 mg once daily) plus a single $P2Y_{12}$ inhibitor (N=709); 2) very-low-dose rivaroxaban (2.5 mg twice daily) plus DAPT (N=709); and 3) warfarin plus DAPT (N=706). Risk differences in stroke and in TIMI major bleeding were simultaneously analyzed to arrive at net clinical benefit (NCB).

Results: Compared to warfarin, both rivaroxaban dosing regimens had comparable risk of TIMI major bleeding (low-dose: -0.86% [95% CI: -2.48% to 0.86%], P=0.30 vs. very-low-dose: -1.17% [95% CI: -2.73% to 0.39%], P=0.14). Risk difference in all-cause stroke between rivaroxaban and warfarin was not significant (low-dose: 0.15% [95% CI: -0.94% to 1.23%], P=0.79 vs. very-low-dose: 0.41% [95% CI: -0.73% to 1.56%], P=0.48). With a non-inferiority margin of 80% or above (equivalent to a risk difference of 2.40%), both rivaroxaban regimens demonstrated similar, favorable NCB against warfarin (low-dose: -1.92% [-3.28% to -0.20%] vs. very-low-dose: -1.74% [-3.09% to -0.17%]).
Conclusions: Bivariate analysis is a novel methodology that allows simultaneous display and assessment of both efficacy and safety outcomes. In the management of AF patients undergoing PCI, rivaroxaban (15 mg once daily or 2.5 mg twice daily) achieved a favorable benefit-to-risk tradeoff over warfarin at the non-inferiority margin of 80% or above.
Figure: NCB of rivaroxaban dosing strategies. Shaded partition above the curve represents lack-of-benefit region.

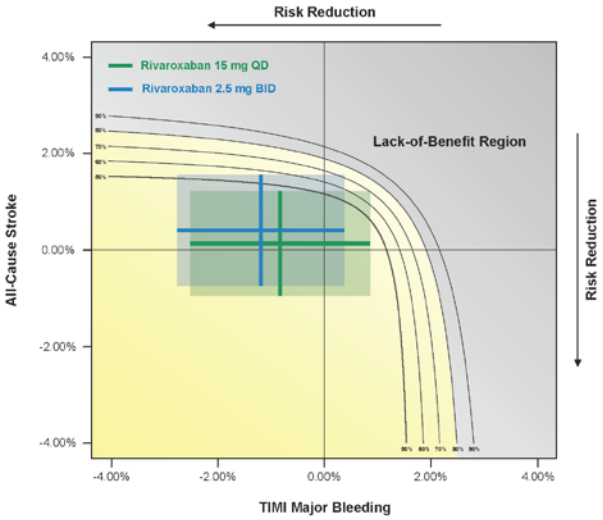

Disclosures: **J. Marszalek:** None. **S. Mehrsefat:** None. **G. Chi:** None.

300 will be presented in the PVD Moderated eAbstract Poster Session. The abstract content is located on page 38.

301

Association of Short and Long Sleep Duration with Carotid Intima-Media Thickness, the Baptist Employee Healthy Heart Study (Behhs)

Muhammad Aziz, Baptist Health South Florida, Miami, FL; Yugandhar Kandimalla, Ocala Regional Medical Ctr, Ocala FL., Ocala, FL; Archana Machavarapu, Ocala Regional Medical Ctr, Ocala, FL; Adnan Younus, Rehan Malik, Baptist Health South Florida, Miami, FL; Mounica Banala, Ocala Regional Medical Ctr, Ocala, FL; Anshul Saxena, Choudhry Humayun, Victor M. Pena, Rana Jaber, Emir Veledar, Khurram Nasir, Baptist Health South Florida, Miami, FL

Objective: Carotid intima media thickness (CIMT) is well-known marker of cerebrovascular & CVD outcomes. Recent literature has discussed association of sleep duration with stroke &CVD, but still limited evidence exists regarding the true relationship of sleep duration with CIMT. The aim of this study is to determine association of short& long sleep duration with CIMT.
Method: Baptist Health South Florida, a not for profit organization, conducted a randomized, non-blinded controlled trial in 2014.This study examined effect of web based interventions on reducing CVD risk in employees. The inclusion criteria were physician diagnosed T2DM and/or Metabolic Syndrome. We used cross sectional data for analysis. Per CDC.gov guidelines, we categorized self-reported sleep duration (hrs) as short (<7), reference (≥7-<9) and long sleep (≥9). CIMT was measured via carotid US screening device by Panasonic CardioHealth Station.

Result: Study population (n=183; 74% female, 49% Hispanic) with mean age 51±10 years. Mean CIMT(mm) in females [0.879±0.15] and males [0.911±0.19] was not different (p>0.05). Atherosclerotic plaque was defined as any obvious focal luminal encroachment > 1.2 mm. In multivariate logistic regression model, per hour increase in sleep duration was associated with twice the odds of increase in CIMT >1.2mm [OR 2.15;95% CI (1.15-4.02)]. However, once we compared the reference sleep with short and long sleep duration categories, we determined, as compared to 7-9 hrs (ref) of sleep, the odds of CIMT >1.2 in those sleeping <7 hrs [OR 1.23; 95% CI (0.27-5.53)] and those sleeping ≥9 hrs [OR 2.91; 95% CI (0.33-25.42)] were not significant in adjusted model.
Conclusion: Although we observed that per hour increase in sleep was related to increase in CIMT >1.2mm (risk of plaque), but we did not find any significant increased risk of plaque in either short or long sleep duration. Longitudinal studies with larger sample size are needed to clarify this association.

Table: Odds ratio for presence of CIMT >1.2 according to "per hour increase in sleep duration" and "sleep duration categories".

Models	Odds of CIMT >1.2 per hour increase in sleep	Sleep duration categories		
		<7 hrs (n=90)	≥7 - <9 hrs (n=73)	≥9 hrs (n=20)
Unadjusted	**1.71(1.11-2.65)**	1.23(0.33-4.54)	Ref	4.31(0.97-19.11)
Model 1	**1.67(1.05-2.65)**	1.41 (0.37-5.29)	Ref	4.68(0.88-24.77)
Model 2	**2.15(1.15-4.02)**	1.23(0.27-5.53)	Ref	2.91(0.33-25.42)

Data adjusted: Model 1: age and gender, Model 1: Model 1+ ethnicity, BMI, blood pressure, fasting glucose, LDL, HDL, triglycerides, current smokers, alcohol intake.

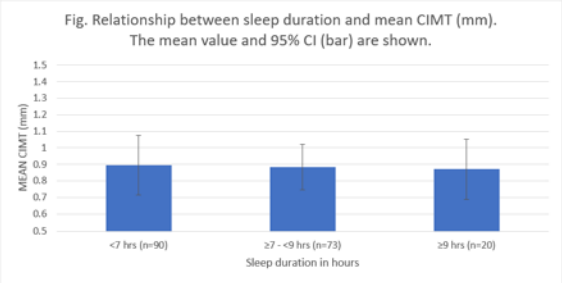

Disclosures: **M. Aziz:** None. **Y. Kandimalla:** None. **A. Machavarapu:** None. **A. Younus:** None. **R. Malik:** None. **M. Banala:** None. **A. Saxena:** None. **C. Humayun:** None. **V.M. Pena:** None. **R. Jaber:** None. **E. Veledar:** None. **K. Nasir:** None.

302

The PAT Ratio is Reduced by Beta-blockers

Ueda Tomohiro, Hiroshima General Hosp, Hiroshima shi, Japan

Background: Flow-mediated dilatation (FMD) of the brachial artery and Peripheral arterial tonometry (PAT) are both methods for assessing endothelial vascular function. FMD measures predominantly nitric oxide mediated vasodilation whereas PAT measures a more complex range of mechanisms. The recent study showed that the sympathetic nervous system plays a significant role in this response. Methods: The study involved 176 subjects (mean age66 ±12 years). Based on the medication of beta-blockers, they were divided into 2 groups: beta-blocker group (n=37) and control group (n=139). Flow mediated vasodilatation (FMD) and nitroglycerine-induced vasodilatation (NID) in the brachial artery was measured by using UNEXEF18G (UNEX CO, Japan), and nitroglycerin mediated vasodilatation (NMD) was used as a control test for FMD. At the same time, PAT ratio was measured by using Endo-PAT 2000 (Itamar Medical, Israel) Results: PAT ratio was significantly impaired in beta-blocker group compared to that in control group (1.5±0.4% vs. 1.9±0.6%, respectively; P<0.05). However, FMD and NMD had no deference in both groups. Multivariable analysis revealed that blood sugar and medication of beta-blockers were independent variables for PAT ratio. Conclusion: These result show that beta-blockers is associated with a tendency towards reduced PAT ratio. PAT needs to be further studied, including the assessment of non-endothelial factor

Disclosures: **U. Tomohiro:** None.

303 will be presented in the PVD Moderated eAbstract Poster Session. The abstract content is located on page 39.

304

Association Between Plaque Morphology and Time Interval After the Neurologic Index Event in Patients with Symptomatic Carotid Stenosis

Pavlos Tsantilas, Andreas Kuehnl, Jaroslav Pelisek, Lars Maegdefessel, Carina Wendorff, Heiko Wendorff, Sofie Schmid, Alexander Zimmermann, Hans-Henning Eckstein, Klinikum Rechts der Isar, Technical Univ of Munich, Munich, Germany

Objectives: Instable plaques are more common in patients with symptomatic carotid stenosis compared to asymptomatic patients. Clinically symptomatic patients are at high risk for a recurrent stroke in the first days after a neurologic index event. Histopathologic plaque stabilisation or remodelling mechanisms of symptomatic plaques are unclear. Therefore, our study aimed to find changes of plaque morphology in dependence of time interval between neurologic index event and plaque removal. **Methods:** Plaques of patients that were removed from surgically treated patients with symptomatic carotid stenosis between 2004 and 2016 were included. Histological analyses of those carotid plaques were performed to assess the type of plaque (American Heart Association classification), the stability of plaque (thickness of the fibrous cap </>200µm), the extent of calcification, inflammation, neovascularization and the deposition of collagen and elastin. Statistical analysis was applied in form of an ordinal regression analysis, adjusted for common risk factors of atherosclerosis. **Results:** Out of 348 included plaques, the patients' median age was 71 (Q1-Q3, 65 - 77) years and 69% were male. Median time interval between index event and plaque removal was 10 days (Q1-Q3, 4-28 days). Most common index event was a transient ischemic attack with 37% (128 of 348), followed by stroke in 28% (97 of 348), amaurosis fugax in 22% (76 of 348) and instable symptoms (crescendo transient ischemic attack, stroke in evolution) in 12% (43 of 348), respectively. The ordinal regression analysis revealed, that the time interval as continuous independent variable had no significant influence on plaque type, plaque stability, extent of calcification, inflammation or neovascularization and the deposition of collagen and elastin. **Conclusions:** The examined plaque morphology features of patients with symptomatic carotid stenosis showed no differences in relation to the time interval between neurologic index event and plaque removal. To find potential symptomatic plaque remodelling mechanisms, currently ongoing molecular and histomorphological analysis aim at identifying novel markers of apoptosis and cell fate-driven mechanisms in fibrous cap-enriched vascular smooth cells.

Disclosures: **P. Tsantilas:** None. **A. Kuehnl:** None. **J. Pelisek:** None. **L. Maegdefessel:** None. **C. Wendorff:** None. **H. Wendorff:** None. **S. Schmid:** None. **A. Zimmermann:** None. **H. Eckstein:** None.

305

Cytokine Response to Concentrated Bone Marrow Aspirate Injections in Patients With Critical Limb Ischemia

S. Keisin Wang, Linden Green, Cliff Babbey, Raghu Motaganahalli, Praveen Kusumanchi, Sunil Tholpady, Andres Fajardo, Michael Murphy, IU Sch of Med, Indianapolis, IN

Objective: No medical intervention is approved for patients who suffer from critical limb ischemia (CLI) without a surgical revascularization option. Concentrated bone marrow aspirate (cBMA) injections have demonstrated safety and efficacy in increasing 1-year amputation-free survival (AFS) in the phase III multicenter, double blind, randomized controlled MOBILE trial. The response to cBMA injection is described herein. **Methods**: A murine (IL-2Rγ$^{-/-}$) hind-limb ischemia model was employed to assay blood and tissue levels of angiogenic markers after MarrowStim™ derived cBMA injection. Responders to therapy were selected by cutaneous laser Doppler. Animals were sacrificed at various time points post-injection during which blood and distal limb tissue was harvested. 10 patients were enrolled into the MOBILE Continuing Access trial from May to December 2016 and received cBMA injections into the ischemic limb. Blood was collected at days 1, 3, 7, 14, 45, 60, and 90. Endothelial progenitor cells (EPCs) and protein markers of tissue ischemia were assayed by FACS and ELISA respectively. **Results**: In mice, cBMA produced a marked increase in gross tissue survival, capillary density, and perfusion compared to the control limb despite low engraftment of human cells. There was no inflammatory infiltration at any of the injection sites. Subanalysis of groups that had differing responses demonstrated crucial increases in FGF-2, VEGF, angiopoietin-2, IL-1β, and TNF-α. 7 subjects donated adequate of blood samples for FACS analysis; of this cohort, 5 patients had demonstrable increases in their EPC to non-EPC ratios immediately post-treatment. No statistically significant changes in FGF, VEGF, ANG1/2, PDGF, and GM-

CSF was observed in the systemic circulation. **Conclusions**: cBMA has demonstrated efficacy in increasing 1-year AFS in CLI patients without surgical revascularization options. However, the response to treatment is variable and further studies are required to predict those who would benefit the most from cBMA.

Disclosures: **S. Wang:** None. **L. Green:** None. **C. Babbey:** None. **R. Motaganahalli:** None. **P. Kusumanchi:** None. **S. Tholpady:** None. **A. Fajardo:** None. **M. Murphy:** None.

306

Impact of Venous Thromboembolism as Independent Predictor of Mortality Among Patients With Gastric Cancer

Harry E Fuentes, Luis H Paz, John Stroger Hosp, chicago, IL; Diana M Oramas, Univ of Illinois at Chicago, chicago, IL; Xavier A Andrade, Yuchen Wang, John Stroger Hosp, chicago, IL; Alfonso J Tafur, NorthShore Univ HealthSystem, Evanston, IL

Background: Cancer-associated thrombosis is a predictor of death. Patients with gastric cancer (GC) are at higher risk for VTE when compared to other solid tumors. There is a paucity of data describing the impact of VTE in GC. **Aim:** To measure the impact of VTE as independent predictor of gastric cancer mortality. **Methods:** Single institution chart review of GC treated patients (2010-15). VTE events were objectively confirmed. GC was ascertained if biopsy proven and metastatic, or on active chemotherapy. Along with cancer specific data, we abstracted risk assessments tools, non-GC specific, validated for VTE and mortality prediction in cancer; including, the Khorana Score (KRS), platelet lymphocyte ratio (PLR) and neutrophil lymphocyte ratio (NLR). Continuous variables are expressed by the by the median (interquartile range). Categorical variables are expressed as percentages. We used SPSS 23, specifically Kaplan-Meir curve and Cox proportional hazard were applied for main objectives. **Results**: We included 112 pts in the analysis, who were predominantly male (66%), 58 (51-64) year-old, with adenocarcinoma (84%) and advanced disease (59%). The median follow-up was 21.3 months (9.5-42.6). We measured high risk of VTE based on the KRS in 59%, 51% had an elevated NLR and 30% had an elevated PLR. VTE occurred in thirteen (12%) patients. The median time from diagnosis to VTE occurrence was 59 days (36-258). After multivariate analysis, the predictors of mortality were: VTE (Hazard Ratio (HR), 2.6; 95% CI, 1.1 to 6.0; p=0.02), Histological type (HR, 3.2; 95% CI, 1.1 to 9.2; p=0.03), Stage (HR, 2.9; 95%CI, 1.4 to 5.8; p<0.01) and PLR (HR, 2.2; 95%CI, 1.3 to 3.9); p<0.01). The one year overall survival of patients with VTE was lower than for those with no VTE (79% vs 41% p<0.05) **Conclusion**: VTE is associated with worse survival among patients with GC. Moreover, this finding was independent of other cancer-specific variables. NLR and KRS were not associated with survival in our GC database.

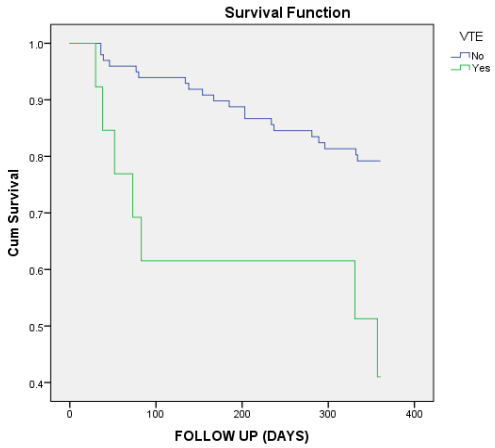

Disclosures: **H.E. Fuentes:** None. **L.H. Paz:** None. **D.M. Oramas:** None. **X.A. Andrade:** None. **Y. Wang:** None. **A.J. Tafur:** None.

307

Circulating sRAGE is Associated with Aortic Dysfunction in Mice Models of Thoracic Aortic Aneurysm

Josephine Galatioto, Mount Sinai Sch of Med, New York, NY; Eric Lai, Univ of Pennsylvania, Philadelphia, PA; Maria Bintanel-Morcillo, Mount Sinai Sch of Med, New York, NY; Tao Wang, Giovanni Ferrari, Reed E Pyeritz, Joseph E Bavaria, **Emanuela Branchetti**, Univ of Pennsylvania, Philadelphia, PA

Backgound. The Receptor for Advanced Glycation End products (RAGE) and its ligands are associated with vascular remodeling and trigger the release of a soluble receptor (sRAGE). We demonstrated that sRAGE is elevated in patients with thoracic aortic disease such as patients with bicuspid aortic valve and Marfan syndromes. Circulating sRAGE in these patients correlates with the presence of a dysfunctional aortic structure without linearly correlating with increasing aortic diameter. We hypothesized that elevated sRAGE levels are the result of structural degeneration during aortic aneurysm formation and that they are affected by pharmacological treatments aimed to inhibit vascular remodeling. **Methods.** Circulating sRAGE was tested by ELISA in two mouse models of thoracic aortic aneurysm (TAA): the AngII chronic infusion model and the hypomorphic $FBN1^{mgR/mgR}$. C57BL6 mice were treated with AngII via osmotic pump for 28 days with or without losartan in drinking water. $FBN1^{mgR/mgR}$ mice were treated with losartan starting from postnatal day 16 (p16). Ascending aorta and blood were collected at day 28 of AngII infusion or at p60 in the hypomorphic model. Aortic dilatation and degeneration were tested by echocardiography and histological analysis. **Results.** Plasma sRAGE is significantly higher in AngII treated animals when compared to controls (118.1± 8.3 vs 45.6±5.01 pg/ml, $p<0.0001$) and is associated with aortic aneurysm formation and increased medial thickening. Similarly, sRAGE levels are higher in $FBN1^{mgR/mgR}$ mice compared to age-matched wild type (1939 ± 320.5 vs 45.6±5.01 pg/ml, $p<0.0001$) in concomitance with elastin degradation (media score 3.5± 0.8 vs 1.03.5± 0.2, $p<0.05$) and proximal aorta enlargement. Plasma sRAGE decreases in AngII and $FBN1^{mgR/mgR}$ mice treated with losartan when compared to age matched untreated or wild type mice (73±24.5 vs 118.1 ± 8.296 pg/ml, $p<0.05$ and 260.7 ± 4.333 vs 1939 ± 320.5 pg/ml, $p<0.001$) together with reduced aorta dilatation, medial thickening and elastin fragmentation. **Conclusion.** sRAGE is elevated in the presence of aortic dilatation in mouse models of TAA, as seen in human aneurysmal patients. These results suggest that sRAGE may be used as a circulating biomarker to assess disease severity in patients with TAA.

Disclosures: **J. Galatioto:** None. **E. Lai:** None. **M. Bintanel-Morcillo:** None. **T. Wang:** None. **G. Ferrari:** None. **R.E. Pyeritz:** None. **J.E. Bavaria:** None. **E. Branchetti:** None.

308

Cardiac Cycle Affects Ultrasound Measurements of Ascending Aortic Diameter in a Marfan Mouse Model

Zheying Chen, Hisashi Sawada, Debra Rateri, Alan Daugherty, Mary Sheppard, Univ of Kentucky, Lexington, KY

Objective:
Ultrasound measurements of aortic diameter are a common endpoint in preclinical studies. However, there is a lack of standardization in both image capture and analysis. For our study, we developed a standardized protocol for measuring ascending aortic diameter and examined effects of cardiac cycle in wild type and fibrillin-1 hypomorphic ($FBN^{mgR/mgR}$) mice.
Methods and Results:
Twelve week old male and female $FBN^{mgR/mgR}$ mice were anesthetized and maintained at a heart rate of 450-550 beats per minute. Ultrasound images were captured using a Vevo 2100 system with a 40MHz tranducer. Images captured were standardized according to two anatomical landmarks: the innominate artery branchpoint and aortic valves. The largest luminal ascending aortic diameter between the sinotubular junction and the innominate artery were measured in mid-systole and end-diastole by two blinded, independent observers.
Aortic diameters were significantly different ($p<0.05$) when comparing systole and diastole within gender and genotype. Interestingly, wild-type male (n=4) and female (n=3) mice exhibited a 19% and 15% expansion of the ascending aorta respectively during systole compared to diastole. This difference was not recapitulated in either male (n=6) or female (n=5) $FBN^{mgR/mgR}$ mice (4% expansion in both; $p<0.05$ vs wild-type). Agreement between observers was excellent ($R^2 = 0.99$) but interobserver variability was a

mean of .09 mm (%CV = 5%)
Conclusion:
As expected, there is a difference in aortic diameters between wild-type and FBN$^{mgR/mgR}$ mice. Luminal aortic diameters in FBN$^{mgR/mgR}$ vs wild-type mice of both genders are affected by cardiac cycle. Mid-systolic aortic expansion in wild-type vs FBN$^{mgR/mgR}$ mice were different. Error introduced by interobserver variability impacts ascending aortic measurements. Altogether, these phenomena may confound analyses of aortic dilation in FBN$^{mgR/mgR}$ mice, especially when studying interventions with modest effect sizes.

	Aortic Diameter (mm)			
	Male		Female	
	Systole	Diastole	Systole	Diastole
Wild-type	1.54 ± 0.08	1.30 ± 0.06	1.35 ± 0.06	1.17 ± 0.06
FBN$^{mgR/mgR}$	2.14 ± 0.20	2.07 ± 0.20	1.68 ± 0.09	1.62 ± 0.11

Disclosures: **Z. Chen:** None. **H. Sawada:** None. **D. Rateri:** None. **A. Daugherty:** None. **M. Sheppard:** None.

308

Cardiac Cycle Affects Ultrasound Measurements of Ascending Aortic Diameter in a Marfan Mouse Model

Zheying Chen, Hisashi Sawada, Debra Rateri, Alan Daugherty, Mary Sheppard, Univ of Kentucky, Lexington, KY

Objective:
Ultrasound measurements of aortic diameter are a common endpoint in preclinical studies. However, there is a lack of standardization in both image capture and analysis. For our study, we developed a standardized protocol for measuring ascending aortic diameter and examined effects of cardiac cycle in wild type and fibrillin-1 hypomorphic (FBN$^{mgR/mgR}$) mice.
Methods and Results:
Twelve week old male and female FBN$^{mgR/mgR}$ mice were anesthetized and maintained at a heart rate of 450-550 beats per minute. Ultrasound images were captured using a Vevo 2100 system with a 40MHz tranducer. Images captured were standardized according to two anatomical landmarks: the innominate artery branchpoint and aortic valves. The largest luminal ascending aortic diameter between the sinotubular junction and the innominate artery were measured in mid-systole and end-diastole by two blinded, independent observers.
Aortic diameters were significantly different ($p<0.05$) when comparing systole and diastole within gender and genotype. Interestingly, wild-type male (n=4) and female (n=3) mice exhibited a 19% and 15% expansion of the ascending aorta respectively during systole compared to diastole. This difference was not recapitulated in either male (n=6) or female (n=5) FBN$^{mgR/mgR}$ mice (4% expansion in both; $p<0.05$ vs wild-type). Agreement between observers was excellent ($R^2 = 0.99$) but interobserver variability was a mean of .09 mm (%CV = 5%)
Conclusion:
As expected, there is a difference in aortic diameters between wild-type and FBN$^{mgR/mgR}$ mice. Luminal aortic diameters in FBN$^{mgR/mgR}$ vs wild-type mice of both genders are affected by cardiac cycle. Mid-systolic aortic expansion in wild-type vs FBN$^{mgR/mgR}$ mice were different. Error introduced by interobserver variability impacts ascending aortic measurements. Altogether, these phenomena may confound analyses of aortic dilation in FBN$^{mgR/mgR}$ mice, especially when studying interventions with modest effect sizes.

	Aortic Diameter (mm)			
	Male		Female	
	Systole	Diastole	Systole	Diastole
Wild-type	1.54 ± 0.08	1.30 ± 0.06	1.35 ± 0.06	1.17 ± 0.06
FBN$^{mgR/mgR}$	2.14 ± 0.20	2.07 ± 0.20	1.68 ± 0.09	1.62 ± 0.11

Disclosures: **Z. Chen:** None. **H. Sawada:** None. **D. Rateri:** None. **A. Daugherty:** None. **M. Sheppard:** None.

309

Blockade of Transforming Growth Factor Beta Activity in Elastase-Induced Aortic Injury in Mice Induces a Human-Like Abdominal Aneurysm

Marc Clement, Fabien Lareyre, Juliette Raffort, Div of Cardiovascular Med, Univ of Cambridge, Cambridge, United Kingdom; Stefanie Pohlod, Inst for Bioengineering, EPFL, Lausanne, Switzerland; Meghana Patel, Div of Cardiovascular Med, Univ of Cambridge, Cambridge, United Kingdom; Bruno Esposito, Inst Natl de la Santé et de la Recherche Médicale, Paris Cardiovascular Res Ctr, Paris, France; Leanne Master, Alison Finigan, Div of Cardiovascular Med, Univ of Cambridge, Cambridge, United Kingdom; Pablo Villabuena, Marco Stamponi, Swiss Light Source, Paul Scherrer Inst, Villigen, Switzerland; Soraya Taleb, Inst Natl de la Santé et de la Recherche Médicale, Paris Cardiovascular Res Ctr, Paris, France; Bram Trashet, Inst for Bioengineering, EPFL, Lausanne, Switzerland; Ziad Mallat, Div of Cardiovascular Med, Univ of Cambridge, Cambridge, United Kingdom

Background: Abdominal aortic aneurysm (AAA) carries important morbidity and mortality and is resistant to medical therapy. Current experimental models do not accurately reproduce the major features of the human disease. There are 2 major categories of mouse models of AAA: those that induce medial dissection, which is not a major characteristic of human AAA, and those that induce aortic dilatation but are self-contained and do not progress to rupture.
Methods: We hypothesized that blockade of TGFβ activity, a guardian of vascular integrity and immune homeostasis, and a major causal factor in genetically triggered thoracic aortic aneurysms in humans, would impair vascular healing in models of 'non-dissecting' abdominal aortic dilatation, and would lead to continuous aneurysmal growth until rupture. We tested this hypothesis in the elastase-induced abdominal aortic dilatation model in mice. We analyzed AAA development and progression using ultrasound in vivo, advanced synchrotron-based ultrahigh resolution imaging ex-vivo, and a combination of biological, histological and flow cytometry-based cellular and molecular approaches in vitro.
Results: We show that systemic blockade of TGFβ activity using a neutralizing mouse monoclonal anti-TGFβ antibody induces a transition from a model of self-contained aortic dilatation to a model of sustained aneurysmal growth culminating in rupture. TGFβ blockade enhances leukocyte infiltration and extracellular matrix degradation, and leads to sustained aneurysmal aortic dilatation, associated with the formation of an intra-luminal thrombus infiltrated with neutrophils, as seen in the human disease. Persistent AAA growth throughout the duration of the experiment is associated with wall disruption without medial dissection, and culminates in fatal aortic wall rupture. Monocyte/macrophage depletion substantially limits AAA severity.
Conclusions: Endogenous TGFβ activity is required for the resolution of elastase-induced aortic injury. We expect that this new model will improve our understanding of the pathophysiology of AAA, and will be useful to identify new therapeutic targets.

Disclosures: **M. Clement:** None. **F. Lareyre:** None. **J. Raffort:** None. **S. Pohlod:** None. **M. Patel:** None. **B. Esposito:** None. **L. Master:** None. **A. Finigan:** None. **P. Villabuena:** None. **M. Stamponi:** None. **S. Taleb:** None. **B. Trashet:** None. **Z. Mallat:** None.

310

ROS Induced Mitochondrioal Dysfunction Causes Endothelial Dyfunction by Downregulation Of SIRT1

Cuk Seong Kim, Su-jung Choi, Harsha Nagar, Shuyu Piao, Seonhee Kim, Ikjun Lee, Sung Min Kim, Chungnam Natl Univ. Sch of Med, Dept of Physiology, Dept of Medical Science, Daejeon, Korea, Republic of

Mitochondrial dysfunction has emerged as the major contributing factor in endothelial dysfunction and vascular disease. However, the key mechanism of mitochondrial dysfunction induced endothelial dysfunction has not to be clear identified. To determine whether mitochondrial dysfunction in endothelial cells play a key role in vascular disease, the phenotype of endothelial specific CRIF1 knock out ($Crif1^{-/-}$) mouse and pathophysiological mechanism in vitro were examined. $Crif1^{-/-}$ mouse showed a lower body weight and cardiac hypertrophy. Down-regulation of CRIF1 in vascular endothelial cell caused disturbances in the mitochondrial OXPHOS (oxidative phosphorylation) complexes, mitochondrial morphology as well as function leading to an increased mitochondrial reactive oxygen species (ROS) production and mitochondrial membrane potential (MMP). In addition, down-regulation of CRIF1 also caused a decrease in Sirt1 expression along with increased eNOS acetylation leading to reduce NO

production. Similar results were obtained in *in vivo* studies using the mouse with CRIF1-deficient vascular endothelial cell. Importantly, endothelium dependent vasorelaxation (EDR) of aortic rings from CRIF1 knock out mouse was considerably less as compared to the wild type counterparts. Also, the EDR was partially recovered following the adSirt1 treated aortic rings from mouse with Crif1-deficient vascular endothelial cell. Taken together, these findings indicate that CRIF1 plays an important role in the maintenance of mitochondrial function and endothelial function via the SIRT1-eNOS pathway.

Disclosures: **C. Kim:** None. **S. Choi:** None. **H. Nagar:** None. **S. Piao:** None. **S. Kim:** None. **I. Lee:** None. **S. Kim:** None.

311

The Long Non-Coding RNA H19 Regulates Experimental Abdominal Aortic Aneurysm Development and Progression

Yuhuang Li, Klinikum rechts der Isar, Technical Univ Munich, Munich, Germany; Hong Jin, Karolinska Instt, Stockholm, Sweden; Albert Busch, Klinikum rechts der Isar, Technical Univ Munich, Munich, Germany; Ekaterina Chernogubova, Alexandra Bäcklund, Anna Olofsson, Suzanne Eken, Changyan Sun, Nancy Simon, Greg Korzunowicz, Per Eriksson, Rebecka Hultgren, Joy Roy, Karolinska Instt, Stockholm, Sweden; Joshua Spin, Philip Tsao, Stanford Univ, Stanford, CA; Lars Maegdefessel, Klinikum rechts der Isar, Technical Univ Munich, Munich, Germany

Background - Long noncoding RNAs (lncRNAs) have emerged as critical epigenetic regulators in various biological processes and diseases. Here we sought to identify and functionally characterize the lncRNA H19 as a novel regulator in abdominal aortic aneurysm development.
Methods and results - We profiled RNA transcript expression in two murine abdominal aortic aneurysm models, Angiotensin II (ANGII) infusion in ApoE-/- mice and porcine pancreatic elastase (PPE) instillation in C57BL/6 wildtype mice. The lncRNA H19 was identified as one of the most highly up-regulated transcripts in both mouse aneurysm models compared to sham-operated controls. This was confirmed by qRT-PCR and *in situ* hybridization. Experimental knock-down of H19, utilizing site-specific antisense oligonucleotides (LNA-GapmeRs) *in vivo*, significantly limited aneurysm growth in both models. Upregulated H19 correlated well with smooth muscle cell (SMC) content and its apoptosis in progressing aneurysms. Of importance, a similar pattern could be observed in human AAA tissue samples, and in a novel preclinical LDLR-/- Yucatan mini-pig aneurysm model. *In vitro* knock-down of H19 markedly decreased apoptotic rates of cultured human aortic SMCs, while overexpression of H19 had the opposite effect. Interestingly, H19-dependent cell fate decisions in SMCs appeared independent of miR-675, which is embedded in the first exon of the H19 gene. A customized transcription factor array and proteomic analysis revealed the hypoxia-inducible factor 1-alpha (HIF1A) and interleukin 1 receptor-like 2 (IL1RL2) as the main downstream effectors being regulated via H19.
Conclusion - The lncRNA H19 is a novel regulator of SMC survival and aortic inflammation in AAA development and progression. Ultimately inhibition of H19 expression might serve as a novel molecular therapeutic target for aneurysm disease.
Key words: Long noncoding RNAs (lncRNAs); abdominal aortic aneurysm; smooth muscle cells (SMCs); Inflammation

Disclosures: **Y. Li:** None. **H. Jin:** None. **A. Busch:** None. **E. Chernogubova:** None. **A. Bäcklund:** None. **A. Olofsson:** None. **S. Eken:** None. **C. Sun:** None. **N. Simon:** None. **G. Korzunowicz:** None. **P. Eriksson:** None. **R. Hultgren:** None. **J. Roy:** None. **J. Spin:** None. **P. Tsao:** None. **L. Maegdefessel:** None.

312

Finite Element Analysis-Derived Biomechanical Rupture Risk Index is Associated With Extracellular Matrix and Structure Organization in the Tunica Media of Abdominal Aortic Aneurysms

Moritz Lindquist Liljeqvist, Antti Siika, Malin Kronqvist, T. Christian Gasser, Per Eriksson, Rebecka Hultgren, Joy Roy, Karolinska Instt, Stockholm, Sweden

Objective: An abdominal aortic aneurysm (AAA) ruptures if the vessel wall stress exceeds its strength, with high mortality as a result. The effect of biomechanical load on AAA gene expression is currently not well understood. **Methods:** Aortic tissue samples from 64 patients with an AAA that had been imaged

with computed tomography angiography (CTA) before surgery were collected from the Stockholm AAA Biobank (STAAAB), separated into intima/media and adventitia wall layers and analyzed with Affymetrix HTA 2.0 microarrays. The aortas were segmented from the CTAs into three-dimensional digital models, which were then subjected to finite element analysis (FEA) without informing the software (VASCOPS A4clinics Research Edition) about age, gender, family history or blood pressure. Peak wall rupture index (PWRI), derived from the FEA, was used as a marker of biomechanical rupture risk. Differential gene expression, adjusted for age and gender, was studied with R. Enriched gene ontology processes were examined for annotated transcripts with GOrilla and REVIGO online tools. **Results:** No transcript was significantly associated with PWRI after 5% false discovery rate correction was performed, in either media nor adventitia. However, there were 1203 and 872 transcripts associated with PWRI at a nominal p-value of < 0.05 in media and adventitia, respectively. Analysis of enriched biological processes using the entire annotated transcript list ranked by fold-change revealed that extracellular matrix and structure organization in the media and nucleic acid metabolism and RNA metabolism in the adventitia, were the most enriched biological processes in aneurysms with high PWRI. **Conclusion:** These results suggest that biomechanical rupture risk associates with expression of extracellular matrix genes as well as the level of bulk gene activity.

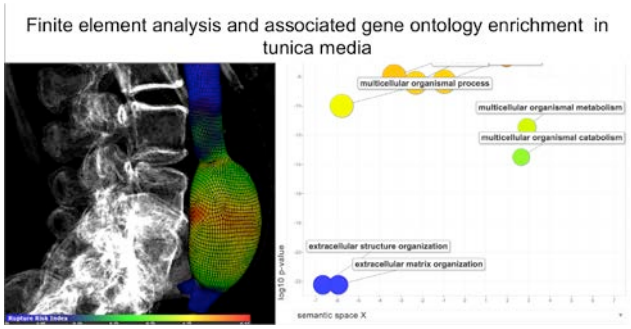

Disclosures: **M. Lindquist Liljeqvist:** None. **A. Siika:** None. **M. Kronqvist:** None. **T. Gasser:** Ownership Interest; Significant; Vascops GmbH, Graz, Austria. Consultant/Advisory Board; Significant; Vascops GmbH, Graz, Austria. **P. Eriksson:** None. **R. Hultgren:** None. **J. Roy:** None.

313 will be presented in the PVD Moderated eAbstract Poster Session. The abstract content is located on page 40.

314

A Stent to Prevent: A Translational Approach Towards Small Abdominal Aortic Aneurysm (AAA) Therapy

Isabel N Schellinger, Univ Medical Ctr Göttingen, Goettingen, Germany; Joshua M Spin, Stanford Univ Sch of Med, Stanford, CA; Gerd Hasenfuss, Univ Medical Ctr Göttingen, Goettingen, Germany; Philip S Tsao, Stanford Univ Sch of Med, Stanford, CA; Uwe Raaz, Univ Medical Ctr Göttingen, Goettingen, Germany

Background: Abdominal aortic aneurysm (AAA) is defined as a permanent dilation of the abdominal aorta that is highly lethal in case of rupture. Current therapeutic approaches are limited to open surgery or stent-based endovascular aortic repair (EVAR) to exclude large sized AAA (>5.5 cm) from the circulation. However, to date there is no effective therapy to prevent small AAA formation and progression. Nonetheless, options for small AAA disease are highly desirable as even small AAA may rupture and app. 70% of all small AAA will grow and eventually require surgical repair.
Objective: Building on our previous experimental research findings we present a novel therapeutic approach for early AAA intervention.
Methods and Results: Our recent biomechanical studies in a murine model of AAA development (elastase model) as well as in human aortae indicate that early AAA growth is critically driven by a stiffness gradient between a stiff AAA segment and the adjacent more compliant aorta. As a promising therapeutic intervention, we found that stiffening of the AAA-adjacent aorta (by external glue application) was sufficient to stop murine AAA formation. In a translational approach we now aim to develop an

intravascular stent prototype that is deployed in the neck region of a developing AAA to increase the mechanical stiffness of the AAA-adjacent aorta. We hypothesize that this intervention will decrease the aortic stiffness gradient towards the AAA segment – thereby preventing further AAA growth. Stent prototypes with varying designs will be tested in a pig model of AAA disease that closely resembles the human anatomic situation.
Conclusion: This project demonstrates a highly promising opportunity to directly translate novel pathomechanistic insights into AAA pathobiology from bench to bedside application and stop early AAA progression in humans.

Disclosures: **I.N. Schellinger:** None. **J.M. Spin:** None. **G. Hasenfuss:** None. **P.S. Tsao:** None. **U. Raaz:** None.

315

Calcium Dose Dependently Influences Endothelial Cell Angiogenesis

Jocelyne Mulangala, Emma J Akers, Peter J Psaltis, Stephen J Nicholls, **Belinda A Di Bartolo**, South Australian Health and Medical Res Inst, Adelaide, Australia

Background: Peripheral artery disease (PAD) is a progressive occlusive disease of the arteries and a vascular complication in diabetes. Vascular calcification (VC) is implicated as a potential driver of PAD, and although the exact mechanisms are unclear, the site and location of calcification within the arterial wall contributes greatly. Long considered a passive process, VC is now recognised as a tightly regulated active process balancing the promotion and inhibition of calcification in the arterial wall. There is little evidence however, to demonstrate the effect of calcification on endothelial cell angiogenesis. This study sought to investigate the effects of calcium as a known inducer of calcification on *in vitro* angiogenesis. **Methods**: Human Coronary Artery Endothelial Cells were cultured and treated with increasing calcium concentrations ($CaCl_2$ 2.45-3.3 mM) for 24h. Proliferation, migration and tubule formation assays were conducted and real-time PCR assessed angiogenic and osteogenic genes. Alkaline phosphotase (ALP) activity was measured in supernatants following treatment. **Results**: High concentrations of calcium reduced cell proliferation with a corresponding increase in ALP production suggesting release of osteogenic stimuli adversely affects cell viability. Mid-range concentrations of calcium induced a significant increase in cell migration (1.0 vs 2.4±0.3, $p<0.05$) while higher concentrations elicited no effect. Calcium treatment demonstrated a dose response where mid-range concentrations increased gene expression of hypoxia-inducible factor-1α (>500 fold), and fibroblast growth factor-2 (>150 fold). This increase corresponded with a decrease (1.0 vs 15.02±4.24; $p<0.0001$) in osteoprotegerin (OPG) at mid-range calcium with a significant increase at the highest concentration (1.0 vs 342±13.27; $p<0.01$) illustrating calcium-induced expression of OPG, a known protective gene in VC, may also regulate angiogenesis. **Conclusion**: This is the first demonstration investigating the effects of calcium on endothelial cell angiogenesis. These findings suggest that calcium can directly affect genes involved in regulating angiogenesis, and could therefore provide an opportunity to develop potential treatments.

Disclosures: **J. Mulangala:** None. **E.J. Akers:** None. **P.J. Psaltis:** None. **S.J. Nicholls:** None. **B.A. Di Bartolo:** None.

317

Satellite Cells Influence Collateral Vessel Formation via Paracrine Effects

Laura Hansen, Wenxue Liu, Giji Joseph, Daiana Weiss, W. Robert Taylor, Emory Univ, Atlanta, GA

Satellite cells are myogenic cells that play a critical role in skeletal muscle repair. They serve as stem cells for muscles, remaining dormant in healthy muscle but activating upon injury resulting in increased proliferation and differentiation into myoblasts. Another key aspect of muscle regeneration is reestablishing vascular supply, but the role of satellite cells in this process is not well established though they are known to produce a number of potential paracrine signals. Thus we hypothesized that satellite cells promote vascular growth through paracrine signaling induced by activation following muscle injury or ischemic damage from diseases such as peripheral artery disease. Using a murine model of hind limb ischemia, we showed that satellite cells increased 3.4 fold ($p<0.01$) in response to ischemia. To determine if satellite cells produce paracrine factors, we used a co-culture system for migration and proliferation. Satellite cells freshly isolated from the ischemic limb led to a 3.5 fold increase in smooth muscle migration ($p<0.0001$) and a 1.3 fold increase ($p<0.01$) in smooth muscle proliferation. Additionally,

cultured satellite cells increased endothelial cell migration 2.8 fold. These results demonstrate the satellite cells produce paracrine factors which can drive both smooth muscle and endothelial cell migration and proliferation which are required for the development of collateral vessels. To test the potential therapeutic capability of satellite cells, alginate encapsulated satellite cells were delivered in the hind limb ischemic model. Using a whole animal in vivo imager to track luciferase expression of the cells, we found the encapsulated cells were viable for up to 2 weeks. The mice that received satellite cells also had significantly increased perfusion (28%, $p<0.05$) at 2 weeks as measured by Laser Doppler imaging. In conclusion our studies have shown that satellite cells increase in response to ischemia, produce paracrine factors that increase vascular cell migration in vitro, and lead to functional increases in perfusion in vivo. We believe these results demonstrate the critical role satellite cells play in collateral vessel formation and may be a potential new therapeutic approach for treating peripheral artery disease.

Disclosures: **L. Hansen:** Research Grant; Modest; NIH F32. **W. Liu:** None. **G. Joseph:** None. **D. Weiss:** None. **W. Taylor:** Research Grant; Modest; NIH grants.

318 will be presented in the PVD Moderated eAbstract Poster Session. The abstract content is located on page 41.

319

Effects of Muscle Stretching on Flow-Mediated Dilation of Popliteal Artery in Patients With Peripheral Artery Disease

Kazuki Hotta, Florida State Univ Coll of Med, Tallahassee, FL; Wayne B Batchelor, James Graven, Vishal Dahya, Thomas E Noel, Akash Ghai, John N Katopodis, William C Dixon IV, Heart and Vascular Ctr, Tallahassee Memorial HealthCare, Tallahassee, FL; Jegghna Chheda, Lia Liberatore, Dept of Nutrition, Food and Exercise Sciences, Florida State Univ Coll of Human Sciences, Tallahassee, FL; Bradley J Behnke, Dept of Kinesiology, Kansas State Univ Coll of Human Ecology, Manhattan, KS; Judy M Muller-Delp, Florida State Univ Coll of Med, Tallahassee, FL

Patients with peripheral artery disease (PAD) frequently have walking impairment due to lower extremity claudication. Our preliminary results in a rat model of aging indicate that a program of daily calf muscle stretching improves endothelium-dependent dilation of soleus muscle arterioles and increases soleus muscle blood flow during exercise. However, the effects of muscle stretching on the function of arteries supplying the legs of PAD patients is unknown. We hypothesized that daily calf muscle stretching improves vascular endothelial function and walking distance in PAD patients. To test our hypothesis, a randomized, non-blinded, crossover study was performed. Four weeks of muscle stretching (30 min/d, 5 days/wk) and 4 weeks of sedentary lifestyle (no stretching) were performed in random order. Thirteen patients with PAD participated in this study (71 ± 2 years old; 7 males and 6 females). During the stretching intervention both ankle joints were maintained at 15o of dorsiflexion using ankle dorsiflexion splints to stretch their calf muscles at home. Flow-mediated dilation (FMD; dilation to post-occlusion reactive hyperemia) and nitroglycerin-induced dilation (dilation to sublingual 0.4 mg nitroglycerin) of the popliteal artery were measured after 4 weeks of muscle stretching and after the no stretching period using ultrasound. A six-minute walk test was also performed to obtain walking distance. After 4 weeks of muscle stretching, FMD and 6-minute walking distance significantly improved as compared to the values measured after 4 weeks of no stretching (FMD: 5.2 ± 0.6 % vs. 3.7 ± 0.4 %, P=0.003 stretching vs. no stretching, 6-minute walking distance: 355 ± 32 m vs. 311 ± 31 m, P=0.007, stretching vs. no stretching; mean ± SE). No difference in nitroglycerin-induced dilation was found between groups (10.9 ± 1.4 vs. 9.9 ± 1.1 %, P=0.54, stretching vs. no stretching). Percentage change of walking distance (%change = [(stretching - no stretching) / no stretching] x 100) significantly correlated with the %change of FMD (R^2=0.65, P=0.03). These results indicate that static calf muscle stretching enhances vascular endothelial function of the popliteal artery, contributing to improvement of walking tolerance in PAD patients.

Disclosures: **K. Hotta:** None. **W.B. Batchelor:** None. **J. Graven:** None. **V. Dahya:** None. **T.E. Noel:** None. **A. Ghai:** None. **J.N. Katopodis:** None. **W.C. Dixon:** None. **J. Chheda:** None. **L. Liberatore:** None. **B.J. Behnke:** None. **J.M. Muller-Delp:** None.

320

Delivery of Hepatocyte Growth Factor mRNA From Nanofibrillar Scaffolds for Treatment of Peripheral Arterial Disease

Ngan F Huang, Luqia Hou, Stanford Univ, Stanford, CA; Cynthia Alcazar, Zachary Strassberg, Veterans Affairs Palo Alto Health Care System, Palo Alto, CA; Michael Hopkins, Stanford Univ, Stanford, CA; Tatiana Zaitseva, Fibralign Corp, Union City, CA; Eduard Yakubov, PhaRNA, LLC, Houston, TX; Michael V Paukshto, Fibralign Corp, Union City, CA

Biological approaches to augment angiogenesis are promising for treatment of peripheral arterial disease (PAD). We propose the use of scaffold-based modified mRNA (mmRNA) delivery as a favorable approach for transient, localized gene delivery. We hypothesized that hepatocyte growth factor (HGF) mmRNA-seeded nanofibrillar scaffolds will enable localized and temporally controlled delivery of mmRNA, leading to augmentation of angiogenesis in a murine model of PAD. To establish the efficacy of mmRNA therapy, mmRNA encoding green fluorescence protein (GFP) was used as a fluorescent reporter for quantification of transfection efficiency. Aligned nanofibrillar collagen scaffolds were loaded with mmRNA and lipofectamine transfection agent. The temporal kinetics of mmRNA release into media was measured by ribogreen assay. To determine the transfection efficiency, human fibroblasts were cultured on the aligned nanofibrillar scaffolds, or on tissue culture plastic, and the efficiency of transfection was measured for up to 7 days and assayed for GFP expression. Based on ribogreen assay, the cumulative release of GFP mmRNA over the course of 14 days was 235 ng/cm scaffold. *In vitro* transfection efficiency on aligned scaffolds (75%) was markedly higher than on tissue culture plastic (45%) after 24h. The persistence of cellular transfection as quantified by western blotting showed GFP expression >5 days post-transfection. Next, to demonstrate therapeutic efficacy for treatment of PAD, scaffolds releasing HGF or GFP mmRNA were transplanted to the site of the murine ischemic hindlimb. At the end of the 14 day experiment, laser Doppler spectroscopy showed that HGF mmRNA scaffold group had a higher mean perfusion ratio (0.32 ±0.10) than the GFP mmRNA scaffold group (0.23±0.14), suggesting that HGF-scaffolds improved blood perfusion. In summary, these data suggest that HGF mmRNA-releasing scaffolds marked improved blood perfusion in a murine model of PAD.

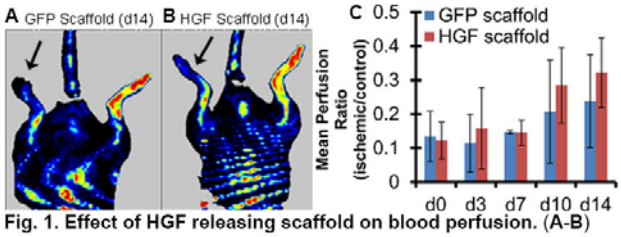

Fig. 1. Effect of HGF releasing scaffold on blood perfusion. (**A-B**) Laser Doppler images of blood perfusion on day 14. (**C**) Mean perfusion ratio (ischemic/control) (n=3). Arrow denotes ischemic limb.

Disclosures: **N.F. Huang:** Research Grant; Modest; US Army Medical Research and Materiel Command (W81XWH-16-C-0009). **L. Hou:** None. **C. Alcazar:** None. **Z. Strassberg:** None. **M. Hopkins:** None. **T. Zaitseva:** None. **E. Yakubov:** None. **M.V. Paukshto:** Research Grant; Modest; US Army Medical Research and Materiel Command (W81XWH-16-C-0009).

321

Central Blood Pressure Regulation in Relation to Hypertension and Adiposity in Youth

Neil E Hultgren, Nicholas G Evanoff, Univ of Minnesota-Sch of Kinesiology, Twin Cities, MN; Alexander M Kaizer, Univ of Minnesota-Sch of Public Health, Twin Cities, MN; Kyle D Rudser, Univ of Minnesota-Sch of Public Helath, Twin Cities, MN; Donald R Dengel, Univ of Minnesota-Sch of Kinesiology, Twin Cities, MN; Aaron S Kelly, Justin R Ryder, Univ of Minnesota-Medical Sch, Twin Cities, MN

Introduction
The relationship between different central BP measurements with hypertension status in youth is not well documented. We hypothesized that measures of central BP would be positively associated with hypertension status in youth independent of adiposity.
Methods
We recruited 149 males and 160 females for this cross-sectional analysis (mean±SD: age = 12.8±2.7;

BMI percentile (%) = 78.5±27.8). Body fat % was measured by dual energy X-ray absorptiometry (DXA) and brachial BP was measured using an automated cuff to calculate systolic BP (SBP) and diastolic BP (DBP). Determined by systolic percentile, there were 238 normotensive (<90th), 29 pre-hypertensive (≥90th - <95th), and 42 hypertensive (≥95th) individuals enrolled. Central BP was determined using the SphygmoCor MM3 system to calculate carotid-aorta SBP (caSBP) carotid-aorta DBP (caDBP) radial-aorta SBP (raSBP) and radial-aorta DBP (raDBP).
Central BP measures were compared across hypertension status groups using ANCOVA, with post-hoc Tukey HSD, adjusted for age, sex, and race. Pearson correlations (unadjusted) and multiple linear regression models, examining the relationship between central BP measures with brachial BP adjusted for age, sex, race, and height, were conducted with further adjustment for body fat % (shown as β±SE).
Results
raSBP, caSBP, raDBP, and caDBP were significantly different between the normotensive and hypertensive groups (all p<0.001). No statistically significant differences were found between normotensive and pre-hypertensive or between pre-hypertensive and hypertensive groups. raSBP and caSBP were correlated to SBP (r=0.59, r=0.62, respectively, p<0.001). raDBP and caDBP were correlated to DBP (r=0.58, r=0.6, respectively, p<0.001). In regression analysis, SBP was positively associated with both raSBP and caSBP (β=0.3±0.06, p<0.001) and (β=0.28±0.08, p<0.001), respectively. DBP was positively associated with raDBP and caDBP (β=0.31±0.06, p<0.001) and (β=0.31 ±0.06, p<0.001), respectively. All associations remained significant after adjustment for body fat %.
Conclusion
These data suggest that central BP, regardless of measurement site, is highly associated with brachial BP and hypertension status in youth independent of adiposity.

Disclosures: **N.E. Hultgren:** None. **N.G. Evanoff:** None. **A.M. Kaizer:** None. **K.D. Rudser:** None. **D.R. Dengel:** None. **A.S. Kelly:** None. **J.R. Ryder:** None.

322

Cost Effectiveness Analysis of Peripheral Arterial Disease Screening With the Ankle-Brachial Index Test

Nathan K Itoga, Hataka Minami, Meena Chelvakumar, Keon Pearson, Matthew W Mell, Eran Bendavid, Douglas K Owens, Stanford Univ, Stanford, CA

Introduction: Screening for asymptomatic PAD (aPAD) with the ankle-brachial index (ABI) test may reduce mortality and disease progression by identifying individuals who may benefit from early initiation of cardiovascular (CV) risk reduction therapies.
Methods: Using a Markov model, we evaluated the cost-effectiveness of initiating medical therapy (e.g. statin & ACE-inhibitor) after a positive ABI screen in adults 65-years old. We modeled progression to symptomatic PAD (sPAD) and CV mortality with and without screening evaluating quality adjust life years (QALY). Cost of the ABI test, physician visit, new medication, and surgery for sPAD were calculated. Our baseline model estimated 96% of patients already eligible for medical therapy given the similar risk factor profiles of aPAD and CV disease. Repeated screening was considered given the imperfect screening test, development of disease with age, and opportunity to re-initiate therapy given limited medication compliance. Variables with uncertainty underwent a tornado analysis to determine variables with large effects.
Results: Our model found an incremental cost of $367 and incremental QALY of 0.0022 with one-time ABI screening resulting in an incremental cost-effectiveness ratio (ICER) of $169,025/QALY over a 35-year period. Removing the benefits of medication on CV mortality increases the ICER by 51%, and removing the benefits of medication on PAD progression increases the ICER by 16%. A tornado diagram shows variables affecting the ICER (Figure). Screening high-risk populations, such as tobacco users where the prevalence of PAD may be 2.5x higher than the general population of 9%, decreases the ICER to $63,500/QALY.
Conclusions: Our cost-effective analysis predicts that one-time ABI screening does not meet generally accepted thresholds for cost effectiveness. Disease prevalence and medication adherence had the largest effects on the ICER and are important to consider in implementing ABI screening.

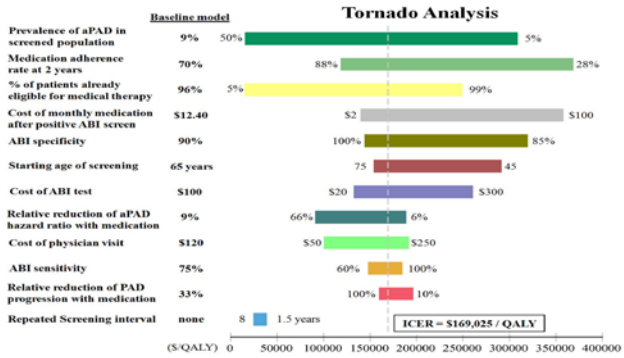

Disclosures: **N.K. Itoga:** None. **H. Minami:** None. **M. Chelvakumar:** None. **K. Pearson:** None. **M.W. Mell:** None. **E. Bendavid:** None. **D.K. Owens:** None.

323

Utilization and Outcomes of Carotid Artery Stenting vs. Carotid Endarterectomy

Parijat S Joy, Univ of Iowa, Iowa City, IA; Gagan Kumar, Northeast Georgia Health System, Gainesville, GA

Introduction: Carotid artery stenting is an alternative to carotid endarterectomy in average surgical-risk symptomatic patients and asymptomatic patients with ≥60% stenosis. We wanted to compare utilization and peri-procedural mortality between these procedures. **Methods:** The 2000-2013 National Inpatient Sample (NIS) was analyzed for admissions when procedures for carotid artery stenting (CAS) or carotid endarterectomy (CEA) were performed. Admissions when both procedures were performed were excluded. Trend of procedures and death during index admission was compared depending on prior cerebrovascular symptoms. **Results:** During the study period, 1991941 patients underwent CEA of which 9.12% were symptomatic and 343,741 patients underwent CAS of which 10.8% were symptomatic. Mean age for CAS vs CEA group was lower among both symptomatic (68.6 vs 69.6 yrs, p<0.001) and asymptomatic patients (70.7 vs 71.2 yrs, p<0.001). More males than females underwent CAS (57% vs 43%) and CEA (58% vs 42%). Both CAS and CEA during same admission was carried out in 20,875 (0.89%) patients. There was a rising trend of both CEA and CAS procedures in symptomatic and asymptomatic patients (ptrend < 0.001)(Figure A1 & B1). Trend of mortality has not changed significantly in all groups except for CEA in asymptomatic patients wherein mortality rate has decreased (ptrend <0.001)(Figure A2 & B2). On multivariable logistic regression analysis, associated conditions significant for mortality in symptomatic patients were atrial fibrillation (OR 2.05, p<0.001), myocardial infarction (OR 1.61, p=0.001) heart failure (OR 1.39, p=0.021) and malnutrition (OR 3.58, p<0.001). Adjusted likelihood of mortality after CAS vs CEA was higher in symptomatic (OR 3.78, p<0.001, C statistic 0.74) and asymptomatic patients (OR 2.00, p<0.001, C statistic 0.80). **Conclusion:** Utilization of CAS and CEA has increased over time. Mortality after CAS vs. CEA during index admission, remains high.

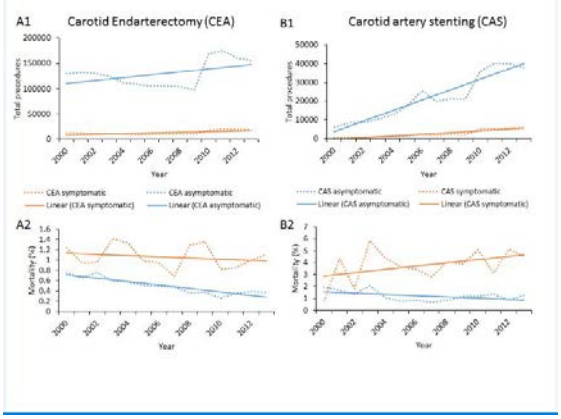

Disclosures: **P.S. Joy:** None. **G. Kumar:** None.

324

Pathological Quantitative Assessment of Plaque Instability in Patients Undergoing Carotid Endarterectomy

Takao Konishi, Hokkaido Cardiovascular Hosp, Sapporo, Japan

Introduction: Instability of carotid atherosclerotic plaques leads to cerebral thromboemboli and ischemic symptoms. However, there has been no specific pathological quantification for the instability of carotid atherosclerotic plaque. The purpose of this study was to quantify atherosclerotic plaque instability in patients undergoing carotid endarterectomy (CEA).
Methods: Carotid plaques were collected after CEA from 67 symptomatic and 15 asymptomatic patients between May 2015 and August 2016. Samples were stained with hematoxylin/eosin and Elastica-Masson (E-Masson). Immunohistochemistry was performed by using an endothelial specific antibody to CD31, CD 34 and PDGFRβ. Plaques were assessed for histopathological characteristics.
Results: Multivariable logistic regression analysis demonstrated that plaque instability was independently associated with the presence of plaque rupture (odds ratio [OR], 9.75, 95% confidence interval [CI]: 1.62 to 58.6, p = 0.013), the minimal fibrous cap thickness (FCT) (OR per 10 μm 0.70, 95% CI: 0.51 to 0.96, p = 0.025), the presence of microcalcification in the fibrous cap (OR 7.82, 95% CI: 1.35 to 45.4, p = 0.022) and the intraplaque microvessels (OR 1.91, 95% CI: 1.02 to 3.57, p = 0.043). If these four independent parameters were combined to a score using the equation derived from the multivariable logistic regression model (Logit(Score) = 0.179 + 2.277 * (insert 1 if plaque rupture present; else 0) - 0.355 * (insert minimal FCT in multiples of 10 μm) + 2.057 * (insert 1 if microcalcification in the fibrous cap present; else 0) + 0.646 * (insert intraplaque microvessels /mm^2), the diagnostic efficiency could be improved to an AUC 0.92 (95% CI: 0.85-0.99, optimal cut-off value 0.814, sensitivity 89.6%, specificity 86.7%, PPV 96.8%, NPV 65.0%, diagnostic accuracy 89.0%).
Conclusions: This study suggested the diagnostic scoring was useful for the quantification of carotid plaque instability in patients undergoing CEA.

Disclosures: **T. Konishi:** None.

325

Usefulness of Peripheral Vascular Disease Assessment on Readmission in a Heart Failure Program Cohort

Hong Seok Lee, Metropolitan Hosp, New York Medical Coll, Univ of California Riverside, New York, NY; Gerald Pekler, Metropolitan Hosp , New York Medical Coll, Univ of California Riverside, New York, NY; Fernand Visco, Metropolitan Hosp, New York Medical Coll, Univ of California Riverside, New York, NY; Amrut Savadkar, Metropolitan Hosp , New York Medical Coll, Univ of California Riverside, New York, NY

Background: Peripheral arterial disease (PAD) was reported to have a relationship with functional capacity in heart failure patients. Heart failure patients presenting with a good functional capacity have been found to have better metabolic equivalents (METs). Recognizing and managing patients' functional capacity surrogates like ankle-brachial index (ABI) and METs will be beneficial to improve the rate of readmission, however, little is known about the relationship with readmission rate in heart failure patients. We assessed readmission rate within 30 days after discharge using functional capacity assessment.
Methods: 860 patients who were followed in the cardiology clinic from 2005 to 2015 were included. We analyzed the 240 patients who were admitted with a diagnosis of acute heart failure. Patients who were unable to cardiac rehabilitation or who had severe lung disease were excluded. Heart failure is classified as a reduced ejection fraction (HFrEF, EF <40) and preserved ejection fraction (HFpEF, EF>=50). MET (Metabolic equivalents) level was used for functional capacity. If ABI was less than 0.9 or over 1.4, patients were regarded to have peripheral arterial disease.We found no significant difference between our HFpEF and HFrEF patients (Mean METS 7.5±0.6 vs 7.4±0.7). ABI did not show any significant difference (1.1±0.2 vs 1.0±0.3). In multiple logistic regression analyses, HFpEF patients with more than 4 MET level were likely to have fewer readmissions rate compared to HFpEF patients with less than 4 METS level [odds ratio (OR): 0.54, confidence interval (CI): 0.35-0.81]. HFpEF patients with ABI between 0.9 and 1.4 had less readmission rate compared to HFpEF with less than 0.9 or more than 1.4 ABI [OR: 0.62, CI: 0.41-0.77] after related risk factors adjustment. **Conclusion:** In conclusion**,** good functional status with better METs and ABI in HFpEF patients was significantly associated with less readmission rate. ABI might be a surrogate factor for assessing functional capacity in HFpEF patients. This result implies that heart failure patients' functional capacity might need to be assessed to decrease readmission rate.

Disclosures: **H. Lee:** None. **G. Pekler:** None. **F. Visco:** None. **A. Savadkar:** None.

327

Blood Vessels Need Ras Signaling to Maintain the Structure Integrity

Wenquan Hu, Ujala Rana, Zhong Liu, Baofeng Zhao, Suresh Kumar, Paula North, Qing (Robert) Miao, Medical Coll of Wisconsin, Milwaukee, WI

The localization of prenylated Ras at the plasma membrane promotes activation of Ras by receptor tyrosine kinases, such as VEGF and FGF receptors. Although Ras has been implicated in angiogenesis, the exact regulatory mechanisms controlling Ras translocation and activation are currently unclear because little is known regarding molecules that control Ras translocation. Nogo-B receptor (NgBR) was identified as a receptor specific for Nogo-B, a cell surface ligand involved in blood vessel remodeling. Our recent study demonstrated that NgBR has a conserved hydrophobic pocket that promotes the membrane accumulation of Ras by directly binding prenylated Ras at the plasma membrane. As we expected, NgBR knockdown in endothelial cells diminishes the membrane localization of Ras and consequently abolishes VEGF/FGF-stimulated activation of Ras and Ras-mediated signalings such as phosphorylation of Akt and ERK. Therefore, NgBR knockout mouse is a unique animal model for examining the effects of Ras plasma membrane localization and Ras signaling on the morphogenesis of endothelial cells. Genetic deletion of NgBR in endothelial cells resulted in embryonic lethality and dilated cerebral blood vessels with fewer pericytes, which resembles the vascular lesion happened in cerebral cavernous malformation (CCM). CCM is characterized by an abnormal cluster of enlarged blood vessels in the brain and spinal cord and caused by dysfunction of three CCM genes (CCM1/2/3), which are required for maintaining endothelial cell (EC) junctions and pericyte recruitment. Our studies showed that NgBR transcript levels decrease in human CCM lesion, and NgBR endothelial specific knockout in mice results in decreased transcription of CCM1/2 in the yolk sac. Additional support for NgBR-CCM1/2 connections comes from studies using cultured human brain microvascular ECs, where loss of NgBR expression also decreases CCM1/2 transcription via NgBR-mediated Ras pathway, which is required for the expression of key transcription factors that are involved in regulating transcription of CCM1/2 genes. Our findings suggest that NgBR-Ras signaling pathway regulates CCM1/2 expression, and that disrupting this signaling pathway results in cerebrovascular malformation.

Disclosures: **W. Hu:** None. **U. Rana:** None. **Z. Liu:** None. **B. Zhao:** None. **S. Kumar:** None. **P. North:** None. **Q. Miao:** None.

This research has received full or partial funding support from the American Heart Association.

328

Coagulation Proteases are Potential Regulators in the Development of Exercise-Related Endofibrosis

Jelle J Posthuma, Jens J Posma, Cardiovascular Res Inst Maastricht, Maastricht Univ Medical Ctr, Maastricht, Netherlands; Goof Schep, Dept of Sports Med, Maxima Medical Ctr, Veldhoven, Netherlands; Mart Bender, Dept of Surgery, Maxima Medical Ctr, Veldhoven, Netherlands; Rene van Oerle, Hugo ten Cate, Henri M Spronk, Cardiovascular Res Inst Maastricht, Maastricht Univ Medical Ctr, Maastricht, Netherlands

Background: High performance athletes can develop symptomatic arterial flow restriction during exercise, caused by endofibrosis. The disease is an poorly understood condition, characterized by fibrosis of the external iliac artery. Pathophysiological processes involved in the development of endofibrosis are unknown. However, evidence shows that coagulation enzymes such as thrombin and factor Xa (FXa) can influence pro-fibrotic processes, mainly mediated through activation of protease activated receptors (PAR). **Aim:** We investigated the immunohistochemical characteristics of endofibrotic lesions to determine the potential role of coagulation proteases and their receptors in development of endofibrosis. **Methods:** 19 arterial endofibrotic specimens were collected during endarterectomy. As controls 20 arterial segments of the external iliac artery were collected post mortem from individuals who donated their body to medical science, with no medical history of cardiovascular disease. Acquired arteries were paraffinized and cut in tissue sections for immunohistochemical staining. Data were analyzed using a Mann-Whitney U test. A 2-tailed $p<0.05$ was considered as statistically significant.

Results: Endofibrotic segments contained a neo-intima, resulting in an intraluminal stenosis (42±14%). Compared to the intima of controls, endofibrotic lesions were highly positive for collagen (47±16% vs 15±5%, p=0.0001) and elastin (38±9% vs 16±4%, p=0.0003). These findings were accompanied by significantly increased alpha smooth muscle actin expression (51±10% vs 36±11%, p=0.01), which morphologically appeared to be myofibroblasts in endofibrotic lesions; which were hardly present in controls. In addition, PAR1 (49±17% vs 22±10%, p=0.0003) and PAR4 (39±8% vs 10±4%, p<0.0001) were upregulated and proenzymes of their activators, prothrombin and factor X were abundantly present in endofibrosis. **Conclusion:** This is the first study to show that myofibroblasts, and the subsequent collagen and elastin production, might be key factors in the development of endofibrosis. The special association suggests that these processes may be regulated through activation of PARs by coagulation proteases, which needs to be established in further studies.

Disclosures: **J.J. Posthuma:** None. **J.J.N. Posma:** None. **G. Schep:** None. **M. Bender:** None. **R. van Oerle:** None. **H. ten Cate:** None. **H.M.H. Spronk:** None.

329

ST266 Attenuates Neointima Formation After Arterial Balloon Angioplasty in Rats

Sina Rahimpour, Xuening Wang, Xiaoyan Liu, Selen C Muratoglu, Univ of Marylnad, Baltimore, MD; Richard Banas, Noveome Biotherapeutics, Inc., Pittsburgh, PA; Si Mai Pham, Univ of Marylnad, Baltimore, MD

OBJECTIVE-Post-angioplasty restenosis due to neointima formation has been attributed to the inflammatory response after acute endoluminal injury. ST266 (Noveome Biotherapeutics, Inc.) a novel secretome derived from proprietary GMP-cultured human Amnion-Derived Multipotent Progenitor (AMP) cells, has been shown to be anti-inflammatory and to promote wound healing. This study examined the therapeutic potential of ST266 in a rat arterial balloon angioplasty model. METHODS-Animals were randomly divided in the following groups (N=7): no-treatment (noTx), systemic ST266, systemic AMPs and local AMP implants. Neointima hyperplasia was induced in the iliac artery of Sprague-Dawley male rats using a 2F Fogarty embolectomy catheter. After surgery, animals in ST266 groups received 0.1, 0.5 or 1ml IV ST266 q.d. In the systemic AMP groups, single-dose (SD) of 0.5 million (M) or 1 M AMPs was injected via Inferior Vena Cava after the angioplasty. In AMP implant experiment 1 M, 5 M or 20 M AMPs were implanted in 300 µL Matrigel (MTG) around the iliac artery after balloon angioplasty. 28 days after the surgery, the iliac arteries were removed for histologic analysis. Re-endothelialization index was measured 10 days after balloon angioplasty. RESULTS-1ml ST266 decreased Neointima/Neointima+Media ratio (N/NM) compared to noTx group (0.34±0.01 vs 0.54±0.04 resp.; *p*=0.004). ST266 also decreased Luminal Stenosis (LS) compared to noTx group (18.18±1.86 vs 39.23±5.75%; *p*=0.008). SD 1 M AMPs decreased LS compared to noTx group (39.23±5.75 vs 19.50±5.35%; *p*=0.033). Significant differences in N/NM were found between 20 M implanted AMPs and noTx group (0.35±0.02 vs 0.54±0.04 resp.; *p*=0.003) and the MTG-only group (0.53±0.05, *p*=0.007). 20 M implanted AMPs decreased the LS (16.78±2.47%) compared to both noTx (39.23±5.75%, *p*=0.001) and MTG-only groups (37.51±8.55%, *p*=0.016). 1ml ST266 significantly increased the re-endothelialization index 10 days after balloon angioplasty compared to noTx group (0.40±0.04 vs 0.14±0.037% resp., *p*=0.002). CONCLUSION-ST266 reduces neointima formation and luminal stenosis and increases the re-endothelialization index after balloon angioplasty. Further research to elucidate the underlying mechanisms is ongoing.

Disclosures: **S. Rahimpour:** None. **X. Wang:** None. **X. Liu:** None. **S.C. Muratoglu:** None. **R. Banas:** None. **S.M. Pham:** None.

330

Autophagy in Vascular Calcification

Cynthia St. Hilaire, Univ of Pittsburgh, Pittsburgh, PA

Vascular calcification accompanies a variety of common cardiovascular-related diseases and correlates with premature death. Vascular calcification is a highly-regulated process but the precise mechanisms inducing this pathology are not fully understood, and currently no treatment exists that halts or reverses vascular calcification. We previously discovered the rare monogenetic disease Arterial Calcification due to Deficiency of CD73 (ACDC) which presents with vessel tortuosity and extensive calcifications in the

medial layer of lower-extremity arteries. To study the mechanisms underlying this disease we previously created ACDC and Control patient iPSCs, and using a teratoma assay discovered that ACDC iPSC teratomas exhibit extensive calcifications, while Control iPSC teratomas do not. Drug screening identified that rapamycin inhibited calcification in this in vivo model. Using our in vitro calcification model with ACDC fibroblasts, we again found that rapamycin inhibited calcification, as well as expression and activity of the key enzyme involved in ectopic calcification, tissue non-specific alkaline phosphatase (TNAP). To corroborate these findings in vascular cells we used coronary artery smooth muscle cells (CASMCs) in our in vitro calcification assay. We found CASMCs calcify in vitro, and that both rapamycin treatment, and importantly, specific activation of autophagy, inhibited calcification in CASMCs. This suggests autophagy as a therapeutic target for the treatment of vascular calcification. Future work will identify how autophagy prevents calcification, and whether rapamycin, which induces autophagy, can be used as a therapy for medial calcification.

Disclosures: **C. St. Hilaire:** None.

331

Are Two Internal Thoracic Grafts Better Than One in Patients With Peripheral Vascular Disease?: Analysis of 858 Cases Between 1996- 2011

Nadav Teich, Refael Mohr, Demitry Pevni, Yael Assaig, Amir Kramer, Nahum Nesher, Yosef Paz, Yanai Ben-Gal, Tel Aviv Sourasky Medical Ctr, Tel-Aviv, Israel

Objectives: Bilateral internal thoracic artery(ITA) grafting is associated with improved survival. However, potential survival benefit of using two ITA`s in patients with peripheral vascular disease(PVD) is questionable due to their short life expectancy and the increased risk of sternal wound infection(SWI) compare to operations incorporating single ITA (SITA).
.The purpose of this study is to compare early and long-term outcome of bilateral ITA grafting(BITA) to that of SITA and vein grafts in PVD patients with multi-vessels coronary disease. **Methods:** Five hundred and thirty three PVD patients who underwent BITA between 1996 and 2011 were compared with 319 who underwent SITA .
Results : SITA patients were more often female, more likely to have Diabetes, chronic obstructive lung disease, unstable angina, previous CABG, renal insufficiency, Cerebro- vascular disease and emergency operation .On the other hand congestive heart failure and triple vessel coronary disease were more prevalent among BITA patients. Operative mortality(3.5% vs. 4.1%, in the SITA and BITA respectively) and occurrences of SWI (6.6% vs 3.9%) and strokes(4.1% vs 6.8%) were not significantly different between groups . BITA patients did not have better Kaplan- Meier 10 year survival (52.1% vs.47.1%, p=0.145) and after propensity score matching(243 well matched pairs) BITA was not associated with better adjusted survival (HR 1.108[95%CI 0.810-1.516] p=0.521)(cox model)
Conclusion: This study does not support routine use of BITA in PVD patients .Earlier mortality from non-cardiac causes, reduces contribution of BITA and increases the influence of PVD and other co-morbidities on survival. Selective use of BITA in lower risk patients might un-mask the benefits of BITA

Disclosures: **N. Teich:** None. **R. Mohr:** None. **D. Pevni:** None. **Y. Assaig:** None. **A. Kramer:** None. **N. Nesher:** None. **Y. Paz:** None. **Y. Ben-Gal:** None.

332

Inhibition of the Enhancer of Zeste Homolog Family Mitigates Intimal Hyperplasia in Rat Carotid Arteries

Mengxue Zhang, Bowen Wang, Go Urabe, Xudong Shi, Lian-Wang Guo, Univ of Wisconsin-Madison, Madison, WI

Rationale: The enhancer of zeste homologs 1 and 2 (EZH1 and EZH2) are histone-lysine N-methyltransferases that modify histones by methylation which leads to transcriptional repression. It has recently been shown that EZH1 and EZH2 play an important role in various cancers. Whether they play a role in recurrent vascular diseases is not known. **Objective:** We assessed whether EZH1 and EZH2 are important contributors to the development of intimal hyperplasia (IH) and restenosis. **Methods and Results**: Following rat carotid balloon angioplasty, EZH2 showed highest expression at day 3 post procedure and then decreased at day 7 in injured arteries, as determined by Western blotting. Change of EZH1 is less prominent. Dual inhibition of EZH1 and EZH2 through peri-adventitial administration of a

selective inhibitor, UNC-1999, effectively inhibited intimal hyperplasia, with ~40% reduction in the ratio of intima to media (I/M). Moreover, in cultured primary rat smooth muscle cells (SMCs) as well as MOVAS cells, pretreatment with 5μM UNC-1999 resulted in a 60% decrease in cell proliferation and ~80% reduction of migration that were stimulated by PDGF-BB. Simultaneous knockdown of EZH1 and EZH2, as well as knockdown of their shared scaffold protein(EED), led to effective inhibition of proliferation and migration of SMCs. However, knockdown of EZH2 alone did not recapitulate the effects of dual inhibition of EZH1 and EZH2. **Conclusions:** This study demonstrates that dual inhibition of EZH1 and EZH2, both histone modifiers, mitigates intimal hyperplasia in vivo and attenuates PDGF-BB stimulated SMC proliferation and migration in vitro.

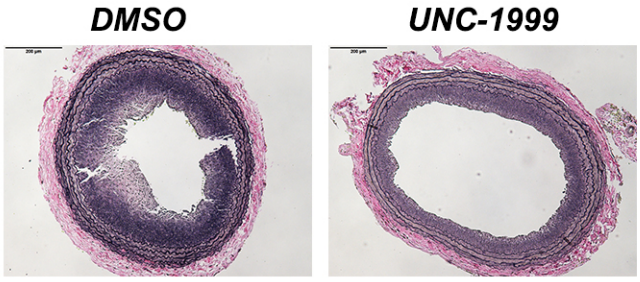

Disclosures: **M. Zhang:** None. **B. Wang:** None. **G. Urabe:** None. **X. Shi:** None. **L. Guo:** None.

333

Hhcy Promotes Myocardial Infarction Induced Myocardiocyte Death via Mitochondria Mediated Inflammasome Activation

Jun Zhou, Xiongwen Chen, Mingxin Tang, Xiaojie Ai, Hong Wang, Xiaofeng Yang, Temple Univ, Philadelphia, PA

Introduction: Elevated level of serum homocysteine (Hcy) has been identified as a risk factor for accelerating progression of cardiovascular disease. Nucleotide-binding oligomerization domain-like receptor pyrin domain-containing protein 3 (NLRP3) inflammasome activation by damaged mitochondria results in caspase-1 dependent inflammatory form of cell death. **Methods and Results:** AMI procedure was performed on hCBS/m*cbs* knockout mice at the age of 10weeks. Caspase-1 activity and myocardiocyte apoptosis were observed at the early stage of post-MI in severe HHcy mice (Hcy,120-220μM). Severe HHcy remarkably aggravated infarction size, cardiomyocyte area, and interstitial fibrosis 6 weeks after MI from 22.7 ± 4.3%, 340 ± 54μm^2, 13.9 ± 1.9% in control mice (Hcy, 7-10μM) to 33.6 ± 6.5%, 485 ± 65μm^2, 26 ± 4.5%, respectively, (*P*=0.035, *P*= 0.041, *P*=0.002). In the meantime, HHcy significantly increased LV cavity dilatation and dysfunction as compared with control mice by echocardiography (5.9 ± 0.2 vs. 4.2 ± 0.4mm, *P*=0.039; LV ejection fraction, 22.6 ± 3.9% vs. 36.8 ± 4.0%, *P*=0.011). Cultured neonatal mouse ventricular myocyte (NMVM) treated with the combination of DL-Hcy (500μM, 48h) and hypoxia (0.5% O2) showed that increased NLRP3 and caspase1 expression and activity, mitochondrial reactive oxygen species (mtROS) and mtDNA production, dissipation of mitochondrial membrane potential, and mitochondrial permeabilization. Moreover, synergetic effect of Hcy and hypoxia led to pronounced accumulation of damaged mitochondrial through suppressing mitophagy of damaged mitochondria. Caspase-1 activity and myocardiocyte death were lessened as NMVMs were administrated with mitochondria-targeted antioxidant Mito-temple and SOD2, whereas caspase-1 inhibition was not able to fully rescue damaged mitochondria. **Conclusion:** Acute myocardial infarction (AMI) initiates an intense inflammatory response in myocardium that promotes myocardiocyte death, ventricular remodeling, and cardiac dysfunction. Hcy accelerates cardiomyocyte death post-MI in part through mitochondrial-mediated NLRP3 inflammasome activation and inflammation, which contributes to adverse cardiac remodeling, ventricular dysfunction, and heart failure.

Disclosures: **J. Zhou:** None. **X. Chen:** None. **M. Tang:** None. **X. Ai:** None. **H. Wang:** None. **X. Yang:** None.

334

Pulmonary Embolism Response Team: Implementation and Outcomes at Northshore University Healthsystems

Omer Iftikhar, Keith Smart, Alya Ahsan, Alfonso Tafur, Northshore Univ HealthSystems, Evanston, IL

Introduction: Pulmonary Embolism Response Team (PERT) protocols are used to expedite risk stratification and management of complex acute pulmonary embolisms (PE). The process varies by institution.
Objective: To quantify mortality outcomes after implementing PERT at our practice (Figure 1).
Methods: 58 patients in our PERT registry were analyzed for parameters seen on table 1. Quantitative data is presented as median and qualitative data as percentages.
Results: Median age was 70.5, with female predominance 65.5% (38 out of 58), PE severity index (PESI) of 101.6, and cancer in 33% (19 out of 58) [Table 1]. 10%(6 out of 58) received thrombolysis and 14%(8 out of 58) received IVC filter. 5 deaths occurred of which 60% (3 patients) were due to cancer progression.
Conclusion: Our PERT algorithm is anchored in right ventricle to left ventricle (RV/LV) ratio on CT reading and does successfully select high risk PE patients. Mortality is similar to that expected by PESI stratification. Prospective comparative evaluation of PERT is needed to see if it affects early mortality.

VARIABLE	N (MEDIAN)	%(IQR)
DEMOGRAPHICS		
AGE	(70.5)	(16)
FEMALE	38	65.5%
COPD	4	6.8%
ACTIVE MALIGNANCY	19	32.7%
CONCOMITANT DVT	37	66.6%
Unilateral	11	19.2%
Bilateral	27	47.3%
PESI		
I	11	18.9%
II	9	15%
III	15	25.8%
IV	11	18.9%
V	12	20.6%
Troponin Elevation	22	40%
Pro-BNP / BNP Elevation	28	68.2%
RV/LV ratio >1	23	48.9%
RV dysfunction on ECHO		
Elevated RVSP (>30)	17	29.3%
Dilated RV	12	20.6%
MANAGEMENT		
Thrombolysis	6	10.3%
Anticoagulation	50	86.2%
DOAC as initial Treatment	3	5.1%
IVC filter	8	14%
OUTCOMES		
4 month Mortality	5	10.6%
Major bleeding	4	8.3%
VTE recurrence	3	5.1%

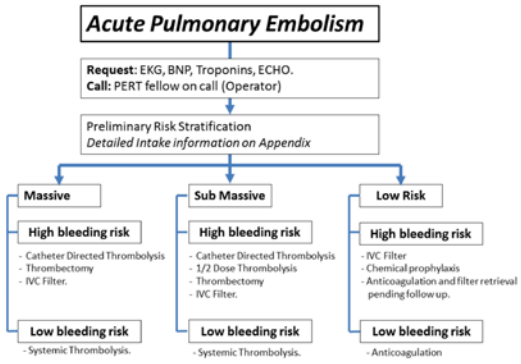

Disclosures: **O. Iftikhar:** None. **K. Smart:** None. **A. Ahsan:** None. **A. Tafur:** None.

336

Prevalence and Risk Factors for Idiopathic Venous Thromboembolism

Patricia Yau, Thomas Maldonado, Juanita Erb, Neel Ranganath, Caroline Sindet-Pederson, Deirdre O'Reilly, Caron Rockman, Jeffrey S. Berger, New York Univ Langone Medical Ctr, New York, NY

Introduction: Venous thromboembolism (VTE) is a major cause of morbidity and mortality in the United States. Despite medical advances in diagnostics and thromboprophylaxis, the incidence of VTE has not substantially decreased over time. Furthermore, many patients are diagnosed with VTE without an identifiable cause.
Objectives: We sought to investigate the prevalence of idiopathic VTE and risk factors associated with this diagnosis.
Methods: Patients diagnosed with deep vein thrombosis (DVT) or pulmonary embolism (PE) were enrolled into a prospective venous thromboembolic center (VTEC) registry at a large tertiary medical center from 7/2015-12/2015. VTE events were considered to be idiopathic if none of the following criteria were met: current pregnancy; current use of hormonal therapy or oral contraceptives, active malignancy; diagnosed thrombophilia; major surgery within 90 days; bed rest, restricted mobility, cast or mold, or serious trauma within 30 days. Patient demographics, comorbidities, social history, family history, laboratory and clinical data were analyzed and compared between groups. Multivariable logistic regression analysis was used to estimate odds of idiopathic VTE.
Results: Of 223 patients with VTE, 93 (41.7%) were determined to be idiopathic. Patients with idiopathic and non-idiopathic VTE were of similar age, race/ethnicity, level of education, type of insurance, and type of VTE (DVT or PE). Patients with idiopathic VTE were more frequently female (68.8% vs. 46.4%; $p < 0.01$), more likely to have a history of COPD (8.6% vs. 1.1%, $p = 0.03$), hyperlipidemia (33.6% vs. 18.3%, $p = 0.02$), and less likely to be on a statin at the time of diagnosis (17.2% vs. 29.3%, $p = 0.05$) than non-idiopathic VTE. After multivariable adjustment, female sex (OR: 2.47, 95% CI 1.35-4.64) and history of varicose veins (OR 2.67, 95% CI 1.15-6.37) were significantly associated with the prevalence of idiopathic VTE.
Conclusions: In a large tertiary medical center, idiopathic VTE occurred in more than 40% of all VTEs. Female sex and history of varicose veins were independently associated with having an idiopathic VTE. These data provide a basis for future investigation into this high-risk population and for further development of prediction models.

Disclosures: **P. Yau:** None. **T. Maldonado:** None. **J. Erb:** None. **N. Ranganath:** None. **C. Sindet-Pederson:** None. **D. O'Reilly:** None. **C. Rockman:** None. **J.S. Berger:** None.

337 will be presented in the PVD Moderated eAbstract Poster Session. The abstract content is located on page 41.

340

Drug-Eluting Balloon Versus Everolimus-Eluting Stent for Restenosis in a Bare-Metal Stent: A Meta-Analysis of Randomized Trials

Akintunde M Akinjero, Icahn Sch of Med at Mount Sinai, New York, NY; Oluwole Adegbala, Seton Hall Univ Sch of Health and Medical Sciences, Englewood, NJ; Tomi Akinyemiju, Univ of Alabama at Birmingham, Birmingham, AL, Birmingham, AL

Background: In-stent restenosis accounts for major morbidity and mortality among patients treated with Bare-Metal Stents (BMS). Early efforts to treat BMS in-stent restenosis with plain balloon angioplasty and first generation drug eluting stents (DES) have been ineffective, leaving drug-eluting balloon (DEB) and second generation DES, such as everolimus eluting stents (EES), as the only remaining options. For BMS in-stent restenosis, studies performed so far have yielded conflicting results, while prior meta-analyses have been influenced by inclusion of observational studies. This is the first meta-analysis to compare EES versus DEB using results from only randomized controlled trials (RCTs).
Methods: A systematic search of PUBMED and EMBASE databases was conducted from first available date to August, 2016 for RCTs comparing DEB with EES. Two reviewers evaluated studies for eligibility and extracted data with binary restenosis rate as the main endpoint. We identified 901 unique citations. Odds ratios were pooled using random-effects modeling. Funnel plots were used to assess publication bias. Heterogeneity was assessed using I^2 statistic. All analysis were performed using Review Manager

(RevMan) version 5.3 (Cochrane Collaboration, 2014).
Results: Three RCTs met study eligibility criteria, with 684 patients and a mean follow-up of 9.5 months. There were 184 and 185 patients in the EES and DEB arms respectively. In pooled analyses, EES was not superior to DEB in binary restenosis rates (pooled odds ratio: 0.76; 95% confidence interval: 0.25-2.32; P=0.14). Heterogeneity was minimal (I^2 = 49%), and the funnel plot did not suggest publication bias.**Conclusion:** In patients with BMS in-stent restenosis, there were no significant differences in binary restenosis rates between EES and DEB. Our results can enhance physician decision-making regarding choice of revascularization tool in this patient population.

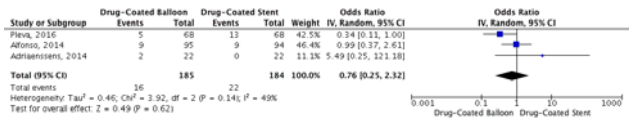

Disclosures: **A.M. Akinjero:** None. **O. Adegbala:** None. **T. Akinyemiju:** None.

342

Coagulation Factor XII Promotes Platelet Consumption in the Presence of Microbial Polyphosphate Under Shear Flow

Jevgenia Zilberman-Rudenko, Stephanie E Reitsma, Chantal P Wiesenekker, Cristina Puy, Oregon Health & Science Univ, Portland, OR; Stephanie A Smith, Univ of Illinois, Urbana, IL; Erik I Tucker, Oregon Health & Science Univ, Portland, OR; Richard J Travers, Univ of Illinois, Urbana, IL; Coen Maas, Rolf T Urbanus, Univ Medical Ctr Utrech, Utrech, Netherlands; David Gailani, Vanderbilt Univ Sch of Med, Nashville, TN; James H Morrissey, Univ of Illinois, Urbana, IL; Andras Gruber, Owen J McCarty, Oregon Health & Science Univ, Portland, OR

Background: Terminal complications of bacterial sepsis include development of consumptive coagulopathy referred to as disseminated intravascular coagulation. Bacterial constituents, including long-chain polyphosphates (polyP), have been shown to activate the contact pathway of coagulation in plasma. Recent work shows that activation of the contact pathway is capable of promoting thrombin generation and platelet activation and consumption in whole blood distal to thrombus formation under shear *ex vivo* and *in vivo*.
Aim: Test the hypothesis that the presence of long-chain polyP in the bloodstream promotes platelet activation and consumption in a coagulation factor (F)XII-dependent manner.
Methods and Results: Presence of long-chain polyP in whole blood promoted platelet aggregation on immobilized collagen surfaces under shear flow. Long-chain polyP enhanced fibrin formation and shortened clotting times of plasma and whole blood. The addition of long-chain polyP promoted platelet P-selectin expression, microaggregate formation and platelet consumption in the bloodstream under shear in a FXII-dependent manner. Moreover, long-chain polyP accelerated thrombus formation on immobilized collagen surfaces under shear flow. Distal to the sites of thrombus formation, platelet consumption was dramatically enhanced in the presence of long-chain polyP in the bloodstream. Inhibiting contact activation of the coagulation pathway reduced fibrin formation on collagen as well as platelet consumption in the bloodstream distal to the site of thrombus formation.
Conclusions: This study demonstrates that bacterial-type long-chain polyP promotes FXII-mediated thrombin generation and platelet activation in the flowing blood and could exaggerate sepsis-associated thrombotic processes, consumptive coagulopathy and thrombocytopenia.

Disclosures: **J. Zilberman-Rudenko:** Research Grant; Modest; F31HL13623001. **S.E. Reitsma:** None. **C.P. Wiesenekker:** None. **C. Puy:** None. **S.A. Smith:** None. **E.I. Tucker:** None. **R.J. Travers:** None. **C. Maas:** None. **R.T. Urbanus:** None. **D. Gailani:** None. **J.H. Morrissey:** None. **A. Gruber:** None. **O.J.T. McCarty:** Research Grant; Modest; R01HL101972, R01GM116184, 13EIA12630000.

This research has received full or partial funding support from the American Heart Association.

344

Comparative Metabolomic Profiling of Thrombotic Myocardial Infarction Reveals a Metabolic Signature Distinct From Non-Thrombotic Myocardial Infarction and Stable Coronary Artery Disease in Human Participants

Andrew P DeFilippis, Univ of Louisville Sch of Med, Div of Cardiovascular Med, Louisville, KY; Patrick J Trainor, Univ of Louisville Sch of Med, Div of Cardiovascular Med and Dept of Bioinformatics, Louisville, KY; Bradford G Hill, Univ of Louisville Sch of Med, Inst of Molecular Cardiology, Louisville, KY; **Alok R Amraotkar**, Univ of Louisville Sch of Med, Div of Cardiovascular Med, Louisville, KY; Shesh N Rai, Univ of Louisville Sch of Public Health, Dept of Bioinformatics and Biostatistics, Louisville, KY; Glenn A Hirsch, Univ of Louisville Sch of Med, Div of Cardiovascular Med, Louisville, KY; Eric C Rouchka, Univ of Louisville Speed Sch of Engineering, Dept of Computer Engineering and Computer Science, Louisville, KY; Aruni Bhatnagar, Univ of Louisville Sch of Med, Div of Cardiovascular Med, Louisville, KY

Background: Current non-invasive diagnostics for acute myocardial infarction (MI) identify myocardial necrosis rather than the primary cause and therapeutic target—plaque disruption and resultant thrombosis. **Aim:** The aim of this study is to identify change specific to plaque disruption and pathological thrombosis. **Methods:** We quantified 1,032 plasma metabolites by mass spectrometry in 11 thrombotic MI, 12 non-thrombotic MI and 15 stable CAD subjects at two acute phase [time of catheterization (T0), six hours (T6)] and one quiescent (>3 months follow-up) time points. A statistical classifier was constructed utilizing (T0) abundances of a parsimonious set of metabolites that demonstrated a significant change between quiescent phase and the acute phase that was distinct from any change seen in non-thrombotic MI or stable CAD subjects. Classifier performance as estimated by 10-fold cross-validation was suggestive of high sensitivity and specificity for differentiating thrombotic from non-thrombotic MI and stable CAD subjects. **Results:** Nineteen metabolites (Table 1) with an intra-subject fold change from time of acute thrombotic MI presentation to the quiescent state were distinct from any change measured in both the non-thrombotic MI and stable CAD subjects undergoing cardiac catheterization over the same time course (false discovery rate <5%). **Conclusions:** We have identified a candidate metabolic signature that differentiates acute thrombotic MI from quiescent state and from acute non-thrombotic MI and stable CAD. Further validation of these metabolites is warranted given their potential as diagnostic biomarkers and novel therapeutic targets for the prevention or treatment of acute MI.

Table 1: Metabolites specific to Thrombotic MI Evidenced by Significant Change from Acute to Quiescent Time-Point

Biochemical	Family	Platform	RI	Mass	*ANOVA*		*Post-Hoc Tests*		
					p-value	q-value	Thromb. vs Non-Thromb.	Thromb. vs sCAD	Non-Thromb. vs sCAD
N-acetylphenylalanine	Amino Acid	LC/MS Neg	2597	206.0823	0.00001	0.00306	0.00072	0.00000	0.07661
Glycine	Amino Acid	GC/MS	1486.9	218.1	0.00003	0.00446	0.00007	0.00002	0.98482
N-acetylvaline	Amino Acid	LC/MS Neg	1704	158.0823	0.00006	0.00650	0.00003	0.00024	0.20156
3-hydroxyisobutyrate	Amino Acid	LC/MS Polar	1619.1	103.0401	0.00009	0.00790	0.00928	0.00002	0.06268
N-acetylleucine	Amino Acid	LC/MS Neg	2400	172.0979	0.00012	0.00915	0.00471	0.00003	0.11955
2-hydroxybutyrate (AHB)	Amino Acid	GC/MS	1169.4	131	0.00022	0.01048	0.03899	0.00006	0.02674
Palmitoyl-linoleoyl-glycerophosphoinositol (1)	Lipid	LC/MS Polar	910	833.5185	0.00025	0.01048	0.00006	0.03846	0.00515
Histidine	Amino Acid	LC/MS Neg	755.9	154.0622	0.00034	0.01192	0.00110	0.00014	0.69936
1-linoleoylglycerophosphoinositol	Lipid	LC/MS Neg	6494	596.2889	0.00062	0.01826	0.00163	0.00027	0.76364
11-dehydrocorticosterone	Lipid	LC/MS Pos	4533.8	345.206	0.00072	0.01992	0.00020	0.00511	0.10644
Cortisol	Lipid	LC/MS Pos	4661.9	363.2166	0.00074	0.01992	0.00086	0.00064	0.82981
Ribonate	Carbohydrate	LC/MS Polar	2425	165.0405	0.00082	0.02130	0.00019	0.02467	0.02553
Unknown 146		LC/MS Pos	1807	207.0175	0.00123	0.02862	0.03483	0.00028	0.10317
Pregnenolonesulfate	Lipid	LC/MS Neg	5100	395.1898	0.00123	0.02862	0.00226	0.00059	0.87066
1-arachidonoylglycerophosphoinositol	Lipid	LC/MS Neg	5482	619.2889	0.00137	0.02974	0.00672	0.00037	0.36496
Corticosterone	Lipid	LC/MS Pos	4851.2	347.2217	0.00195	0.03608	0.01037	0.00055	0.39706
Unknown 225		LC/MS Pos	1962	250.093	0.00234	0.03854	0.00409	0.00105	0.84077
Asparagine	Amino Acid	LC/MS Polar	2951.1	131.0462	0.00295	0.04323	0.01588	0.00081	0.36888
Arachidate (20:0)	Lipid	LC/MS Neg	6295	311.2958	0.00330	0.04733	0.00438	0.00167	0.96597

Abbreviations: Thromb. – Thrombotic MI, Non-Thromb. – Non-Thrombotic MI, sCAD – Stable Coronary Artery Disease

Disclosures: **A.P. DeFilippis:** None. **P.J. Trainor:** None. **B.G. Hill:** None. **A.R. Amraotkar:** None. **S.N. Rai:** None. **G.A. Hirsch:** None. **E.C. Rouchka:** None. **A. Bhatnagar:** None.

This research has received full or partial funding support from the American Heart Association.

345

Detection of Hypercoagulant Condition Caused by Elevated Prothrombin With a Thrombin Generation Assay

William C Chang, U.S. Food and Drug Admin, Silver Spring, MD; Kellie R Machlus, Alisa S Wolberg, Univ of North Carolina, Chapel Hill, NC; Mikhail V Ovanesov, U.S. Food and Drug Admin, Silver Spring, MD

Hypercoagulability resulting from elevated prothrombin is associated with increased thrombosis risk. Patients with elevated prothrombin include those with the G20210A mutation that represents the 2nd most common risk factor for venous thrombosis in European Caucasians. We hypothesized that the commercial thrombin generation assay (TGA), which measures the rate of synthetic thrombin substrate consumption, may detect procoagulant condition caused by elevated prothrombin.
Normal pooled plasma was treated with prothrombin or other coagulation factors to increase their levels to 200% or 400% of normal. TGA was performed using the Calibrated Automated Thrombogram (CAT) platform (Stago, USA) and analyzed with and without correction for substrate consumption. As expected, addition of elevated coagulation factors resulted in elevated TGA as measured by thrombin peak height (TPH) and endogenous thrombin potential (ETP). ETP allowed detection of up to 83% of spiked samples with 200% prothrombin but TPH has failed to distinguish these samples from the procoagulant samples obtained with other coagulation factors.
For samples with 400% prothrombin, CAT failed to return values for TPH for 40% of samples and ETP for 100% of samples but the remaining 60% of TPH values were detected as the procoagulant samples. By analyzing the raw fluorescence data directly, we found that elevated prothrombin, but not other coagulation factors, resulted in thrombin substrate depletion which allowed us to correctly distinguish all samples within our dataset regarding whether or not they had added prothrombin.
We conclude that the commercially available TGA has limited utility in distinguishing samples with elevated prothrombin but additional analysis of data can address this problem. With this additional analysis, TGA may be developable into new point-of-care test to diagnose patients with hypercoagulant conditions undetectable by currently used clotting assays.
Disclaimer: This is an informal communication and represents authors' best judgment. These comments do not bind or obligate FDA.

Disclosures: **W.C. Chang:** None. **K.R. Machlus:** None. **A.S. Wolberg:** None. **M.V. Ovanesov:** None.

346

CD39/CD73 Expressing Exosomes Protect Against Arterial Thrombosis

Roman Covarrubias, Vanderbilt Univ, Nashville, TN; Susanne A Snoek, Arthrogen, Amsterdam, Netherlands; Lin Zhong, Vanderbilt Univ, Nashville, TN; Niels Broekstra, Jonathan D Finn, Arthrogen, Amsterdam, Netherlands; Richard J Gumina, Vanderbilt Univ, Nashville, TN

Objective: To determine whether expression of CD39/CD73 in exosomes protects against ferric chloride-($FeCl_3$) induced arterial thrombosis.
Approach and Results: Ectonucleotidase triphosphate diphosphohydrolase-1 (CD39) and ecto-5'-nucleotidase (CD73) sequentially hydrolyze extracellular ATP or ADP to AMP and AMP to adenosine. We have previously shown that mice with increased CD39 expression are protected against arterial thrombosis. Specifically, increased CD39 expression on circulating monocytes protects against arterial thrombosis. Based on this previous work, we hypothesized that exosomes expressing CD39/CD73 could confer protection against arterial thrombosis and extend the time to arterial occlusion following $FeCl_3$ injury. To test this hypothesis, we stably transfected 293 T cells with mouse CD39 and CD73 or control plasmids then isolated exosomes from the supernatant. Exosomes isolated from mCD39/mCD73 transfected cells showed expression of mCD39 (6.60 µg/ml) and mCD73 (10.8 µg/ml) with a specific activity of 512,936 (U/µg) and 67,406 (U/µg) respectively as shown by phosphate hydrolysis assay (malachite green). To test whether mCD39/mCD73 exosomes protect against arterial thrombosis we infused 9.8×10^{11} CD39/CD73 exosome particles, or control particles, into the jugular vein of wild-type mice 15 minutes prior to $FeCl_3$ injury of the carotid artery. Infusion of mCD39/mCD73 exosomes significantly increased the time to thrombosis when compared to control exosomes in wild-type mice (Figure; control exosomes: 545±15.67 seconds, n=4. mCD39/mCD73 exosomes: 1644±398.3 seconds, n=4. *P*=0.029).
Conclusion: CD39/CD73 expressing exosomes protects mice against arterial thrombosis.

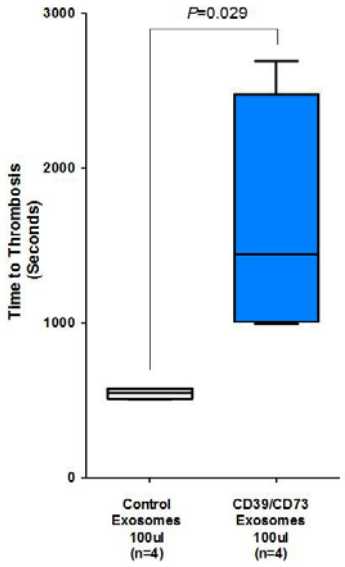

Disclosures: **R. Covarrubias:** None. **S.A. Snoek:** Employment; Significant; Employment provided by Arthrogen.. **L. Zhong:** None. **N. Broekstra:** Employment; Significant; Employment provided by Arthrogen. **J.D. Finn:** Employment; Significant; Employment provided by Arthrogen. **R.J. Gumina:** None.

347

Cigarette Smoking Associated Changes on Platelet Surface

Curtis Lee Lowery III, James D Marsh, **Fusun Kilic**, UAMS, Little Rock, AR

Thirty percent of all deaths from coronary heart disease each year in the US are attributable to cigarette smoking. The acute effects of smoking on the cardiovascular systems are associated with arterial thrombosis. Cigarette smoking produces central nervous system-mediated activation of the sympathetic nervous system, which stimulates secretion of pro-thrombotic molecules, serotonin (5-HT) and catecholamines into the blood at supraphysiological levels. 5-HT and catecholamines activate their platelet-specific receptors in an additive manner to change the platelet biology and physiology. Our studies of blood samples from smokers (collected just after smoking) showed several-fold elevation in plasma 5-HT and catecholamines, and platelet aggregation. To explore smoking-associated changes on platelets, the plasma membrane glycans and proteins were eluted and analyzed in MALDI-MS and LC-MS, respectively. The surface glycans of nonsmokers' platelets were high-mannose-type but those of smokers' platelets were on smokers', sialylated N-glycans. Removing the N-glycan counteracted smoking-mediated platelet aggregation, suggesting that N-glycans play a role in adhesiveness of the platelet surface. MS analysis of the membrane proteins identified enzymes and proteins exclusively on smokers' platelet plasma membrane. These included enzymes involved in glycan biosynthesis and proteins important in membrane trafficking of secretory vesicles. We hypothesize that, upon smoking, glycosylation enzymes normally sequestered in intracellularly, are translocated to the plasma membrane to induce changes in surface glycans. Interestingly, we showed that treating nonsmokers' platelets with 5-HT and catecholamines predisposed them to a prothrombotic state. Furthermore, pharmacological blockade of receptors for 5-HT or catecholamines counteracted the 5-HT-catecholamine-mediated aggregation and alterations in level and composition of surface glycans. Achieving our proposed aims potentially will provide novel biomarkers and pharmacological targets for preventing and treating smoking-associated thrombosis.

Disclosures: **C.L. Lowery:** None. **J.D. Marsh:** None. **F. Kilic:** None.

This research has received full or partial funding support from the American Heart Association.

348

Lys 42, 43, 44 and Arg 12 of Thrombin Activable Fibrinolysis Inhibitor Comprise Thrombomodulin Binding Exosite Essential for Exerting Its Antifibrinolytic Activity

Paul Y. Kim, Chengliang Wu, Alan R. Stafford, James C. Fredenburgh, Jeffrey I. Weitz, McMaster Univ, Hamilton, ON, Canada; Ann Gils, Paul J. Declerck, KU Leuven, Leuven, Belgium

The thrombin-thrombomodulin (TM) complex activates thrombin-activable fibrinolysis inhibitor (TAFI) more efficiently than thrombin or plasmin alone. The exosite on TAFI required for its TM-dependent activation by thrombin has not been identified. Based on previous work by us and others, we generated TAFI variants with one or more of residues Lys 42, Lys 43, Lys 44 and Arg 12 within the activation peptide mutated to alanine. Mutation of one, two, or three Lys residues or the Arg residue alone decreased the catalytic efficiency of TAFI activation by thrombin-TM by 2.4-, 3.2-, 4.7-, and 15.0-fold, respectively, and increased the TAFI concentrations required for half-maximal prolongation of clot lysis times ($K_{1/2}$) by 3-, 4,- 15-, and 24-fold, respectively. Mutation of all four residues eliminated TM binding, decreased the catalytic efficiency of TAFI activation by 45.0-fold, increased the $K_{1/2}$ by 130-fold, and abolished antifibrinolytic activity in a clot lysis assay. When thrombin or plasmin was used as the activator, mutation of all four residues reduced the rate of activation by 1.1- and 4.0-fold compared with wild-type TAFI, respectively, suggesting that the mutation only impacted activation kinetics by thrombin-TM. Surface plasmon resonance data show that mutation of the four residues results in complete loss of binding, either in the presence or absence of thrombin. Together, our findings suggest that these four residues are critical for the interaction of TAFI with the thrombin-TM complex that modulates its antifibrinolytic activity.

Disclosures: **P.Y. Kim:** None. **C. Wu:** None. **A.R. Stafford:** None. **J.C. Fredenburgh:** None. **J.I. Weitz:** None. **A. Gils:** None. **P.J. Declerck:** None.

349

Signatures of Stroke and Bleeding on Left Ventricular Assist Device Support

Tara Shrout, Univ of Kentucky Coll of Med, Lexington, KY; Travis Sexton, Univ of Kentucky Saha Cardiovascular Res Inst, Lexington, KY; Maya Guglin, Susan Smyth, Univ of Kentucky, Lexington, KY

Hypothesis: Platelet function and thromboinflammatory biomarkers will help predict clinical complications in patients on Left Ventricular Assist Device (LVAD) support.
Methods: June 2014-August 2016, 66 patients received Heartmate II(n= 48), Heartware(n=18). Median age 55. 86% Male. Blood collections: baseline (BL); 1, 24, 72, 168-hours and follow-up 30-180-days post-operation. Platelet function analyzed via impedance aggregometry and agonists (thrombin, ADP, collagen, ristocetin). Plasma biomarkers (TNF-a, CD40L, IL-6, CRP, IL-10, IL-1b, PF4, Angiopoietin-1,-2, ST2) analyzed via immunoassays. Clinical data correlated via functional data analysis, multiple linear regression.
Results: Median values reported. Platelets decreased 42.0% (SD 208.0±77;120.9±50)($p<0.001$) while WBC increased 67.1% (SD 8.2 ±2.9;13.7±3.6)($p<0.0001$) BL to 72-hours. Platelet ristocetin aggregation decreased 52% (SE 515.0±79.7;247.1±45.7)($p=0.0006$) BL to 24-hours without BL recovery by day 7. To demonstrate a few biomarkers: IL-6 increased 796.9% (SE 25.4±72.4;227.8 ±94.6)($p=0.004$) BL to 72-hours without BL recovery by follow-up. Angiopoeitin-1 decreased 35% (SE 1279±136.4;837.2±84.7)($p=0.01$) while Angiopoietin-2 increased 235.7% (SE 3143.9±813.5;10555.4±7556.1)($p=0.03$) BL to 72-hours. Angiopoietin-2/angiopoietin-1 was increased 273% from healthy levels at BL (SE 0.46±0.07;1.72±0.65)($p=0.05$) without return by follow-up. One-year outcomes: stroke 18.2%, gastrointestinal bleeding (GIB) 19.7%, thrombosis 9.1%, drive-line infection (DLI) (10.6%) mortality 15.2%. Analysis revealed significant associations of platelet function with GIB and DLI. Significant associations also exist between biomarkers (TNF-a, CD40L, ect) and stroke, GIB, and mortality. Further data will be presented.
Conclusions: LVADs are crucial for patients with limited cardiac function, however significant complications exist. Study results suggest that early platelet function and biomarker analysis may help predict complications such as stroke and bleeding, and thus serve as risk-stratification or targeted therapy tools for patients on LVAD support.

Disclosures: **T. Shrout:** None. **T. Sexton:** None. **M. Guglin:** None. **S. Smyth:** None.

350

Activation of Platelet CLEC-2 in Hematoma Expansion After Intracerebral Hemorrhage: Finding an Effective Dose

Sherrefa R Burchell, Loma Linda Univ, Loma Linda, CA; Loretta Iniaghe, Univ of Benin, Benin, Nigeria; Cesar Reis, Sheryl Aka, Karen Hay, Ronak Raval, John H Zhang, Jiping Tang, Loma Linda Univ, Loma Linda, CA

Intracerebral hemorrhage (ICH) is the least treatable and one of the most disabling stroke subtypes, with both the primary and secondary brain injuries mainly due to hematoma expansion (HE) within the first few hours, followed by an inflammatory and oxidative injury. Almost all ICH patients experience some degree of expansion, and ICH volume can be an independent determinant of mortality and functional outcome. Previous studies found that reduced platelet activity is associated with early ICH growth and worse functional outcomes. The platelet C-type lectin-like receptor 2 (CLEC-2) elicits robust platelet activation upon stimulation. Thus, we hypothesized that activation of CLEC-2 would result in activation and aggregation of platelets, reducing HE, and improving functional outcomes after ICH. We administered two CLEC-2 agonists (Fucoidan and the endogenous ligand Podoplanin) at varying doses after murine ICH and measured hemorrhage volume, brain water content, and behavior. We also collected blood from podoplanin-treated mice and conducted hematologic tests. We further tested Rhodocytin, a known CLEC-2 activator, for whole blood clotting times, platelet functions, and soluble fibrin in human blood samples. We found that treatment with Fucoidan did not reduce hemorrhage volume or brain water content and had no effect on neurological function, compared to vehicle. Further, Podoplanin treatment showed a tendency to reduce brain water content but did not affect hematoma volume or behavior. Our *in vitro* studies showed lower fibrinogen levels with podoplanin treatment, compared to sham and vehicle, but no effect on partial thromboplastin time, prothrombin time, or INR. At higher doses, Rhodocytin resulted in immediate clotting, while at lower doses, it significantly increased soluble fibrin, consistent with initiation of clotting seen in the higher doses. In conclusion, our findings indicate that activation of CLEC-2 at the doses tested does not reduce ICH volume or improve outcomes, but did affect hemostatic parameters. Thus, the agonists may produce favorable outcomes with a different dosing regimen. Further studies are needed to confirm the mechanism by which CLEC-2 is acting in ICH, effective doses, and the effect of altered bleeding parameters.

Disclosures: **S.R. Burchell:** None. **L. Iniaghe:** None. **C. Reis:** None. **S. Aka:** None. **K. Hay:** None. **R. Raval:** None. **J.H. Zhang:** None. **J. Tang:** None.

351

Plasma Phospholipid Transfer Protein Promotes Platelet Aggregation

Xiao-Min Zhao, Taishan Medical Univ, Taian, China, Taian, China; Yun Wang, Shu-Cun Qin, Taishan Medical Univ, Taian, China; **Xian Jiang**, SUNY Downstate Medical Ctr, Brooklyn, NY

Hypothesis: Phospholipid transfer protein (PLTP) has a direct effect on platelet aggregation, since PLTP knockout mice have longer bleeding time. ***Methods and Results:*** Platelets from humans or mice were prepared as were mouse platelet-rich plasma and human recombinant PLTP (rPLTP). In mice, we assessed ADP- and collagen-induced platelet aggregation, phosphatidylserine (PS) externalization, and photothrombosis-induced cerebral infarction. We found that human platelets produce PLTP. Platelet aggregation increased upon PLTP overexpression whereas it decreased with PLTP deficiency in a gene dose-dependent manner. Human rPLTP increased mouse or human platelet aggregation in a dose-dependent manner. PS externalization provides a water/lipid surface for the interaction of coagulation factors, which accelerates thrombosis. Compared with wild type controls, platelets from PLTP transgenic mice had significantly greater amounts of PS on the exterior surface of the plasma membrane, whereas platelets from PLTP-deficient mice had significantly less on the surface, thus influencing fibrinogen binding. Moreover, rPLTP together with ADP significantly increased PS exposure on the plasma membrane of PLTP-deficient platelets, thereby increasing fibrinogen binding. Importantly, PLTP overexpression significantly accelerated the incidence of photothrombosis-induced infarction, whereas PLTP deficiency reduced the incidence. ***Conclusions:*** PLTP promotes PS externalization at the plasma membrane of platelets and accelerates ADP- or collagen-induced platelet aggregation. Thus, PLTP is involved in hypercoagulation. Therefore, PLTP inhibition could be a novel approach for countering thrombosis.

Disclosures: **X. Zhao:** None. **Y. Wang:** None. **S. Qin:** None. **X. Jiang:** None.

354

Clots Are Potent Triggers of Inflammatory Cell Gene Expression: Indications for Timely Fibrinolysis

Robert A Campbell, Adriana Vieira-de-Abreu, Jesse W Rowley, Zechariah G Franks, Matthew T Rondina, Larry W Kraiss, Jennifer J Majersik, Guy A Zimmerman, Andrew Weyrich, Univ of Utah, Salt Lake City, UT

Objective: Blood vessel wall damage often results in the formation of a fibrin clot that traps inflammatory cells, including monocytes. The effect of clot formation and subsequent lysis on the expression of monocyte-derived genes involved in the development and progression of ischemic stroke and other vascular diseases, however, is unknown. Determine if clot formation and lysis regulates the expression of human monocyte-derived genes that modulate vascular diseases. **Approach and Results**: We performed Next Generation RNA sequencing on monocytes extracted from whole blood clots. Thousands of mRNAs were differentially expressed by monocytes from clotted versus unclotted whole blood, including upregulation of interleukin 8 (IL-8) and monocyte chemoattractant protein-1 (MCP-1). Clotted plasma also increased expression of IL-8 and MCP-1, which far exceeded responses observed in LPS-stimulated monocytes. Upregulation of IL-8 and MCP-1 occurred in a thrombin-independent, but fibrin-dependent manner. Fibrinolysis initiated shortly after plasma clot formation (i.e., 1-2 hours) reduced the synthesis of IL-8 and MCP-1, while delayed fibrinolysis was far less effective. Consistent with these *in vitro* models, monocytes embedded in unresolved thrombi from patients undergoing thrombectomy stained positively for IL-8 and MCP-1. **Conclusions:** These findings demonstrate that clots are potent inducers of monocyte gene expression, and that timely fibrinolysis attenuates inflammatory responses. Dampening of inflammatory gene expression by timely clot lysis may contribute to the clinically-proven efficacy of fibrinolytic drug treatment within hours of stroke onset.

Disclosures: **R.A. Campbell:** Research Grant; Significant; American Heart Association (11POST7290019). **A. Vieira-de-Abreu:** None. **J.W. Rowley:** None. **Z.G. Franks:** None. **M.T. Rondina:** Research Grant; Modest; NIA (AG040631), NHLBI (HL092161). **L.W. Kraiss:** None. **J.J. Majersik:** None. **G.A. Zimmerman:** None. **A. Weyrich:** Research Grant; Modest; NHLBI (HL066277), NHLBI (HL112311).

This research has received full or partial funding support from the American Heart Association.

355

Photoluminescent Polylactones Based Nanoscaffolds for Enhancing Reendothelialization

Aneetta E Kuriakose, Priyesh Rajanikant, Upasana Mali, The Univ of Texas at Arlington, Arlington, TX; Dingying Shan, Penn State Univ, State College, PA; Liping Tang, The Univ of Texas at Arlington, Arlington, TX; Subhash Banarjee, UT Southwestern Medical Ctr, Dallas, TX; Jian Yang, Penn State Univ, State College, PA; **Kytai T Nguyen**, The Univ of Texas at Arlington, Arlington, TX

Percutaneous coronary intervention is commonly employed for revascularization. These strategies, however, injure the arterial wall initiating a cascade of inflammatory responses that culminates in restenosis. In our research work, we proposed to use a platelet mimicking fluorescent nano-scaffold system that can cloak an injured artery site from inflammatory cells, capture the endothelial progenitor cells using specialized targeting agents, and promote *in situ* endothelial regeneration. We used photo-luminescent polylactone (BPLP) copolymers such as BPLP-co-poly(L-lactide) (BPLP-PLLA) and BPLP-co-poly(lactic-co-glycolic) acid (BPLP-PLGA50:50 and BPLP-PLGA75:25) to prepare nanoscaffolds; their intrinsic fluorescent properties help us localize and monitor the scaffold's degradation *in vivo* as endothelial regeneration ensues. Our initial studies were focused on optimizing a suitable polymer to be used to make a novel nano-scaffold system.
We fabricated ~200 nm sized BSA-loaded BPLP-polylactone based nanoparticles by standard double emulsion method. BPLP-PLGA based particles released BSA within 14 days, however, BPLP-PLLA showed slow and continued release for 28 days. BPLP-PLGA degraded completely within 4 weeks of study, whereas BPLP-PLLA degraded only 20% during the same time. The cyto-compatibility study showed that the BPLP-PLGA50:50, especially at high concentrations (> 1000µg/ml), is significantly toxic to the human umbilical vein endothelial cells; however, no such toxicity was observed for BPLP-PLGA75:25 and BPLP-PLLA. Hemo-compatibility of the particles demonstrated that they didn't cause any significant lysis of red blood cells, and neither affected blood clotting kinetics compared to that of the control. Furthermore, we observed a minimal number of platelet attachment and activation on BPLP-

PLGA materials compared to that of the glass surface. Based on these initial results we selected BPLP-PLGA 75:25 to fabricate nanoscaffolds. Currently, we are optimizing the effective particle size to enhance their margination towards the arterial wall and other factors, including specialized capturing agents to capture EPC, and growth factor cocktail to improve EPC homing and differentiation at the injured site.

Disclosures: **A.E. Kuriakose:** None. **P. Rajanikant:** None. **U. Mali:** None. **D. Shan:** None. **L. Tang:** None. **S. Banarjee:** None. **J. Yang:** None. **K.T. Nguyen:** None.

356

Adhesion of *Staphylococcus Epidermidis* to Fibrinogen Alters Clot Formation Kinetics and Ultimate Stiffness

Carolyn Vitale, Dept of Pediatrics, Univ of Michigan, Ann Arbor, MI; Tianhui Ma, Michael J. Solomon, Dept of Chemical Engineering, Univ of Michigan, Ann Arbor, MI; J. Scott VanEpps, Dept of Emergency Med, Univ of Michigan, Ann Arbor, MI

Bacterial infection is known to increase the risk for thromboembolism. The mechanism underlying this correlation remains largely unknown. We recently showed that the common pathogen *Staphylococcus epidermidis* retards clot formation, increases clot elasticity and generates a heterogeneous clot structure that remodels over time. Here, we elucidate the mechanism of this process by evaluating the capacity for *S. epidermidis* to bind to fibrinogen as a function of its growth phase. We hypothesized that the effect of *S. epidermidis* on a fibrin clot is related to its propensity toward biofilm formation. Therefore, stationary phase (biofilm-like) *S. epidermidis* will have a more robust effect on clot kinetics and elasticity than exponential phase (planktonic). Furthermore, this difference is mediated by increased adhesion to fibrinogen. Rheometry was used to evaluate the formation and resultant elasticity of fibrin clots with exponential or stationary phase *S. epidermidis*. A functional *in vitro* model was developed to evaluate adhesion of *S. epidermidis* to a fibrinogen coated surface in a continuously flowing environment. Fluorescent labeled exponential and stationary phase *S. epidermidis* were visualized flowing through a parallel plate microfluidic chamber past immobilized fibrinogen. Images were obtained every 3 seconds for 30 min. Bacterial deposition rate and mean adhesion time were quantified by automated image analysis. A paired Student's t-test was used for statistical analysis. Stationary phase *S. epidermidis* retards clot formation and increases resultant elasticity while exponential phase only slightly reduces elasticity. The bacterial deposition rate onto fibrinogen was significantly ($p=0.03$) greater for stationary phase (1741 ± 1513 cells/cm^2 $\cdot$ sec^{-1}) vs exponential phase (676 ± 270 cells/cm^2 $\cdot$ sec^{-1}). The average adhesion time however was similar for exponential and stationary phase cells. Coagulation proteins can provide a framework for bacterial adhesion, biofilm formation and infection. In turn infected thrombi with (biofilm-like) bacteria are stiffer which correlates to more frequent bacterial binding to fibrinogen. This provides a potential molecular mechanism for infection mediated thromboembolic events.

Disclosures: **C. Vitale:** None. **T. Ma:** None. **M.J. Solomon:** None. **J. VanEpps:** None.

360

An Educational Program Improves Cholesterol and Mental Health of Individuals With Hypercholesterolemia

Francisco E Ramirez, Neil Nedley, Nedley Clinic, Weimar, CA

Background Hypercholesterolemia can trigger depressive symptoms. We are reporting on the effect that an educational program has on cholesterol and depression levels. **Methods** A medical clinic trained individuals to run the programs. Those who chose to participate met once a week for 8 weeks for a 2 hour program, which consisted of a 45 minute DVD presentation and a facilitated small group discussion together with weekly practical assignments. The Depression and Anxiety Assessment Test [DAAT] was used. It assessed depression level based on a modified PHQ-9 [Patient Health Questionnaire] test, demographics and participant self reported cholesterol levels and intake of omega-3 foods. No questions were asked about individuals' treatment. The depression was classified according to DSM-5 into 4 categories as none (0-6), mild (7-10), moderate (11-19) or severe (20 or more). The progress was quantified on the category they finished in. The 77 question DAAT questionnaire was administered at baseline and completion. They were taught various healthy lifestyle habits like plant-based diet, exercise, proper rest, bright light, sleep, and avoiding negative thoughts, among other things. **Results** Of 5997

participants that finished the program, 1320 (22%) reported having high cholesterol at baseline, that group had a baseline mean depression level of 13.3 SD 7.4, 76% of them ate omega-3 rich foods. Also at baseline 4060 (68%) reported normal cholesterol, their mean depression was 11.5 SD 7.5, of them 72% ate omega-3 rich foods, 10% did not know their cholesterol levels. The baseline high cholesterol group at the end of the program had an mean depression of 7.1 SD 6.1. Paired samples t-test of before and after was significant $t(1319)=35.7$ with a $p<.001$. The end program of the normal cholesterol group had a mean depression of 6.1 SD 5.8, t-test was significant $t(4059)=53.6$ with a $p<.001$. At the end of the program 26% of the baseline high cholesterol group no longer had hypercholesterolemia. **Conclusion** Hypercholesterolemia seems to be related with higher levels of depression. Those with normal cholesterol improved the most. The program helps lower cholesterol in 1/4 of its participants. Mental health improves in the majority of its participants. Further follow-up is advised.

Disclosures: **F.E. Ramirez:** None. **N. Nedley:** Ownership Interest; Modest; Nedley Health Solutions.

361

Plant-Based Diet and Lifestyle Changes Improve Lipids Among Angina Patients

Francisco E Ramirez, Neil Nedley, Nedley Clinic, Weimar, CA; Albert Sanchez, Weimar Inst, Weimar, CA

Background Angina is an important predictor of heart disease. Lipids can be an important etiological factor of atherosclerosis and angina. We examine the effect that an 18 day medical residential program has on the lipids of such patients.
Methods Participants completed an 18 day program in Weimar, California near Sacramento. Each patient was evaluated by a board certified physician who monitored them during the whole program. Blood samples were taken before and at the end of the program. Results are reported in mg/dl. Among the modalities used in all participants included whole foods plant-based diet, aerobic exercise, proper water intake and hydrotherapy, enough sunlight, avoidance of any addictive substances (tobacco, caffeine, alcohol, etc), breathing exercises, enough rest and psychological, relational and spiritual therapies. The meals were buffet style, 3 times a day with no snacks. Various cooking classes and daily educational lectures were given to empower patients to continue with the changes at home.
Results From $n=2080$ patients, $n=133$ had an angina diagnosis. From the 133 and 116 had complete lab results, 50% percent were males. Results are reported as (mean, SD, median, mode, min, max). Baseline total cholesterol (218, 41, 213, 189, 96, 316), end values (189, 33, 185, 163, 108, 283) t-test $t(115)=11.4$, with significant change $p<.001$, mean difference 28.3. Baseline LDL (137, 37, 128, 117, 53, 227), end values (115, 29, 112, 123, 55, 204), t-test $t(115)=10.2$, with significant change $p<.001$ mean difference 21.6. Baseline HDL (43, 15, 40, 31, 18, 90) end values (42, 12, 39, 33, 21, 76), t-test $t(115)=1.2$ change was not significant, $p=.22$, mean difference .92. Some patients reported decrease in angina symptoms.
Conclusions The program effectively decreases lipids towards a normal range. HDL decreased a little but the change was not significant. Long term follow up should be done on participants of this program to see the long term effect.

Disclosures: **F.E. Ramirez:** None. **N. Nedley:** Ownership Interest; Modest; Nedley Health Solutions. **A. Sanchez:** None.

362

Knockout of NADPH Oxidase 2 Improves Global Metabolism and Endothelial Function in Aging Mice

Lampson M Fan, Div of Cardiovascular Med, Univ of Oxford, Oxford, United Kingdom; **Li Geng**, Jian-Mei Li, Univ of Reading, Reading, United Kingdom

Oxidative stress attributable to the activation of a Nox2-containing NADPH oxidase has been suggested to play a crucial role in the development of aging-associated vascular diseases. However, the mechanism of endothelial Nox2 activation in normal aging process remains unclear. In this study, we investigated the therapeutic potential of targeting Nox2 in improving global metabolism and endothelial function at old age by using age-matched wild-type and Nox2 knockout mice at 3-4 months (young); 11-12 months (middle aged) and 21-22 months (aging). Compared to young mice, middle-aged and ageing wild-type mice had significantly higher blood pressure, hyperglycaemia, hyperinsulinaemia. These were accompanied by oxidative stress in multiple organs including the lung, the liver, the heart and the vessels. The vessel

motor function was examined in an organ bath using aortas isolated from these mice. Endothelium-dependent vessel relaxation to acetylcholine was significantly impaired in aortas of wild-type aging mice, and this was accompanied by increased expressions of Nox2 and markers of inflammation, activation of MAPK and Akt and decreased insulin receptor expression and function. However, these aging-associated disorders in aortas were significantly reduced by knocking out Nox2 in mice. In response to high glucose plus high insulin challenge, coronary microvascular endothelial cells isolated from wild-type mice displayed significantly increased Nox2 expression, oxidative stress and cell senescence, e.g. increased p53 expression and β-galactosidase activity. However, these responses were absent or significantly reduced in the endothelial cells isolated from Nox2 knockout mice. In conclusion, metabolic disorders in particular hyperglycaemia and insulin resistance play an important role in mediating Nox2 activation and oxidative stress in multiple organs in aging. Nox2 is involved in normal aging process-associated vascular inflammation and oxidative damage of endothelial dysfunction.

Disclosures: **L.M. Fan:** None. **L. Geng:** None. **J. Li:** None.

363

Lysosomal Lipid Accumulation and Dysregulation of Downstream Cholesterol Homeostasis in Human Arterial Smooth Muscle Cells

Joshua A. Dubland, Collin S. Pryma, Sima Allahverdian, Ying Wang, Teddy Chan, Gordon A. Francis, Univ of British Columbia, Vancouver, BC, Canada

Background and Hypothesis: Previously we reported that ≥ 50% of the foam cells in human coronary artery atherosclerosis are smooth muscle cell (SMC) derived, and that the rate-limiting cholesterol exporter, ATP-binding cassette transporter protein A1 (ABCA1), has reduced expression in SMCs compared to leukocytes in the intima. Upregulation of ABCA1 expression is dependent on normal flux of lipoprotein-derived cholesterol out of lysosomes and the subsequent generation of 27-hydroxycholesterol (27-OHC). Excess lipoprotein-derived cholesterol is also converted to cholesteryl esters (CE) through the actions of acyl-coA cholesterol acyltransferase (ACAT). Processes by which macrophages store lipoprotein-derived cholesterol in cytosolic and lysosomal compartments are well described, whereas less is known about SMCs. **Hypothesis:** We hypothesize that preferential SMC foam cell formation and the observed derangement in ABCA1 expression are associated with increased lysosomal sequestration of atherogenic lipids. **Methods and Results:** Human aortic SMCs and human monocyte-derived macrophages (HMMs) were loaded with aggregated LDL (agLDL) for 24 hrs, followed by a 24 hr equilibration without lipids to allow processing of lipoproteins. Data are presented as mean±SEM. In response to agLDL, CE content (nmol/mg protein) measured by LC/MS/MS increased from 2.2±1.3 to 277.0±18.2 in HMMs, and 3.5±5.3 to 46.8±14.5 in SMCs (n=9). Confocal microscopy indicated elevated lysosomal lipid accumulation in SMCs compared to HMMs. Levels of 27-OHC (ng/mg protein) as measured by LC/MS/MS increased from 80.9±9.5 to 281.4±22.7 (3.5-fold) in HMMs, and 0.7±0.2 to 1.5±0.3 (1.4-fold) in SMCs (n=9). ACAT activity, measured by the incorporation of ^{14}C-labelled oleate (pmol/mg protein), increased from 21.0±1.7 to 678.1±110.9 (32.2-fold) in HMMs, and 55.6±3.3 to 133.7±15.2 (2.4-fold) in SMCs (n=16). By Western blot, fold change in ABCA1 with exposure to agLDL was 2.3±0.3 in HMMs and 1.3±0.2 in SMCs (n=7-10). **Conclusions:** Accumulation of atherogenic lipids in the lysosomes of SMCs provides a potential mechanism for the reduced ABCA1 expression and preferential formation of foam cells by arterial SMCs.

Disclosures: **J.A. Dubland:** None. **C.S. Pryma:** None. **S. Allahverdian:** None. **Y. Wang:** None. **T. Chan:** None. **G.A. Francis:** None.

364

An NPC1 and NPC2 Independent Pathway Mediates Trafficking of Cholesterol From Lysosomes to the Extracellular Matrix

Xueting Jin, Ying Liu, Natl Institues of Health, Bethesda, MD; Lia Addadi, Weizmann Inst of Science, Rehovot, Israel; Howard S Kruth, Natl Institues of Health, Bethesda, MD

We previously reported that cholesterol-enriched macrophages deposit cholesterol into the extracellular matrix and this process depends on ABCA1 and ABCG1. The extracellular cholesterol deposits can be mobilized by HDL, or ApoA-I, the latter dependent on ABCA1-mediated lipidation of ApoA-I. The objective of the current study was to determine the effects of other genes and inhibitors that affect cellular

cholesterol trafficking on the deposition of extracellular cholesterol. We used a monoclonal antibody that labels cholesterol microdomains to detect the extracellular cholesterol deposits. Progesterone and U18666A previously were shown to induce accumulation of cholesterol within lysosomes, and we found that these agents also blocked macrophage deposition of extracellular cholesterol. Brefeldin A, an inhibitor of golgi and vesicular trafficking, inhibited extracellular cholesterol deposition. On the other hand, vacuolin, an agent that inhibits the fusion between autophagosomes and lysosomes and thereby induces cellular accumulation of autophagosomes, did not inhibit extracellular cholesterol deposition. To examine the effect of mutant genes known to affect cholesterol trafficking, we examined mutant cultured fibroblasts that were cholesterol-enriched by incubation with LDL plus the LXR agonist, T0901317. Like macrophages, normal cholesterol-enriched fibroblasts deposited extracellular cholesterol that was dependent on ABCA1, because ABCA1-deficient fibroblasts did not deposit extracellular cholesterol. While progesterone and U18666A inhibited fibroblast extracellular cholesterol deposition, surprisingly, fibroblasts deficient in NPC1 or NPC2, which also abnormally accumulate cholesterol within lysosomes during cholesterol enrichment, nevertheless, deposited extracellular cholesterol similar to normal fibroblasts. That lysosomal hydrolysis of LDL cholesteryl ester is involved in extracellular cholesterol deposition was shown by substantially reduced extracellular cholesterol deposition by fibroblasts lacking acid cholesteryl ester hydrolase. Our findings indicate that a pathway not dependent on NPC1 or NPC2 mediates trafficking of cholesterol from lysosomes to the extracellular space.

Disclosures: **X. Jin:** None. **Y. Liu:** None. **L. Addadi:** None. **H.S. Kruth:** None.

365

Inhibiting Hmg Coa Reductase Reduces Palmitate-Induced Inflammation in Adipocytes

Asha K Pathak, Chang Yeop Han, Mohamed Omer, Shari Wang, Alan Chait, Univ of Washington, Seattle, WA

Adipose tissue inflammation associates with insulin resistance and increased cardiovascular disease risk. We previously observed that 3T3-L1 adipocytes exposed to palmitate become inflamed and demonstrate increased plasma membrane cholesterol and lipid raft content. It is known that palmitate induces translocation of NAPH oxidase and toll-like receptor 4 into lipid rafts, increasing adipocyte inflammation. However, it is unclear (1) how palmitate alters plasma membrane cholesterol content; and (2) whether increased cholesterol content in the plasma membrane is related to adipocyte inflammation induced by palmitate exposure. We hypothesize that mechanisms involved in increasing plasma membrane cholesterol content after palmitate treatment could be related to cholesterol synthesis and/or ER stress, and that increased cholesterol in lipid rafts is essential for induction of inflammation in adipocytes. To test these hypotheses, differentiated murine 3T3-L1 adipocytes were exposed to palmitate for 24 hours, with and without pre-treatment with HMG-CoA reductase inhibitors (statins) or HDL. RT-PCR was used to evaluate gene expression of inflammation (*Saa3*, *Ccl2*), ER stress (*Bip*, *Chop*), and HMG-CoA reductase (*Hmgcr*). Cholera toxin subunit β staining and flow cytometry were used to evaluate plasma membrane lipid raft content. In differentiated adipocytes, palmitate-induced inflammation neither increased expression of ER stress genes nor HMG-CoA reductase gene expression. However, treatment with 3 different statins (simvastatin, lovastatin, atorvastatin) significantly reduced palmitate-induced adipocyte inflammation as indicated by decreased gene expression of *Saa3* and *Ccl2* (P <0.05). A similar effect was seen with pre-treatment with HDL. Lipid raft content induced by palmitate was decreased by HMG-CoA reductase inhibitors (difference in mean fluorescence intensity P <0.05) and also by pre-treatment with HDL. These findings indicate that ER stress was not involved in increased plasma membrane cholesterol after palmitate-induced inflammation in adipocytes. However, regulating cholesterol content in lipid rafts plays an important role in adipocyte inflammation induced by palmitate.

Disclosures: **A.K. Pathak:** None. **C. Han:** None. **M. Omer:** None. **S. Wang:** None. **A. Chait:** None.

367

Extreme High-Density Lipoprotein Cholesterol Genetics: An Assortment of Large and Small Polygenic Effects

Jacqueline S Dron, Western Univ, London, ON, Canada; Jian Wang, Robarts Res Inst, London, ON, Canada; Cécile Low-Kam, Montréal Heart Inst, Univ de Montréal, Montréal, QC, Canada; Sumeet A Khetarpal, Perelman Sch of Med, Univ of Pennsylvania, Philadelphia, PA; John F Robinson, Adam D McIntyre, Matthew R Ban, Henian Cao, Robarts Res Inst, London, ON, Canada; David Rhainds, Marie-Pierre Dubé, Montréal Heart Inst, Univ de Montréal, Montréal, QC, Canada; Daniel J Rader, Perelman Sch of Med, Univ of Pennsylvania, Philadelphia, PA; Guillaume Lettre, Jean-Claude Tardif, Montréal Heart Inst, Univ de Montréal, Montréal, QC, Canada; Robert A Hegele, Robarts Res Inst, London, ON, Canada

Rationale: Although HDL-C levels are known to have a complex genetic basis, most studies have focused solely on identifying rare variants with large phenotypic effects to explain extreme HDL-C phenotypes.
Objective: Here we concurrently evaluate the contribution of both rare and common genetic variants, as well as large-scale copy number variations (CNVs), towards extreme HDL-C concentrations.
Methods: In clinically ascertained patients with low (*N*=136) and high (*N*=119) HDL-C profiles, we applied our targeted next-generation sequencing panel (LipidSeq™) to sequence genes involved in HDL metabolism, which were subsequently screened for rare variants and CNVs. We also developed a novel polygenic trait score (PTS) to assess patients' genetic accumulations of common variants that have been shown by genome-wide association studies to associate primarily with HDL-C levels. Two additional cohorts of patients with extremely low and high HDL-C (total *N*=1,746 and *N*=1,139, respectively) were used for PTS validation.
Results: In the discovery cohort, 32.4% of low HDL-C patients carried rare variants or CNVs in primary (*ABCA1*, *APOA1*, *LCAT*) and secondary (*LPL*, *LMF1*, *GPD1*, *APOE*) HDL-C–altering genes. Additionally, 13.4% of high HDL-C patients carried rare variants or CNVs in primary (*SCARB1*, *CETP*, *LIPC*, *LIPG*) and secondary (*APOC3*, *ANGPTL4*) HDL-C–altering genes. For polygenic effects, patients with abnormal HDL-C profiles but without rare variants or CNVs were ~2-fold more likely to have an extreme PTS compared to normolipidemic individuals, indicating an increased frequency of common HDL-C–associated variants in these patients. Similar results in the two validation cohorts demonstrate that this novel PTS successfully quantifies common variant accumulation, further characterizing the polygenic basis for extreme HDL-C phenotypes.
Conclusions: Patients with extreme HDL-C levels have various combinations of rare variants, common variants, or CNVs driving their phenotypes. Fully characterizing the genetic basis of HDL-C levels must extend to encompass multiple types of genetic determinants—not just rare variants—to further our understanding of this complex, controversial quantitative trait.

Disclosures: **J.S. Dron:** None. **J. Wang:** None. **C. Low-Kam:** None. **S.A. Khetarpal:** None. **J.F. Robinson:** None. **A.D. McIntyre:** None. **M.R. Ban:** None. **H. Cao:** None. **D. Rhainds:** None. **M. Dubé:** None. **D.J. Rader:** None. **G. Lettre:** None. **J. Tardif:** None. **R.A. Hegele:** None.

368

The GLP-1 Receptor Agonist Liraglutide Improves Autophagy Impairment in the Diabetic Heart

Antoinette Bugyei-Twum, Jennifer Switzer, Krishna K. Singh, Kim A. Connelly, St. Michael's Hosp, Toronto, ON, Canada

Background: Diabetes mellitus is a well-recognized risk factor for the development of heart failure. Although studies with the glucagon-like pepide-1 analog liraglutide—an approved treatment for type 2 diabetes—have demonstrated substantial cardioprotective effects of the drug in both human and experimental diabetes, the underlying mode of action/mechanism of liraglutide remains unclear. Here, we investigate the impact of liraglutide on autophagy—an evolutionary conserved mechanism thought to play an essential role in cell survival during stress—using a rodent model of type 2 diabetes, the Goto Kakizaki (GK) rat.
Methods: Thirty-two weeks old male GK rats and sex/age-matched Wistar controls were treated with liraglutide (0.2 mg/kg/day) or PBS twice daily for 8 consecutive weeks. At 40-weeks of age, cardiac structure/function were assessed by echocardiography and LV tissue samples were collected to assess the expression of inducers/markers of autophagy (mTOR, phospho-mTOR, LC3-I/II, p62, and Beclin-1).

Results: Autophagy was inhibited in the heart of diabetic GK animals when compared to Wistar controls, as confirmed by a significant increase in mTOR expression/activation—a negative regulator of autophagy. This was further confirmed by an observed decrease in the LC3 II/I ratio in diabetic GK animals when compared to controls ($p<0.05$). P62 expression levels, however, were found to be significantly upregulated in GK animals with respect to controls ($p<0.01$); suggesting an impairment or defect in basal autophagy in diabetic GK animals. Liraglutide-treatment—which was associated with an improvement in both HbA1C level and LV hypertrophy in GK animals—resulted a significant reduction in mTOR expression/activation in GK animals when compared to their untreated counterparts. This improvement in autophagy status was further corroborated by an observed increase in LC3 II/I ratio and Beclin-1, as well as a reduction in p62 expression levels.
Conclusion: Overall, our data suggests that the cardioprotective effects of liraglutide may stem from its ability to activate autophagy in the diabetic heart and improve autophagy impairment in the setting of type 2 diabetes.

Disclosures: **A. Bugyei-Twum:** None. **J. Switzer:** None. **K.K. Singh:** None. **K.A. Connelly:** None.

369

Naringenin Supplementation to a Chow Diet Reduces Plasma Lipids and Adiposity, and Suppresses Rer In *Ldlr*$^{-/-}$ Mice Fed a Chow Diet

Amy C Burke, Dawn E Telford, Brian G Sutherland, Jane Y Edwards, Murray W Huff, Robarts Res Inst, London, ON, Canada

Previously, we have shown that intervention by the addition of the citrus flavonoid naringenin to a chow diet enhances the reversal of diet-induced metabolic dysregulation, obesity, and atherosclerosis. However, the metabolic effects of naringenin in the absence of obesity and metabolic dysregulation are unknown. In the present study, we assessed the effect of naringenin supplementation to a chow diet on plasma lipids, adiposity, respiratory exchange ratio (RER), ambulatory activity and tissue lipolysis. For 8 weeks, *Ldlr*$^{-/-}$ mice were fed an isoflavone-free chow diet supplemented with or without 3% naringenin. Over 8 weeks, there was no difference in caloric intake between the two groups. Naringenin supplementation reduced plasma VLDL-cholesterol (C) (-46%; $P<0.05$), VLDL-triglycerides (-43%; $P<0.05$), and LDL-C (-27%; $P<0.05$) compared to mice consuming chow alone. Chow-fed mice maintained body weight, whereas mice fed chow with naringenin were ~1.4 g lighter ($P<0.05$) with significantly reduced adiposity (-48%; $P<0.05$). Histological analysis of epididymal white adipose tissue showed naringenin supplementation reduced adipocyte size and number. Between 6 and 8 weeks of diet, mice were assessed in metabolic cages. Naringenin supplementation had no effect on food intake, ambulatory activity or energy expenditure during both the light and dark cycles. Consistently, naringenin-treated mice had significantly lower RER compared to mice fed chow alone (0.97 vs 0.99; $P<0.05$). This difference was driven by a significant suppression in RER during the light cycle (0.96 vs 1.00; $P<0.05$), but not the dark cycle (0.97 vs 0.98 *N.S*), suggesting an enhanced starvation response. Triglyceride lipolysis was highest in white adipose tissue, followed by liver and muscle. Naringenin supplementation to chow increased the lipolytic rate in adipose, but not in muscle or liver, suggesting reduced adiposity was related to increased expression of ATGL or HSL. In conclusion, compared to chow alone, naringenin supplementation reduced plasma lipids and decreased body weight *via* increased adipose tissue lipolysis and suppressed RER, with no change in energy expenditure.

Disclosures: **A.C. Burke:** None. **D.E. Telford:** None. **B.G. Sutherland:** None. **J.Y. Edwards:** None. **M.W. Huff:** None.

370

Contrast-Induced Nephropathy and Long-Term Outcomes in Patients With Diabetes Undergoing Coronary and Peripheral Angiography and Intervention

Dennis A Hopkinson, Samuel P Powell, Raveen Chawla, Wendy Bottinor, Jeremy S Turlington, Kalpesh Patel, Virginia Commonwealth Univ/McGuire VAMC, Richmond, VA; Peter Danyi, Salem VAMC, Salem, VA; Ion S Jovin, Virginia Commonwealth Univ/McGuire VAMC, Richmond, VA

Background: Patients with diabetes may be at increased risk of contrast-induced nephropathy (CIN) when undergoing coronary and/or peripheral angiography or intervention but there is little data on long-term outcomes. We examined the relationship between diabetes, CIN and long-term outcomes in patients

undergoing coronary and/or peripheral angiography and intervention. Methods and Results: We studied 4070 consecutive, predominantly (98%) male patients undergoing coronary and peripheral angiography and intervention and assessed the association between diabetes, CIN and long-term outcomes including renal dysfunction at 3 months, the need for dialysis and mortality. The mean age of the patients was 66.6 years. Approximately two fifths of the patients (n=1671, 41.05%) were diabetic. Patients with diabetes were the same age but had higher baseline creatinine compared to the patients without diabetes. CIN occurred in 70 (4.19%) diabetic patients and in 64 (2.67%) patients without diabetes at 72 hours after the procedure (odds ratio [OR] 1.59; 95% confidence interval [CI] 1.13 - 2.25; P=0.008). At 3 months, renal dysfunction was seen in 179 (10.71%) diabetic patients versus 174 (7.25%) of the non-diabetic group (OR 1.53, CI 1.23 - 1.91; P=0.0001). After a follow-up of 5 years, 31 (1.86 %) patients with diabetes had developed end-stage renal disease and were started on dialysis versus 13 (0.54 %) of the non-diabetic group (OR 3.47, CI 1.81 - 6.65; P<0.0001). 478 (28.61 %) patients of the diabetic group had died versus 479 (19.97 %) of the non-diabetic group (OR 1.61, CI 1.39 - 1.86; P<0.0001). On multivariate analysis, after adjustment for age, comorbidities, medical therapy and baseline creatinine, the presence of diabetes was significantly associated with CIN (OR 1.50, CI 1.06 - 2.43: p=0.02) and was significantly associated with the incidence of end stage renal disease requiring dialysis (OR 3.64, CI 2.07-10.04; P<0.0001) and with mortality at 5 years (OR 1.58, CI 1.42-2.03, P<0.0001). Conclusion: In this cohort of patients undergoing coronary and/or peripheral angiography and intervention diabetes was associated with CIN, with end-stage renal disease and the need for hemodialysis and was associated with an increased mortality.

Disclosures: **D.A. Hopkinson:** None. **S.P. Powell:** None. **R. Chawla:** None. **W. Bottinor:** None. **J.S. Turlington:** None. **K. Patel:** None. **P. Danyi:** None. **I.S. Jovin:** None.

371

Deficiency in Microrna-155 Leads to Reduced Atherosclerosis, Increased Obesity and Nonalcoholic Fatty Liver Disease--A Novel Mouse Model of Metabolically Healthy Obesity

Candice Johnson, Anthony Virtue, Jahaira Lopez-Pastraña, Ying Shao, Hangfei Fu, Xinyuan Li, Ya-Feng Li, Ying Yin, Jietang Mai, Victor Rizzo, Michael Tordoff, Zsolt Bagi, Huimin Shan, Xiaohua Jiang, Hong Wang, Xiao-Feng Yang, Lewis Katz Sch of Med at Temple Univ, Philadelphia, PA

Metabolically healthy obesity (MHO) describes the phenomenon of overweight and obese patients paradoxically retaining a healthy metabolic profile. The molecular mechanisms underlying MHO remain enigmatic partly due to a dearth of animal models mirroring MHO in patients. Using apolipoprotein E knockout ($ApoE^{-/-}$) mice on high-fat (HF) diet as an atherosclerotic obesity model, we demonstrated: 1) microRNA-155 (miRNA-155, miR-155) is significantly upregulated in aortas of $ApoE^{-/-}$ mice; and miR-155 deficiency in $ApoE^{-/-}$ mice inhibits atherosclerosis; 2) $ApoE^{-/-}$/$miR\text{-}155^{-/-}$ (DKO) mice show HF diet-induced obesity, adipocyte hypertrophy and present with nonalcoholic fatty liver disease (NAFLD); 3) DKO mice demonstrate HF diet-induced elevations of plasma leptin, resistin, fed-state and fasting insulin, increased expression of adipogenic transcription factors, but lack glucose intolerance and insulin resistance. Our results are the first to present a metabolically healthy obesity (MHO) model using DKO mice with features of decreased atherosclerosis, increased obesity and NAFLD. Our findings suggest the mechanistic role of reduced miR-155 expression in MHO and present a new MHO working model based on a single miRNA deficiency in diet-induced obese atherogenic mice. Furthermore, our results serve as a breakthrough in understanding the potential mechanism underlying MHO and provide a new biomarker and novel therapeutic target for MHO-related metabolic diseases.

Disclosures: **C. Johnson:** None. **A. Virtue:** None. **J. Lopez-Pastraña:** None. **Y. Shao:** None. **H. Fu:** None. **X. Li:** None. **Y. Li:** None. **Y. Yin:** None. **J. Mai:** None. **V. Rizzo:** None. **M. Tordoff:** None. **Z. Bagi:** None. **H. Shan:** None. **X. Jiang:** None. **H. Wang:** None. **X. Yang:** None.

This research has received full or partial funding support from the American Heart Association.

372

PPARα/γ Agonist Tesaglitazar Reduces Inflammatory Macrophage Numbers And Induces Adipose Ucp-1 Expression In Diabetic Ob/ob Mice

Victoria Osinski, Univ of Virginia, Charlottesville, VA; Matthew Harms, Jeremie Boucher, AstraZeneca, Mölndal, Sweden; Coleen McNamara, Univ of Virginia, Charlottesville, VA

Rationale: PPARα/γ agonist tesaglitazar effectively improves insulin sensitivity and dyslipidemia in diabetic mice and human subjects. The cellular and molecular mechanisms whereby this occurs remain unclear. Given the established expression of PPARs in macrophages and *in vitro* findings demonstrating attenuated inflammation with PPAR agonism, we hypothesized that tesaglitazar attenuates macrophage-mediated inflammation within the adipose to improve metabolic outcomes in diabetic mice. Methods & Results: To validate that tesaglitazar reduces diabetic symptoms, we treated Ob/ob mice with tesaglitazar or vehicle control for one week and observed significant reductions in fasting blood glucose, insulin, and triglyceride levels with drug treatment when compared to vehicle treatment. Using flow cytometry, we determined that treatment with tesaglitazar results in reduced numbers of total macrophages (CD45+CD11b+F4/80+) in the epididymal and subcutaneous adipose depots. Furthermore, this reduction in macrophages numbers is primarily due to reduced numbers within the M1, or pro-inflammatory, compartment (CD11b+F4/80+CD11c+CD206-) of the macrophage population. Given the established role of inflammation in inhibiting adipocyte Ucp-1 expression, we measured Ucp-1 expression levels in epididymal adipocytes and observed a significant induction of Ucp-1 mRNA expression with tesaglitazar treatment. Conclusion: As anticipated, treatment with tesaglitazar improves insulin sensitivity and dyslipidemia in Ob/ob mice. Interestingly, tesaglitazar treatment also reduced the number of inflammatory macrophages in adipose and induced adipocyte Ucp-1 mRNA expression. Taken together, our findings suggest that tesaglitazar has anti-inflammatory effects indicated by reduced numbers of pro-inflammatory macrophages and increased thermogenic capacity as seen by increased Ucp-1 expression.

Disclosures: **V. Osinski:** None. **M. Harms:** Employment; Significant; Employed at AstraZeneca. **J. Boucher:** Employment; Significant; Employed at AstraZeneca. **C. McNamara:** None.

374

Interleukin-19: A Novel Pro-Angiogenic and Anti-Inflammatory Adipokine

Christine Vrakas, Sheri E Keleman, Rosario Scalia, Michael V Autieri, Lewis Katz Sch of Med, Philadelphia, PA

Uncontrolled inflammation leads to many of the chronic diseases associated with obesity. Due to a lack of oxygen in the tissue, expanding adipose tissue becomes hypoxic and pro-inflammatory. Adipocytes release pro-angiogenic factors in an effort to restore blood flow to the tissue. Presently, little is known about the potential for endogenously expressed anti-inflammatory cytokines to attenuate inflammation and also provide pro-angiogenic effects. IL-19 is uniquely anti-inflammatory, pro-angiogenic and is both expressed by and targets various cells types. IL-19 expression in adipocytes and stromal vascular cells is increased in visceral compared to subcutaneous fat, and is also increased in visceral fat on high fat diet (HFD) compared to normal chow diet. There is no known mechanism to explain the role of IL-19 in adipose tissue expansion, and we hypothesized that IL-19 may have pro-angiogenic and anti-inflammatory properties in expanding adipose tissue. We have identified a gene regulatory factor, Interleukin Enhancer-Binding Factor 3 (ILF3) that is induced in adipocytes and stromal vascular cells by HFD and IL-19 treatment. We found that both IL-19 and VEGF induce ILF3 expression in cultured human endothelial cells (hECs). Proliferation is significantly reduced when ILF3 is knocked down using siRNA in hECs. Furthermore, when ILF3 is knocked down and hECs are stimulated with VEGF several angiogenic cytokines are also decreased. Through immunohistochemistry we found that ILF3 translocates from the nucleus to the cytoplasm in visceral fat of C57BL/6 mice fed a HFD, and remains in the nucleus when fed a normal chow diet. In summary IL-19 may be a unique HFD responsive adipokine functioning to reduce inflammation and increase angiogenesis in expanding adipose tissue. The angiogenic function of IL-19 may work through induction of the gene regulatory factor, ILF3.

Disclosures: **C. Vrakas:** None. **S.E. Keleman:** None. **R. Scalia:** None. **M.V. Autieri:** None.

375

The Intergenic Long Non-Coding RNA RP11-472n13.3 Modulates Interferon-Gamma Signaling and M1 Macrophage Activation

Ying Wang, Chenyi Xue, Muredach Reilly, Hanrui Zhang, Columbia Univ, New York, NY

We aim to interrogate the functions of a subset of human macrophage intergenic long non-coding RNA (lincRNAs) which harbor cardiometabolic trait-associated single nucleotide polymorphisms (SNPs). We have found that one lincRNA RP11-472N13.3 overlaps rs7081678, a SNP significantly associated with central obesity (WHRadjBMI; P=5.57x10^{-6}). RP11-472N13.3 expression is enriched in macrophages relative to other obesity relevant tissues. Thus, RP11-472N13.3 SNPs for obesity may act via its myeloid cell modulation in adipose. In human monocyte-derived macrophage (HMDM), human induced pluripotent stem cell-derived macrophages (IPSDM) and THP1-derived macrophages (THP-1Φ), at RNAseq and Q-PCR, RP11-472N13.3 is abundant in M0 and M2(IL-4) macrophages but markedly suppressed in the M1 state (LPS/IFNγ). RP11-472N13.3 localizes almost exclusively to the cytoplasmic fraction of M0-HMDM. Consistent with GENCODE, our HMDM RNAseq data suggest a single 2-exon isoform. ChIP-seq reveals PU.1 and C/EBP-β binding at RP11-472N13.3 transcription start site. In our HMDM RNAseq (n=30 subjects) data, RP11-472N13.3 expression was inversely correlated with IFNγ-JAK-STAT signaling genes (e.g., *IRF4, IL-12A, IL-23, STAT1, SOCS1, SOCS3*), but not LPS/TLR4 activated genes (e.g., *TNFA, CXCL9, CXCL10, IL1B*)**.** Furthermore, KD of RP11-472N13.3 using siRNA or LNA-ASO in THP-1Φ, amplified expression of IFNγ target genes but not LPS/TLR4 targets during M1 activation (LPS/IFNγ). These data suggest its potential role in modulating IFNγ signaling. Mechanistic studies are needed to examine the molecular mechanisms.

Disclosures: **Y. Wang:** None. **C. Xue:** None. **M. Reilly:** None. **H. Zhang:** None.

This research has received full or partial funding support from the American Heart Association.

376

Nedd4 Regulated Bk Channels in Diabetes Mellitus

DAI-MIN ZHANG, Shao-liang Chen, Yanrong Zhu, Peng Ye, Nanjing First Hosp, Nanjing Medical Univ, Nanjing, China

Big conductance calcium activated potassium(BK) channel plays a critical role in pathophysiological regulation of vascular function. Recent studies indicated that the expression reduction of BK channels in high glucose condition exacerbated vessel dilation, and led to coronary artery diseases, while BK channel expression was reserved in A-kinase anchoring protein(AKAP) knockout mice at same condition. Here, We are to investigate heterologous co-expression of Nedd4 ligase, ubiquitin protein ligase, and KCa1.1 in HEK293 cells. The result shown that co-expression reduced BK current density without modulation of kinetic properties as measured by path clamp techniques. Modulation of current density was dependent on ligase activity and was lost in AKAP knockout mice with diabetes mellitus. Taken together, our data disclose a novel mechanism of KCa1.1 channel regulation that NEDD4 decreased BK channels expression in diabetes mellitus depending on AKAP signal complexity. These findings provide a new insight into potential therapeutic target in vascular diseases, especially in diabetes mellitus.This work was supported by the National Natural Science Foundation of China(Grant No. 8137034)

Disclosures: **D. Zhang:** None. **S. Chen:** None. **Y. Zhu:** None. **P. Ye:** None.

377

Mast Cell Serotonin Controls Subcutaneous Adipose Tissue Browning and Systemic Energy Expenditure in Mice

Xian Zhang, Dept of Med, Brigham and Women's Hosp and Harvard Medical Sch, Boston, MA; Xin Wang, Sch of Biotechnology & Food Engineering, Hefei Univ of Technology, Hefei, China; Guo-Ping Shi, Dept of Med, Brigham and Women's Hosp and Harvard Medical Sch, Boston, MA; Jian Liu, Sch of Biotechnology & Food Engineering, Hefei Univ of Technology, Hefei, China

Adipose tissue browning and systemic energy expenditure provide a defense mechanism against obesity and associated metabolic diseases. In western diet-fed mice, inactivation of mast cells (MCs) ameliorates

obesity and insulin resistance along with improved metabolic rate. Yet, a direct role of MCs in adipose tissue thermogenesis and browning remains unclear. Here we report that, in the context of mice on a chew diet, norepinephrine (NE)-stimulated metabolic rate is increased in MC-deficient *Kit*$^{w\text{-}sh/w\text{-}sh}$ mice and MC-stabilized wide-type (WT) mice. Such functional inactivation of MCs enhances thermogenesis and browning in subcutaneous adipose tissues (SAT), but not in brown (BAT) and epididymal adipose tissues (EAT). MC reconstitution to SAT blocks the aforesaid changes in *Kit*$^{w\text{-}sh/w\text{-}sh}$ mice. Mechanistic studies demonstrate that functional inactivation of MCs not only elevates the numbers of PDGFRα^{+} bipotential adipocyte precursors but also accelerates beige adipocyte differentiation in SAT. Using tryptophan hydroxylase 1 inhibitor, we show that MC-derived serotonin inhibits SAT beige adipocyte biogenesis and systemic energy expenditure. Together, functional inactivation of MCs or inhibition of MC serotonin synthesis in SAT promotes adipocyte browning and systemic energy metabolism in mice.

Disclosures: **X. Zhang:** None. **X. Wang:** None. **G. Shi:** None. **J. Liu:** None.

378

Red Blood Cells from Patients With Type 2 Diabetes Induce Endothelial Dysfunction Through Up-Regulation of Arginase I

Zhichao Zhou, Ali Mahdi, Yahor Tratsiakovich, Oskar Kövamees, Jiangning Yang, John Pernow, Karolinska Instt, Stockholm, Sweden

We previously showed that increased arginase activity is a key mechanism for endothelial dysfunction in patients with type 2 diabetes mellitus (T2DM) thereby arginase inhibition improves endothelial function. Recently, we demonstrated a crucial role of red blood cells (RBCs) in control of cardiac function via an arginase-dependent regulation of nitric oxide export from RBCs, suggesting a direct interaction of RBCs with cardiovascular function. Considering an increase in arginase activity in T2DM, we hypothesized that RBCs induce endothelial dysfunction in T2DM via up-regulated arginase I. Healthy rat aortas were incubated with RBCs from patients with T2DM (T2DM-RBCs) and age-matched healthy subjects (H-RBCs) for 18 h in the absence and presence of the arginase inhibition or scavenging of reactive oxygen/nitrogen species (ROS/RNS). Following the incubation, endothelium-dependent and -independent relaxations (EDR and EIR) were determined using wire myograph. Human internal mammary arteries (IMAs) obtained from non-diabetic patients who underwent cardiac surgery were also incubated with RBCs for functional evaluation. Arginase activity and protein expression were determined in RBCs. EDR was impaired in vessels incubated with T2DM-RBCs (Emax: 43.2±3.0% in aortas, n=8; 32.3±2.7% in IMAs, n=3) but not H-RBCs (Emax: 74.3±3.4% in aortas; 71.5±5.1% in IMAs) in comparison with buffer (Emax: 74.4±2.3% in aortas; 73.1±5.0% in IMAs; $P<0.01$ vs. T2DM-RBCs). EIR was not affected by T2DM-RBCs. The impairment in EDR in rat aortas was fully reversed by inhibition of arginase, ROS and RNS in RBCs. Arginase activity was significantly elevated in T2DM-RBCs. The increased arginase activity was attributed to arginase I, as there was increased arginase I expression in RBCs, whereas no arginase II expression was detected. Moreover, high glucose and RNS stimulation increased arginase activity in H-RBCs, while ROS/RNS scavenging decreased arginase activity in T2DM-RBCs. This study demonstrates a novel mechanism behind endothelial dysfunction that T2DM-RBCs induce endothelial dysfunction via ROS/RNS-dependent up-regulation of arginase I. Targeting arginase I in RBCs may serve as a novel therapeutic tool for treatment of endothelial dysfunction in T2DM.

Disclosures: **Z. Zhou:** None. **A. Mahdi:** None. **Y. Tratsiakovich:** None. **O. Kövamees:** None. **J. Yang:** None. **J. Pernow:** None.

380

SAA Lipidation and Delipidation by Hepatocytes

Ailing Ji, Akinwunmi Akinmusire, Maria C de Beer, Frederick C de Beer, Nancy R Webb, Deneys R van der Westhuyzen, Univ of Kentucky, Lexington, KY

Serum amyloid A (SAA) is one of the most striking acute phase reactants that can rapidly increase 1000-fold in plasma concentration in response to inflammatory cytokines. SAA in lipid-free form exhibits pro-inflammatory activities, but its putative physiological function(s) are poorly understood. SAA is produced and secreted largely by the liver and is present in plasma mainly as an HDL apolipoprotein. The pathways by which SAA is lipidated and incorporated into HDL are poorly understood. Plasma SAA is cleared more rapidly than the other major HDL apolipoproteins, but pathways involved in its delipidation and plasma

clearance have also not been defined. In this study we examined how SAA is lipidated in primary hepatocytes and how such lipidation relates to the formation of nascent HDL particles. Endogenous hepatocyte SAA was lipidated and released from cells as large particles that were distinct from apoA-I-containing nascent HDL's. Unlike apoA-I, formation of these SAA-containing particles was independent of ABCA-I. Similarly, when SAA was exogenously added to cells, SAA was lipidated to form nascent particles that were distinct from apoA-I-containing particles. We further studied the interaction of lipid-free and HDL-bound SAA with hepatocytes. Both in lipid-free form and as part of HDL, SAA exhibited significantly greater binding to cells than apoA-I or apoA-II. Binding studies were also carried out with normal and acute phase HDL's isolated from control and SAA-deficient mice. Together, the results suggested that SAA, unlike apoA-I, is selectively removed from HDL by binding to hepatocytes. These findings may provide new insights into SAA metabolism and function.

Disclosures: **A. Ji:** None. **A. Akinmusire:** None. **M.C. de Beer:** None. **F.C. de Beer:** None. **N.R. Webb:** None. **D.R. van der Westhuyzen:** None.

381

Ideal Cardiovascular Health and Cardiovascular Disease: Heterogeneity Across Event Phenotype and Contribution of Multiple Biomarkers

Bamba Gaye, French Inst of Health and Medical Res, Paris, France; Muriel Tafflet, INSERM, U970, Paris Cardiovascular Res Ctr, Dept of Epidemiology AND Univ Paris Descartes, Sorbonne Paris Cité, Faculté de Médecine, Paris, France; Dominique Arveil, The Strasbourg MONICA Project, Lab d'épidémiologie et de santé publique, EA 3430, Fédération de Médecine Translationnelle de Strasbourg, Univ de Strasbourg, Strasbourg, France, Strasbourg, France; Frank Kee, The UKCRC Ctr of Excellence for Public Health (NI), The Queen's Univ, Belfast-Northern Ireland, Belfast, Ireland; Alun Evans, The UKCRC Ctr of Excellence for Public Health (NI), The Queen's Univ, Belfast-Northern Ireland, Belfast-Northern, Ireland; Philippe Amouyel, The Lille MONICA Project, INSERM, U1167, Inst Pasteur de Lille, Univ Nord de France, UDSL, Lille, 5900, France, Paris, France; Jean Ferrieres, The Toulouse MONICA Project, Toulouse Univ Sch of Med, INSERM UMR 1027, Toulouse, France, Toulouse, France; Jean-Philippe Empana, INSERM, U970, Paris Cardiovascular Res Ctr, Dept of Epidemiology AND Univ Paris Descartes, Sorbonne Paris Cité, Faculté de Médecine, Paris, France

Aims: To investigate whether or not the association between baseline cardiovascular health (CVH) and incident cardiovascular disease (CVD) differs by event phenotypes and to address the mediating effect of inflammatory and haemostatic blood biomarkers.
Methods: The association of ideal CVH with outcomes was computed in 9312 middle-aged men from Northern Ireland and France (whole cohort) in multivariable Cox proportional hazards regression analysis. The mediating effect of baseline blood biomarkers was evaluated in a case control study nested within the cohort after 10 years of follow-up.
Results: After a median follow-up of 10 years, 614 first CHD events and 117 first stroke events were adjudicated. Compared to those with poor CVH, those with an ideal CVH profile at baseline had a 72% lower risk of CHD (HR=0.28; 95% CI: 0.17; 0.46) and a 76% lower risk of stroke (HR=0.24; 95% CI: 0.06; 0.98). No heterogeneity was detected across main CHD and main stroke phenotypes. While significantly lower mean concentrations of hs-CRP, IL-6 (inflammatory markers), and fibrinogen, von Willbrandt factor (haemostatic factors) were noted in the controls with higher CVH status, the association of CVH with incident CHD was not attenuated upon adjustment for these biomarkers.
Conclusion: these results support the universal promotion of ideal CVH for CVD in general and suggest that the lower risk of CHD associated with ideal CVH is independent from inflammatory and haemostatic biomarkers.

Disclosures: **B. Gaye:** None. **M. Tafflet:** None. **D. Arveil:** None. **F. Kee:** None. **A. Evans:** None. **P. Amouyel:** None. **J. Ferrieres:** None. **J. Empana:** None.

382

Transgenic Overexpression of Dimethylarginine Dimethylaminohydrolase 1 Protects from Angiotensin II-induced Cardiac Hypertrophy

Roman N. Rodionov, Silke Brilloff, Natalia Jarzebska, Anne Kolouschek, Univ Ctr for Vascular Med, Technische Univ Dresden, Dresden, Germany; Jens Martens-Lobenhoffer, Stefanie M. Bode-Böger, Inst of Clinical Pharmacology, Otto-von-Guericke Univ, Magdeburg, Germany; Norbert Weiss, Univ Ctr for Vascular Med, Technische Univ Dresden, Dresden, Germany; Andreas Deussen, Irakli Kopaliani, Inst of Physiology, Technische Univ Dresden, Dresden, Germany

Background: ADMA (asymmetric dimethylarginine) is an endogenous inhibitor of nitric oxide synthase. ADMA can be metabolized to citrulline by dimethylarginine dimethylaminohydrolase (DDAH). DDAH1 overexpression lowers ADMA and protects from angiotensin II - induced renal interstitial fibrosis and vascular oxidative stress. The goal of the current study was to test the hypothesis that transgenic overexpression of DDAH1 protects from angiotensin II-induced cardiac hypertrophy. **Methods and Results**: DDAH1 transgenic mice grew and developed normally and had decreased plasma ADMA levels. Angiotensin II was infused for four weeks in the dose of 0.75 mg/kg/day in DDAH1 transgenic mice and wild type littermates via osmotic minipumps. Echocardiography was performed in the first and fourth week after start of the infusion on anaesthetized mice. After 4 weeks of angiotensin II infusion wild type mice developed cardiac hypertrophy. The DDAH1 transgenic mice had higher left ventricular lumen to wall ratio compared to the wild type mice (1.76 ± 0.18 vs 1.15 ± 0.22, $P<0.01$). They also had lower left ventricular posterior wall thickness in systole and diastole as compared to the wild type controls (1.18 ± 0.03 mm vs 1.95 ± 0.16 mm, $P<0.001$ and 0.81 ± 0.03 mm vs 1.62 ± 0.25 mm, $P<0.001$, respectively). **Conclusion**: We demonstrated that upregulation of DDAH1 protects from angiotensin II-induced cardiac hypertrophy. Our findings suggest that ADMA plays a role in angiotensin II - induced myocardial remodeling. Upregulation of DDAH1 might be a potential approach for protection from angiotensin II - induced end organ damage.

Disclosures: **R.N. Rodionov:** None. **S. Brilloff:** None. **N. Jarzebska:** None. **A. Kolouschek:** None. **J. Martens-Lobenhoffer:** None. **S.M. Bode-Böger:** None. **N. Weiss:** None. **A. Deussen:** None. **I. Kopaliani:** None.

383

Patient-Specific Coronary Models Combining Intravascular Ultrasound and Optical Coherence Tomography Lead to More Accurate Plaque Cap Thickness and Stress/Strain Quantifications

Xiaoya Guo, Southeast Univ, Nanjing, China; David Monoly, Emory Univ Sch of Med, Atlanta, GA; Chun Yang, China United Network Comm. Co., Ltd., Beijing, China; Habib Samady, Emory Univ Sch of Med, Atlanta, GA; Jie Zheng, Washington Univ, St. Louis, St. Louis, MO; Liang Wang, Worcester Polytechnic Inst, Worcester, MA; Gary S Mintz, Akiko Maehara, The Cardiovascular Res Fndn, Columbia Univ, New York, NY; Xuan Pei, Zhi-Yong Li, Southeast Univ, Nanjing, China; **Dalin Tang**, Worcester Polytechnic Inst, Worcester, MA; Don P Giddens, Georgia Inst of Technology, Atlanta, GA

Accurate cap thickness and stress/strain quantifications are of fundamental importance for vulnerable plaque research. An innovative modeling approach combining intravascular ultrasound (IVUS) and optical coherence tomography (OCT) is introduced for more accurate patient-specific coronary morphology and stress/strain calculations.
In vivo IVUS and OCT coronary plaque data were acquired from two patients with informed consent obtained. IVUS and OCT images were segmented, co-registered, and merged to form the IVUS+OCT data set, with OCT providing accurate cap thickness. Biplane angiography provided 3D vessel curvature. Due to IVUS resolution (150 μm), original virtual histology (VH) IVUS data often had lipid core exposed to lumen since it sets cap thickness as zero when cap thickness <150 μm. VH-IVUS data were processed with minimum cap thickness set as 50 and 180 μm to generate IVUS50 and IVUS180 data sets for modeling use. 3D fluid-structure interaction models based on IVUS+OCT, IVUS50 and IVUS180 data sets were constructed to investigate the impact of OCT cap thickness improvement on stress/strain calculations.
Figure 1 is a brief summary of results from 27 slices with cap covering lipid cores from 2 patients. Mean cap thickness (unit: mm) from Patient 1 was 0.353 (OCT), 0.201 (IVUS50), and 0.329 (IVUS180), respectively. Patient 2 mean cap thickness was 0.320 (OCT), 0.224 (IVUS50), and 0.285 (IVUS180). IVUS50 underestimated cap thickness (27 slices) by 34.5%, compared to OCT cap values. IVUS50

overestimated mean cap stress (27 slices) by 45.8%, compared to OCT cap stress (96.4 vs. 66.1 kPa). IVUS50 maximum cap stress was 59.2% higher than that from IVUS+OCT model (564.2 vs. 354.5 kPa). Differences between IVUS and IVUS+OCT models for mean cap strain and flow shear stress were modest (cap strain: <12%; FSS <2%).
Conclusion. IVUS+OCT data and models could provide more accurate cap thickness and stress/strain calculations which will serve as basis for plaque research.

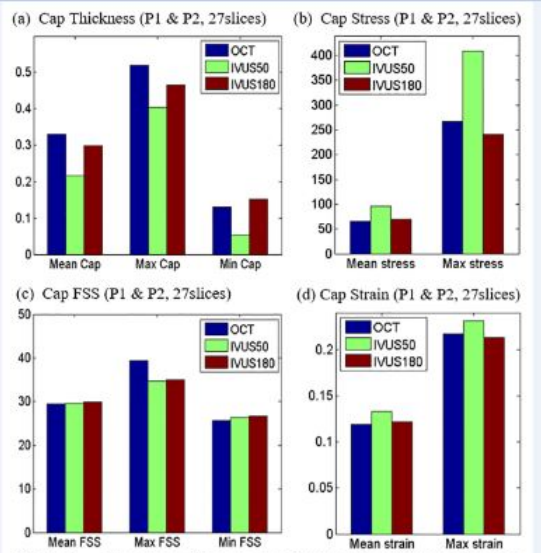

Figure 1. Bar plots of mean, maximum and minimum slice cap thickness, cap stress, strain and flow shear stress (FSS) from 27 slices showing differences from IVUS+OCT, IVUS50 and IVUS180 models. Units: cap: mm; stress: kPa; FSS: dyn/cm^2. Mean cap thickness and max cap thickness are average of slice values. Min cap thickness is min of slice min cap thickness.

Disclosures: **X. Guo:** None. **D. Monoly:** None. **C. Yang:** None. **H. Samady:** None. **J. Zheng:** None. **L. Wang:** None. **G.S. Mintz:** None. **A. Maehara:** None. **X. Pei:** None. **Z. Li:** None. **D. Tang:** Research Grant; Modest; NIH grant R01 EB004759, Jiangsu Province Science and Technology Agency grant BE2016785. **D.P. Giddens:** None.

384

Low Carbohydrate High Protein (LCHP) Diets are Atherogenic by Supplying Excess Amino Acids to Alter the Macrophage mTORC1-Autophagy Signaling Axis

Xiangyu Zhang, Ismail Sergin, Trent Evans, Washington Univ Sch of Med, St. Louis, MO; Astrid Rodríguez Vélez, Univ of Puerto Rico at Mayagüez, Mayagüez, Puerto Rico; Babak Razani, Washington Univ Sch of Med, St. Louis, MO

Low carbohydrate high protein (LCHP) diets are commonly used in weight loss programs. However, the overall health benefits of such regimens are controversial with recent studies even suggesting an increased cardiovascular risk in certain populations. A few reports in animal models corroborate these concerns demonstrating increased LCHP-induced atherosclerosis. Interestingly, the downstream sequelae of such diets on tissues and cellular signaling are largely inferred with relevant mechanisms undefined. We first confirmed in the ApoE-null mouse model that LCHP diets are indeed atherogenic with the development of complex lesions. Using mass spectrometry, we find high protein feeding not only increases serum amino acid levels but increases amino acid load to tissues including the spleen and aorta with resultant activation of the mTORC1 signaling pathway particularly in macrophages. The involvement of mTORC1 is clearly causal as the atherogenic effect of LCHP-feeding is abrogated in macrophage-specific Raptor-null mice. Further mechanistic evaluation of the effects of amino acids on macrophages reveals dichotomous roles on a predominant mTORC1 target, autophagy. Certain amino acids such as Leucine potently activate mTORC1 via recruitment to lysosome and in turn suppress autophagy via ULK1 phosphorylation, whereas others such as glutamine act indirectly by downregulating the transcription of autophagy chaperones including p62/SQSTM1. This combined suppressive effect on autophagy leads to macrophage inflammasome activation and IL-1β release, accumulation of deleterious

protein aggregates, and increased cell death. The in vivo relevance of this LCHP-amino acid-mTORC1-autophagy axis is supported by 1) the absence of increased atherosclerosis in macrophage autophagy-deficient (ATG5-/-) mice fed a LCHP diet, and 2) the absence of reduced atherosclerosis in mice dually deficient in macrophage mTORC1 and autophagy (Raptor/ATG5-/-). Our data provide the first mechanistic details of the deleterious effects of high protein diets on macrophages and the development of atherosclerosis. Incorporation of these concepts in clinical studies will be important to define the vascular effects of dietary protein.

Disclosures: **X. Zhang:** None. **I. Sergin:** None. **T. Evans:** None. **A.R. Vélez:** None. **B. Razani:** None.

385

The Complex Nature of High-Density Lipoprotein Particle Diversity and Population Heterogeneity Necessitates High-Definition Constituent Identification and an Organizational Atlas

Steven G Fried, **Scott W Altmann**, HDL Apomics, Allenhurst, NJ

Introduction: The degree of lipoprotein complexity was unforeseen just a few years ago. Through advances in mass spectrometry it is now recognized that HDL is comprised of >100 proteins and ~200 lipid species in an undetermined number of combinations. These constituents exist in a distribution disequilibrium with each other and to the particle population as a whole. Concealed in this complex particle composition is extensive particle diversity and population heterogeneity and the source of the broad physiology observed with this lipoprotein subclass.
Hypothesis: Science is a systematic enterprise that using mathematics and measurement, creates, builds and organizes knowledge in the form of testable observations, explanations and predictions. The ongoing identification of HDL constituents necessitates an effort to catalogue, categorize, map and relate entities in a structured framework. This will lead to fundamental understanding that advances knowledge and guides HDL biological research, clinical diagnostics and eventual therapeutic strategies.
Methods: Literature analysis was used to produce an HDL proteome reference set. Proteome specific analysis of isoforms, proteolytic products, amino acid modifications and cSNPs were used to prepare a proteoform index. Theoretical tryptic peptide maps were generated and compared to the PeptideAtlas database and available published peptide lists from mass spec studies.
Results: More than 300 non-immunoglobulin proteins were identified from the high-density lipoprotein fraction in published human sample studies. A consensus-based selection process produced an “unofficial” list of 122 genes. UniProtKB was used to expand an index of possible proteoforms and derive a theoretical peptide mass map. The theoretical and empirical mass map demonstrate both consistency and significant differences.
Conclusions: The health benefits of HDL are not in dispute. However, its predictive value is being challenged. The reductionist approach to measuring HDL has proven insufficient and undermines the use of a Precision Medicine model for CAD. Constructing a conceptual framework to unify constituent data is an initial step to resolving the relational context that exists and its functional consequences.

Disclosures: **S.G. Fried:** None. **S.W. Altmann:** Ownership Interest; Significant; Founder/CSO - HDL Apomics.

386

Correlations Between Cardiovascular Disease Risk Factors and Lipid Metabolic Pathways

John R Barr, Zsuzsanna Kuklenyik, Michael Gardner, Christopher Toth, Bryan A. Parks, Jeffery Jones, David Schieltz, Ctrs for Disease Control and Prevention, Atlanta, GA; Michael Andrews, Battelle, Atlanta, GA; Jon Rees, Lisa McWilliams, James L. Pirkle, Ctrs for Disease Control and Prevention, Atlanta, GA

A multiplexed, quantitative analytical workflow was applied to 120 fasting human serum samples collected from 30 normolipidemic, and 90 dyslipidemic donors. The analysis included separation by asymmetric flow field-flow fractionation while collecting fractions with ~1 nm increments of 7-15 nm (HDL), 20-30 nm (LDL) and greater than 30 nm lipoproteins. Size separation was followed by concentration measurements in each size fraction for non-polar lipids (FC, CE and TG), polar lipids (PC, SM, PE and PI), and apolipoproteins (apos A-I, A-II, A-IV, B, C-I, C-II, C-III and E); using three parallel, high throughput, quantitative liquid chromatography-tandem mass spectrometry methods developed in our laboratory. The average hydrodynamic size in each size fraction was also determined by dynamic light scattering. Measuring all major lipid and protein components and the size in all fractions allowed volumetric

estimation of lipoprotein particle numbers (Lp-P). In the LDL size range of 22-26 nm, the calculated mean (N=120 samples) of the average (N=5 fraction/sample) apoB/LDL-P was 1.00 (Stdev=0.31, N=120). The resulting highly comprehensive data set allowed the evaluation of correlations between cardiovascular disease (CVD) risk factors and metabolic pathway specific indicators. For example, multivariate modelling of Total-TG/HDL-C ratios (1.5-17.5) showed negative correlation with HDL-apoC-III/LDL-apoC-III ratios ([Prob>|t|]=0.037) and Total-PC/Total-SM ratios ([Prob>|t|]=0.106) while positive correlation with Total-FC/Total-SM ratios ([Prob>|t|]=0.0125). Correlations in size fractions were also evaluated with [Prob>|t|] criteria <0.1. ApoC-III/Lp-P had positive correlation with both HDL-P and LDL-P levels. ApoC-I/Lp-P correlated negatively with HDL-P but positively with LDL-P levels. ApoE/LDL-P correlated negatively with HDL-P and LDL-P levels but positively with Lp-P in greater than 30 nm size fractions. The models also revealed significant apoC-I/Lp-P*apoC-II/Lp-P, apoC-I/Lp-P*apoC-III/Lp-P, and apoC-III/Lp-P*apoE/Lp-P cross effects. We plan the application of this workflow to samples with known history of atherosclerosis and contribute to the understanding of links between CVD risk and lipid metabolic pathways.

Disclosures: **J.R. Barr:** None. **Z. Kuklenyik:** None. **M. Gardner:** None. **C. Toth:** None. **B.A. Parks:** None. **J. Jones:** None. **D. Schieltz:** None. **M. Andrews:** None. **J. Rees:** None. **L. McWilliams:** None. **J.L. Pirkle:** None.

387

HDL-apolipoprotein A-I Exchange Occurs in the Absence of HDL Particle Remodeling

Mark S Borja, Armen Phelps, Michael N Oda, Children's Hosp Oakland Res Inst, Oakland, CA

Objective: Apolipoprotein A-I (apoA-I) spontaneously exchanges between high-density lipoprotein (HDL)-bound and lipid-free states. This is a key event in reverse cholesterol transport, necessary for *de novo* HDL biogenesis. However, the mechanism of HDL-apoA-I exchange (HAE) is poorly understood. In this study, we test whether HDL remodeling is obligatory to HAE or an independent process.
Method and Results: Recombinant human apoA-I modified with single cysteine mutations were expressed in bacteria and labeled with Alexa 488 and Alexa 647 fluorophores. ApoA-$I_{Alexa647}$ was used to synthesize rHDL particles of defined sizes with phosphatidyl choline (POPC) and cholesterol. Reconstituted HDL of 17.0, 12.2, 9.6, 8.4 and 7.8 nm were obtained. These particles were incubated with excess lipid-free apoA-$I_{Alexa488}$ to initiate HAE, which was quantified using non-denaturing gradient gel electrophoresis to separate HDL particles from lipid-free apoA-I. Gels were imaged using FITC and Cy5 filters. The extent of apoA-$I_{Alexa488}$ binding and apoA-$I_{Alexa647}$ released from HDL was determined by densitometry. HAE occurred without significant changes in rHDL particle size for all subclasses of rHDL. HAE in the forward (lipid-free to bound) direction did not exhibit size dependence, but HAE in the reverse (lipid-bound to free) direction appeared to be size-dependent, with the 8.4 nm rHDL displaying 2-fold higher apoA-$I_{Alexa647}$ dissociation compared to the 17.0 nm particle.
Conclusions: The bidirectional rate of HAE can be measured simultaneously using fluorescent apoA-I probes. Reconstituted HDL particles predominantly retained their size, indicating that apoA-I exchange occurs without remodeling of HDL particles. This result has significant implications as to the possible molecular processes driving apoA-I exchange with HDL.

Disclosures: **M.S. Borja:** None. **A. Phelps:** None. **M.N. Oda:** None.

388

Transcellular Transport of HDL Bearing Gold Nanoparticles Across the Blood Brain Barrier

Skylar T Chuang, Siobanth Cruz, California State Univ, Long Beach, Long Beach, CA; Julia Stab, Sylvia Wagner, Hagen Von Briesen, Fraunhofer Inst for Biomedical Engineering, Sulzbach, Germany; Vasanthy Narayanaswami, California State Univ, Long Beach, Long Beach, CA

The overall objective of this study was to develop a HDL-based multifunctional platform for transport and delivery of highly hydrophobic gold nanoparticles (AuNP) bearing photothermic properties across the blood brain barrier (BBB). We exploited the ability of apolipoprotein E3 (apoE3) to act as a high affinity ligand for the low-density lipoprotein receptor to gain entry into endothelial and glioblastoma cells. The issue of poor aqueous solubility of AuNP of varying diameters (3, 10, or 10 nm) was overcome by integrating them with phospholipids and apoE3, yielding reconstituted rHDL bearing AuNP (rHDL-AuNP). Transmission electron microscopy (TEM) revealed the presence of AuNP embedded in spherical particles. Incubation of human brain microvasculature endothelial cells or glioblastoma cells with rHDL-

AuNP bearing unlabeled or FITC-labeled apoE3 revealed robust uptake of particles that were localized in endocytic/lysosomal vesicles. The transport of rHDL-AuNP across an *in vitro* BBB model developed from primary porcine endothelial cells was examined. The addition of rHDL-AuNP to the luminal side of the cells did not affect the integrity of the BBB as assessed by the localization of key tight junction markers such as occludin, claudins and ZO-1 by immunofluorescence, and, by continual measurement of the transepithelial electrical resistance by impedance spectroscopy under physiological conditions. Lastly, the appearance of fluorescein fluorescence and AuNP in the abluminal side suggested transport of rHDL-AuNP across the neurovascular junction. These findings demonstrate that rHDL bearing apoE3 acts as a detergent in solubilizing and dramatically improving the aqueous solubility of AuNP, facilitates cellular uptake and transcellular transport of rHDL-AuNP across endothelial cells. They are significant since they present rHDL bearing apoE3 as an effective platform for delivering AuNP across the BBB.

Disclosures: **S.T. Chuang:** None. **S. Cruz:** None. **J. Stab:** None. **S. Wagner:** None. **H. Von Briesen:** None. **V. Narayanaswami:** Research Grant; Significant; NIH.

389

The Role of Amadori-Glycation in High Density Lipoprotein Dysfunction and Oxidative Stress in Patients with Diabetes

Takhar Kasumov, Makan Golizeh, Kwangwon Lee, Serguei Ilchenko, NEOMED, Rootstown, OH; Shuhui Wang, Jonathan Smith, Sangeeta Kashyap, Cleveland Clinic Fndn, Cleveland, OH

Objectives Diabetes is associated with HDL dysfunction and oxidative stress. We recently demonstrated that HDL from patients with T2D has reduced anti-oxidant activity and it is pro-inflammatory. Here we used the $^{2}H_2O$-based metabolic labeling approach to test the hypothesis that hyperglycemia-induced glycation contributes to HDL dysfunction and oxidative stress in diet-controlled patients with T2D. ***Methods*** HDL from patients with T2D and age- and BMI-matched healthy controls (n=7/group) was isolated and it's anti-oxidant and cholesterol efflux properties were quantified. ApoAI cross-linking and HDL particle size distribution were anlyzed. HDL proteome composition and post-translational modification of proteins were quantified by shot-gun proteomics aproach. Metabolic $^{2}H_2O$-labeling coupled with high resolution mass spectrometry was applied to quantify HDL turnover and HDL proteome dynamics. ***Results*** Despite significant differences in fasting blood glucose, insulin, insulin resistance and HbA1c, patients with T2D and controls had similar lipid (triglycerides, total cholesterol, and HDL cholesterol) and lipoprotein (apoAI and apoB100) profile. HDL from patients with T2D displayed increased levels of cross-linked apoAI and lipid-poor pre-β1 HDL partcicles. ApoB-depleted serum from T2D patients had reduced PON1 activity and macrophage-cholesterol efflux capacity, and increased levels of lipid peroxidation products measured as TBARS (all $P<0.05$). HDL from patients with T2D was enriched with Amadori glycated apoAI and transferrin (Tf), the key HDL proteins involved in cholesterol and iron transport. The extent of glycations were associated with increased degradation of apoAI and Tf. ApoAI glycation was inversely correlated with ABCA1-induced cholesterol efflux activity of HDL ($r=-0.52$, $P<0.005$), while Tf glycation had positive association with the TBARS levels ($r=0.40$, $P<0.05$). Our *in vivo* HDL flux study demonstrated that glycated apoAI and Tf species were degraded 3 and 10 fold faster than the respective non-modified native proteins. ***Conclusions*** HDL dysfunction and oxidative stress in T2D is related to glycation-induced instability of HDL proteins, including apoAI and Tf.

Disclosures: **T. Kasumov:** None. **M. Golizeh:** None. **K. Lee:** None. **S. Ilchenko:** None. **S. Wang:** None. **J. Smith:** None. **S. Kashyap:** None.

This research has received full or partial funding support from the American Heart Association.

390

The Absence of Abcg5 Abcg8 Reveals a Sexually Dimorphic Adaption to Impaired Biliary Cholesterol Secretion

Jianing Li, Ailing Ji, Ryan E Temel, Deneys R van der Westhuyzen, Gregory A Graf, Univ of Kentucky, Lexington, KY

OBJECTIVE: The ABCG5 ABCG8 (G5G8) sterol transporter is the primary mechanism for biliary cholesterol secretion, but mice maintain fecal sterol excretion in its absence. The mechanism by which mice maintain sterol excretion in the absence of this pathway is not known. Transintestinal cholesterol

excretion (TICE) is an alternative pathway to hepatobiliary secretion. We investigated the impact of G5G8 deficiency on TICE in the absence of Sitosterolemia.
METHODS AND RESULTS: We compared both hepatobiliary and transintestinal cholesterol excretion rates in wild-type (WT) and G5G8 deficient mice of both sexes. WT and G5G8 were maintained on a plant-sterol free diet from the time of weaning to prevent the development of secondary phenotypes associated with Sitosterolemia. Biliary and intestinal cholesterol secretion rates were determined by biliary diversion with simultaneous perfusion of the proximal 10 cm of the small bowel. Among WT mice, biliary cholesterol secretion was greater in female mice compared to males. Conversely, male mice exhibited greater rates of TICE than females. As expected, WT mice had higher biliary cholesterol secretion rates than their G5G8 deficient littermates. However, the decline in biliary cholesterol secretion was far less in male mice compared to females in the absence of G5G8. In female mice, the absence of G5G8 resulted in a two-fold increase in TICE, whereas males were unaffected.
CONCLUSION: Female mice are more dependent upon the biliary pathway for cholesterol excretion, whereas males are more dependent upon TICE. G5G8 independent pathways are present for both biliary and intestinal cholesterol secretion. Female and male mice differ in their adaptation to G5G8 deficiency in order to maintain fecal sterol excretion.

Disclosures: **J. Li:** None. **A. Ji:** None. **R.E. Temel:** None. **D.R. van der Westhuyzen:** None. **G.A. Graf:** None.

391

Sterol Efflux Function and Protein Composition of HDL Associates With Recovery From Stroke

Deanna Plubell, Alexandra Fenton, OHSU, Portland, OR; Clark Wayne, Oregon Health and Science Univ, Portland, OR; Neil A. Zakai, Univ of Vermont, Burlington, VT; Joseph F. Quinn, Nabil J. Alkayed, **Nathalie Pamir**, Oregon Health and Science Univ, Portland, OR

Background: Prospective cohort studies and meta-analyses examining the relationship between HDL-cholesterol (C) and stroke are discordant and question the value of HDL-C as a marker for stroke risk prediction. Other properties of HDL-C such as cholesterol efflux capacity (CEC) and proteome, are less studied.
Methods: We investigated the changes in HDL CEC and proteome to determine if they are associated with improved stroke recovery. Plasma from age- and lipid profile-matched healthy controls (N = 35) and stroke patients were collected at 24 (early, N = 35) and 96 hour (late, N = 20) post stroke, and analyzed with three independent assays to measure macrophage-mediated, ABCA1 and ABCG1-specific sterol efflux, and HDL proteome. Stroke recovery was assessed at 3 months using the Modified Rankin Scores (MRS) and the NIH Stroke Scale (NIHSS).
Results: Both macrophage- and ABCG1-mediated CEC were reduced by 50% (P<0.0001) and 20% (P<0.038) in early and late post stroke samples, respectively, compared to the control group. Patients who had comparable or increased CEC between the two-time points exhibited lower NIHSS and MRS indicating better recovery. Proteomic analysis of HDL indicated a distinct time-dependent remodeling post stroke. Coagulation complement cascade proteins (FGB, FGA, A2M, C3) significantly increased (FDR>0.01) early and returned to control levels later, inflammation proteins (SAA1, SAA2, PON1, C4B) increased early and continued to increase. Interestingly, platelet adhesion proteins (DSG1, JUP, ITGB1, ITGA2, TUBB, DNAH3, PF4) were abundantly present in only later samples.
Conclusion: 1) patients who maintain or improve HDL CEC post stroke exhibit better recovery scores, 2) post stroke HDL proteome remodeling is dynamic with distinct time-dependent protein signatures that may associate with stroke recovery.

Disclosures: **D. Plubell:** None. **A. Fenton:** None. **C. Wayne:** None. **N.A. Zakai:** None. **J.F. Quinn:** None. **N.J. Alkayed:** None. **N. Pamir:** None.

392

The Role of Scavenger Receptor-BI's Transmembrane Domains in Cholesterol Transport: A "Locked Dimer" Strategy

Sarah Proudfoot, Alexandra Chadwick, Emma Allen, Daisy Sahoo, Medical Coll of Wisconsin, Milwaukee, WI

Efficient reverse cholesterol transport requires interactions between high density lipoprotein (HDL) and its receptor, scavenger receptor-BI (SR-BI). SR-BI is an 82 kDa protein with a large extracellular domain anchored by two transmembrane domains (TMDs). Our lab recently solved the NMR structure of SR-BI's C-terminal TMD (C-TMD), a region that mediates SR-BI dimerization. Further, FRET studies suggest HDL-induced movement between neighboring SR-BI monomers, which led to our hypothesis that flexibility between SR-BI TMDs facilitates cholesterol transport. Using structure-guided mutagenesis, we introduced cysteine residues into the C-TMD of full-length SR-BI to create "locked dimers" of the receptor. Total lysate and cell surface expression of WT-, A444C-, L451C-, or G453C-SR-BI were verified in transiently-transfected COS-7 cells by immunoblot analysis and flow cytometry, respectively. Based on the predicted orientation of sulfhydryl side chains relative to the putative dimerization motif, we used immunoblot analysis following electrophoresis under reducing/non-reducing conditions to confirm that A444C- and L451C-SR-BI, but not G453C-SR-BI, formed disulfide bonds. Compared to WT-SR-BI, the locked dimer mutants, A444C- and L451C-SR-BI, exhibited normal selective uptake of [^{3}H]-cholesteryl oleyl ether, despite slightly reduced [^{125}I]-HDL binding. SR-BI-mediated cholesterol efflux to HDL from cells pre-labeled with [^{3}H]-cholesterol was also unaltered by the presence of locked dimers. Finally, we investigated the ability of WT and mutant SR-BI receptors to alter accessibility of membrane free cholesterol to exogenous cholesterol oxidase (as judged by cholestenone levels). L451C- or G453C-SR-BI expression led to reduced cholestenone production compared to WT-SR-BI, suggesting that these mutants may be defective in reorganizing pools of membrane cholesterol. In conclusion, our preliminary data suggest that limiting conformational flexibility between TMDs by forcing locked dimers of SR-BI may not have a major impact on SR-BI-mediated cholesterol transport. However, locked dimers of SR-BI appear to affect the ability of SR-BI to modulate plasma membrane pools of free cholesterol, and this deserves further investigation.

Disclosures: **S. Proudfoot:** None. **A. Chadwick:** None. **E. Allen:** None. **D. Sahoo:** None.

393

Pancreatic Beta Cell Export of miR-375 to High-Density Lipoproteins is Inversely Associated With Insulin Secretion

Leslie R Sedgeman, Vanderbilt Univ, Nashville, TN; Quanhu Sheng, Yan Guo, Kasey C Vickers, Vanderbilt Univ Medical Ctr, Nashville, TN

microRNAs (miRNAs) are critical regulators of glucose metabolism and contribute to the pathogenesis of Type 2 Diabetes (T2D). Recently, we reported that high-density lipoproteins (HDL) transport and deliver functional miRNAs to recipient cells. Here, we report that miR-375 is decreased on HDL in two models of chronic hyperglycemia -- T2D human subjects and Zucker Diabetic Fatty (ZDF) rats. Since miR-375 expression in the islets is 10X greater than in other organs, we tested whether pancreatic beta cells have the ability to export miR-375 to HDL through *in vitro* export assays, incubating HDL with INS1 beta cells or primary human islets. Indeed, we found miR-375 to be readily exported to HDL from INS1 cells and primary islets *in vitro*. To determine if cholesterol transporters contribute to HDL-miR-375 export from beta cells, Abca1, Abcg1 and Scarb1 (SR-BI) were inhibited using siRNAs; however, we found that knockdown of each of these transporters failed to affect the beta cell's ability to export miR-375 to HDL. Nonetheless, enhancing insulin secretion with tolbutamide resulted in the suppression of HDL-miR-375 export, suggesting that miRNA export and insulin secretion are inversely regulated. To determine the roles of Argonaute (Ago) family proteins in HDL-miRNA export, INS1 cells were transfected with siRNAs against *Eif2c1-4* to knockdown Ago1-4. We found HDL-miR-375 export to be suppressed when Ago1, but not Ago2-4, were inhibited, suggesting that miRNA export is downstream of miRNA processing by Ago1. We are currently investigating the relationship between HDL-miR-375 export, insulin secretion, and miRNA processing in pancreatic beta cells to elucidate the mechanism(s) controlling HDL-miR-375 export. Collectively, results suggest that a large fraction of HDL-miRNAs originate from pancreatic beta cells and HDL-miRNAs are exported independent of cholesterol transporters.

Disclosures: **L.R. Sedgeman:** None. **Q. Sheng:** None. **Y. Guo:** None. **K.C. Vickers:** None.

This research has received full or partial funding support from the American Heart Association.

394

Ldl-cholesterol, ApoB100 Kinetics and Atherosclerosis in Ldlr-deficient Yucatan Minipigs: A New Model for Familial Hypercholesterolemia

Dawn E Telford, Amy C Burke, Brian G Sutherland, Cynthia G Sawyez, Jane Y Edwards, Robarts Res Inst, London, ON, Canada; P Hugh Barrett, Univ of Western Australia, Perth, Australia; Roger S Newton, Esperion Therapeutics, Ann Arbor, MI; Murray W Huff, Robarts Res Inst, London, ON, Canada

Lack of animal models with human-like lipoprotein metabolism and pathology has hampered translational research in atherosclerosis. Recently, a model of familial hypercholesterolemia was developed in Yucatan miniature pigs, in which the LDL receptor (LDLR) was deleted through gene targeting of exon 4. The objective of the present study was to determine the plasma lipoprotein response to a high fat diet and the kinetics of apolipoprotein (apo) B metabolism in LDLR-deficient miniature pigs. LDLR+/+ (n=5), LDLR+/- pigs (n=6) and LDLR-/- pigs (n=5) were fed a diet containing 34% kcal from fat and 0.2% cholesterol (C). At 6 weeks, the kinetics of plasma apoB100 (fasting) were measured using stable isotopic techniques and multi-compartmental modeling. In chow-fed pigs, LDL-C was 0.8mM, 1.3mM and 14mM in LDLR+/+, LDLR+/- and LDLR-/- pigs, respectively. On diet for 6 weeks, LDL-C increased 1.3-fold (to 1.09mM), 1.7-fold (to 2.3mM) and 1.2-fold (to 15.8mM) in LDLR+/+, LDLR+/- and LDLR-/- pigs, respectively. The effect of genotype or diet on plasma TG and HDL-C was modest. Compared to LDLR+/+ pigs, VLDL apoB100 pool sizes increased 1.4-fold in LDLR+/- and 1.7-fold in LDLR-/- pigs, due primarily to a decrease in fractional catabolic rates (FCR) of 18% and 63%, respectively. Compared to LDL+/+ pigs, LDL apoB100 pool sizes increased 2.2-fold and 14-fold in LDLR+/- and LDLR-/-, respectively, which was due to both 1.5-fold and 2-fold increases in production rates and 24% and 85% decreases in FCR, respectively. At 23 weeks, raised lesion area in the abdominal aorta was 3.3% in LDLR+/- pigs and 48.5% in LDLR-/- pigs. In the left anterior descending coronary artery, lesion area was $14.7x10^3$ μm^2 in LDLR+/- pigs and $656x10^3$ μm^2 in LDLR-/- pigs. This model should prove useful for translational research in lipoprotein metabolism and atherosclerosis.

Disclosures: **D.E. Telford:** None. **A.C. Burke:** None. **B.G. Sutherland:** None. **C.G. Sawyez:** None. **J.Y. Edwards:** None. **P.H.R. Barrett:** None. **R.S. Newton:** None. **M.W. Huff:** Research Grant; Modest; <10,000.

395

Evaluation of Antibody Responses in Mice Toward Apolipoprotein A-I

Robert H Kline IV, David Henson, **Vincent J Venditto**, Univ of Kentucky, Lexington, KY

Antibodies targeting apolipoprotein A-I (ApoA-I) have been documented in patients suffering from chronic inflammation associated with obesity, autoimmunity and cardiovascular disease (CVD). Anti-ApoA-I antibodies are thought to be serum markers for CVD and not responsible for disease progression, but their exact role is poorly understood. We hypothesize that the antibody response to ApoA-I is highly nuanced with both protective and pathologic antibodies targeting modified or unmodified epitopes. We sought to induce ApoA-I specific autoantibodies in mice targeting specific modified and unmodified epitopes to study their nuanced role in disease progression. To achieve this goal we immunized mice with an immunogenic liposomal formulation containing modified or unmodified peptides derived from ApoA-I. The epitope-specific antibody response toward each epitope and the full length protein were quantified by ELISA. Mice immunized with formulations containing peptide were compared to control mice receiving either peptide or adjuvant alone. Furthermore, antibody responses toward ApoA-I from mice fed normal chow were compared to mice fed a western diet. Our vaccine strategy induced a robust immune response toward the peptide epitopes along with the full length protein. The oxidized peptide also appeared to be more immunogenic than the unmodified, but the mechanism of this observation is unclear. Antibody responses toward ApoA-I were observed after immunization with adjuvant alone suggesting that acute inflammation induces a response to ApoA-I. Studies are currently underway to evaluate the affinity of the anti-ApoA-I antibodies for HDL along with their role in cholesterol efflux and atherosclerosis progression. Correlating these findings with studies in human patients will generate insight into the nuanced antibody responses toward ApoA-I in CVD.

Disclosures: **R.H. Kline:** None. **D. Henson:** None. **V.J. Venditto:** None.

This research has received full or partial funding support from the American Heart Association.

396

Acrolein Modification Weakens the Antimicrobial Activity of Apolipoprotein A1

Paul Weers, Hea J Hong, California State Univ Long Beach, Long Beach, CA

Human apolipoprotein A-I (apoA-I) has been show to exhibit antimicrobial activity by neutralizing lipopolysaccharides and destabilizing inner membranes of gram-negative bacteria. Previous studies showed that acrolein, a highly reactive αβ unsaturated aldehyde generated in cigarette smoking, modifies ε-amino side chains of lysine residues in apoA-I. The current study investigated the effect of acrolein exposure on the structure and antimicrobial activity of apoA-I. Incubation of apoA-I with acrolein using a 1:20 molar ratio, acrolein modification was evident by the appearance of apoA-I oligomers due to intermolecular crosslinking. Increase of the acrolein to protein ratio resulted in heavily cross-linked apoA-I, with protein bands appearing at 63, 98, and 126 kDa. The presence of acrolein-modified lysines in the oligomers was verified through Western blot analysis using mab5F6 antibody that specifically detects acrolein modified lysine residues in proteins. The structural changes of modified apoA-I was analyzed using circular dichroism. The α-helical content of acrolein-modified apoA-I was not significantly different from the unmodified protein. However, the midpoint of guanidine-induced denaturation increased from 0.97 to 1.50 M guanidine upon modification, indicating a significant increase in protein stability. This suggests that while modification did not alter the secondary structure, the protein fold was altered due to cross-linking. To measure the effect of acrolein modification on the interaction with bacterial membranes, binding experiments were performed with phosphatidylglycerol entrapped with calcein. This showed that the percentage of calcein released by apoA-I decreased from 87.5 ± 2.3 % to 4.7 ± 0.13 % when the protein was modified by acrolein. Thus acrolein-modified apoA-I binds phosphatidylglycerol less effectively, possibly due to loss of electrostatic interactions with anionic phospholipid vesicles. In addition, binding of apoA-I to lipopolysaccharides was significantly weaker when the protein was modified by acrolein. These results suggest that apoA-I modification by acrolein results in a protein with a decreased ability to bind to bacterial membranes and is thus less potent as an antimicrobial protein.

Disclosures: **P. Weers:** None. **H.J. Hong:** None.

397

Aldehyde-Modified Hdl Has CD36-dependent Pro-Atherogenic Effects in Macrophages

Rebecca L Holme, Alexandra C Chadwick, Medical Coll of Wisconsin, Milwaukee, WI; Yiliang Chen, Roy L Silverstein, Blood Ctr of Wisconsin, Milwaukee, WI; Daisy Sahoo, Medical Coll of Wisconsin, Milwaukee, WI

The role of high density lipoproteins (HDL) in protecting against cardiovascular disease is compromised when HDL undergoes modification during conditions of oxidative stress; however, the mechanisms underlying these changes in HDL function are not well defined. Reactive aldehydes such as acrolein (a major component in cigarette smoke) or major products of lipid peroxidation such as 4-hydroxynonenal (HNE) or malondialdehyde (MDA) are known to oxidize HDL in cardiovascular disease. To test the hypothesis that modification of HDL with aldehydes impairs HDL's athero-protective functions in macrophages, we first measured the ability of modified HDL to protect against foam cell formation. Cholesterol-loaded peritoneal macrophages isolated from wild-type C57Bl/J mice were incubated with native HDL, acrolein-modified HDL (acro-HDL), HNE-modified HDL (HNE-HDL) or MDA-modified HDL (MDA-HDL) for 24 h. Contrary to native HDL, oxidized forms of HDL were unable to prevent foam cell formation as shown by increased Oil red-O staining. Next, using a Boyden chamber assay, we demonstrated that acro- and MDA-HDL had impaired abilities to promote macrophage migration (64% and 67% of native HDL cell migration, respectively). Finally, using a secreted alkaline phosphatase reporter THP-1 cell-based assay, we determined that acro-HDL promotes activation of the pro-inflammatory NFkappaB pathway. Interestingly, immunoblot and quantitative RT-PCR analyses revealed that incubation of macrophages with acro- and MDA-HDL leads to increased expression of the pro-atherogenic receptor, cluster of differentiation 36 (CD36). Therefore, we repeated the foam cell formation and migration experiments using similar ligands, but this time, in CD36-null peritoneal macrophages. We found that both of these functions were dependent on CD36; however, the extent of the functional changes varied based on the type of oxidative modification present on HDL. In conclusion, modification of

HDL with reactive aldehydes generates a particle that has pro-atherogenic effects in macrophages, many of which are dependent on CD36.

Disclosures: **R.L. Holme:** None. **A.C. Chadwick:** None. **Y. Chen:** None. **R.L. Silverstein:** None. **D. Sahoo:** None.

398

Bile Acid Receptor Activation Ameliorates Metabolic Disorders by Differentially Activating FXR or TGR5

Kavita S Jadhav, Yang Xu, Yanqiao Zhang, Northeast Ohio Medical Univ, Rootstown, OH

Objectives: Activation of the bile acid (BA) receptors farnesoid X receptor (FXR) or TGR5 has beneficial effects on metabolic homeostasis. However, activation of FXR may increase obesity and activation of TGR5 has little effect on lipid metabolism. As such, dual activation of FXR and TGR5 appears to be a more attractive approach for treatment of common metabolic disorders. So far, the role of BA receptor activation in metabolic regulation is not well characterized. **Methods:** We utilized wild-type (WT) mice, *Tgr5*-/- mice, *Fxr*-/- mice, *Apoe*-/- mice and *Shp*-/- mice to investigate whether and how BA receptor activation by INT-767, a semisynthetic agonist for both FXR and TGR5, can prevent or reverse diet-induced metabolic disorders. **Results:** INT-767 reversed HFD-induced obesity and hyperglycemia in a TGR5-dependent manner and inhibited the development of atherosclerosis and non-alcoholic fatty liver disease (NAFLD). Mechanistically, INT-767 improved lipid homeostasis by activation of FXR and increased energy expenditure. Furthermore, activation of FXR inhibited several lipogeneic genes in the liver. We identified peroxisome proliferation-activated receptor γ (PPARγ) and CCAAT/enhancer-binding protein α (CEBPα) as novel downstream targets of FXR. FXR inhibited PPARγ expression by inducing SHP (small heterodimer partner) whereas the inhibition of CEBPα by FXR is SHP-independent. **Conclusions:** BA receptor activation can prevent and reverse obesity, NAFLD and atherosclerosis by specific activation of FXR or TGR5. Our data suggest that compared of activation of FXR or TGR5 alone, dual activation of both FXR and TGR5 is a more attractive strategy for treatment of common metabolic disorders.
Key words: FXR; TGR5; Atherosclerosis; Obesity; NAFLD; Lipogenesis

Disclosures: **K.S. Jadhav:** None. **Y. Xu:** None. **Y. Zhang:** None.

399

High Throughput Comprehensive Volumetric Approach for Determination of Particle Number and Composition of Lipoproteins in Normolipidemic and Dyslipidemic Populations

Zsuzsanna Kuklenyik, John R Barr, James L Pirkle, Ctrs for Disease Control, Atlanta, GA; Cardiovascular Biomarkers Group

Lipoproteins (Lps) are large molecular assembles formed by lipid and apolipoprotein constituents. The physical metric of Lps as metabolically functional entities is particle concentration in serum or plasma (Lp-P). However, the metabolic functions of Lp particles is determined by their lipid/protein composition and structure. To be able to determine both Lp composition and Lp-P, a volumetric approach is required, as demonstrated by Segrest et al and other groups. In this work the volumetric approach was implemented but with applicability to population studies. The workflow included size based separation of Lps by asymmetric flow field-flow fractionation while collecting fractions with 1-1.5 nm increments in the range of 7-15 nm (HDL), 20-30 nm (LDL) and >30 nm Lps (40 fractions in total from 0.1 mL serum aliquots). The average particle size in each fraction was measured by dynamic light scattering. Three high throughput, parallel LC-MS/MS based methods were developed to quantify main non-polar lipids (FC, CE and TG), phospholipids (PC, SM, PE, PI and LPC), and apolipoproteins (apos A-I, A-II, A-IV, B, C-I, C-II, C-III and E). Quantification of particle size and all major Lp components was achieved with 4-15% CVs. Overall accuracy of the methods was demonstrated by ApoB-100/LDL-P molar ratios of 0.7-1.3 (vs. 1 expected) in the 22-26 nm maximum LDL size range. In the 7.5-13 nm size range, ApoA-I/HDL-P was 0.7-3.5 and ApoA-II/HDL-P of 0.5-2.5. Using the calculated Lp-P values, average individual analyte/Lp-P molar ratios were calculated in each fraction. The workflow was applied to 120 patient samples with wide range of Total-C and Total-TG levels. Multivariate response surface modeling was used to show significant correlations among individual lipid/Lp-P and apolipoprotein/Lp-P molar ratios. For example, with

correction for particle size, the correlations of apoC-III/Lp-P and FC/Lp-P with SM/Lp-P, PC/Lp-P, TG/Lp-P and CE/Lp-P were determined, showing the effect of surface lipid and core lipid composition on apoC-III and FC binding to HDL and LDL particles, while also revealing significant cross effects among Lp components. By using <0.1 mL serum or plasma, the workflow is applicable to archived samples collected in large cohort studies.

Disclosures: **Z. Kuklenyik:** None. **J.R. Barr:** None. **J.L. Pirkle:** None.

400

Statin and Ezetimibe Differently Affect Spontaneous Atherothrombotic Occlusion in a Rabbit Model of Plaque Erosion

Tetsuya Matoba, Katsuya Honda, Jun-ichiro Koga, Kaku Nakano, Hiroyuki Tsutsui, Kensuke Egashira, Kyushu Univ, Fukuoka, Japan

Background: Atherothrombosis of a coronary artery with plaque erosion is a major cause of acute coronary syndrome; however, its pathological mechanism and the effects of lipid-lowering therapy are unknown. We have recently reported the CuVIC Trial showing that ezetimibe added to statins improves coronary endothelial function associated with reductions in serum oxysterols in patients after coronary stenting (Takase, et al. ATVB 2017, in press). **Methods and Results**: We performed balloon injury in iliofemoral arteries in male Japanese white rabbits fed with high cholesterol diet and infused with angiotensin II. We examined the occurrence of atherothrombosis by echography 3 times/week, which were subsequently confirmed by angiography. Histochemical analysis revealed the lack of PECAM1-positive endothelial layer in the atherothrombotic sites. In treatment protocol, animals were divided into 3 groups; 1. Control, 2. Ezetimibe 0.6 mg/kg/day, and 3. Rosuvastatin 1.0 mg/kg/day, resulting total cholesterol 2514+/-179, 1716+/-111, and 1403+/-174, respectively after 8 weeks. Oral treatment with Ezetimibe significantly reduced atherothrombotic occlusion. Although there was no difference in the extent of arterial stenosis among 3 groups, treatment with ezetimibe was associated with better re-endothelialization and less tissue factor (TF)-positive areas in the intima. Serum oxysterols including 7-ketocholesterol (7KC) were lower in the Ezetimibe group. Serum from the model rabbits or 7KC induced TF in cultured SMCs. TF induction by the serum from the Ezetimibe group was significantly less compared with other groups. **Conclusions**: We established a valid animal model of spontaneous atherothromobotic occlusion in rabbits, which mimicked plaque erosion observed in human coronary arteries. Reduction in serum oxysterols with ezetimibe may prevent atherothrombosis from plaque erosion, by accelerating re-endothelialization and inhibiting TF expression in injured arteries.

Disclosures: **T. Matoba:** Speakers Bureau; Modest; MSD. **K. Honda:** None. **J. Koga:** None. **K. Nakano:** None. **H. Tsutsui:** None. **K. Egashira:** None.

401

Hypercholesterolemia Induces Pro-Inflammatory Changes in Monocytes Which Are Reversed by PCSK9 Antibody Treatment

Annette E Neele, Sophie J Bernelot Moens, Jeffrey Kroon, Fleur M van der Valk, Jan Van den Bossche, Marten A Hoeksema, Renate M Hoogeveen, Johan G Schnitzler, Academic Medical Ctr, Amsterdam, Netherlands; Marie T Baccara-Dinet, Sanofi, Clinical Development, R&D, Montpellier, France; Garen Manvelian, Regeneron Pharmaceuticals, Tarrytown, NY; Erik S Stroes, Menno P de Winther, Academic Medical Ctr, Amsterdam, Netherlands

Aims: Migration of monocytes into the arterial wall contributes to arterial inflammation and atherosclerosis progression. Since elevated LDL levels have been associated with activation of monocytes, intensive LDL lowering may reverse these pro-inflammatory changes. Subjects with elevated LDL levels are currently treated with statins, which are also described to have pleiotropic effects. Using proprotein convertase subtilisin/kexin type 9 (PCSK9) monoclonal antibodies which selectively reduce LDL we studied the impact of LDL lowering on monocyte phenotype and function in patients with familial hypercholesterolemia (FH). **Methods and Results:** We assessed monocyte phenotype and function using flow cytometry for a broad range of monocyte-relevant markers and a trans-endothelial migration assay in FH patients (n=22: LDL-C 6.8±1.9mmol/L) and healthy controls (n=18, LDL-C 2.9±0.8mmol/L). Interestingly, monocyte chemokine receptor (CCR) 2 expression was approximately 3-fold increased in FH patients compared with controls (ΔMFI 605±214 vs 236±155 P<0.001). CCR2 expression correlated

significantly with plasma LDL-C levels (r=0.709) and positively associated with intracellular lipid accumulation. Monocytes from FH patients also displayed enhanced migratory capacity *ex vivo.* After 24 weeks of PCSK9 monoclonal antibody treatment (n=17), plasma LDL-C was reduced by 49% (from 6.7±1.3 mmol/L to 3.4±1.3 mmol/L *P*<0.001), which coincided with reduced monocyte intracellular lipid accumulation and suppressed CCR2 expression (ΔMFI: baseline 607±209, post PCSK9 mAbs: 207±180, *P*<0.001). Functional relevance was substantiated by the reversal of enhanced migratory capacity of monocytes following PCSK9 monoclonal antibody therapy. All changes were comparable in subjects who were treated with statins (n=14: LDL-C 2.8±0.6mmol/L) indicating that the anti-inflammatory effects were mainly mediated through LDL lowering. **Conclusions:** Elevated LDL levels in FH induce pro-inflammatory changes in monocytes, which is dampened by PCSK9 monoclonal antibody therapy. LDL lowering was paralleled by reduced intracellular lipid accumulation, suggesting that LDL lowering itself is associated with anti-inflammatory effects on circulating monocytes.

Disclosures: **A.E. Neele:** Research Grant; Significant; The Netherlands Heart Foundation (CVON 2011/B019: Generating the best evidence-based pharmaceutical targets for atherosclerosis [GENIUS]). **S.J. Bernelot Moens:** Research Grant; Significant; The Netherlands Heart Foundation (CVON 2011/B019: Generating the best evidence-based pharmaceutical targets for atherosclerosis [GENIUS]). **J. Kroon:** None. **F.M. van der Valk:** None. **J. Van den Bossche:** Research Grant; Significant; Junior Postdoc grant (The Netherlands Heart Foundation (2013T003)), VENI grant (ZonMW (91615052)). **M.A. Hoeksema:** None. **R.M. Hoogeveen:** None. **J.G. Schnitzler:** None. **M.T. Baccara-Dinet:** Employment; Significant; employed by Sanofi. **G. Manvelian:** Employment; Significant; Employed by Regeneron. **E.S.G. Stroes:** Research Grant; Significant; REPROGRAM grant (European commission Horizon2020-PHC-2015: 667837), The Netherlands Heart Foundation (CVON 2011/B019: Generating the best evidence-based pharmaceutical targets for atherosclerosis [GENIUS]. **M.P.J. de Winther:** Research Grant; Significant; The Netherlands Heart Foundation (CVON 2011/B019: Generating the best evidence-based pharmaceutical targets for atherosclerosis [GENIUS]), REPROGRAM grant (European commission Horizon2020-PHC-2015: 667837).

402

Post-transcriptional Regulation of Bile Acid Metabolism by the RNA binding protein ZFP36L1

Elizabeth Tarling, Joan Cheng, Angela Cheng, Pauline Morand, Bethan Clifford, Tamer Sallam, UCLA, Los Angeles, CA; Martin Turner, The Babraham Inst, Cambridge, United Kingdom; **Thomas Vallim**, UCLA, Los Angeles, CA

Bile acids are detergents and important signaling molecules that activate the nuclear receptor FXR to control key metabolic processes, including feedback mechanisms to maintain bile acid homeostasis. Activation of FXR decreases the mRNA levels of several bile acid synthetic genes, including the rate-limiting enzyme *Cyp7a1*. Here we show that *Cyp7a1* mRNA levels are very rapidly reduced following FXR activation, indicative of a post-transcriptional mechanism. We identify the RNA binding protein *Zfp36l1* as an FXR target gene and show that hepatic overexpression of ZFP36L1 in mice decreases *Cyp7a1* mRNA levels. In contrast, *Zfp36l1*$^{L\text{-}KO}$ mice have increased levels of *Cyp7a1* mRNA and biliary bile acids as well as reduced plasma cholesterol levels. *Zfp36l1*$^{L\text{-}KO}$ mice fed a Western diet have reduced diet-induced obesity and steatosis, likely due to impaired lipid absorption, consistent with increased *Cyp7a1* levels. Thus, the ZFP36L1-dependent regulation of bile acid metabolism is an important metabolic contributor of dyslipidemia, obesity and hepatosteatosis.

Disclosures: **E. Tarling:** None. **J. Cheng:** None. **A. Cheng:** None. **P. Morand:** None. **B. Clifford:** None. **T. Sallam:** None. **M. Turner:** None. **T. Vallim:** Consultant/Advisory Board; Significant; Regulus Therapeutics.

This research has received full or partial funding support from the American Heart Association.

404

Induction of MiR133a Expression By IL-19 Targets LDLRAP1 and Reduces Oxidized LDL Uptake in VSMC

Khatuna Gabunia, Allison Herman, Mitali Ray, Sheri Kelemen, Ross England, Raul DeLaCadena, William Foster, Katherine Elliott, Satoru Eguchi, **Michael Autieri**, Temple Univ, Philadelphia, PA

Introduction: The transformation of vascular smooth muscle cells (VSMC) into foam cells leading to increased plaque size and decreased stability is a key, yet understudied step in atherogenesis. We reported that Interleukin-19 (IL-19), a novel, anti-inflammatory cytokine, attenuates atherosclerosis by anti-inflammatory effects on VSMC. We tested the hypothesis that one mechanism was reduction in VSMC foam cell formation. Methods and Results: In this work we report that IL-19 induces expression of miR133a, a muscle-specific miRNA, in VSMC. Although previously unreported, we show that miR133a can target and reduce mRNA abundance, mRNA stability, and protein expression of Low Density Lipoprotein Receptor Adaptor Protein 1, (LDLRAP1), an adaptor protein which functions to internalize the LDL receptor. Mutations in this gene lead to LDL receptor malfunction and cause the Autosomal Recessive Hypercholesterolemia (ARH) disorder in humans. We also show that IL-19 reduces lipid accumulation in VSMC, as well as LDLRAP1 expression and oxLDL uptake in a miR133a-dependent mechanism. We show that LDLRAP1 is expressed in plaque and neointimal VSMC of mouse and human injured arteries. Transfection of miR133a and LDLRAP1 siRNA into VSMC reduces their proliferation and uptake of oxLDL. miR133a is significantly increased in plasma from hyperlipidemic compared with normolipidemic patients. Summary and conclusions: miR133a targets LDLRAP1 3'UTR and reduces its expression. Expression of miR133a in IL-19 stimulated VSMC represents a previously unrecognized link between vascular lipid metabolism and inflammation, and may represent a therapeutic opportunity to combat vascular inflammatory diseases.

Disclosures: **K. Gabunia:** None. **A. Herman:** None. **M. Ray:** None. **S. Kelemen:** None. **R. England:** None. **R. DeLaCadena:** None. **W. Foster:** None. **K. Elliott:** None. **S. Eguchi:** None. **M. Autieri:** None.

405

Synthetic Low Density Lipoprotein Receptor Knockout Mouse Model to Study Atherosclerosis Regression

Debapriya Basu, Yunying Hu, NYU Langone Medical Ctr, New York, NY; Adam E Mullick, Mark J Graham, Ionis Pharmaceuticals, Carlsbad, CA; Shelley Barnhart, Univ of Washington, Seattle, WA; Edward A Fisher, NYU Langone Medical Ctr, New York, NY; Karin E Bornfeldt, Univ of Washington, Seattle, WA; Ira J Goldberg, NYU Langone Medical Ctr, New York, NY

Regression of atherosclerotic plaques occurs when plasma total cholesterol (TC) is markedly reduced. Commonly used animal models of regression include a surgical model of transplantation of atherosclerotic arteries from *Apoe*$^{-/-}$ or *Ldlr*$^{-/-}$ mice to C57BL/6J mice, and the 'Reversa mouse' in which hypercholesterolemia due to deletion of LDL receptor (LDLR) and over-expression of apoB100 is conditionally reversed. These models require either challenging surgeries or time-consuming breeding strategies. We utilized a synthetic method to create and then reverse hypercholesterolemia and atherosclerosis by transient knockdown of hepatic LDLR using antisense oligonucleotides (ASOs). C57BL6/J mice on Western diet were treated once a week for 16 weeks with intraperitoneal injections of LDLR ASO. TC increased to ~600 mg/dl in two weeks, and remained high. After 16 weeks, one group of mice was sacrificed for baseline analysis and the remaining mice were treated with the sense ASO to antagonize any residual LDLR ASO activity. The mice were then either kept on Western diet or switched to chow diet. Within a week, TC decreased to ~150 mg/dl in both regression groups and mice were sacrificed after another week. LDLR mRNA and protein analysis in the baseline group showed that ASO-mediated LDLR deletion was efficient. Similar analysis in both regression groups at the end of the study confirmed recovery of hepatic LDLR expression. Mice in the baseline group had visible plaques in the aortic arch and brachiocephalic artery (BCA). Analysis of the BCA showed that lesion size, visualized by Movat's staining, was not significantly different between the baseline and regression groups. BCA lesions stained for MAC-2, a marker for macrophages, showed reduced macrophage content in both regression groups but more significantly in the Western diet group. Our data show that lesion remodeling and regression, in terms of inflammatory cell content, occur in our model. These changes occur relatively quickly as we analyzed lesions after two weeks of plasma cholesterol reversal. In conclusion, we have

developed a synthetic LDLR hepatic knockout mouse model of atherosclerosis regression that can be used for any genetically modified mouse strain and obviates the need for extensive mouse breeding.

Disclosures: **D. Basu:** None. **Y. Hu:** None. **A.E. Mullick:** Employment; Significant; Ionis Pharmaceuticals. Ownership Interest; Significant; Ionis Pharmaceuticals. **M.J. Graham:** Employment; Significant; Ionis Pharmaceuticals. Ownership Interest; Significant; Ionis Pharmaceuticals. **S. Barnhart:** None. **E.A. Fisher:** None. **K.E. Bornfeldt:** None. **I.J. Goldberg:** None.

406

Flavocoxid a Dual Cox/Lox Inhibitor Reduces Atherosclerosis Development in ApoE KO Mice Fed With a Western High Fat Diet

Alessandra Bitto, Gabriele Pizzino, Giovanni Pallio, Federica Mannino, Natasha Irrera, Domenica Altavilla, Francesco Squadrito, Univ of Messina, Messina, Italy

Flavocoxid is composed by two flavonoids, baicalin and catechin and it exerts anti-inflammatory effect blocking the peroxidase activity of COX1/2 and 5-LOX. This balanced inhibition prevents the development of adverse effects as demonstrated in clinical trials. The antinflammatory effect of flavocoxid was tested in ApoE knock out mice fed with a high fat western diet. Mice (of both sex) were 5 weeks old at the beginning of the experiment and were fed with a high fat diet for 8 weeks. Mice were randomized to receive: vehicle, or simvastatin (40mg/kg/day by oral suspension), or flavocoxid by oral suspension at the human equivalent dose of 500 mg/day (20mg/kg/day) that was previously reported effective in other inflammatory conditions. The body weight, food intake, cholesterol, and triglyceride levels were recorded every week and at the time of sacrifice the thoracic aorta, liver, and blood samples were taken. Flavocoxid supplementation reduced blood levels of triglycerides and cholesterol and the extent of atherosclerotic plaques. In liver samples the mRNA expression of PPAR-alpha and SREBP-1 was significantly affected by flavocoxid supplementation (p less than 0.05 vs untreated ApoE mice), and the western blot analysis demonstrated an increased expression of the AMPK-alpha kinase demonstrating increased cellular metabolism in treated animals (p less than 0.05 vs untreated ApoE mice). The positive results obtained in this pre-clinical model further support the use of flavocoxid to reduce the atherosclerotic burden.

Disclosures: **A. Bitto:** None. **G. Pizzino:** None. **G. Pallio:** None. **F. Mannino:** None. **N. Irrera:** None. **D. Altavilla:** None. **F. Squadrito:** None.

407

High Density Lipoprotein Mediated Protection of Macrophages Against Apoptosis Requires Scavenger Receptor Class B Type 1 Activity and Sphingosine-1-Phosphate

Kevin Chathely, Leticia González, Bernardo Trigatti, McMaster Univ, Hamilton, ON, Canada

BACKGROUND/OBJECTIVES: Prevention of macrophage apoptosis in advanced atherosclerotic lesions can help stop atherosclerosis progression to vulnerable plaques. High density lipoprotein (HDL) can protect macrophages from apoptosis that has been induced by a variety of agents. We hypothesize that this is the consequence of the sphingolipid, sphingosine-1-phosphate (S1P), specifically carried by HDL, and transferred to S1P receptor 1 (S1PR1) on the cells via the HDL receptor, scavenger receptor class B type 1 (SR-B1). **METHODS:** Apoptosis was induced in murine peritoneal macrophages from wild type and different knockout mice with the ER stress inducing agent tunicamycin. Apoptosis was then observed and detected by terminal deoxynucleotidyl transferase mediated dUTP nick end labeling through fluorescent microscopy. All experiments were conducted with an n of 3 or 4. **RESULTS:** Treatment of cells with HDL protected them against tunicamycin induced apoptosis. In contrast, pre-treatment of HDL with S1P lyase, which irreversibly cleaves S1P, eliminated the ability of HDL to protect macrophages. Furthermore, HDL-dependent protection of macrophages against apoptosis required both the HDL receptor SRB1 and the S1PR1. Inhibitor of SRB1's lipid transport activity also prevented HDL dependant protection against apoptosis. **CONCLUSIONS:** These results suggest that the HDL mediated protection of macrophages against apoptosis may involve SRB1 mediated delivery of S1P from HDL to the S1PR1. Understanding the mechanisms by which HDL elicits atheroprotective signalling in macrophages will provide insight into new targets for therapeutic intervention.

Disclosures: **K. Chathely:** None. **L. González:** None. **B. Trigatti:** None.

408

Enzyme Modified LDL Induces Migration and Calcification of Human Coronary Artery SMCs

Bijou Chellan, Marion Hofmann Bowman, Univ of Chicago, Chicago, IL

Background. Enzyme modified LDL (ELDL) is present in human atherosclerotic lesions and is a major foam cell-forming modified LDL for murine vascular smooth muscle cells (SMC) as reported by us previously. Here we study ELDL and its effects on human coronary artery SMC (HCASMC) in vitro. **Methods and Results.** Incubation of HCASMC with 10 µg/ml ELDL (trypsin, cholesterol esterase modified) resulted in significant foam cell formation (analyzed by Oil Red O, lipid measurement) compared to HCASMC incubated with oxidized LDL (200 µg/ml; -75%, $p<0.01$) or native LDL (200 µg/ml; -50%, $p<0.01$). Whole genome gene expression (Illumina Bead Chip HT12v4, analyzed by DAVID v6.8 and IPA) of HCASMC treated with ELDL, oxLDL, LDL, and control (cell culture medium only) showed several top canonical pathways specifically induced by ELDL, together with activated upstream regulators including p38MAPK, NFkB. ERK. Upregulation of ANGPTL4 and BMP-2 -mRNA (22 and 2 fold respectively over native LDL) was verified by qRT-PCR and immunoblotting. ELDL-induced foam cells showed dose dependent (1-20 µg/ml ELDL) increase in migration in collagen coated trans well dishes, which was attenuated by Lacidepine, a known inhibitor of ELDL uptake in murine SMCs. Furthermore, rANGPTL4 also upregulated HCASMC migration dose dependently (1-5 µg/ml for 24 h) and was comparable with the migration induced by ELDL. However, Lacidipine had no effect on rANGPLT4 mediated migration, suggesting that ANGPLT-4 independently of ELDL uptake promotes migration of HCASMC. In calcification assays using MEM with 0.2% FCS and 1.5 mM phosphate, ELDL at 2.5 µg/ml induced more calcification native LDL (>25%, $p<0.01$, analyzed by alizarin red staining and organic extraction, and this was proceeded by increase in BMP-2 mRNA. **Conclusions.** ELDL is highly potent in inducing foam cells in cultured HCASMC. Whole genome expression and bioinformatics analysis indicate up-regulation of pathways linked to osteochondrogenic transformation. BMP-2 and ANGPTL4 are significantly upregulated in ELDL-induced HCASMC foam cells. These results point to the potential of ELDL to induce migratory and osteoblastic effects in HCASMC with potential implications in SMC migration and calcification in human atherosclerosis.

Disclosures: **B. Chellan:** None. **M. Hofmann Bowman:** Research Grant; Modest; R01HL114821.

409

Androgen Inhibits Key Atherosclerotic Processes by Directly Activating *ADTRP* Transcription

Qiuyun Chen, Cleveland Clinic, Cleveland, OH; Chunyan Luo, Huazhong Univ of Science and Technology, Wuhan, China; Kirsten Leineweber, Bayer AG, Wuppertal, Germany; Bo Tang, Huazhong Univ of Science and Technology, Wuhan, China; Weiyi Zhang, Bayer Healthcare Co. Ltd., Beijing, China; Sisi Li, Huazhong Univ of Science and Technology, Wuhan, China; Elisabeth Pook, Bayer AG, Wuppertal, Germany; Shing-Hu Cheung, Bayer Healthcare Co. Ltd., Beijing, China; Martin Bechem, Bayer AG, Wuppertal, Germany; Jing-Shan Hu, Bayer Healthcare Co. Ltd., Beijing, China; Volker Laux, Bayer AG, Wuppertal, Germany; Qing Wang, Cleveland Clinic, Cleveland, OH

Low androgen levels are associated with an increased risk of coronary artery disease (CAD), thrombosis and myocardial infarction (MI), suggesting that androgen has a protective role. However, little is known about the underlying molecular mechanism. Our genome-wide association study identified the *ADTRP* gene encoding the androgen-dependent TFPI regulating protein as a susceptibility gene for CAD and MI. The expression level of *ADTRP* was regulated by androgen, but the molecular mechanism is unknown. Here, we tested the hypothesis that androgen plays a protective role in cardiovascular disease by activating *ADTRP* expression. Luciferase assays with an *ADTRP* promoter luciferase reporter revealed that androgen regulated *ADTRP* transcription. Chromatin-immunoprecipitation showed that the androgen receptor bound to a half androgen response element (ARE) located at +324bp from the *ADTRP* transcription start site. The ARE is required for the transcriptional activation of *ADTRP*. HL-60 monocyte adhesion to EAhy926 endothelial cells (ECs) and transmigration across the EC layer, the two processes critical to development of CAD and MI, were inhibited by androgen, but the effect was reduced by *ADTRP* siRNA and enhanced by overexpression of *ADTRP*. These data suggest that one molecular mechanism by which androgen confers protection against CAD is stimulation of *ADTRP* expression.

Disclosures: **Q. Chen:** None. **C. Luo:** None. **K. Leineweber:** Employment; Significant; >10,000. **B. Tang:** None. **W. Zhang:** Employment; Significant; >10,000. **S. Li:** None. **E. Pook:** Employment; Significant; >10,000. **S. Cheung:** Employment; Significant; >10,000. **M. Bechem:** Employment; Significant; >10,000. **J. Hu:** Employment; Significant; >10,000. **V. Laux:** Employment; Significant; >10,000. **Q. Wang:** Research Grant; Significant; >10,000.

410

Inhibiting Mitochondrial Fission in Progressive Atherosclerosis Protects Against Ischemia/Reperfusion Injury

Simon Duggan, Univ of Bristol, Bristol, United Kingdom

Introduction: Two opposing highly regulated mitochondrial processes, division (fission) and fusion, determine cell-type specific mitochondrial morphology, intracellular distribution and activity. Mitochondrial dysfunction has been implicated in atherogenesis and in cardiac ischemia/reperfusion (I/R) injury.
Hypothesis: We hypothesize that increased mitochondrial fission plays a role in progressive atherosclerosis and protection in I/R injury.
Methods and Results: Male apolipoprotein E knockout mice (ApoE-/-) were fed either a high-fat diet (21% lard & 0.15% cholesterol - HFD) or chow diet for 24 weeks from weaning. Compared to their chow fed littermates, mice fed a HFD demonstrated smaller, shorter and reduced density of left ventricular (LV) interfibrillar mitochondria suggestive of mitochondrial fission by electron microscopy. Furthermore, there was decreased expression of the mitochondrial fusion proteins, optic atrophy 1 and mitofusin 1 and increased fission protein Fis 1. Whilst the proteins Mfn2 and Drp1 were unchanged. On ischemia, LV tissue expression of fission proteins was increased in both groups. In isolated perfused hearts subjected to 30 min ischemia and 120 min reperfusion inhibition of the Drp1-mediated fission with Mdivi-1 (25 µM) at the onset of reperfusion significantly reduced infarct size (n=6/group). Inhibition of the DRP1-mediated fission at serine 637 in langendorff hearts conferred relatively more cardio-protection in the chow fed mice compared to western diet (19.93% ± 2.219%, n=5 versus 29.61% ± 2.517%, n=6; $p < 0.05$). The reduction in myocardial necrosis was corroborated by a significantly reduced release of creatine kinase and recovery of coronary flow.
Conclusion: Inhibiting mitochondrial fission protects hearts against ischemia/reperfusion injury in progressive atherosclerosis.

Disclosures: **S. Duggan:** None.

412

Apelin-13 Enhances Atherosclerotic Plaque Stability in Apoe-Deficient Mice

Rodrigo A Fraga-Silva, École Polytechnique Fédérale de Lausanne, Lausanne, Switzerland; Hugo Seeman, Federal Univ of Minas Gerais, Belo Horizonte, Brazil; Fabrizio Montecucco, Univ of Genoa Sch of Med, Genoa, Italy; Analina Raquel da Silva, Fabienne Burger, Univ of Geneva, Geneva, Switzerland; Fabiana Pereira Costa-Fraga, Léa Anguenot, École Polytechnique Fédérale de Lausanne, Lausanne, Switzerland; François Mach, Univ of Geneva, Geneva, Switzerland; Robson Augusto dos Santos, Rafaela Fernandes da Silva, Federal Univ of Minas Gerais, Belo Horizonte, Brazil; Nikolaos Stergiopulos, École Polytechnique Fédérale de Lausanne, Lausanne, Switzerland

Introduction: Atherosclerosis remains one of the main cause of death worldwide and substantial efforts have been made to identify novel approaches to improve the management of this disorder. Apelin is an endogenous peptidergic family with essential role on the cardiovascular hemostasis and pathologies. Recent studies pointed out a fundamental contribution of Apelin system on atherosclerosis development; however, such reports revealed contradictory data, and to date, it is difficult to accurately define the beneficial or deleterious role of Apelin in atherosclerosis. *Objective:* To better understand the role of Apelin system on atherosclerosis, we aimed to investigate the actions of Apelin-13 treatment on atherosclerotic plaques composition, focusing on features of plaque vulnerability. *Methods:* Apolipoprotein E gene-deleted mice (n=40) were fed with western-type diet for 11 weeks. Atherosclerotic plaque formation was induced in the carotid artery by a shear stress modifier device, which exposed the vessel to distinct patterns of shear stress, resulting in plaque formation with different composition. The mice were treated with Apelin-13 (2 mg/Kg/day) or vehicle for the last 3 weeks of experimental period. *Results:* Apelin-13 treatment did not change atherosclerotic plaque size in the aorta, neither altered the lipid

content of low shear stress and oscillatory shear stress-induced plaques in the carotid. However, Apelin-13 remarkably ameliorated plaque stability by increasing intraplaque collagen content, which was associated with a reduction of MMP-9 expression. Furthermore, Apelin decreased cell infiltration (neutrophil and macrophage) and intraplaque reactive oxygen species content. Interestingly, Apelin-13 treatment reduced total cholesterol, LDL levels and free fatty acids serum levels, while HDL, triglycerides serum levels were not significantly changed. *Conclusion:* Apelin-13 treatment for 3 weeks did not alter the lesion size, but significantly enhances the stable phenotype of atherosclerotic plaques and improved serum lipid profile. These results indicate that activation of Apelin system enhances plaque stability.

Disclosures: **R.A. Fraga-Silva:** None. **H. Seeman:** None. **F. Montecucco:** None. **A.R. da Silva:** None. **F. Burger:** None. **F.P. Costa-Fraga:** None. **L. Anguenot:** None. **F. Mach:** None. **R.A.S. dos Santos:** None. **R.F. da Silva:** None. **N. Stergiopulos:** None.

413

Lipoprotein SCARB1 Intronic Variant Associated with Increased Coronary Heart Disease Risk Affects Cardio-Protective Gene Networks

Diana Golden, UCONN Health, Farmington, CT; Sameet Mehta, Yale Univ, New Haven, CT; Antonina Kolmakova, Annabelle Rodriguez, UCONN Health, Farmington, CT

Introduction: We previously reported a common intronic *SCARB1* (12q24.31) variant, rs10846744, located in an enhancer region, to be significantly associated with coronary artery disease (CAD) in the Multi-Ethnic Study of Atherosclerosis (MESA). RNA-Seq showed expression of the immune checkpoint inhibitor lymphocyte activation gene 3 (*LAG3*, 12p13.31), to be 5-fold lower in carriers of the risk allele, while low plasma LAG3 protein levels were also significantly associated with increased CAD risk in MESA, after multivariate regression analysis.
Hypothesis: That the *SCARB1* rs10846744 variant disrupts long-range transcriptional regulation of *LAG3* disturbing cardio-protective and anti-inflammatory gene networks to promote CAD.
Methods and results: Using functional genomics (HiC global chromatin capture, ChIP-Seq and RNA-Seq) in reference and risk EBV-transformed B lymphocytes to assess 3D chromatin architecture and gene-gene interactions at a 2.5kb resolution, we did not observe direct chromatin contacts between *SCARB1* and *LAG3.* In the reference allele, an enhancer-rich intermediate contact (12q13.13) was found containing genes associated with cholesterol (*SOAT2*) and NR2F2 signaling (*RARG*). This same 12q13.13 region was in direct contact with 22q12.3 (*APOLI)*, an apoprotein associated with HDL and innate immunity. Micro-looping within the rs10846744 12q24.31 region showed direct contacts with other enhancers (*NCOR2*) and cardiovascular loci (*TMEM132B*), while *LAG3* micro-looping on 12p13.31 was associated with immune regulatory networks (*CD4*). Loci associated with viral infection, cytokine production, heart failure and autoimmunity were also identified. NR2F2 disrupted contacts in the risk allele, implicating NR2F2 as a dysfunctional rs10846744 transcriptional repressor altering gene networks. The risk allele included contacts near *PCSK9*, *VLDLR* and 2q33.1, a CAD locus.
Conclusion: Functional genomics of the *SCARB1* rs10846744 enhancer region identified a number of intra- and inter-chromosomal chromatin contacts in reference cells that were markedly disrupted in risk cells. Perturbing NR2F2 and/or genes disrupted in the *SCARB1*-NR2F2 immuno-cardiovascular axis may protect against CAD in the rs10846744 risk population.

Disclosures: **D. Golden:** None. **S. Mehta:** None. **A. Kolmakova:** None. **A. Rodriguez:** Ownership Interest; Significant; Lipid Genomics.

414

Ath28 Congenic Mice Confirm Atherosclerosis Modifying Gene on the Distal End of Chromosome 2

Juying Han, Jonathan D Smith, Cleveland Clinic, Cleveland, OH

Objective- Strain intercrosses between apoE-deficient mice on the AKR (athero-resistant) and DBA/2 (athero-sensitive) strains identified the Ath28 quantitative trait locus (QTL) on the distal end of chromosome 2 (chr 2). We bred congenic mice on the DBA/2 background containing AKR alleles on chr 2 from 172.5 to 180 Mb in order to confirm the presence of atherosclerosis modifying genes in this region.
Methods and Results- We used marker assisted backcrossing to generate DBA/2.AKR (chr 2) apoE-deficient congenic mice. High density genotyping using the MegaMuga array revealed that the AKR strain

donated DNA on chr 2 from 171.5 Mb to the end of the chromosome, with the most distal marker tested at 180 Mb, while DBA/2 markers were found elsewhere in the genome. Mice heterozygote for the congenic interval were intercrossed to generate progeny homozygous for the AKR allele (AA) or the DBA/2 allele (DD). Female and male mice were fed a chow diet and sacrificed at 16 weeks of age. In the females, there was no effect on body weight; the total cholesterol levels trended 13% lower for the DD vs. AA mice ($p=0.07$); and, the HDL-C levels were 55% higher for the DD vs. AA mice ($p=0.05$). Despite having lower total cholesterol levels, the DD mice had 68% larger aortic root lesion areas ($p=0.05$, N=10 and 14 for AA and DD mice, respectively). In the males, the body weight was 12% higher in the DD vs. AA mice ($p<0.01$); the total cholesterol levels were similar in the DD and AA mice; and, the HDL-C levels were 73% higher for the DD vs. AA mice ($p<0.05$). The male DD mice had 27% larger aortic root lesion areas (NS), but we are adding more mice to this study to determine if this is significant (N=6 and 11 for AA and DD mice, respectively). **Conclusions**- Ath28 congenic mice confirm the presence of an atherosclerosis modifying gene on the distal end of chr 2 in chow-fed females. This interval in chr 2 contains over 100 genes. Our prior identification of missense variants between these strains, as well as transcriptomic and eQTL analyses have identified some candidate genes in this interval including *Cstf1, Ctcfl, Zbp1, Ankrd60, Gnas, Cdh4, Ctsz,* and *Rae1*. Further functional genomic studies and creating mice with smaller congenic intervals will be needed in order to narrow the list of candidate genes for in vivo testing.

Disclosures: **J. Han:** None. **J.D. Smith:** None.

415

Repetitive Surgical Procedures in Vascular Patients Are Associated with Perioperative Cardiac Events

Henrike Janssen, Larissa Felgner, Heidelberg Univ Hosp, Heidelberg, Germany; Hans-Jörg Gillmann, Claudia Schrimpf, Saad Rustum, Ralf Lichtinghagen, Hannover Medical Sch, Hannover, Germany; Omke Teebken, Peine Medical Ctr, Peine, Germany; Gregor Theilmeier, Dept Human Med, Faculty of Med and Health Sciences, Univ of Oldenburg, Oldenburg, Germany; Jan Larmann, Heidelberg Univ Hosp, Heidelberg, Germany

Introduction Vascular surgery patients are at risk of myocardial injury after non-cardiac surgery (MINS) associated with perioperative mortality. Underlying mechanisms are largely unknown. In animal models surgery combined with blood loss promotes atherosclerotic lesion progression and plaque destabilization. It is unknown whether repetitive surgery contributes to cardiac risk in patients. ***Hypothesis*** Repetitive surgical procedures in vascular surgery patients are associated with increased MINS rates. ***Methods*** With IRB approval, after obtaining informed consent, pre- and day-1 post-operative (OP) plasma samples were collected from 663 patients undergoing elective aortic-, peripheral vascular or carotid surgery. High-sensitive cardiac troponin T (hs-cTNT) (Roche) was measured pre- and post-OP. Additional 3rd generation cTnT or hs-cTNT measurements were prompted on clinical suspicion for acute coronary syndrome. MINS was defined as any new (delta ≥50%) hs-cTNT ≥50 ng/L or 3rd gen. cTnT >0.03 ng/mL. Data are presented as median (inter quartile range (IQR)) and were compared using Wilcoxon matched-pairs signed tank test. Incidence of the combined endpoint between 1st and 2nd surgeries was compared using one-sided chi square test. $p<0.05$ was considered significant. ***Results*** We identified 40 patients with two repetitive surgical procedures. For 37 patients pre- and post-OP blood samples were available. Median time between surgeries was 53 (43.5-208) days. There were no statistical differences in pre-OP medication or risk factors. Pre-OP hs-cTNT values were slightly higher prior to the 2nd procedure (1st vs. 2nd procedure, 11.2 (6.6-19.9) vs 12.6 (7.9-31.3) ng/l, n=37, $p<0.05$). One patient experienced MINS after the 1st surgery. Five patients reached the endpoint after the 2nd procedure (1st vs 2nd procedure, n=37, $p<0.05$). ***Conclusions*** In vascular patients repetitive surgery is associated with myocardial injury. The underlying mechanisms need to be examined in more detail. However, clinicians should recognize the elevated cardiovascular risk associated with repetitive operations. Among other things, prophylactic strategies for prevention of perioperative cardiac events should focus on patients undergoing repetitive operations.

Disclosures: **H. Janssen:** None. **L. Felgner:** None. **H. Gillmann:** None. **C. Schrimpf:** None. **S. Rustum:** None. **R. Lichtinghagen:** None. **O. Teebken:** None. **G. Theilmeier:** None. **J. Larmann:** None.

416

Targeted Echogenic Liposome Binding Forces Correlate With Atheroma Ultrasound Image Enhancement

Melvin E Klegerman, Susan T Laing, Hyunggun Kim, Patrick H Kee, Melanie R Moody, Shao-Ling Huang, David D McPherson, Univ of Texas Health Science Ctr at Houston, Houston, TX

Background. We have developed echogenic immunoliposomes (Ab-ELIP) as a means of highlighting atheroma at different stages of atherogenesis. We have devised methods to measure conjugated antibody (Ab) binding affinity (targeting efficiency, TE) in order to assess and predict Ab-ELIP imaging enhancement and therapeutic efficacy. We have now constructed an algorithm for calculating binding force from the evaluation data and have tested it relative to ultrasound (US) image enhancement results. **Hypothesis.** One or more Ab-ELIP binding force parameters is predictive of ultrasound imaging enhancement of atheroma in vivo. **Methods.** Ab-ELIP were prepared by conjugating specific MAbs to ELIP. Conjugation efficiency (CE) was then determined by a quantitative immunoblot assay and particle enumeration with a Beckman-Coulter Multisizer to yield CE in molecules Ab/liposome. Conjugated Ab affinity (K_D and K_{assoc}) was derived from ELISA data and used to generate specific TE (CE x relative binding area) and functional avidity (K_{assoc} x specific TE). The functional avidity was then converted to free energy of association using the equation of state ($\Delta G = -RT/nK$). Using specific TE, ΔG in kcal/mole was converted to binding energy in erg/liposome, from which binding forces, E_b, in dyne/liposome were derived. Based on specific TE and Ab molecules per m^2, binding force/liposome was converted to Pascal (10 dyne/cm^2). Finally, dyne/liposome was converted to piconewton (pN)/molecule, a common measure of binding force. **Results.** Using rabbit and miniswine atherosclerotic models, we previously demonstrated US imaging enhancement of atheroma by MAbs specific for ICAM-1, $\alpha_v\beta_3$-integrin and VCAM-1 conjugated to ELIP. Percent image enhancement correlated ($p < 0.05$) with binding force in Pascal, but not in dyne/liposome, indicating the importance of binding area to TE. Binding force in pN/molecule ranged from 311 to 385, which agrees well with the published results of others. **Conclusions.** We have discovered a binding force parameter calculated from CE and TE data that is predictive of Ab-ELIP targeting performance in vivo. The next step, to demonstrate a similar correlation with therapeutic efficacy, will then provide an important tool for clinical Ab-ELIP optimization.

Disclosures: **M.E. Klegerman:** Ownership Interest; Significant; Zymo Pharmaceuticals, LLC. **S.T. Laing:** None. **H. Kim:** Ownership Interest; Significant; Zymo Pharmaceuticals, LLC. **P.H. Kee:** None. **M.R. Moody:** None. **S. Huang:** Ownership Interest; Significant; Zymo Pharmaceuticals, LLC. **D.D. McPherson:** Ownership Interest; Significant; Zymo Pharmaceuticals, LLC.

417

Trf2-Interacting Protein (Terf2ip) S205 Phosphorylation Mediates Atherosclerosis via Orchestrating Endothelial Senescence and Inflammation

Nhat Tu Le, Kyung-Sun Heo, Kyung Ae Ko, Yunting Tao, Tamlyn N Thomas, Raymundo A Quintana Quezada, Keigi Fujiwara, Jun-ichi Abe, Univ of Texas MD Anderson Cancer Ctr, Houston, TX

Telomeric repeat-binding factor 2 (TRF2)-interacting protein (TERF2IP) S205 phosphorylation mediates atherosclerosis (AS) via orchestrating endothelial cell (EC) senescence (Sen) and inflammation. Nhat-Tu Le, Kyung-Sun Heo, Kyung Ae Ko, Yunting Tao,Tamlyn Thomas, Raymundo A Quintana Quezada, Keigi Fujiwara, and Jun-ichi Abe Department of Cardiology, UT MD Anderson Cancer Center **Objective:** Shortened telomere (TL) provokes EC Sen, which is associated with focalized EC inflammation and plaque formation in arteries exposed by disturbed blood flow (d-flow). Although d-flow is known to increase both EC inflammation and Sen, the exact mechanism by which d-flow induces these two different EC pathologies and subsequent AS is poorly understood. **Methods & Results:** TERF2IP, as a member of the sheltrin complex, is not only crucial for DNA double strand break repair at the TL, but also for activation of cytosolic IkB kinase (IKK) and subsequent NF-kB activity. TERF2IP and TRF2 form a stable heterodimer to protect the duplex region of TLs, while activating NF-kB, especially under the d-flow condition. We have discovered that inhibition of p90RSK reduces d-flow-induced EC Sen and inflammation via down-regulating TERF2IP S205 phosphorylation. The nuclear TERF2IP-TRF2 complex protects TLs by repairing DNA damages while the cytosolic complex plays a role in NF-kB activation. When we mutated the TERF2IP phosphorylation site (S205A) in ECs, the nuclear export of the TERF2IP-TRF2 complex was abolished, which inhibited d-flow-induced NF-kB activation and Sen. Both the depletion of TERF2IP by siRNA and S205A mutation inhibited d-flow-induced TERF2 nuclear export, and

residual TRF2 at the TL inhibited d-flow-induced TL dysfunction. The mutation of TERF2IP S205A inhibited cytosolic IKK-NF-kB activation by eliminating the cytosolic TERF2IP-TERF2 complex. The inhibition of d-flow-induced inflammatory adhesion molecule expression and consequent AS were also confirmed in EC-specific TERF2IP knock out mice. **Conclusion:** These results suggest that S205 phosphorylation of TERF2IP induced by p90RSK activation is required for d-flow-induced TL shortening and NF-kB activation via regulating nuclear export of the TERF2IP-TERF2 complex.

Disclosures: **N. Le:** None. **K. Heo:** None. **K. Ko:** None. **Y. Tao:** None. **T. Thomas:** None. **R. Quintana Quezada:** None. **K. Fujiwara:** None. **J. Abe:** None.

This research has received full or partial funding support from the American Heart Association.

418

Co-Culture of Endothelial Cells, Smooth Muscle Cells and Monocytes in Collagen Scaffold: A Novel i*n vitro* Model of Atherosclerosis

Martin Liu, Angelos Karagiannis, Univ of Nebraska Medical Ctr, Omaha, NE; Matthew Sis, Srivatsan Kidambi, Univ of Nebraska Lincoln, Lincoln, NE; Yiannis Chatzizisis, Univ of Nebraska Medical Ctr, Omaha, NE

Objectives: To develop and validate a 3D *in-vitro* model of atherosclerosis that enables direct interaction between various cell types and/or extracellular matrix. **Methods and Results:** Type I collagen (0.75 mg/mL) was mixed with human artery smooth muscle cells (SMCs; $6x10^5$ cells/mL), medium, and water. Human coronary artery endothelial cells (HCAECs; $10^5/cm^2$) were plated on top of the collagen gels and activated with oxidized low density lipoprotein cholesterol (LDL-C). Monocytes (THP-1 cells; $10^5/cm^2$) were then added on top of the HCAECs. Immunofluorescence showed the expression of VE-cadherin by HCAECs (A, B) and α-smooth muscle actin by SMCs (A). Green-labelled LDL-C particles were accumulated in the subendothelial space, as well as in the cytoplasm of HCAECs and SMCs (C). Activated monocytes were attached to HCAECs and found in the subendothelial area (G-I). Both HCAECs and SMCs released IL-1β, IL-6, IL-8, PDGF-BB, TGF-ß1, and VEGF. Scanning and transmission electron microscopy showed the HCAECs monolayer forming gap junctions and the SMCs (D-F) and transmigrating monocytes within the collagen matrix (G-I). **Conclusions:** In this work, we presented a novel, easily reproducible and functional *in-vitro* experimental model of atherosclerosis that has the potential to enable *in-vitro* sophisticated molecular and drug development studies.

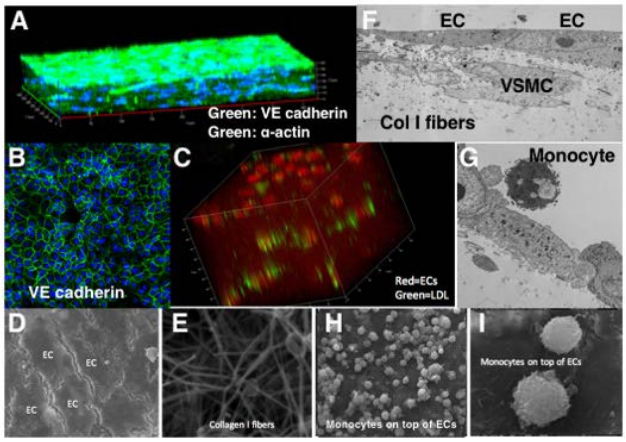

Disclosures: **M. Liu:** None. **A. Karagiannis:** None. **M. Sis:** None. **S. Kidambi:** None. **Y. Chatzizisis:** None.

419

Macrophage Dicer Expression is Required for VEGF-A-induced Arteriogenesis

Chris Mantsounga, Abigail L Healy, Warren Alpert Medical Sch at Brown Univ, Providence, RI; Nicolle Ceneri, Yale Cardiovascular Res Ctr, New Haven, CT; Alan R Morrison, Warren Alpert Medical Sch at Brown Univ, Providence, RI

During ischemia, inflammatory arteriogenesis is determined by macrophage VEGF-A expression. A number of microRNA's have been identified to downregulate VEGF-A and VEGF-mediated angiogenic processes. We sought to determine the microRNA(s) that were most critical to regulating macrophage VEGF-A expression by genetically deleting Dicer in myeloid cells. In a hindlimb ischemia model of angiogenesis and arteriogenesis, we found reduced rescue of hindlimb perfusion in macrophage *Dicer* $^{-/-}$ animals. Surprisingly, this was associated with decreased macrophage VEGF-A production and leaky, dysfunctional arteries as evidenced by microCT angiograms, indicating that Dicer expression and consequent microRNA biogenesis are required for appropriate VEGF-A expression and VEGF-mediated arteriogenesis. The mechanism of reduced macrophage VEGF expression involved decreased VEGF-A mRNA stability with decreased association of VEGF-A mRNA with the RNA-stabilizing protein HuR. Our results support a paradigm shift in the perception of Dicer expression and microRNA biogenesis as a negative regulator of VEGF-A expression and implicate microRNA biogenesis in promoting macrophage VEGF-directed arteriogenesis in response to ischemia. Identification of this novel mechanism of VEGF-A regulation has strong implications in the development of targeted therapeutic strategies that can promote appropriate arteriogenesis in the setting of obstructive vascular disease or inhibit inappropriate arteriogenesis in the setting of malignant oncological diseases.

Disclosures: **C. Mantsounga:** None. **A.L. Healy:** None. **N. Ceneri:** None. **A.R. Morrison:** None.

420

Focal Adhesion Kinase Disrupts Nuclear Factor-kB Signaling and Alleviates Atherogenesis

James Murphy, Steve Lim, Univ of South Alabama, Mobile, AL

Introduction: While we have discovered that focal adhesion kinase (FAK) is critical for global pro-inflammatory gene expression, it remains unclear what role FAK plays in vascular inflammation. Our preliminary data suggested that FAK might regulate a major inflammatory signaling factor, NF-kB. The goals of this study are to investigate the mechanisms underlying FAK-mediated inflammatory gene expression in endothelial cells (ECs), and the effect of FAK inhibition on atherogenesis.
Hypothesis: FAK activity is required for pro-inflammatory gene expression via NF-kB activation in ECs.
Methods: Human aortic ECs (HAoECs) were treated with TNF-α and with/without a FAK inhibitor (FAK-I). Inflammatory gene expression and NF-kB signaling was evaluated via western blot, immunocytochemistry or qRT-PCR. To access vascular inflammation *in vitro*, primary mouse monocytes were used in an adhesion assay on TNF-α stimulated HAoECs. To evaluate the importance of FAK activity in atherogenesis, partial carotid artery ligation was performed in ApoE-/- mice. Mice were fed a high fat/high cholesterol diet and were given either FAK-I or vehicle by oral gavage for two weeks. Both carotid arteries were harvested and analyzed.
Results: We found that FAK activity is required for expression of various pro-inflammatory molecules such as VCAM-1 and MCP-1, and FAK inhibition blocks sustained NF-kB activation. Mechanistically, while FAK inhibition does not block NF-kB activation after 1hr TNF-α stimulation, NF-kB activity significantly reduced after 3hr when compared to TNF-α only. This decrease in NF-kB activity was correlated with a decrease in NF-kB nuclear localization and an increase in IkB protein stability. FAK inhibition reduced monocyte attachment to TNF-α stimulated HAoECs (3.8 vs 22.1 fold). Mice treated with FAK-I showed decreased VCAM-1 expression, macrophage infiltration and lipid accumulation compared to vehicle group.
Conclusion: These results suggest that FAK is critical for global inflammatory gene expression and plays a key role in maintaining sustained NF-kB activity during chronic inflammation in ECs. FAK inhibitors may prove useful as an "anti-inflammatory drug" in the treatment of cardiovascular disease.

Disclosures: **J. Murphy:** None. **S. Lim:** None.

This research has received full or partial funding support from the American Heart Association.

421

Computational Modelling Suggests That Reversing Low HDL May Not Always Lead to Plaque Regression

Mary R Myerscough, Alexander D Chalmers, Univ of Sydney, University of Sydney, NSW, Australia

Introduction: Clinical evidence suggests that high numbers of high density lipoprotein (HDL) particles in the bloodstream and high levels of HDL efficacy, reduce the risk of heart attack and stroke. Experimental evidence suggests that increasing HDL particle number too late in the life of the plaque does not lead to regression but only to reduced rates of plaque growth.
Hypothesis: We postulate that nonlinear dynamics are intrinsic to how cells respond to HDL in reverse cholesterol transport (RCT) from macrophages and foam cells and that these dynamics have consequences for plaque growth, regression and the plaques' responses to changes in the plaque environment, such as changes in low density lipoprotein (LDL) influx.
Methods: We formulated a computational model for the endothelium and the inside of the artery wall. This model consisted of six partial differential equations and associated boundary conditions. We found what conditions led to model plaques remaining small and what led to model plaques growing unboundedly. We also determined the outcomes if the concentration or action of HDL changes at different times in the life of the model plaque.
Results: Model plaques with high concentrations of HDL, highly efficacious HDL and low levels of LDL were small and did not grow. There was a tipping point (or bifurcation point) so that plaques with HDL concentrations below the tipping point grew unboundedly and plaques with HDL concentrations above the tipping point remained small. The position of this tipping point depended on the concentration of modified LDL experienced by the plaque, anti-inflammatory actions of HDL and the phenotypes of macrophages after RCT. Increasing HDL concentration after the model plaque had grown led to plaque regression only if the dynamics of the plaque were such that the model plaque was able to shrink to a small plaque that did not grow. If the reduction in HDL was too late, or not large enough, the model plaque could not regress and continued to grow.
Conclusion: The nonlinear nature of the dynamics of plaque growth and regression may result in outcomes to treatment that seem unexpected or inexplicable. Computational modelling provides a means of exploring the consequences of these dynamics.

Disclosures: **M.R. Myerscough:** None. **A.D. Chalmers:** None.

422

Protease-Activated Receptor 2 is Critical for the Formation and Progression of Atherosclerosis

Shannon Jones, Nathan Robbins, Keith Saum, Samuel Slone, Univ of Cincinnati, Cincinnati, OH; Joel Thompson, Univ of Kentucky, Lexington, KY; Michael Tranter, Univ of Cincinnati, Cincinnati, OH; Nigel Mackman, Univ of North Carolina, Chapel Hill, NC; **A. Phillip Owens III**, Univ of Cincinnati, Cincinnati, OH

Objective: Protease-activated receptor 2 (PAR-2)-dependent signaling results in augmented inflammation and has been implicated in the pathogenesis of several autoimmune conditions. While PAR-2 protein is present in coronary atherosclerotic lesions, the relevance of this finding has not been investigated in experimental models. The objective of this study was to determine the effects of PAR-2 on the development of atherosclerosis. ***Methods and Results:*** Relative expression of PAR-2 is increased in human coronary artery (21 fold) and mouse aortic arch (16 fold) atheromas versus control coronary and aortic arch arteries, respectively (P = 0.001). To determine the effect of PAR-2 deficiency on atherosclerosis, male low density lipoprotein receptor deficient (*Ldlr*$^{-/-}$) mice (8-12 weeks old) that were *Par-2*$^{+/+}$ or *Par-2*$^{-/-}$ were fed a fat and cholesterol-enriched diet for 12 (n = 10 each group) or 24 weeks (n = 5 each group). PAR-2 deficiency attenuated atherosclerosis in the aortic sinus and aortic root with no effects on total plasma cholesterol concentrations or lipoprotein distributions after 12 (P = 0.000433) and 24 (P = 0.037) weeks. These reductions were attributable to **both** hematopoietic and non-hematopoietic-derived PAR-2 from analysis of bone marrow experiments (n = 15 for each of 4 chimeric groups; P < 0.05). Mechanistic studies using ex vivo macrophages show that activation of PAR-2 results in augmented foam cell formation and apoptosis with treatment of oxidized low-density lipoprotein in conjunction with decreased expression of the nuclear receptor LXR-alpha and several cholesterol transporters. In addition, PAR-2 activation of ex-vivo cultured vascular smooth muscle cells (VSMCs) augments their transition to a macrophage-like state (after cholesterol treatment) via upregulation of

human antigen R (HuR) and resultant stabilization of the transcription factor Krüppel-like factor 4 (KLF4). ***Conclusion:*** Our results indicate PAR-2 deficiency significantly attenuates the initiation (12 weeks) and reduces the progression (24 weeks) of atherosclerosis potentially via regulation of both lipid efflux from macrophages and the phenotypic modulation of VSMCs.

Disclosures: **S. Jones:** None. **N. Robbins:** None. **K. Saum:** None. **S. Slone:** None. **J. Thompson:** None. **M. Tranter:** None. **N. Mackman:** None. **A. Owens III:** None.

423

Telomerase Deficiency in Hematopoietic Stem Cells Decreases Atherosclerosis by Silencing STAT3-Dependent Inflammation in Macrophages

Hua Qing, Elizabeth Heywood, Karrie L Jones, Genevieve Doyon, Dennis Bruemmer, Univ of Pittsburgh, Pittsburgh, PA

OBJECTIVE: Telomerase Reverse Transcriptase (TERT), the catalytic subunit of telomerase, supports critical cellular responses required for tissue remodeling. Previous studies established that TERT expression is induced in activated macrophages and during experimental and human atherosclerosis formation. In the present study, we investigated the role of TERT for atherosclerosis development and macrophage inflammation. **APPROACH AND RESULTS:** TERT-deficient mice were crossbred with LDL-receptor-deficient (LDLr-/-) mice to generate first generation G1TERT-/-LDLr-/- offsprings, which were then further intercrossed to obtain third generation G3TERT-/-LDLr-/- mice. G1TERT-/-LDLr-/- mice revealed no telomere shortening while severe telomere attrition was evident in G3TERT-/-LDLr-/- mice. When fed an atherogenic diet, G1TERT-/-LDLr-/- and G3TERT-/-LDLr-/- mice were both protected from atherosclerosis formation compared to their wildtype controls, indicating that genetic TERT-deletion prevents atherosclerosis, and formation of the disease is not affected by telomere attrition. Similarly, atherosclerosis development was decreased in chimeric LDLr-/- mice with TERT deletion in hematopoietic stem cells after bone marrow transplantation. TERT deficiency reduced macrophage accumulation in atherosclerotic lesions and altered chemokine expression, including CXC1/2/3, CCL3, CCL5, CCL21, CCR7, IL-6, and IL-1α. In isolated macrophages, sequence analysis of silenced inflammatory gene promoters indicated that TERT deletion altered signal transducer and activator of transcription 3 (STAT3)-dependent chemokine expression and recruitment of phosphorylated STAT3 to its target promoters. Mechanistically, TERT expression was necessary and sufficient to maintain STAT3 phosphorylation. Finally, we demonstrate that TERT deletion induces transcription of PIAS and SOCS3, both are endogenous inhibitors of STAT3 pathway. **CONCLUSIONS**: We propose that genetic TERT deficiency decreases atherosclerosis formation by silencing inflammatory chemokine transcription through inactivation of the STAT3 signaling pathway.

Disclosures: **H. Qing:** None. **E. Heywood:** None. **K.L. Jones:** None. **G. Doyon:** None. **D. Bruemmer:** None.

This research has received full or partial funding support from the American Heart Association.

424

An IFNg-regulated Macrophage Protein Network Links Type 2 Diabetes to Atherosclerosis

Catherine A Reardon, Amulya Lingaraju, Kelly Q Schoenfelt, Guolin Zhou, Univ of Chicago, Chicago, IL; Ning-Chun Liu, Ilona Babenko, Jay Heinecke, Tomas Vaiser, Andrew Hoofnagle, Univ of Washington, Seattle, WA; Lev Becker, Univ of Chicago, Chicago, IL

Type 2 diabetics have a higher risk for atherosclerosis, but the mechanisms underlying the increased risk are poorly understood. Macrophages, which are activated in type 2 diabetes (T2D) and have a role in all stages of atherogenesis, are an attractive link. Our hypothesis is that T2D promotes macrophage dysfunction to promote atherosclerosis. To investigate the relationship between T2D and macrophage dysfunction, we used a proteomics approach to identify dysregulated proteins secreted from peritoneal macrophages in a diet induced mouse model of obesity and insulin resistance in the absence of hypercholesterolemia. Twenty-seven T2D responsive proteins were identified that predict defects in many of the critical functions of macrophages in atherosclerosis (e.g. decreased apoE- cholesterol efflux; decreased MFGE8 – efferocytosis, increased MMP12- matrix degradation). The macrophages from lean and obese mice were not lipid loaded, but the obese macrophages accumulated significantly more

cholesterol when exposed to high levels of atherogenic lipoproteins in vitro suggesting that dysregulation of the T2D responsive proteins in diabetic mice render macrophages more susceptible to cholesterol loading. Importantly, many of these same protein changes, which were present in atherosclerotic *Ldlr-/-* mice with T2D, were normalized when these mice were fed non-diabetogenic hypercholesterolemic diets. Thus, foam cell formation in the presence and absence of T2D produces distinct effects on macrophage protein levels, and hence function. Further, we identify IFNγ as a mediator of the T2D responsive protein dysfunction. IFNγ, but not other cytokines, insulin or glucose, promote the T2D responsive protein dysregulation and increased susceptibility to cholesterol accumulation in vitro and the dysregulation is not observed in macrophage foam cells obtained from obese, diabetic IFNγ receptor 1 knockout animals. We also demonstrate that IFNγ can target these proteins in arterial wall macrophages *in vivo*. These studies suggest that IFNγ is an important mediator of macrophage dysfunction in T2D that may contribute to the enhanced cardiovascular risk in these patients.

Disclosures: **C.A. Reardon:** None. **A. Lingaraju:** None. **K.Q. Schoenfelt:** None. **G. Zhou:** None. **N. Liu:** None. **I. Babenko:** None. **J. Heinecke:** None. **T. Vaiser:** None. **A. Hoofnagle:** None. **L. Becker:** None.

425

Is Adventitial Thickening a Pathogenic Factor in Aortic Atherosclerosis?: A Controlled Transesophageal Echocardiographic Study

Luis P Roldan, UNM, Albuquerque, NM; **Paola C Roldan**, Univ of Colorado, Denver, CO; Brennan N Gibbs, Richard Snider, Michelle D Ratliff, Clifford R Qualls, Carlos A Roldan, UNM, Albuquerque, NM

Background. Aortic (Ao) atherosclerosis is common in systemic lupus erythematosus (SLE), is best assessed by transesophageal echocardiography (TEE), and is characterized by increased intima-media thickness (IMT) and plaques. Although TEE may also allow characterization of Ao adventitial thickness (AT), there is limited data on the pathogenic role of adventitial thickening in Ao atherosclerosis.
Methods. 68 SLE patients (62 women, age 36 ± 12 years) and 25 age-and-gender matched healthy controls (22 women, age 34 ± 11 years) underwent multiplane TEE. At a depth of 3-4 cm using narrow sector scan, 2-dimensional guided M-mode images were obtained to assess the presence of plaques, IMT outside of plaques, AT outside of plaques, and AT in plaques at three different levels of the thoracic Ao (proximal, mid, distal). At each aortic level, 3 IMT and 3 AT measurements were taken during end diastole using electronic calipers. These measurements were then averaged. Unaware of subjects' clinical data, one observer assessed for IMT and plaques while a second observer assessed AT. For purpose of analysis, intima-media thickening was defined as >1 mm which is >2SD above the corresponding overall mean IMT in controls (0.66 ± 0.17 mm), and adventitial thickening as >1.07 mm which is >2SD above the corresponding overall mean AT in controls (0.81 ± 0.13 mm). Plaques were defined as focal-protruding IMT >50% of the surrounding vessel wall at any aortic level.
Results. As shown in **Table 1A,** intima-media thickening and plaques were greater in patients than in controls. Similarly, adventitial thickening was more common in patients than in controls. In addition, AT was greater in patients with intima media thickening, plaques, and intima-media thickening or plaques (**Table 1B)**. Furthermore, AT was greater in plaques than AT outside of plaques (**Table 1C**).
Conclusion. Adventitial thickening is a pathogenic factor of Ao atherosclerosis in SLE.

Table 1A: Aortic Intima-Media Thickening, Plaques, and Adventitial Thickening in Patients and Controls		
Patients (N = 68)	**Controls (N = 25)**	**P Value**
Subjects with Intima-Media Thickening (>1mm)		
16 (24%)	1 (4%)	0.03
Subjects with Plaques		
17 (25%)	0	0.003
Subjects with Intima-Media Thickening or Plaques		
23 (34%)	1 (4%)	0.003
Subjects with Adventitial Thickening (>1.07 mm)		
10 (15%)	0	0.057
1B: Adventitial Thickness (mm) in Patients with and without Aortic Atherosclerosis		
Intima-Media Thickening (N = 16)	**No Intima-Media Thickening (N = 52)**	**P value**
0.93 ± 0.24	0.75 ± 0.26	0.02
Plaques (N = 17)	**No Plaques (N = 51)**	
0.90 ± 0.30	0.76 ± 0.25	0.09
Intima-Media Thickening or Plaques (N = 23)	**No Intima-Media Thickening or Plaques (N = 45)**	
0.91 ± 0.30	0.74 ± 0.24	0.02
1C: Adventitial Thickness (mm) in Patients with Plaques		
In Plaques	**Outside of Plaques**	
1.32 ± 0.17	0.98 ± 0.28	*0.0002

*Paired t-test.

Disclosures: **L.P. Roldan:** None. **P.C. Roldan:** None. **B.N. Gibbs:** None. **R. Snider:** None. **M.D. Ratliff:** None. **C.R. Qualls:** None. **C.A. Roldan:** None.

426

Overexpression of Tissue-nonspecific Alkaline Phosphatase (TNAP) Accelerates Coronary Artery Disease in the Setting of Hypercholesterolemia in Mice

Filippo Romanelli, AnthonyMarco Corbo, New York Inst of Technology Coll of Osteopathic Med, Old Westbury, NY; Maryam Salehi, Sanford Res, Sioux Falls, SD; Manisha C. Yadav, Sanford Burnham Prebys Medical Discovery Inst, La Jolla, CA; Soha Salman, David Petrosian, Omid J. Rashidbaigi, Maria Plummer, New York Inst of Technology Coll of Osteopathic Med, Old Westbury, NY; Ilian Radichev, Sanford Res, Sioux Falls, SD; Anthony B. Pinkerton, José Luis Millán, Sanford Burnham Prebys Medical Discovery Inst, La Jolla, CA; Alexei Y. Savinov, Sanford Res, Sioux Falls, SD; Olga V. Savinova, New York Inst of Technology Coll of Osteopathic Med, Old Westbury, NY

Objective - Vascular calcification in asymptomatic individuals is an independent predictor of coronary heart disease (CHD). It is therefore plausible that vascular calcification plays a direct pathophysiological role in atherosclerosis, an underlying cause of CHD. The purpose of this study was to examine the contribution that vascular calcification has on the development of coronary atherosclerosis in a mouse model of familial hypercholesterolemia. *Approach and Results* - Calcification was induced by overexpression of tissue-nonspecific alkaline phosphatase (TNAP) in endothelial cells of mice harboring a point mutation in the low density lipoprotein receptor (*ldlr,* wicked high cholesterol, WHC). Mice were fed an atherogenic diet; echocardiographic and biochemical data were collected longitudinally. Atherosclerosis and vascular calcification were analyzed histologically in the aorta, aortic sinus and coronary arteries. TNAP mice were also treated with a combination of an atherogenic diet and a specific inhibitor of TNAP (SBI-425). Combined with the *ldlr* mutation and an atherogenic diet, TNAP-driven arterial calcification led to severe atherosclerosis with 100% morbidity characterized by occlusive coronary artery disease, pathological cardiac hypertrophy with dilated LV and reduced ejection fraction (EF). We detected an interaction between vascular calcification and atherosclerosis in mice with endothelial TNAP overexpression. This interaction was particularly prominent in coronary circulation. Targeting TNAP activity therapeutically helped improve survival and heart function of endothelial TNAP overexpressor mice, however the incomplete inhibition of TNAP by SBI-425 was a limitation of this study. *Conclusions* - Vascular calcification *via* TNAP overexpression in endothelial cells promotes coronary atherosclerosis and is pathogenic under conditions of hypercholesterolemia.

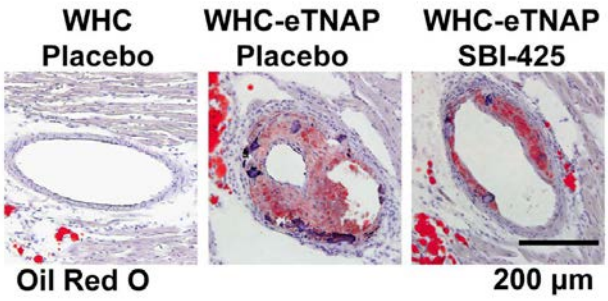

Disclosures: **F. Romanelli:** None. **A. Corbo:** None. **M. Salehi:** None. **M.C. Yadav:** None. **S. Salman:** None. **D. Petrosian:** None. **O.J. Rashidbaigi:** None. **M. Plummer:** None. **I. Radichev:** None. **A.B. Pinkerton:** None. **J. Millán:** None. **A.Y. Savinov:** None. **O.V. Savinova:** None.

427

Histopathological and Molecular Effects of SIRT3 Deletion in Advanced Calcific Aortic Valve Disease

Carolyn M Roos, Michael A Hagler, Grace C Verzosa, Bin Zhang, Hirokazu Fujimoto, Jordan D Miller, Mayo Clinic, Rochester, MN

Increasing age is the greatest risk factor for development and progression of calcific aortic valve disease (CAVD), and mitochondrial dysfunction has been implicated in the pathogenesis of cardiovascular calcification. Previous findings by our group suggested a significant reduction in expression of multiple sirtuin (SIRT) isoforms in normocholesterolemic aged mouse aortic valves, however, it is unclear if losses in SIRT3—a major mitochondrial SIRT isoform—modulates progression of aortic valve calcification. Therefore, we hypothesized that loss of SIRT3 in a hypercholesterolemic mouse model of CAVD will result in augmented calcium burden in aortic valve, increased osteogenic signaling, and impaired aortic valve function. To test this we used mice that were $Ldlr^{-/-}/ApoB^{100/100}$ mice that were either wild-type (LA-$SIRT3^{+/+}$) or null for SIRT3 (LA-$SIRT3^{-/-}$) and fed a western diet (TD88137) for 12 months. Alizarin red was used to quantitate calcium burden, qRT-PCR was used to measure changes in mRNA levels, and high-resolution echocardiography was used to assess aortic valve function (cusp separation distance). In line with our hypothesis, we observed a substantial increase in calcium burden in LA-$SIRT3^{-/-}$ mice compared to their LA-$SIRT3^{+/+}$ littermates(11.7±4.0, 4.8±1.8; respectively). Interestingly, expression of Runx2 and osterix—classic markers of osteogenic differentiation—were decreased in LA-$SIRT3^{-/-}$ mice compared to their LA-$SIRT3^{+/+}$ littermates. Expression of Msx2, were markedly increased in aortic valve tissue from LA-SIRT3-deficient mice. Despite these histological and molecular changes, SIRT3 deletion did not alter cusp separation distance (LA-$SIRT3^{+/+}$ = 0.81±0.04; LA-$SIRT3^{-/-}$ = 0.81±0.02). Collectively, this data suggest losses in SIRT3 can contribute to accelerated valve calcification through unclear molecular mechanisms, but these changes are not sufficient to drive reductions in cusp separation distance. Additional experiments delineating the histopathological and molecular sequelae of SIRT3 deletion will be critical to understanding its role in the pathogenesis of CAVD.

Disclosures: **C.M. Roos:** None. **M.A. Hagler:** None. **G.C. Verzosa:** None. **B. Zhang:** None. **H. Fujimoto:** None. **J.D. Miller:** None.

428

Role of Thrombospondin-1 in Atherosclerotic Complications Associated With Metabolic Syndrome

Soumyadip Sahu, Rituparna Ganguly, Brianna Rea, Abigail Cerroni, Amy Mathias, Priya Raman, Northeast Ohio Medical Univ, Rootstown, OH

Atherosclerosis is the leading cause of increased morbidity and mortality in metabolic syndrome (MetS), a constellation of risk factors that include hyperglycemia and visceral obesity. Individuals with MetS have increased incidence of vascular smooth muscle cell (VSMC) migration and proliferation, a key characteristic of VSMC phenotypic transition. We previously reported that high glucose and high leptin,

mimicking hyperglycemia and obesity, independently upregulate a potent proatherogenic matricellular protein, thrombospondin-1 (TSP-1), expression in VSMCs. The goal of the present study was to investigate the role of TSP-1 in development of atherosclerosis in MetS. We generated a mouse model of combined MetS and atherosclerosis (*KKAy*$^{+/-}$/ApoE$^{-/-}$) by crossing obese hyperglycemic agouti yellow *KKAy*$^{+/-}$ mice with atherosclerotic ApoE$^{-/-}$ mice. Upon weaning, yellow *KKAy*$^{+/-}$/ApoE$^{-/-}$ mice and age-matched black *KKAy*$^{-/-}$/ApoE$^{-/-}$ littermates were maintained on regular chow diet from 4-18 wks of age. Mice were euthanized after an overnight fasting; blood, aortae and heart were collected for lipid profiling, immunoblotting and atherosclerotic lesion studies. Yellow *KKAy*$^{+/-}$/ApoE$^{-/-}$ mice showed significant increase in body weight, blood glucose and plasma lipid levels vs. black *KKAy*$^{-/-}$/ApoE$^{-/-}$ littermates. Aortic root morphometry demonstrated increased lesion burden (Oil red O) and neointimal thickening (H & E) in MetS *KKAy*$^{+/-}$/ApoE$^{-/-}$ vs. non-MetS *KKAy*$^{-/-}$/ApoE$^{-/-}$ mice. Immunohistochemistry further revealed co-localization of α-SMA (SMC marker) and PCNA (proliferation marker) expression in aortic roots of *KKAy*$^{+/-}$/ApoE$^{-/-}$ vs. *KKAy*$^{-/-}$/ApoE$^{-/-}$ mice. Notably, lesion formation was associated with an increase in TSP-1 expression in aortic vessels. Consistently, TSP-1 and PCNA expression were elevated in aortic SMC (aSMC) primary cultures derived from obese diabetic *KKAy*$^{+/-}$ mice vs. lean non-diabetic *KKAy*$^{-/-}$ littermates. Finally, incubation of aSMC with a TSP-1 blocking peptide reduced PCNA and vimentin (SMC synthetic marker) expression coupled with attenuated SMC proliferation in obese diabetic *KKAy*$^{+/-}$ mice. Together, these results suggest a putative role of TSP-1 in accelerated atherosclerosis and VSMC phenotypic transition in MetS.

Disclosures: **S. Sahu:** None. **R. Ganguly:** None. **B. Rea:** None. **A. Cerroni:** None. **A. Mathias:** None. **P. Raman:** None.

429

The Effects of Fluvastatin and Methyl-β-Cyclodextrin-Mediated Cholesterol Depletion on the Biomechanics of Vascular Smooth Muscle Cells in Atherosclerosis

Hanna J Sanyour, Zhongkui Hong, Univ of South Dakota, Sioux Falls, SD

Atherosclerosis is a leading cause of death worldwide. Phenotypic shifting, alteration in cell adhesion, and migration toward inflammatory site of blood vessel wall are all critical contributions of vascular smooth muscle cells (VSMC) to the progression of atherosclerosis. Knowing that cholesterol is a main participant of fatty deposition in atherosclerotic lesions, cholesterol's role in orchestrating cell migration, mechanics and spreading has grown more apparent. Growing evidences suggests that cholesterol loaded into VSMC in atherosclerosis is much larger than previously known, and about 40% of the total foam cells in the atherosclerotic plaque were VSMC-derived. Emerging studies have increasingly categorized cholesterol as major player in regulating VSMC stiffness and N-Cadherin mediated cell-cell adhesions. Modulating their activity or expression may block VSMC migration during the progression of atherosclerosis. In this study, the effects of a 3-hydroxy-3-methylglutaryl-coenzyme-A reductase inhibitor, fluvastatin and Methyl-β-Cyclodextrin-Mediated (MβCD) cholesterol depletion on VSMCs N-cadherin adhesion and cellular stiffness were addressed. VSMCs cholesterol quantification and lactate dehydrogenase assays demonstrated significant reduction in total cellular cholesterol content by approx. 67% for fluvastatin and 40% for MβCD. The atomic force microscope (AFM) was used to investigate real time adhesion and stiffness of living VSMCs. A proprietary software package written in Matlab was used to estimate Young's modulus of the cell cortex. Cell adhesion was measured for 50-70% confluent cells with N-Cadherin coated stylus AFM probes on an AFM mounted on an inverted microscope. Our results suggested that fluvastatin and MβCD mediated cholesterol depletion increased N-cadherin mediated cell adhesion force by approx. 27% and 17% respectively. In addition, fluvastatin and MβCD respectively reduced VSMCs stiffness by approx. 24% and 29 % compared to control VSMCs. Altogether, the knowledge that we obtained in this project may lead to a novel therapeutic strategy that could potentially control and block VSMC migration and prevent atherosclerotic plaque formation by deciphering and regulating N-cadherin mediated adhesion

Disclosures: **H.J. Sanyour:** None. **Z. Hong:** None.

430

Myeloid RANK Deletion Accelerate the Development of Atherosclerosis in ApoE Deficient Mice with Chronic Kidney Disease

Marta Scatena, Will Driscoll, Luz Wigzell, Heather Striegel, Michael E Rosenfeld, Univ of Washington, Seattle, WA

Objective: Chronic kidney disease (CKD) greatly increases the risk of cardiovascular disease morbidity and mortality. Mounting data has identified the receptor activator of NF-κB (RANK) pathway as an important mediator of the accelerated atherosclerosis and vascular calcification observed in CKD. Here we investigated the role of myeloid RANK in a model of CKD accelerated atherosclerosis and vascular calcification in apolipoprotein E-deficient mice (apoE$^{-/-}$). *Methods and results:* We used the Lys M promoter to conditionally delete granulocyte and monocyte RANK in atherogenic apoE$^{-/-}$ mice. To induce CKD *RANK$^{(flox/flox)}$LysM$^{(cre/+)}$Apoe$^{(-/-)}$* (apoE$^{\Delta RANK}$) and *LysM$^{(cre/+)}$Apoe$^{(-/-)}$* (apoE^{CTL}) underwent a two-step surgical procedure to achieve 5/6th nephrectomy. Additional control animals underwent sham surgeries. Blood urea nitrogen (BUN) levels were elevated approximately two-fold in the CKD mice relative to sham-operated mice regardless of genotype. CKD was accompanied by a trend toward lower body weight, as well as slightly elevated circulating phosphate levels at the time of sacrifice. CKD induced a 47% elevation of plasma cholesterol levels in the apoE$^{\Delta RANK}$ and apoE^{CTL} mice, with no significant difference in cholesterol levels between the apoE$^{\Delta RANK}$ and apoE^{CTL} CKD mice. Interestingly, CKD resulted in elevated triglycerides in apoE$^{\Delta RANK}$ mice, but not in apoE^{CTL} mice. CKD mice age 22 and 34 weeks had larger average lesional cross-section areas in the root of the aorta as compared to sham operated mice ($p<0.001$ and $p=0.03$). Most importantly, the aortic root lesions in CKD apoE$^{\Delta RANK}$ mice were significantly larger than those from apoE^{CTL} CKD mice. In all genotypes and disease conditions we observed very little vascular calcification. *Conclusions:* These results suggest an atheroprotective role for myeloid RANK signaling in CDK-dependent lesion acceleration.

Disclosures: **M. Scatena:** None. **W. Driscoll:** None. **L. Wigzell:** None. **H. Striegel:** None. **M.E. Rosenfeld:** None.

This research has received full or partial funding support from the American Heart Association.

431

Nlrp3 Inflammasome Inhibits Cholesterol Efflux in Macrophages by Downregulating Gpr109a Expression. A Novel Proatherogenic Mechanism

Gantsetseg Tumurkhuu, Jargalsaikhan Dagvadorj, Wenxuan Zhang, Timothy Crother, Kenichi Shimada, Moshe Arditi, Shuang Chen, Cedars Sinai Medical Ctr, Depts of Pediatrics and Med, Div of Infectious Diseases and Immunology, and Infectious and Immunologic Diseases Res Ctr (IIDRC), Los Angeles, CA

Recent studies suggest that Nlrp3 inflammasome activation plays a critical role in the development of atherosclerosis and *Chlamydia pneumoniae (Cpn*) infection has been shown to accelerate atherogenesis. Herein, we asked whether Cpn infection induced acceleration is via Nlrp3 inflammasome activation in hypercholestrolemia mouse model. *Nlrp3$^{-/-}$Ldlr$^{-/-}$*, *Casp1$^{-/-}$Ldlr$^{-/-}$* and *Ldlr$^{-/-}$* mice were infected intranasally with *Cpn* followed by western diet (WD) for 16 weeks. *Ldlr$^{-/-}$* mice *infected with Cpn* infection had markedly increased lesion size in the aortic sinus and aorta *en face* compared to WD only group. Casp1 activation in lesion macrophages in *Ldlr$^{-/-}$* mice was also increased in *Cpn* group *vs* controls. *Nlrp3$^{-/-}$Ldlr$^{-/-}$* or *Casp1$^{-/-}$Ldlr$^{-/-}$* mice with and without *Cpn* resulted in significantly smaller of plaques in aortic root and aorta compare to *Ldlr$^{-/-}$* mice. However, no difference was observed between *Cpn* infected and uninfected groups in the double knockout animals. Furthermore, foam cell formation of *Nlrp3$^{-/-}$,* and *Casp1$^{-/-}$* peritoneal macrophages after treatment with OxLDL and *Cpn* was significantly reduced when compared with WT cells. Interestingly, expression levels of the cholesterol efflux transporter, ATP-binding cassette A1 (ABCA1), was increased by RT PCR and western analysis in the KO macrophages. Further investigations found that the niacin receptor Gpr109a, a known positive regulator of ABCA1, was upregulated in Nlrp3 KO macrophages during foam cell formation. Hydroxy-butyrate, an activating ligand of GPR109, was produced by macrophages after *Cpn* infection indicating a feedback loop. Intact IL-1 signaling suppressed Gpr109a expression suggesting a pathway by which the inflammasome and IL-1β could enhance foam cell formation. In aortic root lesions, macrophage expression of Gpr109a was increased in *Nlrp3$^{-/-}$Ldlr^{-}* mice compare with *Ldlr$^{-/-}$* mice on WD and infected with *Cpn*. In conclusion, the activation of the NLRP3 inflammasome negatively regulate Gpr109a receptor and its downstream cholesterol efflux transporter ABCA1, which leads to more foam cell formation and acceleration of

atherosclerosis in *Ldlr*$^{-/-}$ mice.
This work was supported by the National Institutes of Health grant HL111483 (to S. Chen)

Disclosures: **G. Tumurkhuu:** None. **J. Dagvadorj:** None. **W. Zhang:** None. **T. Crother:** None. **K. Shimada:** None. **M. Arditi:** None. **S. Chen:** None.

This research has received full or partial funding support from the American Heart Association.

433

Map Kinase Phosphatase-5 Deficiency in Macrophages Protects Against Atherogenesis

Xinbo Zhang, Yale Univ Sch of Med, New Haven, CT; Cheng Zhang, Temple Univ Sch of Med, Philadelphia, PA; Bo Tao, Lei Zhang, Anton M. Bennett, Yale Univ Sch of Med, New Haven, CT; **Jun Yu**, Temple Univ Sch of Med, Philadelphia, PA

Objective- To determine the role of macrophage MAP Kinase Phosphatase-5 (MKP-5) in the pathogenesis of atherosclerosis. **Approach and Results**- Lethally irradiated LDLR$^{-/-}$ mice were transplanted with wild-type (WT) or MKP-5 deficient (MKP-5$^{-/-}$) bone marrow and subjected to high-fat feeding. Mice transplanted with MKP-5$^{-/-}$ bone marrow developed smaller atherosclerotic lesions accompanied by decreased lipid deposition and macrophage content compared to WT. Lack of MKP-5 in macrophages led to decreased plasma levels of interleukin-1α (IL-1α) and IL-7, elevated anti-inflammatory cytokines IL-1 receptor antagonist (IL-1rn) and IL-4. Mechanistically, lack of MKP-5 in macrophages inhibited ox-LDL-induced foam cell formation through enhanced cholesterol efflux mediated by increased expression of ATP-binding cassette transporters ABCA1 and ABCG1. **Conclusions**-These data suggest that the macrophage MKP-5 deficiency reduces atherosclerosis progression and foam cell formation through amelioration of cholesterol efflux and inhibition of inflammation.

Disclosures: **X. Zhang:** None. **C. Zhang:** None. **B. Tao:** None. **L. Zhang:** None. **A.M. Bennett:** None. **J. Yu:** None.

This research has received full or partial funding support from the American Heart Association.

434

The Majority of Outpatients with Severe Hypercholesterolemia at an Academic Tertiary Centre Have Not Been Screened for FH

Ezim Ajufo, Masako Ueda, Erik Hossain, Tracey Sikora, Scott M Damrauer, Emil M deGoma, Kristen Dilzell, Stephanie DerOhannessian, Marina Cuchel, Daniel J Rader, Univ of Pennsylvania, Philadelphia, PA

Background: National and International guidelines recommend, as a minimum, that individuals with LDL-C ≥190mg/dL are asked about a family history of ASCVD and hypercholesterolemia to screen for familial hypercholesterolemia (FH), a monogenic condition that carries considerable ASCVD risk. However, FH is grossly underdiagnosed and undertreated in the US. One reason for this may be failure to screen severely hypercholesterolemic individuals for FH.
Hypothesis: We evaluated the hypothesis that poor identification of FH might be due to inadequate screening for FH among individuals with severe hypercholesterolemia.
Methods: An EHR query was used to identify active adult patients in the University of Pennsylvania outpatient EHR database (N=310 802) with LDL-C≥220mg/dL, excluding secondary causes of hypercholesterolemia. The EHR was then systematically reviewed for structured notation of family history information.
Result: The query identified 3,475 individuals with severely elevated LDL-C. Among them, only 47.9% (1666) had family history data relating to ASCVD (968), hypercholesterolemia (336) or both (362) in the EHR. The history was positive in 94.2% (1569) of these cases. Overall, patients with LDL-C ≥220mg/dL were more likely to be screened (OR 1.57; 95% CI 1.47-1.68) than those with LDL <220mg/dL. Within the former group, the odds of being screened were higher in Caucasians (OR 1.52; 95% CI 1.33-1.75), with more severe LDL-C elevation or a history of ASCVD (OR 1.36; 95% CI 1.10 - 1.67). Conversely, the presence of diabetes (OR 0.73; 95% CI 0.61-0.86) or hypertension (OR 0.82; 95% CI 0.72-0.94), made screening less likely to occur. Interestingly, the setting of clinical care was also important; individuals seen in secondary care (OR 1.68; 95% CI 1.41-2.26), general (OR 1.69, 95% CI 1.47-1.95) or preventative cardiology (OR 1.82; 95% CI 1.47-2.25) were more likely to be screened. Finally, statin prescription was

more common in those screened (OR 1.39; 95% CI 1.16-1.88), but this did not affect LDL-C goal achievement.
Conclusion: At a large academic centre, the majority of outpatients with severe hypercholesterolemia had no record of being screened for FH. This report sheds light on factors that might be relevant to the underdiagnosis of FH in the US.

Disclosures: **E. Ajufo:** None. **M. Ueda:** None. **E. Hossain:** None. **T. Sikora:** None. **S.M. Damrauer:** None. **E.M. deGoma:** None. **K. Dilzell:** None. **S. DerOhannessian:** None. **M. Cuchel:** None. **D.J. Rader:** None.

435

An Electronic Health Records Query for Severe Hypercholesterolemia Identifies Individuals With Undiagnosed Clinical and Molecular FH at a Tertiary Academic Centre

Ezim Ajufo, Masako Ueda, Tracey Sikora, Emil M deGoma, Kristen Dilzell, Anna Raper, Stephanie DerOhannessian, Erik Hossain, Megan L Mucksavage, Marina Cuchel, Daniel J Rader, Univ of Pennsylvania, Philadelphia, PA

Background: Familial hypercholesterolemia (FH) is a common heritable disorder of elevated low density lipoprotein cholesterol (LDL-C) with an estimated prevalence of 1/200-300 in the US; however, fewer than 10% of cases have been identified. We wanted to examine whether a simple EHR query for severe hypercholesterolemia could be used to identify clinically and genetically defined cases of FH.
Objectives/Purpose: We tested the hypothesis that querying the EHR using an LDL-C criterion would be a novel way to screen for and ultimately identify undiagnosed cases of FH.
Methods: An EHR screening query was used to identify active adult patients with LDL-C $\geq$ 220 mg/dL in the University of Pennsylvania outpatient EHR database. Patients with secondary causes of hypercholesterolemia and those who had previous genetic testing for FH were excluded. The query identified 3,475 individuals, 120 were subsequently consented and enrolled for molecular testing. This was performed with next-generation sequencing using Progenika's SEQPRO LIPO IS platform, targeting *LDLR, APOB, PCSK9* and *LDLRAP1*. A literature search was performed to gather information on identified *LDLR* variants of unknown significance (VUS). In addition, *in-silico* analysis was employed to evaluate the pathogenicity of the *LDLR* and *LDLRAP1* VUS.
Results: Among the 120 subjects, 53 (44.2%) met the Dutch Lipid Clinic Network (DLCN) criteria for probable or definite clinical FH. Molecularly, 19 FH-related pathogenic mutations were found in 18 (15%) individuals. Four had a common *APOB (*R3500Q) mutation, 14 had a *LDLR* mutation. One individual had a double heterozygous mutation in *PCSK9* and *LDLR.* In addition, 17 *LDLR* VUS were identified in 16 (13.9%) individuals. A literature review and *in-silico* analysis predicted that 8 VUS found in 10 subjects were "disease causing". Therefore, a total of 28 (24.3%) subjects from our cohort carried either a FH causal mutation or likely pathogenic variant. Overall, 59 subjects (49.2%) in our cohort were ascertained to have either a clinical or molecular diagnosis of FH.
Conclusion: The use of an EHR screening query for severe hypercholesterolemia was a novel, low investment but relatively high yield approach for identifying undiagnosed cases of FH at a tertiary academic centre.

Disclosures: **E. Ajufo:** None. **M. Ueda:** None. **T. Sikora:** None. **E.M. deGoma:** None. **K. Dilzell:** None. **A. Raper:** None. **S. DerOhannessian:** None. **E. Hossain:** None. **M.L. Mucksavage:** None. **M. Cuchel:** None. **D.J. Rader:** None.

437

Endothelial Cell Gene Expression in Hypertensive Mice

Stephen J Wilson, Kate L Lowe, Michael P Bokoch, Yoga Srinivasan, Roland S Wu, Shaun R Coughlin, Univ of California, San Francisco, San Francisco, CA

Hypertension is the major risk factor for premature cardiovascular disease, morbidity and mortality. It is the leading cause of death and disability globally, contributing to cardiovascular and renal diseases, including stroke, heart failure, coronary heart disease, and chronic kidney disease. We sought to determine the transcriptional changes that occur in cardiac endothelial cells secondary to hypertension, using ribosomal profiling of mice expressing the ribosomal protein Rpl22 tagged with the hemagglutinin (HA) epitope under control of Tie2-Cre (Tie2-Cre:RiboTag mice). Immunoprecipitation of HA-Rpl22 from

heart tissue isolated from Tie2-Cre:RiboTag mice resulted in an approximate 10-fold enrichment of endothelial genes (Pecam-1, VE-cadherin) relative to genes highly expressed in cardiomyocytes (Tnnt2, Fabp3) as assessed by RT-PCR. Subsequently, Tie2-Cre:RiboTag mice were implanted with osmotic pumps delivering saline or angiotensin II (1000ng/kg/min) for 4 weeks. Angiotensin II infusion significantly increased blood pressure ($p<0.0001$, n=7-8) resulting in an increased heart to body weight ratio (6.07 ± 0.48 vs 8.14 ± 0.73; $p<0.05$, n=7-8). Transcriptomes from Tie2-Cre positive cells within the heart were isolated using Ribotag ribosomal immunoprecipitation and RNA-seq was performed. Five hundred and eighty seven differentially expressed genes were detected (fold change >1.5, $p<0.05$, n=3), representing pathways such as extracellular matrix metabolism, angiogenesis and fatty acid transport. Analysis of hypertension associated gene expression in endothelial cells across different organs may reveal the mechanism of hypertension-associated diseases.

Disclosures: **S.J. Wilson:** None. **K.L. Lowe:** None. **M.P. Bokoch:** None. **Y. Srinivasan:** None. **R.S. Wu:** None. **S.R. Coughlin:** None.

438

Macrophages in a BAPN/AT2 Induced Model of Murine Aneurysm are Predominantly Lyve-1 and Tim-4 Negative

John S Byrne, Rickvinder Besla, Angela Li, Edouard Al-chami, Karen Legg, Emily Chen, Maral Ouzounian, Thomas Lindsay, Clint Robbins, Univ of Toronto, Toronto, ON, Canada

Macrophages are key effector cells in aneurysm progression. Aneurysm macrophages may derive from monocyte recruitment and turnover of resident cells. We tested the hypothesis that aneurysm macrophages have a non-resident (lyve-1/tim-4 negative) phenotype.
C57/Bl6 mice were administered beta-aminoproprionononitrile (BAPN) and angiotensin-2 (AT2). At four weeks, whole aortas were excised, photomicrographed, and single cell suspensions created for immunophenotyping with flow cytometry. Results were compared to wild-type controls.
BAPN/AT2 causes aortic dilatation ($p<0.01$) with maximal aneurysmal degeneration at the suprarenal aorta (wild-type control aortic diameter 0.93±0.03mm, n=8; BAPN/AT2 2.00±0.10mm, n=23; $p<0.0001$). BAPN/AT2 significantly increased aortic cd45+ myeloid-lymphoid cells and cd11b+ f4/80+ macrophages ($p<0.02$). Maximal aneurysm diameter correlated positively with aortic cell numbers of cd45+ myeloid-lymphoid cells ($R=0.8168$, $p<0.001$) and macrophages ($R=0.5977$, $p=0.02$). In wild-type, aortic macrophages are predominantly lyve-1 positive (67±3%, n=10). Whilst overall macrophage numbers are increased in aneurysm, the percentage of lyve-1 positive macrophages is significantly reduced (40±3%, n=18; $p<0.001$). The number of lyve-1 negative macrophages ($R=0.6875$, $p=0.02$), correlated with maximal suprarenal aortic diameter. In controls and aneurysm, lyve-1 positive, but not lyve-1 negative, macrophages are also tim-4 positive.
In a BAPN/AT2 murine aneurysm model, aortic cd45+ myeloid-lymphoid cells and macrophages are increased and cell counts correlate with maximal aortic dilatation. Wild-type murine aortic macrophages are predominantly lyve-1/tim4 positive, with a significant relative increase in lyve-1/tim4 negative macrophages in aneurysm, suggesting lyve-1/tim-4 may indicate a resident macrophage phenotype.

Disclosures: **J.S. Byrne:** None. **R. Besla:** None. **A. Li:** None. **E. Al-chami:** None. **K. Legg:** None. **E. Chen:** None. **M. Ouzounian:** None. **T. Lindsay:** None. **C. Robbins:** None.

439

High Dimensional Single-Cell Immune Contexture of Human Atherosclerotic Plaques and Blood

Adeeb Rahman, Aleksey Chudnovskiy, El-ad David Amir, Seunghee Kim-Schulze, Jennifer R Li, Christian Pina, Noah Moss, Romain Remark, Sacha Gnjatic, Peter Faries, Miriam Merad, **Chiara Giannarelli**, Icahn Sch of Med at Mount Sinai, New York, NY

Atherosclerosis is a disease characterized by immune infiltration of the arterial wall in response to tissue damage and systemic inflammation. In the era of precision medicine, is essential to gain insights on immune contexture of atherosclerotic tissue taking into account disease-specific cell variation in patients. We applied high-dimensional technologies for the analysis of multiple parameters at the single-cell level in clinical samples of patients undergoing carotid endatherectomy (CEA, n=15). Using time-of-flight mass-cytometry (CyTOF), we simultaneously analyzed 32 parameters at the single-cell level in peripheral blood mononuclear cells (PBMCs) and atherosclerotic-tissue associated immune cells of the same

patient.
Using viSNE, we mapped single-cell heterogeneity into two dimensions to discriminate PBMCs and tissue-associated CD45+ immune cells. Next, we employed Phenograph to cluster cells into phenotypically related populations, which were annotated based on canonical marker expression patterns.
We identified several major immune subsets including two subsets of macrophages ($CD163^{low}$ and $CD163^{high}$), monocytes, dendritic cells (DCs), B and T cells. The most prevalent CD45+ cells identified in atherosclerotic tissue were $CD4^+$ (25.8%) and $CD8^+$ (25.2%) T cells, macrophages (12.8%), monocytes (7.7%) and B (2.1%) cells. Using a regression analysis similar to that employed by CITRUS, we determined that macrophages and a subset of CD8 T cells characterized by low expression of CD127 were selectively enriched in tissue vs. blood. Multiplexed immunohistochemistry confirmed that T cells comprised a major portion of the CD45+ cells in atherosclerotic tissue, even more abundant than macrophages.
This study of deep phenotyping across-atherosclerotic tissue and blood demonstrate a significant T cell tissue infiltration of a specific subset of CD8 T cells. This suggests that adaptive T cell immunity plays a critical role in advanced atherosclerosis. The extension of this systems biology analysis pipeline to larger datasets can improve our understanding of the core mechanisms of chronic inflammation in atherosclerosis.

Disclosures: **A. Rahman:** None. **A. Chudnovskiy:** None. **E. Amir:** None. **S. Kim-Schulze:** None. **J.R. Li:** None. **C. Pina:** None. **N. Moss:** None. **R. Remark:** None. **S. Gnjatic:** None. **P. Faries:** None. **M. Merad:** None. **C. Giannarelli:** None.

441

Macrophage CD40 in Atherosclerosis, Obesity and Multiple Sclerosis

Annelie Shami, Suzanne Aarts, Academic Medical Ctr, Univ of Amsterdam, Amsterdam, Netherlands; Christina Bürger, Inst for Cardiovascular Prevention (IPEK), Ludwig-Maximilians Univ Munich, Munich, Germany; Pascal Kusters, Susan van den Berg, Tom Seijkens, Academic Medical Ctr, Univ of Amsterdam, Amsterdam, Netherlands; Gijs Kooij, Dept of Molecular Cell Biology and Immunology, Neuroscience Campus Amsterdam, VU Univ Medical Ctr, Amsterdam, Netherlands; Christian Weber, Norbert Gerdes, Inst for Cardiovascular Prevention (IPEK), Ludwig-Maximilians Univ Munich, Munich, Germany; Menno de Winther, Esther Lutgens, Academic Medical Ctr, Univ of Amsterdam, Amsterdam, Netherlands

Introduction: The co-stimulatory dyad CD40-CD40L plays a central role in fine-tuning immune reactions in atherosclerosis, obesity-induced inflammation and multiple sclerosis (MS). Inhibition of CD40 in atherosclerosis and experimental autoimmune encephalomyelitis (EAE) ameliorates disease outcome, whereas CD40-deficiency in a diet induced obesity (DIO) model worsens insulin resistance and induces excessive adipose tissue inflammation. Although inhibition of CD40 has powerful effects, we do not know which CD40 expressing cell-type is responsible for the amelioration/aggravation of disease. As myeloid CD40 is known to play a role in leukocyte trafficking, which is important in atherosclerosis, obesity and neuro-inflammation, we hypothesize that myeloid CD40 is important in these disease modalities.
Methods: To investigate the role of myeloid CD40 in atherosclerosis, obesity and EAE we have generated macrophage specific LysM-CD40flfl$^-$(ApoE-/-), and dendritic cell/adipose tissue macrophage specific CD11C-CD40flfl). Atherosclerosis was induced by aging the LysM-CD40flfl$^-$ApoE-/- mice until 30 weeks. EAE was induced in LysM-CD40flfl mice by subjecting them to myelin oligodendrocyte glycoprotein peptide (MOG35-55), and LysM-CD40flfl and CD11c-CD40flfl mice were subjected to a 60% high fat diet for 18 wks.
Results: LysM-CD40flfl$^-$ApoE-/- mice showed a significant reduction in atherosclerotic plaque area, with a reduced macrophage accumulation. Loss of macrophage CD40 in EAE results in a significant decrease in the neurological symptoms of EAE, and a majority of the LysM-CD40flfl mice were fully protected against EAE. LysM-CD40flfl mice subjected to DIO showed an increase in macrophage accumulation in the visceral adipose tissue, but did not affect adipose tissue mass, insulin tolerance, or plasma triglyceride concentrations. The CD11CcreCD40flfl mice exhibited a decrease in visceral adipose tissue weight, an increased lipid content in the liver and slightly decreases leukocyte numbers and pro-inflammatory gene expression in the adipose tissue.
Conclusions: Macrophage CD40 is an important driver of atherosclerosis and EAE. Macrophage CD40 is protective in obesity-induced inflammation, but is probably not the key player.

Disclosures: **A. Shami:** None. **S. Aarts:** None. **C. Bürger:** None. **P. Kusters:** None. **S. van den Berg:** None. **T. Seijkens:** None. **G. Kooij:** None. **C. Weber:** None. **N. Gerdes:** None. **M. de Winther:** None. **E. Lutgens:** None.

442

FOXO1/Notch Signaling Modulates Ambient Ultrafine Particle Impaired Vascular Repair

Kyung In Baek, René R. Sevag Packard, UCLA, Los Angeles, CA; Arian Saffari, USC, Los Angeles, CA; Zhao Ma, Anh Phuong Luu, Hilary Yen, Andrew Pieterson, Jeffrey J Hsu, UCLA, Los Angeles, CA; Bin Ren, Medical Coll of Wisconsin, Milwaukee, WI; Constantinos Sioutas, USC, Los Angeles, CA; Rongsong Li, Tzung K Hsiai, UCLA, Los Angeles, CA

Introduction: Exposure to ultrafine particles (UFP, d < 0.1 μm), redox-active components of particular matter ($PM_{2.5}$), promotes endothelial dysfunction. Notch signaling in endothelial cells (EC) regulates differentiation and proliferation of vasculature. FOXO1 interacts with Notch signaling by enhancing assembly of activation complex during induction of Notch signaling. Whether UFP impair vascular repair by modulating FOXO1/Notch signaling axis remains elusive.
Hypothesis: We hypothesized that UFP impairs vascular repair by attenuating Notch signaling via inhibition on FOXO1.
Methods and results: Control transgenic *Tg(fli1:gfp)* zebrafish embryos underwent tail amputation at 3 days post fertilization (dpf) developed complete vascular repair at 3 days post amputation (dpa), whereas exposure to UFP, or treatment with ADAM10 inhibitor to prevent Notch activation, or micro-injection of dominant negative(DN) Notch1b mRNA disrupted vascular network and impaired regeneration (*P < 0.05, n=20). By crossing the Notch reporter line *Tg(tp1:gfp)* with the *Tg(flk1:mCherry)* line, we demonstrated UFP inhibits endothelial Notch signaling on the amputated site at 3 dpa. Micro-injection of NICD mRNA only partially rescued endothelial Notch activity and impaired vascular repair in the presence of UFP (*P < 0.05, n=20). FOXO1 MO significantly inhibited Notch signaling, mimicking the UFP-impaired vascular repair. Injection of FOXO1 mRNA accentuated Notch activity and rescued UFP-impaired vascular repair. In human aortic endothelial cells, UFP suppressed FOXO1 expression and the co-localization with NICD, but not Master-Mind Like 1(MAML) or active NICD expression (*P < 0.05, n=3). As a corollary, UFP exposure induced dose and time-dependent reduction in Notch reporter activity, FOXO1 mRNA expression and the expression of Notch signaling related genes including the Notch ligand Dll4 and Notch target HES1. (*P < 0.05, n=3).
Conclusions: In conclusion, UFP attenuated FOXO1/Notch cooperation to modulate Notch signaling and impaired vascular repair in embryonic zebrafish.

Disclosures: **K. Baek:** None. **R.R. Packard:** None. **A. Saffari:** None. **Z. Ma:** None. **A.P. Luu:** None. **H. Yen:** None. **A. Pieterson:** None. **J.J. Hsu:** None. **B. Ren:** None. **C. Sioutas:** None. **R. Li:** None. **T.K. Hsiai:** None.

443

Absence of Pro-Protein Convertase Subtilisin/Kexin 6 Increases Flow-Mediated Outward Remodeling in the Mouse Common Carotid Artery

Samuel Röhl, Anders Arner, Kenneth Caidahl, Ulf Hedin, Ljubica Perisic Matic, Anton Razuvaev, Karolinska Instt, Stockholm, Sweden

Objective: Proprotein convertases (PCSKs) process matrix metalloproteases and cytokines but their function in vasculature is largely unknown. Previously, we demonstrated upregulation of PCSK6 in atherosclerotic plaques, localization to smooth muscle cells in the fibrous cap and positive correlation to inflammation, extracellular matrix remodeling and cytokines. Here, our aim was to evaluate the effects of PCSK6 on flow-mediated vascular remodeling in mice using high-frequency ultrasound and myography.
Materials and Methods: PCSK6 -/- and C57Bl/6J mice were compared in this study divided in baseline control and increased flow groups. Increased flow was created in the right common carotid artery (CCA) by ligation of the left CCA. All animals were subjected to high-frequency ultrasound examination prior to surgery, at 3 and 5 weeks after surgery. Upon euthanization 6 weeks post-surgery the right CCA was harvested for myography evaluation, subsequently fixed at optimal stretch and prepared for histological evaluation.
Results: The vascular circumference at optimal stretch in myography was strongly correlated (Pearson

r=0.74, p<0.001) and in agreement with the diastolic circumference measured by high-frequency ultrasound in examined animals. A significant increase in diastolic circumference was seen at 3 and 5 weeks after surgery in PCSK6 -/- mice with increased flow compared to PCSK6 -/- control group (1.6±0.15 mm vs 1.4±0.08 mm, p<0.05 and 1.7±0.09 mm vs 1.4±0.12 mm, p<0.01). Myography revealed a significant increase in circumference at optimal stretch (1.7±0.21 mm vs 1.4±0.08 mm, p<0.05) in PCSK6 -/- mice subjected to increased flow compared to PCSK6 -/- control group. A significant flow-mediated increase in medial contractility was identified (0.68±0.14 mN/mm vs 0.45±0.11 mN/mm, p<0.05) in C57Bl/6J mice compared to C57Bl/6J control where as an absence of flow-mediated increase in medial contractility was seen in PCSK6 -/- mice.
Conclusion: Absence of PCSK6 increases outward remodeling and reduces medial contractility in response to increased blood flow.

Disclosures: **S. Röhl:** None. **A. Arner:** None. **K. Caidahl:** None. **U. Hedin:** None. **L. Perisic Matic:** None. **A. Razuvaev:** None.

444

A Six-Microrna Panel Identified as a Potential Biomarker for Early-Stage Atherosclerotic Lesions

Genesio Karere, Jeremy Glenn, Dept of Genetics, Texas Biomedical Res Inst, San Antonio, TX; Samuel Galindo, Dept of Genetics, Southwest Natl Primate Res Ctr, Texas Biomedical Res Inst, San Antonio, TX; Roy Garcia, Frederic Chevalier, Dept of Genetics, Texas Biomedical Res Inst, San Antonio, TX; Edward Dick, Laura Cox, Dept of Genetics, Southwest Natl Primate Res Ctr, Texas Biomedical Res Inst, San Antonio, TX

Introduction Atherosclerosis is a progressive disease, and it's the common cause of cardiovascular disease (CVD). CVD is the leading cause of morbidity and mortality in the US. It is important to detect early-stage asymptomatic atherosclerosis prior to progression to plaques. However, it is not feasible to obtain target tissues from humans with early-stage atherosclerosis. We tested the hypothesis that a panel of microRNAs (miRNAs) expressed in atherosclerotic lesions and expressed in plasma of the same baboons are potential biomarkers indicative of initiation and progression of atherosclerosis. **Methods and Results** We used small RNA-Seq to identify miRNA expression profiles in atherosclerotic lesions and in plasma of baboons. We challenged adult baboons (n=24) with a high cholesterol, high fat (HCHF) diet for two years. After the diet challenge, common iliac arteries were harvested, fixed in 10% buffered formalin and stained with Sudan IV. We observed interesting fatty streak lesion variations, including early stage (EGES), flat (F) and raised (R) lesions, corresponding, respectively, to AHA lesion types I, II and V. We identified 45 miRNAs differentially expressed in fatty streak lesions (ES vs F=0; ES vs R =36; F vs R=9), and 43 miRNAs in plasma of the same animals (ES vs F=0; ES vs R =21; F vs R=22). Further, we observed that miR-30-5p, miR-340-5p, miR-548-5p and let-7-3p were expressed in flat lesions as well as in plasma, whereas miR-30-5p and miR-21-5p were expressed in raised lesions and in plasma. FDR < 0.05. **Conclusions** We conclude that a panel of six miRNAs differentially expressed in fatty streak lesions and differentially expressed in plasma of the same animals is a potential biomarker indicative of initiation and progression of atherosclerosis in baboons. Future studies will focus on translating baboon findings to humans.

Disclosures: **G. Karere:** None. **J. Glenn:** None. **S. Galindo:** None. **R. Garcia:** None. **F. Chevalier:** None. **E. Dick:** None. **L. Cox:** None.

This research has received full or partial funding support from the American Heart Association.

445

Venous Adventitial Cells May Protect Against Human Vein Graft Stenosis

Michael Sobel, Lihua Chen, Gale Tang, **Richard D Kenagy**, Univ of jWashington, Seattle, WA

Introduction: A $p27^{Kip1}$ single nucleotide polymorphism (SNP) is associated with vein graft failure. The protective genotype (AA) is associated with slower growth of human saphenous vein adventitial cells, but not of smooth muscle cells (SMCs). We investigated the influence of patient clinical characteristics on the migration of adventitial cells and SMCs from vein tissue and the interaction between adventitial cells and SMCs on cell growth.
Methods and Results: Tissue explants of the adventitia and intima/media were prepared from samples

of vein used for leg bypass, and the number of cells emerging from explants was counted over time (15 replicates/vein, 43 veins). Correlating migration with clinical characteristics of the patient, the degree of leg ischemia was an important factor. Migration of adventitial cells was slower with more severe ischemia (AAI<0.6; N=12) compared to milder ischemia (AAI≥0.6; N= 31): 37.0 ± 4.9 vs 53.8 ± 7.7 cells/explant day 7; mean ± SEM, P<.03). Migration of SMCs from the intima/media explants showed no influence of ischemia (19.1 ± 3.0 vs 24.1 ± 6.1; P=.12). The p27 SNP genotype, diabetes, smoking, and wounds/infection bore no correlation with migration. To test cell interactions, adventitial cells and SMCs from 11 veins were seeded in triplicate on opposite sides of 0.4 um Transwell filters that prevent cell migration (6 AA and 5 CC p27 SNP genotypes), such that the same or different cells were opposed. Cells were counted for a Day4/Day1 proliferation ratio. Compared to AA SMCs, AA adventitial cells significantly inhibited AA SMC growth (10.9 ± 2.5% inhibition; P<.01). In contrast, CC adventitial cells did not significantly inhibit CC SMC growth (4.1 ± 3.5% inhibition, P=.20).
Conclusions: Migration of adventitial cells, but not SMCs, from vein tissue is inhibited by increased ischemia. This suggests that adventitial cells may be beneficial, since more severe ischemia has been associated with poorer graft patency. Supporting this, adventitial cells with the protective AA genotype (but not the CC genotype) inhibit the growth of SMCs. These data suggest that adventitial cells and their in situ precursors may inhibit intimal hyperplasia and graft failure by inhibiting SMC proliferation in a p27 SNP genotype-dependent manner.

Disclosures: **M. Sobel:** None. **L. Chen:** None. **G. Tang:** None. **R.D. Kenagy:** None.

446

Cellular Uptake of Glycol Chitosan Nanoparticles in Idiopathic Pulmonary Fibrosis Fibroblasts in Response to the Collagen-Rich Microenvironment

Richard Nho, Ji-Young Yhee, Univ of Minnesota, Minneapolis, MN

Idiopathic pulmonary fibrosis (IPF) is a fatal lung disease characterized by the presence of persistent fibrotic fibroblasts which have apoptosis-resistant properties in response to cell death inducing conditions including type I collagen rich matrix. Although selective targeting of fibrotic fibroblasts is a feasible concept for the effective therapy of IPF, no reliable drug carriers for targeting IPF fibroblasts have been reported. To address this limitation, biodegradable glycol chitosan nanoparticles (CNPs) were utilized as a carrier system for selective targeting of IPF patients-derived fibroblasts. Primary human lung fibroblasts from non-IPF and IPF patients (n = 6/group) were treated with various doses (50−450 μg/ml) of CNPs, and the subcellular localization of CNPs was examined as a function of time (3, 6, and 30 h) with a confocal microscope. CNPs were found in the cytoplasm of fibroblasts at 30 h post-treatment on tissue culture plates in the absence of collagen while the intracellular CNPs were clearly observed at 3 h post-treatment. Importantly, the cellular uptake of the CNPs was significantly increased at 3, 6, and 30 h post-treatment, when control and IPF fibroblasts were cultured on collagen, suggesting that fibroblast and collagen interaction promotes the CNP's cellular internalization process. Clathrin-mediated endocytosis, caveolae-mediated endocytosis, and macropinocytosis were then suppressed by chlorpromazine (30 μM), genistein (100 μM), or amiloride (50 μM), respectively to elucidate the underlying mechanism of cellular uptake of CNPs in fibroblasts on the collagen matrix. Amiloride pre-treatment remarkably reduced the cellular internalization of CNPs in fibroblasts cultured on the collagen matrix. Furthermore, additional results also showed that sodium-hydrogen exchanger 1 (NHE-1) and PI3K play important roles in the increased cellular uptake of CNPs in the lung fibroblasts on the collagen matrix, suggesting that the subcellular localization of CNPs is largely due to the macropinocytosis. We propose that our approach can be a promising tactic for targeted delivery of therapeutics to the fibrotic fibroblasts residing in collagen matrix, which may lead to the improved treatment outcomes of this deadly disease.

Disclosures: **R. Nho:** None. **J. Yhee:** None.

447

Deep Transcriptomic Analysis of Human Vascular Cells Identifies Risk Genes for Common Vascular Diseases

Sylvia T Nurnberg, YoSon Park, Jordi Vaquero-Garcia, Univ of Pennsylvania, Philadelphia, PA; Milos Pjanic, Stanford Univ, Stanford, CA; Susanna Elwyn, John Pluta, Wei Zhao, Stephanie Testa, Yoseph Barash, Christopher Brown, Univ of Pennsylvania, Philadelphia, PA; Thomas Quertermous, Stanford Univ, Stanford, CA; Daniel Rader, Univ of Pennsylvania, Philadelphia, PA

The most recent Genome-wide Association Study (GWAS) meta-analysis has reported a total of 58 genomic loci to be statistically significantly associated with genetic susceptibility to Coronary Artery Disease (CAD) (Consortium, 2015). Many of these loci also associate with other phenotypes, with the majority being lipid traits (Tada et al., 2014). But also hypertension, stroke (Dichgans et al., 2014) and migraine (Pickrell et al., 2016) appear to share genetic determinants with CAD.
To functionally annotate the genomic loci harboring these association SNPs we sequenced the transcriptomes of 20 same donor human coronary artery endothelial (EC) and smooth muscle cell (SMC) lines. Deep RNA-Sequencing was used to assess Differential Gene Expression, Differential Splicing and Allele-Specific Expression. Focusing on GWAS loci for vascular phenotypes (CAD, stroke, migraine) we identified genes which display allele-specific differences in mRNA expression or splicing. We propose these genes as suitable targets for follow up studies.
Consortium, C.A.D. (2015). A comprehensive 1000 Genomes-based genome-wide association meta-analysis of coronary artery disease. Nature genetics 47, 1121-1130.
Tada, H., Won, H.H., Melander, O., Yang, J., Peloso, G.M., and Kathiresan, S. (2014). Multiple associated variants increase the heritability explained for plasma lipids and coronary artery disease. Circulation Cardiovascular genetics 7, 583-587.
Dichgans, M., Malik, R., Konig, I.R., Rosand, J., Clarke, R., Gretarsdottir, S., Thorleifsson, G., Mitchell, B.D., Assimes, T.L., Levi, C., et al. (2014). Shared genetic susceptibility to ischemic stroke and coronary artery disease: a genome-wide analysis of common variants. Stroke; a journal of cerebral circulation 45, 24-36.
Pickrell, J.K., Berisa, T., Liu, J.Z., Segurel, L., Tung, J.Y., and Hinds, D.A. (2016). Detection and interpretation of shared genetic influences on 42 human traits. Nature genetics 48, 709-717.

Disclosures: **S.T. Nurnberg:** None. **Y. Park:** None. **J. Vaquero-Garcia:** None. **M. Pjanic:** None. **S. Elwyn:** None. **J. Pluta:** None. **W. Zhao:** None. **S. Testa:** None. **Y. Barash:** None. **C. Brown:** None. **T. Quertermous:** None. **D. Rader:** None.

448

***Etv2-Mir130a-Jarid2* Cascade Regulates Vascular Patterning During Embryogenesis**

Bhairab N Singh, Lillehei Heart Inst, Minneapolis, MN; Naoyuki Tahara, Yasuhiko Kawakami, Dept of Genetics, UMN, Minneapolis, MN; Naoko Koyano-Nakagawa, Wuming Gong, Mary Garry, Daniel Garry, Lillehei Heart Inst, Minneapolis, MN

Remodeling of the pre-existing primitive vasculature is necessary for the formation of a complex branched vascular architecture. However, the factors that modulate these processes are incompletely defined. Previously, we defined the role of microRNAs (miRNAs) in endothelial specification. In the present study, we further examined the *Etv2-Cre* mediated ablation of *Dicer*$^{L/L}$ and characterized the perturbed vascular patterning in the embryo proper and yolk-sac. We mechanistically defined an important role for *miR-130a*, an Etv2 downstream target, in the mediation of vascular patterning and angiogenesis *in vitro* and *in vivo*. Inducible overexpression of *miR-130a* resulted in robust induction of vascular sprouts and angiogenesis with increased uptake of acetylated-LDL. Mechanistically, *miR-130a* directly regulates *Jarid2* expression by binding to its *3'-UTR* region. CRISPR/Cas9 mediated knockout of *miR-130a* showed increased levels of *Jarid2* in the ES/EB system. Further, the levels of *Jarid2* transcripts were increased in the *Etv2-null* embryos at E8.5. In the *in vivo* settings, injection of *miR-130a* specific morpholinos in zebrafish embryos resulted in perturbed vascular patterning with reduced levels of endothelial transcripts in the *miR-130a* morphants. qPCR and *in situ hybridization* techniques demonstrated increased expression of *jarid2a* in the *miR-130a* morphants *in vivo*. These findings demonstrate a critical role for *Etv2-miR-130a-Jarid2* in vascular patterning both *in vitro* and *in vivo*.

Disclosures: **B.N. Singh:** None. **N. Tahara:** None. **Y. Kawakami:** None. **N. Koyano-Nakagawa:** None. **W. Gong:** None. **M. Garry:** None. **D. Garry:** None.

450

Monocytic Glutaredoxin 1 Protects Mice Against Obesity, Hyperglycemia and Atherosclerosis

Kevin Downs, Sina Tavakoli, John D Short, Huynh N Nguyen, Reto Asmis, UTHSCSA, San Antonio, TX

Overexpression of glutaredoxin 1 (Grx1) protects monocytes from metabolic stress-induced priming, i.e. dysregulation and hypersensitization to chemokines (Ullevig et al. ATVB 2012). To address the role of monocytic Grx1 in mice and in the development of atherogenesis and obesity, we transplanted bone marrow (BM) from either wild-type (WT) or $Grx1^{-/-}$ donor mice into atherosclerosis-prone $LDLR^{-/-}$ mice and fed these mice a high-fat diet (HFD) for up to 20 weeks. $Grx1_{Leuko}{}^{-/-}$ mice showed accelerated weight gain after 9 weeks followed by early onset of hyperglycemia. After 6 weeks on HFD, atherosclerotic lesions were slightly larger in $Grx1_{Leuko}{}^{-/-}$ mice than in WT mice, but the differences did not reach statistical significance. However, after 20 weeks, $Grx1_{Leuko}{}^{-/-}$ mice showed 36% larger lesions than WT-BM recipients, and monocyte chemotaxis *in vivo* was increased 1.6-fold. Furthermore, compared to WT-BM recipients, adipose tissues and livers of $Grx1_{Leuko}{}^{-/-}$ mice also showed increased macrophage content and elevated tissue inflammation as determined by IHC and qRT-PCR-based gene array. Adipose tissue in particular, showed significant increases in the expression of proinflammatory genes in addition to an increased abundance of proinflammatory “crown-like” structures. In contrast, genes associated with inflammation resolving macrophages were significantly suppressed. Macrophages isolated from $Grx1^{-/-}$ mice and stimulated with INFγ+TNFα also showed increased expression of pro-inflammatory M1-associated genes, whereas M2-associated genes were suppressed in $Grx\text{-}1^{-/-}$ macrophages activated with IL-4. Furthermore, macrophages from $Grx1^{-/-}$ mice exposed to metabolic stress also display increased protein *S*-glutathionylation, enhanced hypersensitization to chemokine, and impaired autophagy compared to macrophages from wild-type mice. Taken together, our data show that loss of monocytic Grx1 worsens monocyte priming in response to HFD-induced metabolic stress and accelerates the infiltration of dysfunctional monocyte-derived macrophages into tissues, such as aorta, liver and adipose tissues. We conclude that monocytic Grx1 is critical for maintaining metabolic homeostasis in mice and protects mice against obesity and atherogenesis.

Disclosures: **K. Downs:** None. **S. Tavakoli:** None. **J.D. Short:** None. **H.N. Nguyen:** None. **R. Asmis:** None.

This research has received full or partial funding support from the American Heart Association.

452

Serine Carboxypeptidase 1 Mediates Vascular Remodeling by Increasing Inflammatory Cell Infiltration

Ting-Hein Lee, Chang Gung Univ, Kwei-Shan Tao-Yuan, Taiwan; Joseph Miano, Aab Cardiovascular Res Inst, Univ of Rochester Sch of Med and Dentistry, Rochester, NY

In pathological vascular remodeling, contractile vascular smooth muscle cells (VSMCs) switch their phenotype to highly proliferative and migratory states leading to neointimal formation. Inflammatory cell recruitment and infiltration, which is dependent on the increased expression of adhesion molecules on the endothelial cells, is a key event to initiate SMC phenotypic modulation in vascular remodeling. Serine carboxypeptidase 1 (scpep1), a novel protease containing the putative catalytic triad (Ser-Asp-His) common to all members of the serine protease family, has been proved to be involved in vascular remodeling by promoting SMC proliferation and migration in a catalytic triad-dependent manner. To determine whether Scpep1 modulates leukocyte adhesion and infiltration, a flow-induced model of vascular remodeling was conducted in wild-type (WT) or Scpep1 knockout (KO) mice. Scpep1-null mice show a decreased number of infiltrated leukocytes into the intima and media compared to WT mice. Further, mice devoid of Scpep1 show a dramatic reduction of vascular cell adhesion molecule-1 (VCAM-1) and intercellular cell adhesion molecule-1 (ICAM-1) expression in vessels in comparison with that of WT mice. Consistent with our in vivo data, the expression levels of ICAM-1 and VCAM-1 on human umbilical vein endothelial cells (HUVECs) transfected with SiRNA against Scpep1 were significantly decreased after TNF-α treatment. Taken together, these data suggest that Scpep1 may increase leukocyte extravasation by increasing the expression of VCAM-1 and ICAM-1 adhesion molecules.

Disclosures: **T. Lee:** None. **J. Miano:** None.

454

Myeloid CD98hc Deficiency Reduces Atherosclerotic Plaque Development via Impaired Proliferation of Macrophages

Sara McCurdy, William A Boisvert, Univ of Hawaii, John A. Burns Sch of Med, Honolulu, HI

Macrophage accumulation is a key process affecting all stages of atherosclerosis. Whether these cells accumulate in plaque solely by recruitment of monocytes from circulation or by proliferation within the plaque is an important question that has garnered much interest in recent years. Originally identified as a lymphocyte activation marker, CD98hc (SLC3A2) is a transmembrane protein involved in cell proliferation and survival *via* integrin signaling and MAP kinase activation. We hypothesized that CD98hc deficiency in myeloid cells would have a protective effect on atherosclerosis development and plaque composition by limiting macrophage proliferation. For the studies described, we utilized mice with myeloid-specific deletion of the CD98hc (*CD98hc$^{fl/fl}$LysMCre^{+}*) to determine the effects of CD98hc deficiency on macrophage function in the context of atherosclerosis. We performed *in vitro* assays to investigate the role of CD98hc in the proliferation and survival of primary mouse bone marrow derived macrophages. Although we found no differences in the number of bone marrow cells isolated from control or CD98hc$^{-/-}$ animals, after differentiation with MCS-F for 7 days, the number of macrophages obtained from CD98hc$^{-/-}$ mice was approximately 80% lower ($7.2 \pm 2.2 \times 10^6$ vs. $42.4 \pm 4.6 \times 10^6$ per mouse) compared to control mice. Proliferation assays *in vitro* using EdU revealed approximately 50% (15.4 ± 2.5% vs. 7.5±1.8%) reduced cell proliferation in CD98hc$^{-/-}$ macrophages compared to control cells that could not be rescued with the addition M-CSF. In a 6-week atherosclerosis study using *Ldlr$^{-/-}$CD98hc$^{fl/fl}$LysMCre^{+}* mice, Oil-Red O staining of whole aortae as well as aortic sinus sections showed that atherosclerotic plaque development was reduced compared to *Ldlr$^{-/-}$CD98hc$^{fl/fl}$LysMCre^{-}* control mice. Additionally, immunohistochemical staining of atherosclerotic tissues revealed a reduction in macrophage abundance and proliferation within the plaque of *Ldlr$^{-/-}$CD98hc$^{fl/fl}$LysMCre^{+}* mice compared to control mice. These findings support an important role of CD98hc in macrophage proliferation within the plaque environment, and provide a novel target for reducing atherosclerosis.

Disclosures: **S. McCurdy:** None. **W.A. Boisvert:** None.

This research has received full or partial funding support from the American Heart Association.

455

HDL-Small RNA Gene Regulatory Networks Alter T Cell Signalling in Systemic Lupus Erythematosus

Danielle L Michell, Jared L Moore, Michelle J Ormseth, Shilin Zhao, Quanhu Sheng, C. Michael Stein, Amy S Major, Kasey C Vickers, Vanderbilt Univ Medical Ctr, Nashville, TN

Systemic Lupus Erythematosus (SLE) is a debilitating disease primarily in women involving complex T and B cell dysregulation. SLE presents with dysfunctional HDL and we have previously found that HDL-microRNAs (miRNA) are significantly altered in SLE; however, miRNAs are just one of many types of small non-coding RNAs (sRNA). As such, we hypothesized that HDL-sRNA cargo and cell-to-cell communication in SLE extend beyond miRNAs. Using high-throughput sRNA sequencing (sRNA-seq), we found that tRNA-derived sRNAs (tDRs) were highly abundant on HDL and were significantly altered in SLE subjects (n=9) compared to controls (n=8, $P<0.05$). In addition, circulating levels of angiogenin, an RNaseIII enzyme responsible for tDR cleavage from parent tRNAs, was also found to be significantly increased in plasma ($P<0.05$) from SLE subjects compared to controls. To determine if tDRs are altered in CD4+ T cells in SLE subjects, real-time PCR was used to quantify candidate tDRs, and we found that tDR-GlyGCC levels were significantly increased 4.2-fold in SLE ($P<0.01$) and readily exported to HDL. Strikingly, total RNAseq, *in silico* analysis, and mRNA sequencing suggested that ROCK2, a critical regulator of CD4+ T cell differentiation, is a direct tDR-GlyGCC target gene which was confirmed with gene reported (luciferase) assays. Moreover, activated human CD4+ T cells transfected with tDR-GlyGCC mimetics, demonstrated reduced ROCK2 protein levels and STAT3 phosphorylation, and consequently reduced inflammatory cytokine secretion (IL-17 and IL-21; $P<0.05$). To determine if T cell exported tDR-GlyGCC is transferred between cells by HDL, *ex vivo* studies were completed using Trans-PhotoActivatable-Ribonucleoside-CrossLinking-ImmunoPrecipitation high-throughput Sequencing (Trans-PAR-CLIPseq). Using this approach, we found a cassette of CD4+ T cell-originating sRNAs, including

tDR-GlyGCC, that were transferred by HDL to recipient immune cells. Here, we demonstrate that HDL facilitates intercellular transfer of tDRs between immune cells and a critical role for tDR-GlyGCC in regulating T cell signalling.

Disclosures: **D.L. Michell:** None. **J.L. Moore:** None. **M.J. Ormseth:** None. **S. Zhao:** None. **Q. Sheng:** None. **C. Stein:** None. **A.S. Major:** None. **K.C. Vickers:** None.

This research has received full or partial funding support from the American Heart Association.

456

Rage Suppresses Angiogenesis and Blood Flow Recovery After Hind Limb Ischemia in Diabetic Mice Through Modulation of Macrophage Inflammation and Macrophage-endothelial Interactions

Raquel Lopez Diez, Qing Li, Huilin Li, Shi Fang Yan, Ann Marie Schmidt, New York Univ, New York, NY

Peripheral vascular disease is a condition characterized by atherosclerotic narrowed arteries distal to the aorta which triggers an acute or critical limb ischemia. Development of ischemic PVD has been considered one of the principal complications of diabetes, leading to amputation of digits and limbs. Advanced glycation end products (AGE) ligands and their receptor (RAGE) have been implicated in multiple key mechanisms underlying diabetes and diabetic complications, including hypoxia and ischemia/reperfusion injury. We tested the hypothesis that vascular recovery after hind limb ischemia would be rescued by deficiency of RAGE, at least in part through modulation of macrophage dysfunction. Wild type (WT) and *Ager* deficient mice were rendered diabetic with streptozotocin, and subjected to unilateral hind limb ischemia. Previous results showed an increased accumulation and expression of AGEs and RAGE in ischemic muscle, especially in diabetic WT mice. Attenuated angiogenesis and impaired blood flow recovery were also observed, in parallel with reduced early inflammatory macrophage infiltration into ischemic muscle in the WT diabetic mice. We performed flow cytometry to analyze circulating monocyte subsets: pro-inflammatory Ly6G/C^{hi} and anti-inflammatory Ly6G/C^{lo}. Work by others reported higher levels of monocytes in diabetes in the baseline state without injury; our data indicate that the increase is mostly attributed to the pro-inflammatory Ly6G/C^{hi} population, being significantly lower in the *Ager*$^{-/-}$ diabetic mice. After seven days of ischemia to the unilateral hind limb, lower levels of circulating pro-inflammatory Ly6G/C^{hi} monocytes were found in both WT and *Ager* deficient diabetic mice. After four weeks of injury, the pro-inflammatory monocytes levels were significantly recovered to baseline levels in *Ager*$^{-/-}$ mice, whereas WT mice failed to reacquire their baseline levels. *In vitro* studies using murine endothelial cells and murine macrophages revealed that RAGE suppressed macrophage-endothelial cell interaction, particularly in diabetes-relevant concentrations of D-glucose. These data suggest unique ischemia-dependent mechanisms in hind limb ischemia through RAGE down-regulation of the early adaptive immune response.

Disclosures: **R. Lopez Diez:** None. **Q. Li:** None. **H. Li:** None. **S. Yan:** None. **A. Schmidt:** None.

457

Selective Epidermal Growth Factor Receptor Inhibition in Cd4+ T Cells Induces Anergy and Limits Atherosclerosis Development

Lynda Zeboudj, Mikael Maître, Lea Guyonnet, Ludivine Laurans, Jeremie Lemarie, Andreas Giraud, Simon Bourcier, Wared Nour-Eldine, Alain Tedgui, Ziad Mallat, Pierre-Louis Tharaux, Hafid Ait-Oufella, INSERM UMR970, Paris, France

Background. Several Epidermal Growth Factor receptor (EGFR) inhibitors have been successfully developed for the treatment of cancer. They inhibit tumor cell survival, proliferation and migration. EGFR is also expressed by leukocytes, but little is known about its role in the modulation of the immune response. We aimed to determine whether EGF-R expressed on CD4$^+$ T cells is functional, and to address the consequences of EGF-R inhibition in atherosclerosis, a T cell-mediated chronic inflammatory disease of the vascular wall.
Method and results. Mouse CD4$^+$ T cells expressed Egfr, and the EGFR tyrosine kinase inhibitor AG-1478 blocked *in vitro* T cell proliferation and Th1/Th2 cytokine production. *In vivo*, treatment of *Ldlr*$^{-/-}$ mice with the Egfr inhibitor Erlotinib for 8 weeks induced T cell anergy, reduced T cell infiltration within atherosclerotic lesions and protected against atherosclerosis. Selective deletion of Egfr in CD4$^+$ T cells resulted in decreased T cell proliferation and activation both *in vitro* and *in vivo*, as well as reduced IFN-γ,

IL-17A, IL-4 and IL-10 production. Atherosclerotic lesion size was reduced by 2-fold in irradiated *Ldlr*$^{-/-}$ mice reconstituted with bone marrow from *Cd4Cre Egfr*$^{lox/lox}$ mouse, compared to *Cd4Cre Egfr*$^{+/+}$ chimeric mice, after 4, 6 and 12 weeks of high fat diet, associated with marked reduction in T cell infiltration in atherosclerotic plaques. Finally, human blood T cells expressed EGFR and EGFR inhibition reduced T cell proliferation both *in vivo* and *in vitro*.
Conclusion. EGFR is expressed by human and mouse CD4^{+} T cells. EGFR pharmacological inhibition or genetic invalidation induced T cell anergy *in vitro* and *in vivo*, and reduced atherosclerosis development. Our results suggest that targeting EGFR may be a novel strategy to combat atherosclerosis.

Disclosures: **L. Zeboudj:** None. **M. Maître:** None. **L. Guyonnet:** None. **L. Laurans:** None. **J. Lemarie:** None. **A. Giraud:** None. **S. Bourcier:** None. **W. Nour-Eldine:** None. **A. Tedgui:** None. **Z. Mallat:** None. **P. Tharaux:** None. **H. Ait-Oufella:** None.

458

Role of Colony Stimulating Factor 1 Receptor in Graft Vascular Disease

Vanessa Almonte, Oriyanhan Wunimenghe, Dario F Riascos-Bernal, Prameladevi Chinnasamy, Smitha Jayakumar, Nicholas E Sibinga, Albert Einstein Coll of Med, Bronx, NY

Heart and kidney transplants are effective treatments for end-stage organ failure, but their long-term success is limited by graft vascular disease (GVD), the leading cause of solid organ transplant failure. This process manifests as concentric thickening of vessel walls due to neointimal hyperplasia in the donor organ, characterized by expansion of cells, notably smooth muscle-like cells (SMLCs) and macrophages (MPs), which accumulate, proliferate, and eventually occlude the lumen of arteries. Our lab recently reported that loss of colony stimulating factor-1 (CSF1) expression in either donor or recipient mice limits GVD, and showed that SMLCs isolated from neointimal lesions express high levels of CSF1 and its receptor, CSF1R. While CSF1-mediated activation of CSF1R has been studied extensively in MP biology, its role in SMLCs and GVD has not been well characterized. We hypothesize that CSF1R activation in neointimal MPs and SMCs occurs after organ transplantation and promotes the development of GVD.
To test this idea, carotid arteries from 8-12 week old C57/B6J male mice were transplanted orthotopically into female or male mice. At day 30 post transplantation, sex-mismatched transplants developed significant neointimal lesions not seen in sex-matched controls. Neointimal, adventitial, and to a lesser extent medial cells were positive for CSF1R and CD68, which were scarcely detected in control untransplanted arteries. Cells in the media of transplanted vessels co-stained for smooth muscle alpha actin (SMA) and calponin. SMA-positive cells were found in neointimal lesions, with few cells co-expressing calponin. Proliferation, assessed by Phospho-histone H3 staining, was evident in cells of uncertain origin in the media and neointima. In conclusion, H-Y antigen-driven histoincompatibility in this mouse transplant model yielded vascular lesions that resemble GVD, with significant neointima formation, preservation of medial cells, and evidence of CSF1R expression and of cell proliferation. Future studies will focus on lineage tracing of smooth muscle and myeloid cells to evaluate neointimal cell origins, plus genetic depletion of CSF1R in these cell lineages to determine the requirement for CSF1R expression in the development of GVD.

Disclosures: **V. Almonte:** None. **O. Wunimenghe:** None. **D.F. Riascos-Bernal:** None. **P. Chinnasamy:** None. **S. Jayakumar:** None. **N.E.S. Sibinga:** None.

459

O-Linked N-Acetylglucosamine Promotes Vascular Smooth Muscle Cell Dedifferentiation and Intimal Hyperplasia

Ashley J Bauer, Kristen L Leslie, Allison C Ostriker, Kathleen A Martin, Yale Univ, New Haven, CT

Vascular smooth muscle cells (VSMCs) exhibit a unique phenotypic plasticity that underlies numerous cardiovascular pathologies. Platelet-derived growth factor (PDGF) promotes VSMC dedifferentiation characterized by proliferation and decreased contractile protein expression while the mTORC1 inhibitor and stent therapeutic rapamycin inhibits these effects. The enzyme O-linked N-Acetylglucosamine (O-GlcNAc) Transferase (OGT) adds O-GlcNAc modifications to serine or threonine in proteins and has been implicated in cardiovascular diseases. We hypothesized that OGT may regulate VSMC plasticity. We found that OGT and O-GlcNAc expression were associated with dedifferentiation, as both were decreased by rapamycin, but increased with PDGF treatment in human coronary artery SMCs. Knocking

down OGT *in vitro* increased contractile marker expression at the mRNA and protein levels, including MYH11, CNN, TGLN, and ACTA2, while decreasing VSMC proliferation. Conversely, OGT overexpression inhibited expression of MHY11, CNN, and TGLN. Consistent with a role in dedifferentiation, immunostaining revealed that OGT and O-GlcNAc were increased following femoral artery endothelial denudation injury in C57BL/6 mice. Notably, smooth muscle-specific OGT knockout attenuated neointima formation relative to controls in a carotid artery ligation model of intimal hyperplasia. In conclusion, these findings indicate that PDGF and vascular injury increase OGT expression and O-GlcNAc modifications in SMCs in vitro and in vivo, leading to OGT-dependent transcriptional repression of contractile marker expression and promotion of intimal hyperplasia.

Disclosures: **A.J. Bauer:** None. **K.L. Leslie:** None. **A.C. Ostriker:** None. **K.A. Martin:** None.

460

Intra- and Inter-Day Reproducibility of Low-Flow Mediated Constriction Response in Young Adults

Michelle M. Harbin, Univ of Minnesota, Twin Cities, Minneapolis, MN; Joseph D. Ostrem, Concordia Univ - St. Paul, St. Paul, MN; Nicholas G. Evanoff, Aaron S. Kelly, Donald R. Dengel, Univ of Minnesota, Twin Cities, Minneapolis, MN

PURPOSE: When assessing vasomotor endothelial function of the brachial artery by reactive hyperemia, blood flow is stopped and creates a period of low-flow mediated constriction (L-FMC). Little is known about how this parameter influences flow-mediated vasodilation (FMD). The purpose of this study was to better understand this relationship and to determine the intra- and inter-day reproducibility of brachial L-FMC in healthy adults. **METHODS:** Brachial L-FMC and FMD were measured on 26 healthy, young adults (13 males, 13 females; 24.6 ± 2.7 years). Each subject had two assessments conducted on two separate visits, separated by a minimum of seven days. Brachial artery pre-occlusion baseline diameter was imaged during rest and prior to cuff-occlusion. Continuous imaging of the artery was captured during the last 20 seconds of cuff-occlusion to 180 seconds post-cuff release. An L-FMC was considered present if the relative change from pre-occlusion baseline to L-FMC artery diameter was less than -0.1%. Peak FMD was measured as the greatest 10-second average in brachial artery diameter following occlusion compared to pre-occlusion baseline. **RESULTS**: Overall, there was a strong, positive correlation between increased brachial L-FMC and blunted FMD (visit 1 test 1: r=0.758, p<0.001; visit 1 test 2: r=0.706, p<0.001; visit 2 test 1: r=0.836, p<0.001; visit 2 test 2: 0.857, p<0.001). The reproducibility of intra- and inter-day L-FMC diameter were ICC = 0.627, CV = 54.4% and ICC = 0.734, CV = 43.5%, respectively. **CONCLUSION**: The results of the present study suggest that the degree of vasoconstriction to low-flow conditions influences the subsequent maximal dilation during reactive hyperemia. However, L-FMC in young adults is variable as evidenced by the weak inter- and intra-day reproducibility of the measure. Further research is needed to study brachial L-FMC reproducibility among varying subject populations and the implications L-FMC has on the interpretation of FMD results.

Disclosures: **M.M. Harbin:** None. **J.D. Ostrem:** None. **N.G. Evanoff:** None. **A.S. Kelly:** None. **D.R. Dengel:** None.

461

A Novel Model of Spontaneous Arteriovenous Fistula Formation

Yukinobu Ito, Makoto Yoshida, Akita Univ Graduate Sch of Med, Akita, Japan; Hirotake Masuda, Ogachi Central Hosp, Ogachi, Japan; Hiroshi Nanjo, Akiteru Goto, Akita Univ Graduate Sch of Med, Akita, Japan

Aims: Most In vivo angiogenesis studies have been performed by setting an ischemic condition, or by administrating angiogenic factors such as vascular endothelial growth factor. Unexpectedly, we discovered to spontaneously create new blood vessels by just suturing an arterial graft patch in the jugular vein, using a rabbit model. In general, arteriovenous malformations consist of tangles of arteries and veins that are often connected by a fistula. However, the causes and mechanisms of these clinical entities are not fully understood. The purpose of this study is to show the methods used to produce the model, and then to report the chronological processes involved in the development of this neovasculature and the change of endogenous angiogenic factors. **Methods and Results:** We performed to suture an arterial graft patch into the rabbit vein. Within a month after the surgery, dense (nidus-like) neovasculature was formed around the patch. Angiography and pulse-oximeter analyses demonstrated that the blood, which flew into the new vessels, was arterial blood. It means that arteriovenous shunt has

been formed. Pathological evaluation revealed multiple branching vessels sprouting out from the patch suture site, and numerous dilated vessels devoid of sphincter muscle in the surrounding connective tissue. We determined, by FISH analysis, that these branches had originated from the graft itself. The endogenous angiogenic factors, such as VEGF, have soared immediately after the surgery. **Conclusion:** This is the first *in vivo* model of spontaneous arteriovenous fistula formation via the creation of neovasculature. These findings exemplify the difference between the arterial and venous intima, and we believe that this difference could be key to understanding human vascular anomaly diseases and the basic principles of vascular network formation, angiogenesis and/or vasculogenesis.

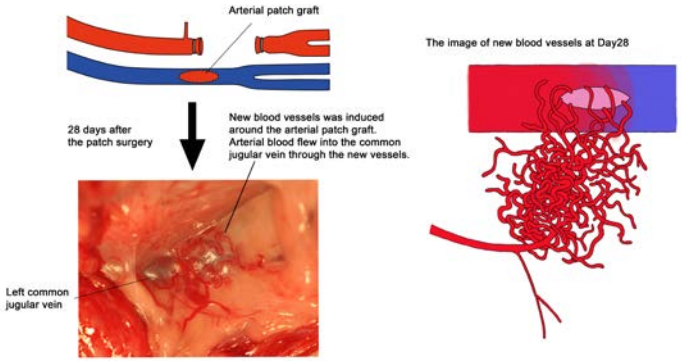

Disclosures: **Y. Ito:** Research Grant; Significant; A grants-in-aid of the Cardiovascular Research Fund. **M. Yoshida:** None. **H. Masuda:** None. **H. Nanjo:** Research Grant; Significant; JSPS KAKENHI Grant Numbers JP26350811. **A. Goto:** None.

462

Expression, Phosphorylation and Interaction Partners of the Transcription Factor Grainyhead-like 3 in the Endothelium

Stefanie Kohlgrüber, Nadine Dyballa-Rukes, Sabine Metzger, IUF - Leibniz Res Inst for Environmental Med, Duesseldorf, Germany; Anh Nguyen, Jim Garmey, Coleen McNamara, Robert M. Berne Cardiovascular Res Ctr, Univ of Virginia - Sch of Med, Charlottesville, VA; Judith Haendeler, Joachim Altschmied, IUF - Leibniz Res Inst for Environmental Med, Duesseldorf, Germany

The transcription factor Grainyhead-like 3 (GRHL3) regulates apoptosis, migration and NO-bioavailability and thus, critical functions of endothelial cell, which are impaired in many cardiovascular diseases. However, due to the lack of a good antibody, all experiments concerning the regulation of GRHL3 itself were performed on the RNA level. After establishing a new antibody, we analyzed the GRHL3 protein in aortic sections of ApoE-deficient mice fed a high fat diet, a model for atherosclerosis. The diet resulted in a reduction of GRHL3 levels in the endothelium, which was corroborated *ex vivo* in endothelial cells treated with LDL. This simulated high fat diet also led to a decrease in endothelial NO-synthase. As the activity of transcription factors is regulated by post-translational modifications and protein-protein interactions, we analyzed the phosphorylation of GRHL3 and identified potential interaction partners. Using a combination of immunoprecipitation and -blotting we demonstrated for the first time that GRHL3 is phosphorylated on tyrosine residues. Furthermore, this phosphorylation was NO-inducible and Src-kinase-dependent. After characterization of the modified residues, we will assess their relevance by determining the impact of phospho-mimetic and non-phosphorylatable mutants on functional parameters of endothelial cells. To identify potential interaction partners of GRHL3 we immunoprecipitated the protein and analyzed the co-precipitated proteins by mass spectrometry. We identified the DBHS-proteins NONO and SFPQ, which have been implicated in the regulation of transcription and alternative splicing. The interaction with these two proteins was validated by co-immunoprecipitation. As a next step, we will overexpress and downregulate these proteins in endothelial cells to evaluate their cross-talk with GRHL3. Taken together our findings demonstrate (i) a downregulation of GRHL3 in a disease setting, (ii) a Src-kinase dependent, NO-inducible phosphorylation and (iii) an interaction with other gene-regulatory proteins. The analysis of the functional consequences of these different aspects of GRHL3 regulation will further shed light on the GRHL3 network in the endothelium and thus, its functions in the vasculature.

Disclosures: **S. Kohlgrüber:** None. **N. Dyballa-Rukes:** None. **S. Metzger:** None. **A. Nguyen:** None. **J. Garmey:** None. **C. McNamara:** None. **J. Haendeler:** None. **J. Altschmied:** None.

463

The Key Regulatory Elements for SM22 Transcription

Maozhou Yang, Wayne State Univ, Detroit, MI; Soren Warming, Genentech Inc., South San Francisco, CA; Jianbin Shen, Hong Jiang, Wayne State Univ, Detroit, MI; Hui J Li, Univ of Massachusetts, Worcester, MA; Steve Krawetz, **Li Li**, Wayne State Univ, Detroit, MI

Gene transcription is controlled by an array of transcriptional regulatory elements. SM22 gene regulation has been widely used to characterize the molecular mechanisms of smooth muscle cell (SMC) phenotypic modulation during cardiovascular development and in vascular diseases. Our previous studies show that the proximal CArG box (CArGnear) in the SM22 promoter is required for its transcription in arterial smooth muscle cells (SMC). However, the role of the CArG box in visceral SMCs has not yet been explored. Here we aim to determine the role of CArG boxes in regulating S*M22* transcription in both vascular and visceral SMCs. Using bacterial chromosome (BAC) recombineering, we knock-in a *lacZ* reporter into a *SM22* BAC to trace SM22 transcriptional activities in transgenic mice. Anatomic/histology analyses show that the *lacZ* expression patterns in the BAC transgenic mice recapitulate that of the endogenous *SM22* transcription during embryogenesis and in adult. Similar to the endogenous *SM22* regulation, the expression of *lacZ* is highly sensitive to vascular remodeling: carotid injury abolishes lacZ expression in the arterial wall. Using seamless BAC recombineering mutagenesis, we generate mutations in the proximal and/or distal CArG box in the SM22-lacZ-BAC. Consistent with our previous results, we find that mutating the CArGnear box disrupts the *lacZ* expression in the aorta; this mutation also drastically reduces its expression in visceral SMCs including stomach, uterus and bladder. Interestingly, mutating the distal CArG (CArGfar) box does not affect the lacZ expression in arterial, venous and visceral SMCs. Mutating both CArG boxes nearly abolishes *lacZ* expression in all SMCs. This study provides evidence supporting the generation of SM22 knockout mice by mutating the CArG boxes in the SM22 promoter using the CRISPR technology.

Disclosures: **M. Yang:** None. **S. Warming:** None. **J. Shen:** None. **H. Jiang:** None. **H.J. Li:** None. **S. Krawetz:** None. **L. Li:** None.

464

Cellular and Molecular Characterisation of Human Endothelial Progenitors in vivo Defined Based on Self-Renewal and Colony Forming Potential Identifies Notch Signaling as a Key Pathway

Jatin Patel, Abbas Shafiee, Ho Yi Wong, Josue Alexis, Kiarash Khosrotehrani, The Univ of Queensland, Brisbane, Australia

Background: Although endothelial progenitors have long been described, there remains significant controversy around their identity *in vivo*. The endothelial colony forming (ECFC) assays suggested a hierarchy among endothelial cells *in vivo*. Our aim was to systematically test different endothelial cell populations sorted from the human placenta, a highly vascularised tissue, based on various cell surface markers for their ECFC potential. **Methods and Results:** Upon sorting based on key markers CD45, CD34 and CD34 it was easily established that most ECFC potential was concentrated in the CD45-CD34+ fraction. Among this population, single cell culture assays (>300 wells per cell type) were performed on sorted CD31neg, CD31int and CD31hi cells. Only the CD31int cells were able to grow high proliferative potential ECFC. CD31neg populations contained mesenchymal stem cells (MSC) whereas CD31hi cells only produced mature endothelial clusters. RNA sequencing of each fraction identified Notch signalling as a key driver of endothelial progenitors as opposed to MSC. When the CD31int population was further characterised it was found to be expressing VE-Cadherin as predicted by the RNAseq, however, was not in contact with the circulation as it did not stain for lectins injected intravenously. In accordance the self-renewing fraction of ECFC cultures *in vitro* was dependent on Notch signalling and controlled the expression of IL33 and CDKN1C (p57) to maintain progenitors in quiescence. This was validated *in vitro* and *in vivo* by performing shRNA and pharmacological inhibition of the different pathways. **Conclusion:** Our study uncovers a population of endothelial progenitors *in vivo* at the cellular and molecular level and identified a novel role for Notch signalling in maintaining progenitor self-renewal *in vivo* and *in vitro*.

Disclosures: **J. Patel:** Ownership Interest; Modest; Angiostem. **A. Shafiee:** None. **H. Wong:** None. **J. Alexis:** None. **K. Khosrotehrani:** Ownership Interest; Modest; Angiostem.

465

Nicotine Differentially Influences Segmental Aortic Stiffening

Markus U Wagenhaeuser, Stanford Univ, Stanford, CA; Isabel N Schellinger, Univ of Goettingen, Goettingen, Germany; Sabina P Guenther, Univ of San Francisco, San Francisco, CA; Takuya Yoshino, Kensuke Toyama, Yosuke Kayama, Alicia Deng, Alexander M Zoellner, Stanford Univ, Stanford, CA; Uwe Raaz, Univ of Goettingen, Goettingen, Germany; Joshua M Spin, Philip S Tsao, Stanford Univ, Stanford, CA

Background: Arterial stiffness is a major risk factor for various cardiovascular diseases and contributes to the development of abdominal aortic aneurysms (AAA). In this context, differential aortic stiffening of adjacent aortic segments increases aortic wall stress and accelerates the disease. Smoking is a major risk factor for AAA, in part due to nicotine. In this study, we investigated aortic stiffening of the thoracic and abdominal aorta and analyzed stiffness-related gene expression.
Methods: 36 WT mice (C57BL/6) mice were infused with nicotine or PBS using osmotic mini pumps for 42 days. Thoracic segment (TS) and abdominal segment (AS) aortic stiffness were analyzed using ultrasound (M-Mode and PW). TS and AS were further investigated by *ex vivo* myograph measurements. Gene expression for TMIP2, MT1-MMP, MMP2, collagen type I and type III was performed for both segments separately.
Results: Myograph measurements revealed increased strain within the AS after 2 weeks ($p<.05$) in response to nicotine (vs. PBS), but no stiffening of the TS. After 6 weeks, the AS showed additional increases in strain with nicotine ($p<.05$); however, only minor increases in stiffness could be observed for the TS. Ultrasound M-Mode results confirmed the myograph results. Nicotine treatment also led to increased aortic pulse wave velocity (PWV) after 2 weeks ($p<.05$) and 6 weeks ($p<.05$). Gene expression analysis revealed up-regulation in the TS and AS of MT1-MMP and MMP2 after 2 weeks of nicotine, while TIMP2 was downregulated, and collagen type I and type III were up-regulated in both TS and AS ($p<.05$). After 6 weeks, there were no longer significant differences in either segment for any of these genes.
Discussion: Aortic stiffening in response to nicotine varies between the TS and AS segment over a time course of 6 weeks. This leads to an increased stiffness gradient between the TS and AS. Gene expression changes in stiffness-related genes occurred in response to nicotine, although no difference appeared between the segments. We conclude that the difference in stiffness development for TS and AS could be based on a different basic morphological structure involving elastin and collagen load, and that these responses may in part explain nicotine's role in promoting AAA.

Disclosures: **M.U. Wagenhaeuser:** None. **I.N. Schellinger:** None. **S.P. Guenther:** None. **T. Yoshino:** None. **K. Toyama:** None. **Y. Kayama:** None. **A. Deng:** None. **A.M. Zoellner:** None. **U. Raaz:** None. **J.M. Spin:** None. **P.S. Tsao:** None.

466

CX3CR1 Down Regulation Reduces Venous Neointimal Hyperplasia Formation in a Murine Hemodialysis Vascular Access Model

Binxia Yang, Sreenivaslisu Kilari, Deborah L McCall, Mayo Clinic, Rochester, MN; John Broadwater, Steven Kerr, Lynn Pantages, Mary Mcfarland, Boehringer Ingelheim Pharmaceuticals, Inc, Ridgefield, CT; Sanjay Misra, Mayo Clinic, Rochester, MN

Introduction Venous neointimal hyperplasia (VNH) is a major cause of hemodialysis arteriovenous fistula (AVF) vascular access failure. CX3CR1 mediates macrophage infiltration into the vasculature. Mice were used which had been genetically engineered to knock in the human CX3CR1 gene. **Hypothesis** The hypothesis to be tested is that increased CX3CR1 gene expression results in VNH formation associated with AVF. **Methods** We used 50 CX3CR1 knock in mice which were divided into 2 groups: 1. CX3CR1 antibody (30 mg/kg administered intraperitoneally two times per week) or vehicle (equal amount of volume used for CX3CR1 antibody administered intraperitoneally). AVFs were created by connecting the carotid artery to ipsilateral jugular vein 28 days after nephrectomy was performed to induce chronic kidney disease. Histology and Immunohistochemistry analysis at the outflow vein of AVF were performed to assess the pathological changes. **Results:** There was a significant decrease in neointima area in the outflow veins of AVF in CX3CR1 antibody group compared to the vehicle group at day 28 (43085 ± 12678 vs. 58963.4 ± 9273 μm^2, $P<0.05$). There was a significant decrease in the ratio of neointima/media+adventitia area in the outflow veins of AVF in CX3CR1 antibody group compared to the

vehicle group at day 28 (0.34 ± 0.1 vs. 0.61 ± 0.1, P<0.05). Cell density in neointima area in CX3CR1 group outflow veins was significantly lower than the vehicle group at day 14 (9600 ± 1000 vs. 13000 ± 3000 /mm^2, P<0.01). There was a significant decrease in the average CD68-positive cell density in the CX3CR1 group outflow veins compared to the vehicle group (0.96 ± 0.34 vs.15.9 ±10, P<0.001) at day 14. **Conclusion** Decreasing CX3CR1 significantly reduces macrophages infiltration and results in a significant reduction in VNH. This study provides a rationale for using CX3CR1 antibody in reducing VNH formation.

Disclosures: **B. Yang:** None. **S. Kilari:** None. **D. McCall:** None. **J. Broadwater:** None. **S. Kerr:** None. **L. Pantages:** None. **M. Mcfarland:** None. **S. Misra:** Other; Significant; This research was funded by Boehringer Ingelheim Pharmaceuticals, Inc.

467

Fibronectin Extradomain B (FN-EDB) Expression is Specific to the Atherosclerotic Lesion Types III, IV, and V, and the FN-EDB targeting Nanomedicine Enhances Atherosclerotic Plaque Detection and Local Delivery of Model Drug Cargo

Mikyung Yu, Renata Leitao, Xiaoding Xu, Phei Er Saw, Carleena Angelica Ortega, Kevin Si, Suyeon Ahn, Jerry Liu, Azita Lotfi, In-Hyun Lee, Won-Il Choi, Mirna Brayner, Jinjun Shi, Morteza Mahmoudi, Ctr for Nanomedicine and Dept of Anesthesiology, Brigham and Women's Hosp, Harvard Medical Sch, Boston, MA; Sanyong Jon, Dept of Biological Sciences, Korea Advanced Inst of Science & Technology, Daejon, Korea, Republic of; Frederick Schoen, Dept of Pathology, Brigham and Women's Hosp, Harvard Medical Sch, Boston, MA; Omid Farokhzad, Ctr for Nanomedicine and Dept of Anesthesiology, Brigham and Women's Hosp, Harvard Medical Sch, Boston, MA

Background: The Fibronection extradomain B (FN-EDB) is upregulated during tissue remodeling and has been postulated as a potential biomarker for atherosclerosis, yet a systematic investigation for the presence of FN-EDB in plaque has not been reported. We hypothesized that the FN-EDB expression would intensify in advanced plaques; furthermore the engineering of FN-EDB-targeted nanoparticles (FN-EDB-NPs) could enable the imaging/diagnosis and local delivery of therapeutic payloads to plaques.
Methods: The amount of FN-EDB in atherosclerotic (*n*=143) and normal arteries (*n*=43) of human tissue specimen (ages: 40 to 85 years) was histologically stained and quantified using FN-EDB specific bi-podal peptide ($APT_{FN\text{-}EDB}$). Next, FN-EDB-NPs were developed by immobilization of $APT_{FN\text{-}EDB}$ on nanoparticles surface containing Gd-DTPA for MRI imaging. These NPs were administered to apolipoprotein E-deficient mice fed a western diet and the brachiocephalic arteries were visualized with MRI. The mice were sacrificed and the ascending to the descending thoracic aortas and the aortic roots of the mice were studied for Gd, FN-EDB, and FN-EDB-NPs quantification. The utility of FN-EDB-NPs for drug delivery was evaluated using Cyanine, as a model small molecule drug, and NPs biodistribution and pharmacokinetics were studied.
Results: The FN-EDB positive area was significantly greater in the atherosclerotic tissues than in the normal arteries (*P*<0.001). It was particularly specific to the Type III (*P*<0.01), IV (*P*<0.01) and V lesions (*P*<0.001) compared to the Type I and II lesions. The FN-EDB expression indicated a positive correlation with macrophage infiltration and neoangiogenesis. T1-weighted images of the atherosclerosis mouse models (*n*=86) revealed substantial FN-EDB-NPs accumulation in plaques compared to the control NPs, Magnevist® or wild type C57BL/6J mice (*n*=21). Additionally, FN-EDB-NPs significantly enhanced the blood circulation time ($t_{1/2}$: ~ 6 h) and plaque accumulation (up to 72 h) of a model drug.
Conclusions: Our findings offer the first evidence that FN-EDB expression is specific to the Type III, IV and V lesions and suggest that the FN-EDB-NPs could be a promising platform for targeted imaging/diagnosis and therapy of atherosclerosis.

Disclosures: **M. Yu:** None. **R. Leitao:** None. **X. Xu:** None. **P. Saw:** None. **C. Ortega:** None. **K. Si:** None. **S. Ahn:** None. **J. Liu:** None. **A. Lotfi:** None. **I. Lee:** None. **W. Choi:** None. **M. Brayner:** None. **J. Shi:** None. **M. Mahmoudi:** None. **S. Jon:** None. **F. Schoen:** None. **O. Farokhzad:** None.

468

Smooth Muscle Cells Accelerate Endothelial Regeneration Through a Protein Kinase C-delta-Dependent Secretion of CXCR2 Ligands

Ting Zhou, Jun Ren, Matthew B Parlato, Bernard Y Binder, Noel Phan, Qiwei Wang, Danielle Stewart, Kartik Gupta, Conner Feldman, Yi Si, Zhenjie Liu, Nader Sheibani, William L Murphy, Bo Liu, UW-Madison, Madison, WI

Background: Efficient regeneration of denuded endothelial cells (ECs) is an important process that counteracts the pro-stenotic activities. Unfortunately, this natural healing process is frequently compromised by disease conditions such as diabetes. Protein kinase C-delta (PKCδ) plays a complex role in the arterial injury response by regulating apoptosis of vascular smooth muscle cells (SMCs) as well as production of chemokines capable of attracting resident and circulating cells. In this study, we explored whether SMCs participate in endothelial repair through a PKCδ-dependent paracrine mechanism.
Methods and Results: Following balloon injury to the rat carotid, SMC-specific gene transfer of *Prkcd* accelerated reendothelialization compared to the empty vector, reflected by a larger area excluded from Evans blue measured 14 days post injury (59.60±5.01% vs 25.38±7.52%). In contrast, SMC-specific knockdown of endogenous *Prkcd* delayed reendothelialization compared to the non-targeting shRNA control (41.31±6.54% vs 70.31±5.97%). *In vitro*, media conditioned by AdPKCδ-infected SMCs increased endothelial wound healing without affecting their proliferation and viability. In addition, SMCs in a PKCδ-dependent fashion attracted circulating angiogenic cells (CACs), a cell population that promotes neovascularization via production of angiogenic factors. A PCR-based array analysis identified *Cxcl1* and *Cxcl7* among others as PKCδ-mediated chemokines produced by SMCs. Blocking CXCL7 or CXCR2 significantly inhibited endothelial wound healing and CAC migration in response to AdPKCδ-infected SMC conditioned media. *In vivo*, PKCδ overexpression in SMCs following balloon injury increased CXCL7 production and stimulated CACs recruitment to injured arteries. Furthermore, insertion of a *Cxcl7* cDNA in the lentiviral vector that carries a *Prkcd* shRNA overcame the negative effects of *Prkcd* knockdown on reendothelialization.
Conclusions: Regeneration of denuded endothelium involves multiple cell types from the vascular wall as well as circulation. SMCs stimulate reendothelialization in a PKCδ-dependent paracrine mechanism, likely through CXCL7-mediated recruitment of ECs from uninjured endothelium and CACs from circulation.

Disclosures: **T. Zhou:** None. **J. Ren:** None. **M.B. Parlato:** None. **B.Y. Binder:** None. **N. Phan:** None. **Q. Wang:** None. **D. Stewart:** None. **K. Gupta:** None. **C. Feldman:** None. **Y. Si:** None. **Z. Liu:** None. **N. Sheibani:** None. **W.L. Murphy:** None. **B. Liu:** None.

This research has received full or partial funding support from the American Heart Association.

473

Dissecting Aortic Aneurym in Angiotensin II - Infused Mice: The Mechanisms Behind Lesion Variability

Bram Trachet, EPFL, Lausanne, Switzerland; Alessandra Piersigilli, Weill Med Cornell, New York, NY; Lydia Aslanidou, Rodrigo A Fraga-Silva, Jessica Sordet-Dessimoz, EPFL, Lausanne, Switzerland; Pablo Villanueva-Perez, PSI, VIlligen, Switzerland; Marco F Stampanoni, PSI, Villigen, Switzerland; Nikolaos Stergiopulos, EPFL, Lausanne, Switzerland; Patrick Segers, Ghent Univ, Gent, Belgium

Angiotensin II-infused mice develop dissecting aneurysms, characterized by intramural rather than intraluminal thrombus, suprarenal rather than infrarenal lesions, medial dissections rather than circumferential elastin degradation and a variability in lesion shape that remained as yet unexplained. In order to provide insight into these intriguing lesions we scanned murine aortas at baseline and after 10, 18 and 29 days of Angiotensin II infusion, both in vivo (ultrasound, micro-CT) and ex vivo (phase-contrast X-ray tomographic microscopy). Dissecting aneurysms of varying severity occurred in 31/34 mice. All of these were characterized by a medial tear near the ostium of thoracic and abdominal aortic side branches, with a predilection for the left and ventral aspects of the ostium of the celiac artery. In 25/31 animals an intramural hematoma was formed. Fully ruptured branch ostia occurred significantly more often in the supraceliac aorta, affecting in particular the left suprarenal artery (the first branch cranial to the celiac artery, 23/25). Animals with a thoracic tear (6/31) had significantly larger intramural hematoma than animals with an abdominal tear ($p<0.05$), and the length of the hematoma correlated to the number of ruptured side branches ($r^2=0.78$). In 11 mice a parallel false channel was formed. The volume of free-

flowing intramural blood in the false channel was significantly larger for left than for ventral tears, but was not related to the length of the tear. Our data suggest that (i) medial tears are the primary event in dissecting AAA formation, (ii) an intramural hematoma is formed if the adventitia covering the medial tear dissects and leads to the accumulation of intramural blood from ruptured side branches, (iii) adventitial dissection and hematoma formation progress in the direction of least resistance/smallest side branches (i.e. cranial of the celiac artery) and (iv) a false channel is formed if the radial expansion of the adventitia due to blood flowing out of the medial tear acts in the same (leftward) direction as the expansion due to a ruptured left suprarenal artery. We conclude that Ang II-infused mice can be a valuable model to study the under-researched role of side branches in the formation and progression of aortic dissections.

Disclosures: **B. Trachet:** None. **A. Piersigilli:** None. **L. Aslanidou:** None. **R.A. Fraga-Silva:** None. **J. Sordet-Dessimoz:** None. **P. Villanueva-Perez:** None. **M.F.M. Stampanoni:** None. **N. Stergiopulos:** None. **P. Segers:** None.

474

Early Events in Dissecting Aneurysms Induced by Angiotensin-II Infusion: The Geometry-Driven Aspect of a Multifaceted Problem

Lydia Aslanidou, **Bram Trachet**, Mauro Ferraro, EPFL, Lausanne, Switzerland; Alessandra Piersigilli, Weill Med Cornell, New York, NY; Rodrigo Fraga-Silva, Jessica Sordet-Dessimoz, EPFL, Lausanne, Switzerland; Pablo Villanueva-Perez, Marco Stampanoni, PSI, Villigen, Switzerland; Patrick Segers, Ghent Univ, Ghent, Belgium; Nikolaos Stergiopulos, EPFL, Lausanne, Switzerland

While research on dissecting aneurysms in Angiotensin-II infused mice spans more than a decade, the temporal sequence of initial events still remains unclear. Recent findings in our group suggested that focal medial tears at the vicinity of suprarenal side branches are the primary event in disease formation. In this study we used a combined experimental-computational approach to investigate the hypothesis that initial events of dissecting AAAs originate at branching sites along the aorta. Male apolipoprotein-deficient mice were infused with Angiotensin-II (n=11) and saline 0.9% (n=6) for 3 days and scanned with contrast-enhanced microCT prior to sacrifice. One animal presented an in-vivo rupture during the microCT scan, and was rescanned after 2.5 hours to observe real-time morphological changes. In all other animals, the excised aortic tissue was imaged with Phase Contrast X-Ray Tomographic Microscopy (PCXTM) at 6.5um isotropic resolution. An automatic morphing code was developed to map the ex-vivo geometry onto the in vivo geometry, and a finite element simulation yielded a stress distribution that represents an estimation of the wall tension, not only due to the pressurization, but also due to the local stretch field. We found that the nanoparticulate microCT contrast agent had infiltrated the aortic wall in 11/11 Ang-II infused animals, while no infiltration was observed in 6/6 control mice. The infiltration affected at least one pair of intercostal arteries in 11/11 mice, and in 9/11 mice the coeliac region was also affected. Image-guided histology allowed us to determine the circumferential distribution of microlesions at branching sites, including disruption of elastin fibers, apoptotic cell appearance, subintimal leukocyte infiltration and intramural hematomas. In the animal whose aorta had ruptured during the in vivo scan, the initial hematoma had originated around 3 pairs of intercostal arteries and quickly propagated afterwards. Mouse-specific finite element simulations revealed a co-location of computed peak stresses at the vessel wall and histologically identified vascular damage. We conclude that the aortic geometry, and side branches in particular, play a pivotal role in the onset of dissecting AAA.

Disclosures: **L. Aslanidou:** None. **B. Trachet:** None. **M. Ferraro:** None. **A. Piersigilli:** None. **R. Fraga-Silva:** None. **J. Sordet-Dessimoz:** None. **P. Villanueva-Perez:** None. **M. Stampanoni:** None. **P. Segers:** None. **N. Stergiopulos:** None.

475

Novel Gene Therapy Facilitates Critical Limb Ischemia Reperfusion in Mouse Hindlimb Gangrene Model

Punam P Parikh, Roberta Lassance-Soares, Manuela Regueiro, Hongwei Shao, Yan Li, **Zhao-Jun Liu**, Omaida C. Velazquez, Univ of Miami, Miami, FL

Lack of a reliable animal hindlimb gangrene model limits molecular investigation of critical limb ischemia. We sought to develop a mouse hindlimb gangrene model, used to assess the efficacy of novel gene therapy. We hypothesized that priming ischemic hindlimb tissue with E-selectin/adeno-associated virus

(AAV) enhances therapeutic angiogenesis and attenuates gangrene.
We tested two methods to induce hindlimb gangrene. First, FVB mice underwent femoral artery ligation (FAL) to achieve critical limb ischemia. Second, FVB underwent combined FAL and administration of NG-nitro-L-arginine methyl ester (L-NAME), nitric oxide synthase inhibitor, which further reduces hindlimb perfusion. Prior to FAL and L-NAME use, gangrene-induced mice were intramuscularly administered E-selectin/AAV (treatment) or LacZ/AAV (control) to the hindlimb. Gangrene was assessed with a standardized ischemia score ranging from 0 (no gangrene) to 11 (forefoot gangrene), recorded on postoperative day (POD)'s 2,7,14. Hindlimb reperfusion using Laser doppler imaging was quantified by mean perfusion of ligated:non-ligated limb on same POD's. Live animal Dil perfusion plus laser scanning confocal microscopy quantified limb neovascularization.
Most FVB did not develop gangrene with FAL-only (n=2/8, 25% gangrene incidence). Combined FAL and L-NAME consistently induced hindlimb gangrene (n=14/14, 100% gangrene incidence). Laser doppler imaging score on POD 7 for E-selectin/AAV (n=7) and LacZ/AAV (n=7) was 0.41 vs 0.27 (P=0.071) and on POD 14 was 0.54 vs 0.29 (P=0.017). Dil perfused ligated hindlimb in E-selectin/AAV and LacZ/AAV revealed significantly higher mean neovascularization intensity score of 44 vs 21 (P=0.037). Dil perfused non-ligated limb in respective mice demonstrated mean intensity score of 50 vs 25 (P=0.006). Mean limb ischemia score on POD 2,7,14 for E-selectin/AAV and LacZ/AAV was 1.9, 2.9, 3.7 vs 2.7, 3.9, 5.3 (P=0.104).
We developed a highly reliable mouse hindlimb gangrene model where E-selectin-based novel gene therapy improved limb reperfusion and neovascuclarization in critical limb ischemia. This hindlimb gangrene model can be used to further understand Redox pathways contributing to gangrene, facilitating future translational studies.

Disclosures: **P.P. Parikh:** None. **R. Lassance-Soares:** None. **M. Regueiro:** None. **H. Shao:** None. **Y. Li:** None. **Z. Liu:** None. **O.C. Velazquez:** None.

476

Exercise Induced Pulmonary Hypertension in Patient Presenting With Acute Cardiac Symptoms

Zulfiqar A Qutrio Baloch, Brandon Regional Hosp, Brandon, FL; Shabber Abbas, R-Endocrinology, Hamilton, NJ; Abbas Ali, West Virginia Univ, Morgantown, WV; Syed Imran Zaidi, East Tennessee Univ, Johnson city, TN; Sumera Bukhari, Seton Hall Univ, Trenton, NJ

Introduction: Patients presenting with symptoms of angina, dyspnea, and fatigue with negative cardiac and pulmonary test findings are often investigated with exercise right heart catheterization. Patients displaying pulmonary hypertension or exercise-induced pulmonary hypertension (EIPH) were isolated and studied further to elaborate upon similarities and differences with patients with normal pressures.
Hypothesis: EIPH may be an under-recognized cause of cardiac complaints.
Methods: Clinical data was obtained from 172 randomly and retrospectively selected patients including data on hemodynamics, cardiopulmonary exercise testing (CPET), and echocardiogram findings. Patients with EIPH had a resting mean pulmonary arterial pressure below 25 mmHg and on exercise above 25 mmHg. Patients with resting pulmonary hypertension were stratified into WHO group 1 (pulmonary arterial) and WHO group 2 (due to left heart). Prior response to treatment with long-acting nitrates was also reviewed.
Results: 27 patients had EIPH, 24 had WHO group 1 pulmonary hypertension, 37 had WHO group 2 pulmonary hypertension, 54 did not have pulmonary hypertension, and 30 did not have any exercise data. No significant differences were found across any groups in resting or exercise CPET performance. The mean age of those with pulmonary hypertension was 71.67 years and 58.89 for those without ($p<0.01$). Both had a mean left ventricular ejection fraction between 53-
57%. The mean VO2 max for those with resting pulmonary hypertension or EIPH was below 20 ml/kg/min. For every 1-year increase in age the odds of developing EIPH increased by 1.08. The use of long-acting nitrate was associated with improvement of symptoms in symptomatic patients. Most of the EIPH patients were noted to have exercise-induced diastolic dysfunction and many also had concomitant chronotropic incompetance.
Conclusions: EIPH represents those who have negative left-heart stress cardiac findings yet have underlying abnormalities significant enough to require symptomatic treatment during exercise. This includes diastolic dysfunction and chronotropic incompetency. Cardiovascular performance was found to be equally poor in patients with EIPH as compared to those with resting pulmonary hypertension.

Disclosures: **Z.A. Qutrio Baloch:** None. **S. Abbas:** None. **A. Ali:** None. **S. Imran Zaidi:** None. **S. Bukhari:** None.

478

Altered Blood Flow and Anatomic Variations Increase the Translational Value of the PPE Murine Aneurysm Model

Albert Busch, Lars Maegdefessel, Dept for Vascular and Endovascular Surgery, Univ Hosp Rechts der Isar, Munich, Germa, Munich, Germany

Introduction: Abdominal aortic aneurysm (AAA) is an individual and socioeconomic burden in the aging society. Treatment relies on surgical exclusion of the dilated aorta by open or endovascular repair only. For research purposes, animal models are necessary and the elastase induced aneurysm model (PPE) has gained much attention for it closely mimics endstage human aneurysm disease. However, to improve the translational value of this model we conducted a couple of modifications in relation to human aneurysm morphology.
Materials and Methods: In 10-week-old male C57BL/6J wild-type mice the classic PPE procedure with local perfusion of porcine pancreatic elastase in order to induce aneurysm was modified using flow alteration by partial ligation of the iliac artery or the aorta. Additionally, careful exploration of the abdominal aortic branches allowed PPE induction at the suprarenal and iliac level. Molecular biology, ultrasound and immunistochemistry were used to evaluate the results.
Results: Aortic blood flow restriction (PPE 2.0) significantly increases murine AAA diameter and affects the localization of vascular wall remodeling. Suprarenal aortic dissection allows inducing a more proximal aneurysm (PPE 3.0) similar to the angiotensin II induced aneurysm model. Separate investigation for canonical activation of transforming growth factor ß in these two embryologically distinct segments shows no difference. Creating an aorto-iliac bifurcated aneurysm (PPE 4.0) completes the mimicry of human aneurysm morphologies.
Conclusion: PPE is the most important model for AAA research and the ß-versions PPE 2.0, 3.0 and 4.0 modifying its morphology further increase the translational value.

Disclosures: **A. Busch:** None. **L. Maegdefessel:** None.

479

Smc Phenotype Switch Targeting Apoe is a Therapeutic Target in Popliteal Aneurysm

Albert Busch, **Ekaterina Chernogubova**, Yuhuang LI, Udo Lorenz, Dept for Vascular and Endovascular Surgery, Univ Hosp Rechts der Isar, Munich, Germa, Munich, Germany; Joy Roy, Karolinska Inst, Munich, Sweden; Rebecka Hultgren, Karolinska Inst, Stockholm, Sweden; Lars Maegdefessel, Dept for Vascular and Endovascular Surgery, Univ Hosp Rechts der Isar, Munich, Germa, Munich, Germany

Introduction: Popliteal artery aneurysm (PAA) is an individually highly fatal disease, causing ischemia and eventual major amputation, mainly in 50-70 year old males. It is the most frequent peripheral artery aneurysm and correct treatment is challenging for clinicians, since both open and endovascular repair have only modest success rates, depending on the clinical presentation. In comparison to other aneurysm entities, little is known about its specific pathogenesis.
Material and Methods: 30 Human PAA and popliteal artery samples were analyzed by immunohistochemistry, mRNA and miRNA expression analysis and protein assays on the OLink platform in order to identify key features of the disease and crucial pathways involved. Furthermore, a novel murine model of PAA is characterized for future applications in basic research.
Results: Vascular smooth muscle cells loose their contractile phenotype along with significant inflammatory and proteolytic changes in the vessel wall architecture. Extensive tissue remodeling with high cell turnover rates is a unique feature in comparison to AAA. This correlates with highly abundant expression of the apolipoproteins E and CI suggestive to have a pro-proliferative effect in peripheral vascular tissue. Additionally, array-based screening on gene and protein level revelaed the pentraxin-related protein 3 as a potential biomarker and soluble inducer of neutrophil homing. Other targets of interest in relation to ApoE were fatty acid binding protein 4 and Insulin growth facto binding protein 2. These findings are emphasized by a specific case of a solely mechanically induced PAA in a young male.
Conclusion: Pathogenesis of PAA shows similar histologic features than AAA, yet differs in potential pathways involved. Increased cell turnover in the aneurysmal neck area suggests evaluation of alternative treatment strategies, targeting key processes in its pathogenesis.

Disclosures: **A. Busch:** None. **E. Chernogubova:** None. **Y. Li:** None. **U. Lorenz:** None. **J. Roy:** None. **R. Hultgren:** None. **L. Maegdefessel:** None.

480

Aortic Microcalcification Associates with Aortic Elastin Fragmentation in Marfan Syndrome

Shaynah Wanga, Stijntje Hibender, Academic Medical Ctr, Amsterdam, Netherlands; Yanto Ridwan, Erasmus Medical Ctr, Rotterdam, Netherlands; Cindy van Roomen, Mariska Vos, Ingeborg van der Made, Academic Medical Ctr, Amsterdam, Netherlands; Nicole van Vliet, Erasmus Medical Ctr, Rotterdam, Netherlands; Romy Franken, Maarten Groenink, Aeilko H Zwinderman, Barbara J Mulder, Carlie J de Vries, Academic Medical Ctr, Amsterdam, Netherlands; Jeroen Essers, Erasmus Medical Ctr, Rotterdam, Netherlands; **Vivian de Waard**, Academic Medical Ctr, Amsterdam, Netherlands

Marfan syndrome (MFS) is a genetic connective tissue disorder, in which aortic rupture is the major cause of death. MFS patients with an aortic diameter below the advised limit for prophylactic surgery (<5cm) may unexpectedly experience an aortic dissection or rupture, despite yearly monitoring. Hence, there is a clear need for improved prognostic markers to predict such aortic events. We hypothesize that elastin fragments play a causal role in aortic calcification in MFS and that microcalcification serves as a novel marker for aortic disease severity. To address this hypothesis, we analyzed MFS patient and mouse aortas. MFS patient aortic tissue showed enhanced microcalcification in areas with extensive elastic lamina fragmentation in the media. A causal relationship between medial injury and microcalcification was revealed by studies in vascular smooth muscle cells (SMCs); elastin peptides were shown to increase the activity of the calcification marker alkaline phosphatase (ALP) and reduce the expression of the calcification inhibitor matrix gla protein (MGP) in human SMCs. In murine $Fbn1^{C1039G/+}$ MFS aortic SMCs, ALP mRNA and activity was upregulated when compared to wildtype SMCs. The elastin peptide-induced ALP activity was prevented by incubation with lactose as inhibitor of the elastin receptor complex, and a MEK1/2 kinase inhibitor, indicating downstream involvement of ERK1/2 phosphorylation. Histological analyses in MFS mice revealed macrocalcification in the aortic root, while the ascending aorta contained microcalcification, as identified with the near-infrared fluorescent bisphosphonate probe OsteoSense-800. Significantly, microcalcification correlated strongly with aortic diameter, aortic distensibility, elastin breaks and phosphorylated ERK1/2. In conclusion, microcalcification co-localizes with aortic elastin degradation in MFS aorta of man and mice, where elastin-derived peptides induce a calcification process in SMCs via the elastin receptor complex and ERK1/2 activation. We propose microcalcification as a novel imaging marker to monitor local elastin degradation and thus predict aortic events in MFS patients.

Disclosures: **S. Wanga:** None. **S. Hibender:** None. **Y. Ridwan:** None. **C. van Roomen:** None. **M. Vos:** None. **I. van der Made:** None. **N. van Vliet:** None. **R. Franken:** None. **M. Groenink:** None. **A.H. Zwinderman:** None. **B.J.M. Mulder:** None. **C.J.M. de Vries:** None. **J. Essers:** None. **V. de Waard:** None.

481

Pharmacological Inhibition of Calpain Attenuates Mineralocorticoid Receptor Agonist and High Salt-Induced Abdominal Aortic Aneurysm Incidence and Aortic Rupture in Mice

Aida Javidan, Weihua Jiang, Venkateswaran Subramanian, Univ of Kentucky, Lexington, KY

Background and Objective: Recently, we demonstrated that pharmacological and genetic inhibition of calpains, a class of calcium-activated neutral cysteine proteases, attenuated angiotensin II (AngII)-induced abdominal aortic aneurysms (AAAs) in mice. A newly identified non-invasive model of aneurysm has been developed in mice using deoxycorticosterone acetate (DOCA) coated pellets and oral administration of high salt. It is interesting to note that in this model, systemic administration of renin angiotensin inhibitors had no effect on aneurysm formation. The purpose of this study was to test whether pharmacological inhibition of calpain would influence AAA formation induced by mineralocorticoid receptor agonism and high salt in mice. ***Methods and Results:*** To determine whether calpain inhibition influenced DOCA and high salt-induced AAAs, 9 month old male C57BL/6 mice were administered calpain inhibitor, BDA-410 (30 mg/kg/day) or vehicle (n=10 per group) by oral gavage 1 week before DOCA pellet implantation and throughout the subsequent 21 days. Mice were implanted with DOCA pellets (50mg/ mouse for 21 days) and maintained on high salt (0.9% NaCl and 0.2% KCl) water. Calpain inhibition significantly suppressed AAA incidence (defined as increase in aortic diameter or AAA rupture; Vehicle = 60% vs BDA = 20%; $P<0.05$) compared to the vehicle group. Calpain inhibition also significantly

protected DOCA + high salt-induced aortic rupture (Vehicle = 6/10 vs BDA = 1/10; P<0.05) in mice. ***Conclusion:*** These data demonstrate that calpain activation plays a critical role in not only AngII-induced, but also aldosterone pathways accelerated AAA formation in mice.

Disclosures: **A. Javidan:** None. **W. Jiang:** None. **V. Subramanian:** None.

This research has received full or partial funding support from the American Heart Association.

482

IDH2 Deficiency Induces Oxidative Stress and Vascular Inflammation

Seonhee Kim, Su-jeong Choi, Harsha Nagar, Shuyu Piao, Ikjun Lee, Sungmin Kim, Cuk-Seong Kim*, Chungnam Natl Univ. Sch of Med, Dept of Physiology, Dept of Medical Science, Daejeon, Korea, Republic of

Isocitrate dehydrogenase 2 (IDH2) plays an essential role protecting cells against oxidative stress-induced damage. A deficiency in IDH2 leads to mitochondrial dysfunction and the production of reactive oxygen species (ROS) in cardiomyocytes and endothelial cells. However, the physiological function of IDH2 in vascular system is mostly unknown In this study, we investigated whether IDH2 knockdown causes mitochondrial dysfunction and vascular inflammation *in vitro* and *in vivo*. IDH2 knockdown decreased the expression of mitochondrial oxidative phosphorylation (OXPHOS) complexes I, II and III, which lead to increased mitochondrial superoxide. In addition, the levels of fission and fusion proteins (Mfn-1, OPA-1, and Drp-1) were significantly altered and MnSOD expression also was decreased by IDH2 knockdown. Furthermore, knockdown of IDH2 decreased eNOS phosphorylation and nitric oxide (NO) concentration in endothelial cells. Interestingly, treatment with Mito-TEMPO, a mitochondrial-specific superoxide scavenger, recovered mitochondrial fission-fusion imbalance and blunted mitochondrial superoxide production, and reduced the IDH2 knockdown-induced decrease in MnSOD expression, eNOS phosphorylation and NO production in endothelial cells. Endothelium-dependent vasorelaxation was impaired, and the concentration of bioavailable NO decreased in the aortic ring in IDH2 knockout mice. These findings suggest that IDH2 deficiency induces endothelial dysfunction through the induction of dynamic mitochondrial changes and impairment in vascular function. Key words: IDH2, mitochondria, endothelial cells, ROS

Disclosures: **S. Kim:** None. **S. Choi:** None. **H. Nagar:** None. **S. Piao:** None. **I. Lee:** None. **S. Kim:** None. **C. Kim*:** None.

484

Multimerization of BAFF Regulates B Cell Function and Growth of Aortic Aneurysms

Vlad Serbulea, Philipp Jakobs, Srabani Sahu, Prasad Srikakulapu, Coleen A McNamara, Gorav Ailawadi, Gilbert R Upchurch Jr., Norbert Leitinger, **Akshaya K Meher**, Univ of Virginia, Charlottesville, VA

B cell activating factor (BAFF) regulates differentiation and survival of B cells by binding to the surface receptors BAFF receptor (BR3), transmembrane activator and CAML interactor (TACI) and B cell maturation antigen (BCMA). During differentiation, intracellular metabolic reprogramming is crucial, such as, naïve B cells are metabolically quiescent, whereas, antibody producing plasma cells are metabolically active. We have reported that depletion of B cells protects mice from abdominal aortic aneurysm (AA), however it is not clear how B cells promote AA growth. BAFF exists as a 3mer (binds only to BR3) or as a 60mer (binds to BR3, TACI and BCMA). Therefore, we hypothesize that BAFF multimerization regulates the immune and metabolic phenotype of B cells by binding to BAFF receptors and modulate AA growth. Immunohistology was performed on AA tissues collected from patients undergoing open AA repair. Experimental AA was induced by elastase perfusion of abdominal aorta or angiotensin II infusion (1000 ng/kg/min) method in 8 weeks old male C57BL/6 or apolipoprotein E knockout mice, respectively. Western blotting, flow cytometry and Seahorse extracellular flux assays were used to determine immune and metabolic changes in B cells in response to recombinant BAFF 3mer and 60mer. BR3+ B cells were detected in the milieu of BAFF in human AAs. Mouse AAs demonstrated significant infiltration (>50/section) of CD138+ plasma B cells, but few (4-10/section) CD20+ B cells. In vitro, BAFF 3mer induced canonical NF-kB, whereas, 60mer induced both canonical and non-canonical NF-kB signaling. Moreover, the 3mer significantly decreased mitochondrial density, oxygen consumption rate, and surface expression of IgD and IgM indicating a metabolically quiescent state of B cells. However, these

parameters were significantly increased by the 60mer similar to plasma cells. Anti-BR3 IgG1, but not a control IgG1 antibody decreased BAFF 60mer-induced oxygen consumption rate by 50%. In a pilot study (n=10/group), anti-BR3 IgG1, but not the control IgG1 aggravated angiotensin II-induced AA growth. Altogether, our results suggest that BAFF 3mer and 60mer oppositely regulate immune and metabolic phenotype of B cells and inhibition of BAFF-BR3 signaling is detrimental for AA growth.

Disclosures: **V. Serbulea:** None. **P. Jakobs:** None. **S. Sahu:** None. **P. Srikakulapu:** None. **C.A. McNamara:** None. **G. Ailawadi:** None. **G.R. Upchurch Jr.:** None. **N. Leitinger:** None. **A.K. Meher:** None.

This research has received full or partial funding support from the American Heart Association.

485

On the Relative Effectiveness of Machine Learning and Statistical Methods in Predicting Abdominal Aortic Aneurysm Rupture in the Asian Population

Tejas Canchi, Nanyang Technological Univ, Singapore, Singapore; **Sourav S Patnaik**, Univ of Texas at San Antonio, San Antonio, TX; E Y Ng, Dinesh K Srinivasan, Nanyang Technological Univ, Singapore, Singapore; Sriram Narayanan, Tan Tock Seng Hosp, Singapore, Singapore; Ender A Finol, Univ of Texas at San Antonio, San Antonio, TX

Background: Abdominal Aortic Aneurysms (AAA) have a high risk of mortality if they rupture, making it one of the leading causes of death in elderly men. Hence, a better prediction method is necessary to identify high rupture risk patients. **Methods:** Retrospective data (clinical and AAA geometric parameters) were collected of 114 Asian AAA patients from an IRB approved database. We applied a novel machine learning algorithm (MLA) to predict AAA rupture by generating a decision tree of rupture risk predictors. For comparative analysis, a binary logistic regression (backward stepwise Wald) was also performed. The rupture status was the dependent variable for both methods; each method provided the highest weighted risk factors and effectiveness of classification as assessed by Receiver Operating Characteristic (ROC) curves. **Results:** For the MLA, the most significant risk factors were DAAA (maximum diameter) (> 57 mm), presence of hypertension, D4 (diameter at the iliac bifurcation) (> 23.7 mm), age (> 79 years), and D3 (right common iliac artery diameter) (> 14 mm), as seen in Fig. 1a. Similarly, the backward stepwise logistic regression analysis showed a strong association for rupture with DAAA (O.R. 2.635), L1 (distance between the lowest renal artery and the iliac bifurcation) (O.R. 1.658), D3 (O.R. 1.876), NL (AAA neck length) (O.R. 0.294), and age (O.R. 0.681). The MLA exhibited a lower classification accuracy (80.7% vs. 99.2%) and area under the curve (ROC analysis) (56.3% vs. 98.2%) when compared to the regression analysis, as seen in Fig. 1b. **Conclusions:** This is the first known report of predictive rupture risk in the Asian AAA patient population using MLA and statistical methods. Although the MLA did not provide improved classification accuracy compared to a standard statistical method, the risk factors obtained from both methods were similar. Future studies will aim at improving the prediction ability of MLA in a racially diverse AAA patient population.

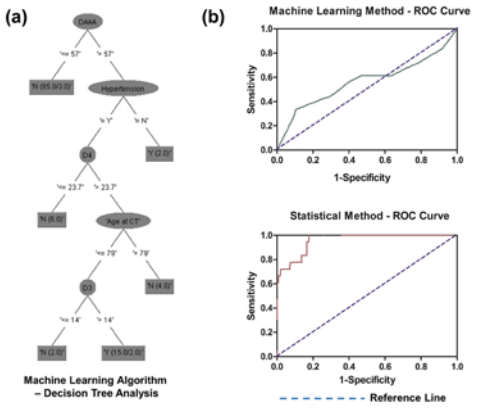

Figure 1: (a) Decision Tree Analysis from the Machine Learning Algorithm (MLA); (b) receiver operator characteristic curves (ROC) from MLA and statistical method, respectively.

Disclosures: **T. Canchi:** None. **S.S. Patnaik:** None. **E.Y.K. Ng:** None. **D.K. Srinivasan:** None. **S. Narayanan:** None. **E.A. Finol:** None.

486

A Novel Synthetic Glycolipid TLR4 Antagonist (FP7) Negatively Regulates in vitro and in vivo Hematopoietic and Non-Hematopoietic Vascular Toll Like Receptor 4 Signalling

Charys Palmer, Anglia Ruskin Univ, Cambridge, United Kingdom; Francesco Peri, Univ of Milano-Bicocca, Milan, Italy; Frank Neumann, Innaxon, Tewkesbury, United Kingdom; **Grisha Pirianov**, Anglia Ruskin Univ, Cambridge, United Kingdom

Objectives: The toll-like receptors (TLRs), including TLR4, have been shown to play a crucial role in vascular inflammatory based diseases. The main goal of this study was to determine the potential of FP7, a synthetic glycolipid active as TLR4 antagonist, to modulate hematopoietic and non-hematopoietic vascular TLR4 proinflammatory signalling. **Methods:** Human umbilical vein endothelial cells (HUVEC), THP-1 monocytes, THP-1-derived macrophages and Angiotensin II-infused Apo E deficient mice were *in vitro* and *in vivo* models respectively. Western blotting, antibody array and ELISA approaches were used to explore the effect FP7 on TLR4 functional activity on two levels: modulation of TLR4-induced mitogen activated protein kinases (MAPK) and p65 NF-kB activity and expression of TLR4 dependent proinflammatory proteins in response to liposaccharide (LPS) and ligands of sterile inflammation; minimally oxidized LDL (moxLDL) and small fragments of hyaluronan (sfHA). **Results**: Following activation of TLR4 by ligands of non-sterile and sterile inflammation, *in vitro/in vivo* data revealed that FP7 inhibited MAPK and p65 NF-kB phosphorylation associated with down regulation of specific TLR4 dependent proinflammatory proteins proteins, such as MCP-1, ICAM-1, RANTES, MIP-1 gamma, KC etc. In addition to inhibition of LPS-induced TLR4 signalling, FP7 negatively regulated TLR4 activation in response to ligands of sterile inflammation; moxLDL and sfHA (*in vitro*) and Angiotensin II infusion (*in vivo*). **Conclusions:** These results demonstrate the ability of FP7 to negatively regulate in vitro and in vivo hematopoietic and non-hematopoietic vascular TLR4 signalling, suggesting the potential therapeutic use of this novel TLR4 antagonist for pharmacological intervention of vascular inflammatory based diseases such as atherosclerosis and aneurysm.

Disclosures: **C. Palmer:** None. **F. Peri:** None. **F. Neumann:** None. **G. Pirianov:** None.

487 will be presented in the PVD Moderated eAbstract Poster Session. The abstract content is located on page 42.

489

A Data Driven Approach to Identify Subtypes of Abdominal Aortic Aneurysm With Distinct Clinical and Genetic Characteristics

Zi Ye, Erin Austin, Iftikhar Kullo, Mayo Clinic, Rochester, MN

Background: Abdominal aortic aneurysm (AAA) is a complex and heterogeneous disorder. We hypothesized that dense phenomapping using electronic health records (EHR) can identify subtypes of AAA with distinct clinical and genetic characteristics. **Methods & Results:** AAA cases (n=1108) and controls (n=4694) were identified from the Mayo vascular disease biorepository and had available high-density genotyping data. 132 Candidate genetic variants ($p < 10E-5$) associated with atherosclerotic cardiovascular disease (ASCVD) or AAA were selected from GWAS catalog. Using model-based Gaussian-mixture cluster analysis of 46 clinical features from 6 data domains, 24 data elements, 204 variables (including age, sex, vital signs, laboratory data, medication use, family history), spanning over 20 years of observational time in the EHR, we identified two subtypes of AAA: subtype 1(S1, n=421) with faster AAA growth rate (baseline size adjusted mean difference, 95% CI: 0.013, 0.001 to 0.020 cm / year faster, $p = 0.03$), higher all-cause mortality (age & sex adjusted hazard ratio, 95% CI: 1.36, 1.09 - 1.70, $p < 0.01$) than subtype 2 (S2, n=687). As compared with the controls, thyroid disorder / rheumatoid or osteoarthritis / infectious conditions were uniquely associated with increased odds ratio for S1; ASCVD / hyperlipidemia / hypertension were uniquely associated with increased odds ratio for S2. After adjustment for all group-specific diseases, genetic variants in *CDKN2B-AS1, NOA1-REST, ERG, ZNF335-MMP9* and *SMAD3* were associated with S1 and variants in *MMP12, DAB2IP, LHFPL2, LPA, FSTL5* and *SORT1* were associated with S2 (all FDR $p < 0.05$). After adjustment for disease comorbidities and genetic variants differently associated with S1 and S2, the increased risk for all-cause death of S1 than S2 and

the difference in AAA expansion rate in subgroups attenuated (Both p-values > 0.09) **Conclusions:** We identified two subtypes of AAA with different rates of aneurysm expansion and all-cause mortality, which were associated with subtype-specific disease comorbidities and genetic markers, suggesting the potential of leveraging EHR to facilitate individualized medicine in patients with AAA.

Disclosures: **Z. Ye:** None. **E. Austin:** None. **I. Kullo:** None.

490

Quantitative and Dynamic Measurements of Aortic Wall of Acute Type-A Aortic Dissection With X-Ray Phase-Contrast Tomography

Koki Yokawa, Kobe Univ Hosp, Kobe, Japan; Takuro Tsukube, Japanese Red Cross Kobe Hosp, Kobe, Japan; Naoto Yagi, Masato Hoshino, Japan Synchrotron Radiation Res Inst / SPring-8, Sayo, Japan; Yutaka Nakashima, Japanese Red Cross Fukuoka Hosp, Fukuoka, Japan; Kazunori Nakagawa, Kyushu Univ, Graduate Sch of Med, Fukuoka, Japan; Yutaka Okita, Kobe Univ Hosp, Kobe, Japan

OBJECTIVES: We previously reported excellent findings of X-ray phase-contrast tomography (PCX) for visualization of the formalin-fixed human aortic wall samples, and PCX enabled to demonstrate changes of tunica media in acute type A aortic dissection (AADA) . This study evaluates quantitative and dynamic measurements of fresh aortic wall samples of AADA with this modality. **METHODS:** Fresh human aortic samples of the ascending aorta (n=7) were obtained during emergent aortic repair for AADA. Formalin-fixed human aortic walls of AADA (n=15) and normal aorta (n=15) were also investigated. PCX is approximately 1000 times more sensitive than absorption-contrast X-ray imaging and effective resolution of PCX is 11.7 μm. Quantitative and dynamic measurement has been developed to visualize changes in imaging of fresh aortic wall under various tensile force to simulate physiological condition, in which aortic wall is stretched according to blood pressure.**RESULTS:** In normal aorta, quantitative measurement of density of the media was 1.095±0.003(g/cm3), and no different between intimal side (1.083±0.002) and adventitial side (1.085±0.003). On contrast, in formalin-fixed aorta of AADA, the medial density was 1.063±0.027, significantly lower than normal aorta (Figure-1), and different between intimal side and adventitial side (1.061±0.008 vs 1.081±0.011, respectively; p<0.005). In fresh sample of AADA, distribution of the medial density was equal to that of formalin-fixed aorta and differences of the medial density were clearly observed with elevation of tensile force of the aortic wall (Figure-1). These differences in density within tunica media were well correlated with distribution of elastic fibers and existence of cystic medial necrosis in pathological analysis. **CONCLUSIONS:** X-ray phase-contrast tomography was a strong modality to understand aortic structures and pathogenesis of acute type A aortic dissection.

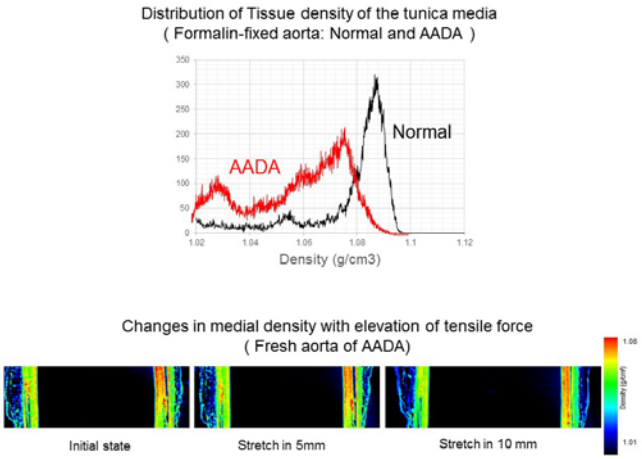

Disclosures: **K. Yokawa:** None. **T. Tsukube:** None. **N. Yagi:** None. **M. Hoshino:** None. **Y. Nakashima:** None. **K. Nakagawa:** None. **Y. Okita:** None.

491

Racial Disparities in the Trends of Acute Myocardial Infarction Outcomes Among Medicaid Patients, 2007-2011

Oluwole M Adegbala, Englewood Hosp and Medical Ctr, Bergerfield, NJ; Akintunde Akinjero, Icahn Sch of Med, Mount Sinai, NY; Samson Alliu, Maimonides Medical Ctr, Brooklyn, NY; Adeyinka Charles Adejumo, Univ of Massachusetts,, Worcester, MA; Emmanuel Akintoye, Wayne State Univ, Detroit, MI; David Otuada, Univ of Alabama, Birmingham, AL; Tokunbo Ajayi, John Hopkins Med, Howard County General Hospital, DC; Nnaemeka Onyeakusi, Bronx-Lebanon Hosp Ctr, Bronx, NY; Eseosa Edo-Osagie, Englewood Hosp and Medical Ctr, Bergerfield, NJ; Modupeoluwa Durojaiye, Univ of Alabama, Birmingham, AL; Edgar Lichstein, Albert Einstein Coll of Med, Bronx, NY; Tomi Akinyemiju, Univ of Alabama, Birmingham, AL

Background
Although, in-hospital mortality from acute myocardial infarction (AMI) have declined in the United States recently, there is a gap in knowledge regarding racial differences in this trend. We sought to evaluate the effect of race on the trends in outcomes after Acute Myocardial Infarction among Medicaid patients in a nationwide cohort from 2007-2011
Methods
We extracted data from the Nationwide Inpatient Sample (NIS) for all hospitalizations between 2007 and 2011 for Medicaid patients aged 45 years or older with principal diagnosis of AMI using ICD-9-CM codes. Primary outcome of this study was all cause in-hospital mortality. We then stratified hospitalizations by racial groups; Whites, African Americans and Hispanics, and assessed the time trends of in-hospital mortality before and after multivariate analysis.
Results
The overall mortality from AMI among Medicaid patients declined during the study period (8.80% in 2007 to 7.46% in 2011). In the adjusted models, compared to 2007, in-hospital mortality from AMI for Medicaid patients decreased across the 3 racial groups; Whites (aOR= 0.88, CI=0.70-0.99), African Americans (aOR=0.76, CI=0.57-1.01), Hispanics (aOR=0.87, CI=0.66-1.25). While the length of hospital stay declined significantly among African American and Hispanic with 2 days and 1.76 days decline respectively, the length of stay remained unchanged for Whites. There was non-significant increase in the incidence of stroke across the various racial groups; Whites (aOR= 1.23, CI=0.90 -1.69), African Americans (aOR=1.10, CI=0.73 -1.64), Hispanics (aOR=1.03, CI=0.68-1.55) when compared to 2007.
Conclusion
In this study, we found that in-hospital mortality from AMI among Medicaid patients have declined across the racial groups. However, while the length of stay following AMI declined for African Americans and Hispanics with Medicaid insurance, it has remained unchanged for Whites. Future studies are necessary to identify determinants of these significant racial disparities in outcomes for AMI.

Disclosures: **O.M. Adegbala:** None. **A. Akinjero:** None. **S. Alliu:** None. **A.C. Adejumo:** None. **E. Akintoye:** None. **D. Otuada:** None. **T. Ajayi:** None. **N. Onyeakusi:** None. **E. Edo-Osagie:** None. **M. Durojaiye:** None. **E. Lichstein:** None. **T. Akinyemiju:** None.

493

Correlation Between Cannabis Use and the Prevalence of Cerebrovascular Disease (Cva); Analysis from the National Inpatient Sample (NIS) 2012-2014

Samson E Alliu, Maimonides Medical Ctr, Brooklyn, NY; Adeyinka Adejumo, Univ of Massachusetts Medical Sch, Worcester, MA; Modupeolowa Durojaiye, Univ of Alabama at Birmingham, Birmingham, AL; Oluwole Adegbala, Englewood Hosp and Medical Ctr, Englewood, NJ; Tokunbo Ajayi, Johns Hopkins Med, Howard County General Hosp, Columbia MD, Columbia, MD; Nnaemeka Onyeakusi, Bronx-Lebanon Hosp, Bronx, NY; Lawrence Wolf, Stephan Kamholz, Jacob Shani, Maimonides Medical Ctr, Brooklyn, NY; Edgar Lichstein, Albert Einstein Coll of Med, Bronx, NY

Background: With increasing legalization of cannabis, there is a growing number of cannabis users in the US. Cannabidiol - a component of cannabis with no psychoactive or cognitive effect has been proven in animal models to have vasodilatory and anti-inflammatory effect on the blood vessels. However, in clinical literature, the association between cerebrovascular accident **(**CVA) and cannabis remains inconclusive.
Objective: To examine if there is a difference in the prevalence of CVA among patients who use

cannabis and non-users.
Methods: We identified patients > 18 years (N=12,114,360) from the 2012 -2014 National Inpatient Sample database. Using the ICD-9 code, we categorized patients using cannabis (non-dependent and dependent users) and non-users. Our outcome of interest was prevalence of CVA in this population. Logistic regression analysis was performed to assess the association between cannabis use and CVA. Using multivariate regression model, we adjusted for known confounders of CVA; age, gender, race, insurance type, socioeconomic status, tobacco use, cocaine use, alcohol abuse, amphetamine use, hyperlipidemia, diabetes, hypertension, renal failure, prior history of CVA and family history of CVA.
Results: From our study sample **(**12,114,360 hospitalized patients), 2.1% (253,752) had a diagnosis of CVA, 1.48% (179,576) were non-dependent cannabis users and 0.21% (25,968) dependent users. Among hospitalized patient, non-dependent cannabis use was associated with an 8% increased odds of CVA (AOR 1.08 [1.03-1.13]) compared to non-users. However, dependent cannabis use was associated with a 60% decreased odds of CVA (AOR 0.40 [0.31-0.49]) compared to non-users. Also, In-group comparison shows a 60% decreased odds of CVA among dependent cannabis users (AOR 0.36[0.29-0.46]) compared to non-dependent cannabis users.
Conclusions: Non-dependent cannabis use was associated with a slightly increased odd of CVA while dependent cannabis use was independently protective against CVA. Our study used the largest repository of clinical information to explore this association, however we recommend more clinical study to explore this correlation in other to maximize the pharmacological benefit of cannabidiol in cannabis for the prevention of CVA.

Disclosures: **S.E. Alliu:** None. **A. Adejumo:** None. **M. Durojaiye:** None. **O. Adegbala:** None. **T. Ajayi:** None. **N. Onyeakusi:** None. **L. Wolf:** None. **S. Kamholz:** None. **J. Shani:** None. **E. Lichstein:** None.

494

Safety of Chelation Therapy with Edta in Patients With Critical Limb Ischemia: A Pilot Trial of Limb Preservation in Diabetic Patients

Ivan A Arenas, Ian Ergui, Gervasio A Lamas, Mount Sinai Medical Ctr Miami Beach, Miami, FL

Critical limb ischemia (CLI) carries a one year 30% risk of amputation and 25% risk of mortality. Toxic metals are associated with peripheral artery disease and overall cardiac mortality. In The Trial to Assess Chelation Therapy (TACT), EDTA-based chelation improved outcomes in patients with coronary artery disease, with a particular benefit observed in diabetic patients. Here we present the preliminary findings of an open label study aimed at evaluating the safety of EDTA-based chelation, as used in TACT, in diabetic patients with CLI. Methods: Diabetic patients with CLI Rutherford stage 4 to 5, ≥ 75% stenosis in two or more infra-popliteal arteries and skin perfusion pressure of <40 mmHg in the affected limb were enrolled. Participants received 40 infusions of disodium EDTA over the course of a year, with the first 20 infusions administered bi-weekly and subsequent infusions administered weekly. Laboratory safety assessments were conducted at nine of the infusion visits. Lower extremity pressures and skin perfusion pressures were obtained at baseline and after 20 and 40 infusions using the SensiLase PAD-IQ. HIPAA compliant photographs along with clinical and quality of life questionnaires were also collected. Results: Three patients (2 women and 1 man) out of 10 planned patients have completed forty EDTA-based infusions. The mean (SD) age and creatinine clearance were 80(7) years and 55(3) mL/min, respectively. All patients had detectable levels of toxic metals in urine; lead was the most abundant toxic metal in the chelated urine. The lowest baseline tissue perfusion pressure in the affected limb was 22, 17 and 19 mmHg for each of the three patients, respectively. Patients have been followed up for an average of 61 (14) weeks. There have been no side effects related to therapy. No patient has been amputated or developed an acute cardiac event. One patient had a PTCA of her affected leg and underwent a debridement of a non-healing ulcer. No significant changes have been detected in skin perfusion pressures during follow up. Conclusions: Preliminary findings of this open label trial suggest that EDTA treatment in CLI patients is safe. Moreover, after more than a year of follow up, no patient has required any amputation or had any cardiovascular event.

Disclosures: **I.A. Arenas:** None. **I. Ergui:** None. **G.A. Lamas:** Research Grant; Significant; NIH Grant. TACT Principal Investigator.

495

Mouse Model of Mesenteric Ischemia Secondary to Vascular Calcification and Atherosclerosis

Konstantinos Damiris, Filippo Romanelli, NYIT Coll of Osteopathic Med, Old Westbury, NY; Alexei Savinov, Sanford Res Ctr, Sioux Falls, SD; José Luis Millan, Sanford Burnham Prebys Medical Discovery Inst, La Jolla, CA; Jes Kuruvilla, Olga V Savinova, NYIT Coll of Osteopathic Med, Old Westbury, NY

Objective- Atherosclerosis is a leading cause of chronic mesenteric ischemia (CMI), defined as intestinal hypoperfusion resulting from stenosis of mesenteric arteries. Symptoms of CMI range from non-specific abdominal pain and weight loss to aversion of food resulting in cachexia. In this study we aim to define intestinal ischemia and its effects on gastrointestinal structure and function in an *in vivo* model of atherosclerosis. *Hypothesis*- Overexpression of tissue-nonspecific alkaline phosphatase (TNAP) under conditions of hypercholesterolemia in a mouse model will lead to atherosclerosis causing intestinal ischemia. *Methods and Results*- We have previously established that endothelial TNAP overexpression (eTNAP) results in calcification of medium-sized arteries including mesenteric. In this study eTNAP was combined with a point mutation in the low-density lipoprotein receptor (*ldlr^*WHC). When fed an atherogenic diet (Paigen's diet, starting at 8 weeks of age), WHC-eTNAP mice developed acute body weight loss (>15% from baseline), whereas WHC mice continued to gain weight. Examination of the mesenteries of WHC-eTNAP demonstrated eccentric vascular remodeling and stiffening, as well as calcification of atherosclerotic plaques (n=4). Mesenteric arteries of WHC were not affected (n=3). WHC-eTNAP (n=2) mice developed extensive atherosclerosis of submucosal arterioles in the colon where most vessels were narrowed or occluded. Examination of the small intestine in WHC-eTNAP mice showed structurally distressed villi accompanied with an increase in goblet cells and fragmentation of the epithelial layer possibly reflecting cell death. The colon demonstrated loss of goblet cells and signs of denuding of the epithelium. *Conclusion*- Atherosclerosis induced by overexpression of TNAP causes occlusion of mesenteric arteries as well as structural pathology in the small and large intestine

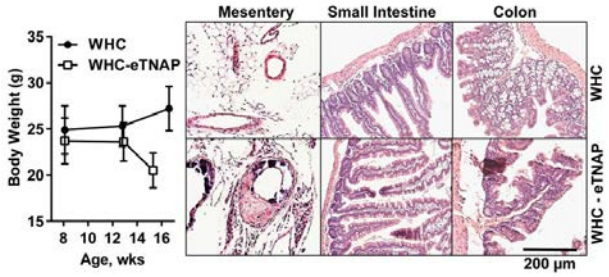

Disclosures: **K. Damiris:** None. **F. Romanelli:** None. **A. Savinov:** None. **J. Millan:** None. **J. Kuruvilla:** None. **O.V. Savinova:** None.

496 will be presented in the PVD Moderated eAbstract Poster Session. The abstract content is located on page 43.

497

Sex Differences in the Relationship Between Pro-Inflammatory Adipokines, Chemerin and Resistin, and Carotid Atherosclerotic Plaque Instability

Karina Gasbarrino, Russell Yanofsky, McGill Univ, Montreal, QC, Canada; Carina Sancho, Univ de Montréal, Montreal, QC, Canada; Fanny Jaunet, Polytech Nice-Sophia, Biot, France; Huaien Zheng, McGill Univ, Montreal, QC, Canada; Chi Lai, John Veinot, Univ of Ottawa Heart Inst, Ottawa, ON, Canada; Stella S. Daskalopoulou, McGill Univ, Montreal, QC, Canada

Introduction: Sex differences in plaque morphology and composition exist; men develop more unstable plaques than women. Yet, stroke kills more women than men. Despite these differences, no sex-specific guidelines for carotid disease management exist. Thus, markers that reflect sex-specific morphological features in the plaque should be explored for better prediction of stroke risk. Pro-inflammatory adipokines, chemerin and resistin, influence vascular function. Herein we are the first to investigate sex differences in

the relationship between carotid plaque instability and the expression of these adipokines. ***Methods:*** Subjects with ≥50% carotid stenosis scheduled for a carotid endarterectomy were recruited from McGill-affiliated hospitals. Pre-operative plasma chemerin and resistin levels were measured using ELISA. Stability of carotid plaque specimens was assessed by two gold standard histological classifications. Stable and unstable plaques were immunostained for chemerin, chemerin's receptor (ChemR23), and resistin. Digital and semi-quantifications assessed the % area of expression as well as staining intensity (mild to high) and % of positively stained macrophages/foam cells. Plaque mRNA expression was assessed by quantitative PCR. Sex-hormone analyses are ongoing. ***Results:*** Men (n=171) had more unstable plaque features, i.e., greater hemorrhage (P=0.022), lipid core size (P<0.001), inflammation (P=0.007), cap infiltration (P=0.006), and less fibrous tissue (P<0.001) than women (n=79). Circulating chemerin and resistin levels were similar between men and women and no sex differences were observed in relation to plaque instability. The % area of chemerin and resistin staining in the plaque was greater in unstable *vs* stable plaques in men only (P=0.040; P=0.005, respectively). Similarly, greater intensity in chemerin, ChemR23, and resistin staining was associated with plaque instability in men only (P<0.001; P=0.013; P=0.033, respectively). In contrast, lower resistin plaque mRNA expression was associated with plaque instability in women only (P=0.040). ***Conclusion:*** Our results suggest the possibility of a sex-dependent regulatory mechanism underlying the connection between these adipokines and plaque instability.

Disclosures: **K. Gasbarrino:** None. **R. Yanofsky:** None. **C. Sancho:** None. **F. Jaunet:** None. **H. Zheng:** None. **C. Lai:** None. **J. Veinot:** None. **S.S. Daskalopoulou:** None.

498

In vivo Assessment of Murine Valvular and Vascular Calcification Using ^{18}F Sodium Fluoride Micro Positron-Emission Tomography and Computed Tomography

Jeffrey J. Hsu, Alexander Wu, Jinxiu Lu, Soban Umar, Linda L. Demer, Yin Tintut, UCLA, Los Angeles, CA

Calcific aortic valvular and vascular disease (CAVVD) is associated with increased morbidity and mortality. In addition to the commonly practiced computed tomography (CT) to evaluate for the presence of CAVVD, recent work has demonstrated the use of ^{18}F-sodium fluoride positron-emission tomography (^{18}F-PET) to assess both valvular and vascular calcification in humans. In this pilot study, we combined ^{18}F μPET and μCT to assess for aortic valvular and aortic arch calcification *in vivo*. Aged *Apoe*$^{-/-}$ mice (n=5) were injected with ~200 μCi ^{18}F-sodium fluoride and, one hour later, were imaged with fused μPET-μCT (Figure A,C). Intravenous contrast was used for the μCT studies to assist with anatomic localization (Figure B,D). To assess valvular hemodynamics, direct cardiac catheterization was performed on the mice to determine the peak-to-peak pressure gradient (PPG) across the aortic valve, between the left ventricle and aorta (Figure E,F). All mice were found to have aortic arch calcification present on both μPET and μCT imaging. In mice with aortic valve calcification specifically identified on μPET-μCT (Figure A-D, red arrows), there was increased ^{18}F uptake in the heart and aorta (58.8 ± 7.7 %ID/cc) compared to the mouse without aortic valve calcification (16.2 %ID/cc). Additionally, in the mice with aortic valve calcification, the mean transvalvular PPG was 9.7 ± 2.5 mmHg, and in the mouse without valvular calcification, the PPG was 3.3 mmHg. Alizarin red staining of histological sections from the aortic valves and aortic roots from these mice was performed to assess for the presence of calcium mineral. In conclusion, these findings suggest that the use of ^{18}F μPET-μCT in small animals provides a method to determine the presence of CAVVD *in vivo*. Future studies will determine whether changes in ^{18}F μPET-μCT signal reliably correlate with meaningful changes in CAVVD.

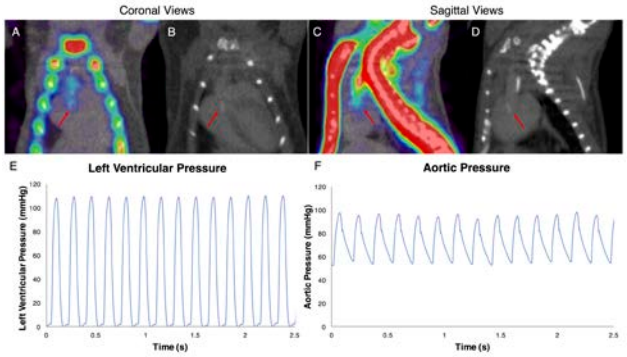

Disclosures: **J.J. Hsu:** None. **A. Wu:** None. **J. Lu:** None. **S. Umar:** None. **L.L. Demer:** None. **Y. Tintut:** None.

499

Lipoprotein(A) and Carotid Intimal Medial Thickness

Hiroaki Ikezaki, Yuya Yokota, Ernst J Schaefer, Katalin V Horvath, Bela F Asztalos, Jean Mayor Human Nutrition Res Ctr on Aging at Tufts Univ, Boston, MA; Norihiro Furusyo, Kyushu Univ Hosp, Fukuoka, Japan

Introduction: Atherosclerotic cardiovascular disease (ASCVD) is a leading cause of death and disability in both Japan and the United States. Carotid intimal medial thickness (CIMT) has been used as a marker of ASCVD risk. We examined various specialized lipoprotein parameters to determine their utilities for predictor of CIMT progression.
Methods: Using plasma samples obtained from fasting men and women (n=2245) living in the Fukuoka area of Japan, (median age 59 years), at baseline we measured direct high density lipoprotein cholesterol (HDL-C), HDL2-C, HDL3-C, low density lipoprotein cholesterol (LDL-C), small dense LDL-C (sdLDL-C), triglycerides (TG), LDL-triglycerides (LDL-TG), lipoprotein(a) or Lp(a), and adiponectin. All assays were measured on an automated high throughput platform (Olympus AU400) using assay kits from the Denka Seiken Corporation (Niigata, Japan) and had within and between run coefficients of variations of < 5%. Blood pressure, body mass index, use of medications, and history of hypertension, dyslipidemia and diabetes were also assessed. CIMT of the common carotid artery was assessed bilaterally at baseline and after 5 years of follow up used trained technicians with analysis coefficients of variation of < 10%. Participants using statin therapy at baseline and during follow up were excluded.Results: After controlling for age and gender, only Lp(a) was significantly associated with change in CIMT over a 5 year period in this population. The data indicated that for every 1 log unit higher Lp(a) level at baseline, there was a 0.06 mm increase in CIMT over 5 years (p=0.02). While relationships were seen with other parameters and CIMT change, none of these other relationships reached statistical significance at p<0.05. We also observed significant relationships (p<0.05) between CIMT progression and age, gender, current smoking, history of hypertension, treatment of hypertension.Conclusions: Our data indicate that lipoprotein (a) as measured by immunoassay in an important predictor of the progression of atherosclerosis in the common carotid arteries of middle aged and elderly Japanese men and women, and serves as a valuable marker of ASCVD risk.

Disclosures: **H. Ikezaki:** None. **Y. Yokota:** None. **E.J. Schaefer:** None. **K.V. Horvath:** None. **B.F. Asztalos:** None. **N. Furusyo:** None.

500

Treatment of Arterial Embolization for Pulmonary Arteriovenous Malformations With and Without Osler Disease

Yasutaka Kawamura, Harue Hosp, Fukui, Japan; Motoji Fukazawa, Shinya Hasegawa, Awa Regional Medical Ctr, Chiba, Japan; Yukio Chiba, Hayashi Hosp, Fukui, Japan

Purpose: We report cases with pulmonary arteriovenous malformations (PAVM) treated with transcatheter arterial embolization. The clinical features of PAVM and the indication, techniques and

longterm outcome of the embolization therapy were assessed.
Patients: Six patients (age ranges from 44 to 67, five women and a man) had diagnosed as PAVM. Two patients diagnosed as definite HHT: Hereditary Hemorrhagic Telangiectasia (Rendu-Osler-Weber Syndrome) with epistaxis and family history and one as possible HHT associating hemorrhagic skin telangiectasias and abnormally enlarged the internal thoracic artery. Indication of the pulmonary arterial embolization therapy: Four patients had the episodes of cerebral infarction, one developed cerebellar ataxia, and another patient was proved the decreased PaO_2. Two patients revealed the enlargement of PAVM. CT and 3-dimensional CT angiography (CTA) was obtained on 64-multi-detector row unit (Toshiba, Aquilion64, Japan) with bolus injection of contrast agent. The transcatheter pulmonary arterial embolization was performed with microcatheter system (TERUMO, Japan) and 0.035 coils of 6, 4, 3mm in diameter (Boston Scientific, USA). **Results**: After the selective catheterization for PAVM, all feeding arteries > 3 mm in diameter was embolized. Since coil size selection was crucial for the safe and productive procedure, the size of feeding arteries had been carefully estimated on CTA date in advance. All patients were successfully treated without any problems during and after the procedure. One patient with HHT, three years after the treatment of 4.3cm PAVM, showed the recurrent PAVM of 0.5mm in diamete. The other patient showed a small vessel emerged distal to the embolized PAVM draining to the pulmonary vein. These lesions were too small to consider the clinical management and had been followed up with no change. **Conclusion**: The pulmonary arterial embolization therapy for PAVM was discussed. The treatments were successful, however, some recurrences were noted. We did not thoroughly embolized the distal side of PAVM because to minimize the normal lung damage and to avoid the migration of coils. Deliberate clinical follow-up should be required and should apply the additional treatment, if necessary.

Disclosures: **Y. Kawamura:** None. **M. Fukazawa:** None. **S. Hasegawa:** None. **Y. Chiba:** None.

501

Prevalence of Ascending Aorta Atherosclerosis as Detected by Echocardiography and Computed Tomography in Patients Referred for Atrial Fibrillation Ablation

Efstratios Koutroumpakis, Benjamin Schwartz, John Espey, Elizabeth Rau, David Steckman, Mikhail Torosoff, Albany Medical Coll, Albany, NY

Introduction: The prevalence and significance of thoracic aorta atherosclerosis in AF patients has not been clearly defined in the literature. There are scant reports supporting an association of atherosclerotic aortic plaque burden with embolic phenomena and recurrence of AF post ablation. Two modalities of aortic atherosclerosis detection include computed tomography (CT) and echocardiography.
Hypothesis: The prevalence of ascending aorta atherosclerosis in AF patients is high and CT performs better than transthoracic echocardiography in its detection.
Methods: We investigated prevalence of ascending aorta atherosclerosis by CT and transthoracic echocardiography in 76 consecutive patients referred for AF ablation (67.1% males, 62.9 +/- 9.8 years old, 6.6% active smokers, 75% paroxysmal AF, 13.1% with LV ejection fraction (EF) <50%, 61.8% with hyperlipidemia, 55.8% with hypertension, 10.5% with diabetes, 2.6% with chronic kidney disease, and 1 patient with peripheral artery disease). The pre-ablation echocardiograms and cardiac CT scans, originally performed for left atrial mapping and evaluation of left atrial appendage thrombus, were reviewed in a blinded fashion for the presence of aortic atherosclerosis.
Results: Out of 76 AF ablation patients, 27 (35.5%) had evidence of ascending aorta atherosclerosis by CT and 43 (56.6%) by echocardiography. Using CT as the gold standard, echocardiography had a sensitivity of 70.4% and a specificity of 51% in identification of ascending aorta atherosclerosis. Positive and negative predictive values were 44.2% and 75.8%, respectively. A total of 16 patients (21.1%) had AF recurrence post ablation, out of which 6 (37.5%) had evidence of aortic atherosclerosis on CT (vs 21/49 [42.9%] in the non-recurrence group).
Conclusions: Ascending aorta atherosclerosis is common in patients referred for AF ablation. Transthoracic echocardiography likely overestimates its prevalence. Aortic atherosclerosis as detected by CT was not significantly associated with AF recurrence post ablation. More studies investigating clinical implications and best treatment approach to subclinical aortic therosclerosis in patients with AF are needed.

Disclosures: **E. Koutroumpakis:** None. **B. Schwartz:** None. **J. Espey:** None. **E. Rau:** None. **D. Steckman:** None. **M. Torosoff:** None.

502

Effect of Intensive Versus Standard Blood Pressure Control on Stroke and Serious Adverse Event: A Bivariate Analysis on the Net Clinical Benefit

Jolanta Marszalek, Louis A. Weiss Memorial Hosp, Chicago, IL; Sara Mehrsefat, Johns Hopkins Univ, Sch of Med, Baltimore, MD; Gerald Chi, Beth Israel Deaconess Medical Ctr, Harvard Medical Sch, Boston, MA

Background: Intensive blood pressure (BP) control is associated with a reduced risk of stroke but a greater risk of serious adverse event (SAE), thereby offsetting the benefit-to-risk ratio of this strategy.
Methods: Using a previously described method of bivariate analysis, efficacy and safety outcomes were collectively analyzed as net clinical benefit (NCB) based on data from three randomized controlled trials comparing intensive versus standard BP control among 17,115 patients (ACCORD, SPS3, and SPRINT trials). Bivariate risk difference was assessed by the minimum distance from NCB curve to 95% CI of risk difference in all-cause stroke and SAE.
Results: Compared to standard BP target, intensive strategies reduced all-cause stroke by 0.70% (95% CI: 0.19% to 1.21%; P = 0.007) and increased SAE by 1.85% (95% CI: 1.35% to 2.34%; P < 0.0001). With a non-inferiority margin of 25%, standard strategy was preferable with respect to NCB in diabetics (bivariate risk difference: 1.29% [0.40% to 2.31%]) and in patients without diabetes or prior stroke (1.55% [0.76% to 2.37%]). Among patients with stroke history, intensive strategy failed to achieve non-inferiority in NCB (-0.18% [-1.01% to 0.83%]).
Conclusions: Bivariate analysis is a novel method that allows simultaneous display and assessment of efficacy and safety outcomes. Among patients with cardiovascular risk factors, intensive BP control failed to demonstrate a favorable risk-benefit profile against standard BP control with respect to the tradeoff between stroke and SAE.

Figure 1. Net clinical benefit of intensive vs standard BP control

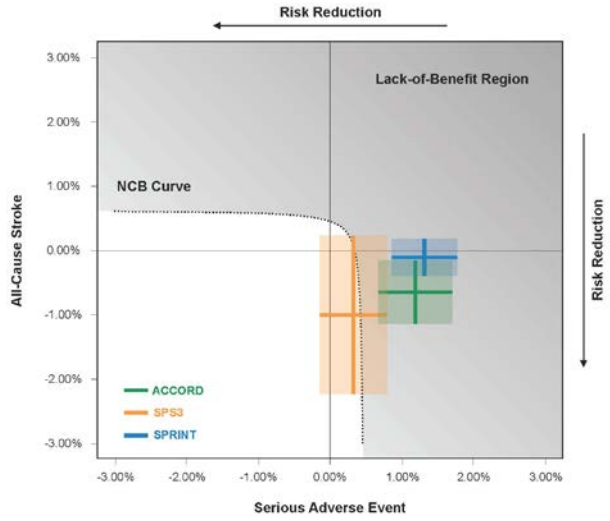

Figure 2. Forest plot of bivariate risk difference in stroke and SAE

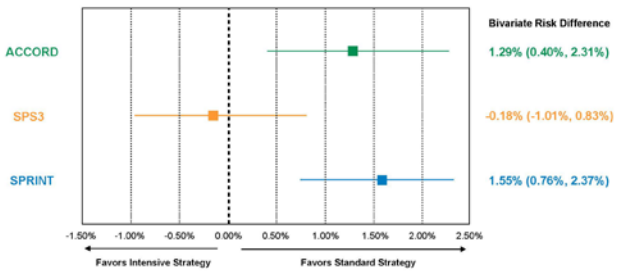

Disclosures: **J. Marszalek:** None. **S. Mehrsefat:** None. **G. Chi:** None.

504

Regional Variations of Ischemic Stroke in The United States

Prateeth Pati, Adnan Khalif, Balaji Shanmugam, UPMC Mercy, Pittsburgh, PA

Geographic Distribution of Acute Ischemic Stroke admissions in the United States
Background:The geographic distribution of acute ischemic stroke in the United States has not been evaluated, unlike the association shown with acute MI by Patel et al., (International Journal of Cardiology, 2014, 172.3). Our study looked at the geographic distribution and seasonal variation of acute ischemic stroke using the National Inpatient Sample (NIS) from 2011 - 2013.
Methods:Adult admissions with a primary diagnosis of acute ischemic stroke were extracted from the NIS database using the ICD 9 code 434.91 from 2011 - 2013. Admission information included hospital region (West, South, Mid-Atlantic and Northwest) and seasonal admission rates (Winter=December-February, Spring=March-May, Summer=June-August, Fall=September-November). A Chi square analysis was used to analyze differences in categorical variables (we assumed a normal distribution of 25% per region).
Results:A total of 120714 admissions were identified (weighted = 603361). There were more cases of acute ischemic stroke in the South (41.52 percent of admissions) compared to the mid Atlantic (21.4), Northwest (17.98) or West (19.08) with a p value < 0.0001. Each year between 2011 to 2013 showed a higher rate of admissions for acute ischemic stroke in the South. Taking the years into summation showed no statistically significant difference in seasonal variation in any of the regions.div>Conclusion:Our study shows a higher number of admissions for acute ischemic stroke in the South, but failed to show any seasonal differences. However, there are several studies that suggest a preponderance of admissions for acute myocardial infarction during the winter season, Spencer et al., (Journal of the American College of Cardiology, 1998, 31.2.) Further studies are needed to identify why there is a significant regional difference in the admission rates for acute ischemic stroke.

Disclosures: **P. Pati:** None. **A. Khalif:** None. **B. Shanmugam:** None.

505

Incidence of Major Bleeding in a Real-World Population of 57,070 Nonvalvular Atrial Fibrillation Patients Treated with Rivaroxaban

Frank Peacock, Baylor Coll of Med, Houston, TX; Manesh Patel, Duke Univ Health System and Duke Clinical Res Inst, Durham, NC; **Zhong Yuan**, Janssen Res and Development, Titusville, NJ; Nicholas Sicignano, Kathleen Hopf, Health ResTx LLC, Trevose, PA; Sally Tamayo, Naval Medical Ctr Portsmouth, Portsmouth, VA

Introduction: Rivaroxaban, a direct factor Xa inhibitor approved in 2011, reduces the risk of stroke and systemic embolism in patients with nonvalvular atrial fibrillation (NVAF). Phase 3 results from the registration trial showed a major bleeding (MB) rate of 3.6 per 100 person-years. **Objective:** To evaluate MB incidence among NVAF patients taking rivaroxaban in a post-approval clinical setting. **Methods:** From January 1, 2013 to June 30, 2016, over 10 million electronic medical records from the Department of Defense Military Health System were queried. A validated MB case-finding algorithm (Cunningham) was used to identify MB-related hospitalizations. Major bleeding incidence, patient characteristics, comorbid conditions, concomitant medications, bleeding management, and fatal bleeds were assessed. **Results:** Of 57,070 rivaroxaban users with NVAF, 1,914 experienced a MB event, with incidence of 2.60 (95% CI 2.49-2.72) per 100 person-years. Patient characteristics and subgroup bleeding rates are displayed in Table 1. There were 62 patients who experienced fatal bleeding, and the mean (SD) age at time of death was 79.3 (7.6) years. Among those who died, 74.2% had intracranial hemorrhage, 22.6% had gastrointestinal hemorrhage, and 3.2% had bleeding in other sites. **Conclusion:** The incidence, pattern, and management of MB in rivaroxaban users with NVAF in a large and diverse population were generally consistent with the findings from the registration trial. Fatal bleeding was rare.

Table 1.

		MB Cases N=1,914	Patients without MB N=55,156
Mean Age (SD), years		78.7 (8.2)	76.7 (10.3)
Male, *n* (%)		995 (52.0)	31,053 (56.3)
MB Incidence Rate [a] per 100 person-years (95% CI)		2.60 (2.49-2.72)	
MB Incidence Rate by Bleed Site per 100 person-years (95% CI)	Intracranial	0.23 (0.19-0.26)	
	Gastrointestinal	2.22 (2.11-2.33)	
	Other/Unspecified	0.16 (0.14-0.19)	
Fatal [b] MB Incidence Rate per 100 person-years (95% CI)		0.08 (0.07-0.11)	
Transferred to ICU, *n* (%)		825 (43.1)	
Blood Transfusion Received, *n* (%)		900 (47.0)	
Presence of Comorbidities, *n* (%)	Hypertension	1,661 (86.8)	34,914 (63.3)
	Coronary Heart Disease	951 (49.7)	15,609 (28.3)
	Diabetes	710 (37.1)	13,899 (25.2)
	Heart Failure	702 (36.7)	10,314 (18.7)
	Renal Disease	488 (25.5)	8,549 (15.5)
	Prior Ischemic Stroke	149 (7.8)	2,261 (4.1)
Mean (SD) CHA_2DS_2-VASc score		4.5 (1.5)	3.4 (1.6)
Mean (SD) HAS-BLED Score [c]		2.9 (1.1)	2.0 (1.1)
Concomitant Medications [d] *n* (%)	Statins	1,135 (59.3)	34,693 (62.9)
	Proton Pump Inhibitors	800 (41.8)	25,151 (45.6)
	SSRIs	291 (15.2)	9,873 (17.9)

MB=Major Bleeding; SD=Standard Deviation; CI=Confidence Interval; CHA_2DS_2-VASc= Congestive heart failure, hypertension, age >75 years, diabetes mellitus, prior stroke or TIA or systemic embolism, vascular disease, age 65-75 years, sex-female; Scores range from 0-9. [a] MB incidence rate was calculated for all first major bleeds. [b] During patient's hospitalization for the MB event. [c] INR values were not available, the variable for labile INRs was dropped from the algorithm resulting in a maximum possible modified HAS-BLED score of 8 rather than 9 [d] The 3 most frequently prescribed medications among MB patients

Disclosures: **F. Peacock:** Research Grant; Modest; Abbott, Alere, Banyan, Cardiorentis, Janssen, Portola, Pfizer, Roche, The Medicine's Company, ZS Pharma. Ownership Interest; Modest; Comprehensive Research Associates LLC, Emergencies in Medicine LLC. Consultant/Advisory Board; Modest; Alere, Cardiorentis, Ischemia Care, Janssen, Phillips, Portola, Prevencio, The Medicine's Company, ZS Pharma. **M. Patel:** Research Grant; Modest; Heart Flow Technologies, Janssen, Johnson & Johnson, AstraZeneca, National Heart Lung and Blood Institute, Agency for Healthcare Research and Quality. Consultant/Advisory Board; Modest; AstraZeneca, Bayer, Otsuka. **Z. Yuan:** Employment; Significant; Janssen Research and Development. Ownership Interest; Modest; Johnson & Johnson. **N. Sicignano:** Employment; Significant; Employee of Health ResearchTx LLC, which has a business agreement with Janssen. **K. Hopf:** Employment; Significant; Independent contractor for Health ResearchTx LLC, which has a business agreement with Janssen.. **S. Tamayo:** None.

506

Intramural Structural Changes in Human Femoropopliteal Arteries With Age

William Poulson, Alexis Rogers, Rishi Batra, Paul Deegan, Alexey Kamenskiy, Jason MacTaggart, Univ of Nebraska Medical Ctr, Omaha, NE

Introduction:
Femoropopliteal artery (FPA) disease is common and therapeutic interventions and reconstructions leave significant room for improvement. Models of arterial growth and remodeling can help better understand the pathophysiology of FPA disease, but they require detailed data on arterial structural composition to produce accurate predictions. The goal of this work was to quantify intramural collagen and elastin in human FPAs and determine how these constituents change with age.
Methods:
FPAs were obtained from 32 tissue donors without hallmarks of peripheral artery disease (average age 50±18 years, age range 15-72 years). Longitudinal pre-stretch, wall thickness and lumen diameter were used to calculate *in situ* volume of tissue in a 1cm-long arterial segment. Arteries were fixed in formalin and sectioned in both transverse and longitudinal directions. Elastin and collagen contents were quantified with image analysis using Verhoeff-Van Gieson and Masson's Trichrome stained slides scanned at 10x.
Results:

Ageing was associated with an increase in *in situ* tissue volume of 31mm^3 per decade of life, and increases in the overall wall and tunica media thicknesses of 94μm and 19μm per decade of life respectively (p=0.01). Volume fraction of elastin did not change with age (p=0.49) and remained at 4.8±1.6%, although elastic fibers did become more fragmented (p<0.01). Amorphous medial collagen increased with age from occupying 35±11% of the media at ages younger than 30 years, to 54±9% of the media at ages older than 60 years. This translated into an increase of 4.1% in medial collagen per decade of life (p<0.01). Volume fraction of fibrillar adventitial collagen did not change with age (p=0.09) and remained at 34±7%.

Conclusions:

In human FPAs, arterial walls thicken and collagen content increases with age. Though total elastin content remains stable, elastic fiber architecture deteriorates with aging. Quantification of intramural structural changes in human FPAs across age groups can be instrumental for developing models of arterial growth and remodeling that can help better understand the pathophysiology of peripheral artery disease.

Disclosures: **W. Poulson:** None. **A. Rogers:** None. **R. Batra:** None. **P. Deegan:** None. **A. Kamenskiy:** None. **J. MacTaggart:** None.

507

Glutamic Acid May Not Contribute to the Mechanism in Which Saccharina Japonica Attenuates Hypertension in 2-Kidney, 1-Clip Renovascular Hypertensive Rats

Yukiko Segawa, Kobe Womens Univ, Kobe, Japan; Hiroko Hashimoto, Osaka Seikei Junior Coll, HigashiYodogawa, Japan; Saki Maruyama, Tomoko Osera, Nobutaka Kurihara, Kobe Womens Univ, Kobe, Japan

Objective: Saccharina japonica (SJ), one of brown algae, is cultivated or grows wild in Japan and neighbor countries. The extract “dashi” is used for soup stock in Japan. We reported the decreases in blood pressure (BP) both by the intake of SJ diet and by dashi extracted from SJ (DASHI) in 2-kidney, 1-clip renovascular hypertensive (2K1C) rats. Some researchers have suggested that alginic acid (AA) may be involved in the mechanism of the SJ effect. However, DASHI contains AA as much as 5%(5 of 100) of what the original SJ contains. Thus, the antihypertensive effects by SJ in 2K1C may be through the other contents of SJ. SJ is rich in Glutamic acid (GA) which is one of the umami, the intake of which was reported to decrease BP in human in epidemiologic studies. GA is eluted from the SJ into the DASHI when extracting DASHI from SJ. Therefore, we hypothesized that GA in DASHI contributes to the mechanism of BP decreased by DASHI diet in 2K1C rats. In this study, we observed BP in 2K1C rats fed a diet containing GA as much as that in the SJ diet which had decreased BP in the previous study. Methods: Male Sprague-Dawley rats (6wks) were treated with sham operation (SHAM) or clipping the left renal artery (2K1C). After surgery, the rats started receiving a control diet (C) or a diet containing L-GA (G) for 6 weeks. The systolic BP (SBP) was measured by a tail-cuff method every week. At the end, mean arterial BP (MAP) was measured in each rat under anesthesia. Result: Six weeks after the surgery, SBP was significantly higher in 2K1C-C than in SHAM-C (163±2 vs 111±5 mmHg, p<0.05). In 2K1C-G (171±7), it showed no significant difference compared with 2K1C-C and was significantly higher than that in SHAM-C (p<0.05). At the end of the protocol, MAP showed the similar results to SBP. Conclusion: Glutamic acid may not contribute to the mechanism of alleviating hypertension by dietary SJ and SJ extract in 2K1C.

Disclosures: **Y. Segawa:** Research Grant; Modest; Society for Research on Umami Taste(2016-2017). **H. Hashimoto:** None. **S. Maruyama:** None. **T. Osera:** None. **N. Kurihara:** Research Grant; Modest; YUKIYOSHI INSTITUTE(2016).

508

Peripheral Artery Disease is Associated With Frailty in Patients With Chorionic Hemodialysis

Hidemi Takeuchi, Michihiro Okuyama, Haruhito A. Uchida, Nozomu Otaka, Yuki Kakio, Yuka Okuyama, Ryoko Umebayashi, Hitoshi Sugiyama, Jun Wada, Okayama Univ Graduate Sch of Med, Dentistry and Pharmaceutical Sciences, Okayama, Japan

Objective: The clinical condition of frailty is a common problem in the elderly population. Chronic hemodialysis (HD) patients often have peripheral artery disease (PAD) as a vascular complication.

However, the relationship between PAD and frailty in Japanese HD patients remains unknown. The aim of this study was to identify the relationships among PAD and risk factors in Japanese chronic HD patients. **Method:** This study was a multi-center, cross-sectional and observational investigation which was conducted at 6 institutions, including 5 general hospitals and 1 private clinic. Subjects were all chronic HD patients who regularly visited the institutions. To evaluate frailty, we used the modified Fried's frailty phenotype adjusted for Japanese as the self-reported questionnaire, and measured each physical domain. Furthermore, we calculated ankle-brachial index (ABI) to define PAD. PAD was defined as ABI < 0.9 in our study. **Result:** Of the 542 patients in all institutions, 362 were enrolled in this study. Sixty-two patients (17.1%) were categorized as PAD group and 300 patients (82.9%) as non-PAD group. In the PAD group, the prevalence of frailty was significantly higher than in the non-PAD group (34% vs 18%). Non-shunt side grip strength was significantly stronger in the non-PAD group (23.6 kg vs 17.0 kg, $P<0.0001$). Thigh circumferences (the mean of both sides) were also significantly larger in the non-PAD group (41.7 cm vs 39.7 cm, $P=0.0054$). Univariate regression analyses showed that frailty, age, number of oral medicine, and history of myocardial infarction (MI) had significant correlations with PAD. Multivariate logistic regression analysis demonstrated that the factors independently associated with PAD were as follows: frailty (OR = 2.061, 95% C.I. 1.091-3.894) and MI (OR = 3.742, 95% C.I. 2.051-6.831). **Conclusion:** PAD is associated with frailty in HD patients.

Disclosures: **H. Takeuchi:** None. **M. Okuyama:** None. **H.A. Uchida:** None. **N. Otaka:** None. **Y. Kakio:** None. **Y. Okuyama:** None. **R. Umebayashi:** None. **H. Sugiyama:** None. **J. Wada:** None.

509

Comparison of Drug Elluting Stent and Per Cutenaeous Transluminal Angioplasty in Patients With Infra-Popliteal Peripheral Arterial Disease

Rahul Vasudev, MeetKumar Sheth, Priyank Shah, St Joseph's Regional Medical center, Paterson, NJ; Upamanyu Rampal, St Joseph's Regional Medical center, Cedar Grove, NJ; Hiten Patel, St Joseph's Regional Medical center, Clifton, NJ; Fayez Shamoon, Mahesh Bikkina, Hartaj Virk, St Joseph's Regional Medical center, Paterson, NJ

Introduction: Drug-eluting Stent(DESs) have demonstrated improved patency and freedom from target lesion revascularization compared with Bare-Metal stents or Percutaneous Transluminal Angioplasty(PTA); however, the effect on clinical outcome parameters, such as limb salvage and wound healing, remains unidentified. We present a direct comparison of clinical outcomes in patients who underwent DES vs PTA.
Methods: We collected data of patients who underwent infra-popliteal arterial interventions at our institution. Clinical end points analyzed were all cause mortality, target vessel revascularization, primary vessel patency, and target limb major and minor amputations. Differences between two groups were analyzed by chi square for categorical variables and t test for continuous variables. Statistical significance was considered for P values less than .05 in a 2-sided test.
Results: Total of 83 cases, n=42 in DES group and n=41 in PTA group were analyzed. Mean age was 71.6 years (range 49-95). Out of the total 83 patients in the study 45 had a history of diabetes (54%) and 51 (61%) were current /past smokers. Average follow up period of 14 months for both the groups. Primary vessel patency was defined as absence of ≥50% restenosis on follow up. During the follow up period vessel patency in DES group [69% (n=29/42)] was significantly higher as compared to 36% (15/41) in PTA group (P=0.04, odds ratio 3.867, 95% Confidence interval: 1.5 - 9.6). Target vessel revascularization in DES group was 24% (10/42) as compared to 32% (13/28) in PTA group (P=0.47, odds ratio 0.67, 95% confidence interval: 0.26 - 1.77). Target limb amputation was 10% (4/42) in DES group as compared to 24% (10/41) in PTA group (P = 0.085), odds ratio 0.33, 95% confidence interval: 0.09 - 1.14). All cause mortality in both the groups were at 10%, 4/42 in DES group and 4/41 in PTA group (P=1, odds ratio 0.97, 95% confidence interval: 0.23 - 4.19).
Conclusion: To conclude primary vessel patency was superior in DES group as compared to PTA group. Target limb amputation rates were higher in PTA group but not statistically significant. Target vessel revascularization and all cause mortality were similar in both the groups. Thus primary treatment with DES should be considered in patients with infra-popliteal PAD.

Disclosures: **R. Vasudev:** None. **M. Sheth:** None. **P. Shah:** None. **U. Rampal:** None. **H. Patel:** None. **F. Shamoon:** None. **M. Bikkina:** None. **H. Virk:** None.

511

High Signal Intensity on Diffusion Weighted Magnetic Resonance Imaging Reflects Acuity of Deep Vein Thrombus

Toshihiro Gi, Atsushi Yamashita, Faculty of Med, Univ of Miyazaki, Miyazaki, Japan; Yasuyoshi Kuroiwa, Koga General Hosp, Miyazaki, Japan; Yuko Konishi, Taketoshi Asanuma, Faculty of Veterinary Med, Univ of Miyazaki, Miyazaki, Japan; Takuroh Imamura, Koga General Hosp, Miyazaki, Japan; Yujiro Asada, Faculty of Med, Univ of Miyazaki, Miyazaki, Japan

Objective: Acuity of deep vein thrombus/ thrombosis (DVT) may affect effectiveness of anti-thrombotic therapy. However, the acuity of DVT is not reliably detected by current noninvasive imaging techniques. This study investigated whether diffusion weighted magnetic resonance (MR) imaging can detect DVT and define the acuity of thrombus in patients with DVT and a rabbit model of venous thrombus.
Methods: Diffusion weighted MR imaging was performed with a 1.5-T MR system in 8 patients with DVT. Venous thrombus was induced in rabbit jugular vein by endothelial denudation and 10 minutes blood stasis with a balloon catheter. The thrombus was imaged with a 3.0-T MR system at 4 hours and at 1, 2 and 3 weeks, and the jugular veins were histologically assessed.
Results: All patients were detected DVT with diffusion weighted MR imaging, and the DVT showed high or mixed high and iso signal intensity on the diffusion sequence. The rabbit venous thrombi were rich in erythrocyte and fibrin at 4 hours, and showed focal organizing reaction at 1 and 2 weeks, and was replaced by fibrous tissue at 3 weeks. The rabbit thrombi showed high signal intensity on diffusion weighted MR imaging at 4 hours, mixed high and iso signal intensity at 1 and 2 weeks, or mixed iso and low signal intensity at 3 weeks. The signal intensity was positively correlated with erythrocyte and fibrin contents, and negatively correlated with macrophage and collagen contents.
Conclusions: Diffusion weighted MR imaging can detect DVT and high signal intensity on the sequence may reflect acuity of DVT.

Disclosures: **T. Gi:** None. **A. Yamashita:** None. **Y. Kuroiwa:** None. **Y. Konishi:** None. **T. Asanuma:** None. **T. Imamura:** None. **Y. Asada:** None.

512

Predictors of Mortality in Cancer-Associated Calf Deep Vein Thrombosis

Juan P Salazar Adum, Univ de Cuenca, Cuenca, Ecuador; Luis Diaz-Quintero, NorthShore Univ HealthSystem, Evanston, IL; Harry E Fuentes, John H. Stroger Jr. Hosp of Cook County, Chicago, IL; Alfonso Tafur, Benjamin Lind, Joseph Caprini, NorthShore Univ HealthSystem, Evanston, IL

Background: Venous thromboembolism (VTE) is a leading cause of mortality in cancer patients. The outcomes of patients with cancer-associated calf deep vein thrombosis (CDVT), including mortality data, are less understood compared with proximal thrombosis.
Aim: To characterize predictors of mortality among cancer-associated CDVT patients.
Methods: Single institution inception cohort of cancer-associated CDVT patients who presented with thrombosis distal to popliteal level confirmed objectively by ultrasound, computed tomography or VQ scan were independently reviewed. Active cancer was defined as metastatic disease or use of chemotherapy at diagnosis. The Khorana risk score (KRS) suggested for DVT and mortality prediction in cancer was abstracted based on laboratory tests and cancer type at diagnosis. Institutional review board approval was obtained prior to the analysis. Categorical variables are expressed as percentages and continuous variables as median (interquartile range). SPSS software version 22 was used and Chi-square, Mann–Whitney U and Cox proportional hazard were applied.
Results: One hundred nine patients (Men=44 (40%), Age>65=89 (82%), BMI>30=25 (23%), Smoker=59 (54%)) were included. The majority had a low or intermediate KRS (30%-64% respectively). Forty-seven percent died during a median follow-up time of 2.5 years (0.5-3.1). After multivariate analysis, the predictors of mortality were found to be: smoking (Hazard Ratio 2.3; 95%CI 1.2-4.7), metastasis (HR 5.8; 95%CI 2.9-11.7), gastrointestinal cancer (HR 3.9; 95%CI 1.8-8.5), and lung cancer (HR 4.1 95%CI 1.7-10.3). VTE specific variables not associated with mortality included: bilateral CDVT, concomitant pulmonary embolism, multiple vein involvement, filter placement, or a surgery-associated event.
Conclusion: Cancer-specific variables and smoking predicted mortality among CDVT patients in this cohort. Neither the KRS nor VTE specific characteristics were predictive of death. A larger study is necessary to further explore these findings.

Disclosures: **J.P. Salazar Adum:** None. **L. Diaz-Quintero:** None. **H.E. Fuentes:** None. **A. Tafur:** None. **B. Lind:** None. **J. Caprini:** None.

514

Sex-Related Disparities in Outcomes After Myocardial Infarction Among Patients With Atrial Fibrillation: Evidence From a Nationwide Study

Akintunde M Akinjero, Icahn Sch of Med at Mount Sinai, New York, NY; Oluwole Adegbala, Seton Hall Univ Sch of Health and Medical Sciences at Englewood Hosp and Medical Ctr, Englewood, NJ; Tomi Akinyemiju, Univ of Alabama at Birmingham, Birmingham, AL

Background: The overall mortality rate after acute myocardial infarction (AMI) is falling in the United States. However, outcomes remain unacceptably worse in females compared to males. It is not known how coexisting atrial fibrillation (AF) modify outcomes among the sexes. We sought to examine the association of sex with clinical characteristics and outcomes after AMI among patients with AF.
Methods: We accessed the Healthcare Cost and Utilization Project (HCUP) Nationwide Inpatient Sample (NIS), to extract all hospitalizations between 2007 and 2011 for patients above 18yrs with principal diagnosis of AMI and coexisting diagnosis of AF using ICD 9-CM codes. The NIS represents the largest all-payer hospitalization database in the United States, sampling approximately 8 million hospitalizations per year. We also extracted outcomes data (length of stay (LOS), stroke and in-hospital mortality) after AMI among Patients with AF. We then compared sex differences. Univariate and Multivariate analysis were conducted to determine the presence of statistically significant difference in outcomes between men and women.
Results: A total of 184,584 AF patients with AMI were sampled, consisting of 46.82% (86,420) women and 53.13% (98,164) men. Compared with men, women with AF and AMI had a greater multivariate-adjusted risk for increased stroke rate (aOR=1.51, 95% CI=1.45-1.59), and higher in-hospital mortality (aOR=1.12, 95% CI=1.09-1.15). However, female gender was not significantly associated with longer LOS (aOR=-0.22, 95% CI= -0.29-(-0.14).
Conclusion: In this large nationwide study of a population-based cohort, women experienced worse outcomes after AMI among patients with AF. They had higher in-hospital mortality and increased stroke rates. Our findings highlight the need for targeted interventions to improve these disparities in outcomes.

Table 1. Multivariate Adjusted Odds Ratios For the influence of Female gender on the In-Hospital Outcomes Among Patients Hospitalized for MI and Afib.

Outcomes	Model [a] COR/β (95% CI)	Model [b] AOR/β (95% CI)
Stroke	**1.53 (1.46 – 1.61)**	**1.51 (1.45 – 1.59)**
LOS	**- 0.25 (-0.32 - (–0.17))**	**-0.22 (-0.29 – (-0.14))**
In-Hospital Mortality	**1.12 (1.09 – 1.15)**	**1.12 (1.09 – 1.15)**

[a] Unadjusted Model; COR = Crude Odds Ratios
[b] Adjusted for race, sex, age, insurance type, median household income national quartile for patient ZIP Code, and Comorbidities using Modified Deyo Comorbidity index
β = as regression coefficient indicating number of days
Bold indicates significance p value ≤ 0.05.

Disclosures: **A.M. Akinjero:** None. **O. Adegbala:** None. **T. Akinyemiju:** None.

516

Chromosome 18p Deletion Inhibits Platelet Aggregation

Andrew D Meyer, Anjana Raghunath, Patricia Heard, Jannine Cody, Univ of Texas Health, San Antonio, TX

Inappropriate platelet function is a significant risk factor for cardiovascular disease, the leading cause of death in the United States. Although abnormal platelet function has a strong genetic component, very few human genes have been linked to platelet function. Mice with a homozygous deletion of *EMILIN2* (Elastin Microfibril Interface Located Protein2) gene, located on Chromosome 18p, have a significant decrease in platelet function and clot formation. However, deletion or inactivation of only one copy of a gene is most relevant to human disease modeling. Our hypothesis is that blood samples from people with single 18p deletions that include *EMILIN2* will have decreased platelet function compared to healthy individuals. We conducted a case-control study of nine adult individuals with chromosome 18p deletions matched with healthy men and women (n=20). Routine coagulation measurements were performed on a STAGO STA-R instrument. Platelet aggregation was measured with whole blood impedance aggregometry and

Thromboelastography with PlateletMapping using the manufacturers' protocols. There was no significant difference in platelet count, prothrombin time, partial thromboplastin time, d-dimer, or fibrinogen between individuals with a single 18p gene copy number and normal controls. However, platelet aggregation was impaired in individuals with 18p deletions compared to normal controls in response to collagen and arachidonic acid (ASPI), respectively (p<0.0001, Figure 1). Moreover, Thromboelastography with PlateletMapping was decreased in individuals with 18p deletions compared to normal controls for ADP and ASPI, (p<0.001). Individuals with one copy of 18p have decrease platelet function compared to normal controls. These results identify a novel human genetic loci linked to a specific phenotype of platelet function. Future will studies will determine if this gene can be used for diagnostic or therapeutics for cardiovascular disease.

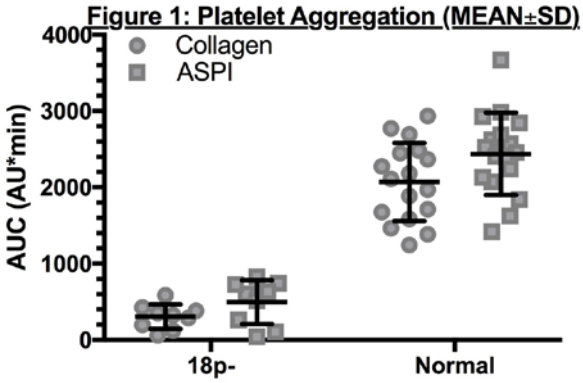

Disclosures: **A.D. Meyer:** Research Grant; Significant; NCATS/CTSA Pilot Project. **A. Raghunath:** None. **P. Heard:** None. **J. Cody:** Research Grant; Modest; NCATS/CTSA Pilot Project.

517

Differential Redox Profiles Due to Endothelial Heterogeneity During Oxidative Stress

Bandana Shrestha, Christopher B. Pattillo, Louisiana Health Science Ctr -Shreveport, Shreveport, LA

Atherosclerosis, a chronic inflammatory disease characterized by plaque formation in vascular walls results in perfusion complications culminating in ischemia and induced angiogenesis. Interestingly, atherosclerosis is known largely to be an arterial disease with a preference in vascular beds, often affecting more arteries than veins. A significantly different pattern exists between the endothelial cells of these major blood vessels, highlighting the possibility of intrinsic differences between arterial and venous micro-environments including vascular endothelial cells themselves leading to variable responses during pathogenesis. Although isolated primary cells have been shown to lose some in-vivo characteristics under cell culture conditions, our data proves that these heterogeneous cell types retain the ability to differentially sense redox states. Oxidative stress is one of the key players associated with progression of atherosclerosis, marked by over-production of reactive oxygen species (ROS) and reduction in endogenous antioxidants such as glutathione (GSH). GSH, a major free radical scavenger prevents ROS damage by reducing ROS while being oxidized into glutathione disulfide (GSSG). GSSG is then recycled back to its reduced form under normal physiological conditions, hence maintaining an optimum GSH:GSSG ratio. This ratio is known to be deregulated during redox imbalance seen with oxidative stress during disease, due to decreasing GSH and increasing GSSG levels. Our experiments using Mouse Aorta Endothelial Cells (MAECs) and mouse Vena Cava Endothelial cells (VCECs) to represent arterial and venous endothelial cells display differences in this GSH:GSSG ratio as well, implicating differential redox states within these vessel types. Additionally, differences in oxidative stress related responses with regards to cell proliferation, migration, adhesion molecule expression and leukocyte recruitment in endothelial cells of arteries and veins further highlight the possibility of drastically different predispositions to atherosclerosis. Thus, endothelial cell heterogeneity between arteries and veins may lead to differential redox profiles and altered physiological functions during oxidative stress.

Disclosures: **B. Shrestha:** None. **C.B. Pattillo:** None.

This research has received full or partial funding support from the American Heart Association.

518

Coronary Thrombus Leukocytes of Acute Coronary Syndrome Patients Trans-Differentiate Into Endothelial Cell-Like Angiogenic Cells

Hangfei Fu, Nish Vadalia, Eric R Xue, Candice Johnson, Jun Yu, Xiaofeng Yang, Hong Wang, Temple Univ Lewis Katz Sch of Med, Philadelphia, PA

Current angiogenic therapies for cancers and cardiovascular diseases have not yet achieved expected benefits, which reflects the need for improved understanding of angiogenesis. In this study, we focused on solving the problem of whether tissues have different angiogenic potentials (APs) in physiological conditions; and how angiogenesis is regulated in various disease conditions. In healthy and diseased human and mouse tissues, we profiled the expression of 163 angiogenic genes, including transcription regulators (TRs), growth factors and receptors (GF/Rs), cytokines and chemokines (C/Cs), and proteases and inhibitors (P/Is). TRs were categorized as inflammatory, homeostatic, and endothelial cell-specific TRs, and C/Cs were categorized as pro-angiogenic, anti-angiogenic, and bi-functional C/Cs. We made the following findings: *1)* human heart, muscle, eye, pancreas, and lymph node are among the tissues with the highest APs; *2)* tissues with high APs have more active angiogenic pathways and angiogenic C/C responses; 3*)* inflammatory TRs dominate regulation of all angiogenic C/Cs; homeostatic TRs regulate all to a lower extent, while endothelial cell-specific TRs mainly regulate pro-angiogenic and bi-functional C/Cs; *4)* tissue AP is positively correlated with the expression of oxygen sensors PHD2 and HIF1B, VEGF pathway gene VEGFB, and stem cell gene SOX2; *5)* cancers of the digestive system tend to have increased angiogenesis dominated by endothelial cell-specific pro-angiogenic pathways, while lung cancer and prostate cancer have significantly decreased angiogenesis; *6)* endothelial cell-specific pro-angiogenic pathways are significantly increased in thrombus-derived leukocytes in patients with acute coronary artery disease. Our results demonstrate that thrombus-derived leukocytes are partially “hijacked” to become endothelial cell-like angiogenic cells that directly promote angiogenesis after myocardial infarction; and that certain solid tumors may be more sensitive to anti-angiogenic therapies than others.

Disclosures: **H. Fu:** None. **N. Vadalia:** None. **E.R. Xue:** None. **C. Johnson:** None. **J. Yu:** None. **X. Yang:** None. **H. Wang:** None.

519

Inhibition of von Willebrand Factor Activity Does Not Delay Cutaneous Wound Healing

Kristen Gorman, Laura Sommerville, George Pitoc, Duke Univ, Durham, NC; Dougald M Monroe III, Univ of North Carolina, Chapel Hill, NC; **Maureane Hoffman**, Duke Univ, Durham, NC

Introduction: Physiologically, von Willebrand Factor (VWF) recruits platelets to sites of injury by binding to exposed collagen and platelet GPIbα, particularly at sites of high shear. VWF is critical to hemostasis, since complete deficiency leads to bleeding as severe as hemophilia. Conversely, VWF plays a key role in arterial thrombosis, as in myocardial infarction and stroke. Despite being an attractive therapeutic target, no agents directed against VWF are currently available. Our group is testing an RNA aptamer that blocks VWF binding to GPIbα as an antithrombotic. We have previously shown that leukocyte influx and cutaneous healing are impaired in a mouse model of hemophilia. We have also found that wound healing is delayed in mice given target specific oral anticoagulants. The purpose of the current study was to determine whether inhibiting VWF would similarly impair wound healing. Methods: We used C57BL/6J mice administered vehicle or VWF aptamer. At the dose selected, aptamer prolonged the saphenous vein bleeding time for the expected 10 day healing period. Healing was assessed in a skin punch biopsy model. Wound size was measured daily, and following sacrifice the wound area harvested for histology. Inflammation (in the absence of tissue injury) was induced by topical application of cantharidin for 24 hours, followed by tissue harvesting. Results: The in vivo efficacy of the aptamer was verified, since bleeding remained prolonged to a level slightly less severe than hemophilia at the end of the experiment (10 days after wounding). There was no difference in time to healing between control and aptamer-treated mice, with all wounds healed at 10 days. There was also no statistically significant difference in wound size at any time. Cantharidin induced a similar level of cellular influx in treated and control mice. Aptamer-treated mice exhibited a slight amount of inflammation-induced hemorrhage, though not the gross hemorrhage observed in thrombocytopenic mice. Conclusion: Inhibition of VWF activity does not delay cutaneous wound closure, despite inducing a severe hemostatic defect. Compared to other

antithrombotic strategies, an aptamer against VWF could avert some undesirable side effects on host defense and tissue repair.

Disclosures: **K. Gorman:** None. **L. Sommerville:** None. **G. Pitoc:** None. **D.M. Monroe:** None. **M. Hoffman:** None.

520

Acoustic Tweezing Thromboelastometry

Daishen Luo, Damir Khismatullin, R. Glynn Holt, Tulane Univ, New Orleans, LA

Background: Critical care patients such as trauma and major surgery patients often develop coagulopathy due to depletion of both pro- and anti-coagulants. They are at high risk of both bleeding and thrombotic complications and require monitoring of their coagulation status. The contact of a blood sample with artificial surfaces and its exposure to clot activators, which happen in all commercially available coagulation analyzers, may lead to improper assessment of blood coagulation and thus errors in predicting bleeding/thrombosis risks.
Objective: Real-time assessment of whole blood or blood plasma coagulation by novel non-contact acoustic tweezing technology.
Method: 4-5 microliter drops of whole blood collected from healthy volunteers or commercial control plasma were levitated in air by acoustic radiation forces. Their coagulation kinetics including reaction time, fibrin network formation time (FNFT), clot formation time and maximum clot strength was assessed from mechanical (drop shape) and photo-optical (light intensity) data. FNFT was determined as a difference between mechanical and photo-optical reaction times.
Results: Whole blood samples were exposed to pro- or anti-coagulants during levitation in the acoustic tweezing device. Changes in the coagulation status between different experimental groups were detected within 10 minutes. Similarly, less than 7 minutes was required to detect significant changes in reaction time, clot formation time and maximum clot strength between low, normal, and high fibrinogen level control plasma samples. FNFT was shown to be significantly reduced in plasma samples with a higher level of Factor XIII.
Conclusions: The acoustic tweezing technology integrates photo-optical tests used in plasma coagulation assays with viscoelastic tests used in whole blood analysis. Its key disruptive features are the increased reliability and accuracy due to non-contact measurement, small sample volume requirement, relatively short procedure time (<10 minutes), and the ability to assess the level of Factor XIII function from FNFT measurements. Our technology addresses a current lack of reliable methods to measure blood coagulation in patients with coagulopathy.

Disclosures: **D. Luo:** Other Research Support; Significant; Altria fellowship. **D. Khismatullin:** None. **R. Holt:** None.

This research has received full or partial funding support from the American Heart Association.

521

A Pilot Study Comparing Anti-Inflammatory Effects of Tranexamic Acid and Epsilon Aminocaproic Acid in Pediatric Congenital Heart Surgery

Nirbhay Parashar, Tarek Nafee, Cheryl Lefaiver, Christine Steffensen, Vince Rizzo, Vibhash Kumar, Chawki ElZein, Andrew Van Bergen, Advocate Children's Hosp, Oak Lawn, IL

Background: Antifibrinolytic agents are frequently used during pediatric heart surgery with cardiopulmonary bypass (CPB) to reduce transfusions. There are no studies comparing anti-inflammatory effects of antifibrinolytic agents, tranexamic acid (TXA) and Epsilon Aminocaproic acid (EACA). We compared the two agents in pediatric patients undergoing redo sternotomy with CPB.**Aim:** To compare anti-inflammatory effects of tranexamic acid versus aminocaproic acid in pediatric patients undergoing redo sternotomy and cardiopulmonary bypass.
Methods: We conducted a randomized, double blind pilot study, comparing 10 subjects in each group receiving EACA and TXA. A cytokine panel was used to measure 13 inflammatory markers in pre, immediate post and 24 hours post-CPB period. Between group comparisons were tested with Mann-Whitney U tests and within group comparisons with Friedman tests.
Results: Sample characteristics were comparable in both groups. Post CPB, plasma levels of 7 markers

increased significantly ($p<0.05$) in both groups, including MCP-1; 3 increased significantly ($p<0.03$) in the EACA group alone, including GM-CSF; and 3 did not change over time (Table 1). No difference was found between groups for markers except for IL-10, which was significantly higher in EACA group post CPB. While absolute values of markers, chest tube output and volume of blood product needs were lower in TXA group, the differences were not statistically significant.
Conclusion: There was no significant difference in anti-inflammatory profiles between EACA and TXA in this pilot study. GM-CSF and MCP-1 were increased in our study post CBP which has not been described in previous studies.

		Time Period			
Marker	Group	pre CBP	immediate post CBP	24 hr post CBP	*p*
GM-CSF	TXA	3.6 (2.7-6.7)	5.8 (3.9-8.4)	5.1 (3.1-8.8)	0.07
	EACA	5.4 (2.1-11)	7.3 (5.3-13)	5.1 (1.6-9.5)	*≤ 0.001*
	p	0.52	0.26	0.94	
MCP-1	TXA	184.7 (133-228.6)	308.6 (256.4-507.9)	180 (92.3-235)	*0.007*
	EACA	224.6 (170.7-323.4)	251.9 (218.6-385.5)	180.2 (109.8-221.1)	*0.002*
	p	0.17	0.26	0.94	
IL-10	TXA	3 (2.3-6)	1047.6 (646.4-1996.8)	6.2 (4.5-33.3)	*≤ 0.001*
	EACA	3.2 (2.2-6.5)	2338.3 (1995.5-2839.3)	13.3 (5.5-27.2)	*≤ 0.001*
	p	1.00	*0.03*	0.70	

Table1 (values of markers in pg/ml)

Disclosures: **N. Parashar:** None. **T. Nafee:** None. **C. Lefaiver:** None. **C. Steffensen:** None. **V. Rizzo:** None. **V. Kumar:** None. **C. ElZein:** None. **A. Van Bergen:** None.

522

Activated FXI Regulates the Catalytic Activity of Adamts13 by Removing the CUB Domains

Cristina Puy, Kathleen S. Garland, Toshiaki Shirai, Stephanie E. Reitsma, Jevgenia Zilberman-Rudenko, András Gruber, Owen J.T. McCarty, Oregon Health & Science Univ, Portland, OR

Background: ADAMTS13 cleaves and inactivates von Willebrand factor (VWF), which binds collagen, facilitating platelet adhesion under vascular injury. But is still uncertain how ADAMTS13 activity is regulated. Thrombin and plasmin have been shown to cleave ADAMTS13. Based on the fact that elevated levels of FXI is an independent risk factor for deep vein thrombosis and ischemic stroke, we hypothesize that FXIa inactivates ADAMTS13 leading to platelet aggregation and thrombus formation. **Aim**: To determine the functional role of inactivation of ADAMTS13 by FXIa. **Methods and results:** Recombinant ADAMTS13 (250 nM) was incubated with FXIa (50 nM) for increasing times (0-3 hours) at 37^{o}C before being analyzed by western blot using an anti-ADAMTS13 antibody against the two CUB domains (C-terminal) or against the metalloproteinase (MET) domain (N-terminal). Our results show that FXIa caused the disappearance of the ADAMTS13 band (~200 kDa) and the appearance of a band at ~150 kDa when the samples were analyzed with the anti-MET antibody and a ~50 kDa band when the samples were analyzed with the anti-CUB antibody. The presence of aprotinin, which inhibits FXIa activity, blocked the degradation of ADAMTS13. Kallikrein or FXIIa were unable to cleave ADAMTS13. Using a cell surface immunoassay we observed that after incubation with FXIa, the detection of the CUB domain from ADAMTS13 was lost from endothelial cells surface. The incubation of ADAMTS13 with FXIa caused an increase in ADAMTS13 activity as measured by a fluorogenic substrate (FRETS). **Conclusion**: ADAMTS13 circulates in a closed conformation, which is maintained by a CUB-spacer domain binding interaction. ADAMTS13 becomes conformationally activated through interaction of its CUBs domains with VWF. Here we show that FXIa-mediated deletion of ADAMTS13-CUB domains enhances its capacity to cleave FRETS and blocks the interaction with VWF. Our results suggest that FXIa may limit ADAMTS13-mediated VWF inactivation.

Disclosures: **C. Puy:** None. **K.S. Garland:** None. **T. Shirai:** None. **S. Reitsma:** None. **J. Zilberman-Rudenko:** None. **A. Gruber:** None. **O.J. McCarty:** None.

This research has received full or partial funding support from the American Heart Association.

523

Ultrasound Assisted Thrombolysis Versus Catheter Directed Thrombolysis: A Meta-Analysis

Syed Imran M Zaidi, Abdul Ahad Khan, Hemang B Panchal, East Tennessee State Univ, Johnson City, TN; Zulfiqar Qutrio Baloch, Brandon Regional Hosp, Brandon, FL; Enambir Josan, Timir K Paul, East Tennessee State Univ, Johnson City, TN

Introduction: Deep venous thrombosis (DVT) and pulmonary embolism (PE) have many methods of treatment including anti-coagulation, thrombectomy and thrombolysis. Thrombolysis can be achieved via systemic or local thrombolytic agents, with standard local thrombolysis achieved via catheter insertion in proximity to the thrombus and delivery of thrombolytic agents. Ultrasound-assisted catheter thrombolysis (UAT) is a relatively newer form of thrombolysis which utilizes ultrasonic energy, along with local thrombolytics to help in thrombus breakdown. The objective of our meta-analysis is to compare UAT and catheter directed thrombolysis (CDT) for treatment of DVT and PE.
Methods: PubMed database was searched through January 2017. Three studies (n=156) comparing UAT (n=99) and CDT (n=57) for thrombolysis were included. End points were > 50% thrombus lysis, bleeding (moderate and severe), and mortality on short term follow up (<1 year). The relative risk (RR) or mean difference (MD) with 95% confidence interval (CI) was computed and p<0.05 was considered as a level of significance.
Results: Thrombolysis success rate was similar with UAT and CDT (RR 1.06, CI 0.89-1.27, p=0.49). Moderate and severe bleeding events were similar with both groups (RR 0.71, CI 0.27-1.87, p=0.49). Mortality on short term follow up was significantly lower in UAT as compared to CDT (RR 0.47, CI 0.23-0.95, p=0.04).
Conclusions: The results of our meta-analysis demonstrated no difference in thrombolysis success rate or bleeding events when using UAT Vs CDT, however short term mortality was significantly lower with UAT. Further controlled trials with larger sample sizes are required to assess the possible benefit of using ultrasonic energy for venous thrombolysis.

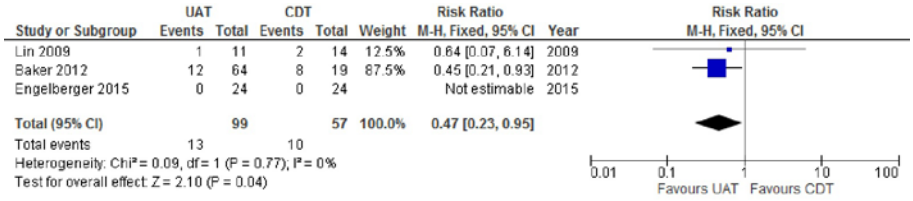

Disclosures: **S.M. Zaidi:** None. **A. Khan:** None. **H.B. Panchal:** None. **Z. Qutrio Baloch:** None. **E. Josan:** None. **T. K Paul:** None.

524

Identification of Roles for the Rho-Specific Guanine Nucleotide Dissociation Inhibitor (RhoGDI) Ly-Gdi in Platelet Function

Anh T Ngo, Marisa L Thierheimer, Özgün Babur, Anne D Rocheleau, Xiaolin Nan, Owen J McCarty, **Joseph Aslan**, Oregon Health & Science Univ, Portland, OR

Introduction: Upon activation, platelets undergo specific morphological alterations critical to hemostatic plug and thrombus formation via actin cytoskeletal reorganizations driven by the Rho GTPases Rac1, Cdc42 and RhoA. Here we investigate roles for Rho-specific guanine nucleotide dissociation inhibitor proteins (RhoGDIs) in regulating platelet function. **Methods and Hypothesis:** Through an approach combining pharmacology, cell biology and systems biology methods we assessed the hypothesis that RhoGDI proteins regulate Rho GTPase-driven platelet functions downstream of platelet integrin and glycoprotein receptors. **Results:** We find that platelets express two RhoGDI family members, RhoGDI and Ly-GDI. Antibody interference and platelet spreading experiments suggest a specific role for Ly-GDI in platelet function. Intracellular staining and super resolution microscopy assays find that Ly-GDI displays an asymmetric, polarized localization that largely overlaps with Rac1 and Cdc42 as well as microtubules and protein kinase C (PKC) in platelets adherent to fibrinogen. Signaling studies based on interactome and pathways analyses also support a regulatory role for Ly-GDI in platelets, as Ly-GDI is phosphorylated at PKC substrate motifs in a PKC-dependent manner in response to the platelet collagen receptor

glycoprotein (GP)VI-specific agonist collagen-related peptide. Notably, inhibition of PKC diffuses the polarized organization of Ly-GDI in spread platelets relative to its colocalization with Rac1 and Cdc42. **Conclusion:** In conclusion, our results support roles for Ly-GDI as a localized regulator of Rho GTPases in platelets and link PKC and Rho GTPase signaling systems to platelet function.

Disclosures: **A.T.P. Ngo:** None. **M.L.D. Thierheimer:** None. **Ö. Babur:** None. **A.D. Rocheleau:** None. **X. Nan:** None. **O.J.T. McCarty:** None. **J. Aslan:** None.

This research has received full or partial funding support from the American Heart Association.

525

Integration of Platelet Agonist Signaling During the Hemostatic Response in vivo

Jian Shen, Soochow Univ, Suzhou, China; Sara Sampietro, Jie Wu, Univ of Pennsylvania, Philadelphia, PA; Juan Tang, Shanghai Inst of Biomedical Sciences, Shanghai, China; Chelsea N. Matzko, Univ of Pennsylvania, Philadelphia, PA; Chaojun Tang, Soochow Univ, Suzhou, China; Ying Yu, Shanghai Inst of Biomedical Sciences, Shanghai, China; Lawrence F. Brass, Univ of Pennsylvania, Philadelphia, PA; Li Zhu, Soochow Univ, Suzhou, China; **Timothy J Stalker**, Univ of Pennsylvania, Philadelphia, PA

The local microenvironment within an evolving hemostatic plug shapes the distribution of soluble platelet agonists, resulting in a gradient of platelet activation emanating from the site of injury. While thrombin and ADP mediated platelet activation are clearly critical for establishment of this gradient, it remains unclear to what extent there is overlap of these and other platelet signaling pathways in time and space. In other words, does a single agonist dominate the platelet activation state within specific regions of a hemostatic plug, or do multiple agonist pathways need to be integrated to produce the gradient of platelet activation observed? Further, how do the relationships among different agonists change in the face of anti-platelet or anti-coagulant therapy and what are the consequences for hemostatic plug organization? Here, we used a combination of genetic and pharmacologic approaches coupled with real-time intravital imaging to examine how thrombin, thromboxane A_2, $P2Y_{12}$ and epinephrine signaling are coordinated in time and space to regulate the development of platelet activation gradients at a site of vascular injury in vivo. We found that both thromboxane A_2/TP signaling and ADP/$P2Y_{12}$ signaling are required for accumulation of minimally activated platelets in the outer shell region of hemostatic plugs. Interestingly, dual inhibition of both thromboxane and $P2Y_{12}$ signaling did not have an additive effect, but rather was similar to inhibition of either pathway alone. Epinephrine, which activates a Gi signaling pathway similar to ADP/$P2Y_{12}$, was completely dispensable for hemostatic plug formation, even in the absence of $P2Y_{12}$ signaling. Finally, inhibition of $P2Y_{12}$ in the setting of sub-maximal thrombin activity revealed no role for $P2Y_{12}$ signaling in the development of robust platelet activation within the hemostatic plug core region. Taken together, these data shed new light on the way multiple platelet signaling pathways are integrated during the hemostatic response in vivo, and predict the outcome of therapeutically targeting specific platelet signaling pathways alone and in combination on hemostatic plug organization.

Disclosures: **J. Shen:** None. **S. Sampietro:** None. **J. Wu:** None. **J. Tang:** None. **C.N. Matzko:** None. **C. Tang:** None. **Y. Yu:** None. **L.F. Brass:** Research Grant; Significant; The Medicines Company. **L. Zhu:** None. **T.J. Stalker:** Research Grant; Significant; The Medicines Company.

526

Thromboembolic Phenomenon in a Patient With Unexplained Transverse Aortic Thrombus

Hazem Alhawasli, Alan Brown, Lutheran General Hosp, Park Ridge, IL

A 55 year-old Caucasian male, with no known past medical history, presented to the ER complaining of left upper extremity pain with finger tingling and difficulty speaking that started 8 hours before presentation, while driving his car. In the ER, physical exam was remarkable for mild expressive aphasia with difficulty finding words. His left arm was tender without any edema or erythema and normal range of motion. His left hand fingertips appeared cyanotic (Picture 1), however his radial and ulnar pulses were intact bilaterally. Laboratory evaluation revealed a platelet count 1,416,000/mcl, and normal PT/INR and PTT. CT of the brain showed no intracranial bleed. MRI of the brain showed multiple small sub-acute infarcts in the left occipital lobe, left basal ganglia and bilateral cerebellar hemispheres suggesting a shower of emboli. Because of a concern for possible aortic dissection by the ER physician, a CT angiogram of the chest was done. It revealed a large filling defect (up to 3.1 cm) in the distal transverse

thoracic aorta, consistent with non-occlusive thrombus adjacent to the origin of the left subclavian artery (Picture 2). Subsequently, TEE was done and again showed a large mobile thrombus attached to the inferior posterior wall of the transverse thoracic aorta (Picture 3). Given the extremely mobile and large sized thrombus, with high risk for further embolization, the patient underwent surgery with excision of the aortic thrombus (Picture 4). The patient had an uncomplicated post-operative course and warfarin was started empirically post-operatively.
Further Hematology work up was suggestive of Essential Thrombocytosis. The patient was started on hydroxyurea.
On his 3-week follow up appointment, his platelet count decreased to 202,000/mcl. Anti-coagulation was continued for 3 months. His neurologic symptoms significantly improved with only mild residual left hand finger tips claudication which resolved by 1 month post discharge.

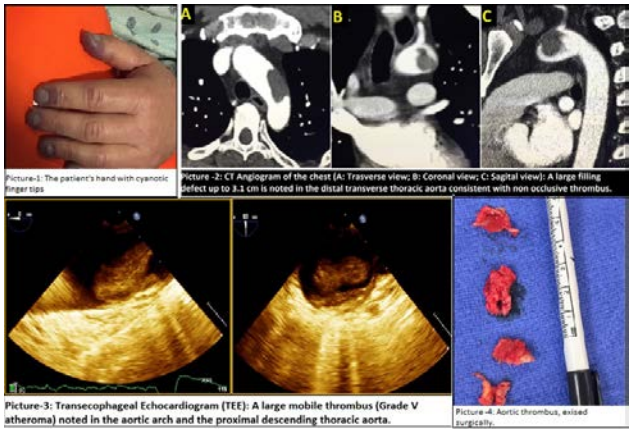

Picture-1: The patient's hand with cyanotic finger tips

Picture -2: CT Angiogram of the chest (A: Trasiverse view; B: Coronal view; C: Sagital view): A large filling defect up to 3.1 cm is noted in the distal transverse thoracic aorta consistent with non occlusive thrombus.

Picture-3: Transecophageal Echocardiogram (TEE): A large mobile thrombus (Grade V atheroma) noted in the aortic arch and the proximal descending thoracic aorta.

Picture-4: Aortic thrombus, exised surgically.

Disclosures: **H. Alhawasli:** None. **A. Brown:** None.

527

The Functional Significance of the Adenosine A_{2b} Receptor in the Internal Mammary Artery

Stephen R Archacki, Qing K Wang, CCF, Cleveland, OH

Objective— The endothelium is the initial target that leads to cardiovascular disease. Knowing that the internal mammary arteries (IMA) are resistant to the development of atherosclerosis, which contrasts with coronary arteries (Cor) which are athero-prone, we hypothesize that genes over-expressed in the endothelial cells (ECs) of between these two arteries will identify genes that resist atherosclerosis.
Methods and Results—Microarray analysis showed over 1,000 differentially expressed in the ECs of IMA vs Cor. The most statistically significant different gene was the adenosine A_{2B} receptor. This indicates the A_{2B} receptor may be involved in a resistance to atherosclerosis. Western blot analysis showed higher A_{2B} expression in the IMA than in coronary arteries with or without disease from proteins harvested from these human arteries and ECs. Overexpression of A_{2B} in ECs blunted: monocyte adhesion, cell adhesion molecule expression, migration, and the transendothelial migration of monocytes-- processes directly associated with the development of atherosclerosis. Knockdown of A_{2B} expression by siRNA promoted these processes.
Conclusions—ECs derived from the IMA and Cor are distinctly different in gene expression, which may be responsible for their differential sensitivities for atherosclerosis. This study defined how the A_{2B} receptor may act as an atherosclerotic-resistance gene, which blunted monocyte adhesion and cell adhesion molecule expression, EC migration and retarded the transendothelial migration of monocytes.

Disclosures: **S.R. Archacki:** None. **Q.K. Wang:** None.

528

Selectin-Binding Peptide Conjugate Molecule Decreases Murine Deep Vein Thrombosis Formation

Andrea M Chambers, James R Wodicka, Gurneet S Sangha, Purdue Univ, Lafayette, IN; Alyssa Panitch, Univ of California, Davis, Davis, CA; Craig Goergen, Purdue Univ, Lafayette, IN

Introduction: Deep vein thrombosis (DVT) affects 300,000 to 600,000 people annually with a recurrence in 20-50% after 10 years. Treatment is managed through anticoagulant drugs, but side effects occur due to systemic administration. The venous endothelium is thought to perpetrate thrombosis, especially through endothelial cell surface adhesion receptors P-selectin and E-selectin. In this study, a selectin receptor-binding molecule (EC-SEAL), made with a selectin-binding peptide and dermatan sulfate backbone was used to evaluate thrombus prevention in the infrarenal vena cava (IVC) of a mouse over 24 hours using high frequency ultrasound.
Purpose: P-selectin and E-selectin have exemplified a link between DVT, leukocyte accumulation and rolling, and platelet binding. Thus, the purpose was to evaluate the ability of EC-SEAL to reduce leukocyte and platelet binding, and subsequently DVT, in a mouse model by blocking the corresponding endothelial cell receptors.
Methods: A surgical murine model of thrombosis was induced by IVC stenosis with non-absorbable 6-0 silk suture and a 30-gauge needle (male C57BL/6; 10.8 ± 0.2 weeks old). The stenosis led to a 90% reduction in blood flow through the vessel. Within 10 minutes of suture placement around the IVC, 100 µl of saline (n = 6), EC-SEAL (n = 4), or heparin (n = 6) were systemically injected via the tail vein. Thrombus was observed before surgery, 6 hours and 24 hours after surgery using the Vevo 2100 high frequency ultrasound (FUJIFILM VisualSonics Inc.). Thrombus volume and IVC volume were analyzed using 3D ultrasound images, while thrombus weight was measured *ex vivo*.
Results and Conclusions: Six hours after post-ligation, the mean thrombus percentage (thrombus volume/total IVC volume) was 63.1±5.3% for saline, 25.8±11.2% for EC-SEAL, and 26.1±11.4% for heparin. EC-SEAL and heparin groups had significantly lower 6-hour mean thrombus percentage ($p < 0.05$; ANOVA with a Tukey HSD post-hoc). The 24-hour mean thrombus percentage and thrombus weight were not statistically significant. The data suggest EC-SEAL reduces thrombus at 6 hours while avoiding reduced clotting time side effects associated with heparin. Further work will be needed to determine the true potential for EC-SEAL as a DVT treatment.

Disclosures: **A.M. Chambers:** None. **J.R. Wodicka:** Ownership Interest; Modest; James Wodicka is one of the inventors of EC-SEAL and would receive royalties on potential future earnings. **G.S. Sangha:** None. **A. Panitch:** Ownership Interest; Significant; EC-SEAL is licensed to Symic Biomedical; Alyssa Panitch is a founder of Symic Biomedical. Consultant/Advisory Board; Modest; Alyssa Panitch is one of the inventors of EC-SEAL and would receive royalties on potential future earnings. Consultant/Advisory Board; Significant; Alyssa Panitch is an scientific Advisory board member of Symic Biomedical. **C. Goergen:** None.

529

Statin Therapy Decreases Vascular Inflammation and Prolongs Patency in Murine Arteriovenous Fistula

Jie Cui, Harkamal S Jhajj, Cardiovascular Res Ctr, Massachusetts General Hosp, Harvard Medical Sch, Boston, MA; **Chase W Kessinger**, Cardiovascular Res Ctr/Massachusetts General Hosp, Boston, MA; Jason McCarthy, Ctr of Systems Biology and Cardiovascular Res Ctr, Massachusetts General Hosp, Harvard Medical Sch, Boston, MA; Farouc A Jaffer, Cardiovascular Res Ctr, Massachusetts General Hosp, Harvard Medical Sch, Boston, MA

Background:AVFs are the lifeline of dialysis patients, but can often occlude. The most common cause of AVF failure is inflammation-driven neointimal hyperplasia and thrombosis. Here, we investigated whether statin therapy with well-recognized anti-inflammatory properties can improve murine AVF patency, and further assessed the anti-inflammatory effects.Methods: One week prior to AVF creation, mice were randomized to oral atorvastatin 1.14mg/kg/day or control 100ul PBS (both n=10), administered by daily gavage. AVF were created using an end-to-side internal jugular vein and carotid artery anastomosis. AVF blood flow was measured (Transonic blood flow probe) at day 0 and weekly thereafter until occlusion (blood flow < 0.1ml/min). On day 6, CLIO-VT680, an inflammatory cell-targeted fluorescent nanoparticle, was injected intravenously (10mg/kg). 24 hours later, in vivo survival epifluorescence molecular imaging was performed to visualize inflammatory cell in the AVF venous outflow limb. Histopathological

assessment of AVF was performed in on day 7 and 14 mice (6 statin each, 6 control each) to assess venous outflow area, AVF scarring via collagen, and adventitial macrophage content.Results: At day 7, the in vivo venous outflow cellular inflammation signal (CLIO-VT680 TBR) was significantly lower in statin-treated mice (3.5±0.16 vs 4.5±0.5 PBS, p=0.02). Adventitial macrophage content was significantly lower in statin group at day 14 (p=0.01). Positive AVF remodeling, a desirable feature for clinical AVF patency, was higher in the statin group as compared to the PBS group (p=0.02 at week 1, p=0.002 at week 2). In vivo, statin-treated animals exhibited greater AVF blood flow (BF) preservation from day 7 to day 14 (ΔAVF BF +0.14±0.2 ml/min vs. -0.79±0.32 ml/min PBS, p=0.02). The ΔAVF BF from day 7 to day 14 correlated inversely and significantly with the day 7 CLIO-VT680 cellular inflammation (r=-0.56, p=0.02), indicating that baseline inflammation may predict AVF failure. Kaplan Meier survival analysis showed median AVF patency in mice treated with statin was 28 days compared to 14 days in PBS treated group (p<0.05).Conclusion: Statin therapy prolongs AVF patency and preserves AVF blood flow in association with diminished AVF cellular inflammation.

Disclosures: **J. Cui:** None. **H.S. Jhajj:** None. **C.W. Kessinger:** None. **J. McCarthy:** None. **F.A. Jaffer:** None.

530

In vivo DVT Inflammation Presages Vein Wall Injury, and is Ameliorated by Statin Therapy

Chase W Kessinger, Guanming Qi, Ahmed Tawakol, MGH/Harvard Medical Sch, Boston, MA; Peter K. Henke, Univ of Michigan, Ann Arbor, MI; Farouc A. Jaffer, MGH/Harvard Medical Sch, Boston, MA

OBJECTIVE: Inflammation mediates early venous thrombosis (VT) resolution and can induce vein wall scarring (VWS), a key driver of the morbid post-thrombotic syndrome (PTS). Statins exhibit anti-inflammatory properties, and may positively impact VWS after VT. However, whether early inflammation contributes to this process and can be detected is not known. In this study, we hypothesized that early VT inflammation detected by 18F-fludeoxyglucose (FDG) positron emission tomography/computed tomography (PET/CT) could predict subsequent VWS and that both VT inflammation and VWS would be attenuated by statin therapy.
METHODS: Stasis VT was induced by complete ligation in male C57BL/6J mice (n=55) in either the infrarenal inferior vena cava (IVC, n=42) or right jugular vein (n=13). IVC VT mice were randomized to statin or control groups. Statin (rosuvastatin 5mg/kg) was given by oral gavage starting one day prior to VT induction; control mice received PBS. All mice underwent survival FDG-PET/CT venography imaging on day 2. FDG-PET inflammation signals (standard uptake value (SUV), SUVmax, target-to-background ratios (TBR)) were measured. Picrosirius red staining of day 14 VT sections measured vein wall collagen/thickness. Ex vivo VT tissue gamma counting of a subgroup was performed at day 2. Whole-thrombus protein/mRNA and VT tissue sections assessed neutrophil content.
RESULTS: FDG-PET/CT at day 2 revealed increased FDG uptake in jugular VT over the contralateral sham surgery vein (p<0.001). Statin-treated mice showed a decrease in FDG-PET SUV, SUVmax and TBR (p<0.05 for all). Whole-thrombus analyses and tissue section immunostaining showed reduced thrombus neutrophil content at day 2, without reducing GLUT1 or MPO expression (p>0.05). At day 14, statin therapy significantly reduced VWS (p=0.02). In mice undergoing survival imaging, the day 2 FDG-PET VT inflammation signal correlated significantly with the magnitude of day 14 VWS (IVC VT r=0.74, p<0.001) and jugular models of VT (r=0.62, p=0.02).
CONCLUSIONS: Quantitative FDG inflammation imaging demonstrates that early VT inflammation presages subsequent VWS, and is ameliorated by prophylactic statin therapy. The overall findings support the concept that statins and could reduce VWS and PTS.

Disclosures: **C.W. Kessinger:** None. **G. Qi:** None. **A. Tawakol:** None. **P.K. Henke:** None. **F.A. Jaffer:** None.

531

Association of D-Dimer with Oxidized Phospholipids, Antibodies to Oxidation-Specific Epitopes and Plaque Morphology in Coronary Artery Disease

HEMA KOTHARI, Anh T Nguyen, Univ of Virginia Health System, Charlottesville, VA; Yohei Hisada, Univ of North Carolina, Chapel Hill, NC; Xiaohong Yang, Sotirios Tsimikas, Univ of California San Diego, La

Jolla, CA; Nigel Mackman, Univ of North Carolina, Chapel Hill, NC; Angela Taylor, Coleen A McNamara, Univ of Virginia Health System, Charlottesville, VA

Objective: Lp(a) is the prominent lipoprotein carrier of oxidized phospholipids (OxPLs) in plasma and OxPLs on Lp(a) are thought to contribute to its atherothrombotic effects. IgM antibodies to oxidation-specific epitopes (OSE) block proinflammatory properties of OxPLs and higher plasma levels in humans associate with reduced CAD and lower risk of cardiovascular (CV) events. Coronary thrombosis upon rupture of an unstable plaque leads to CV events. We hypothesize that plasma D-dimer, a marker of thrombosis, associates inversely with IgM antibodies to OSE and positively with OxPLs on apoB-100 (OxPL-apoB), Lp(a) and indices of unstable plaques as determined by VH-IVUS.
Methods and Results: OxPL-apoB, Lp(a) and IgM to OSE (phosphocholine-BSA (PC-BSA) and a malondialdehyde (MDA) mimotope) were measured in 106 subjects with stable CAD undergoing angiography. The plasma D-dimer level was 367.8 ng/mL (range 78.3- 2098.8 ng/mL) and 37 subjects had D-dimer levels (mean ± SD; 918.52 ± 482.81 ng/mL) above the threshold for healthy subjects (>500 ng/mL). D-dimer positively associated with OxPL-apoB (r=0.45, p=0.001) and Lp(a) (r=0.44, p=0.001; n=50) and inversely associated with IgM antibodies to PC-BSA and MDA mimotope (r=0.25, p=0.01 and r=0.20, p=0.04 respectively). Moreover, D-dimer associated inversely with plaque fibrosis (r=0.21, p=0.03), positively with coronary artery calcium (r=0.30, p=0.002) and trended to associate positively with necrosis (r=0.15, p=0.13) in univariate analysis. In multivariable analysis, significant association between D-dimer and calcium persisted while association with fibrosis was nearly significant (p=0.07). Notably, in subjects with D-dimer levels above 500 ng/mL, these associations were stronger (fibrosis; r=-0.45, p=0.006, calcium; r= 0.39, p=0.016, necrosis; r=0.45, p= 0.005).
Conclusions: Our results suggest associations between Lp(a), OxPLs and potentially atheroprotective IgM antibodies to OSE and markers of thrombosis. While associations are modest and a larger study is needed, results raise the interesting possibility that plasma D-dimer may identify subjects prone to Lp(a)/OxPL-induced subclinical thrombosis, which may increase risk for future adverse events.

Disclosures: **H. Kothari:** None. **A. Nguyen:** None. **Y. Hisada:** None. **X. Yang:** None. **S. Tsimikas:** None. **N. Mackman:** None. **A. Taylor:** None. **C. McNamara:** None.

This research has received full or partial funding support from the American Heart Association.

535

Gender Dictates the Relationship Between Clinical Markers of Lipid Metabolism and Immune Function

Catherine J Andersen, Fairfield Univ, Fairfield, CT; Terrence M. Vance, The State Univ of New York Plattsburgh, Plattsburgh, NY

Dyslipidemias and leukocytosis are associated with cardiovascular disease and immune disorders. Mechanistic studies have shown lipoprotein metabolism to play a significant role in the regulation of atherosclerosis development and leukocyte activation, whereas lipid-lowering treatments have been shown to exert beneficial anti-inflammatory and immunomodulatory effects in clinical trials. However, the relationship between clinical markers of lipid metabolism and immune function has not been extensively evaluated at the population level. Thus, we analyzed data from National Health and Nutrition Examination Surveys 1999-2004 to determine whether blood lipids could be used to predict clinical leukocyte counts, and whether there was a relationship between blood lipids, statin use, and prevalence of antinuclear antibodies (ANA) – the most common form of autoantibodies. After adjusting for age, serum cotinine, BMI, waist circumference, race/ethnicity, statin use, and survey cycle, we observed a strong positive linear trend between serum triglycerides vs. blood lymphocyte and basophil counts (cells/μL) in men and women (> 20 years old; n= 5,647), whereas a positive trend between monocytes vs. triglycerides and lymphocytes vs. total cholesterol and LDL-cholesterol was only detected in women. In multiple regression models, a 10% increase in total cholesterol, LDL-cholesterol, and triglycerides was associated with a predicted 1.6%, 0.6%, and 1.4% increase in blood lymphocyte counts in women, respectively, whereas no relationship was observed in men. In a population subsample (n = 1,526), we further found that women were more likely to be positive for ANA as compared to men (women: 17.4% vs. men: 11.7%); however, we did not observe significant associations between the odds of being ANA positive and serum levels of total cholesterol, LDL-cholesterol, or HDL-cholesterol in either men or women. Interestingly, we found that women who take statins have significantly lower odds of being ANA positive (OR 0.25; 95% CI 0.09-0.76), whereas no significant associations between statin use and ANA prevalence was observed in

men. Together, these findings suggest blood lipids and statin usage may be better predictors of clinical markers of immune function in women.

Disclosures: **C.J. Andersen:** None. **T.M. Vance:** None.

536

Poor Correlation Between FMD and PAT-Ratio in Patients With Metabolic Syndrome

Ueda Tomohiro, JR Hiroshima Hosp, Hiroshima shi, Japan

Background: Flow mediated dilatation (FMD) and peripheral arterial tonometry (PAT) are commonly used methods for assessing endothelial function in a research setting but it is unclear how well they correlate. The aim of this study is to compare and correlate these methods in patients with metabolic syndrome. Methods: The study involved 105 subjects (mean age68±10 years) with metabolic syndrome. Based on the results of coronary angiography, they were divided into 2 groups: a study group with coronary lesions (n=68) and a control group without coronary lesions (n=37). Flow mediated vasodilatation (FMD) and nitroglycerine-induced vasodilatation (NID) in the brachial artery was measured by using UNEXEF18G (UNEX CO, Japan). At the same time, PAT ratio was measured by using Endo-PAT 2000 (Itamar Medical, Israel) Results: FMD was not correlated with PAT ratio by Spearman`s analysis. FMD was significantly impaired in the study group compared to that in the control group (3.9±1.8% vs. 2.6±1.5%, respectively; P<0.001). However, NID and PAT ratio had no deference in the two groups. Multivariable analysis revealed that FMD (odds ratio: 0.53, 95% confidence interval [CI]: 0.31-0.90) were independent variables for CAD in metabolic syndrome patients. Conclusion: This study showed that poor correlation between FMD and PAT in patients with metabolic syndrome. PAT may not be used as a substitute for FMD as a measure of endothelial function

Disclosures: **U. Tomohiro:** None.

537

Dock2 Deficiency Mitigates High-Fat Diet-Induced Obesity by Reducing Adipose Tissue Inflammation While Increasing Energy Expenditure

Xia Guo, Feifei Li, Zaiyan Xu, Shi-You Chen, The Univ of Georgia, Athens, GA

Obesity is a public health problem as its association with type 2 diabetes, cardiovascular disorders and many other diseases. Adipose tissue inflammation is frequently observed and plays a vital role in obesity and insulin resistance. Dedicator of cytokinesis 2 (DOCK2) has shown proinflammatory effect in several inflammatory diseases, but its role in obesity remain unknown. To explore the function of DOCK2 in obesity and insulin resistance, wild-type (WT) and DOCK2 knockout (DOCK2-/-) mice were fed with chow or high-fat diet (HFD) for 12 weeks. Metabolic, biochemical and histologic analyses were performed. DOCK2 expression was robustly up-regulated in adipose tissue in WT mice given HFD. DOCK2-/- mice were protected against HFD-enhanced body weight gain with an improved metabolic homeostasis and insulin resistance. In addition, DOCK2 deficiency attenuated adipose tissue and systemic inflammation accompanied by a reduced macrophage infiltration. Moreover, DOCK2 deficiency induced the adipose tissue browning and increased energy expenditure as shown by the up-regulation of metabolic genes in DOCK2-/- mice. Our data indicated that DOCK2 deficiency can protect mice from HFD-induced obesity, metabolic disorders, and insulin resistance. Therefore, targeting DOCK2 may be a potential therapeutic strategy for treating obesity-associated diseases.

Disclosures: **X. Guo:** None. **F. Li:** None. **Z. Xu:** None. **S. Chen:** None.

This research has received full or partial funding support from the American Heart Association.

538

Gum Arabic Acutely Inhibit PCSK9 and Upregulate LDLr in HepG2

Hatim Abulola, Stacey Dybel, **Chinedu Ochin**, Univ of Massachusetts Lowell, Lowell, MA; Mohamed Ali, Ahfad Univ for Women, Omdurman, Sudan; Mahdi Garelnabi, Univ of Massachusetts Lowell, Lowell, MA

Introduction: Gum arabic (GA) (Acacia Senegal) is widely used agent in both the pharmaceutical and food industries as an emulsifier and stabilizer. It is a branched complex polysaccharide molecule rich in calcium, potassium, and magnesium in addition to other minerals. Its aqueous solution is either neutral or slightly acidic. Human intake of GA with atorvastatin was reported to significantly reduce plasma low density lipoprotein, and triglyceride. This study is designed to test mechanism (s) of its action on HepG2 cell. **Hypothesis:** The plasma lipids reduction associated with GA intake is likely associated with PCSK9/LDLr mechanism. **Methods:** Gum Arabic was dissolved in water and irradiated under UV light for 5 hours. Three final concentrations: 5ng/ml, 100ng/ml and 500 ng/ml were used for treatment of HepG2 cells at 6 hours, 12 hours and 24 hours using 12 well plates. Following treatment cells were collected into Trizol® solution; RNA was extracted for gene expression following Trizol® supplier protocol. cDNA was synthesized and the expression of PSCK9, LDLR and other related genes were tested using real time PCR. **Results:** The use of viscous (soluble) fiber (e.g., oats, guar, pectin, and psyllium) as therapeutic dietary options to enhance lowering of LDL cholesterol in primary and secondary prevention of CHD was well known, however there is no study to date that have shown the GA cholesterol lowering mechanism(s). In this study cell treated with GA for six hours has resulted in approximately 50 fold reductions of PCSK9 gene expression across the various concentrations, and approximately 25 fold up regulation of LDLr gene. Prolonged treatments beyond the six hours have shown differential responses. **Conclusions:** This study demonstrates that Gum Arabic has acute anti PCSK9 properties, as well as beneficial LDLr modulation effects. Our data explain the modulatory mechanism of Gum Arabic plasma LDL lowering effects associated with its intake in humans.

Disclosures: **H. Abulola:** None. **S. Dybel:** None. **C. Ochin:** None. **M. Ali:** None. **M. Garelnabi:** None.

539

Lipogenesis Regulates the Response of Cardiac Muscle to Ischemic Stress Through Sarcoplasmic Reticulum Calcium Atpase

Larry D. Spears, Babak Razani, Katsuhiko Funai, Chu Feng, Haowei Song, Clay F. Semenkovich, Washington Univ Sch of Med, St. Louis, MO

Dysfunctional calcium homeostasis is a hallmark of heart failure, a sequela of myocardial infarction (MI). Previous research has shown that mice deficient in cardiac fatty acid synthase (FAS), the rate-limiting enzyme for de novo lipogenesis, have dysfunctional calcium signaling and a predisposition to heart failure. Yet the mechanisms linking endogenous lipid synthesis, myocardial calcium homeostasis, and cardiac function remain poorly understood. A major step in calcium handling is the transport of cytosolic calcium back into the sarcoplasmic reticulum (SR) by sarcoplasmic reticulum calcium ATPase (SERCA), and recent evidence suggests that SR lipid composition can affect SERCA function. To determine whether FAS plays a role in SERCA activity in the heart, we evaluated FASKard (FAS Knockout in the Myocardium) mice in the setting of experimental myocardial infarction (MI). Deletion of heart FAS caused a decrease in SERCA activity in younger adult (4 months) and aged (12 months) mice when compared to control (Ctrl) mice of the same age. Lipidomic analysis of the SR showed the reduced SERCA activity in FASKard mice was due to an altered SR phospholipid composition, leading to an imbalance of SR phosphatidylcholine to phosphatidylethanolamine phospholipid ratios. This altered ratio of SR phospholipids was due to a decrease in the abundance of specific phosphatidylethanolamine phospholipid species. MI caused a decrease in SERCA activity in both Ctrl and FASKard mice hearts. FASKard mice after MI had impaired survival with concomitantly decreased SERCA activity compared to Ctrl mice after MI. FASKard MI mice also had a perturbed ratio of SR phosphatidylcholine to phosphatidylethanolamine phospholipids compared to Ctrl MI mice, due to a decrease in certain phosphatidylethanolamine phospholipids. Additionally, MI induced FAS expression in the myocardium. These findings suggest that myocardial de novo lipogenesis is critical to the maintenance of the SR phospholipid composition, SR-mediated calcium homeostasis, and blunting the development of heart failure, particularly ischemic cardiomyopathy. Furthermore, FAS regulation of the SR lipid composition represents a novel therapeutic strategy in the treatment of heart failure.

Disclosures: **L.D. Spears:** None. **B. Razani:** None. **K. Funai:** None. **C. Feng:** None. **H. Song:** None. **C.F. Semenkovich:** None.

540

Activation of Srebp1c Processing is Required in Flx-Induced Hepatic Lipid Accumulation

Jing Xiong, Nanjing Medical Univ, Nanjing, China

Fluoxetine (FLX), a typical drug belonging to the category of selective serotonin reuptake inhibitors (SSRI), is the most widely prescribed psychoactive drug in the treatment of depression and other mood disorders. It has been demonstrated that the administration of FLX increases the possibility of weight gain and dyslipidemia. We find previously that dysregulation of lipogenic and lipolytic genes is critical in FLX-promoted hepatic lipid accumulation. Therefore, a chronic mild stress depression model and cultured primary mouse hepatocytes were used to investigate the effects and underlying mechanisms of FLX on the promoted hepatic lipid accumulation. The evidence have shown that FLX increases the concentrations of triglyceride (TG) and total cholesterol (TC) in the liver tissues of depressive mice, while only increases TG in the liver tissues of normal mice. FLX induces lipid accumulation in both normal and depressive mice by upregulating the lipogeneic genes Acetyl-CoA carboxylase 1 (ACC1) and Fatty acid synthase (FAS) expression and downregulating the lipolytic genes carboxylesterase 1 (CES1) and CES2. Using primary cultured mouse hepatocytes, it is shown that FLX promotes the expression of transcription factor SREBP1c as well as its proteolytic cleavage and nuclear translocation. FLX significantly suppresses SREBP1c proteolytic cleavage in hepatocytes after the incubation lasting as short as 3 hours, which is a more prompt way than the elevated expression of SREBP1c. Further experiments show that the specific inhibitors of proteases S1P and S2P attenuate FLX-induced SREBP1c activation and hepatic lipid accumulation. As SCAP (SREBP cleavage-activating protein) escorts SREBPs from the endoplasmic reticulum to the Golgi complex where proteases cleave SREBPs and therefore is required for SREBP activation, we find that FLX promotes the protein level of SCAP in a concentration- and time-dependent manner. In conclusion, FLX directly acts on the hepatocytes by facilitating the expression and proteolytic activation of SREBP1c to promote hepatic lipid accumulation. The findings not only provide new insight into the understanding of the mechanisms for SSRI-mediated dyslipidemia effects, but also suggest a novel therapeutic target to interfere.

Disclosures: **J. Xiong:** None.

542

Effects of 1-Methylnicotinamide on Inflammatory and Lipid Biomarkers

Jean-claude Tardif, Montreal Heart Inst, Montreal, QC, Canada; Sameh Fikry, Sameh Fikry Med Professional Corp, Waterloo, ON, Canada; Ginette Girard, Diex Res Sherbrooke Inc., Sherbrooke, QC, Canada; Tania Discenza, Annik Fortier, Montreal Health Innovations Coordinating Ctr, Montreal, QC, Canada; Eugenio A Cefali, Cortria Corp, Waltham, MA; Marie-Claude Guertin, Montreal Health Innovations Coordinating Ctr, Montreal, QC, Canada

Background: 1-methylnicotinamide, a nicotinic acid metabolite, is TRIA-662's active component. As part of a pilot study, we assessed TRIA-662's effects on inflammatory biomarkers and blood lipids. **Methods:** Patients aged 18-80 years with mean serum triglycerides (TG) 2.26-5.65 mmol/L, low-density lipoprotein-cholesterol levels not needing drug therapy, and stable diet and exercise regimens were randomized to TRIA-662 or placebo (PBO, 3:1) up-titrating to 6 g daily orally for 14 weeks. Outcomes were treatment compliance and changes from baseline in inflammatory biomarkers and blood lipids. **Results:** The 71 randomized patients were 54±12 years old, 54% were male, 48% were obese, 37% had hypertension, 25% dyslipidemia, and 7% diabetes. Treatment compliance and study completion (95% CI) were reached in 87.1% (79.3, 95.0%) and 87.3% (79.6, 95.1%) of patients overall, respectively. Adjusted geometric mean percent change (95% CI) from baseline in high-sensitivity C-reactive protein was -15.66% (-28.40, -0.66%) with TRIA-662 (p=0.0419 vs baseline) and 1.21% (-13.95, 19.05%) with PBO. The between-group difference of -16.67% (-33.59%, 4.57%) in favor of TRIA-662 did not reach significance (p=0.1130). The effect of TRIA-662 on tumor necrosis factor (TNF) alpha was influenced by the baseline value: For a baseline TNF value of 3.30 pg/mL (third quartile), the adjusted mean change (95% CI) was -0.65 (-0.92, -0.38) pg/mL, corresponding to a 20% decrease, with TRIA-662 and 0.31 (-0.32, 0.95) pg/ml, corresponding to a 9% increase with PBO, with a between-group difference of -0.97 (-1.65, -0.29) pg/mL

(p=0.0076). The adjusted mean changes from baseline in adiponectin were 0.55 µg/mL (0.23, 0.86 µg/mL) corresponding to a 6% increase for TRIA-662 and -0.06 µg/mL (-0.53, 0.42 µg/mL) corresponding to a 0.7% decrease for PBO (p=0.0391 between groups). Geometric mean TG value at baseline was 3.36 mmol/L. The adjusted geometric mean percent change (95% CI) in TG was -9.01% (-15.91%, -1.54%) for TRIA-662 and -2.09% (-13.03, 10.24%) for PBO (p=0.3088 between groups). Baseline HDL-C was 1.01 ± 0.28 mmol/L, and the difference in change over time was not significant between groups (p=0.8242). **Conclusion:** TRIA-662 favourably affected inflammatory biomarkers in this pilot study.

Disclosures: **J. Tardif:** Research Grant; Significant; Amarin, Astra-Zeneca, DalCor, Eli-Lilly, Merck, Pfizer, Roche, Servier, Cymabay, Sanofi. Honoraria; Significant; Astra-Zeneca, DalCor, Pfizer, Roche, Sanofi, Servier. Ownership Interest; Modest; DalCor. **S. Fikry:** None. **G. Girard:** None. **T. Discenza:** None. **A. Fortier:** None. **E.A. Cefali:** Employment; Significant; Vice President, Clinical Development, Cortria Corporation. **M. Guertin:** None.

543

Myeloperoxidase Induces Endothelial Dysfunction via Activation of Calpain

Zienab Etwebi, Gavin Landesberg, Rosario Scalia, Temple Univ, Philadelphia, PA

Myeloperoxidase (MPO) is a peroxidase enzyme secreted by activated leukocytes, which has been associated with endothelial dysfunction and insulin resistance. The calcium dependent protease calpain has also been linked to vascular disease in insulin resistance and type 2 diabetes. Accordingly, we tested the hypothesis that endothelial expressed calpains play a role in MPO-induced endothelial dysfunction and vascular inflammation. Mouse lung microvascular endothelial cells (MMVEC) were stimulated with 10 nM MPO for 30, 60, 120, 180, and 240 minutes. Expression levels of Vascular Cell Adhesion Molecule 1 (VCAM-1), 5' AMP Activated Protein Kinase (AMPK), Protein Kinase B (PKB) (Akt), endothelial Nitric Oxide (eNOS) phosphorylation at serine 1177 (Se1177), Protein Phosphatase 2 (PP2A), and calpains were measured by immunoblot analyses. MPO time dependently activated µ-calpain (P<0.0001 vs control) but not m-calpain. MPO also significantly increased PP2A protein levels (P<0.001), decreased AMPK phosphorylation (P<0.01), AKT phosphorylation (P<0.05), and eNOS phosphorylation at (Se1177) (P<0.01), while significantly increased VCAM-1 protein levels (P<0.01). Pretreatment of MMVECs with the selective calpain inhibitor ZLLal (100 µM) prevent MPO-induced calpain activation (P<0.0001 vs MPO alone). Inhibition of calpain activity also preserved AMPK phosphorylation, eNOS phosphorylation, and PP2A levels, in the face of MPO (P<0.001 versus MPO alone). Calpain inhibition also prevented upregulation of VCAM-1. Using an *ex vivo* leukocyte adhesion assay we also found leukocytes failed to adhere to the vascular endothelium of MPO treated aortas isolated from µ-calpain deficient mice (p<0.001 versus aortas isolated from WT mice). Taken together, our data first demonstrate a primary role for µ-calpain in endothelial dysfunction induced by leukocyte derived MPO.

Disclosures: **Z. Etwebi:** None. **G. Landesberg:** None. **R. Scalia:** None.

544

Diabetes Mellitus Impacts on Vascular Calcification in Peripheral Arterial Disease Patients but Does Not Further Activates Osteogenic Markers in Beta-Glycerophosphate Stimulated Vascular Smooth Muscle Cells

Elisangela Farias-Silva, Cynthia A Mendes, Hosp Albert Einstein, São Paulo, Brazil; Luciana A Pescatore, InCor/FMUSP, São Paulo, Brazil; Maria Claudina C Andrade, Luciana S Carmo, Youri E Almeida, Marcela A Kaminagakura, Mônica Koga, Nelson Wolosker, Marcel Liberman, Hosp Albert Einstein, São Paulo, Brazil

Introduction: Diabetes mellitus (DM) accelerates vascular calcification (VC) in peripheral arterial disease (PAD), increasing limb ischemia and amputation risk. Although DM and VC implicates in PAD, the mechanisms underlying vascular smooth muscle cells (SMC) osteochondrogenic differentiation in this setting are scarce. **Objectives:** To assess VC and osteogenic mRNA/protein expression (Msx2, Runx2 and ALPL) in arteries and in primary SMC isolated from PAD patients with DM (n=3), without DM (n=2) and individuals without PAD (control [CTL], n=2) that underwent amputation. **Methods**: Ethical committee approved study and patients signed informed consent**.** 5-7th passages SMC were incubated without (untreated) or with β-glycerophosphate 10mM (β-GP) for 48h (mRNA expression), 72h (protein expression) and 14 days (calcification). In addition, we performed tissue immunofluorescence and Alizarin

Red S. **Results:** Untreated PAD+DM SMC increased calcification (4.6±1.2) in comparison to PAD without DM patients (2.5±0.2) and CTL individuals (1.0±0.07). β-GP further increased calcification in respective groups (51.3±4.7; 13.5±1.1 and 9.8±1.2). Msx2 mRNA expression decreased in CTL SMC after β-GP (48h) and did not change in PAD without DM and in PAD+DM SMC. Msx2 protein expression decreased in all groups after calcifying medium (72h). Moreover, Runx2 mRNA expression increased in β-GP-treated PAD+DM SMC and ALPL mRNA expression augmented in β-GP-treated SMC from PAD without DM patients. However, Runx2 and ALPL protein expression was not modulated by calcifying medium (72h) in all groups. Interestingly, immunofluorescence of arterial samples demonstrated increased osteochondrogenic protein expression (Msx2, Runx2 and ALPL) around calcifying foci in PAD+DM group (+++) *versus* PAD without DM (++) and *versus* CTL (+) patients. Coincidently, PAD+DM group showed augmented vascular calcification ($19x10^4 \pm 10x10^4$; $7x10^4 \pm 2x10^4$; $3x10^3 \pm 10^{-2} \mu m^2$). **Conclusion:** We demonstrated increased calcification in arteries from amputated PAD+DM patients and in respective SMC without and with calcifying medium. Although we found augmented osteochondrogenic protein expression in the vessel wall from PAD+DM individuals this was not robustly shown in isolated SMC *in vitro*.

Disclosures: **E. Farias-Silva:** None. **C.A. Mendes:** None. **L.A. Pescatore:** None. **M.C. Andrade:** None. **L.S. Carmo:** None. **Y.E. Almeida:** None. **M.A. Kaminagakura:** None. **M. Koga:** None. **N. Wolosker:** None. **M. Liberman:** None.

545

Cinnamon Extract Inhibit Lipids and Inflammation by Modulation of Transcription Factors: *in vivo* Model

Zeynep Tuzcu N/A, Cemal Orhan, Nurhan Sahin, Kazim Sahin, Firat Univ, Elazig, Turkey; **Vijaya Juturu**, OmniActive Health Technologies Inc, Morristown, NJ

OBJECTIVES: CNM (CNM) polyphenol has antioxidant and anti-inflammatory properties. Therefore, we hypothesized CNM decrease heart disease risk factors and may enhance anti- inflammatory properties in rats fed a diet containing CNM. In this study, we evaluated the effects of CNM polyphenol on insulin resistance (IR), hyperlipidemia, hepatic transcription factors expressions [sterol regulatory element-binding protein1c (SREBP-1c), liver X receptor-α (LXR-α), nuclear factor kappa B p65 (NF-κB p65), nuclear factor-E2-related factor-2 (Nrf2)] in rats fed high fat diet (HFD). **METHOD:** Twenty-eight Wistar rats were allocated into four groups; (i) normal control; animals fed with normal chow (C) (ii) CNM (C+CNM 100 mg/kg b.wt.), (iii) HFD (42% of calories as fat, high fat diet [HFD]), and (iv) HFD + CNM for 12 weeks. Blood analysis for triglycerides (TG) and cholesterol (CHOL), glucose, insulin, malonaldehyde (MDA a marker of oxidative stress [OS]) were estimated. Body weight, visceral fat and liver weight recorded and liver MDA assessed. SREBP-1c, LXR-α, ATP-citrate lyase (ACLY), fatty acid synthase (FAS), NF-κB p65 expressions and decreased the PPAR-α, p-IRS-1, Nrf2, HO-1 proteins were evaluated by Western blotting. **RESULTS:** HFD rats of the liver had increased SREBP-1c, LXR-α, ATP-citrate lyase (ACLY), fatty acid synthase (FAS), NF-κB p65 expressions and decreased the PPAR-α, p-IRS-1, Nrf2, HO-1 expressions compared to control group. CNM supplementation decreased body weight (8.4%), visceral fat (36.6%), liver weight (17.7%), serum glucose and insulin concentrations, lipid profile ($P < 0.05$), and serum and liver MDA (23.3% and 25.4 %) concentration compared to HFD rats ($P < 0.05$). CNM decreased hepatic SREBP-1c (18.1 %), LXRα (27.9%), ATP-citrate lyase (ACLY, 22.7 %), fatty acid synthase (FAS, 15.8 %), NF-κB p65 (23.3%) and enhanced the PPAR-α, IRS-1 (72.7 %), Nrf2 (111.7 %) and HO-1 (72.1 %) proteins in HFD rat livers ($P < 0.05$). **DISCUSSION:** These results suggest CNM supplementation reduces hyperlipidemia, inflammation, and oxidative stress through activating transcription factors (SREBP-1c, LXR-α, NF-κB, and Nrf2) and anti-oxidative defense signaling pathway.

Disclosures: **Z. Tuzcu:** None. **C. Orhan:** None. **N. Sahin:** None. **K. Sahin:** Research Grant; Modest; OmniActive Health Technologies Ltd. India. **V. Juturu:** Employment; Significant; Employee.

546

Metformin Significantly Increased Survival Rate in Patients With Diabetes and Comorbid Heart Disease

Longjian Liu, Darryl Brown, Drexel Univ Dornsife Sch of Public Health, Philadelphia, PA; Barbara Simon, Howard J. Eisen, Drexel Univ Coll of Med, Philadelphia, PA

Objective: We assessed the hypothesis that metformin use significantly decreases risk of all-cause and heart disease (HD) mortality in patients with diabetes mellitus (DM).
Methods: Subjects with DM aged ≥30 (n=3612) participating in 1999 -2010 National Health and Nutrition Examination Surveys, who had anti-DM drug therapy information, and were followed up by December 2011 were analyzed. Baseline DM, coronary heart disease (CHD) and heart failure (HF) were defined as a physician-diagnosis of the disease(s). Death from HD was classified using ICD10:I20-I25).
Results: Mean (SD) age of 3612 participants was 63.1 (13.02), 83.4% (3056/3612) were under anti-DM therapies, and 20.3% was in metformin monotherapy, 4.9% in metformin combination (MCO), 24.8% in insulin, 45.4% in thiazolidinedione, sulfonylurea, and combinations, and 4.7% in any other antidiabetic drugs therapies. Baseline CHD and HF rates were 11.38% and 9.13%. At the end of follow-up, 1024 died from all-cause (21.86%), and 222 died from HD. Multivariate Cox's proportional hazard regression analysis indicated that diabetic patients with comorbid HD (CHD and/or HF) had significant higher all-cause mortality than those without. However, these excess mortalities were significantly reduced in patients with metformin therapies than their counterparts without metformin. The hazard ratios (HR, 95%CI) of metformin use versus those without for all-cause mortality was 0.53 (0.38-0.76, p=0.001). Diabetic patients with CHD and with metformin therapies had a significantly lower 10-year all-cause mortality than those without metformin (33% vs. 64%, p<0.001). Similarly, diabetic patients with HF and with metformin therapies had a significantly lower 10-year all-cause mortality than their counterparts (42.8% vs. 73.1%, p<0.001). The effects of metformin on all-cause mortality were positively modified after adjusting dyslipidemia and insulin resistance.
In conclusion, metformin significantly increased survival rates from all-cause mortality in diabetic patients with comorbid CHD and/or HF. The mortality risk reduction may be partially explained by an effect of metformin on a reduction of dyslipidemia and insulin resistance.

Disclosures: **L. Liu:** None. **D. Brown:** None. **B. Simon:** None. **H.J. Eisen:** None.

547

Glycocylated Hemoglobin Targets Among Diabetics and Cardiovascular Disease: Do We Need to Change Focus?

Ebenezer T Oni, Siva Buddhavarapu, Kunal Nangrani,, Ricky Patel, Chinelo Madubum, Raja Chand, Tanyka Sam, Brooklyn Hosp Ctr, Brooklyn, NY

Background:
Diabetes is an established risk factor for cardiovascular disease (CVD). Glycosylated hemoglobin (HbA1C) targets are surrogate markers to monitor disease progression and guide treatment. While HbA1C targets are relevant in ascertaining glycemic control, the relationship of the established cutoffs and cardiovascular disease risk are not clear.
Methods:
We conducted a step wise logistic regression from a cohort of 1,065 diabetic patients attending the Ambulatory Care Clinic at The Brooklyn Hospital Center between 2012- 2014. CAD was defined as a diagnosis of coronary artery disease in the health records.
Results: Twelve percent were females, 9% of the individuals achieved an HbA1C target ≤ 7%., and 12% had a history of CAD. Thirty-eight percent were taking metformin, 18% were on insulin. Only 7% of individuals with CAD had their A1C at target. Both a linear regression of HbA1C and logistic regression of HbA1C > 7% did not show any significant association with CAD, See table 1.
Conclusion: This cross-sectional analysis of diabetic patients on treatment did not show an association between glycosylated hemoglobin and CAD. It is therefore imperative for future studies to evaluate the relationship between HbA1C and cardiovascular outcomes and ascertain the usefulness of this marker to guide CVD treatment strategies in diabetics.
Model 1-unadusted, Model 2- adjusted for BMI, Model 3- adjusted for BMI, LDL, HDL, gender, Metformin use, insulin use.

	Odds Ratio	95% CI	P-value
Model 1	0.73	0.36 – 1.50	0.40
Model 2	0.78	0.38 – 1.59	0.49
Model 3	0.89	0.31 – 2.59	0.84

Disclosures: **E.T. Oni:** None. **S. Buddhavarapu:** None. **K. Nangrani,:** None. **R. Patel:** None. **C. Madubum:** None. **R. Chand:** None. **T. Sam:** None.

548

Molecular Mechanism Behind Protein S Deficiency in Obese Patients

Vijaya S Pilli, LSU Health Sience Ctr, New Orleans, LA

Introduction: Protein S is a vitamin K-dependent plasma protein, produced mainly in the liver; Protein S circulates in the blood at a concentration of 450 nM. Protein S is an anticoagulant, serving as a cofactor for APC and TFPI, and as an inhibitor of Factor IX (FIXa). Protein S deficiency causes deep vein thrombosis (DVT), increased risk of inflammation and, because DVT is a complication commonly observed in obese individuals, Protein S deficiency might be associated with obesity. **Aim:** To identify a correlation between Protein S deficiency and obesity, and identify the probable molecular mechanism behind the Protein S deficiency in the obese subjects. **Methods:** Immunoblots, ELISA, EMSA, CHIP, aPTT assay, and thrombin generation assay. **Results:** By ELISA, we measured a decrease in Protein S level in obese mice compared with wild type mice. In obesity, the liver becomes hypoxic, thus, we hypothesized that hypoxia and hypoxia inducible factor 1 alpha (HIF1α) may regulate Protein S expression in obesity. We found that a high fat diet induced HIF1α stability in mice. HIF1α levels were inversely proportional to Protein S levels, suggesting that HIF1α is a negative regulator of Protein S expression. We further identified a putative HIF1α binding site in the Protein S promoter, and, by using *in vitro* and *in vivo* assays, we demonstrated that HIF1α binds directly to the Protein S promoter and suppresses transcription. We further confirmed HIF1α-mediated Protein S transcriptional regulation *in vivo,* Plasma Protein S levels are increased in the liver-specific HIF1α knockout mouse whereas, liver-specific overexpression of HIF1α reduced the concentration of Protein S in the plasma. **Conclusion:** We conclude that HIF1α regulates Protein S expression in mouse liver and in obesity. Inhibition of HIF1α or intravenous injection of Protein S may reduce the occurrence of DVT in obese individuals.

Disclosures: **V.S. Pilli:** None.

549

Visceral Adipose Tissue Associates With Coronary Plaque Burden Beyond Cardiovascular Risk Factors in Psoriasis

Joshua P Rivers, Amit K Dey, Jonathan H Chung, Anshuma Rana, Abhishek Chaturvedi, Justin A Rodante, Joseph B Lerman, Martin P Playford, Jianhua Yao, Marcus Y Chen, David A Bluemke, Tiffany M Powell-Wiley, Nehal N Mehta, NIH, Bethesda, MD

Background: Psoriasis (PSO), a chronic inflammatory disease associated with increased cardiovascular (CV) risk, provides a reliable human model to study inflammatory atherogenesis. PSO has been known to be associated with cardiometabolic dysfunction including adipose tissue dysfunction. Recently, visceral adiposity (VAT) was shown to be associated with increased CV events, but whether VAT is associated with subclinical atherosclerosis as assessed by coronary plaque burden has not been characterized.
Hypothesis: We hypothesized that VAT volume by CT is associated with total burden (TB) and more specifically with non-calcified burden (NCB) by CCTA.
Methods: Consecutive PSO patients (N=68) underwent CT scans to measure abdominal adiposity. VAT volume was quantified from the level of the diaphragm to the pubic symphysis and reported in volume. Coronary plaque characterization was performed by CCTA (Toshiba 30 slice) via QAngio CT software (Medis, The Netherlands). The relationship of VAT with TB and NCB was analyzed using unadjusted and adjusted multivariable regression models (STATA 12).

Results: The cohort was middle-aged, predominantly male, at low CV risk by FRS with mild to moderate PSO by skin disease severity (Table 1). VAT volume associated with both TB (beta coefficient= 0.49, p-value <0.001) and NCB (beta coefficient= 0.51, p-value <0.001). This relationship remained significant after adjustment for cardiovascular risk factors for TB (beta coefficient= 0.28, p-value = 0.004) and NCB (beta coefficient = 0.34, p-value <0.001).
Conclusions: Directly quantified VAT directly associated with TB and NCB independent of cardiovascular risk factors. These findings suggest that adipose tissue dysfunction may in part contribute to the high CV events observed in psoriasis and support efforts to provide weight control as a strategy to reduce CV disease in psoriasis.

Table 1: Description of Psoriasis Cohort.

Parameter (n=68)	
Demographics and medical history	
Age, years	52.2 ± 12.4
Sex, males	39 (57)
Ethnicity, whites	61 (90)
Hypertension	21 (31)
Hyperlipidemia	45 (66)
Type-2-Diabetes	9 (13)
Current tobacco use	5 (7)
Lipid treatment	28 (41)
Clinical and laboratory values	
Systolic blood pressure, mmHg	124.8 ± 12.7
Body mass index, kg/m^2	29.9 ± 5.3
Waist-to-hip ratio	0.93 ± 0.09
Framingham risk score	4 (2-7)
Total cholesterol, mg/dL	178.9 ± 35.9
HDL cholesterol, mg/dL	54.4 ± 16.9
LDL cholesterol, mg/dL	98.2 ± 32.2
Triglycerides, mg/dL	109 (79.5-141)
Insulin, mIU/mL	15.6 ± 9.5
Glucose, mg/dL	102.8 ± 20.1
Homeostatic Model Assessment of Insulin Resistance	3.2 (2.0-5.0)
C-reactive protein, mg/L	1.4 (0.7-4.1)
Psoriasis severity and treatment	
Psoriasis area severity index score	5.2 (3.0-8.4)
Systemic or biologic treatment	26 (38)
Coronary artery burdens	
Total Burden (x100), mm^2	1.20 ± 0.49
Non-Calcified Burden (x100), mm^2	1.15 ± 0.46
Dense Calcified Burden (x100), mm^2	0.02 (0.007-0.04)
Adiposity by computed tomography	
Subcutaneous adiposity, cm^3	211.4 ± 113.1
Visceral adiposity, cm^3	178.7 ± 98.0

Note: Values reported in the table as mean±standard deviation (mean ± S.D.) or median (interquartile change) [median (IQR)] for continuous variables and as n (%) for categorical variables.

Disclosures: **J.P. Rivers:** None. **A.K. Dey:** None. **J.H. Chung:** None. **A. Rana:** None. **A. Chaturvedi:** None. **J.A. Rodante:** None. **J.B. Lerman:** None. **M.P. Playford:** None. **J. Yao:** None. **M.Y. Chen:** None. **D.A. Bluemke:** None. **T.M. Powell-Wiley:** None. **N.N. Mehta:** None.

550

Alteration of Glycolysis Metabolite Levels and Impaired Hypoxic Response in Diabetic Atherosclerosis

Atsushi Yamashita, Yunosuke Matsuura, Faculty of Med, Miyazaki Univ, Miyazaki, Japan; Yan Zhao, Hokkaido Univ, Sapporo, Japan; Takashi Iwakiri, Faculty of Med, Miyazaki Univ, Miyazaki, Japan; Kazuaki Yamasaki, Hokkaido Univ, Sapporo, Japan; Chihiro Sugita, Faculty of Pharmaceutical Sciences, Kyusyu Univ of Health and Welfare, Nobeoka, Japan; Chihiro Koshimoto, Miyazaki Univ, Miyazaki, Japan; Kazuo Kitamura, Faculty of Med, Miyazaki Univ, Miyazaki, Japan; Keiichi Kawai, Inst of Medical, Pharmaceutical and Health Sciences,Kanazawa Univ, Kanazawa, Japan; Nagara Tamaki, Graduate Sch of Med, Hokkaido Univ, Sapporo, Japan; Songji Zhao, Yuji Kuge, Hokkaido Univ, Sapporo, Japan; Yujiro Asada, Faculty of Med, Miyazaki Univ, Miyazaki, Japan

Objective: Diabetes mellitus accelerates atherosclerosis that causes most cardiovascular events. Several metabolic pathways are considered to contribute to the development of atherosclerosis, but comprehensive metabolic alterations to atherosclerotic arterial cells remain unknown. The present study investigated metabolic status and their relationship to vascular histopathological changes in the atherosclerotic arteries of rabbits with alloxan-induced diabetes.

Approach and Results: Diabetic atherosclerosis was induced in rabbits ilio-femoral arteries by injecting alloxan (100 mg/kg), injuring the arteries using a balloon, and feeding with a 0.5% cholesterol diet. Plaque burden, macrophage content, and hypoxic areas were more prevalent in arteries with diabetic, than non-diabetic atherosclerosis. Metabolomic analyses highlighted 12 metabolites that were significantly altered between diabetic and non-diabetic atherosclerosis. A half of them were associated with glycolysis metabolites, and their levels were decreased in diabetic atherosclerosis. The uptake of glucose evaluated as ^{18}F-fluorodeoxyglucose in atherosclerotic lesions increased according to increased macrophage content or hypoxic areas in non-diabetic, but not diabetic rabbits. Despite profound hypoxic areas, the nuclear localization of hypoxia-inducible factor-1α decreased and the number of apoptotic cells increased in diabetic atherosclerotic lesions.
Conclusions: Altered glycolysis metabolism and an impaired response to hypoxia in atherosclerotic lesions under conditions of insulin-dependent diabetes might be involved in the development of diabetic atherosclerosis.

Disclosures: **A. Yamashita:** None. **Y. Matsuura:** None. **Y. Zhao:** None. **T. Iwakiri:** None. **K. Yamasaki:** None. **C. Sugita:** None. **C. Koshimoto:** None. **K. Kitamura:** None. **K. Kawai:** None. **N. Tamaki:** None. **S. Zhao:** None. **Y. Kuge:** None. **Y. Asada:** None.

552

Aberrant Expression of MicroRNA-378a Induces Hepatic Insulin Resistance via Activation of ER Stress and the dsRNA Activated Protein Kinase PKR

Xiao Cheng, Yongyan Song, Qiaozhu Su, Univ of Nebraska-Lincoln, Lincoln, NE

microRNAs(miRNAs) are noncoding RNAs with a length of 19 to 25 nt that are involved in posttranscriptional gene regulation by binding to the 3'-untranslated regions (3'-UTR) of target mRNA and impacting diverse cellular processes, including cell differentiation, energy metabolism and chronic inflammation. MicroRNA-378a (miR-378a) has been reported to be involved in adipose tissue browning and cancer development. However, its role in cellular stress signaling and hepatic insulin resistance has not yet been investigated. Here we reported that expression of hepatic miR-378a was upregulated by metabolic inflammatory inducers, such as high fructose feeding, bacterial lipopolysaccharide (LPS) and inflammatory cytokine TNFα. The elevated miR-378a subsequently targeted the 3'-UTR of PPARα which compromised mitochondrial fatty acid β-oxidation and induced mitochondrial and ER stress. miR-378a was further found to directly interacted with the dsRNA binding motifs within the dsRNA activated protein kinase PKR and activated the kinase to sustain the inflammatory stress and blunt the insulin signaling in hepatocytes. Genetic depletion of miR-378a rescued hepatocytes from mitochondrial and ER stress, systemic inflammation and insulin resistance induced by fructose and LPS. **Conclusion:** This study, for the first time, demonstrates that miR-378a is involved in mediating the metabolic inflammatory response in the onset of insulin resistance. This study further unveils a novel finding that miR-378a is capable of directly interacting with and activating a protein kinase PKR to sustain the stress signaling between mitochondria and ER. This discovery greatly broadens the physiological function of miR-378a by demonstrating that, in addition to regulate its target genes on the mRNA level, miRNA-378a is able to interact with RNA binding protein(s) and exerts its regulatory effect directly on the protein levels. Results from this study may provide rationale for using miR-378a as a pharmaceutical target in the treatment of insulin resistance.

Disclosures: **X. Cheng:** None. **Y. Song:** None. **Q. Su:** None.

555

Functional Characterization Uncovered Novel Loss-of-function Mutations in ABCA1

Xin Bi, James McParland, Univ of Pennsylvania, Philadelphia, PA; Jian Wang, Adam D McIntyre, Robert A. Hegele, Robarts Res Inst, London, ON, Canada; Daniel J. Rader, Marina Cuchel, Univ of Pennsylvania, Philadelphia, PA

Objectives: *ABCA1* encodes the membrane protein ATP-binding cassette transporter A1 (ABCA1), a pivotal player in nascent HDL formation via its ability to facilitate cholesterol and phospholipid efflux to apolipoprotein A-I (ApoA-I). *ABCA1* variants are frequently found in subjects with primary hypoalphalipoproteinemia, however, their pathogenicity and causal link with the clinical phenotype are not always known. **Methods:** *In silico* analysis (Mutation Assessor, PANTHER, PolyPhen-2, PROVEAN,

SIFT, and VEST) were performed to predict the functional consequences of *ABCA1* missense variants found in our cohort of hypoalphalipoproteinemia. A subset of novel *ABCA1* variants were generated *in vitro* through site-directed mutagenesis and their abilities in mediating lipid efflux to apoA-I were determined using standard methods. **Results:** A total of 32 mutations in *ABCA1* were identified, among which 15 were classified as missense, 9 as nonsense or frameshift, 7 as intronic, and 1 as "no-protein". We selected 5 variants that were labeled as pathogenic or possibly pathogenic by in silico analysis to conduct functional studies. Two newly identified mutations in ABCA1, a nonsense mutation (p.E1005X) and a missense mutation (p.S2046R), resulted in complete loss of the canonical lipid efflux function of ABCA1 (2.5% and 1.8% of wild type cholesterol efflux level respectively). These results were concordant with the phenotypic characteristics of the carriers. Three additional mutations (p.G750W and p.R1341T and p.I1085F) resulted in only a partial loss of function (66-75% of wild type cholesterol efflux level). These results were somewhat discordant with the phenotype of the heterozygote carriers (HDL-C levels of 16, 14 and 38 mg/dl respectively), suggesting the presence of additional causal factors. **Conclusions:** These results support E1005X and S2046R as ABCA1 loss-of-function mutations and highlight the need to conduct functional studies on unknown variants to determine their pathogenicity.

Disclosures: **X. Bi:** None. **J. McParland:** None. **J. Wang:** None. **A.D. McIntyre:** None. **R.A. Hegele:** None. **D.J. Rader:** None. **M. Cuchel:** None.

556

Lipoprotein Remodeling and Cholesterol Exchange Monitored Using Fluorescent Lipids and Proteins

Edward B Neufeld, Nicolas O Francone, Gizem Yilmaz, Scott M Gordon, Denis O Sviridov, Lipoprotein Metabolism Section, NHLBI NIH, Bethesda, MD; Maureen Sampson, Dept of Clinical Chemistry, Clinical Chemistry Section,NIH, Bethesda, MD; Stephen J Demosky Jr, Milton Pryor, Marcelo J Amar, Alan T Remaley, Lipoprotein Metabolism Section, NHLBI NIH, Bethesda, MD

We developed a sensitive and robust *in vitro* method to monitor lipoprotein cholesterol and protein exchange and lipoprotein remodeling, using non-exchangeable fluorescent phosphatidylethanolamine (PE) as a lipoprotein marker. We applied this method to monitor the exchange of unesterified cholesterol (FC) and apoA-I among isolated human lipoproteins and synthetic lipoprotein-X (LpX). Fluorescent FC, but not PE, rapidly equilibrated between VLDL and HDL, and transferred almost entirely from VLDL or HDL to LDL. Fluorescent apoA-I bound specifically to HDL and remodeled fluorescent PE and FC-labeled LpX into a new lipoprotein particle that contained both fluorescent lipids and apoA-I. LpX-derived fluorescent PE incorporated into plasma HDL only. The incorporation of LpX-derived fluorescent FC into plasma lipoproteins was similar to fluorescent FC alone, consistent with remodeling of LpX to HDL with concomitant exchange of FC between lipoproteins. LPL remodeled fluorescent PE and FC-tagged VLDL into a new particle containing both fluorescent lipids and apoA-I. We also developed a model system to study lipid transfer *in vitro* and *in vivo* by depositing lipids on calcium silicate hydrate crystals to form dense lipid coated donor particles that are readily separated from acceptor membranes and can be used as a surrogate for cell-dependent cholesterol efflux. These methodologies can readily be applied to study the other members of the vast lipoprotein proteome and the wide variety of remodeling events involved in lipoprotein-mediated lipid homeostasis in health and disease.

Disclosures: **E.B. Neufeld:** None. **N.O. Francone:** None. **G. Yilmaz:** None. **S.M. Gordon:** None. **D.O. Sviridov:** None. **M. Sampson:** None. **S.J. Demosky:** None. **M. Pryor:** None. **M.J. Amar:** None. **A.T. Remaley:** None.

557

Type 2 Diabetes is Associated With Impaired High-Density Lipoprotein Endothelial Protective Function

Tomas Vaisar, Erica Couzens, Arnold Hwang, Andrew N Hoofnagle, Univ of Washington, Seattle, WA; Carolyn E Barlow, Laura F DeFina, Cooper Inst, Dallas, TX; Francis Kim, Univ of Washington, Seattle, WA

Aim: One of the hallmarks of diabetes is impaired endothelial function. High density lipoproteins (HDL) can exert protective effects on endothelium stimulating NO production and protecting from inflammation. Previous study suggested that HDL in obese people with diabetes and metabolic syndrome and markedly

low HDL-C lost endothelial protective function. We aimed to test whether type 2 diabetes impairs HDL endothelium protective functions in people with otherwise normal lipid profile. **Methods:** In a case-control study (n=40 per group) nested in the Cooper Center Longitudinal Study, we isolated HDL and measured its ability to stimulate activity of endothelial nitric oxide synthase (eNOS; phosphorylation of Ser1177) in endothelial cells and the ability of HDL to suppress inflammatory response of endothelial cells (NFkB activation). Additionally, we also measured by LCMS levels of sphingosine-1-phosphate (S1P) and plasma P-selectin by ELISA. **Results:** The HDL in people with type 2 diabetes lost almost 40% of its ability to stimulate eNOS activity (P<0.001) and 20% of its ability to suppress inflammation in endothelial cells (*P*<0.001) compared to non-diabetic controls despite similar BMI and lipid profile (HDL-C, LDL-C, TC, TG).The ability of HDL to stimulate eNOS activity was negatively associated with plasma levels of P-selectin, an established marker of endothelial dysfunction (r=−0.32, *P*<0.001). Furthermore, sphingosine-1-phosphate (S1P) levels were decreased in plasma of people with diabetes (*P*=0.017) and correlated strongly with HDL-mediated eNOS activation. **Conclusions:** Collectively, our data suggest that HDL in individuals with type 2 diabetes loses its ability to maintain proper endothelial function independent of HDL-C, perhaps due to loss of S1P, and may contribute to development of diabetic complications.

Disclosures: **T. Vaisar:** None. **E. Couzens:** None. **A. Hwang:** None. **A.N. Hoofnagle:** None. **C.E. Barlow:** None. **L.F. DeFina:** None. **F. Kim:** None.

This research has received full or partial funding support from the American Heart Association.

558

PCPE2 Promotes Adipocyte Maturation via Regulation of SR-BI Activity

Hao Xu, Sushma Kaul, Elisa Maruko, Kaniz Fatema, Med Coll of Wisconsin, Milwaukee, WI; Craig A Glastonbury, Kerrin Small, King's Coll London, London, United Kingdom; Michael J Thomas, Mary Sorci-Thomas, Med Coll of Wisconsin, Milwaukee, WI

Procollagen C-endopeptidase enhancer protein 2 (PCPE2) is an enhancer protein that enhances the cleavage of the C-termini of procollagen by bone morphogenetic protein 1. But the function of PCPE2 is not limited to collagen maturation. Recently our lab reported that PCPE2 increased HDL-associated cholesteryl ester uptake via scavenger receptor class B type 1 (SR-BI), an HDL cholesterol receptor highly expressed in adipose tissue. Interestingly, TwinsUK study in human provided data showing that PCPE2 mRNA is highly correlated with adipose tissue distribution. Further, our lab observed a reduced size of visceral fat pad in PCPE2 deficient mice despite its indifference in body weight compared to the wild type. To study the molecular and cellular mechanisms of how PCPE2 regulates SR-BI function and how it affects adipose tissue formation, we generated PCPE2 knockout ($PCPE2^{-/-}$) cell line from murine preadipocyte 3T3-L1 cell using CRISPR-Cas9 technology. Induction of 3T3-L1 cell to differentiate into mature adipocyte increases the expression of both PCPE2 and SR-BI hand in hand around 3 fold, which parallels the process of lipid droplet formation. Immunofluorescence studies showed that PCPE2 is distributed all over the cell in mature adipocyte, while SR-BI is mostly distributed along the cytoplasmic and lipid droplet membranes, in addition to the perinuclear region. More interestingly, $PCPE2^{-/-}$ 3T3-L1 cell shows an impairment in lipid droplet formation during the induction of differentiation, with less than 10% of cells generating lipid droplets, and the size of lipid droplet being only about 50% of that in wild type. Although $PCPE2^{-/-}$ 3T3-L1 cell expresses SR-BI at a higher level compared with wild type cell, nearly 50% of the SR-BI in wild type cell are in homodimer structure while $PCPE2^{-/-}$ 3T3-L1 cell has almost none SR-BI multimer, indicating that SR-BI in $PCPE2^{-/-}$ 3T3-L1 cell is inactive. Taken together, we concluded that PCPE2 plays a critical role in keeping SR-BI in active conformation, which, in turn, controls adipocyte maturation. Whether this effect is associated with collagen maturation will be assessed in our future studies.

Disclosures: **H. Xu:** None. **S. Kaul:** None. **E. Maruko:** None. **K. Fatema:** None. **C.A. Glastonbury:** None. **K. Small:** None. **M.J. Thomas:** None. **M. Sorci-Thomas:** None.

559

Exploiting Macrophage Autophagy-Lysosomal Biogenesis With the Natural Sugar Trehalose as a Therapy for Atherosclerosis

Ismail Sergin, Xiangyu Zhang, **Trent D Evans**, Babak Razani, Washington Univ in St. Louis, St. Louis, MO

The autophagy-lysosome system is a catabolic cellular mechanism that degrades dysfunctional proteins and organelles. In atherosclerosis, there is mounting evidence that this process is rendered dysfunctional particularly in plaque macrophages and is an important trigger for plaque progression. In an effort to characterize practical inducers of macrophage degradative capacity, we now describe the unique vascular benefits of a natural sugar called trehalose, a recognized autophagy inducer with a currently unknown mechanism of action. Trehalose-treated macrophages display enhanced autophagy via a process that involves lysosomal stress and resultant activation of TFEB, the master transcriptional regulator of autophagy-lysosomal biogenesis. We find an important downstream effect of trehalose to be the induction of p62-dependent selective autophagy of cytotoxic polyubiquitinated protein aggregates and dampening of IL-1β/inflammasome function. We confirm the relevance of these in vitro observations in several pro-atherogenic (ApoE-/-) mouse models. Administration of trehalose during eight weeks of Western diet feeding potently induces autophagy and TFEB in plaque macrophages with concomitant reductions in polyubiquitinated protein aggregate burden along with significantly reduced plaque size and complexity. Importantly, these findings are completely abrogated in mice deficient in macrophage autophagy (ATG5-/-) or the selective autophagy chaperone (p62-/-). Further detailed pharmacokinetic evaluation of trehalose shows that physiologically relevant concentrations are indeed achievable in mice. Taken together, our data support the serious consideration of this safe and natural sugar as a potent inducer of macrophage degradative capacity in the treatment of atherosclerotic vascular disease.

Disclosures: **I. Sergin:** None. **X. Zhang:** None. **T.D. Evans:** None. **B. Razani:** None.

560

Ideal Cardiovascular Health and Subclinical Markers of Carotid Structure and Function the Paris Prospective Study III

Bamba Gaye, INSERM, U970, Paris Cardiovascular Res Ctr, Dept of Epidemiology AND Univ Paris Descartes, Sorbonne Paris Cité, Faculté de Médecine, Paris, France; Hazrije Mustafic, Dept of Cardiology, Univ Hosp of Geneva, Switzerland (H.M.), Geneva, Switzerland; Stéphane Laurent, INSERM, U970, Paris Cardiovascular Res Ctr, Dept of Epidemiology AND APHP, Georges Pompidou European Hosp, Pharmacology Depts,, Paris, France; Marie-Cécile Perier, INSERM, U970, Paris Cardiovascular Res Ctr, Dept of Epidemiology, Paris, France; Frédérique Thomas, Preventive and Clinical Investigation Ctr, Paris, France; Muriel Tafflet, INSERM, U970, Paris Cardiovascular Res Ctr, Dept of Epidemiology, Paris, France; Bruno Pannier, Preventive and Clinical Investigation Ctr, Paris, France; Pierre Boutouyrie, INSERM, U970, Paris Cardiovascular Res Ctr, Dept of Epidemiology AND APHP, Georges Pompidou European Hosp, Pharmacology Depts,, Paris, France; Xavier Jouven, INSERM, U970, Paris Cardiovascular Res Ctr, Dept of Epidemiology AND Dept of Cardiology, Univ Hosp of Geneva, Switzerland (H.M.), Paris, France; Jean-Philippe Empana, INSERM, U970, Paris Cardiovascular Res Ctr, Dept of Epidemiology AND Univ Paris Descartes, Sorbonne Paris Cité, Faculté de Médecine, Paris, France

Objective—We hypothesized that subclinical markers of vascular structure and function, which are independent predictors of cardiovascular disease, would be less frequent in subjects with ideal than poor cardiovascular health (CVH) as defined by the American Heart Association (AHA).
Approach and Results—Carotid parameters were measured using high-precision echotracking device in 9155 nonreferred participants attending a health checkup in a large health center in Paris (France) between 2008 and 2012. According to the AHA, participants with 0 to 2, 3 to 4, and 5 to 7 metrics (smoking, physical activity, body mass index, diet, blood glucose and total cholesterol, blood pressure) at the ideal level were categorized as having poor, intermediate, and ideal CVH. Carotid parameters were dichotomized according to their median value, and multivariable logistic regression analysis was performed. Mean age was 59.55 (SD 6.3) years; 39% were females, and ideal CVH was present in 10.11% of the study participants. After adjustment for age, sex, education, and living alone and compared with a poor CVH, an ideal CVH was associated with lower common carotid artery intima–media thickness (odds ratio=1.64; 95% confidence interval 1.40, 1.93), absence of carotid plaques (odds ratio=2.14; 95%

confidence interval 1.60, 2.87), lower Young's elastic modulus (odds ratio=2.43; 95% confidence interval 2.07, 2.84), and higher carotid distensibility coefficient (odds ratio=2.90; 95% confidence interval 2.47, 3.41).
Conclusions—In community subjects aged 50 to 75 years, ideal CVH was associated with substantially less arterial stiffness and thickness. These associations might contribute to the lower risk of cardiovascular diseases in subjects with ideal CVH.

Disclosures: **B. Gaye:** None. **H. Mustafic:** None. **S. Laurent:** None. **M. Perier:** None. **F. Thomas:** None. **M. Tafflet:** None. **B. Pannier:** None. **P. Boutouyrie:** None. **X. Jouven:** None. **J. Empana:** None.

561

GITR Activation Promotes Regulatory CD4+ T-cell Responses and Stimulates Leukocyte Recruitment in Atherosclerotic Plaques

Annelie Shami, Academic Medical Ctr, Univ of Amsterdam, Amsterdam, Netherlands; Svenja Meiler, Holger Winkels, Norbert Gerdes, Inst for Cardiovascular Prevention (IPEK), Ludwig-Maximilians Univ Munich, Munich, Germany; Esther Lutgens, Academic Medical Ctr, Univ of Amsterdam, Amsterdam, Netherlands

Glucocorticoid-induced tumor necrosis factor receptor family-related protein (GITR) - a costimulatory molecule - is expressed on CD4(+) effector memory T cells and regulatory T cells as well as antigen-presenting cells and mast cells; while its ligand (GITRL) is mainly found on antigen-presenting cells and endothelial cells. However, the definitive role of GITR in atherosclerosis is not fully understood. Our hypothesis is that signaling through GITR plays a vital role in atherosclerosis progression.
Low-density lipoprotein receptor-deficient mice ($Ldlr^{-/-}$) with B-cell-restricted overexpression of GITRL (*Gitrl*^{tg}) fed a high-cholesterol diet showed a profound increase in both CD4(+) effector memory T cells and regulatory T cells in secondary lymphoid organs in comparison to wild-type controls. Additionally, the number of regulatory T cells was significantly enhanced in the thymus and aorta of these mice along with increased GITRL and interleukin-2 transcript levels. Atherosclerotic lesions of $Ldlr^{-/-}Gitrl^{tg}$ mice contained more total $CD3^+$ T cells as well as $Foxp3^+$ regulatory T cells overall, leading to significantly less severe atherosclerosis.
Conversely, atherosclerosis was found to be less severe in mice deficient in apolipoprotein E and GITR ($ApoE^{-/-}$ $GITR^{-/-}$). Atherosclerotic lesions in these mice were found to contain less macrophages and CD3-positive T-cells. Perfusion assays using two-photon excitation microscopy revealed less wild type leukocyte adhesion on GITR-deficient endothelium, with a further reduction in adhesion by GITR-deficient leukocytes to both wild type and GITR-deficient endothelia. Finally, expression of GITR expression in human plaque tissue was significantly increased in ruptured plaques.
In conclusion, these data indicate that continuous GITR stimulation through B cell GITRL acts protective in a mouse model of atherosclerosis by regulating the balance between regulatory and effector memory CD4(+) T cells, while GITR activation on endothelial cells promotes atherogenesis by stimulating leukocyte recruitment into the plaque.

Disclosures: **A. Shami:** None. **S. Meiler:** None. **H. Winkels:** None. **N. Gerdes:** None. **E. Lutgens:** None.

562

Human Carotid Atherosclerosis Plaque Progression and Vessel Material Stiffness at Follow Up Had Positive Correlation: An in vivo Vessel Stiffness MRI Follow Up Study

Qingyu Wang, Sch of Biological Science and Medical Engineering, Southeast Univ, Nanjing, China; **Dalin Tang**, Worcester Polytechnic Inst, Worcester, MA; Gador Canton, Univ of Washington, Seattle, WA; Jian Guo, Sch of Biological Science and Medical Engineering, Southeast Univ, Nanjing, China; Xiaoya Guo, Southeast Univ, Nanjing, China; Thomas S Hatsukami, Div of Vascular Surgery, Univ of Washington, Seattle, WA; Kristen L Billiar, Zheyang Wu, Worcester Polytechnic Inst, Worcester, MA; Chun Yuan, Dept of Radiology, Univ of Washington, Seattle, WA

It is hypothesized that artery stiffness may be associated with plaque progression. However, in vivo vessel material stiffness follow-up data is lacking in the literature.
In vivo 3D multi-contrast and Cine magnetic resonance imaging (MRI) carotid plaque data were acquired from 8 patients with follow-up (18 months) with written informed consent obtained. Cine MRI and 3D thin-layer models were used to determine parameter values of the Mooney-Rivlin models for the 81slices from

16 plaques (2 scans/patient) using our established iterative procedures. Effective Young's Modulus (YM) values for stretch ratio [1.0,1.3] were calculated for each slice for analysis.
Stress-stretch ratio curves from Mooney-Rivlin models for the 16 plaques and 81 slices are given in Fig. 1. Average YM value of the 81 slices was 411kPa. Slice YM values varied from 70 kPa (softest) to 1284 kPa (stiffest), a 1734% difference. Average slice YM values by vessel varied from 109 kPa (softest) to 922 kPa (stiffest), a 746% difference. Location-wise, the maximum slice YM variation rate within a vessel was 306% (139 kPa vs. 564 kPa). Average slice YM variation rate within a vessel for the 16 vessels was 134%. Average variation of YM values from baseline (T1) to follow up (T2) for all patients was 61.0%. The range of the variation of YM values was [-28.4%, 215%]. For progression study, YM increase ($YMI=YM_{T2}-TM_{T1}$) showed negative correlation with plaque progression measured by wall thickness increase (WTI), (r= -0.6802, p=0.0634). YM_{T2} showed strong negative correlation with WTI (r= -0.7764, p=0.0235). Correlation between YM_{T1} and WTI was not significant (r= -0.4353, p= 0.2811).
Conclusion In vivo carotid vessel material properties have large variations from patient to patient, along the vessel segment within a patient, and from baseline to follow up. Use of patient-specific, location specific and time-specific material properties could potentially improve the accuracy of model stress/strain calculations.

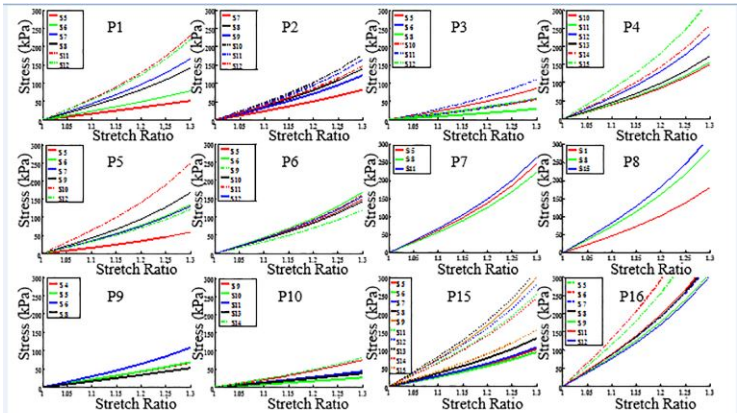

Figure 1. Stress-Stretch Ratio curves from Mooney-Rivlin Models using parameter values determined from Cine MRI selected from 16 plaque samples studied.

Disclosures: **Q. Wang:** None. **D. Tang:** Research Grant; Significant; National Institute of Biomedical Imaging and Bioengineering R01 EB004759, National Science Foundation (DMS-0540684). **G. Canton:** Research Grant; Significant; National Science Foundation (DMS-0540684). **J. Guo:** None. **X. Guo:** None. **T.S. Hatsukami:** None. **K.L. Billiar:** Research Grant; Modest; National Institute of Biomedical Imaging and Bioengineering R01 EB004759. **Z. Wu:** None. **C. Yuan:** Research Grant; Modest; NSF grant DMS-0540684.

563

Serum Amyloid A3 is a High Density Lipoprotein-associated Acute Phase Protein

Maria C De Beer, Ailing Ji, Victoria P Noffsinger, Preetha Schridas, Frederick C De Beer, Lisa R Tannock, Nancy R Webb, Univ. of Kentucky, Lexington, KY

Acute phase serum amyloid (SAA) is a family of evolutionarily conserved, secreted proteins that exerts innate functions relevant to vascular disease. In humans, two SAA isoforms (SAA1 and SAA2) are highly induced in the liver and extrahepatic tissues under the regulation of inflammatory cytokines. During severe inflammation, SAA1/2 levels can increase $\geq$1000-fold in plasma, where it is found associated with HDL. Mice produce an additional acute phase SAA, SAA3, which is thought to be produced mainly by adipocytes and macrophages and has not previously been found circulating on HDL. The goal of this study was to investigate whether SAA3 serves as a third liver-derived, HDL-associated acute phase SAA in mice. Using isoform-specific oligonucleotide primers for qRT-PCR, we determined that SAA3 is transcriptionally induced to a similar extent (~2500-fold) compared to SAA1.1/2.1 (~6000-fold) in livers of C57BL/6 mice 19 hr after lipopolysaccharide (LPS) injection (100 µg/mouse). SAAs were also robustly induced in fat tissue (SAA1/2~100-fold; SAA3~400-fold). The analysis of primary mouse hepatocytes and *in situ* hybridization of mouse liver sections indicated that liver-derived SAAs are produced by hepatocytes and not other stromal cells, including Kupffer cells. All 3 SAA isoforms were detected in

plasma of LPS-injected mice, although SAA3 levels were ~20% of SAA1/2. After separation by FPLC, virtually all of plasma SAA1/2 eluted with the HDL fraction, whereas ~15% of plasma SAA3 appeared to be lipid poor/free. HDL isolated from acute phase mouse plasma by density gradient ultracentrifugation was subjected to isoelectric focusing to determine the relative recovery of the various SAA isoforms. Whereas the bulk of plasma SAA1.1 was found in the d=1.063-1.21 fraction, only ~50% of SAA2.1 and ~10% of SAA3 was recovered after ultracentrifugation. These findings suggest that SAA3 may be more loosely associated with HDL compared to SAA1.1/2.1, which may give rise to lipid poor/free SAA3 that is susceptible to more rapid clearance in vivo. We conclude that SAA3 is a major hepatic acute phase SAA in mice that may produce systemic effects during inflammation. Future studies investigating SAA pathobiology in mice must take into account the previously under-studied SAA3.

Disclosures: **M.C. De Beer:** None. **A. Ji:** None. **V.P. Noffsinger:** None. **P. Schridas:** None. **F.C. De Beer:** None. **L.R. Tannock:** None. **N.R. Webb:** None.

564

Structure-Function Studies of ApoA-I Mimetic Peptides for ABCA1-Dependent Cholesterol Efflux and HDL Formation

Rafique M Islam, George Mason Univ, Natl Insts of Health, Fairfax, VA; Mohsen Permousa, Natl Inst of Health, Rockville, MD; Scott Gordon, Denis Sviridov, Natl Inst of Health, Bethesda, MD; Richard W Pastor, Natl Inst of Health, Rockville, MD; Alan T Remaley, Natl Inst of Health, Bethesda, MD

To examine the mechanism of action of ApoA-I mimetics, we designed 4 peptides with a variable number of E, L, K and A residues and determined their ability to form HDL-like particle and promote ABCA1-dependent cholesterol efflux. They were named based on a unique physical
property:
N=ELK-neutral
(EKLKELLEKLLEKLKELL),
H=ELK-hydrophobic
(EKLLELLKKLLELLKELL),
P=ELK-positive
(EKLKALLEKLKAKLKELL),
Neg=ELK-negative
(EELKEKLEELKEKLEEKL). CD-spectroscopy showed that H and P were mostly helical in an aqueous buffer (52% and 22%, respectively), and in a TFE-containing solvent, mimicking a lipid environment, all peptides showed greater than 40% helicity. In DMPC vesicle solubilization assay, we observed following order: P>N>H>>Neg. By non-denaturing gel electrophoresis, N, H, P formed approximately 8, 8, and 18 nm size lipid particles, respectively when combined with DMPC. However, Neg did not form any detectable particle. A mixture of natural lipids (PC:SM:LysoPC:PE:PS:PI; mol% 55:12:5:10:8:10), intended to simulate ABCA1 lipid membrane microdomain, yielded similar results . Using BHK-ABCA1 transfected cells, cholesterol efflux studies showed following results: H>N>>P, whereas Neg peptide was inactive. All-atom MD simulation of N carried out on a 12–nm disc containing POPC:cholest (200:20), 26 peptides, and initially placed in belt-like configuration as head-to-tail dimers, the starting structure was maintained for at least 3 µ-sec, indicated a strong preference for this configuration. However, when N was initially oriented in a picket-fence configuration, it distorted to a belt-like pattern within 1 µ-sec. For Neg, both starting configurations were much less stable with dimers losing their connectivity and monomers migrating to the top and bottom of the disc, leaving large hydrophobic patches of acyl chains exposed. Cross-linking studies were consistent with the ability of H and N to form dimers to stabilize the HDL structure, and thereby, were also consistent with simulation. Together, we show that a net neutral charge, a relatively large hydrophobic moment (0.78), and a broad hydrophobic face (180 degrees) are optimum features for an apoA-I mimetic peptide to promote cholesterol efflux and to stabilize a nascent discoidal HDL structure.

Disclosures: **R.M. Islam:** None. **M. Permousa:** None. **S. Gordon:** None. **D. Sviridov:** None. **R.W. Pastor:** None. **A.T. Remaley:** None.

565

Ambient Ultrafine Particle Digestion Alters Gut Microbiota in Association With Increased Atherogenic Lipid Metabolites

Rongsong Li, Jieping Yang, UCLA, Los Angeles, CA; Arian Saffari, USC, Los Angeles, CA; kyung Baek, Jonathan Jacobs, Joseph Pisegna, Zhaoping Li, UCLA, Los Angeles, CA; Constantinos sioutas, USC, Los Angeles, CA; Mohamad Navab, Tzung Hsiai, UCLA, Los Angeles, CA

Ambient particulate matter (PM) exposure is associated with atherosclerosis and inflammatory bowel disease. Ultrafine particles (UFP, d_p< 0.1-0.2 µm) are redox active components of PM. We hypothesized that orally ingested UFP promoted atherogenic lipid metabolites in both the intestine and plasma via altered gut microbiota composition. Low density lipoprotein receptor-null (*Ldlr*$^{-/-}$) mice on a high-fat diet were orally administered with vehicle control or UFP (40 µg/mouse/day) for 3 days a week. After 10 weeks, UFP ingested mice developed macrophage and neutrophil infiltration in the intestinal villi, accompanied by elevated cholesterol but reduced coprostanol levels in the cecum, as well as elevated atherogenic lysophosphatidylcholine (LPC 18:1) and lysophosphatidic acids (LPAs) in the intestine and plasma. At the phylum level, Principle Component Analysis revealed significant segregation of microbiota compositions which was validated by Beta diversity analysis. UFP-exposed mice developed increased abundance in Verrocomicrobia but decreased Actinobacteria, Cyanobacteria, and Firmicutes as well as a reduced diversity in microbiome. Spearman's analysis negatively correlated Actinobacteria with cecal cholesterol, intestinal and plasma LPC18:1, and Firmicutes and Cyanobacteria with plasma LPC 18:1. Thus, ultrafine particles ingestion alters gut microbiota composition, accompanied by increased atherogenic lipid metabolites. These findings implicate the gut-vascular axis in a atherosclerosis model.

Disclosures: **R. Li:** None. **J. Yang:** None. **A. Saffari:** None. **K. Baek:** None. **J. Jacobs:** None. **J. Pisegna:** None. **Z. Li:** None. **C. sioutas:** None. **M. Navab:** None. **T. Hsiai:** None.

566

MicroRNA-146a Deficiency Prevents PCSK9 Gain-of-Function Mutation-induced Hypercholesterolemia in Mice

Shayan Mohammadmoradi, Aida Javidan, Weihua Jiang, Jessica Moorleghen, Venkateswaran Subramanian, Univ of Kentucky, Lexington, KY

Background and Objective: Mimetic mediated activation of microRNA 146a (miR-146a) reduces atherosclerosis via suppression of nuclear factor-κB-driven inflammation in mice. The purpose of this study was to determine whether miR-146a influences plasma cholesterol in hypercholesterolemic mice. **Methods and results:** To induce hypercholesterolemia, female C57BL/6 miR-146a WT (n=8) and miR-146a KO (n=8) mice were injected intraperitoneally with an adeno-associated viral vector (AAV) expressing the proprotein convertase subtilisin/kexin type 9 (PSCK9 D377Y) gain-of-function mutant at a dose of 3 x 10^{10} genomic copies/mouse. After infection, mice were fed a Western diet (21% wt/wt milk fat; 0.15% wt/wt cholesterol) for sixteen weeks, and plasma PCSK9 and total cholesterol concentrations were monitored monthly using an enzymatic assay. Plasma PCSK9 concentrations were profoundly increased 4 weeks post injection (Baseline: WT - 179 ± 12 vs KO - 207 ± 12; Week 4: WT - 1700 ± 148 vs KO - 2689 ± 305 ng/ml) and remained significantly high during 16 weeks (WT - 882 ± 142 vs KO - 718 ± 109 ng/ml; p<0.05 vs baseline) of Western diet feeding. Consistent with increased plasma PCSK9 concentrations, plasma cholesterol concentrations were increased in both groups of mice. Interestingly, miR-146a KO group mice showed less significant increase in plasma cholesterol compared to WT group (Baseline: WT - 88 ± 3 vs KO - 83 ± 3; Week 4: WT - 328 ± 25 vs KO - 195 ± 18 mg/dl) irrespective of the comparable plasma PCSK9 concentrations. Also, lipoprotein distribution analysis with size exclusion gel chromatography revealed that miR-146a KO mice showed a strong reduction in high density lipoprotein (HDL) particles while very low density lipoprotein (VLDL) and low density lipoprotein (LDL) particles were not affected. **Conclusion:** Our findings suggests that miR146a plays a critical role in the regulation of HDL particles in PCSK9 gain-of-function mutant-induced hypercholesterolemia in mice. Future studies will identify gene targets influenced by miR-146a in regulating HDL-cholesterol in hypercholesterolemic mice.

Disclosures: **S. Mohammadmoradi:** None. **A. Javidan:** None. **W. Jiang:** None. **J. Moorleghen:** None. **V. Subramanian:** None.

This research has received full or partial funding support from the American Heart Association.

567

Genetic and Clinical Heterogeneity of Marked High Density Lipoprotein Deficiency

Eliana Polisecki, Andrew S Geller, Taylor Sacco, Margaret R Diffenderfer, Bela F Asztalos, Boston Heart Diagnostics, Framingham, MA; Sotirios K Karathanasis, MedImmune, Gaithersburg, MD; Robert A Hegele, Western Univ, London, ON, Canada; Ernst J Schaefer, Boston Heart Diagnostics, Framingham, MA

Aim: Our goal was to assess the population prevalence, genetics and clinical phenotypes of subjects with marked HDL deficiency.
Methods: 200 subjects (26% female, mean age 52 years) with serum HDL-C < 20 mg/dL, fasting triglycerides (TG) < 600 mg/dL, C reactive protein (CRP) < 10 mg/L, myeloperoxidase (MPO) < 1000 pmoles/L, HbA1c < 8.0%, liver transaminases < 120 U/L, and not taking anabolic steroids were studied. Lipids, inflammation markers, liver enzymes, and HDL particles were assessed; and sequencing of 31 lipid metabolism genes including *ABCA1, APOA1, LCAT*, and *LPL* was done.
Results: HDL-C < 20 mg/dl was observed in 473 (0.35%) men (n=135,912) and 140 (0.089%) women (n=160,964) in our population over one year. In this low HDL group, 6.4% had elevated CRP, 4.4% had abnormal liver function, 4.2% had elevated HbA1c, 1.0% had elevated MPO, 0.5% had elevated TG, and 11.5% of men were taking anabolic steroids. These subjects were excluded. The 200 subjects studied had plasma values of LDL-C 102, HDL-C 15, TG 239, and apoA-I 76 mg/dL, with a marked deficiency of very large and large α-1 and α-2 HDL. *ABCA1* mutations were found in 38 subjects (19.0%; 29 heterozygotes, 6 compound heterozygotes, 3 homozygotes). *APOA1* mutations were found in 10 subjects (5.0%; 9 heterozygotes, 1 homozygote). *LCAT* mutations were found in 17 subjects (8.5%; 13 heterozygotes, 3 compound heterozygotes, 1 homozygote). In addition, 11 subjects (5.5%) had the *LPL* N318S variant, and 13 subjects (6.5%) had the *ABCA1* c.-279 C>G variant. Premature coronary heart disease (CHD) was observed in some subjects with *ABCA1 and APOA1* mutations. Neuropathy was observed in some subjects with *ABCA1* mutations, and kidney failure was observed in the subject with the homozygous *LCAT* mutation.
Conclusions: Marked HDL deficiency occurred in 0.2% of our population and can be associated with liver disease, inflammation, diabetes, severe hypertriglyceridemia, and the use of anabolic steroids. In the absence of these conditions, mutations in *ABCA1, APOA1, or LCAT* were found in 32% of subjects studied. Premature CHD was seen in some subjects with *ABCA1 or APOA1* mutations, neuropathy was seen in some subjects with *ABCA1* mutations, and kidney failure was observed in some subjects with *LCAT* mutations.

Disclosures: **E. Polisecki:** Research Grant; Modest; x. **A.S. Geller:** Research Grant; Modest; x. **T. Sacco:** Research Grant; Modest; x. **M.R. Diffenderfer:** Research Grant; Modest; x. **B.F. Asztalos:** Research Grant; Modest; x. **S.K. Karathanasis:** Employment; Significant; x. **R.A. Hegele:** None. **E.J. Schaefer:** Research Grant; Modest; x.

568

Lipidomic Comparison of Hyperglycemic and Normal Subjects Using Absolute Quantitation of >700 Lipid Species

Jon Rees, Susan Kuklenyik, Michael Gardner, David Schieltz, Bryan A Parks, Jeffrey Jones, Christopher Toth, Lisa McWilliams, Michael Andrews, John R Barr, CDC, Atlanta, GA

The presence of diabetes mellitus in patients significantly increases the risk of cardiovascular disease, among many negative health outcomes. Several research groups have reported lipid species anomalies in subjects showing insulin resistance, including higher concentrations of sphingomyelin species relative to normal controls. Advances in lipidomic methodologies has allowed for the profiling of numerous lipid species in a single extraction and analytical run. We used the SCIEX Lipidyzer platform to determine the absolute concentration of 770 distinct lipid species from 52 subjects categorized into hyperglycemic (n=30) and normal subjects (n=22). Lipid species were determined from the following classes: cholesterol esters (CE), ceramides (CER), diacylglycerols (DAG), dihydroceramide (DCER), free fatty acids (FFA), hexosylceramides (HCER), lactosylceramides (LCER), lysophosphatidylcholines (LPC), lysophosphatidylethanolamines (LPE), phosphatidylcholines (PC), phosphatidylethanolamines (LPE), sphingomyelins (SM), and triacylglycerols (TAG).
After normalizing by the sum of total apolipoprotein A and apolipoprotein B (to account for the possibility of reduced particle number due to medicinal intervention), lipids both by class and species were

compared using one way analysis of variance. On a class level, relative to normal subjects, hyperglycemic patients showed increased levels of CER and FFA. Individual lipid species of these classes that were higher in hyperglycemic patients include CER(18:0), CER(20:0), CER(24:1), FFA(16:0), FFA(16:1), FFA(18:0), FFA(18:1), FFA(18:2), FFA(18:3), and FFA(20:3) Differences were also found in SM concentrations between hyperglycemic and normal patients resulting in a higher the SM/PC ratio, indicating changes in the lipid fluidity of the shell in lipoprotein particles of hyperglycemic patients. On a species level, SM(16:0), SM(18:1), and SM(24.1), were elevated in hyperglycemic subjects relative to normal subjects. This finding of elevated unsaturated SM species in hyperglycemic patients is at odds with other studies where it was found that the saturated SM moieties were elevated in insulin resistant subjects.

Disclosures: **J. Rees:** None. **S. Kuklenyik:** None. **M. Gardner:** None. **D. Schieltz:** None. **B.A. Parks:** None. **J. Jones:** None. **C. Toth:** None. **L. McWilliams:** None. **M. Andrews:** None. **J.R. Barr:** None.

569

Albuminuria, the HDL Proteome, and Prevalent Coronary Artery Calcium in Type 1 Diabetes

Baohai Shao, Leila Zelnick, Jake Wimberger, John Brunzell, Jonathan Himmelfarb, Karin E. Bornfeldt, Ian H. de Boer, Jay W. Heinecke, Univ of Washington, Seattle, WA

Patients with type 1 diabetes (T1D) are at high risk of atherosclerotic cardiovascular disease (CVD). Albuminuria is strongly associated with CVD risk and fully accounts for the excess overall mortality risk in some T1D cohorts. One important contributor might be alterations of the HDL proteome. In the current study, we tested the hypotheses that albuminuria is associated with alterations in the HDL proteome in T1D, and that these alterations are associated with prevalent CVD. We performed a cross-sectional study of 191 Diabetes Control and Complications Trial/Epidemiology of Diabetes Interventions and Complications (DCCT/EDIC) participants selected according to levels of urine albumin excretion (67 persistent normoalbuminuria, 64 persistent microalbuminuria, and 60 persistent macroalbuminuria). We used targeted proteomics and isotope dilution tandem-mass spectrometry to quantify the concentration of 47 proteins in HDL. Adjusting for age, sex, DCCT treatment group, duration of diabetes, lipid-lowering medications, renin-angiotensin system inhibitors, smoking, BMI, and HbA1c, and after accounting for multiple comparisons, six proteins in HDL were significantly associated with albuminuria (2 increased and 4 decreased). For example, compared to normoalbuminuria, macroalbuminuria was associated with 57% and 177% higher AMBP (P=0.0003) and PTGDS (P=0.0006), respectively, and 28% and 27% lower PON1 (P=0.002) and PON3 (P=0.008), respectively. Furthermore, PON1 and PON3 in HDL were strongly and negatively associated with the presence of coronary artery calcium, with odds ratios per 1-SD difference of 0.63 (0.43-0.92, 95% CI, P=0.02) for PON1 and 0.59 (0.40-0.87, 95% CI, P=0.008) for PON3. Our observations indicate that the HDL proteome is remodeled in albuminuric patients with T1D, and that these alterations in HDL's protein cargo may mediate, in part, the relationship of albuminuria with CVD. Because PON1 and PON3 are anti-atherogenic in hypercholesterolemic mice, our data suggest that low levels of PON1 and PON3 in HDL increase the risk of atherosclerosis in diabetic humans. In future studies, it will be important to determine whether reductions of PON1 and PON3 in HDL predict the risk of future CVD in subjects with T1D.

Disclosures: **B. Shao:** None. **L. Zelnick:** None. **J. Wimberger:** None. **J. Brunzell:** None. **J. Himmelfarb:** None. **K.E. Bornfeldt:** None. **I.H. de Boer:** None. **J.W. Heinecke:** None.

570

Macrophage Catabolism of Aggregated Lipoproteins Using a Novel Extracellular Compartment Regulates Lipid Accumulation During Atherosclerosis

Rajesh K Singh, Abigail S Haka, Valeria C Barbosa-Lorenzi, Arky Asmal, Frederik Lund, Yuquan Xiong, Harvey F Chin, Inna Grosheva, Timothy Hla, Frederick R Maxfield, Weill Cornell Medical Coll, New York, NY

Despite impressive advances in research, prevention, and treatment, atherosclerotic vascular disease remains the leading cause of death in the developed world. Mechanisms of cholesterol accumulation in the arteries have been studied intensively, but the *in vivo* contributions of different pathways leading to lipid accumulation and foam cell formation are not understood. In the arteries, low-density lipoprotein (LDL) is aggregated and bound to the extracellular matrix. When such aggregated LDL is presented to

macrophages, they form a novel acidic, hydrolytic compartment that is topologically extracellular, to which lysosomal enzymes are secreted. Such compartments are observed *in vivo* in murine atherosclerotic plaque macrophages interacting with cholesterol rich deposits. Using state-of-the-art quantitative and high resolution microscopy techniques, characterization of compartment morphology reveals how macrophages use local actin polymerization to drive plasma membrane remodeling at the interface with aggregated LDL. This leads to sequestration of aggregated LDL into topologically convoluted structures that allow acidification, catabolism and internalization of LDL. We find that a TLR4/MyD88/Syk/PI3 kinase/Akt dependent signaling pathway in macrophages regulates the formation of such catabolic compartments. Consistent with this, deficiency of TLR4 *in vivo* can protect macrophages from lipid accumulation in murine atherosclerotic plaques. Herein, we provide compelling evidence for a novel form of catabolism that macrophages use to degrade aggregated LDL *in vivo* during atherosclerosis and this process leads to foam cell formation, cell death and promotes disease progression.

Disclosures: **R.K. Singh:** None. **A.S. Haka:** None. **V.C. Barbosa-Lorenzi:** None. **A. Asmal:** None. **F. Lund:** None. **Y. Xiong:** None. **H.F. Chin:** None. **I. Grosheva:** None. **T. Hla:** None. **F.R. Maxfield:** None.

This research has received full or partial funding support from the American Heart Association.

571

Short Term Taste Preference for Cholesterol Rich Diet in ABCA1 Null Mice

Maki Tsujita, Shinya Ugawa, Nagoya City Univ Graduate Sch of Medical Scienses, Nagoya, Japan; Shinji Yokoyama, Nutritional Health Science Res Ctr, Chubu Univ, Kasugai, Japan

Background: Plasma HDL particle is one of the essential player for maintaining cholesterol homeostasis in mammal. Even though cholesterol can be ubiquitously biosynthesized upon requirement, cholesterol in diet is efficiently used to maintain cholesterol homeostasis which implicates existence of sensing system for cholesterol in diet. The study of taste preference on cholesterol was not well explored. In this project we examined taste preference in mice using a novel method called dual diet test (DDT) system. Methods: Chow pellets of 1.2% cholesterol or 0.02% Acesulfame potassium (AmK, calorie-free sweet molecule) were prepared based on standard mouse chow, CE-2(0.2% cholesterol, Crea Japan). The mouse chow tray was divided into three sections. Water nozzle was set in the center section. Each chow was weighed then set ether right or left section. One session was composed by 1-3 days and remaining chow was weighed to calculate consumption of each chow diet. The diet position was switched randomly at each session. The operation was performed between ZT9-ZT10 when mice were less active in a day. To avoid social isolation stress, 2-5 littermates were placed per cage. Results: C56B/6 wild type mice and LCAT null mice significantly preferred 1.2% cholesterol containing chow compared to control chow during 6 sessions by 18-28 weeks old littermates (n=16, n=8, respectively). These mice also significantly preferred AmK-chow compared to the control chow. ABCA1 null and ABCA1 heterozygote mice exhibited significance on the preference of 1.2% cholesterol in the first 3 sessions but not for the later sessions. Repeating the experiment after interval period improved their cholesterol preference in ABCA1 null mice. No gender difference was observed. Preferences to AmK-chow were significant in all trials. Conclusions: The preference in higher cholesterol or sweet in diet were detected at this novel DDT system, significantly. In ABCA1 null or heterozygote mice, long-term preferences to high cholesterol diet were abolished perhaps due to their lack of focus on cholesterol-rich chow of which less reward to these mice. In this experiment, mice synchronized in consuming higher cholesterol containing diet indicating mice are sensing cholesterol as a preferred tastant.

Disclosures: **M. Tsujita:** None. **S. Ugawa:** None. **S. Yokoyama:** None.

572

The Effect of Inflammation and Soluble Epoxide Hydrolase Inhibition on Fatty Acid Epoxide Incorporation Into VLDL

Rachel E Walker, Pennsylvania State Univ, University Park, PA; Olga V Savinova, New York Inst of Technology, Old Westbury, NY; Theresa L Pedersen, Advanced Analytics, Davis, CA; John W Newman, USDA ARS Western Human Nutrition Res Ctr, Davis, CA; Gregory C Shearer, Pennsylvania State Univ, University Park, PA

OBJECTIVE: We have previously observed fatty acid epoxides, a class of potent anti-inflammatory oxylipins, in circulating VLDL. The source of these epoxides is unknown. Cytochrome P450 (CYP450) produces them via oxygenation of polyunsaturated fatty acids (PUFAs), and soluble epoxide hydrolase (sEH) converts them to diols. Our objectives were 1) to investigate if incorporation of epoxides into VLDL occurs via hepatic VLDL synthesis and 2) to determine if incorporation is modulated by inflammation or by inhibition of hepatic sEH.
APPROACH AND RESULTS: A 2×2 factorial design was used for treatment assignment. Livers were isolated from rats treated with pro-inflammatory lipopolysaccharide (LPS, 10 mg/kg ip) or saline. AUDA, an inhibitor of sEH (10 µM), was included or excluded in the perfusate (Control, N=3; LPS, N=4; AUDA, N=4; LPS+AUDA, N=4). Livers were perfused for 180 minutes. VLDL was isolated by ultra-centrifugation, then analyzed by LC-MS/MS for oxylipin content. Analyzed epoxides and diols were derived from alpha-linolenic acid (ALA), linoleic acid (LA), arachidonic acid (AA), eicosapentaenoic acid (EPA), and docosahexaenoic acid (DHA). Two-way ANOVA's were used with triglyceride concentration as a covariate. Concentrations (nM) are reported as mean [95% CI]. DHA-derived epoxides increased with AUDA treatment (3.91 [3.01, 5.07]) compared to livers without AUDA (2.06 [1.58, 2.67]) (p=0.004), but other epoxides were unchanged by AUDA. EPA and ALA-derived epoxides decreased with LPS treatment (0.32 [0.22, 0.47]; 2.44 [2.07, 2.87]) compared to animals without LPS (0.73 [0.46, 1.16]; 3.28 [2.71, 3.96]) (p=0.01; 0.02). AA and DHA-derived diols decreased with LPS treatment (1.01 [0.82, 1.25]; 0.21 [0.17, 0.26]) compared to animals without LPS (1.46 [1.15, 1.86]; 0.31 [0.24, 0.39]) (p=0.03; 0.03).
CONCLUSIONS: Treatment with LPS and AUDA have significant effects on incorporation of epoxides and diols into VLDL, supporting hepatic incorporation controlled by inflammation. Inflammation decreased select EPA- and ALA-derived epoxides. In contrast, sEH inhibition increased only DHA-derived epoxides. Surprisingly, in VLDL only epoxides derived from omega-3 fatty acids were affected by either inflammation or inhibition of sEH.

Disclosures: **R.E. Walker:** None. **O.V. Savinova:** None. **T.L. Pedersen:** None. **J.W. Newman:** None. **G.C. Shearer:** None.

573

Human Microrna-548p Decreases apoB Secretion and Lipid Synthesis

Liye Zhou, Mahmood Hussain 11203, SUNY Downstate Medical Ctr, Brooklyn, NY

Objective: MicroRNAs (miRs) play important regulatory roles in lipid and lipoprotein metabolism. ApoB, as the only essential scaffolding protein in the assembly of very low density lipoproteins, is a target to treat hyperlipidemia and atherosclerosis. We aimed to find out miRs that reduce apoB expression. **Approach:** Bioinformatics analyses predicted that hsa-miR-548p can interact with apoB mRNA.MiR-548p mimic and control were transfected in human and mouse hepatoma cell lines to test its role in regulating apoB secretion and mRNA expression levels. Site-directed mutagenesis was used to identify the interacting site of miR-548p in human apoB 3´-untranslated region. Fatty acid oxidation and lipid syntheses were examined in miR-548p overexpressing cells to investigate its function in lipid metabolism. **Results:** Experimentally, we observed that miR-548p significantly reduces apoB secretion from human hepatoma cells in time and dose dependent manner. Mechanistic studies showed that miR-548p interacts with the 3´-untranslated region of human apoB mRNA to enhance posttranscriptional degradation. Bioinformatics algorithms suggested two potential binding sites of miR-548p on human apoB mRNA. Site-directed mutagenesis studies revealed that miR-548p targets site II involving both seed and supplementary sequences. MiR-548p had no effect on fatty acid oxidation but significantly decreased lipid synthesis in human hepatoma cells by reducing the expression of HMGCR and ACSL4 enzymes involved in cholesterol and fatty acid synthesis. In summary, miR-548p reduces lipoprotein production and lipid synthesis by reducing expression of different genes in human hepatoma cells. **Conclusion:** These

studies suggest that miR-548p could be useful in treating atherosclerosis, hyperlipidemia and hepatosteatosis.

Disclosures: **L. Zhou:** None. **M. Hussain:** None.

This research has received full or partial funding support from the American Heart Association.

574

High-Density Lipoproteins Suppress Amyloid Beta Induced Human Brain Microvascular Endothelial Cell Activation

Emily B Button, Jerome Robert, Sophie K Stukus, Guilaine Boyce, Ebrima Gibbs, Catherine Cowan, Wai Hang Cheng, Sonja Soo, Brian Yuen, Kevin Kang, Arvin Bahrabadi, Iva Kulic, Gordon Francis, Neil Cashman, Cheryl L Wellington, Univ of British Columbia, Vancouver, BC, Canada

Introduction
Epidemiological studies suggest a link between plasma high-density lipoprotein (HDL) cholesterol levels and Alzheimer's disease (AD) risk through mechanisms that are not understood. We hypothesize that HDL protects against AD through actions at the blood-brain-barrier. HDL has vasoprotective functions in large peripheral arteries, however, it is unknown if these functions extend to cerebral vessels to reduce the contribution of cerebrovascular dysfunction in AD pathogenesis. We investigated *in vitro* interactions between HDL and amyloid beta (Aβ), the toxic peptide known to accumulate in AD, in peripheral and brain-derived endothelial cells (EC).
Methods
HDL was isolated by density gradient ultracentrifugation and added to human umbilical vein endothelial cells (HUVEC) or human cerebral microvascular endothelial cells (hCMEC/D3). Cell activation was measured by counting adhered labelled peripheral blood mononuclear cells (PBMC) after stimulation with tumour necrosis factor α (TNFα) or Aβ. Aβ binding and uptake into cells was measured using ELISA and immunofluorescence. All experiments included at least 4 independent replicates.
Results We demonstrate that HDL attenuates Aβ-induced EC activation independent of nitric oxide production, miR-233 and changes in adhesion molecule expression. Rather, HDL acts through scavenger receptor BI to block Aβ uptake into ECs and, *in vitro*, can maintain Aβ in a soluble state. We validated our results using three dimensional engineered vessels composed of primary human endothelial and smooth muscle cells. Following Aβ addition to the abluminal (brain) side, we demonstrated that HDL circulated within the lumen attenuates EC activation, again independent of intracellular adhesion molecule changes.
Conclusions We show that the anti-inflammatory activities of HDL extend to cerebrovascular endothelial cells and work to suppress Aβ-induced activation through a novel mechanism involving the inhibition of Aβ binding and uptake into cells through SR-BI. The protective role for HDL against Aβ may explain the epidemiological evidence supporting a protective effect of high plasma HDL cholesterol levels against dementia.

Disclosures: **E.B. Button:** None. **J. Robert:** None. **S.K. Stukus:** None. **G. Boyce:** None. **E. Gibbs:** None. **C. Cowan:** None. **W. Cheng:** None. **S. Soo:** None. **B. Yuen:** None. **K. Kang:** None. **A. Bahrabadi:** None. **I. Kulic:** None. **G. Francis:** None. **N. Cashman:** None. **C.L. Wellington:** None.

575

ApoE Determines the Functional Fate of ApoC-III: Hepatic Clearance vs. Lipase Activity

Bastian Ramms, Chelsea Nora, Norah Al-assam, Univ of California, San Diego, La Jolla, CA; Mark Graham, Ionis Pharmaceuticals, Carlsbad, CA; **Philip Gordts**, Univ of California, San Diego, La Jolla, CA

Clearance of triglyceride (TG)-rich lipoproteins (TRLs) is mediated by three main receptors syndecan-1 (SDC1), low-density lipoprotein receptor (LDLR) and LDLR-related protein 1 (LRP1). Previous studies revealed that interactions of apolipoprotein (apo) E and apoA-V on TRLs with heparan sulfate chains of SDC1 are required for TLR clearance. ApoC-III is another apolipoprotein and emerging factor in regulating TG metabolism. We recently showed that apoC-III inhibits hepatic TRL clearance through the LDLR/LRP1 axis and that apoC-III accumulates on TRLs in mutant mice lacking functional SDC1 (*Ndst1*$^{f/f}$*Alb-Cre*$^{+}$), suggesting that apoC-III enriched TRLs are preferentially cleared by SDC1. In this study we determined the impact of apoE, a common ligand for all three receptors, on apoC-III metabolism. In *Apoe*$^{-/-}$*Ndst1*$^{f/f}$*Alb-Cre*$^{+}$ mice antisense oligonucleotide (ASO) lowering of apoC-III reduced

plasma TG levels. In contrast to *Ndst1*$^{f/f}$*Alb-Cre*$^{+}$ mice the apoC-III ASO was not associated with improved hepatic TRL clearance in [^{3}H]retinol excursion studies in *Apoe*$^{-/-}$*Ndst1*$^{f/f}$*Alb-Cre*$^{+}$ mice. Binding and uptake experiments in primary hepatocytes with apoE-deficient TRLs were not affected by the presence or absence of apoC-III. Reconstitution of the same TRLs with apoE inhibited clearance only of apoC-III enriched TRLs indicating that apoE is essential for apoC-III-mediated inhibition of TRL clearance. Further analysis revealed that apoC-III ASO improved lipase activity in *Apoe*$^{-/-}$*Ndst1*$^{f/f}$*Alb-Cre*$^{+}$ mice. It remains to be determined if apoC-III lowering in the absence of apoE stimulates lipoprotein lipase or hepatic lipase or both. In conclusion we demonstrate that apoC-III blocks TRL clearance in an apoE-dependent manner and inhibits lipase activity in the absence of functional apoE.

Disclosures: **B. Ramms:** None. **C. Nora:** None. **N. Al-assam:** None. **M. Graham:** Employment; Significant; Ionis Pharmaceuticals. **P. Gordts:** Research Grant; Significant; Ionis Pharmaceuticals.

This research has received full or partial funding support from the American Heart Association.

576

Salicylamine, A γ-ketoaldehyde Scavenger, Improves HDL Function and Reduces Atherosclerosis in Apoe Deficient Mice

Jiansheng Huang, Patricia Yancey, Lei Ding, Youmin Zhang, John Oates, Venkataraman Amarnath, Jackson Roberts II, Sean Davies, MacRae F. Linton, Vanderbilt Univ, Nashville, TN

Background: Lipid peroxidation products impair the cholesterol efflux capacity of high-density lipoprotein (HDL) and promote the development of atherosclerosis. The impact of inhibition of malondialdehyde (MDA)-HDL adduct formation by scavengers on HDL function and whether small molecule aldehyde scavengers protect against the development of atherosclerosis was examined.
Methods and Results: Western blot analysis of ApoAI revealed that the amount of ApoAI crosslinking increased with MDA concentration. In the presence of LPS, MDA-HDL (HDL modified by 1mM MDA) versus control HDL stimulated 2- and 1.8-fold more expression of TNF-α and IL-1β in *Apoe-/-* macrophages demonstrating that MDA-HDL has reduced anti-inflammatory function. HDL-mediated macrophage cholesterol efflux was decreased by ~ 42%, 55%, 70%, and 80%, respectively, for HDL modified with 0.125 mM, 0.25 mM, 0.5 mM, and 1mM MDA, demonstrating that MDA modification of HDL affects its cholesterol efflux capacity in a dose dependent manner. Analysis by Western blot demonstrated that 5mM of salicylamine (SAM) and 5mM of pentylpyridoxamine (PPM), γ-ketoaldehyde scavengers, attenuated MDA mediated crosslinking of apoA-I in HDL (molar ratio of MDA and HDL is 1:5) by 60% and 80 % ($P<0.05$), respectively. Both SAM and PPM maintained the cholesterol efflux capacity of MDA treated HDL in *Apoe-/-* macrophages. In addition, pretreatment of LDL with SAM prevented MDA-ApoB adduct formation, and compared to incubation with LDL containing MDA-ApoB adducts, SAM treatment resulted in 57% less cholesterol accumulation in J774 macrophages. Importantly, administration of the ketoaldehyde scavenger, SAM, versus the nonreactive analogue, 4-SAM, to *Apoe-/-* mice consuming a Western diet for 16 weeks reduced the extent of proximal aortic atherosclerosis by 28% ($P<0.05$).
Conclusions: Treatment with salicylamine, a γ-ketoaldehyde scavenger: 1) inhibits MDA-ApoA1 adduct formation thereby preserving HDL cholesterol efflux capacity; 2) prevents MDA-apoB100 formation resulting in less macrophage cholesterol accumulation; 3) reduces atherosclerosis in *Apoe*$^{-/-}$ mice. These results support the therapeutic potential of salicylamine in the treatment of atherosclerotic cardiovascular disease.

Disclosures: **J. Huang:** None. **P. Yancey:** None. **L. Ding:** None. **Y. Zhang:** None. **J. Oates:** None. **V. Amarnath:** None. **J. Roberts II:** None. **S. Davies:** None. **M.F. Linton:** None.

577

MicroRNA-30c Reduces Plasma Cholesterol in Different Hypercholesterolemic and Hyperglycemic Mouse Models

Sara Irani, Jahangir Iqbal, SUNY Downstate Medical Ctr, New York, NY; **M.Mahmood Hussain**, Winthrop Univ Hosp, Mineola, NY

High plasma cholesterol levels are found in several metabolic disorders and their reductions are advocated to reduce risk of atherosclerosis. A way to lower plasma lipids is to curtail lipoprotein assembly

and secretion; however, this is associated with steatosis. We have shown that microRNA-30c (miR-30c) reduces Western diet-induced hypercholesterolemia and atherosclerosis in C57BL/6J and *Apoe*$^{-/-}$ mice with no obvious adverse effects by reducing hepatic lipoprotein production and lipid synthesis. Here, we tested the effect of miR-30c on plasma lipids, transaminases and hepatic lipids in five different mouse models. Hepatic delivery of miR-30c reduced MTP activity but did not affect plasma cholesterol, triglyceride and glucose in chow-fed C57Bl6J and streptozotocin-induced diabetic, normolipidemic mice. However, hepatic delivery of miR-30c to chow fed leptin deficient (*ob/ob*) and leptin receptor deficient (*db/db*) hypercholesterolemic and hyperglycemic type 2 diabetic mice reduced cholesterol in total plasma and VLDL/LDL by ~ 28%and ~ 25%, respectively, without affecting phospholipid, triglyceride and glucose levels. Interestingly, these mice had lower plasma transaminases and creatine kinases indicating possible beneficial effects. Mechanistic studies showed that miR-30c reduced hepatic MTP activity and lipid synthesis. Moreover, miR-30c significantly lowered plasma cholesterol and atherosclerosis in Western-diet fed low density lipoprotein receptor knockout mice with no effect on plasma triglyceride, glucose and transaminases, suggesting that miR-30c can be a potential therapeutic agent for homozygous familial hypercholesterolemia. In all these studies, hepatic lipid levels were similar in control and miR-30c injected mice. These studies indicate that miR-30c reduces plasma cholesterol in diet-induced and diabetic hyperholesterolemic mice but not in normocholesterolemic mice. Thus, miR-30c may be beneficial in lowering plasma cholesterol in different metabolic disorders independent of the origin of hypercholesterolemia.

Disclosures: **S. Irani:** None. **J. Iqbal:** None. **M. Hussain:** None.

This research has received full or partial funding support from the American Heart Association.

579

In vitro Models Concur with Clinical Results to Confirm Pleiotropic Mechanisms of Action for Gemcabene

Daniela C Oniciu, Charles L Bisgaier, Gemphire Therapeutics Inc., Livonia, MI

Introduction. Gemcabene, a fraudulent fatty acid, induces biological properties in nonclinical models, of which many translate to clinical findings in dyslipidemia patients. Its known mechanism of action includes reduction of the overall hepatic *de novo* triglyceride and cholesterol synthesis, and increase in VLDL clearance. Clinical benefits in various human populations infer that other mechanisms are involved that warrant evaluation.
Methods and Results. We assessed the gemcabene effects in other molecular mechanistic models, particularly to study inhibition of human ATP Citrate Lyase (hACL), apolipoprotein gene expression in Sandwich-Cultured Transporter Certified™ Human Hepatocytes (SCHH), and expression of genes related to inflammation and cell signaling.
Gemcabene, MEDICA-16, palmitic acid and their CoA thioesters were studied in a recombinant hACL in vitro assay system. Gemcabene-CoA thioester, but not the parent compound, inhibited recombinant hACL activity in vitro in a dose-dependent manner, in agreement with results obtained with palmitoyl-CoA and palmitic acid. Unlike palmitic acid, MEDICA-16, and bempedoic acid, gemcabene does not form a CoA ester in human hepatocytes: radioisotope studies show 98.8% parent gemcabene.
Further, gemcabene potential on the gene expression of lipogenesis and inflammation markers was assessed in SCHH. Gemcabene showed significant regulation of HMG-CoA synthase 2 (HMGCS2) and CRP mRNAs. A marked induction response of the HMGCS2 mRNA content was observed, ranging from 2.26- to 2.73-fold ($p \leq 0.05$) over control in SCHH treated with all concentrations of gemcabene (500, 1000, and 1500 µM). Also, a clear and statistically significant (p-value ≤ 0.05) concentration-related suppression response of CRP mRNA content was observed, ranging from (-2.58)- to (-2.65)-fold below control in SCHH treated with 1000 and 1500 µM gemcabene.
Finally, RT-PCR analysis of liver samples from STAM™ mice treated with gemcabene revealed its downregulating effect on inflammatory, lipogenic, lipoprotein metabolism, and cell signaling genes: TNF-α, MCP-1, NF-κB, ApoC-III, and ACC1.
Conclusion. Gemcabene manifests its pharmacological profile in lipid management and inflammation by multiple mechanisms of action.

Disclosures: **D.C. Oniciu:** Employment; Significant; employee. **C.L. Bisgaier:** Employment; Significant; employee.

580

Acidic Domain of ApoB-100 and Other Short Negatively Charged Peptides Anchored to Lipoproteins Cause Hypertriglyceridemia in Mice

Denis O Sviridov, Puja Terse, Anna Wolska, Scott M Gordon, Alan T Remaley, NIH, Bethesda, MD

Human Apolipoprotein B-100 (ApoB-100) is the main protein of VLDL and LDL particles in plasma. It is a large 4536 amino acid protein with various structural domains, such as the LDL-receptor binding motif and multiple proteoglycan binding sites, all of which have a high positive charge. A search of the primary amino acid sequence of ApoB-100 revealed the presence of the following acidic domain: DMDEDDD (AA 3985-3991). We hypothesized that this motif could affect the interaction of ApoB-containing lipoproteins with liver and or possibly GPIHBP1, which also contains an acidic domain that interacts with the positive charged motifs on VLDL. We synthesized a fluorescent tagged DMDEDDD peptide and conjugated it at the N-terminus with two molecules of alpha-tocopherol to serve as an anchor to lipoprotein particles. After adding the peptide to human plasma, it was found to readily bind to all lipoproteins, as determined by FPLC analysis. VLDL incubated with the peptide showed an increased negative charge and lost its ability to bind to heparin as determined by chromatography on a HiTrap™ heparin column. The peptide injected in LDLr-KO mice (30 mg/kg) caused a rapid 3-fold increase in plasma triglycerides within 1 h and the triglyceride elevation persisted for at least 24 h. A similarly designed negative charged peptide attached to tocopherol (EEEEEEEE) also raised triglycerides in mice but a neutral charged control peptide (KEKEKEKE) did not. To understand the mechanism, we tested the above peptides for their ability to inhibit LPL, using an in vitro assay with intralipid as a substrate and found that negative charged peptides inhibited lipolysis (IC_{50}=50 uM), but the neutral control peptide did not. We are now investigating other potential mechanisms for how acidic peptides may cause hypertriglyceridemia. In summary, a peptide based on an acidic domain on ApoB-100 appears to cause hypertriglyceridemia in mice by inhibition of LPL and possibly by interfering with proteoglycan binding of lipoproteins. These results may be relevant in understanding VLDL metabolism and for the design of therapeutic apolipoprotein mimetic peptides.

Disclosures: **D.O. Sviridov:** None. **P. Terse:** None. **A. Wolska:** None. **S.M. Gordon:** None. **A.T. Remaley:** None.

581

Smooth Muscle Cell Specific Loss of the Pluripotency Factor Oct4 Enhances Atherosclerosis via Shifting Smooth Muscle Cells to a Less Migratory, but More Proinflammatory Phenotype

Olga A Cherepanova, Gabriel Falcao Alencar, Svyatoslav M Tkachenko, Stefan Bekiranov, Gary K Owens, Univ of Virginia, Charlottesville, VA

Atherosclerosis is the leading cause of death in Western civilization accounting for more than 40% of all deaths. Despite reduced death rates due in part to statin treatment, there is little understanding of the molecular and cellular mechanisms that can help to reverse atherosclerotic development and/or decrease the chances of plaque rupture with associated clinical sequelae such as myocardial infarction or stroke. We recently demonstrated a functional role of the pluripotency factor OCT4 in smooth muscle cells (SMCs) during atherosclerosis, in that SMC-specific conditional *Oct4* knockout mice exhibit marked alterations in lesion size and cellular composition within atherosclerotic lesions of *Apoe*$^{-/-}$ high-fat diet fed mice, including a thinner fibrous cap, increased necrotic core and increased intra-plaque hemorrhage. Results of SMC-lineage tracing studies show that these changes were likely due to marked reductions in SMC number within lesions including in the fibrous cap area, as well as significant increases in macrophage-like (LGALS3^{+}) SMCs within the tunica media. Further studies show that inactivation of *Oct4* in SMCs nearly completely abrogated the pro-atherogenic oxidized phospholipid POVPC-induced migration of SMCs *in vitro* and outgrowth of SMCs from aortic explants *ex vivo.* RNA-seq and ChIP-seq analyses of lesion specimens from *Apoe*$^{-/-}$ high-fat diet fed mice and cultured SMCs treated with POVPC or 1% O_2 hypoxia show that loss of *Oct4* in SMCs was associated with marked activation of genes associated with inflammation and phagocytosis, and suppression of genes associated with cell migration, including extracellular matrix proteins, matrix metalloproteinases and multiple axon guidance molecules. Moreover, loss of *Oct4* significantly increased ability of SMCs to phagocyte red blood cells in response to oxidized LDL treatment *in vitro*. Results advance our understanding of mechanisms by which OCT4 expression in SMCs impacts atherosclerosis lesion development and may help identify novel potential therapeutic targets for treatment of atherosclerosis.

Disclosures: **O.A. Cherepanova:** None. **G. Falcao Alencar:** None. **S.M. Tkachenko:** None. **S. Bekiranov:** None. **G.K. Owens:** None.

This research has received full or partial funding support from the American Heart Association.

582

The CCR7+ PDGFRa+ Cell Population is Increased in Regressing Atherosclerotic Plaques

France Dierick, Talin Ebrahimian, Stefania Simeone, David Simon, Veronique Michaud, Stephanie Lehoux, Lady Davis Inst, Montreal, QC, Canada

Introduction: Atherosclerosis is characterized by the accumulation of lipids, cells and fibers in the arterial wall. Atherosclerotic plaques form in regions of low blood flow, whereas vessels exposed to high blood flow remain lesion-free. We created a surgical mouse model, arteriovenous fistula (AVF), which increases blood flow in the brachiocephalic artery (BCA) specifically, without altering serum lipid levels. Methods & Results: LDLR KO mice were placed on a high-fat diet (HFD). Control mice were sacrificed at week 12. Sham and AVF surgery was performed at week 12 and mice were kept on a HFD for a further 1-4 weeks. We found that high blood flow is beneficial and leads to a significant ~50% regression of BCA plaque size in AVF mice compared with Controls, by week 4. We performed flow cytometry to characterize the different cell populations within Sham and AVF plaques. At day 7 after surgery, there was no difference in macrophage (F4/80+) or dendritic cell (CD11c+) content between Sham and AVF. However, we found a significant, 4-fold increase in the total number of CD45-/CCR7+/PDGFRa+ cells in the BCA plaques of AVF mice vs Shams ($p<0.01$). No such change was observed in the aortic sinus plaques of AVF or Shams. CCR7 was previously found to be overexpressed in regressing plaques upon an abrupt lowering of plasma lipids, but in CD45+ cells. In our model, plasma lipids remained high and CCR7+ cells instead expressed PDGFRa, a perivascular and multi-lineage differentiation marker. This cell population also expressed mesenchymal stem cell markers (CD90, CD44, CD34) and CD68. Conclusion: Our data point to an unexpected increase in the CD45-/CCR7+/PDGFRa+ cell population in the early plaque regression process. They suggest that mesenchymal-type cells may promote regression in plaques exposed to high blood flow.

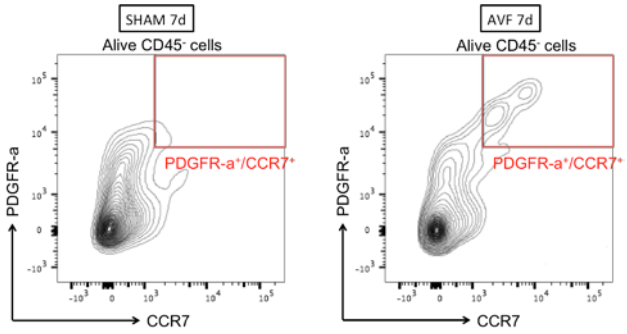

Disclosures: **F. Dierick:** None. **T. Ebrahimian:** None. **S. Simeone:** None. **D. Simon:** None. **V. Michaud:** None. **S. Lehoux:** None.

584

Allograft Inflammatory Factor-1 is Required for NfκB Pathway Activity in Macrophages and Atherosclerosis

Lander Egaña-Gorroño, Prameladevi Chinnasamy, Nicholas Sibinga, Albert Einstein Coll of Med, Bronx, NY

Introduction: In preliminary studies, we found that Allograft inflammatory factor-1 (AIF1) supports MΦ migration, phagocytosis, survival and pro-inflammatory cytokine secretion. Moreover, AIF1 limits necrotic core formation in atherosclerotic lesions *in vivo*. Nuclear Factor-κB (NFκB)-mediated signal transduction has been established at different stages of atherosclerosis. We hypothesize that AIF1-regulated

processes in atherosclerosis may be mediated through effects on NFκB signaling.
Methods: Bone marrow (BM) derived MΦs were isolated and immortalized from wt and *Aif1*$^{-/-}$ mice and stimulated with oxidized-LDL (50 ug/ul; oxLDL). Lysates were immunoblotted for total and phosphorylated (active) p65 NFκB, and for total and phosphorylated forms of the IκBα repressor. *Aif1* expression in mouse Raw 264.7 cells was knocked down (KD) using siRNA, and NFκB reporter activity, measured by a luciferase reporter, was assessed after adding LPS+IFN-γ. Immunohistochemical analysis for phospho-p65 NFκB was performed in atherosclerotic lesions (aortic roots) from *Apoe*$^{-/-}$ (SKO) and *Apoe*$^{-/-}$*;Aif1*$^{-/-}$ (DKO) mice maintained on high fat diet for 16 weeks.
Results: In AIF1-deficient BMMΦs stimulated with oxLDL, we found no differences in the levels of total p65 NFκB and IκBα, but interestingly, phospho-p65 NFκB levels were significantly reduced and phospho-IκBα levels increased compared to wt cells (P<0.05). AIF1 KD using siRNA significantly reduced NFκB activity compared to scrambled control (scrambled control vs. AIF1 KD; 40% vs. 22% luciferase activity, P<0.05), and this impairment was rescued with the addition of AIF1 cDNA. *In vivo*, NFκB phospho-p65 staining showed that in comparison to SKO samples, DKO aortic roots had decreased phospho-p65 NFκB (SKO vs. DKO; 7.0 vs. 4.0 +nuclei/aortic root, P<0.05).
Conclusions: AIF1 is required for NFκB activation in MΦs and moreover, AIF1 enhances NFκB activity in atherosclerotic lesions *in vivo*. Because NFkB has been closely linked to both cytokine expression and cell survival signaling, these results point to a critical role for AIF1 in pro-inflammatory MΦ functions. Future studies involve identifying the precise steps of the pathway controlled by AIF1, and the mechanisms by which AIF1 affects NFκB signaling.

Disclosures: **L. Egaña-Gorroño:** None. **P. Chinnasamy:** None. **N. Sibinga:** None.

585

Mathematical Modelling of Monocytes and Monocyte-Derived Cells in Inflammation Shows Cholesterol Biomagnification as a Determinant of Atherosclerotic Plaque Fate

Hugh Ford, Univ of Sydney, Sydney, Australia

Efferocytosis recycles substances, such as cholesterol, from apoptotic monocytes and monocyte-derived macrophages (Mo/Mphi) back into the Mo/Mphi population. Without net removal, these substances will concentrate within successive generations of Mo/Mphis --- a biomagnification process seldom explored in inflammation. We propose that biomagnification of cholesterol within the Mo/Mphi population is an important feature of atherosclerotic plaque progression by gradually enhancing inflammation and necrosis over time.
We have developed a mathematical model of Mo/Mphi in inflammation where a population of Mo/Mphi is modelled with a distribution of internalised lipids in the population. We use this to explore the relationship between cholesterol accumulation and plaque fate. Although the number of Mo/Mphis in the plaque remains stable when the rates of recruitment and proliferation are balanced by apoptosis and egress, lipid dynamics (such as cholesterol bioaccumulation) within this system may change. The model can be used to investigate the conditions when lipids are and are not stably trafficked between Mo/Mphi and apoptotic Mo/Mphi. Destabilisation of lipid dynamics results in a continuous throughput of material from Mo/Mphi and apoptotic Mo/Mphi to the necrotic core. These conditions include the amount of modified LDL relative to HDL, the propensity of Mo/Mphi to replicate and to leave the plaque. Surprisingly Mo/Mphi proliferation provides a highly protective mechanism by halving accumulated cholesterol between two daughter cells and doubling the phagocytic capacity of the parent cell. Overall the technique of mathematical modelling offers novel insights into both plaque pro- and regression. We will conclude with a discussion on how the theory of biomagnification extends to all innate inflammatory systems.

Disclosures: **H. Ford:** None.

586

CD40L on T Cells is a Major Contributor to Atherosclerosis in Hyperlipidemic Mice

Norbert Gerdes, Univ Clinic Duesseldorf, Duesseldorf, Germany; Christina Buerger, Holger Winkels, Christian Weber, LMU Munich, Munich, Germany; Esther Lutgens, AMC Amsterdam, Amsterdam, Netherlands

Atherosclerosis is a lipid driven chronic inflammatory disease of the arterial wall, involving both innate and adaptive immune responses. Specialized immune cells such as monocytes, B cells, T cells and dendritic

cells (DCs) contribute to disease progression or control the inflammatory responses. The CD40-CD40L dyad was identified as an efficient modulator of cellular immune responses. CD40 is a member of the tumor necrosis factor receptor (TNFR) superfamily and is activated by CD40 ligand (CD40L). CD40 and CD40L both are expressed on the majority of immune and non-immune cells associated with atherosclerosis. However, the specific contribution of CD40-CD40L signaling on the different single cell types towards atherosclerosis progression remains undefined. Here, we aimed to investigate the cell type-specific mechanisms of CD40-CD40L interactions in atherosclerosis by generating mice with a conditional ablation of CD40L on T cells. Hyperlipidemic mice with a T cell-specific deficiency of CD40L developed significantly smaller atherosclerotic lesions in the ascending after 28 weeks of chow diet, and following 6 weeks of a cholesterol-enriched diet when compared to their littermate controls. Changes in lesion size were accompanied by a modified anti-inflammatory plaque phenotype, characterized by an increased proportion of smooth muscle cells and a reduced number of pro-inflammatory immune cells, such as macrophages and T cells. T cell CD40L-deficient mice displayed systematically reduced expression of pro-inflammatory cytokines such as IL-1β, IL-2, IL-12, and IFNγ, and increased expression of anti-inflammatory cytokines IL-10 and TGFβ. This anti-inflammatory milieu was paralleled a change in the development and activation status of the T cells with mice lacking CD40L on T cells displaying a reduction in the expression of cytokines and gene markers associated with the activation of T cells (e.g., IL-2, CD69). This change was also reflected within the T cell populations which had a reduced proportion of activated effector T cells and an increased ratio of naïve T cells. Thus, our study ascribes CD40L on T cells a central role in atherosclerosis.

Disclosures: **N. Gerdes:** None. **C. Buerger:** None. **H. Winkels:** None. **C. Weber:** None. **E. Lutgens:** None.

587

Absence of Coronary Calcium on Non-contrast Enhanced, Non ECG-gated CT Correlates with Non-obstructive Coronary Artery Disease. A Retrospective Data Analysis of Liver Transplant Recipients

Hilda M Gonzalez-Bonilla, Akanksha Thakkar, Antonio Duran, Alpana Senapati, Nakul Gupta, Paulino Alvarez, Su Min Chang, Houston Methodist, Houston Texas, TX

Background Coronary angiography (CAG) remains the gold standard to diagnose coronary artery disease (CAD). However, it is associated with multiple risks and its utility is not well defined in the liver transplant population. Alternatives to evaluate for CAD such as coronary artery calcium score (CACS) are being increasingly investigated. **Hypothesis** To determine if the absence of coronary arterial calcium (CACS=0) on non-contrast, non-ECG gated chest CT scan can exclude obstructive CAD in liver transplant patients. **Methods** We performed a retrospective analysis of data collected from liver transplant recipients. We included patients who had a CT chest without contrast and CAG less than one year apart. Agatston score was derived from non-IV contrast, non-ECG gated chest CT's utilizing the syngo.via platform (Siemens Healthcare). CACS was compared against CAG. Patients with coronary stents were excluded. We determined NPV, PPV, sensitivity and specificity of using CACS = 0 as predictor of the absence of obstructive CAD. **Results** Mean age at date of transplant was 59.03 and males accounted for 68.8% of our population. The negative predictive value for CACS=0 as a predictor of non-obstructive CAD was 100%. Positive predictive value for CACS≥1 was 6.8%. Sensitivity and specificity for the correlation between CACS and CAD were 100% and 33% respectively (Figure 1). CACS was stratified into four subgroups based severity, and we found that all patients with obstructive CAD had scores >400 (Figure 2). **Conclusion** The absence of coronary arterial calcium (CACS=0) on non-contrast, non ECG gated chest CT has a high negative predictive value and can exclude the presence of obstructive CAD.

Figure 1. Correlation between CACS and CAD

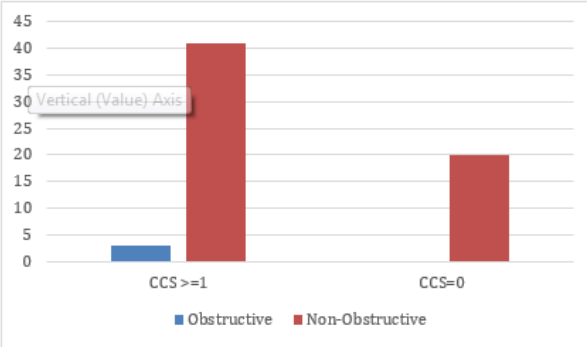

Figure 2. CAG result and CACS categories

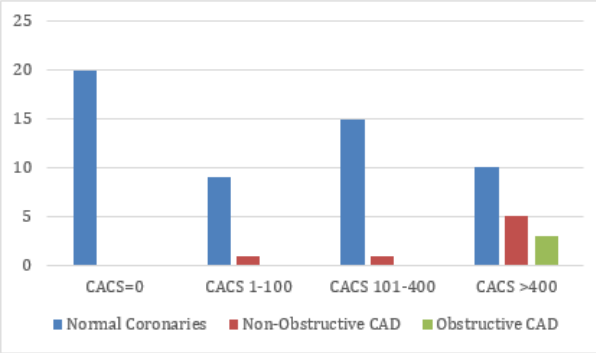

Disclosures: **H.M. Gonzalez-Bonilla:** None. **A. Thakkar:** None. **A. Duran:** None. **A. Senapati:** None. **N. Gupta:** None. **P. Alvarez:** None. **S. Chang:** None.

588

Nuanced Antibody Responses to Apolipoprotein A-I in Patients With Cardiovascular Disease

David M Henson, Vincent Venditto, Univ of Kentucky, Lexington, KY

Antibodies targeting apolipoprotein A-I (ApoA-I) have been identified in patients with cardiovascular disease (CVD). Anti-ApoA-I antibodies are thought to be markers of disease, but their exact role is unclear. We hypothesize that antibodies targeting ApoA-I are both protective and pathologic and unraveling the nuanced response to ApoA-I will provide insight into improved risk stratification of patients suffering from CVD. To test our hypothesis we screened serum samples by ELISA collected from patients with CVD to identify anti-ApoA-I antibody responses toward the full length protein along with immunogenic epitopes including the lecithin cholesterol acyl transferase (LCAT) domain and the C-terminal peptide of ApoA-I. These epitopes are of particular interest due to their propensity to undergo oxidative post-translational modification. Antibodies were affinity-purified toward ApoA-I, and their role in reverse cholesterol transport elucidated. Our data indicate that serum collected from patients with CVD enrolled in multiple clinical trials possess a highly nuanced immune response. We find that these antibody responses change over time in some patients who present with an AMI and antibodies correlate with outcomes. The mechanisms of these observed effects are currently under investigation. A full report on correlations between patient characteristic and antibody level will be presented. This work highlights the complexities of anti-ApoA-I antibodies in patients, which will guide development of a CVD risk stratification tool.

Disclosures: **D.M. Henson:** None. **V. Venditto:** None.

This research has received full or partial funding support from the American Heart Association.

589

Host-Genotype Shaped Microbiome Modulates Development of Atherosclerosis

Kazuyuki Kasahara, Lindsay L Traeger, Kymberleigh A Romano, Julia H Kreznar, Eugenio I Vivas, Univ of Wisconsin-Madison, Madison, WI; Margarete Mehrabian, Aldons J Lusis, Univ of California, Los Angeles, Los Angeles, CA; Federico E Rey, Univ of Wisconsin-Madison, Madison, WI

Genetic variation drives phenotypic diversity and determines predisposition to cardiovascular disease. Previous work revealed a large degree of variation on atherosclerosis susceptibility among 100 inbred strains of mice from the Hybrid Mouse Diversity Panel (HMDP). Additionally, each HMDP inbred strain shows a distinct microbiota composition. Here, we assessed the contributions of the gut microbiome to the development of atherosclerosis. Cecal samples from four HMDP strains showing disparate atherosclerosis phenotypes were transplanted into groups of *ApoE*$^{-/-}$ germ-free mice. Transplanted *ApoE*$^{-/-}$ mice were maintained on a high-plant polysaccharide diet containing 0.2% cholesterol for 8 weeks and analyzed for atherosclerotic lesions, microbiome, and metabolome. We found that mice colonized with cecal microbes from two HMDP donors prone to atherosclerosis development exhibited larger lesions compared to recipient mice colonized with samples from donors that show little signs of atherosclerosis. Metabolomic analyses of plasma from transplanted mice and metagenomic analyses of cecal contents from the transplanted and 24 HMDP donor mice identified microbial functions that are associated with the severity of disease. Altogether, our work provides novel insights into how microbes contribute to the development of cardiovascular disease and suggest that host genotype may select for microbial communities that modulate progression of atherosclerosis.

Disclosures: **K. Kasahara:** None. **L.L. Traeger:** None. **K.A. Romano:** None. **J.H. Kreznar:** None. **E.I. Vivas:** None. **M. Mehrabian:** None. **A.J. Lusis:** None. **F.E. Rey:** None.

590

Autophagy is Required for Endothelial Atheroprotective Signaling Under Physiological Flow

Marouane Kheloufi, Anne-Clemence Vion, Adel Hammoutene, Johanne Poisson, Juliette Lasselin, Cecile Devue, Isabelle Pic, Inserm u970, Paris, France; Nicolas Dupont, Inserm u845, Paris, France; Johanna Busse, Konstantin Stark, Medische Klinik I, Klinikum der Univ München, München, Germany; Xavier Loyer, Inserm u970, Paris, France; Michele Souyri, CNRS; UMR7622, Paris, France; Benoit Viollet, Inserm U1016, Paris, France; Pierre Julia, Service de Chirurgie Cardiaque et Vasculaire - Hôpital Européen Georges Pompidou, AP-HP, Paris, France; Alain Tedgui, Inserm u970, Paris, France; Patrice Codogno, Inserm U845, Paris, France; Chantal M. Boulanger, Pierre-Emmanuel Rautou, Inserm u970, Paris, France

Objective: Preferential development of atherosclerotic lesions in areas of low shear stress is associated with increased endothelial inflammation, apoptosis and senescence. On the contrary, high shear stress areas are protected from plaque development, but the mechanisms remain elusive. Autophagy is a protective mechanism allowing recycling of defective organelles and proteins to maintain cellular homeostasis. Our aim was to understand the role of autophagy in athero-protective effects of high shear stress.
Approach and Results: We used the parallel plate chamber system in vitro to generate different shear stress conditions on endothelial cell deficient or not in autophagy (shRNA Atg5 vs. control) and examined autophagic flux in cells transfected with RFP-GFP-LC3 plasmid. Endothelial autophagy was silenced in *Atg5*$^{flox/flox}$*; VE-cadherin-cre* mice. We first demonstrated in human and murine arteries and in cultured endothelial cells that atheroprotective shear stress activates endothelial autophagic flux. On the opposite, endothelial cells exposed to atheroprone low shear stress displayed inefficient autophagy, associated with activation of mTOR, inhibition of AMPKα pathways and blockade of the autophagic flux. Interestingly, plaque burden augmented specifically in areas usually atheroresistant in *ApoE*$^{-/-}$ hypercholesterolemic mice deficiency in endothelial autophagy. Both in cultured endothelial cells and in transgenic mice, deficiency in endothelial autophagy was associated with a defect in endothelial alignment with flow direction, a hallmark of endothelial cell health. Deficiency in endothelial autophagy increased endothelial senescence and TNFα-induced inflammation under high shear stress conditions. These effects were associated with impaired KLF2 activation. In transgenic mice, endothelial senescence and apoptosis was augmented in high shear stress areas of the descending thoracic aorta when compared to control littermate mice.

Conclusions: Altogether, these results show that adequate endothelial autophagic flux under high shear stress limits atherosclerotic plaque formation by preventing inflammation, senescence and apoptosis.

Disclosures: **M. Kheloufi:** None. **A. Vion:** None. **A. Hammoutene:** None. **J. Poisson:** None. **J. Lasselin:** None. **C. Devue:** None. **I. Pic:** None. **N. Dupont:** None. **J. Busse:** None. **K. Stark:** None. **X. Loyer:** None. **M. Souyri:** None. **B. Viollet:** None. **P. Julia:** None. **A. Tedgui:** None. **P. Codogno:** None. **C. Boulanger:** None. **P. Rautou:** None.

591

Absence of Nicotinamide Nucleotide Transhydrogenase Exacerbates Atherosclerosis in Mice

Aimee E Vozenilek, Matthew Vetkoetter, Xinggui Shen, Matthew D Woolard, Ronald L Klein, A Wayne Orr, **David M Krzywanski**, LSU Health Science Ctr - Shreveport, Shreveport, LA

Oxidant stress contributes to endothelial cell injury and inflammation that are hallmarks of early stage atherosclerosis. Emerging evidence implicates mitochondrial reactive oxygen species (ROS) as important contributors to this oxidant stress and differences in mitochondrial function may augment this process. We have shown that variation in mitochondrial function and ROS production associated with ethnicity contributes to endothelial and vascular dysfunction. To model these distinct mitochondrial redox phenotypes we used C57Bl/6N (6N) and C57Bl/6J (6J) mice that also display unique mitochondrial functional properties due to the differential expression nicotinamide nucleotide transhydrogenase (NNT). Mice were treated with adeno-associated virus encoding a gain-of-function form of proprotein convertase subtilisin/kexin type 9 (PCSK9) that leads to hypercholesterolemia, increased LDL levels, and atherosclerosis in mice. PCSK9 treatment and 8 weeks of high fat diet led to increases in plasma lipids in both 6N and 6J mice. However, 6J animals displayed significantly higher levels of fat deposition in the vasculature and increased plaque size in the carotid sinus. 6N mice co-treated with the mitochondria targeted superoxide dismutase mimetic MitoTEMPO for the final 4 weeks of the experiment displayed reduced plasma lipids, but no impact on fat deposition or plaque size was observed. In contrast, MitoTEMPO increased vascular fat deposition and plaque size in 6J mice consistent with a more severe atherosclerotic phenotype. Increased mitochondrial ROS was confirmed by demonstrating elevated vascular superoxide in 6J versus 6N animals and that this difference is exacerbated on high fat diet. MitoTEMPO diminished vascular superoxide production to near baseline levels in both groups, yet increased plaque size and fat deposition in 6J mice suggests a role for hydrogen peroxide in this process. These data indicate that loss of NNT and changes in mitochondrial function increase vascular ROS production and exacerbate lipid deposition and plaque development in the early stages of atherosclerosis.

Disclosures: **A.E. Vozenilek:** None. **M. Vetkoetter:** None. **X. Shen:** None. **M.D. Woolard:** None. **R.L. Klein:** None. **A.W. Orr:** None. **D.M. Krzywanski:** None.

592

Constitutive CD40-Signaling in Dendritic Cells Limits Atherosclerosis by Provoking Inflammatory Bowel Disease and Ensuing Cholesterol Malabsorption

Pascal J Kusters, Tom T Seijkens, Academic Medical Ctr, Amsterdam, Netherlands; Holger Winkels, La Jolla Inst for Allergy and Immunology, La Jolla, CA; Marion J Gijbels, Academic Medical Ctr, Amsterdam, Netherlands; Christian Weber, Norbert Gerdes, Ludwig-Maximilians Univ, Munich, Germany; Esther Lutgens, Academic Medical Ctr, Amsterdam, Netherlands

The co-stimulatory molecule CD40 is a major driver of atherosclerosis. It is expressed on a wide variety of cell types including mature dendritic cells (DCs) and required for optimal T cell activation and expansion. It remains undetermined if and how CD40 on DCs impacts the pathogenesis of atherosclerosis. Here we examined the effects of constitutively active CD40 in DCs on atherosclerosis, using low-density lipoprotein-deficient *(Ldlr$^{-/-}$)* bone-marrow chimeras that express an engineered latent membrane protein 1 (LMP)/CD40 fusion protein conferring constitutive CD40 signaling under control of the CD11c promoter (*DC-CD40ca*). As expected, *DC-CD40ca/Ldlr$^{-/-}$* chimeras showed increased antigen presenting capacity on DCs and increased T cell numbers. However, they developed extensive neutrophilia compared to *wt/ldlr$^{-/-}$* chimeras. Despite overt T cell expansion and neutrophilia we observed a reduction in cDC frequency and a dramatic reduction in atherosclerosis (*CD40wt/ldlr$^{-/-}$* 22076±3763 μm^2 vs. *DC-CD40ca/ldlr$^{-/-}$* 2511±1256 μm^2). Further analyses revealed that cholesterol and triglyceride levels decreased by 37% and 60%, respectively, in *DC-CD40ca/Ldlr$^{-/-}$* chimeras. Moreover, *DC-CD40ca/Ldlr$^{-/-}$*

chimeras developed inflammatory bowel disease characterized by massive transmural influx of leukocytes and lymphocytes, resulting in villous degeneration and lipid malabsorption. Constitutive activation of CD40 in DCs results in inflammation of the gastrointestinal tract, thereby impairing lipid uptake, which consequently results in attenuated atherosclerosis.

Disclosures: **P.J.H. Kusters:** None. **T.T.P. Seijkens:** None. **H. Winkels:** None. **M.J.J. Gijbels:** None. **C. Weber:** None. **N. Gerdes:** None. **E. Lutgens:** None.

593

High-Monounsaturated Fat Mediterranean-Type Diet Reduces Foamy Monocyte Formation and Atherosclerosis in Ldlr-/- Mice on High-Cholesterol Diet

Zeqin Lian, Xiao-yuan Dai Perrard, William Lagor, Baylor Coll of Med, Houston, TX; Frank Sacks, Harvard Sch of Public Health, Boston, MA; Christie Ballantyne, Huaizhu Wu, Baylor Coll of Med, Houston, TX

A large randomized clinical trial (PREDIMED) showed that adding “healthy monounsaturated fat (MUF)” to Mediterranean diet (MedD) by supplementation with extra virgin olive oil or nuts led to a reduction in atherosclerotic cardiovascular events, but the mechanisms remain incompletely understood. Hyperlipidemia, a major risk factor for atherosclerosis, may induce lipid accumulation in circulating monocytes, leading to formation of foamy monocytes (FMs), which contribute to atherosclerosis. We hypothesize that high-MUF MedD reduces FM formation and therefore inhibits atherogenesis associated with hyperlipidemia. To test this, LDLR-/- mice were fed western-type high-saturated fat, high-cholesterol diet (WD) (21% milkfat containing 13.3% saturated fat and 5.9% MUF; 0.2% cholesterol), high-MUF MedD with high cholesterol (HC-MedD, 21% fat [from extra-virgin olive oil, walnuts, almonds, and hazelnuts] containing 2.6% saturated fat and 13.4% MUF; 0.2% cholesterol), or normal diet (ND, control). At 3 months, mice on HC-MedD had similar body weight gain but significantly lower liver/body weight index compared to mice on WD. Plasma triglyceride levels were significantly lower in mice on HC-MedD (318 ± 31 mg/dL, n=13) than on WD (769 ± 60 mg/dL, n=9, $P<0.05$ vs HC-MedD group). Total cholesterol levels tended to be lower in mice on HC-MedD (2088 ± 180 mg/dL) than on WD (3092 ± 220 mg/dL). Compared to mice on WD, mice on HC-MedD had lower proportions of FMs and lower side scatter values (491 ± 11 vs 555 ± 3 in WD group, n=10/group, $P<0.001$), indicating less lipid, in FMs. Lipid accumulation in FMs of LDLR-/- on WD accelerated conversion of monocyte subsets from CD11c-CD36+ to CD11c+CD36+, leading to increased ratio of CD11c+CD36+ to CD11c-CD36+ monocytes in mice on WD (2.6 ± 0.3, n=10) vs ND (1.3 ± 0.2, n=9, $P<0.01$). In contrast, this ratio was not increased in mice on HC-MedD (1.4 ± 0.1, n=10) compared to mice on ND, and was lower than that in mice on WD ($P<0.01$). Oil red O staining of en face aorta showed 27% decrease in lesion areas in mice on HC-MedD vs on WD ($P<0.05$). In summary, compared to WD high in saturated fat and cholesterol, high-MUF MedD with high cholesterol lowered triglyceride levels, inhibited FM formation, and reduced atherosclerotic lesion size in LDLR-/- mice.

Disclosures: **Z. Lian:** None. **X. Perrard:** None. **W. Lagor:** None. **F. Sacks:** None. **C. Ballantyne:** None. **H. Wu:** None.

This research has received full or partial funding support from the American Heart Association.

594

Matrix Gla Protein Associates With Coronary Artery Calcification and Increases in Subacute Myocardial Infarction Together With Inflammatory Activation by Tumor Growth Factor-β1

Antonio Eduardo Pesaro, Carlos Vicente Serrano Jr, Marcelo Katz, Carolina Pereira, Cristovao L Mangueira, Ana Eduarda Z. de Carvalho, Karina L Salmazi, Cesar H Nomura, Marcelo Franken, **Marcel Liberman**, Hosp Albert Einstein, Sao Paulo, Brazil

Osteogenic Proteins (OP) and atherosclerotic inflammation modulate vascular calcification. Patients with acute myocardial infarction (MI) demonstrate higher inflammation and develop accelerated coronary artery calcification (CAC), compared to stable coronary artery disease patients. We aimed to: (a) test the association of OP and inflammatory proteins with CAC in individuals assessed for primary cardiovascular prevention; (b) evaluate these biomarkers in acute and subacute phases post-MI. We prospectively enrolled 170 patients, divided in 3 groups: (1) primary prevention patients who underwent ambulatory

coronary computed tomography with a CAC score ≥ 100, n=100; (2) primary prevention patients with a CAC score=zero, n=30; (3) post-MI patients, n=40, during acute (3±1 days post-MI) and subacute (46±17 days post-MI) phases. Serum OP (osteoprotegerin, RANKL, fetuin-A and Matrix Gla protein [MGP]) and serum inflammatory proteins (C-reactive protein, oxidized LDL, tumoral necrosis factor-α and tumor growth factor [TGF]-β1) were measured by ELISA. Associations of plasma OP and inflammatory proteins levels with CAC were adjusted by age, sex and use of statins. In the post-MI group, all biomarkers were compared both in acute vs. subacute phases and in acute phase vs. CAC zero group. Compared to CAC zero, patients with CAC score ≥ 100 were older, predominantly men and had higher rates of hypertension and diabetes. After adjusted analysis, only MGP was associated with a CAC score ≥ 100 (OR 1.48 [95% CI 1.01-2.16; per 100ng/ml increase; p=0.047). Serum MGP and TGF-β1 were higher in subacute phase compared to acute phase post-MI (median [25-75 percentile], 342 vs. 279ng/ml respectively; p=0.01 and 711 vs. 492pg/ml; p=0.03). All biomarkers were similar in acute phase post-MI vs. CAC zero. In conclusion, serum MGP was associated with higher CAC in primary cardiovascular prevention patients. After MI, both serum MGP and TGF-β1 levels increased in the subacute phase. Our findings unveiled a potential role for MGP as a biomarker of CAC in primary cardiovascular prevention. Additionally, this clinical study unfolds further mechanistic hypothesis of how increased TGF-β1 and MGP may modulate vascular inflammation and CAC progression in subacute MI patients.

Disclosures: **A. Pesaro:** None. **C. Serrano Jr:** None. **M. Katz:** None. **C. Pereira:** None. **C.L.P. Mangueira:** None. **A.Z. de Carvalho:** None. **K.L.C. Salmazi:** None. **C.H. Nomura:** None. **M. Franken:** None. **M. Liberman:** None.

595

Gender Difference Was Present in the Production of Cytokines in Mice With PM Exposure

Xuanyou Liu, Yichao Xiao, Qingyi Zhu, Meng Jiang, Yunyan Duan, Hong Hao, Joseph D Abraham, Qinghua Sun, Zhenguo Liu, The Ohio State Univ Medical Ctr, Columbus, OH

Gender difference is present in a variety of diseases especially cardiovascular diseases like coronary artery diseases (**CAD**). It is well known that males tend to suffer from CAD earlier than females for largely unknown reasons. Oxidative stress and inflammation are considered an important mechanism for the development of cardiovascular diseases. Cytokines including interleukin (IL)-6 and tumor necrosis factor-α (TNF-α) play an important role in oxidative stress and inflammation. Ambient fine particulate matter (**PM**) exposure is closely associated with cardiovascular diseases and oxidative stress. The present study was designed to determine if there was a gender difference in the production of cytokines in the mice with PM exposure. Both male and female wild-type C57BL/6 mice (8-10 weeks) were exposed to PM2.5 for 6 weeks via intranasal approach with PBS as the control. Serum concentrations of the cytokines including IL-6, IL-1β, and TNF-α were measured with ELISA in the mice before and after PM exposure. There was no difference between male and female mice in the serum levels of IL-6, IL-1β, or TNF-α at the baseline. As expected, PM exposure substantially increased the serum levels of IL-6, IL-1β, and TNF-α both in male and female mice (by up to 6 times). However, their serum concentrations were significantly higher in male mice than in the females by 64.2%, 26.5%, and 30.7% for IL-6, IL-1β, and TNF-α, respectively ($p < 0.05$, $n = 10$). Similar changes in the inflammatory infiltrations in the lungs were observed in the male and female mice with PM exposure. The data from the present study demonstrated that more cytokines were produced in male mice than in the females with PM exposure. The clear gender difference in the serum levels of cytokines in response to PM exposure may partially contribute to the gender difference in the development of cardiovascular diseases. Further studies are needed to investigate the mechanisms related to the gender difference in the response to PM exposure.

Disclosures: **X. Liu:** None. **Y. Xiao:** None. **Q. Zhu:** None. **M. Jiang:** None. **Y. Duan:** None. **H. Hao:** None. **J.D. Abraham:** None. **Q. Sun:** None. **Z. Liu:** None.

597

Effect of Electronic Cigarettes on Cardiovascular Health

Marina V Malovichko, Abhinav Agarwal, Millicent Winner, Michel Smith, Srinivas Sithu, Univ of Louisville, Louisville, KY; Terry Gordon, New York Univ, Louisville, NY; Aruni Bhatnagar, Daniel Conklin, Univ of Louisville, Louisville, KY; Lung-Chi Chen, New York Univ, Louisville, NY; Sanjay Srivastava, Univ of Louisville, Louisville, KY

Electronic cigarettes (E-cig) are battery operated devices used for the delivery of aerosolized nicotine. Unlike conventional cigarettes, E-cig do not contain tar and several other chemicals abundant in conventional cigarettes, and have therefore become extremely popular over the last decade. However, little is known about the health effects of E-cig. To examine the effect of E-cig on cardiovascular health we exposed 8-week old C57BL/6 (C57; maintained on normal chow) and apoE-KO mice (maintained on Western diet) to filtered air or E-cig (36 mg/ml nicotine aerosolized in glycerol/propylene glycol, 50/50, v/v) for 12 weeks (3 h/day; 7 days a week). Total suspended particle (TSP) mass concentration (124 ± 14 mg/M^3) particle size (0.67 µM) and total carbon (33.1 %TSP) were kept constant. Cotinine was undetectable in the plasma of air exposed mice, but the plasma cotinine levels were 11.7±1.2 and 38.7±3.6 ng/ml in E-cig exposed C57 and apoE-KO mice respectively. Exposure to E-cig did not affect the body weight of C-57 or apoE-KO mice. Complete blood count showed that total leukocyte levels were decreased by 28 percent ($P<0.05$) in E-Cig exposed mice as compared with air exposed mice. However, flow cytometric analyses of immune cells showed that levels of CD4+ T-cells, CD8+ T-cells, B-Cells and monocytes in E-cig exposed mice were comparable with air exposed. E-cig had no effect on circulating endothelial progenitor cells, insulin resistance, platelet monocyte aggregates and plasma lipoproteins and cytokines in C57 mice. Similarly, plasma cholesterol (E-cig 1088±61 vs air 1102±61 mg/dL) and triglyceride (E-cig 95±9 vs air 77±5 mg/dL) levels of E-cig exposed apoE-KO mice were comparable with air exposed controls. However, the aortic lesion area of E-cig exposed apoE-KO mice was 1.2 fold higher than the air exposed mice ($P<0.05$). Collectively, these data suggest that electronic cigarettes moderately increase aortic atherosclerosis without affecting plasma lipids, insulin resistance, systemic inflammation and platelet activation.

Disclosures: **M.V. Malovichko:** None. **A. Agarwal:** None. **M. Winner:** None. **M. Smith:** None. **S. Sithu:** None. **T. Gordon:** None. **A. Bhatnagar:** None. **D. Conklin:** None. **L. Chen:** None. **S. Srivastava:** None.

598

Carotid Artery Ultrasound Texture, Cardiovascular Risk Factors, and Subclinical Arterial Disease: The Multi-Ethnic Study of Atherosclerosis (Mesa)

Carol Mitchell, Claudia E Korcarz, Matthew Tattersall, Adam D Gepner, Univ of Wisconsin Madison, Madison, WI; Wendy S Post, Johns Hopkins Hosp, Baltimore, MD; Joel D Kaufman, Robyn L McClelland, Univ of Washington, Seattle, WA; James H Stein, Univ of Wisconsin Madison, Madison, WI

Background Ultrasound texture “contrast” can be used to characterize the arterial wall non-invasively. Texture contrast provides information about the distribution and gray level differences of the pixels in the arterial wall and may describe early changes related to arterial injury. We determined if ultrasound texture contrast was associated with cardiovascular disease (CVD) risk factors and subclinical arterial disease. **Methods** We evaluated ultrasound images of the distal right common carotid artery from a convenience sample of 151 participants from the first examination of the Multi-Ethnic Study of Atherosclerosis, a population-based cohort of individuals without clinical CVD. Images were digitized, normalized, and standardized to a pixel density of 20/mm. Plaque texture analysis software (LifeQ Medical, Cyprus) used the gray level difference statistics method to determine the contrast of the far wall of the carotid intima-media complex. Multivariable linear regression models (adjusted for age, sex and race/ethnicity) were used to examine relationships between contrast, CVD risk factors (age, BMI, total cholesterol, high-density lipoprotein cholesterol [HDL-C], low-density lipoprotein cholesterol, triglycerides, hypertension, diabetes mellitus, smoking, glomerular filtration rate, C-reactive protein, interleukin-6, D-dimer, fibrinogen, alcohol consumption, education level, physical activity level, statin use), carotid intima-media thickness (IMT), coronary artery calcium (CAC), and CVD risk score. **Results** The 151 participants were mean (standard deviation) 68.1 (9.2) years old (54% female; 31% Hispanic, 28% Black, 10% Chinese, and 31% White). In models that included age, sex, and race, contrast was associated independently with age (beta [standard error] -0.9 [0.4] per year; p=0.02), HDL-C (0.6 [0.2] per mg/dL; p=0.02), C-reactive protein (-2.3 [0.9] per mg/L; p=0.02), and carotid IMT (-1.3 [0.4] microns; p=0.001). Other CVD risk factors and CAC

were not associated independently with contrast. **Conclusions** Lower contrast, an ultrasound texture feature, is associated with increasing age, lower HDL-C, higher CRP, and higher carotid IMT, supporting its potential use for evaluating arterial injury and CVD risk.

Disclosures: **C. Mitchell:** Other; Modest; Davies Publishing Inc., authorship for two echocardiography textbooks, currently under review, may have future royalties, Elsevier, author textbook chapters, may have future royalties, Wolters Kluwer, author textbook chapters, may have future royalties. **C.E. Korcarz:** None. **M. Tattersall:** None. **A.D. Gepner:** None. **W.S. Post:** None. **J.D. Kaufman:** None. **R.L. McClelland:** None. **J.H. Stein:** Other; Significant; Wisconsin Alumni Research Foundation-patent related to carotid wall thickness and vascular age.

This research has received full or partial funding support from the American Heart Association.

599

Extracellular Vesicles Secreted by Atherogenic Macrophages Transfer Microrna to Inhibit Cell Migration

My-Anh Nguyen, Denuja Karunakaran, Michele Geoffrion, Univ of Ottawa Heart Inst, Ottawa, ON, Canada; Henry S Cheng, Toronto General Res Hosp Inst, Toronto, ON, Canada; Ljubica Perisic Matic, Ulf Hedin, Karolinska Inst, Stockholm, Sweden; Lars Maegdefessel, Technical Univ Munich, Munich, Germany; Jason E Fish, Toronto General Res Hosp Inst, Toronto, ON, Canada; Katey J Rayner, Univ of Ottawa Heart Inst, Ottawa, ON, Canada

During inflammation, macrophages secrete vesicles carrying RNA, protein and lipids as a form of extracellular communication. In the vessel wall, extracellular vesicles (EVs) have been shown to be transferred between vascular cells during atherosclerosis, however, the role of macrophage-derived EVs in promoting atherogenesis is not known. Here, we **hypothesize** that atherogenic macrophages secrete microRNAs (miRNA) in EVs to mediate cell-cell communication and promote pro-inflammatory and pro-atherogenic phenotypes in recipient cells. **Results**: We isolated EVs from mouse and human macrophages treated with an atherogenic stimulus (oxidized LDL) and characterized the EV-derived miRNA expression profile. Using microarrays and Q-PCR, we confirmed the enrichment of miR-146a, miR-128, miR-185, miR-365 and miR-503 in atherogenic EVs compared to controls. Live-cell imaging demonstrated that macrophage-derived EVs are taken up and transfer exogenous miRNA (*C. elegans)* to naive recipient macrophages. Bioinformatic analysis suggests that atherogenic EV-derived miRNAs are predicted to target genes involved in cell migration and adhesion pathways. Indeed, treatment of naïve macrophages with EVs from atherogenic but not control macrophages inhibited the migration of naïve cells towards a chemokine stimulus (80% decrease in migration, $p \leq 0.01$). *In vivo*, delivery of EVs also abolished LPS-induced emigration of mouse peritoneal macrophages. Moreover, inhibition of miR-146a (using anti-miR oligonucleotides or miR-146a$^{-/-}$ macrophages), the most enriched miRNA in atherogenic EVs, reduced the inhibitory effect of EVs on macrophage migratory capacity. EV-mediated delivery of miR-146a repressed the expression of target genes IGF2BP1 and HuR in recipient cells, and knockdown of IGF2BP1 and HuR using siRNA reduced macrophage migration, highlighting the importance of these EV-miRNA targets in regulating macrophage motility. Notably, expression of miR-146a was elevated in mouse and human atherosclerotic lesions compared to controls. **Thus,** EV-derived miRNAs from atherogenic macrophages, in particular miR-146a, may accelerate the development of atherosclerosis by decreasing cell migration and promoting macrophage entrapment in the vessel wall.

Disclosures: **M. Nguyen:** None. **D. Karunakaran:** None. **M. Geoffrion:** None. **H.S. Cheng:** None. **L.P. Matic:** None. **U. Hedin:** None. **L. Maegdefessel:** None. **J.E. Fish:** None. **K.J. Rayner:** None.

600

Deposition of Endothelial Cell-derived Fibronectin by Alpha5beta1 Integrins Mediates Oxidized LDL-induced Proinflammatory Gene Expression and Early Atherosclerosis

Arif Yurdagul Jr., Jonette M Green, Zaki Al Yafeai, LSU Health Sciences Ctr - Shreveport, Shreveport, LA; Patrick A. Murphy, UCONN Medical Sch, Framington, CT; **A. Wayne Orr**, LSU Health Sciences Ctr - Shreveport, Shreveport, LA

Subendothelial basement membrane remodeling to a fibronectin-rich matrix precedes lesion development, and endothelial cell interactions with fibronectin prime inflammatory responses to a variety

of atherogenic stimuli. However, the mechanisms regulating early atherogenic fibronectin accumulation remain unknown. We now show that treating endothelial cells with oxidized LDL (oxLDL) potently induces endothelial fibronectin deposition through activation of the fibronectin-binding integrin α5β1, as inhibiting α5β1 (blocking antibodies, α5 knockout cells) completely abrogates oxLDL-induced fibronectin deposition *in vitro*. Inducible endothelial-specific deletion of α5 integrins significantly blunts endothelial proinflammatory gene expression at atheroprone sites and diminishes atherosclerotic plaque formation in ApoE knockout mice, suggesting an important role for this integrin in early endothelial activation. However, endothelial α5 deletion surprisingly enhances fibronectin staining in the endothelial layer, potentially due to leak of plasma-derived fibronectin. Plasma fibronectin differs from cell-derived fibronectin due to the lack of two alternatively spliced domains, termed extradomain A (EIIIA) and extradomain B (EIIIB). Interestingly, loss of endothelial cell-derived fibronectin (fibronectin siRNA) completely inhibits oxLDL-induced VCAM-1 expression, and only rescue with cell-derived fibronectin, but not plasma fibronectin, reverses this inhibitory effect. This effect appears to be due to the presence of EIIIA and EIIIB domains, as endothelial cells isolated from EIIIA/EIIIB knockout mice also show reduced oxLDL-induced proinflammatory responses. However, it is unclear whether this response is due to specific EIIIA/EIIIB receptors or due to altered integrin signaling, as limiting the presence of cell-derived fibronectin prevents integrin α5 localization to focal adhesions and reduces fibronectin fibril length. Taken together, our data demonstrate that oxLDL stimulates α5 integrin-dependent deposition of endothelial-derived fibronectin into the subendothelial matrix and suggest that the source of fibronectin regulates the subsequent endothelial cell proinflammatory responses.

Disclosures: **A. Yurdagul:** None. **J.M. Green:** None. **Z. Al Yafeai:** None. **P.A. Murphy:** None. **A.W. Orr:** None.

This research has received full or partial funding support from the American Heart Association.

601

Global and Liver Specific Bmal1 Deficient Mice Regulate Intestinal Lipid Absorption

Xiaoyue Pan, Mahmood Hussain, Winthrop Univ Hosp, Mineola, NY

Circadian rhythms controlled by clock genes affect plasma lipids, known risk factors for atherosclerosis. Clock and Bmal1 are critical clock genes that positively regulate circadian rhythms. We have shown that Clock plays an important role in lipid absorption. Additionally, we showed that global ablation of *Bmal1* in *Apoe*$^{-/-}$ and *Ldlr*$^{-/-}$ mice, and liver-specific ablation of Bmal1 in *Apoe*$^{-/-}$ (L-*Bmal1*$^{-/-}$*Apoe*$^{-/-}$) mice increases atherosclerosis. However, it is unknown whether Bmal1 regulates intestinal lipid absorption. We studied cholesterol and triglyceride absorption in normal and lipase-inhibited *Bmal1*$^{-/-}$ and *Bmal1*$^{-/-}$*Apoe*$^{-/-}$ mice with global Bmal1 deficiency and compared it with *Bmal1*$^{+/+}$ and *Bmal1*$^{+/+}$*Apoe*$^{-/-}$, respectively. To study the effect of liver-specific Bmal1 deficiency, studies were performed in L-*Bmal1*$^{-/-}$ and L-*Bmal1*$^{-/-}$*Apoe*$^{-/-}$ mice and data were compared with *Bmal1*$^{fl/fl}$ and *Bmal1*$^{fl/fl}$*Apoe*$^{-/-}$ mice. In addition, enterocytes isolated from these mice were used to study uptake and secretion of cholesterol and oleic acid. Further, protein and mRNA levels of candidate genes involved in lipid uptake, lipoprotein assembly and secretion were quantified.
Both normal and lipase-inhibited *Bmal1*$^{-/-}$ mice absorbed significantly higher amounts of cholesterol and triglyceride. Further, uptake and secretion of cholesterol and fatty acids by enterocytes was increased in *Bmal1*$^{-/-}$ mice. As reported previously, liver-specific Bmal1 ablation increased VLDL production. Surprisingly, postprandial plasma lipids were also significantly increased in L-*Bmal1*$^{-/-}$ mice than in control *Bmal1*$^{fl/fl}$ mice. Further, enterocytes isolated from L-*Bmal1*$^{-/-}$ took up more lipids and secreted more lipoproteins. Moreover, in vivo lipid absorption in L-*Bmal1*$^{-/-}$ was increased. Gene expression quantifications revealed that intestinal MTP, DGAT1, CD36 and NPC1L1 mRNA levels were increased in global and hepatic Bmal1 deficient animals.
Global and liver-specific ablation of Bmal1 increases intestinal lipoprotein production by increasing the expression of genes involved in lipid uptake and lipoprotein assembly. These data for the first time suggest that intestinal lipoprotein assembly is regulated by hepatic Bmal1.

Disclosures: **X. Pan:** None. **M. Hussain:** None.

This research has received full or partial funding support from the American Heart Association.

602

High-Density Lipoprotein Protects Macrophages Against Apoptosis Through BH3-only Bcl-2 Family Member Bim

Alexander Qian, Pei Yu, Leticia Gonzalez, Bernardo Trigatti, McMaster Univ, Hamilton, ON, Canada

Macrophage apoptosis contributes to the formation of necrotic cores within atherosclerotic lesions, increasing the susceptibility of atherosclerotic plaques to rupture and the risk of cardiovascular events. In advanced atherosclerotic plaques, lipid-laden foam cells are exposed to a diverse number of apoptosis inducers, including prolonged endoplasmic reticulum (ER) stress. The pro-apoptotic BH3-only protein Bim has been reported to mediate apoptosis in response to ER stress induction in a variety of cells including macrophages. Treatment of macrophages with high-density lipoprotein (HDL) protects them against apoptosis induced by a variety of stressors. We hypothesize that HDL mediated protection against macrophage apoptosis occurs via pathways that regulate Bim activity. To test this, thioglycollate-elicted peritoneal macrophages were treated in lipoprotein deficient culture with different apoptosis inducers in the absence or presence of HDL. Cell apoptosis was assessed by cleaved caspase 3 staining and terminal deoxynucleotidal transferase dUTP nick end labeling. Treatment of mouse peritoneal macrophages in culture with 50μg/ml of human HDL protected against apoptosis induced by tunicamycin ($P<0.05$) without affecting ER stress markers, Grp78, Grp94 and CHOP. Peritoneal macrophages from mice deficient in Bim were less susceptible to apoptosis induced by treatment with either tunicamycin or 7-ketocholesterol. Furthermore, treatment with HDL provided no additional protection to apoptosis in Bim KO macrophages. Our results suggest that protection of macrophage apoptosis by HDL is regulated through pathways involving the activity of BH3-only Bcl-2 family member Bim.

Disclosures: **A. Qian:** None. **P. Yu:** None. **L. Gonzalez:** None. **B. Trigatti:** None.

603

Induction of Dendritic Cell-Mediated Activation of T Cells From Atherosclerotic Plaques by Human Heat Shock Protein 60

Mizanur Rahman, Karolinska Instt, Stockholm, Sweden; Johnny Steuer, Peter Gillgren, Section of Vascular Surgery, Dept of Surgery, Södersjukhuset, Inst of Clinical Science and Education, Karolinska Instt, Stockholm, Sweden, Stockholm, Sweden; Anquan Liu, Johan Frostegård, Karolinska Instt, Stockholm, Sweden

Objective: Atherosclerosis, the major cause of cardiovascular disease (CVD) is characterized by presence of activated immunocompetent cells, including dendritic cells (DCs) and T cells; dead cells and oxidized low density lipoprotein (OxLDL) in the atherosclerotic plaques. Heat shock protein (HSP), especially HSP60, is implicated in atherosclerosis. We reported that Annexin A5 (ANXA5) inhibits atherosclerosis-manifestations in apolipoprotein E-/- mice. Here we study HSP60 effects on human DCs and T cells.
Methods and results: Human DCs were treated with HSP60 and naïve autologous T cells were co-cultured with thus pre-treated DCs. HSP60 induced DC-activation and T cell proliferation as determined by FACScan, gene-activation and cytokine production. HSP60-induced T cell activation was partly MHC class II-dependent. T cells exposed to HSP60-treated DCs produced IFN-γ, IL-17 but not TGF-beta. HSP60 did not promote expression of Toll like receptors 2 or 4. ANXA5 inhibited HSP60-effects on DCs and T cells and partly bound HSP60. Further, OxLDL induced HSP 60 was abolished by ANXA5. Experiments on DC and T cells derived from carotid atherosclerotic plaques from patients with symptomatic carotid disease gave similar results as from blood donors.
Conclusions: Our data show that HSP60 induces an MHC class II-dependent activation of blood- and plaque derived T cells which are mostly of Th1 type. HSP60 could thus be an important T cell antigen in plaques, and mediate oxLDL:s immunogenic effects on DC-T cell activation, promoting plaque rupture and clinical manifestations of CVD. ANXA5 inhibits these effects.

Disclosures: **M. Rahman:** None. **J. Steuer:** None. **P. Gillgren:** None. **A. Liu:** None. **J. Frostegård:** None.

604

Genetic Deletion of Interleukin-19 Exacerbates Atherogenesis and Inflammatory Gene Expression in *Ldlr*$^{-/-}$ Mice

Mitali Ray, Khatuna Gabunia, Christine Vrakas, Farah Kako, Sheri E. Kelemen, Allison Herman, Michael V. Autieri, Temple Univ Sch of Med, Philadelphia, PA

IL-19 is an anti-inflammatory interleukin and a member of the IL-10 family. Our laboratory has previously shown that IL-19 treatment is able to decrease atherosclerotic plaque burden in *Ldlr*$^{-/-}$ mice through polarization of T cells and macrophages to their anti-inflammatory phenotypes. We hypothesized that lack of IL-19 would exacerbate atherosclerosis. We observed that the absence of IL-19 results in increased plaque burden in *Ldlr*$^{-/-}$ x *Il19*$^{-/-}$ (DKO) mice when compared to *Ldlr*$^{-/-}$ controls after 14 weeks of high fat diet (HFD) administration by *en face* and Oil Red O staining of aorta and aortic root. In a rescue study wherein DKO mice were placed on HFD for 14 weeks and simultaneously injected i.p. with 10ng/g/day of mIL-19 or PBS, DKO mice injected with mIL-19 had significantly less plaque than PBS controls. To test our hypothesis that exacerbated plaque in the DKO was due to an increased pro-inflammatory environment, we performed gene expression analysis from spleen and arch from *Ldlr*$^{-/-}$ and DKO mice after 14 weeks of HFD, as well as a series of *in vitro* experiments in isolated *Ldlr*$^{-/-}$ and DKO VSMCs and BMDMs. qRT-PCR analysis revealed DKO mice have a global and more dramatic local polarization of T cells and macrophages to pro-inflammatory Th1 and M1 phenotypes in the spleen and aortic arch. We stimulated cultured VSMCs and BMDMs with pro-inflammatory stimulus, TNFα, and found that DKO VSMCs express greater levels of TNFα and MCP-1 mRNA compared to *Ldlr*$^{-/-}$ controls. DKO BMDMs also exhibit increased expression levels of TNFα, as well as IL-1β when compared to *Ldlr*$^{-/-}$. Gene expression analysis also demonstrated increased levels of pro-inflammatory mRNA binding protein, human antigen R (HuR) in the DKO spleen and arch. HuR stabilizes pro-inflammatory transcripts by binding ARE elements in the 3' UTR. Utilizing the RNA synthesis inhibitor actinomycin D in cultured BMDM and VSMC, we observed increased mRNA stability of inflammatory genes in DKO cells when compared to *Ldlr*$^{-/-}$ by qRT-PCR. These data suggest that IL-19 is an atheroprotective cytokine which dampens inflammatory gene expression by modulation of mRNA stability.

Disclosures: **M. Ray:** None. **K. Gabunia:** None. **C. Vrakas:** None. **F. Kako:** None. **S.E. Kelemen:** None. **A. Herman:** None. **M.V. Autieri:** None.

This research has received full or partial funding support from the American Heart Association.

605

Diastolic Blood Pressure Predicts Coronary Plaque Volume in Patients with Coronary Artery Disease

Mohamad Saleh, Abdulhamied Alfaddadgh, Harvard Medical Sch, Beth Israel Deaconess Medical Ctr, Boston, MA; Tarec Elajami, Mount Sinai Medical Ctr, Miami, FL; Hasan Ashfaque, Francine Welty, Harvard Medical Sch, Beth Israel Deaconess Medical Ctr, Boston, MA

Introduction: Hypertension is a major risk factor for coronary artery disease (CAD) and is associated with increased morbidity and mortality. The effect of systolic vs. diastolic blood pressure (BP) on coronary plaque volume has not been reported. Coronary blood flow occurs during diastole; shear stress affects plaque formation. **Hypothesis:** Diastolic BP may be a better predictor of plaque volume than systolic BP. **Methods:** 285 subjects with stable CAD underwent coronary computed tomographic angiography to assess the indexed volume (plaque volume [mm3] divided by segment length [mm]) of fatty, fibrous, non-calcified, calcified and total coronary plaque. Segments with significant calcium-blooming artifact were excluded. A backward linear regression model adjusted for age, gender, BMI, estimated glomerular filtration rate, total cholesterol, LDL-C, HDL-C and triglycerides. **Results:** Mean (SD) age was 63.1 ± 7.7 years (18% female). A significant increase was observed in volume of all plaque components across diastolic BP tertiles except for calcified which was borderline (p= 0.069) (Table). In contrast, there was no difference in systolic tertiles. In multivariate regression, diastolic BP tertile was a significant independent predictor of volume of all plaque components - fatty (β= 0.075; p=0.038), fibrous (β= 0.178; p= 0.004), non-calcified (β= 0.256; p= 0.008), calcified (β= 0.081; p= 0.007) and total (β= 0.353; p= 0.002) whereas no association was observed between systolic BP tertile and volume of any plaque component (Table). **Conclusion:** In patients with CAD, diastolic BP tertile independently predicts coronary plaque volume whereas systolic BP tertile does not. Since coronary blood flow occurs during diastole, a possible

mechanism for the difference between systolic and diastolic BP is increased shear stress during diastolic blood flow. Therefore, control of diastolic BP may be an important factor in determining plaque volume.

Table. Comparison of Indexed Plaque Volumes (mean ± SD) by Tertiles of Systolic and Diastolic Blood Pressure Plaque Component[a]

	Systolic Blood Pressure Tertiles					
	1st Tertile (≤ 118 mmHg)	2nd Tertile (119-130 mmHg)	3rd Tertile (> 130 mmHg)	p-value for trend	Multivariate Regression	
	Mean ± SD	Mean ± SD	Mean ± SD		β	p-value
Fatty	9.5 ± 5.3	10.0 ± 6.4	9.7 ± 5.7	0.747	0.015	0.544
Fibrous	16.7 ± 9.3	17.1 ± 10.6	17.4 ± 9.8	0.622	0.043	0.294
Non-calcified	26.1 ± 14.4	27.1 ± 16.8	27.1 ± 15.3	0.664	0.061	0.335
Calcified	5.2 ± 4.4	5.5 ± 5.1951	5.6 ± 4.6	0.653	0.010	0.629
Total	30.9 ± 17.1	32.5 ± 20.7148	32.6 ± 18.2	0.522	0.082	0.287

	Diastolic Blood Pressure Tertiles					
	1st Tertile (≤ 68 mmHg)	2nd Tertile (69-76 mmHg)	3rd Tertile (> 76 mmHg)		Multivariate Regression	
	Mean ± SD	Mean ± SD	Mean ± SD	p-value for trend	β	p-value
Fatty	9.0 ± 5.4	9.3 ± 5.6	10.9 ± 6.2	0.024	0.075	**0.038**
Fibrous	15.4 ± 9.4	16.4 ± 9.5	19.4 ± 10.4	0.004	0.178	**0.004**
Non-calcified	24.4 ± 14.6	25.7 ± 15.0	30.3 ± 16.4	0.008	0.256	**0.008**
Calcified	5.4 ± 4.6	4.3 ± 3.5	6.6 ± 5.6	0.069	0.081	**0.007**
Total	29.3 ± 17.7	30.0 ± 17.2	37.0 ± 20.4	0.004	0.353	**0.002**

[a] indexed plaque volume expressed as mm^3 divided by length of segment in mm

Disclosures: **M. Saleh:** None. **A. Alfaddadgh:** None. **T. Elajami:** None. **H. Ashfaque:** None. **F. Welty:** None.

606

Reciprocal Gene-Gene Regulation Between GWAS Genes *ADTRP* and *MIA3* Contributing to Susceptibility of Coronary Artery Disease

Fan Wang, Cleveland Clinic Lerner Res Inst, Cleveland, OH; Chunyan Luo, Xiang Ren, Tie Ke, Chengqi Xu, Subo Qin, Bo Tang, Yufeng Yao, Huazhong Univ of Science and Technology, Wuhan, China; Qiuyun Chen, Qing K Wang, Cleveland Clinic Lerner Res Inst, Cleveland, OH

Genome-wide association studies (GWAS) have identified >60 genomic loci for coronary artery disease (CAD), including *ADTRP* (regulator of TFPI and coagulation) and *MIA3* (involved in ER trafficking of collagens). In this study, we hypothesized that some GWAS genes form a molecular regulatory network involved in the pathogenesis of CAD. Global microarray analysis showed that *ADTRP* regulated expression of *MIA3* and *PIK3R3* encoding the regulatory subunit 3 of PI3K. *ADTRP*-mediated up-regulation of *PIK3R3* activates AKT, resulting in up-regulation of *MIA3*. Knockdown of *ADTRP* expression promoted oxidized-LDL-mediated monocyte adhesion to endothelial cell (EC) and transendothelial migration of monocytes, inhibited EC proliferation and migration, and increased apoptosis, which was reversed by expression of constitutively active AKT1, while the over-expression of *ADTRP* in ECs blunted these processes. Knockdown of *MIA3* expression also promoted monocyte adhesion to ECs and transendothelial migration of monocytes. However, knockdown of *MIA3* increased *ADTRP* expression, suggesting that *MIA3* negatively regulates *ADTRP* expression. Genetically, no significant interaction between *ADTRP* SNP rs6903956 and *MIA3* SNP rs17465637 was detected in 2,185 CAD patients and 2,156 non-CAD controls by classical two-locus genotypic analysis, relative excess risk due to interaction or INTERSNP programs. We have recently found that one molecular mechanism for gene-gene interaction is positive cyclic cross-regulation of gene expression: Gene A positively regulates gene B, whereas gene B also positively regulates gene A. Here we have identified a different scenario in which gene A positively regulates gene B, but gene B negatively regulates gene A, thereby resulting in lack of gene-gene interaction. In conclusion, we have uncovered a novel molecular signaling pathway involving *ADTRP* and *MIA3* for the pathogenesis of CAD. We show that *ADTRP* positively regulates *PIK3R3* expression, which leads to activation of AKT and up-regulation of *MIA3*, thereby regulating endothelial cell functions directly relevant to atherosclerosis. These results further support that positive cyclic cross-regulation of gene expression is a molecular mechanism for gene-gene interaction.

Disclosures: **F. Wang:** None. **C. Luo:** None. **X. Ren:** None. **T. Ke:** None. **C. Xu:** None. **S. Qin:** None. **B. Tang:** None. **Y. Yao:** None. **Q. Chen:** None. **Q.K. Wang:** None.

608

Macrophage-Associated Lipin-1 Contributes to Atherosclerosis

Aimee E Vozenilek, Louisiana State Univ Health Sciences Ctr-Shreveport, Shreveport, LA; Aaron R Navratil, Univ of California San Diego, San Diego, CA; Brian Finck, Washington Univ Sch of Med, Saint Louis, MO; A. Wayne Orr, **Matthew D Woolard**, Louisiana State Univ Health Sciences Ctr-Shreveport, Shreveport, LA

OBJECTIVE: Macrophage pro-inflammatory responses induced by oxidized low-density lipoproteins (oxLDL) mediate atherosclerosis progression. However, how oxLDL causes macrophages to become pro-inflammatory is still enigmatic. Macrophage foam cell formation induced by oxLDL requires glycerolipid synthesis. Lipin-1, a key enzyme in the glycerolipid synthesis pathway, contributes to oxLDL-elicited pro-inflammatory responses in a macrophage cell line. The objective of this study was to determine if myeloid-associated lipin-1 contributes to atherogenesis and asses its role in oxLDL-mediated signaling in macrophages**APPROACH AND RESULTS:** We developed mice lacking lipin-1 in myeloid cells and used adeno-associated viral vector 8 expressing the gain-of-function mutation of mouse proprotein convertase subtilisin/kexin type 9 (AAV8-PCSK9) to induce hypercholesterolemia and plaque formation. Mice lacking myeloid-associated lipin-1 had reduced atherosclerotic burden compared to control mice despite similar plasma lipid levels. Stimulation of bone marrow-derived macrophages with oxLDL activated a persistent PKCα/βII-ERK1/2-cJun signaling cascade that contributed to macrophage pro-inflammatory responses. Bone marrow-derived macrophages lacking lipin-1 failed to activate this PKCα/βII-ERK1/2-cJun signaling cascade. **CONCLUSIONS:** Our data demonstrates that myeloid-associated lipin-1 is atherogenic, likely through persistent activation of a PKCα/βII-ERK1/2-cJun signaling cascade that contributes to foam cell pro-inflammatory responses. Taken together these results suggest that oxLDL-induced foam cell formation and oxLDL-induced macrophage pro-inflammatory responses are not separate outcomes of oxLDL-stimulation of macrophages, but rather lipid synthesis that contributes to foam cell formation also influences macrophage inflammatory responses.

Disclosures: **A.E. Vozenilek:** None. **A.R. Navratil:** None. **B. Finck:** None. **A.W. Orr:** Research Grant; Modest; Collaborator R01HL131844. **M.D. Woolard:** Research Grant; Modest; Principal investigator La CATS 1 U54 GM104940, Principal Investigator NIH R01HL131844.

612

High Dimensional Single-Cell Intracellular Signaling Identifies CCL5 as a Potential Key Driver of Myeloid Cell Reprogramming in Atherosclerotic Patients

Adeeb Rahman, Letizia Amadori, Seunghee Kim-Schulze, Pauline Mury, Noah Moss, Jennifer Li, Christian Pina, Peter Faries, Miriam Merad, **Chiara Giannarelli**, Icahn Sch of Med at Mount Sinai, New York, NY

Atherosclerosis is a disease characterized by chronic inflammation. However, identifying new molecularly targeted interventions in human atherosclerosis has proven difficult. In this study, we used phosphoCyTOF to comprehensively characterize functional responses of peripheral immune populations in human atherosclerosis at the single-cell level. Healthy PBMCs were exposed to plasma of patients with atherosclerosis (n=20) or healthy donors (n=10) and the activation of major signaling pathways across all major immune subsets using 18 surface markers and 10 intracellular phospho-proteins. Using viSNE we visualized and defined 10 major immune cell populations: B cells, Basophils, CD1c DCs, CD4 T cells, CD8 T cells, CD14 and CD16 monocytes, NK cells, NKT cells, and pDCs. Next, we evaluated the relative expression of 10 phospho-proteins (IkBa, pCREB, pERK1/2, pMAPKAP2, pp38, pPLCg2, pS6, pSTAT1, pSTAT3, and pSTAT5) across this immunological map and visualized functional pathways that were differentially induced in response to plasma of atherosclerotic patients vs. healthy donors. Monocytes exhibited the greatest immune activation, showing increased phosphorylation of p38, MAPKAP2, ERK1/2, CREB and S6 in response to atherosclerotic plasma. To identify plasma cytokines responsible for this effect, we measured a panel of 41 cytokines and identified CCL5, CXCL10 (IP-10), CXCL1 (GRO), PDGF-AA and PDGF-BB as the most differentially expressed in atherosclerotic vs. healthy plasma. PhosphoCyTOF analysis showed that only CCL5 reproduced the phosphorylation pattern induced by atherosclerotic plasma in monocytes, an effect that was completely inhibited by a CCL5 blocking antibody (Fig. 1). These results suggest that CCL5 in plasma of patients with atherosclerotic disease drives specific innate immune cell signaling functions that mark the inflammatory response in atherosclerotic disease.

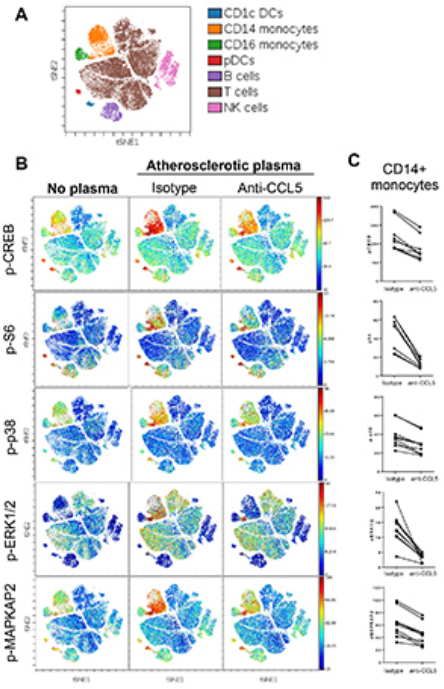

Fig. 1. Effect of CCL5 inhibition on innate immune responses to atherosclerotic plasma. (A). viSNE plot colored to show cell type identity. **(B).** viSNE plots of a representative sample show the effect of CCL5 inhibition using a blocking antibody on the phosphorylation of intracellular kinases activated by atherosclerotic plasma in healthy PBMCs. **(C).** Summary dot plots show the effect of CCL5 inhibition on the phosphorylation of intracellular kinases in $CD14^+$ monocytes across 8 patients.

Disclosures: **A. Rahman:** None. **L. Amadori:** None. **S. Kim-Schulze:** None. **P. Mury:** None. **N. Moss:** None. **J. Li:** None. **C. Pina:** None. **P. Faries:** None. **M. Merad:** None. **C. Giannarelli:** None.

613

In Vitro Microvessels to Study the Platelet-Endothelium Interface

Jevgenia Zilberman-Rudenko, Oregon Health & Science Univ, Portland, OR; Andrew D Wong, Johns Hopkins Univ, Baltimore, MD; Daniel E Sallee, Stephanie E Reitsma, Cristina Puy, Toshiaki Shirai, Annachiara Mitrugno, Oregon Health & Science Univ, Portland, OR; Peter C Searson, Johns Hopkins Univ, Baltimore, MD; Owen J McCarty, Oregon Health & Science Univ, Portland, OR

Background: Under normal conditions, endothelial cells (ECs) govern blood flow dynamics including providing a barrier between blood and tissue and regulating platelet aggregation and thrombin generation in the bloodstream. In turn, blood components, primarily platelets and coagulation factors such as thrombin, regulate EC barrier integrity. The breakdown of EC barrier function is a hallmark of a variety of vascular diseases. In sepsis, for example, the dysfunction of vascular ECs has been correlated with poorer outcomes due to hemorrhage and multi-organ failure associated with consumption of platelets and coagulation factors into clots within the microcirculation, a condition termed disseminated intravascular coagulation (DIC).
Aim: Develop an endothelialized flow chamber to study the platelet-endothelium interface.
Methods and Results: We developed a 3D-chamber with a perfuseable cylindrical microvessel embedded in an extracellular matrix (ECM) material. This model allows for the study of the role of thrombin generation and platelet aggregation in endothelial barrier leak development and repair in healthy as well as inflamed microvessels. Incorporation of subendothelial matrix proteins in these 3D-microvessel devices expands the capacity of the microfluidic studies to investigate blood cell extravasation and enables the control of physical parameters such as transmural pressure and interstitial flow through the ECM.
Conclusion: This model may provide insight into the pathophysiology of different disease states and serve as an expedient platform for therapy design and testing.

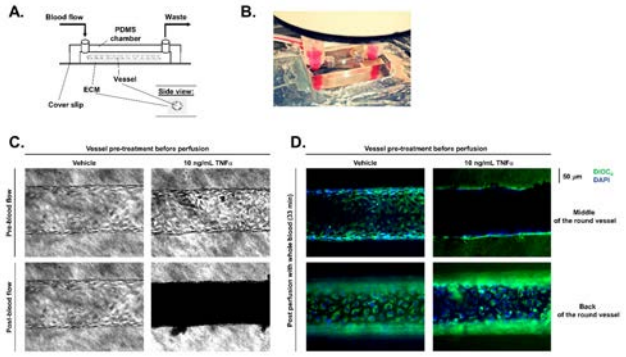

The platelet-endothelium interface under shear flow. Diagram (**A**) and an experimental prototype (**B**) of a 3D-perfuseable device. Microvessel phenotype (following treatment with vehicle or 10 ng/mL TNFα) pre- and post- perfusion with recalcified whole blood for 33 min as visualized by differential interference contrast, DIC, (**C**) and fluorescence microscopy (**D**).

Disclosures: **J. Zilberman-Rudenko:** Research Grant; Modest; F31HL13623001. **A.D. Wong:** None. **D.E. Sallee:** None. **S.E. Reitsma:** None. **C. Puy:** None. **T. Shirai:** None. **A. Mitrugno:** None. **P.C. Searson:** None. **O.J.T. McCarty:** Research Grant; Modest; R01HL101972, R01GM116184, 13EIA12630000.

This research has received full or partial funding support from the American Heart Association.

614

Shear Stress-Induced Glycolytic Metabolites Promote Vascular Repair

Kyung In Baek, Rongsong Li, David Liem, Tyler Beebe, UCLA, LA, CA; Jianguo Ma, Beihang Univ, Beijing, China; Howard Choi, Nelson Jen, Hilary Yen, Peipei Ping, Tzung K Hsiai, UCLA, LA, CA

Introduction: Hemodynamic shear stress is intimately linked with transcriptomic and epigenomic changes to maintain endothelial homeostasis. Metabolomics studies have led to emergent metabolic biomarkers and therapeutic targets. Whether shear stress modulates metabolomic pathway to promote vascular repair remains to be investigated.
Hypothesis: We hypothesized that shear stress regulates VEGF receptor-PKCε-PFKFB3 signaling-mediated glycolytic metabolites to promote vascular repair.
Method and Results: Both pulsatile (PSS: 23 ± 8 dyn·cm^{-2} at 1 Hz) and oscillatory shear stress (OSS: 0.1 ± 3 dyn·cm^{-2} at 1 Hz) up-regulated PKCε expressions and the activity (*P < 0.05, n=3), whereas silencing VEGFR2 with siRNA, or treating with VEGFR inhibitor, Cediranib, attenuated shear stress-mediated PKCε expression in human aortic endothelial cells(HAEC). Constitutively active (CA)-PKCε adenovirus infection enhanced tube formation assessed by Matrigel as well as significantly increased PFKFB3 expressions promoting glycolysis, whereas the dominant negative(DN) PKCε resulted in opposite effects. Co-localization of PKCε and PFKFB3 expression was demonstrated in the endothelium of aortic arch and thoracic aorta in a New Zealand White rabbit model. In the zebrafish tail amputation model, reduction of shear stress via *GATA-1a* morpholino oligonucleotide(MO) injection and inhibition of PKCε expression via PKCε MO impaired vascular repair between the dorsal aorta and the dorsal longitudinal anastomotic vessel at 3 days post amputation(dpa). PKCε mRNA rescued *GATA-1a* MO-mediated impairment of vascular repair (*P < 0.01, n=20, **P < 0.05, n=5). Metabolomic analysis in HAEC applied to PSS and OSS revealed modulation of a number of metabolites including increased glycolytic metabolite dihydroxyacetone, which was blocked by PKCε siRNA. Treatment with dihydroxyacetone rescued PKCε-impaired vascular repair.
Conclusion: In conclusion, shear stress-mediated VEGFR-PKCε-PFKFB3 signaling increased glycolytic metabolites to mediate vascular repair.

Disclosures: **K. Baek:** None. **R. Li:** None. **D. Liem:** None. **T. Beebe:** None. **J. Ma:** None. **H. Choi:** None. **N. Jen:** None. **H. Yen:** None. **P. Ping:** None. **T.K. Hsiai:** None.

615

Transactivation of EGFR by TGFβ Induces Hypertension by Increasing Arteriolar Myogenic Response

Daniela Carnevale, Sapienza Univ of Rome and IRCCS Neuromed, Pozzilli (IS), Italy; Manuel Casaburo, Stefania Fardella, IRCCS Neuromed, Pozzilli (IS), Italy; Dario Bizzotto, Univ of Padova, Pozzilli (IS), Italy; Francesco Da Ros, Univ of Padova, Padova, Italy; Giuseppe Cifelli, Gualtiero Innocenzi, IRCCS Neuromed, Pozzilli (IS), Italy; Giorgio Bressan, Univ of Padova, Padova, Italy; Giuseppe Lembo, Sapienza Univ of Rome and IRCCS Neuromed, Pozzilli, Italy

Myogenic tone (MT) is an intrinsic property of arteriolar smooth muscle cells (SMCs) that contract when intraluminal pressure is increased. MT is a relevant physiological mechanism to maintain stable blood flow through important organs like kidney and brain, thus preventing organ damage that could derive from increase in blood pressure (BP). On the other hand, enhancement of the basal MT could raise BP by increasing systemic vascular resistance, thus further contributing to hypertension. Several studies in animal models suggest that primary dysfunctions in SMCs can directly cause abnormalities in BP. However, in hypertensive animal models investigated so far, the increment of MT is accompanied by a stronger response to G protein coupled receptor (GPCR) agonists, thus making it difficult to distinguish whether increased vascular resistance and BP are primary effects of a more robust MT or the consequence of increased reactivity to agonists. Here we show an increased MT in mice deficient of *Emilin1* , an extracellular inhibitor of TGFβ signaling, displaying a phenotype of spontaneous hypertension. We also found that the higher TGFβ signaling in *Emilin1* deficient SMCs stimulates heparin binding epidermal growth factor (HB-EGF) expression and subsequent transactivation of the EGF receptor. When step-increases in intraluminal pressure are applied to mesenteric resistance arteries (MRA), the combined stimulation of mechanosensor and EGF transactivation results into activation of transient receptor potential classical type 6 (TRPC6) and melastatin type 4 (TRPM4) channels, stimulation of voltage dependent calcium channels (VDCC). To put our data into translational perspective, we measured MT on resistance arteries isolated from hypertensive patients and untreated normotensives, finding increased MT and TGFβ signaling in the former group. In addition, by using an antibody neutralizing EGFR signaling we found a normalization of the increased MT, thus confirming the relevance of TGFβ-EGFR pathway in humans. Overall our results suggest that primary increase of MT induced by TGFβ-EGFR transactivation can cause hypertension and that higher TGFβ-EGFR signaling and MT are common alterations of resistance arteries of hypertensive patients.

Disclosures: **D. Carnevale:** None. **M. Casaburo:** None. **S. Fardella:** None. **D. Bizzotto:** None. **F. Da Ros:** None. **G. Cifelli:** None. **G. Innocenzi:** None. **G. Bressan:** None. **G. Lembo:** None.

616

Potentiation of Endothelium-Dependent Vasodilation by Adenylate Cyclase Type 9 Inactivation is Associated with Increased Endothelial Cell Signaling in Mouse Femoral Arteries

Yohann Rautureau, Adeline Raigneault, Uy Kurunradeth, Daniel Rivas, Marie-Eve Higgins, Eric Thorin, Eric Rhéaume, Jean-Claude Tardif, Montreal Heart Inst, Montreal, QC, Canada

Adenylate cyclase (AC) activity in vessels is associated with vasodilation. The AC family includes 10 members of which AC9 is the least studied. We recently demonstrated that *Adcy9* inactivation in mice protects from atherosclerosis in the aorta and potentiates endothelium-dependent vasodilation (EDV) to acetylcholine (ACh) in femoral arteries (FA). Our objectives were 1) to determine *Adcy9* expression in FA; 2) investigate endothelial signalling pathways associated with *Adcy9* inactivation-induced potentiation of ACh-induced EDV; and 3) to assess the effect of *Adcy9* inactivation on EDV during flow-mediated dilation (FMD).
FA were isolated from 8 to 13 week-old *Adcy9*-inactivated (*Adcy9*^{Gt}) and wild-type (WT) littermate mice. *Adcy9* expression was studied in WT FA tissue section by *in situ* hybridization (ISH) using *Adcy9* and negative control probes. Diameter of pressurized (80 mmHg) FA (internal diameter 288±3 µm) was studied in response to ACh (n=7-14) and shear stress (n=12) up to 20 dynes/cm^2 after preconstriction with phenylephrine. To study the role of endothelial signalling pathways in response to ACh-induced EDV, FA were incubated in absence or presence of inhibitors for nitric oxide (NO) synthase (L-NNA 0.1 µM), cyclooxygenase (meclofenamate 1 µM) and endothelial hyperpolarization (TRAM-34 10 µM plus apamin 0.1 µM).
ISH with *Adcy9* probe resulted in numerous dots in the vascular wall of the FA. Meclofenamate and the

combination of TRAM-34 plus apamin decreased maximal (E_{max}) EDV to ACh, respectively, by 40 and 17% in *Adcy9*^{Gt} (P<0.01) but had no effect in WT mice. L-NNA reduced E_{max} to ACh by 26% in WT (P<0.01) and 50% in *Adcy9*^{Gt} (P<0.01). *Adcy9* inactivation tended to increase FMD to shear stress ranging from 6 to 20 dynes/cm^2: At 10 dynes/cm^2, FMD was increased from 25.4±4.9% in WT to 37.4±4.9% in *Adcy9*^{Gt} mice (P=0.083, n=12 per group).
In conclusion, our data show that FA express *Adcy9* and that *Adcy9* inactivation increases the effects of endothelial NO, hyperpolarization and cyclooxygenase pathways in EDV. A numerical increase in FMD in Adcy9^{Gt} compared to WT confirms the potentiating effect of *Adcy9* inactivation on EDV. The potentiation of endothelial dilatory pathways appears to be associated with the anti-atherosclerotic effects of *Adcy9* inactivation.

Disclosures: **Y. Rautureau:** None. **A. Raigneault:** None. **U. Kurunradeth:** None. **D. Rivas:** None. **M. Higgins:** None. **E. Thorin:** None. **E. Rhéaume:** None. **J. Tardif:** Research Grant; Significant; Amarin, Astra-Zeneca, DalCor, Eli Lilly, Esperion, Ionis, Merck, Pfizer, Roche, Sanofi, Servier. Honoraria; Significant; DalCor, Pfizer, Sanofi, Servier. Other; Modest; Patent genotype dependent effects of dalcetrapib, Equity in DalCor.

617

Inhibitors of Beta-Catenin Signaling Limit Growth of Vascular Smooth Muscle Cells

Dario F Riascos-Bernal, Jordana N Gross, Prameladevi Chinnasamy, Nicholas E Sibinga, Albert Einstein Coll of Med, Bronx, NY

Smooth muscle cell (SMC) growth is essential for artery formation during development and significantly contributes to neointima formation after vascular injury in adulthood. We recently showed, using a tissue-specific deletion and knock-in of mutant alleles, that beta-catenin (b-ctn) signaling function is essential for SMC growth and artery formation; moreover, protein interactions mediated by its C-terminus domain are required for assembly of the arterial wall, while b-ctn N-terminus interactions are dispensable. Inhibitors of b-ctn have been developed, but their effects on vascular SMC growth have not been fully tested. We hypothesize that inhibitors that disrupt protein interactions mediated by the b-ctn C-terminus domain will impair b-ctn signaling and limit growth of vascular SMCs. We evaluated growth of mouse aortic SMCs and human coronary artery SMCs in culture using AlamarBlue after exposure to increasing concentrations (0.01 to 10 micromolar) of several validated b-ctn inhibitors or vehicle control: PKF118-310 (disrupts the b-ctn/TCF interaction), ICG001 (disrupts the b-ctn C-terminus/CBP interaction), XAV939 (promotes the b-ctn destruction complex), and carnosic acid (disrupts the b-ctn N-terminus/BCL9 interaction). We also evaluated the effect of these inhibitors on b-ctn transcriptional activity in SMCs using a TOPflash reporter system. We found that PKF118-310 (p<0.05 vs. vehicle), ICG001 (p<0.05 vs. vehicle), and XAV939 (p<0.05 vs. vehicle), but not carnosic acid, limit mouse (n=16 independent cultures) and human (n=8 independent cultures) SMC growth in a dose-response manner. PKF118-310 exhibited the most potent inhibitory effect. We also found that PKF118-310, ICG001, and XAV939, but not carnosic acid, inhibit b-ctn transcriptional activity in arterial SMCs in culture. In conclusion, pharmacological inhibition of b-ctn signaling, particularly blocking the b-ctn C-terminus output, inhibits growth of vascular SMCs in culture, providing a rationale to test these inhibitors in models of vascular injury as they hold promise as novel therapies for cardiovascular disease.

Disclosures: **D.F. Riascos-Bernal:** None. **J.N. Gross:** None. **P. Chinnasamy:** None. **N.E.S. Sibinga:** None.

This research has received full or partial funding support from the American Heart Association.

618

Hypoxia Inducible Factor 1a Stabilization in Autosomal Dominant Hyper IgE Syndrome Fibroblasts Rescues Impaired Ability to Support Angiogenesis

Alex F Grubb, Lab of Cardiovascular Regenerative Med, Ctr for Molecular Med, NHLBI, NIH: Cleveland Clinic Lerner Coll of Med:, Bethesda, MD; Natalia I Dmitrieva, Lab of Cardiovascular Regenerative Med, Ctr for Molecular Med, NHLBI NIH,, Bethesda, MD; Avram Walts, Guibin Chen, Lab of Cardiovascular Regenerative Med, Ctr for Molecular Med, Bethesda, MD; Xue Zhang, Xujing Wang, Bioinformatics and Systems Biology Core, Systems Biology Ctr, Bethesda, MD; Alexandra F Freeman, Steve M Holland, Lab

of Clinical Infectious Diseases, NIAID, NIH, Bethesda, MD; Manfred Boehm, Lab of Cardiovascular Regenerative Med, Ctr for Molecular Med, Bethesda, MD

Background: Autosomal dominant Hyper-IgE syndrome (AD-HIES) is a rare primary immunodeficiency caused by dominant negative mutations in signal transducer and activator of transcription 3 (STAT3), a mediator of widespread physiological processes. It is characterized by dermatitis, recurrent infections, elevated IgE, poor post-surgical healing, and connective tissue abnormalities. How STAT3 deficiency leads to this phenotype, however, is not known. Current treatment options are limited to antimicrobials for infection control. The aim of this study was to investigate which of STAT3's many functions are dis-regulated in AD-HIES, and where potential targets for therapy may lie.
Methods: We used skin fibroblasts (SF) from 3 AD-HIES patients and 3 normal volunteers. To evaluate potentially affected pathways, we utilized RNA- Seq and subsequent Gene Set Enrichment (GSEA) and pathway analysis (Pathway Studio, GeneGo Metacore). Endothelial cell tube formation assay was used to assess ability of AD-HIES SFs to support angiogenesis.
Results: GSEA and pathway analysis showed deficiencies in signaling pathways linked to wound healing, extracellular matrix remodeling and angiogenesis including targets of Hypoxia Inducible Factor 1a (HIF1a) (P values for enrichments < 0.001). Therefore, we hypothesized that AD-HIES SFs have impaired ability to support angiogenesis due to deficient Hif1a-dependent secretion of matrix proteases and growth factors. Indeed, AD-HIES SF secreted up to 5 times less matrix metalloprotease 1, 3, and 9, placental growth factor and fibroblast growth factors 1 and 2 (Luminex Multiplex, n=3-9, P<0.05). Culture medium from AD-HIES SFs failed to fully support tube formation by endothelial cells resulting in lower number of junctions, meshes, and total tubule length (n=6, P<0.005). Stabilization of Hif1a in AD-HIES SFs by prolyl hydroxylase inhibitor dimethyl fumarate restored its transcriptional activity leading to increased number of junctions, meshes, and tubule length (n=12, P<0.05)
Conclusion: AD-HIES SFs have deficiencies in pro-angiogenic signaling pathways that lead to decreased growth factor secretion and angiogenesis. Stabilization of HIF1a corrects this deficiency and is an enticing target for future therapy.

Disclosures: **A.F. Grubb:** None. **N.I. Dmitrieva:** None. **A. Walts:** None. **G. Chen:** None. **X. Zhang:** None. **X. Wang:** None. **A.F. Freeman:** None. **S.M. Holland:** None. **M. Boehm:** None.

620

Circulating miRNAs a Novel Tool to Assess BAG3 Related Dilated Cardiomyopathy

Rocio Toro, Sch of Med of Cadiz, Cadiz, Spain; Marta Saura, Dept of Systems Biology (Physiology), Univ of Alcalá, Sch of Med (IRYCIS), Alcala de Henares (Madrid), Spain; David De Gonzalo, Vicenta Llorente-Cortes, Group of Lipids and Cardiovascular Pathology, Biomedical Res Inst Sant Pau (IIB Sant Pau), Barcelona, Spain; Felix Rosa-Longobardo, Alipio Mangas, Sch of Med of Cadiz, Cadiz, Spain; Jose Luis Zamorano, Cardiology Dept, Univ Hosp Ramón y Cajal (IRYCIS), Madrid, Spain; Carlos Zaragoza, Cardiology Dept, Univ Francisco de Vitoria/Hosp Ramón y Cajal Res Unit (IRYCIS), Cadiz, Spain

Background
A new familial dilated cardiomyopathy (DCM) was recently found related to mutations in the antiapoptotic BAG3 gene. MicroRNAs (miRNAs) are short non-coding RNAs playing significant roles in cardiac disease, including DCM, thus representing new potential targets of treatment. However, no previous study has evaluated the clinical association between BAG3-related DCM and circulating miRNAs.
Purpose
We aimed to evaluate whether the clinical association between BAG3-related familial DCM and the circulating miRNA profile may represent a new tool for the diagnosis and progression assessment of the disease.
Methods
Detailed clinical and echocardiographic information was obtained from 21 patients with familial DCM carrying the BAG3 mutation and 21 age-matched healthy subjects. RNA was isolated from peripheral blood and analysed using ultrasequencing. Bioinformatic analysis was performed to explore the potential molecular pathways related to the miRNA profile.
Results
To determine the miRNA profile in BAG3-associated DCM, the analysis of 1759 circulating miRNA was performed in symptomatic and asymptomatic patients with BAG3 mutation, and compared to healthy age-matched subjects. The expression profiles showed significant differences between controls and BAG3 mutation carriers: miRNAs 3191-3p, 6769b-3p, 1249-ep, 154-5p, 6855-5p, and 182-5p were at least 2-fold downregulated in patients compared to healthy subjects. Endogenous gene targets of these miRNAs

are now under investigation, highlighting miR-182-5p,and its target Ankyrin G.
Conclusions
miRNAs emerge as a novel tool to differentiate healthy subjects and patients with BAG3-related DCM. Of particular interest is the downstream analysis of endogenous miRNA targets, the Ankyrin G gene. Further investigation regarding the contribution of Ankyrin G and other target genes of the miRNA profile described in BAG3-related DCM will be a key step to deeply understand the contribution of miRNAs in the pathophysiology of familial DCM.

Disclosures: **R. Toro:** None. **M. Saura:** None. **D. De Gonzalo:** None. **V. Llorente-Cortes:** None. **F. Rosa-Longobardo:** None. **A. Mangas:** None. **J. Zamorano:** None. **C. Zaragoza:** None.

621

Basic Fibroblast Growth Factor Helps to Maintain the Stemness of Rat Multipotent Adult Progenitor Cells Partially via Erk1/2 Signaling

Qingyi Zhu, Meng Jiang, Xuanyou Liu, Yichao Xiao, Hong Hao, Abraham Joseph, Davis Heart and Lung Inst, Columbus, OH; Shenghua Zhou, The Second Xiangya Hosp of Cardiology, Changsha, China; Jiangjun Guan, Zhenguo Liu, Davis Heart and Lung Inst, Columbus, OH

Bone marrow mesenchymal stem cells are one of the important sources for cell replacement therapies. The outcome of the cell-based therapies is determined by a variety of factors including the source of the cells and their functional status. The functional status is usually measured by the expression of stem cell specific marker Oct-4 (stemness), differentiation potential (multipotency), and production of paracrine factors. It could be beneficial to keep the stem cells in a multipotent state for their optimal therapeutic outcome. The present study was to investigate the effect of basic fibroblast growth factor (bFGF) on the stemness of bone marrow stem cells and related mechanism. Rat multipotent adult progenitor cells (MAPCs) were used as the source of bone marrow stem cells, and induced to differentiate in vitro with (bFGF:5ng/ml and 20ng/ml) and without bFGF for up to 7 days. The expression of Oct4 and endothelial markers including Flk1, VWF and CD31, and smooth muscle cell markers including α-SMA, SM22 and CNN1 were determined with real-time (RT) PCR and western blot. We observed that both transcriptional (as reflected by RT-PCR) and protein expression (by western blot) of Oct4 was maintained at relatively stable levels in the cells treated with bFGF during the early phase of differentition. On the other hand, the expression of Flk1, VWF, CD31 and α-SMA, SM22, CNN1 were significantly decreased in the cells with the presence of bFGF. Treatment with bFGF significantly increased the phosphorylation of Erk1/2, not Akt nor STAT3, in the cells. Inhibition of Erk1/2 phosphorylation with PD98059 partially but significantly attenuated the effect of bFGF on Oct4 expression in the cells. These data suggest that bFGF could be able to maintain the bone marrow stem cells in their undifferentiated state in vitro partially through Erk1/2 signaling-mediated mechanism.

Disclosures: **Q. Zhu:** None. **M. Jiang:** None. **X. Liu:** None. **Y. Xiao:** None. **H. Hao:** None. **A. Joseph:** None. **S. Zhou:** None. **J. Guan:** None. **Z. Liu:** None.

622

Cd44 Plays an Important Role in Regulating Heart Failure Induced Lung Vascular Remodeling and Who Type-2 Pulmonary Hypertension

Xinyu Weng, Wenhui Yue, Dongzhi Wang, Cardiovascular Dept, Shanghai Tenth Renmin Hosp, Shanghai, China; Huan Wang, Univ Minnesota, Minneapolis, MN; Yawei Xu, Cardiovascular Dept, Shanghai Tenth Renmin Hosp, Shanghai, China; **Yingjie Chen**, Univ Minnesota, Minneapolis, MN

End-stage left ventricular failure or chronic heart failure (CHF) causes severe lung inflammation, vascular remodeling, WHO type-2 pulmonary hypertension, and right ventricular hypertrophy. However, the molecular mechanism of CHF-induced lung inflammation and remodeling is largely unknown. CD44 is a member of the hyaluronate receptor family of cell adhesion molecules, which has been shown to play a selective role in controlling macrophage and lymphocyte migration. Here we demonstrated that end-stage CHF causes a dramatic increase of CD44 expression in heart and lung in human and mice. Histological staining shows that CD44 is predominantly expressed in leukocytes such as macrophages. Flow cytometry analysis further demonstrates that CD44 is predominantly expressed in F4/80 positive macrophages, CD4+, and CD8+ T cells. CD44 expression is dramatically increased in activated T cell subsets. To further determine the physiological role of CD44 in CHF-induced lung remodeling and type-2

pulmonary hypertension, we studied the effect of CD44 blockade on type-2 pulmonary hypertension development in a group of mice with existing moderate left ventricular failure without apparent lung remodeling. Interestingly, we found that blockade CD44 with blocking antibodies (Abs) significantly attenuate the development of lung vascular and interstitial leukocyte infiltration, lung vascular remodeling, fibrosis, and increase of right ventricular hypertrophy. Blockade CD44 signaling also significantly attenuated further decline of left ventricular ejection fraction in mice with existing LV failure. In addition, we demonstrated that induction of T regulatory cells with IL-2 and IL-2 Abs complex significantly attenuated the infiltration of CD44 positive leukocytes in lung tissue, lung vascular remodeling, lung fibrosis, and right ventricular hypertrophy in mice with existing moderate left ventricular failure. Together, these data indicate an important role of CD44 in left ventricular failure-induced lung inflammation, and type-2 pulmonary hypertension, suggesting that inhibition of CD44 may attenuate heart failure progression and type-2 pulmonary hypertension.

Disclosures: **X. Weng:** None. **W. Yue:** None. **D. Wang:** None. **H. Wang:** None. **Y. Xu:** None. **Y. Chen:** None.

This research has received full or partial funding support from the American Heart Association.

623

Hyperhomocysteinemia Potentiates Inflammatory Monocyte Differentiation and Vascular Dysfunction in Type 2 Diabetic Mice

Pu Fang, Xiaohua Jiang, Xiaofeng Yang, Hong Wang, Temple Univ, Philadelphia, PA

Hyperhomocysteinemia (HHcy) is associated with increased diabetic cardiovascular diseases. In this study, we investigated the effects of type 2 diabetes mellitus (T2DM), HHcy and their combination on inflammatory monocyte (MC) differentiation and vascular function.
We established an atherosclerosis-susceptible T2DM+HHcy compound mouse model. T2DM was induced in db/db mice by spontaneous mutation (average blood glucose 493 mg/dL). HHcy was established by feeding the mice a high fat+high methionine diet (HF+HM, 8 weeks). Methionine is the homocysteine (Hcy) precursor, which elevated plasma Hcy level to 129 µM. Plasma Hcy level was lowered by vitamin therapy employing a HF+HM+high vitamin diet (HF+HM+HV), which reduced plasma Hcy levels from 129 µM to 42 µM. HHcy aggravated T2DM-impaired endothelial-dependent vessel relaxation to acetylcholine, which was completely abolished by endothelial nitric oxide synthase (eNOS) inhibitor N^G-nitro-L-arginine methyl ester. HHcy potentiated T2DM-induced inflammatory monocytes ($CD45^+CD11b^+Ly6C^+$ MCs) in aorta isolated from compound mice. Severe HHcy- and T2DM-induced mononuclear cells (MNCs), $CD11b^+$ MCs, $CD11b^+Ly6C^{middle+high}$ inflammatory MCs and M1 macrophages (MØs) were potentiated by the combination of HHcy and T2DM in mouse bone marrow (BM), peripheral blood, and spleen. Folate based Hcy-lowering therapy (HF+HM+HV) reversed systemic MNC, MC, inflammatory MC and MØ and aortic inflammatory MC increases in T2DM mice. Finally, bone marrow transplantation (BMT) using lentivirus-shLy6C transduced BM cells, which decreased blood $Ly6C^+$ inflammatory MCs, resulted in ameliorated endothelial-dependent vessel relaxation. In conclusion, our data suggested that HHcy accelerated T2DM-induced systemic inflammatory MC and MØ differentiation, aortic inflammatory MC infiltration, and vascular dysfunction.

Disclosures: **P. Fang:** None. **X. Jiang:** None. **X. Yang:** None. **H. Wang:** None.

This research has received full or partial funding support from the American Heart Association.

624

Accumulation of Advanced Glycation End Products is Associated With Structural Degeneration of Bioprosthetic Heart Valves

Antonio Frasca, Children's Hosp of Philadelphia, Philadelphia, PA; Emanuela Branchetti, Perelman Sch of Med at the Univ of Pennsylvania, Philadelphia, PA; Juan B Grau, Univ of Ottawa Heart Inst, Ottawa, ON, Canada; Matthew J Gillespie, Robert J Levy, Children's Hosp of Philadelphia, Philadelphia, PA; Giovanni Ferrari, Perelman Sch of Med at the Univ of Pennsylvania, Philadelphia, PA

Introduction: Bioprosthetic heart valves (BHV) are widely used but frequently limited by structural valve degeneration (SVD), necessitating re-operation. Calcification is by far the best-studied SVD mechanism, but recent studies suggest that oxidative stress contributes to SVD. Advanced glycation end products

(AGEs), formed by the ligation of sugar derivatives to proteins under oxidative conditions, mediate tissue degeneration in cardiovascular diseases. AGEs effect tissue damage through cross-linking and degradation of extracellular matrix proteins including collagen, a major structural component of BHV, as well as through exacerbation of inflammatory cell stimulation. **Hypothesis:** We hypothesize that AGEs accumulate in BHVs and are associated with oxidative stress-based SVD **Methods:** We performed immunohistochemistry for AGEs and specifically carboxymethyl lysine (CML) on sections of fixed, paraffin-embedded samples of degenerated bioprosthetic heart valves from 7 patients in the Penn Cardiac Bioregistry (4 male, 3 female, ages 40-83) and 4 short-term experimental Melody valve leaflets deployed in branch pulmonary arteries of 3 sheep. We correlated these results with levels of the circulating AGE receptor sRAGE via ELISA for patient BHV explants and with oxidized amino acid levels quantitated by mass spectrometry of di-tyrosine for experimental sheep BHV explants. **Results:** There was diffuse accumulation of AGEs in both clinical SVD and sheep explants of BHV. Immunohistochemistry reveals clear AGE and CML staining in all tested valves versus minimal to absent staining in unimplanted control samples. Staining intensity qualitatively correlated with overall di-tyrosine accumulation as well as sRAGE levels that were elevated in BHV patients. Notably, local staining for AGE in BHV is intensified in areas of calcification, thickening, and apparent inflammatory infiltration as well as in areas with structural damage. **Conclusions:** Extensive AGE accumulation was observed in both BHV explanted for SVD and sheep explants compared to controls, supporting the view that AGEs are associated with SVD pathophysiology. The association of AGE accumulation with di-tyrosine in BHV suggests that oxidative stress is a major mechanism of BHV SVD.

Disclosures: **A. Frasca:** None. **E. Branchetti:** None. **J.B. Grau:** None. **M.J. Gillespie:** None. **R.J. Levy:** None. **G. Ferrari:** None.

This research has received full or partial funding support from the American Heart Association.

625

Modest Elevations of Extracellular Sodium Activate Dendritic Cells and Contribute to Hypertension

Natalia Barbaro, Jason Foss, Sergey Dikalov, David Harrison, **Annet Kirabo**, Vanderbilt Univ Coll of Med, Nashville, TN

Recently, it has become apparent that sodium can accumulate in the interstitium of hypertensive humans and animals, and such high salt concentrations drive immune cells toward a pro-inflammatory phenotype through poorly defined mechanisms. We hypothesized that dendritic cells (DCs) are activated by modest elevations of extracellular sodium via formation of IsoLGs leading to hypertension. Isolated mouse splenic DCs were cultured in media with either normal salt (NS, 150 mM NaCl), high salt (HS, 190 mM NaCl) or HS plus the gp91ds-tat peptide which inhibits assembly of NADPH oxidase for 24 hours. DCs exposed to HS demonstrated a marked increase in superoxide production compared to NS (146.3±9.5 vs. 100.0±5.0 % control, $p<0.001$). This was NADPH oxidase dependent because incubation with the gp91ds-tat peptide prevented this effect. Using flow cytometry, we found that DCs cultured in HS had a significantly higher expression of CD86 and more IsoLG-protein adducts than those cultured in NS. These effects were not mimicked by an equiosmolar concentration of mannitol. Western blot analysis of protein extracts from DCs indicated HS markedly increased phosphorylation of the NADPH oxidase subunit $p47^{phox}$ and association of $p47^{phox}$ with $gp91^{phox}$. Importantly, we found that the salt-activated DCs promote production of cytokines interferon gamma and interleukin 17 by primed T cells. To determine whether these salt-activated DCs promote hypertension, mice received adoptive transfer of splenic DCs that were cultured for 24 hours in either NS (n = 6); HS (n = 5); or HS plus an IsoLG scavenger (n = 6). Mice were then implanted with radiotelemeters to measure mean arterial pressure (MAP) and infused with a subpressor dose (140 ng/kg/min) of angiotensin II (AngII) for two weeks. This caused no increase in MAP in mice that received NS DCs (+0.8 +/- 3.3 mmHg), whereas MAP increased significantly with AngII infusion in mice that received HS DCs (+13.4 +/- 5 mmHg). This pro-hypertensive effect of salt on DCs was attenuated by scavenging of IsoLGs (-3.3 +/- 4.4 mmHg) during salt exposure. These findings provide a mechanistic link between salt, inflammation and hypertension involving increased oxidative stress and IsoLG production in DCs.

Disclosures: **N. Barbaro:** None. **J. Foss:** None. **S. Dikalov:** None. **D. Harrison:** None. **A. Kirabo:** None.

This research has received full or partial funding support from the American Heart Association.

626

Apabetalone (Rvx-208), a Selective Bet Protein Inhibitor, Reduces Expression of Acute Phase Response Markers *in vitro* and in Patients With Cardiovascular Disease and Chronic Kidney Disease

Ewelina Kulikowski, Sylwia Wasiak, Dean Gilham, Laura Tsujikawa, Christopher Halliday, Ravi Jahagirdar, Resverlogix Corp., Calgary, AB, Canada; Mike Sweeney, Jan Johansson, Resverlogix Corp., San Francisco, CA; Norm Wong, Resverlogix Corp., Calgary, AB, Canada

Apabetalone is an inhibitor of the epigenetic readers bromodomain and extraterminal (BET) proteins, currently in a phase 3 outcomes trial in patients with cardiovascular disease (CVD) and diabetes mellitus. A post hoc analysis of phase 2b trials demonstrated a 55% relative risk reduction in major adverse cardiac events in CVD patients. Elevated inflammatory markers correlate with CVD. Inflammation also accompanies chronic kidney disease (CKD) and CKD patients are at risk of CVD. Previous research has shown that apabetalone modulates pathways that contribute to chronic inflammation, including the acute phase response (APR). Here, pathway analysis of gene microarrays showed downregulation of APR by apabetalone in primary human hepatocytes (PHH). Real-time PCR and ELISA analysis of RVX-208 treated PHHs confirmed that APR genes that correlate with CVD are suppressed by 20 to 95%, including CRP, ceruloplasmin (CP), serum amyloid P (SAP), PAI-1, alpha 2-macroglobulin (A2M), complement C2, C3 and C5, MBL2, serum amyloid A and interleukin 18. Apabetalone decreased IL-6-induced expression of CP, SAP and A2M, with most striking effects on CRP (-75%). Apabetalone also decreased LPS-induced expression of SAP in a mouse endotoxemia model. To assess effects of apabetalone on inflammatory mediators in CVD patients, SOMAscan™ 1.3K proteomic analysis was performed on plasma from phase 2b ASSERT (12 weeks; n=25) and ASSURE (26 weeks; n=47) clinical trials. This approach identified APR as the top downregulated pathway by apabetalone in both trials. APR biomarkers are elevated in CKD patients where they correlate with disease progression. To gain insight into the pharmacodynamics of the APR response to apabetalone, stage 4 CKD patients (n=8) received a single dose of the drug followed by plasma proteomics at several time points. At 12h post dose, APR was significantly downregulated by apabetalone. Of note, CRP was decreased in CKD patients after 12h of treatment (-7%, p=0.04) versus baseline, as well as in ASSERT (-43%, p=0.01) and ASSURE (-21%, p=0.02) trials versus placebo. Downregulation of the APR pathway by apabetalone may lead to reduced chronic inflammation in CVD and CKD patients and contribute to the reduction in MACE in patients with high residual CVD risk.

Disclosures: **E. Kulikowski:** Employment; Significant; Resverlogix Corp.. Ownership Interest; Modest; Resverlogix Corp. **S. Wasiak:** Employment; Significant; Resverlogix Corp.. Ownership Interest; Modest; Resverlogix Corp. **D. Gilham:** Employment; Significant; Resverlogix Corp.. Ownership Interest; Modest; Resverlogix Corp. **L. Tsujikawa:** Employment; Significant; Resverlogix Corp.. Ownership Interest; Modest; Resverlogix Corp. **C. Halliday:** Employment; Significant; Resverlogix Corp.. Ownership Interest; Modest; Resverlogix Corp. **R. Jahagirdar:** Employment; Significant; Resverlogix Corp.. Ownership Interest; Modest; Resverlogix Corp. **M. Sweeney:** Employment; Significant; Resverlogix Corp.. Ownership Interest; Modest; Resverlogix Corp. **J. Johansson:** Employment; Significant; Resverlogix Corp.. Ownership Interest; Modest; Resverlogix Corp. **N. Wong:** Employment; Significant; Resverlogix Corp.. Ownership Interest; Modest; Resverlogix Corp..

627

Human Osteopontin Isoforms Differentially Promote Neovascularization in Response to Ischemia via Macrophage Recruitment and Survival

Grace S.H. Lee, Courtney M. Caroti, Giji Joseph, Daiana Weiss, Hector F. Salazar, Zoe Shin Yee Lok, W. Robert Taylor, **Alicia N Lyle**, Emory Univ, Atlanta, GA

Background: Coronary and peripheral artery diseases result in vessel occlusion and ischemia, initiating neovascularization to restore blood flow and preserve function. We previously established that osteopontin (OPN), a matricellular cytokine, is critical to ischemia-induced neovascularization. Unlike rodents, humans express 3 OPN isoforms (a, b, and c); however, the roles of these isoforms in neovascularization and cell migration remain undefined. *Methods and Results:* Using a murine model of hindlimb ischemia in $OPN^{-/-}$ mice and $1.5x10^6$ lentivirus particles expressing OPNa, OPNb or OPNc delivered IM, we found that OPN isoforms have different effects on functional perfusion recovery *in vivo*. OPNa increased limb perfusion 30.4%±0.8 and OPNc by 70.9%±6.3, as measured by laser Doppler

perfusion imaging (d14; p<0.001 vs. LVGFP). Increases in perfusion translated to significant increases in functional limb use in OPNa and OPNc treated animals (61.1%±8.2; 76.2%±9.7; p<0.05), as assessed by voluntary running wheel use, and was not due to isoform expression differences (ELISA, n=6, p=ns). While OPN isoforms did not differentially affect angiogenesis, OPNa and OPNc significantly increased arteriogenesis (enlargement of arterioles), as measured by the increase in SM α-actin positive vessels in the small (200 - 700 μm^2; 47.2%±6.1; 55.9%±6.7) and large artery (1000 - 2500 μm^2; 54.2%±6.1; 76.5%±10.9) ranges *in vivo* (n=9; p<0.001 vs. OPNb). We hypothesized that OPN isoform-dependent effects on arteriogenesis are due to differential effects on macrophage function. OPN isoforms did not differentially affect macrophage polarization and all 3 isoforms increased macrophage survival (64.9%±1.1 - 78.6%±1.9 vs. control; p<0.0001). However, OPNa and OPNc both increased macrophage migration, where OPNc was the more potent migratory stimulus (n=4, p<0.001 vs. no trx, OPNa, OPNb). *Conclusion:* In conclusion, human OPN isoforms exert divergent effects on neovascularization through differential effects on arteriogenesis and macrophage migration and survival. Altogether, these data support that human OPN isoforms may represent novel therapeutic targets to improve neovascualrization and preserve tissue function in obstructive artery disease patients.

Disclosures: **G.S. Lee:** None. **C.M. Caroti:** None. **G. Joseph:** None. **D. Weiss:** None. **H.F. Salazar:** None. **Z. Shin Yee Lok:** None. **W. Taylor:** None. **A.N. Lyle:** None.

628

Circulating Exosomes Isolated from Septic Mice Induce Endothelial Hyperpermeability Through Promoting Podosome Cluster Formation

Xingjiang Mu, Xiaohong Wang, Kobina Essandoh, Yutian Li, Amanda M Pugh, Jiangtong Peng, Shan Deng, Esam S Salem, Charles C Caldwell, Guo-Chang Fan, Univ of Cincinnati, Cincinnati, OH

Introduction: Septic shock increases vascular permeability, leading to multiple organ failure and higher mortality. Reactive oxygen species (ROS) have been shown to promote both actin cytoskeleton reorganization resulting in vascular leakage and the formation of podosome, an actin-based dynamic membrane structure. Interestingly, recent studies have shown that circulating exosomes from septic patients contained higher levels of ROS than healthy ones. In this study, we hypothesized that septic exosomes can transfer exosomal ROS to endothelial cell (EC) to promote the generation of podosomes, leading to hyperpermeability.
Methods: C57BL/6 mice (20-25g) were subjected to CLP surgery or injection with LPS (25 μg/g). Sham-operated or PBS-treated mice were used as controls. Exosomes were isolated from sera, collected at 3 h post-CLP or post-LPS-injection. Podosomes were identified by co-immunostaining F-actin/cortactin following stimulation with PMA, thrombin and exosomes. Transendothelial electrical resistance (TEER) analysis was performed to monitor the change of EC monolayer permeability. The ROS levels in exosomes and ECs were measured by using a ROS-Glo H_2O_2 Assay kit.
Results: First, we observed that thrombin and PMA both stimulated podosome cluster formation at the cell periphery in (30-36%, 90-108 of 300) ECs, which correlated well with reduction (40.5-50.7%, 6-7.5 of 14.8) in TEER values (n=4, p<0.01). Next, we discovered that septic exosomes collected at 3 h post-CLP or post-LPS-injection contained significantly higher amount of H_2O_2 which can be transferred into ECs, leading to 1.5-fold increase of H_2O_2 in ECs (n=6, p<0.01). Moreover, treatment of ECs with septic exosomes remarkably increased the percentage of cells carrying podosome clusters (20.3%, 51 of 251) compared to controls (9.5%, 24 of 252 n=4, p<0.01). Meanwhile, the TEER value was reduced by 27.6% (3.4 of 12.3) upon septic exosome stimulation (n=4, p<0.01). By contrast, scavenging H_2O_2 in septic exosomes significantly attenuated their effects on podosome cluster formation and EC monolayer TEER.
Conclusion: septic exosomes can stimulate the formation of podosome clusters in ECs through transferring exosomal H_2O_2, leading to endothelial hyperpermeability.

Disclosures: **X. Mu:** None. **X. Wang:** None. **K. Essandoh:** None. **Y. Li:** None. **A.M. Pugh:** None. **J. Peng:** None. **S. Deng:** None. **E.S.B. Salem:** None. **C.C. Caldwell:** None. **G. Fan:** None.

628

Circulating Exosomes Isolated from Septic Mice Induce Endothelial Hyperpermeability Through Promoting Podosome Cluster Formation

Xingjiang Mu, Xiaohong Wang, Kobina Essandoh, Yutian Li, Amanda M Pugh, Jiangtong Peng, Shan Deng, Esam S Salem, Charles C Caldwell, Guo-Chang Fan, Univ of Cincinnati, Cincinnati, OH

Introduction: Septic shock increases vascular permeability, leading to multiple organ failure and higher mortality. Reactive oxygen species (ROS) have been shown to promote both actin cytoskeleton reorganization resulting in vascular leakage and the formation of podosome, an actin-based dynamic membrane structure. Interestingly, recent studies have shown that circulating exosomes from septic patients contained higher levels of ROS than healthy ones. In this study, we hypothesized that septic exosomes can transfer exosomal ROS to endothelial cell (EC) to promote the generation of podosomes, leading to hyperpermeability.
Methods: C57BL/6 mice (20-25g) were subjected to CLP surgery or injection with LPS (25 μg/g). Sham-operated or PBS-treated mice were used as controls. Exosomes were isolated from sera, collected at 3 h post-CLP or post-LPS-injection. Podosomes were identified by co-immunostaining F-actin/cortactin following stimulation with PMA, thrombin and exosomes. Transendothelial electrical resistance (TEER) analysis was performed to monitor the change of EC monolayer permeability. The ROS levels in exosomes and ECs were measured by using a ROS-Glo H_2O_2 Assay kit.
Results: First, we observed that thrombin and PMA both stimulated podosome cluster formation at the cell periphery in (30-36%, 90-108 of 300) ECs, which correlated well with reduction (40.5-50.7%, 6-7.5 of 14.8) in TEER values ($n=4$, $p<0.01$). Next, we discovered that septic exosomes collected at 3 h post-CLP or post-LPS-injection contained significantly higher amount of H_2O_2 which can be transferred into ECs, leading to 1.5-fold increase of H_2O_2 in ECs ($n=6$, $p<0.01$). Moreover, treatment of ECs with septic exosomes remarkably increased the percentage of cells carrying podosome clusters (20.3%, 51 of 251) compared to controls (9.5%, 24 of 252 $n=4$, $p<0.01$). Meanwhile, the TEER value was reduced by 27.6% (3.4 of 12.3) upon septic exosome stimulation ($n=4$, $p<0.01$). By contrast, scavenging H_2O_2 in septic exosomes significantly attenuated their effects on podosome cluster formation and EC monolayer TEER.
Conclusion: septic exosomes can stimulate the formation of podosome clusters in ECs through transferring exosomal H_2O_2, leading to endothelial hyperpermeability.

Disclosures: **X. Mu:** None. **X. Wang:** None. **K. Essandoh:** None. **Y. Li:** None. **A.M. Pugh:** None. **J. Peng:** None. **S. Deng:** None. **E.S.B. Salem:** None. **C.C. Caldwell:** None. **G. Fan:** None.

629

IFN-Gamma-Dependent Repression of TET2 in Allograft Vasculopathy Exacerbates VSMC Activation

Allison Ostriker, Kathleen Martin, Yale, New Haven, CT

Coronary allograft vasculopathy (CAV) occurs in 50% of heart transplant recipients at 10 years after surgery. Allograft failure secondary to CAV accounts for 30% of deaths in heart transplant recipients. CAV is characterized by concentric intimal hyperplasia (IH) in the graft vasculature that causes ischemic injury to the myocardium. T cell-derived INF-γ is a well-established driver of IH in CAV. The molecular mechanisms of IFN-γ-dependent phenotypic modulation of vascular smooth muscle cells (VSMCs) in CAV are not fully elucidated.
Our group recently showed that TET methylcytosine dioxygenase 2 (TET2) is a master regulator of VSMC phenotype. We hypothesized that IFN-γ modulates TET2 expression and/or function in VSMCs in CAV. We found, using a minor histocompatibility mismatch aorta graft model of allograft vasculopathy, that TET2 expression was decreased in the graft neointima relative to aortic VSMCs prior to grafting. Lineage tracing studies showed that TET2 activity was decreased in donor VSMC-derived cells present in the neointima. Nuclear localization of phospho-STAT1 correlated with TET2 repression in these cells suggesting that IFN-γ signaling may mediate repression of TET2. Further, we found that IFN-γ was sufficient to repress TET2 expression in human and mouse VSMCs in vitro. TET2 repression by IFN-γ was not repressed by rapamycin, an mTOR inhibitor known to be effective against CAV but which has significant side effects.
We hypothesized that IFN-γ signaling directly represses TET2. IFN-γ rapidly induced activation of STAT1 in VSMCs in vitro. Transcription factor binding site prediction suggested potential STAT1 binding sites on the TET2 promoter in both human and mouse. ChIP-PCR confirmed that STAT1 occupancy occurs at the

TET2 promoter in response to IFN-γ.
Studies are ongoing to determine if STAT1 directly negatively regulates TET2 transcription in response to IFN-γ, and if TET2 overexpression can rescue the effect of IFN-γ on VSMC activation and IH in in vivo models of allograft vasculopathy. Since IFN-γ-dependent repression of TET2 is not reversed by rapamycin, elucidating this pathway represents an opportunity for developing complementary therapies to mTOR inhibition that may result in improved outcomes and fewer side effects.

Disclosures: **A. Ostriker:** None. **K. Martin:** None.

This research has received full or partial funding support from the American Heart Association.

630

Cst1 Discriminates Between Senescence Due to Replicative and Stress-Induced Endothelial Cell Aging

Sadaf Afreen, Karl E Herbert, Univ of Leicester, Leicester, United Kingdom

Introduction Senescence comprises the cellular and molecular changes leading to compromised functionality of organs. The presence of senescent endothelial cells in human atherosclerotic lesions suggests a contribution to vascular pathology. Better understanding of endothelial senescence will help identify its role in endothelial dysfunction. In this study gene expression changes were assessed in human endothelial cells following induction of senescence either by replicative or peroxide-induced stress and genes identified that were differentially expressed to be used as biomarkers of endothelial aging. Methods Replicative senescent endothelial cells (REPS) were established by passaging human umbilical vein endothelial cells (HUVECs) up to 25 population doublings and stress-induced premature senescence (SIPS) was induced by treating HUVECs with tertiary butyl hydrogen peroxide (t-BHP) for 1 hr for consecutive 3 days. Senescence was confirmed by staining with senescence marker SA β-gal and p53 expression through Western blotting. Gene expression changes were confirmed by qPCR using Taqman probes. Results REPS and SIPS cells were found to be 71 % (912 of 1285) and 81 % (980 of 1210) positive for SA-beta gal staining respectively, compared to young endothelial cells (10 % (130 of 1308); Fig1). CST1 was identified as highly expressed gene (90 fold) in REPS but not SIPS of endothelial cells in microarray gene expression analysis. Further validation using qPCR showed a 164 fold increase in CST1 expression (fig2) in REPS endothelial cells only. Conclusion In conclusion, this study confirms that CST1 as a new marker of replicative senescence in human endothelial cells.

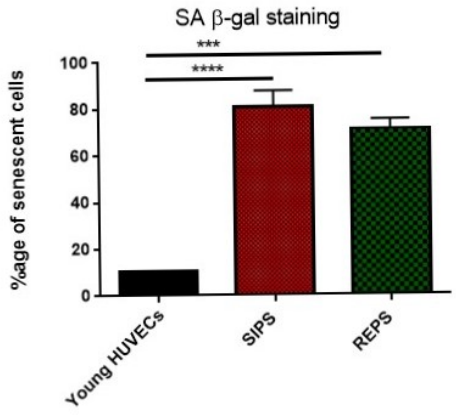

Fig1

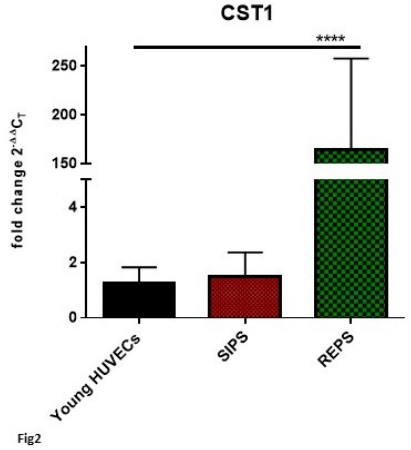

Disclosures: **S. Afreen:** None. **K.E. Herbert:** None.

631 will be presented in the PVD Moderated eAbstract Poster Session. The abstract content is located on page 43.

632

Aortic Dilatation in Marfan Syndrome: A Result of Amplification of Molecular Mechanisms of Aging?

Michael A Hagler, Grace Casaclang-Verzosa, Bin Zhang, Carolyn Roos, Nassir Thalji, Jordan Miller, Mayo Clinic, Rochester, MN

Marfan syndrome (MFS) is a genetic disease with a mutation for the microfibrillar constituent protein fibrillin-1 being the most prevalent. MFS is often associated with progressive aortic root dilation, ultimately progressing to aortic aneurysm and dissection. While recent work has shown that increased angiotensin-II receptor type-1 and transforming growth factor beta (TGF-β) signaling contributes to aneurysm formation in aorta, efficacious therapeutic targets remain elusive. Given previous reports of progeriod phenotypes in a subset of Marfan patients, we sought to determine whether there are molecular changes that are consistent with accelerated aging in a mouse model of Marfan syndrome. In mice carrying a loss-of-function mutation in fibrillin-1, we assessed aortic root dimensions by echocardiography and gene expression levels of TGF-β1-3, runt related transcription factor 2 (RUNX2), and the cellular senescent marker CDKN2A by quantitative real time PCR at 3 and 14 months of age. As expected, aortic sinus dimensions did not change significantly with aging in wild type mice, but increased dramatically in fibrillin-1 mutant mice compared to wild-type littermate controls and with age ($p < 0.05$ for both). TGF-β1 ligand expression paralleled age and disease-dependent changes in aortic dimensions, however TGF-β2 and TGF-β3 mRNA levels did not. Aortic dilatation was associated with increased gene expression of RUNX2 with aging and in marfanoid mice. Interestingly, fibrillin-1 mutant mice demonstrated marked increases in expression of the anti-proliferative cell-cycle checkpoint protein CDKN2A at both time points, and correlated with changes in TGF-β1 (R^2=0.54) and RUNX2 (R^2=0.69) mRNA. CDNK2A gene expression patterns, however, demonstrated a poor correlation with expression of TGF-β2 and TGF-β3 (R^2=0.04 and 0.06. respectively). Collectively, these data lend insight into novel mechanisms that may regulate development of aortic root dilation in patients MFS and are the first to implicate increased senescent cell burden in Marfan syndrome. Furthermore, we propose that clearance of senescent cells could be a viable therapeutic intervention to slow progression aortic root-dilation and aneurysm in patients with Marfan syndrome.

Disclosures: **M.A. Hagler:** None. **G. Casaclang-Verzosa:** None. **B. Zhang:** None. **C. Roos:** None. **N. Thalji:** None. **J. Miller:** None.

633

Protein Kinase D Regulates VEGFR-2 Transcriptional Activity in Endothelial Cells Through AP-2β

Luke H. Hoeppner, Hormel Inst, Univ of Minnesota, Austin, MN; Resham Bhattacharya, Univ of Oklahoma Health Sciences Ctr, Oklahoma City, OK; Ying Wang, Ramcharan Singh Angom, Enfeng Wang, Shamit Dutta, Heike R. Doeppler, Mayo Clinic, Jacksonville, FL; Isobel A. Scarisbrick, Mayo Clinic, Rochester, MN; Peter Storz, Debabrata Mukhopadhyay, Mayo Clinic, Jacksonville, FL

Vascular endothelial growth factor A (VEGF) signals primarily through its cognate receptor VEGFR-2 to control vasculogenesis and angiogenesis. Dysregulation of these physiological processes contributes to the pathologies of heart disease, stroke, and cancer. Protein kinase D (PKD) plays a crucial role in the regulation of angiogenesis by modulating endothelial cell proliferation and migration. In human umbilical vein endothelial cells (HUVEC) and human blood outgrowth endothelial cells (BOEC), knockdown of PKD-1 or PKD-2 downregulates VEGFR-2 and significantly inhibits VEGF-induced endothelial cell proliferation and migration. We sought to determine the molecular mechanism through which PKD modulates VEGFR-2 expression. Based on bioinformatics data, activating enhancer binding protein 2 (AP2) binding sites exist within the VEGFR-2 promoter. Thus, we hypothesized PKD may downregulate VEGFR-2 through AP2-mediated transcriptional repression of the VEGFR-2 promoter. Indeed, AP2β binds the VEGFR-2 promoter upon PKD knockdown in HUVEC as evident by chromatin immunoprecipitation assay. Luciferase reporter assays using serial deletions of AP2β binding sites within the VEGFR-2 promoter revealed transcriptional activity negatively correlated with the number of AP2β binding sites, thus confirming negative regulation of VEGFR-2 transcription by AP2β. Next, using siRNA, we demonstrated that upregulation of AP2β decreased VEGFR-2 expression and loss of AP2β enhanced VEGFR-2 expression. *In vivo* studies confirmed this finding as we observed increased VEGFR-2 immunostaining in the dorsal horn of the spinal cord of embryonic day 13 AP2β knockout mice. We hypothesize that PKD directly regulates AP2β function by serine phosphorylation and ongoing studies are being conducted to determine phosphorylation sites in AP2β directly regulated by PKD. Taken together, we demonstrate AP2β negatively regulates VEGFR-2 transcription and VEGFR-2 is a major downstream target of PKD. Our findings describing how PKD regulates angiogenesis may contribute to the development of therapies to improve the clinical outcome of patients afflicted by heart disease, stroke, and cancer.

Disclosures: **L.H. Hoeppner:** None. **R. Bhattacharya:** None. **Y. Wang:** None. **R. Angom:** None. **E. Wang:** None. **S. Dutta:** None. **H.R. Doeppler:** None. **I.A. Scarisbrick:** None. **P. Storz:** None. **D. Mukhopadhyay:** None.

This research has received full or partial funding support from the American Heart Association.

634

Partial Genetic Disruption of mTOR Signaling Does Not Improve Vascular Endothelial Function in Hypercholesterolemic Mice

Aiham H Jbeli, Sanford Sch of Med - Univ of South Dakota, Sioux Falls, SD; Bin Zhang, Carolyn M. Roos, Jordan D. Miller, Mayo Clinic, Rochester, MN

Endothelial cell senescence promotes inflammation and impairs endothelium-dependent vasodilation. While aging, hypercholesterolemia, and caloric excess are known to drive cellular senescence in part through activation of mTOR, it is unknown whether reducing mTOR signaling can improve vasomotor function in aging mice. Here, we used hypercholesterolemic mice ($Ldlr^{-/-}/apoB^{100/100}$, or LA) carrying intact copies of mTOR (LA-$mTOR^{+/+}$) or were deficient in one copy of mTOR (LA- $mTOR^{+/-}$). Mice were fed Western Diet for 6 or 12 months, and vasomotor function in aorta was evaluated using isolated organ chamber baths. Maximum relaxation to acetylcholine (MR_{ACH}) was progressively impaired from 6 months to 12 months in LA-$mTOR^{+/+}$ mice (55±4% and 30±4%, respectively). In contrast to our hypothesis, however, MR_{ACH} was not significantly improved in LA-$mTOR^{+/-}$ mice at either time point (62±3% and 35±5%, respectively). Interestingly, a subgroup analysis showed significant improvement in MR_{ACH} in male mice at the 6-month point (male LA-$mTOR^{+/+}$ mice = 30 ± 9% vs male LA-$mTOR^{+/-}$ mice = 55±4%; $p < 0.01$), whereas vasomotor function in female mice was nearly identical across groups. There was no significant difference at the 12-month point (male LA-$mTOR^{+/+}$ mice = 19 ± 3% vs male LA-$mTOR^{+/-}$ mice = 22 ± 5%). Relaxation to acetylcholine was attenuated by L-NAME at 6 months and 12 months (but identical between genotypes) and relaxation to nitroprusside was identical between strains at each time point, suggesting that changes in endothelial function were not masked by compensatory mechanisms

(e.g., endothelium-derived hyperpolarizing factors). Furthermore, reduction of mTOR did not elicit changes in maximal tension generated in response to Prostaglandin $F_{2\alpha}$ at either time point. Collectively, despite compelling evidence from in vitro model systems, genetic reduction of mTOR signaling *in vivo* does not appear to be sufficient to improve vasomotor function in our model of aging hypercholesterolemic mice**.** Our data do, however, shed light on a potential role of sex in dictating phenotypic changes in early to moderate stages of disease, which warrants further investigation.

Disclosures: **A.H. Jbeli:** None. **B. Zhang:** None. **C.M. Roos:** None. **J.D. Miller:** None.

635

Role of Micro RNA-21 in Venous Neointimal Hyperplasia (VNH): Implications in Targeting MiR-21 For VNH Treatment

Sreenivasulu Kialri, Binxia Yang, Deborah McCall, Sanjay Misra, Mayo Clinic, Rochester, MN

The exact molecular mechanisms involved in hemodialysis arteriovenous fistula (AVF) failure caused by venous neointimal hyperplasia (VNH) are not clear. It has been observed that there is an accumulation of extracellular matrix and up regulation of pro-fibrotic genes accompanied with presence of fibroblasts, smooth muscle cells, and inflammatory cells in the stenotic veins. Previous studies have demonstrated that adventitial and medial fibroblasts have a pivotal role(s) in VNH formation. MicroRNA-21 (miR-21) contributes to fibroblast to myofibroblast differentiation and dysregulation of miR-21 plays a pathological role in failure of coronary artery bypass grafts. The aim of the present study was to determine the role of miR-21 in VNH associated with AVF. We assessed miR-21 expression using qRT-PCR in the outflow veins of AVFs compared to control (contralateral jugular veins) veins in the C57BL/6J mice with chronic kidney disease (CKD). MiR-21 expression was upregulated accompanied with down regulation of miR-21 target genes; PPAR-α, PTEN and TIMP-3. In addition, gene expression of fibroblast specific protein (FSP) -1, TGF (transforming growth factor) -β1, matrix metalloproteinases (MMP)-2, -9, collagen-I, and IV were significantly increased at day 7 after AVF creation. Immunohistochemistry revealed that there was a significant increase in proliferating cell index (Ki-67) and fibroblast index (FSP-1) in the outflow veins of AVFs. Hypoxia has been shown to increase fibroblast to myofibroblast differentiation and this is predicted to be an early step in VNH formation. Therefore we assessed miR-21 expression in hypoxic ($1\%O_2$) mouse pulmonary vein fibroblasts compared to normoxic cells *in vitro* and it was found that miR-21and TGF-β1 significantly elevated with down regulation of miR-21 target genes PTEN and TIMP-3. Furthermore, miR-21 knockdown in hypoxic fibroblasts attenuated TGF-β1 expression with a significant upregulation of genes targeted by miR-21 compared to controls. Together these results indicate that upregulation of miR-21 expression may result in fibroblast to myofibroblast differentiation resulting in VNH formation.

Disclosures: **S. Kialri:** None. **B. Yang:** None. **D. McCall:** None. **S. Misra:** Research Grant; Significant; NIH RO1: HL 98967.

636

Regulation of Galectin-3 Expression in Pulmonary Vascular Smooth Muscle by Dna Methylation

Xueyi Li, Feng Chen, Stephen Haigh, Yusi Wang, Zsuzsana Bordan, David Stepp, Neal Weintraub, Scott Barman, David Fulton, Augusta Univ, Augusta, GA

Pulmonary Arterial Hypertension (PAH) is characterized by excessive vascular cell proliferation, inward remodeling and increased stiffness and inflammation of the pulmonary blood vessels. We found that galectin-3 (Gal-3) is upregulated in PA from multiple models of PAH including monocrotaline (MCT), MCT + pneumonectomy, and SUGEN/hypoxia rats as well as in human PAH and correlated with severity of disease. Gal-3 is a β-galactoside binding lectin implicated in signaling pathways regulating cell proliferation, inflammation and fibrosis, but its role in PAH is poorly defined. Confocal analysis revealed the majority of Gal-3 expression in the media of PA of both rodent models and humans. Selective inhibitors of Gal-3 attenuated PAH in MCT-treated rats and reduced indices of proliferation, fibrosis and increased apoptosis in PA. Overexpression of Gal-3 in PASMC increased proliferation, migration and expression of profibrotic molecules and protected from apoptosis. Acute exposure of cultured HPASMC with various mitogens and factors important in the development of PAH, failed to increase Gal-3 expression. In contrast, PASMC isolated from rats with PAH exhibited an enduring capacity for increased proliferation and expressed higher levels of Gal-3 suggesting an epigenetic mechanism regulating Gal-3

expression. We found that treatment of PASMC with inhibitors of DNA methylation robustly increased Gal-3 expression in control human and rat PASMC but not in MCT-derived PASMC. Methylation analysis of DNA isolated from PA using MeDIP-qPCR and pyrosequencing revealed hypomethylation of Gal-3 proximal promoter. Analysis of DNA methyltransferase expression in PA revealed a significant loss of only Dnmt3A expression in hypertensive PA. To assess the role of local methylation in the regulation of Gal-3 expression we used CRISPR-dCas9. Targeted Gal-3 promoter methylation using multiple RNA guides and dCas9-Dnmt3A-Dnmt3L effectively reduced Gal-3 expression in SMC isolated from MCT rat PA and reversed the excessive proliferation. These results advance an important role of methylation-dependent mechanisms in Gal-3 signaling and provide a mechanism for the enduring changes in vascular cell behavior observed in PAH.

Disclosures: **X. Li:** None. **F. Chen:** None. **S. Haigh:** None. **Y. Wang:** None. **Z. Bordan:** None. **D. Stepp:** None. **N. Weintraub:** None. **S. Barman:** None. **D. Fulton:** None.

This research has received full or partial funding support from the American Heart Association.

637

Role of Nuclear Smooth Muscle Alpha-Actin in the Differentiation of Vascular Smooth Muscle Cells

Shuangtao Ma, Dianna M Milewicz, The Univ of Texas Health Science Ctr at Houston McGovern Medical Sch, Houston, TX

Although the function of the cytoplasmic smooth muscle (SM) α-actin in contractile units has been well characterized in vascular SMCs, whether the SM α-actin is present in the nucleus and its nuclear function are yet to be determined. Our previous study discovered the mutations in *ACTA2*, which encodes SM α-actin, predispose to both thoracic aortic disease and occlusive vascular diseases (stroke and coronary artery disease). We hypothesize that nuclear SM α-actin is critical for differentiation of SMCs. The cytoplasmic and nuclear fractions of mouse SMCs were isolated and the SM α-actin was detected in both cytosol and nucleus by immunoblotting. Moreover, both cytoplasmic and nuclear SM α-actin were dramatically upregulated during the differentiation of SMCs stimulated with TGF-β. Two-dimensional gel electrophoresis, which can separate actin isoforms based on distinct isoelectric points, was used to show that the ratio of SM α-actin to β-actin was increased in nuclear fraction when compared to cytoplasmic fraction with differentiation of SMCs, driven by serum starvation and TGF-β treatment. Furthermore, differentiation was associated with a significantly higher nuclear to cytoplasmic ratio of SM α-actin, indicating SM α-actin accumulates in the nucleus during differentiation. Co-immunoprecipitation experiments identified that nuclear SM α-actin is a component of the chromatin remodeling complex, Ino80, and the immunofluorescence confirmed co-localization of SM α-actin and Ino80 in the nucleus. To investigate the transcriptional function of nuclear SM α-actin, we performed the chromatin immunoprecipitation quantitative PCR, which revealed that the SM α-actin, but not β-actin, accumulated to the promoter region of SMC differentiation markers, including *Myh11*, *Cnn1*, and *Tagln*, during the differentiation of SMC. As expected, the *Acta2* mutant SMCs (pArg149Cys) disrupt the differentiation of SMCs based on decreased contractile protein levels and increased proliferation. Furthermore, specific *Acta2* missense mutations disrupt the ability for SM α-actin to localize to the nucleus. Taken together, our study found the SM α-actin concentrates into the nucleus of SMCs and may play a role in chromatin remodeling required for differentiation of SMCs.

Disclosures: **S. Ma:** None. **D.M. Milewicz:** None.

This research has received full or partial funding support from the American Heart Association.

638

Novel Role of 4-Hydroxy-2-Nonenal Mediated Mitochondrial Stress Signaling in Ischemia and Reperfusion Injury

Sumitra Miriyala, Mini Chandra, Manikandan Panchatcharam, Christopher Kevil, Md Shenuarin Bhuiyan, Jonathan Fox, LSU Health Sciences Ctr - Shreveport, Shreveport, LA

Myocardial infarction is the single most prevalent cause of morbidity and mortality among adults. Excess generation of reactive oxygen species plays a major role in the cellular response to cardiac

ischemia/reperfusion (I/R) injury. Accumulated evidence indicates that oxidative stress in mitochondria plays an important role in I/R injury, but how mitochondrial redox mechanisms are involved in cardiac dysfunction remains unclear. Manganese Superoxide Dismutase (MnSOD), an antioxidant enzyme that catalyzes the conversion of superoxide radicals (O_2•-) in mitochondria. The absence of *SOD2* (a gene that encodes MnSOD) is found to be embryonic lethal in animal models due to impairment of mitochondrial function, most noticeably in the heart. In our investigation, we found MnSOD mimetic, MnTnBuOE-2-PyP^{5+} distributed 3-fold more in mitochondria than in cytosol. The exceptional ability of MnTnBuOE-2-PyP^{5+} to dismute O_2•- parallels its ability to reduce ONOO− and CO3−. Based on our initial results, we have generated mice that specifically lack MnSOD in cardiomyocytes (Mhy6-SOD2$^{\Delta}$). These mice showed early mortality ~6 months due to cardiac mitochondrial dysfunction. FACS analyses using Mito-Tracker Green indicated that the mass of mitochondria per cell was slightly decreased in the Mhy6-SOD2$^{\Delta}$ to the wild type. We then examined oxidative phosphorylation levels in Mhy6-SOD2$^{\Delta}$ v.s. wild type using a Seahorse XF analyzer. The rate of oxygen consumption per cells was significantly lower in Mhy6-SOD2$^{\Delta}$ cardiomyocytes than that in wild type. The most noticeable difference in the O_2 consumption was found in the presence of FCCP (H+ ionophore/uncoupler). 4-hydroxy-2-nonenal (HNE) adduction of mitochondrial apoptosis-inducing factor (AIFm2) inactivates the NADH oxidoreductase activity of AIFm2 and facilitates its translocation from mitochondria. His 174 on AIFm2 is the critical target of HNE adduction that triggers this functional switch. HNE adduction and translocation of AIFm2 from mitochondria following I/R injury are attenuated by superoxide dismutase mimetics. These results identify a previously unrecognized role of the MnSOD-HNE-AIFm2 axis, with important consequences for mitochondrial stress signaling, especially in cardiac I/R injury.

Disclosures: **S. Miriyala:** None. **M. Chandra:** None. **M. Panchatcharam:** None. **C. Kevil:** None. **M. Bhuiyan:** None. **J. Fox:** None.

640

Overexpression of Vasohibin-2 Exacerbates Development of Angiotensin II-Induced Thoracic Aortic Aneurysms Independent of VeEGF

Michihiro Okuyama, Dept. Cardiovascular Surgery, Okayama Univ Hosp, Okayama, Japan; Haruhito A Uchida, Dept. of Chronic Kidney Disease (CKD) and Cardiovascular Disease (CVD), Okayama Univ, Graduate Sch of Med, Dentistry and Pharmaceutical Sciences, Okayama, Japan; Ryoko Umebayashi, Yuki Kakio, Hidemi Takeuchi, Katsuyuki Tanabe, Dept. of Nephrology, Rheumatology, Endocrinology and Metabolism, Okayama Univ, Graduate Sch of Med, Dentistry and Pharmaceutical Sciences, Okayama, Japan; Yasufumi Sato, Dept. of Vascular Biology, Inst of Development, Aging, and Cancer, Tohoku Univ, Sendai, Japan; Jun Wada, Dept. of Nephrology, Rheumatology, Endocrinology and Metabolism, Okayama Univ, Graduate Sch of Med, Dentistry and Pharmaceutical Sciences, Okayama, Japan

Objective: Chronic angiotensin II (AngII) infusion promotes both thoracic (TAAs) and abdominal aortic aneurysms (AAAs) in mice. Vasohibin-2 (VASH2) is known to cause angiogenesis at the sprouting front of neovascularization. The purpose of this study was to examine whether VASH2 influenced AngII-induced TAAs.
Methods: Male C57BL/6J mice (10-week-old) were injected with VASH2 or LacZ expressing adenovirus (Ad; 7.5 x 10^9 vp/100 μL) via tail vein at 2 week intervals. One week after the first injection, subcutaneous infusion of either AngII (1,000 ng/kg/min) or saline by mini osmotic pumps was started for 3 weeks. Consequently, mice were divided into 4 groups: AngII + Ad VASH2 (n=22), AngII + Ad LacZ (n=21), saline + Ad VASH2 (n=10), saline + Ad LacZ (n=8). Next, in order to examine whether VASH2 affected TAAs via VEGF regulation, bevacizumab was intraperitoneally administrated into mice; AngII + Ad VASH2 + saline (n=15), AngII + Ad VASH2 + bevacizumab (n=15). TAAs were evaluated in all mice by *en face* method. Third, human aortic smooth muscle cells (hSMCs) were infected with Ad VASH2 or Ad LacZ, stimulated with or without AngII to evaluate further mechanism.
Result: Intima area of aortic arch was significantly larger in AngII + Ad VASH2 group than in AngII + Ad LacZ group (19.78 ± 0.40 mm^3 vs 17.74 ± 0.44 mm^3, $P < 0.001$). Gelatin zymography demonstrated that AngII upregulated latent MMP-2 expression, and activated MMP-2 most prominently in AngII + VASH2 group. Protein expression of p21 and p53 in thoracic aortas was enhanced in AngII + VASH2 group. Positive TUNEL staining was observed in thoracic aortic wall of AngII + VASH2 group. No significant difference in intima area of aortic arch between AngII + Ad VASH2 + saline group and AngII + Ad VASH2 + bevacizumab group. In vitro, the same results were observed regarding protein expression of p21 and p53, and TUNEL staining. In addition, Annexin-V staining was detected only in AngII + VASH2 group.

Conclusion: Overexpression of VASH2 accelerated development of AngII-induced TAAs in vivo. VASH2-induced cell apoptosis may influence AngII-induced TAA formation independent of VEGF.

Disclosures: **M. Okuyama:** None. **H.A. Uchida:** None. **R. Umebayashi:** None. **Y. Kakio:** None. **H. Takeuchi:** None. **K. Tanabe:** None. **Y. Sato:** None. **J. Wada:** None.

641

Protein Disulfide Isomerase-A1 Overexpression Enhances Vascular Calcification in Mice

Luciana A Pescatore, Patricia Nolasco, Heart Inst, Univ of São Paulo Sch of Med, São Paulo, Brazil; Elisângela Farias-Silva, Hosp Albert Einstein, São Paulo, Brazil; Leonardo Jensen, Carolina G Fernandes, Heart Inst, Univ of São Paulo Sch of Med, São Paulo, Brazil; Youri E Almeida, Luciana S Carmo, Hosp Albert Einstein, São Paulo, Brazil; Laurindo R Laurindo, Heart Inst, Univ of São Paulo Sch of Med, São Paulo, Brazil; Marcel Liberman, Hosp Albert Einstein, São Paulo, Brazil

Vascular calcification (VC) is an active pathophysiological process promoting enhanced morbidity and mortality without effective therapy. Oxidative stress and endoplasmic reticulum (ER) stress support cardiovascular calcification progression. We showed previously that the ER redox chaperone protein disulfide isomerase-A1 (PDI) is required for agonist-driven Nox NADPH oxidase activation. Oxidant levels and expression of Nox subunits and PDI are upregulated in calcifying rabbit valves. We hypothesized that PDI supports VC. We recently developed a new PDI overexpression mouse model (TgPDI) in FVB background (WT). To investigate whether TgPDI mice show increased VC, we challenged 20 week-old TgPDI mice with Vitamin-D_3 (VitD) for 14 days. Also, we incubated primary vascular smooth muscle cells (VSMC) isolated from WT or TgPDI mice with mineralizing medium (β-glycerophosphate 10mM + $CaCl_2$ 6mM). TgPDI results were compared to those from respective WT littermates. We tested distinct VitD doses. At $9x10^4$IU/day, WT mice depicted negligible increases in calcification area (median 0.07% to 0.36% aorta cross-sectional area, p=ns, n=5), while TgPDI showed enhanced calcification (median 0.20 to 3.63 % area, $p<0.05$, n=4). The sum of calcification areas across all mice showed a 2.6-fold increase in TgPDI. TgPDI mice did not develop aortic valve stenosis or change in ascending aorta peak wave velocity at echocardiography. *In vitro,* VSMC phenotype marker expression (SM22 and alpha-actin) was enhanced in TgPDI vs. WT cells at baseline, while calcifying stimulation for 3 or 7 days decreased such VSMC marker expression both in WT and in TgPDI VSMC. Conversely, calcifying stimulation for 3 or 7 days showed no effects on ER stress marker expression (GRP78, GRP94). To assess whether these findings apply to humans, we examined femoral arteries from diabetic and non-diabetic patients with peripheral arterial disease, which showed increased arterial calcification and marked coincident PDI overexpression in samples from diabetic patients. In conclusion, PDI overexpression *in vivo* associates with enhanced VC after VitD calcifying stimulus. PDI and its associated signaling proteins deserve further study as potential therapeutic targets in VC progression.

Disclosures: **L.A. Pescatore:** None. **P. Nolasco:** None. **E. Farias-Silva:** None. **L. Jensen:** None. **C.G. Fernandes:** None. **Y.E. Almeida:** None. **L.S. Carmo:** None. **L.R. Laurindo:** None. **M. Liberman:** None.

642

Specific Protein Kinase C Isoforms Are Critical Mediators of Physiologic Downregulation of Perivascular Tissue Factor

Laura Sommerville, Kristen Gorman, Duke Univ Medical Ctr, Durham, NC; Dougald Monroe, Univ of North Carolina, Chapel Hill, NC; Maureane Hoffman, Veterans Affairs and Duke Univ Medical Ctrs, Durham, NC

Tissue factor (TF) is a procoagulant and transmembrane receptor for FVII(a) that is upregulated in pathological conditions. We recently demonstrated that perivascular TF is downregulated around angiogenic vessels near a cutaneous wound. The goal of this study was to identify mechanisms that mediate TF loss. Primary cultures of human pericytes express high levels of TF. TF expression was lost during culture with phorbol-12 myristate 13-acetate (PMA) for 8 hours, and was maintained for 24 hours. This model recapitulates the pattern of downregulation observed *in vivo*. Using qRT-PCR we assessed changes in TF gene expression in response to PMA. TF mRNA decreased 4- and 6-fold at 8 and 12 hours after treatment ($p<0.01$), and remained 2-fold lower in treated cells after 24 hours ($p<0.05$). Inhibiting *de novo* transcription with actinomycin D showed that degradation of TF mRNA was similar in PMA- and vehicle-treated groups (p=ns). Thus, downregulation of TF mRNA occurs primarily through

inhibition of its synthesis. We next identified a physiologic mediator of TF downregulation using specific inhibitors against PMA-responsive signaling proteins. Two different inhibitors against Protein Kinase C (PKC) were used: Go6983, which inhibits isoforms α, β, δ, ε, μ, and ζ, and GFX, which inhibits α, β, ε, and γ. Both inhibitors significantly attenuated PMA-mediated transcriptional downregulation ($p<0.001$). Based on overlap of inhibited isoforms, this suggests a minimal role for ζ, μ, δ, and γ, while one or more of the α, β, and ε isoforms appear to be critical mediators of TF mRNA synthesis inhibition. Since the timing of TF protein loss is not fully explained by transcriptional inhibition, we investigated the role of protein degradation in TF loss. When protein synthesis was inhibited by cyclohexamide, addition of PMA shortened the half-life of pericyte TF from 11 hours to 5 hours ($p<0.001$). This indicates that increased protein degradation contributes to PMA-induced loss of TF expression. Both Go6983 and GFX significantly attenuated TF protein degradation also. Taken together, our data show that TF downregulation is mediated by transcriptional inhibition and protein degradation, and PKC α, β, and ε have emerged as potential mediators of both mechanisms.

Disclosures: **L. Sommerville:** None. **K. Gorman:** None. **D. Monroe:** None. **M. Hoffman:** None.

This research has received full or partial funding support from the American Heart Association.

643

CX_3CR1 Identifies Adventitial Macrophage Progenitor Cells (AMPCS), a Local Source of Self-Renewing Macrophages in Postnatal Murine Arteries

Deborah F Toledo, Anna Williamson, Nisha Schwarz, Sanuja Fernando, Belinda Di Bartolo, Stephen J Nicholls, Peter J Psaltis, Discipline of Med, Univ of Adelaide & Vascular Res Ctr, Heat Health Theme, South Australian Health and Medical Res Inst, Adelaide, Australia

Background: Macrophages are integral to vascular biology and disease. Although traditional paradigms assert that vascular macrophages originate from circulating monocytes, recent data suggest that some are seeded in utero from CX_3CR1^+ progenitors, and are maintained postnatally by local self-renewal. We previously identified a novel population of locally-maintained adventitial macrophage progenitor cells (AMPCs) as a source of self-renewing macrophages in adult mouse arteries.
Hypothesis: AMPCs express CX_3CR1 and do not derive from definitive hematopoiesis.
Methods: Single-cell disaggregates were prepared from postnatal murine aortas. AMPC content was assessed by macrophage colony-forming unit (CFU-M) assays. Flow cytometry together with fluorescence activated cell sorting (FACS) were used to investigate the immunophenotypic profile of AMPCs and fate-mapping to assess their origins.
Results: CFU-M prevalence in C57BL/6J aortic cells was highest in neonatal mice (~100 per 10^5 cells), and diminished progressively with age (~55/10^5 at 3w, ~15/10^5 at 12w, ~5/10^5 at 52w, $n>4$, $P<0.01$). Secondary replating of single cells from aortic CFU-M revealed striking self-renewal capacity, with 1 in 10 cells forming new CFU-M ($n=8$). Undifferentiated CFU-M displayed >95% expression of the stem cell markers Sca-1 and c-Kit, and high levels of CX_3CR1, but did not acquire the monocyte/macrophage markers CD11b or F4/80 until treated with macrophage-colony stimulating factor ($n=6$). Mice deficient in CX_3CR1 ($Cx_3cr1^{GFP/GFP}$) produced fewer CFU-M than heterozygous ($Cx_3cr1^{+/GFP}$) littermates (8.7±0.7 vs 15.3±0.7 per 10^5, $P<0.001$, $n>7$). FACS selection confirmed that CFU-M forming AMPCs were exclusively contained within a CX_3CR1^+ subpopulation that did not express either CD11b or F4/80 ($n=3$). Finally, CFU-M analysis from $Flt3^{Cre}xRosa^{mT/mG}$ mice demonstrated that AMPCs arise from a $FLT3^{-ve}$ source, indicating that their origins are independent of definitive hematopoiesis ($n=4$).
Conclusion: Clonogenic, self-renewing murine AMPCs express CX_3CR1 but not the monocyte/macrophage markers CD11b and F4/80. The high prevalence of AMPCs in neonatal aorta is consistent with prenatal seeding from CX_3CR1^+ progenitors, independent of definitive hematopoiesis.

Disclosures: **D.F. Toledo:** None. **A. Williamson:** None. **N. Schwarz:** None. **S. Fernando:** None. **B. Di Bartolo:** None. **S.J. Nicholls:** None. **P.J. Psaltis:** None.